MOLECULAR AND CELLULAR MECHANISMS IN REPRODUCTION AND EARLY DEVELOPMENT

EDITED BY: Rafael A. Fissore, Adam Burton and Karin Lykke-Hartmann
PUBLISHED IN: Frontiers in Cell and Developmental Biology

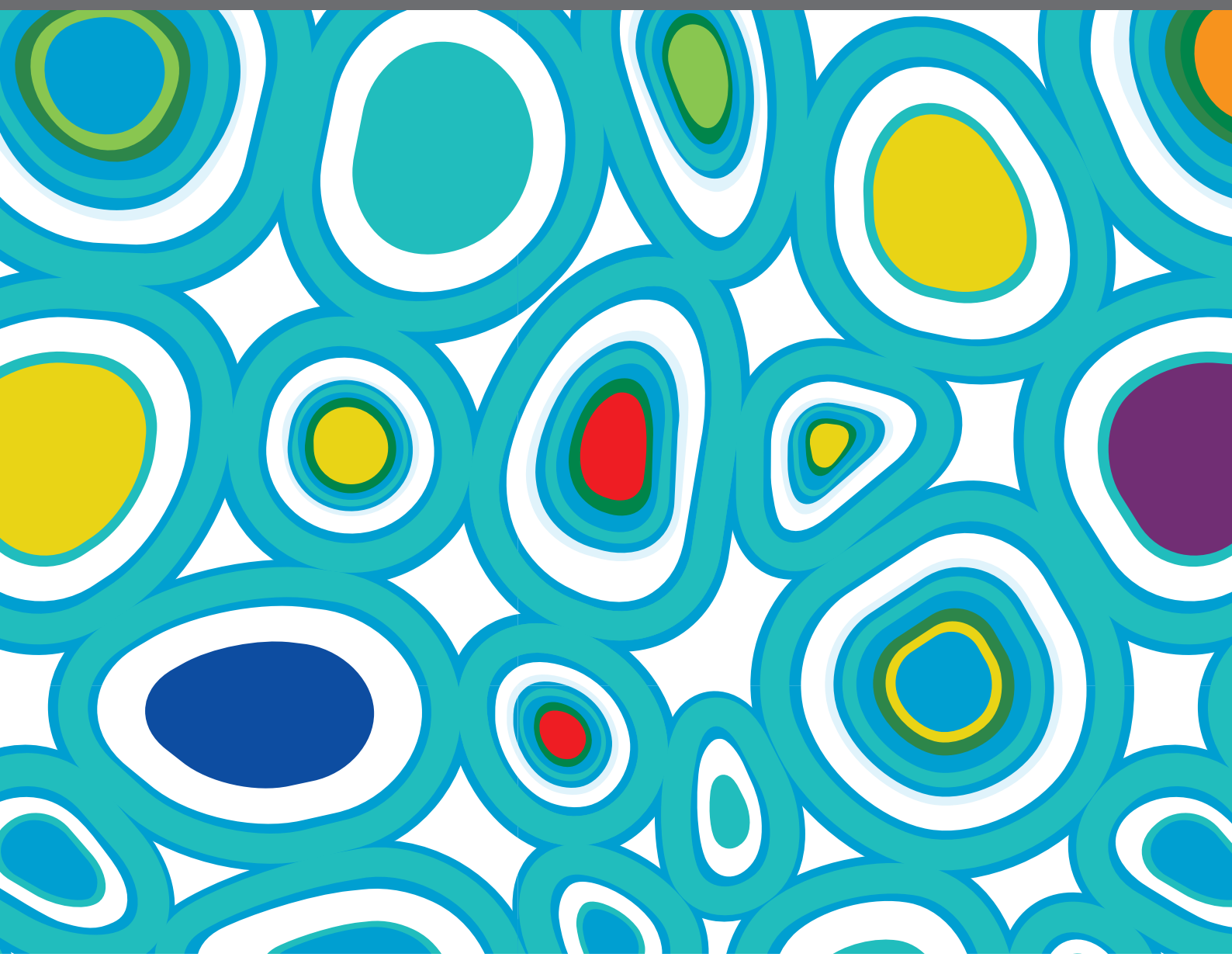

frontiers Research Topics

ISSN 1664-8714
ISBN 978-2-88945-944-5
DOI 10.3389/978-2-88945-944-5

About Frontiers

Frontiers is more than just an open-access publisher of scholarly articles: it is a pioneering approach to the world of academia, radically improving the way scholarly research is managed. The grand vision of Frontiers is a world where all people have an equal opportunity to seek, share and generate knowledge. Frontiers provides immediate and permanent online open access to all its publications, but this alone is not enough to realize our grand goals.

Frontiers Journal Series

The Frontiers Journal Series is a multi-tier and interdisciplinary set of open-access, online journals, promising a paradigm shift from the current review, selection and dissemination processes in academic publishing. All Frontiers journals are driven by researchers for researchers; therefore, they constitute a service to the scholarly community. At the same time, the Frontiers Journal Series operates on a revolutionary invention, the tiered publishing system, initially addressing specific communities of scholars, and gradually climbing up to broader public understanding, thus serving the interests of the lay society, too.

Dedication to Quality

Each Frontiers article is a landmark of the highest quality, thanks to genuinely collaborative interactions between authors and review editors, who include some of the world's best academicians. Research must be certified by peers before entering a stream of knowledge that may eventually reach the public - and shape society; therefore, Frontiers only applies the most rigorous and unbiased reviews.
Frontiers revolutionizes research publishing by freely delivering the most outstanding research, evaluated with no bias from both the academic and social point of view. By applying the most advanced information technologies, Frontiers is catapulting scholarly publishing into a new generation.

What are Frontiers Research Topics?

Frontiers Research Topics are very popular trademarks of the Frontiers Journals Series: they are collections of at least ten articles, all centered on a particular subject. With their unique mix of varied contributions from Original Research to Review Articles, Frontiers Research Topics unify the most influential researchers, the latest key findings and historical advances in a hot research area! Find out more on how to host your own Frontiers Research Topic or contribute to one as an author by contacting the Frontiers Editorial Office: researchtopics@frontiersin.org

MOLECULAR AND CELLULAR MECHANISMS IN REPRODUCTION AND EARLY DEVELOPMENT

Topic Editors:
Rafael A. Fissore, University of Massachusetts, Amherst, United States
Adam Burton, Helmholtz Center Munich - German Research Center for Environmental Health, Germany
Karin Lykke-Hartmann, Aarhus University, Denmark

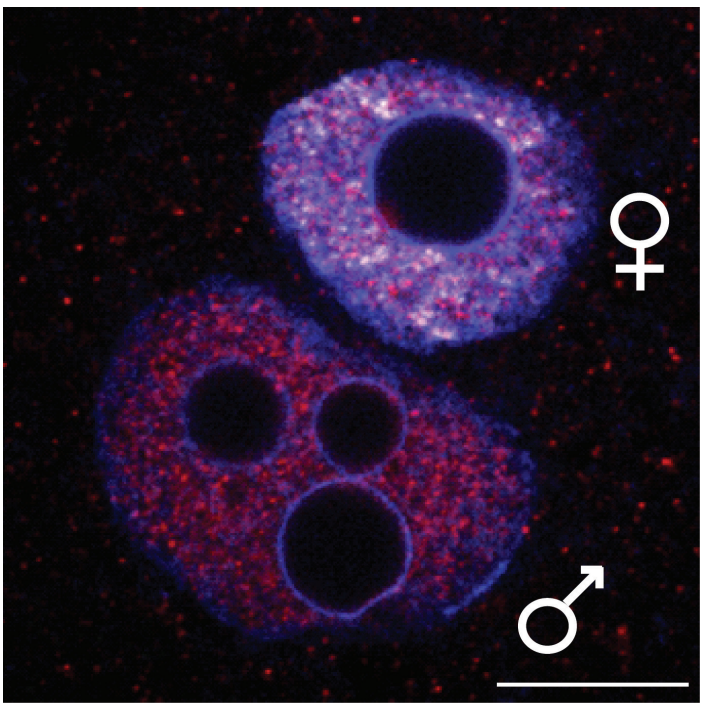

The image is a single confocal section of the pronuclei of a mouse zygote (PN3 stage), stained with anti 5-methylcytosine (grayscale), anti 5-hydroxymethylcytosine (red) and DAPI (blue). The scale bar represents 10µm. Image: Jonathan Adam Burton.

The Research Topic aims to support progress towards understanding the different sets of developmental processes that are absolutely required to complete all the steps essential for successful embryonic development, under physiological conditions. We sought contributions that dealt with single cells, interaction between cells as well as intra- and extracellular signal transduction. The Research Topic presents original studies covering experimental and theoretical approaches, descriptions of new methodologies, reviews and opinions.

Citation: Fissore, R. A., Burton, A., Lykke-Hartmann, K., eds. (2019). Molecular and Cellular Mechanisms in Reproduction and Early Development. Lausanne: Frontiers Media. doi: 10.3389/978-2-88945-944-5

Table of Contents

frontiers in Cell and Developmental Biology

EDITORIAL
published: 20 March 2019
doi: 10.3389/fcell.2019.00036

Editorial: Molecular and Cellular Mechanisms in Reproduction and Early Development

Rafael A. Fissore[1], *Adam Burton*[2] *and Karin Lykke-Hartmann*[3,4,5]*

[1] Department of Veterinary and Animal Sciences, University of Massachusetts, Amherst, MA, United States, [2] Institute of Epigenetics and Stem Cells, Helmholtz Zentrum München, München, Germany, [3] Department of Biomedicine, C Aarhus University, Aarhus, Denmark, [4] Department of Clinical Medicine, Aarhus University, Aarhus, Denmark, [5] Department of Clinical Genetics, Aarhus University Hospital, Aarhus, Denmark

Keywords: male and female gametes, Ca^{2+} signaling, fertilization, chromosomes, histones, folate, human pluripotent stem cells

Editorial on the Research Topic

Molecular and Cellular Mechanisms in Reproduction and Early Development

The growth and division of gamete cells are prerequisites for successful fertility and have received increasing attention in research communities (Skinner, 2005; Da Silva-Buttkus et al., 2008; Shah et al., 2018).

In the early 1950s, Austin and Chang independently described the changes that are required for the sperm to fertilize oocytes *in vivo*. During capacitation, sperm undergo a change in the motility pattern called hyperactivation (Yanagimachi, 1970). In this issue of Frontiers, a comprehensive review addresses the importance of this in the male gamete and the changes that occur in sperm during their transit through the male and female reproductive tracts by complex signaling cascades with focus on the principal molecular mechanisms that govern human sperm capacitation (Puga Molina et al). Sperm are both transcriptionally and translationally silent, therefore post-translational modifications are essential to regulate their function. In this issue for Frontiers, a study shows that that O-GlcNAc transferase (OGT), the enzyme responsible for O-GlcNAcylation, is present in the testis, epididymis, and immature caput sperm, which indicates that modulation of O-GlcNAcylation takes place during sperm maturation and suggest a role for this post-translational modification in this process (Tourzani et al).

Already during embryo development in the mother's uterus, the pool of oocytes is established, maintained, and stored. The pool of the earliest primordial (resting) follicles is almost completely laid down in ovaries during fetal life and constitutes at any moment in time the reproductive potential of a female (Skinner, 2005; Da Silva-Buttkus et al., 2008; Shah et al., 2018). Once activated, the primordial follicles grow in size, and the flat layer of surrounding granulosa cells, which is characteristic for primordial follicles, transforms into cubic granulosa cells, typical of activated primary follicles (Skinner, 2005; Da Silva-Buttkus et al., 2008; Shah et al., 2018). Activation of the primordial follicles occurs in a hormone-independent manner (Edson et al., 2009; Tingen et al., 2009). The PI3K/Akt/mTOR pathways are known players in this transition (Goto et al., 2007; Reddy et al., 2008; Jagarlamudi et al., 2009; Adhikari et al., 2013; Makker et al., 2014; Cheng et al., 2015b; Hsueh et al., 2015), and are regulated by phosphatase and tensin homologs deleted on chromosome 10 (PTEN), the tuberous sclerosis complex (TSC1/2) and recently, the HIPPO signaling (Kawamura et al., 2013; Cheng et al., 2015a; Kawashima and Kawamura, 2018), synergistically with the phosphatidylinositol 3-kinase (PI3K)/AKT pathway (Grosbois and Demeestere, 2018). Several contributions in this issue for Frontiers describe new signaling pathwaysas potential regulators of the primordial-to-primary transition in human follicles, with a new view on how androgens might contribute (Ernst et al.; Steffensen et al.).

OPEN ACCESS

Edited and reviewed by:
Philipp Kaldis,
*Agency for Science, Technology and Research (A*STAR), Singapore*

***Correspondence:**
Karin Lykke-Hartmann
kly@biomed.au.dk

Specialty section:
This article was submitted to Cell Growth and Division, a section of the journal Frontiers in Cell and Developmental Biology

Received: *07 February 2019*
Accepted: *27 February 2019*
Published: *20 March 2019*

Citation:
Fissore RA, Burton A and Lykke-Hartmann K (2019) Editorial: Molecular and Cellular Mechanisms in Reproduction and Early Development. Front. Cell Dev. Biol. 7:36. doi: 10.3389/fcell.2019.00036

Egg activation at fertilization in mammalian eggs is caused by a series of transient increases in the cytosolic free calcium (Ca^{2+}) concentration, referred to as Ca^{2+} oscillations (Stricker, 1999). These Ca^{2+} oscillations are initiated by a sperm specific phospholipase Czeta isoform, PLCζ that hydrolyses its substrate PIP_2 to produce the Ca^{2+} releasing messenger $InsP_3$. In this issue of Frontiers, a study shows that PLCζ induce Ca^{2+} Oscillations in mouse eggs, which involve a positive feedback cycle of Ca^{2+} induces $InsP_3$ formation from cytoplasmic PIP_2 (Sanders et al). This manuscript also suggests that the site of InsP3 production by PLCζ is from PIP_2-containig cytoplasmic vesicles spread throughout the cytoplasm, which is diametrically different from the site of PIP_2 hydrolysis by other PLCs. Oocyte maturation is associated with changes in the electrical properties of the plasma membrane and alterations in the function and distribution of ion channels. Therefore, variations on the pattern of expression, distribution, and function of ion channels and transporters during oocyte maturation are fundamental to reproductive success. In this issue for Frontiers, a review comprehensively discusses the role of ion channels during oocyte maturation, fertilization and early embryonic development, and how ion channel studies in *Xenopus* oocytes, an extensively studied model of oocyte maturation, translate into a greater understanding of the role of ion channels in mammalian oocyte physiology (Carvacho et al).

Chromosome dynamics during meiotic prophase I are associated with a series of major events such as chromosomal reorganization and condensation, pairing/synapsis and recombination of the homologs, and chromosome movements at the nuclear envelope (NE). The linker of nucleoskeleton and cytoskeleton (LINC) complexes are important constituents of the NE that facilitate in the transfer of cytoskeletal forces across the NE to individual chromosomes. In this issue for Frontiers, a review summarizes the findings of recent studies on meiosis-specific constituents and modifications of the NE and corresponding nucleoplasmic/cytoplasmic adaptors being involved in NE-associated movement of meiotic chromosomes, as well as describing the potential molecular network of transferring cytoplasm-derived forces into meiotic chromosomes in model organisms (Zeng et al.), aiming to increase our understanding of the NE-associated meiotic chromosomal movements in plants.

The newly formed 1-cell embryo (the zygote) undergoes its first mitotic cell division to form the 2-cell stage embryo, a transition mainly controlled by maternal factors stored in the oocyte (Zheng and Liu, 2012). Folates have been shown to play a crucial role for proper development of the embryo as folate deficiency has been associated with reduced developmental capacity such as increased risk of fetal neural tube defects and spontaneous abortion. In this issue for Frontiers, a study shows that maternally contributed FOLR1 protein appears to maintain ovarian functions, and contribute to preimplantation development combined with embryonically synthesized FOLR1 (Strandgaard et al).

Packaging DNA into chromatin allows for mitosis and meiosis, prevents chromosome breakage and controls gene expression and DNA replication (Borsos and Torres-Padilla, 2016). Histones contribute to eukaryotic chromatin structure and function in a well-known manner (Harr et al., 2016). Interestingly, free histones also have antimicrobial functions (Kawasaki and Iwamuro, 2008). For example, histones in amniotic fluid appear to fight bacteria by neutralizing the lipopolysaccharide (LPS) of microbes that gain access to this fluid (Witkin et al., 2011). The possible benefits of mitigating extracellular histone cytotoxicity have been outlined for the reproductive tract and other organs, however, in this issue of Frontiers, an opinion article reassesses previously published data to support the notion that uterine histone secretion fosters early embryo development in multiple ways (Van Winkle).

The regulation of signaling pathways by Ca^{2+} occurring at the earliest stages of development is not only important in fertilization, but also for human pluripotent stem cells (hPSC) maintenance (Todorova et al., 2009). The Ca^{2+} P-type ATPases, the plasma membrane calcium ATPases (PMCAs) and the sarco/endoplasmic reticulum Ca^{2+} ATPase (SERCAs), which reside in different compartments of the cell and along with other Ca^{2+} transporting system, contribute to the regulation of the intracellular Ca^{2+} concentration. In this issue for Frontiers, a study uses hPSCs to generated neural stem cells (NSCs) of the central and peripheral nervous system and investigated the main neural progenitor states for the presence of PMCAs using RNA sequencing (RNA-seq) and immunofluorescent labeling, and show that dynamic change in ATPase expression correlates directly with the stage of differentiation (Chen et al). These data have important implications for understanding the role of Ca^{2+} in development and potentially how disease states, which disrupt Ca^{2+} homeostasis, can result in global cellular dysfunction.

We hope that the articles in this topic will be of interest to researchers working in development and cell biology, providing basis for further discussion on this area to initiate new research questions that will contribute to our further understanding of cell growth and division in developmental contexts.

AUTHOR CONTRIBUTIONS

KL-H was the Guest editor of this Research Topic, inviting co-editors AB and RF working with them to define the subjects to be treated. They identified and invited leaders in specific research fields to contribute their work to the Research Topic. They acted as handling editors of manuscripts in the topic. KL-H wrote the Editorial with input from the other co-editors.

FUNDING

Research in KL-H laboratory is supported by the Danish Council for Independent Research | Medical Sciences (6120-00027B9) and the Novo Nordisk foundation (NNF160C0022480).

ACKNOWLEDGMENTS

We are very grateful to all authors who contributed toward this issue.

REFERENCES

Adhikari, D., Risal, S., Liu, K., and Shen, Y. (2013). Pharmacological inhibition of mTORC1 prevents over-activation of the primordial follicle pool in response to elevated PI3K signaling. *PLoS ONE* 8:e53810. doi: 10.1371/journal.pone.0053810

Borsos, M., and Torres-Padilla, M. E. (2016). Building up the nucleus: nuclear organization in the establishment of totipotency and pluripotency during mammalian development. *Genes Dev.* 30, 611–621. doi: 10.1101/gad.273805.115

Cheng, Y., Feng, Y., Jansson, L., Sato, Y., Deguchi, M., Kawamura, K., et al. (2015a). Actin polymerization-enhancing drugs promote ovarian follicle growth mediated by the Hippo signaling effector YAP. *FASEB J.* 29, 2423–2430. doi: 10.1096/fj.14-267856

Cheng, Y., Kim, J., Li, X. X., and Hsueh, A. J. (2015b). Promotion of ovarian follicle growth following mTOR activation: synergistic effects of AKT stimulators. *PLoS ONE* 10:e0117769. doi: 10.1371/journal.pone.0117769

Da Silva-Buttkus, P., Jayasooriya, G. S., Mora, J. M., Mobberley, M., Ryder, T. A., Baithun, M., et al. (2008). Effect of cell shape and packing density on granulosa cell proliferation and formation of multiple layers during early follicle development in the ovary. *J. Cell Sci.* 121, 3890–3900. doi: 10.1242/jcs.036400

Edson, M. A., Nagaraja, A. K., and Matzuk, M. M. (2009). The mammalian ovary from genesis to revelation. *Endocr. Rev.* 30, 624–712. doi: 10.1210/er.2009-0012

Goto, M., Iwase, A., Ando, H., Kurotsuchi, S., Harata, T., and Kikkawa, F. (2007). PTEN and Akt expression during growth of human ovarian follicles. *J. Assist. Reprod. Genet.* 24, 541–546. doi: 10.1007/s10815-007-9156-3

Grosbois, J., and Demeestere, I. (2018). Dynamics of PI3K and Hippo signaling pathways during *in vitro* human follicle activation. *Hum. Reprod.* 33, 1705–1714. doi: 10.1093/humrep/dey250

Harr, J. C., Gonzalez-Sandoval, A., and Gasser, S. M. (2016). Histones and histone modifications in perinuclear chromatin anchoring: from yeast to man. *EMBO Rep.* 17, 139–155. doi: 10.15252/embr.201541809

Hsueh, A. J., Kawamura, K., Cheng, Y., and Fauser, B. C. (2015). Intraovarian control of early folliculogenesis. *Endocr. Rev.* 36, 1–24. doi: 10.1210/er.2014-1020

Jagarlamudi, K., Liu, L., Adhikari, D., Reddy, P., Idahl, A., Ottander, U., et al. (2009). Oocyte-specific deletion of Pten in mice reveals a stage-specific function of PTEN/PI3K signaling in oocytes in controlling follicular activation. *PLoS ONE* 4:e6186. doi: 10.1371/journal.pone.0006186

Kawamura, K., Cheng, Y., Suzuki, N., Deguchi, M., Sato, Y., Takae, S., et al. (2013). Hippo signaling disruption and Akt stimulation of ovarian follicles for infertility treatment. *Proc. Natl. Acad. Sci. U.S.A.* 110, 17474–17479. doi: 10.1073/pnas.1312830110

Kawasaki, H., and Iwamuro, S. (2008). Potential roles of histones in host defense as antimicrobial agents. *Infect. Disord. Drug Targets* 8, 195–205. doi: 10.2174/1871526510808030195

Kawashima, I., and Kawamura, K. (2018). Regulation of follicle growth through hormonal factors and mechanical cues mediated by Hippo signaling pathway. *Syst. Biol. Reprod. Med.* 64, 3–11. doi: 10.1080/19396368.2017.1411990

Makker, A., Goel, M. M., and Mahdi, A. A. (2014). PI3K/PTEN/Akt and TSC/mTOR signaling pathways, ovarian dysfunction, and infertility: an update. *J. Mol. Endocrinol.* 53, R103–R118. doi: 10.1530/JME-14-0220

Reddy, P., Liu, L., Adhikari, D., Jagarlamudi, K., Rajareddy, S., Shen, Y., et al. (2008). Oocyte-specific deletion of Pten causes premature activation of the primordial follicle pool. *Science* 319, 611–613. doi: 10.1126/science.1152257

Shah, J. S., Sabouni, R., Cayton Vaught, K. C., Owen, C. M., Albertini, D. F., and Segars, J. H. (2018). Biomechanics and mechanical signaling in the ovary: a systematic review. *J. Assist. Reprod. Genet.* 35, 1135–1148. doi: 10.1007/s10815-018-1180-y

Skinner, M. K. (2005). Regulation of primordial follicle assembly and development. *Hum. Reprod. Update* 11, 461–471. doi: 10.1093/humupd/dmi020

Stricker, S. A. (1999). Comparative biology of calcium signaling during fertilization and egg activation in animals. *Dev. Biol.* 211, 157–176. doi: 10.1006/dbio.1999.9340

Tingen, C., Kim, A., and Woodruff, T. K. (2009). The primordial pool of follicles and nest breakdown in mammalian ovaries. *Mol. Hum. Reprod.* 15, 795–803. doi: 10.1093/molehr/gap073

Todorova, M. G., Fuentes, E., Soria, B., Nadal, A., and Quesada, I. (2009). Lysophosphatidic acid induces Ca2+ mobilization and c-Myc expression in mouse embryonic stem cells via the phospholipase C pathway. *Cell. Signal.* 21, 523–528. doi: 10.1016/j.cellsig.2008.12.005

Witkin, S. S., Linhares, I. M., Bongiovanni, A. M., Herway, C., and Skupski, D. (2011). Unique alterations in infection-induced immune activation during pregnancy. *BJOG* 118, 145–153. doi: 10.1111/j.1471-0528.2010.02773.x

Yanagimachi, R. (1970). The movement of golden hamster spermatozoa before and after capacitation. *J. Reprod. Fertil.* 23, 193–196.

Zheng, W., and Liu, K. (2012). Maternal control of mouse preimplantation development. *Results Probl. Cell Differ.* 55, 115–139. doi: 10.1007/978-3-642-30406-4_7

Conflict of Interest Statement: The authors declare that the research was conducted in the absence of any commercial or financial relationships that could be construed as a potential conflict of interest.

frontiers in Cell and Developmental Biology

ORIGINAL RESEARCH
published: 10 August 2018
doi: 10.3389/fcell.2018.00085

Transcripts Encoding the Androgen Receptor and IGF-Related Molecules Are Differently Expressed in Human Granulosa Cells From Primordial and Primary Follicles

Line L. Steffensen[1], *Emil H. Ernst*[1†], *Mahboobeh Amoushahi*[1], *Erik Ernst*[2,3] *and Karin Lykke-Hartmann*[1,4,5*]

[1] Department of Biomedicine, Aarhus University, Aarhus, Denmark, [2] The Fertility Clinic, Horsens Hospital, Horsens, Denmark, [3] The Fertility Clinic, Aarhus University Hospital, Aarhus, Denmark, [4] Department of Clinical Medicine, Aarhus University, Aarhus, Denmark, [5] Department of Clinical Genetics, Aarhus University Hospital, Aarhus, Denmark

Bidirectional cross talk between granulosa cells and oocytes is known to be important in all stages of mammalian follicular development. Insulin-like growth factor (IGF) signaling is a prominent candidate to be involved in the activation of primordial follicles, and may be be connected to androgen-signaling. In this study, we interrogated transcriptome dynamics in granulosa cells isolated from human primordial and primary follicles to reveal information of growth factors and androgens involved in the physiology of ovarian follicular activation. Toward this, a transcriptome comparison study on primordial follicles (n = 539 follicles) and primary follicles (n = 261 follicles) donated by three women having ovarian tissue cryopreserved before chemotherapy was performed. The granulosa cell contribution in whole follicle isolates was extracted *in silico*. Modeling of complex biological systems was performed using IPA® software. We found the granulosa cell compartment of the human primordial and primary follicles to be extensively enriched in genes encoding IGF-related factors, and the Androgen Receptor (AR) enriched in granulosa cells of primordial follicles. Our study hints the possibility that primordial follicles may indeed be androgen responsive, and that the action of androgens represents a connection to the expression of key players in the IGF-signaling pathway including IGF1R, IGF2, and IGFBP3, and that this interaction could be important for early follicular activation. In line with this, several androgen-responsive genes were noted to be expressed in both oocytes and granulosa cells from human primordial and primary follicle. We present a detailed description of *AR* and *IGF* gene activities in the human granulosa cell compartment of primordial and primary follicles, suggesting that these cells may be or prepare to be responsive toward androgens and IGFs.

Keywords: human granulosa cells, transcriptome, follicle development, AR, IGF

OPEN ACCESS

Edited by:
Eiman Aleem,
College of Medicine Phoenix,
University of Arizona, United States

Reviewed by:
Rajprasad Loganathan,
School of Medicine, Johns Hopkins University, United States
Ahmed Waraky,
University of Gothenburg, Sweden

****Correspondence:***
Karin Lykke-Hartmann
kly@biomed.au.dk

†Present Address:
Emil H. Ernst,
Department of Obstetrics and Gynaecology, Herning Hospital, Herning, Denmark

Specialty section:
This article was submitted to Cell Growth and Division, a section of the journal Frontiers in Cell and Developmental Biology

Received: *03 April 2018*
Accepted: *18 July 2018*
Published: *10 August 2018*

Citation:
Steffensen LL, Ernst EH, Amoushahi M, Ernst E and Lykke-Hartmann K (2018) Transcripts Encoding the Androgen Receptor and IGF-Related Molecules Are Differently Expressed in Human Granulosa Cells From Primordial and Primary Follicles. Front. Cell Dev. Biol. 6:85. doi: 10.3389/fcell.2018.00085

INTRODUCTION

Female fertility is dependent on continuous (monthly) activation of primordial follicles from the resting dormant follicle pool. A primordial follicle is made up by an oocyte surrounded partly by flattened granulosa cells. As the primordial follicle is activated, it transforms into a primary follicle, where the oocyte is now surrounded by a complete layer of cubical granulosa cells. The primordial to primary follicle transition is a delicate and tightly regulated balance between activating and inhibiting factors with contribution from numerous different molecular pathways, but the mechanisms are not yet completely understood (Wandji et al., 1996). Bidirectional communication between the somatic granulosa cells and the oocyte is a fundamental part of both dormancy and activation, as well as the establishment of an optimal intrafollicular microenvironment (Eppig, 2001).

The essential role of androgens in normal ovarian function has been recognized for decades. Androgens play a key role by being the precursor of estradiol, however increasing evidence emphasize that the direct actions of androgens likewise are central for normal follicular development (Lebbe and Woodruff, 2013). It has been suggested that androgen sensitivity in early pre-antral follicles influence the primordial follicle recruitment (Vendola et al., 1999a; Stubbs et al., 2005; Yang et al., 2010). In the intraovarian communication, androgens may play a necessary role (Lebbe and Woodruff, 2013; Gervasio et al., 2014). Androgens bind the androgen receptor (AR) and exert the classical androgen response by genomic induction of transcription of several genes including *AR* itself, creating an autocrine loop between ligand and receptor (Weil et al., 1998; Gelmann, 2002). Besides the direct genomic effects, androgen signaling is also known to induce rapid non-genomic pathways via cytosolic AR and the mitogen-activated protein kinase extracellular signal-related kinase (MAPK/ERK) pathway (Kousteni et al., 2001). A balanced androgen level is however crucial, and exposure to excess androgens is associated with ovarian dysfunction. A large group of women suffering from ovarian dysfunction is women suffering from polycystic ovary syndrome (PCOS), a common endocrine disorder, in which hyperandrogenism is a key feature (Franks, 1995). Morphologically, polycystic ovaries have an increased percentage of growing follicles and "stockpiling" of the primary follicles compared to controls (Webber et al., 2003; Maciel et al., 2004). Moreover, clinical evidence from women exposed to androgen excess due to congenital adrenal hyperplasia (Hague et al., 1990) or exogenous testosterone treatment in female-to-male transsexuals (Spinder et al., 1989; Becerra-Fernández et al., 2014) underlines this picture by increased prevalence of morphologically polycystic ovaries compared to controls. Polycystic ovaries are also a common trait in prenatally androgenized sheep, an animal model for PCOS (Padmanabhan and Veiga-Lopez, 2013). Lambs born to dihydrotestosterone (DHT) or testosterone treated ewes showed the same pattern of dysfunctional early follicular development as the women suffering from PCOS. These examples emphasize the involvement of androgens in the early follicular development. In this follicular-phase gonadotropins are not obligatory, while local growth factors may play an important role. Insulin-like growth factor (IGF) signaling is a prominent candidate and may be connected to androgen-signaling. In the human ovary both IGF1 and IGF2 act as ligands for IGF receptor 1 (IGF1R) (Willis et al., 1998), and IGF2 expression is more prominent compared to other species (Mazerbourg et al., 2003). Rhesus monkeys treated with testosterone showed an increase in the fraction of activated primary follicles and a 5-fold increase in IGF1R mRNA in the oocytes of primordial follicles, as well as an elevation in the intra-oocyte IGF1 signaling (Vendola et al., 1999a,b). Likewise, pigs treated with the anti-androgen Flutamide reduced the mRNA and protein expression of IGF1R in the oocyte, and showed delayed primordial follicle activation (Knapczyk-Stwora et al., 2013). In preantral follicles isolated from women suffering from PCOS, an enhanced expression of IGF1R mRNA and protein was noted compared to controls (Stubbs et al., 2013). In the IGF-signaling system IGF binding proteins (IGFBPs) have in recent years received increased attention, because of their potential active modulating role of IGF-bioavailability. This is in contrast to the conventional idea about IGFBPs as simple carrier proteins. The IGFBPs bind IGF and sequester the binding of IGF to its receptors. This modulating role might be important in terms of shifting from the dormant to the activated follicular stage (Hu et al., 2017).

We hypothesize that primordial follicles may be androgen responsive based on the presents of components supporting androgen signaling, and that the action of androgens could be closely connected to the expression of key players in the IGF-signaling such as IGF1R, IGF2, and IGFBP3.

RESULTS

The global RNA transcriptomes representative for granulosa cells from primordial and primary follicles (http://users-birc.au.dk/biopv/published_data/ernst_et_al_GC_2017/) (Ernst et al., 2018) revealed 12.872 and 11.898 transcripts in granulosa cells from primordial and primary follicles, respectively (Ernst et al., 2018). The lists were further processed to exclude transcripts that were not consistently expressed in all patients and lists representative of stage-specific consistently expressed genes (SSCEGs) were generated. We applied this strict filter to only include analysis of genes that were consistent between patients included in this study, but certainly does not rule out that additional genes could be relevant. The SSCEGs analysis of the granulosa cell transcriptome revealed 1695 transcripts in primordial follicles and 815 transcripts in primary follicles. We further applied strict bioinformatic filters, and quality control to ensure specificity in output transcriptomes, and confirmed the presence of known granulosa cell-specific factors, as well as the absence of oocyte-specific factors. The SSCEGs lists in granulosa cells from primordial and primary follicles (Ernst et al., 2018) were used to extract genes differentially expressed genes (DEG) between the two cell populations.

The "Androgen Signaling" Pathway

We identified the most enriched and significant Canonical Pathways in granulosa cells from primordial and primary follicles

TABLE 1 | "Androgen Signaling" pathway annotations—granulosa cells from primordial follicles.

Gene name	Gene symbol	FPKM mean value	*p*-value
RNA Polymerase II Subunit D	*POLR2D*	2,508	0,186
G Protein Subunit Alpha 12	*GNA12*	1,573	0,195
G Protein Subunit Alpha Q	*GNAQ*	4,444	0,121
RNA Polymerase II Subunit J	*POLR2J*	2,812	0,066
General Transcription Factor IIH Subunit 2	*GTF2H2*	3,333	0,165
CDK Activating Kinase Assembly Factor	*MNAT1*	1,618	0,157
G Protein Subunit Alpha I2	*GNAI2*	1,574	0,184
G Protein Subunit Gamma 11	*GNG11*	1,521	0,038
Protein Kinase C Iota	*PRKCI*	4,140	0,027
Androgen Receptor	*AR*	3,134	0,012
Protein Kinase C Eta	*PRKCH*	3,709	0,172
G Protein Subunit Gamma 5	*GNG5*	3,200	0,003
Protein Kinase D3	*PRKD3*	1,538	0,174
Protein Kinase C Beta	*PRKCB*	2,157	0,112
Protein Kinase C Alpha	*PRKCA*	4,440	0,087

"Androgens Signaling" pathway annotation of the 15 transcripts identified in granulosa cells from primordial follicles. FPKM mean values were calculated based on triplicate expression values of the same transcript using a one-sample t-test. The p-value is indicative of the consistency in expression pattern across triplicates.

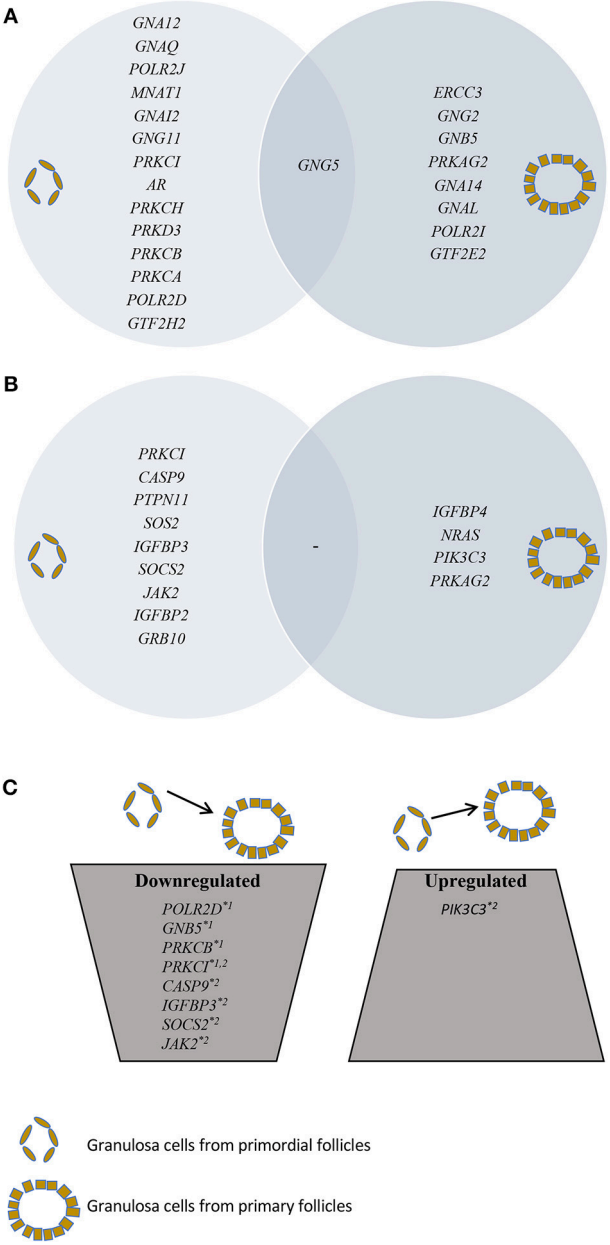

FIGURE 1 | Presentation of SSCEGs and DEGs in granulosa cells from primordial and primary follicles. **(A)** Presentation of SSCEGs from the "AR Signaling" Pathway that are significantly expressed in granulosa cell from primordial and primordial follicles, as indicated, and the number in the middle representing SSCEG in both stages. **(B)** Presentation of SSCEGs from the "IGF1 Signaling" Pathway that are significantly expressed in granulosa cell from primordial and primary follicles, as indicated, and number in the middle representing SSCEG in both stages. **(C)** Presentation of DEGs from both "AR Signaling" (Noted *1) and "IGF1 Signaling" (Noted *2) pathways.

(Ernst et al., 2018). To further analyze the 'Androgen Signaling' Pathways, we used the Ingenuity Pathway Analysis (IPA®) analysis software, which can be used to determine the most significant pathways and the genes allocated with each pathway. We found "Androgen Signaling" from Canonical Pathways significantly and differentially enriched in granulosa cells from both primordial and primary follicles (**Table 1**).

In granulosa cells from primordial follicles, the "Androgen Signaling" was highly enriched (p = 3,97E-02) with 15 genes assigned (*POLR2D, GNA12, GNAQ, POLR2J, GTF2H2, MNAT1, GNAI2, GNG11, PRKCI, AR, PRKCH, GNG5, PRKD3, PRKCB, PRKCA*), including the androgen receptor *(AR)* (**Table 1**; **Figure 1A**). The *AR* transcript is low-to-moderately expressed (mean FPKM value of 3.13) with a p-value of $p = 0.012$, indicating that the *AR* transcript is consistently expressed in the samples tested.

The "Androgen Signaling" was also enriched in granulosa cells from primary follicles (p = 3,42E-02) with nine genes (*POLR2I, ERCC3, GNG2, GNB5, PRKAG2, GTF2E2, GNA14, GNG5, GNAL*) assigned (**Table 2**; **Figure 1A**). In granulosa cells from primary follicles, the *AR* transcript levels is very low (mean FPKM value is 1.65) and was not consistently expressed in our samples ($p = 0.39$).

Differentially Expressed Genes in the "Androgen Signaling" Pathway

During the primordial to primary follicle transition, "Androgen Signaling" was non-significantly down-regulated (p = 5,65E-01). However, four genes (*PRKC1, POLR2D, GNB5,* and *PRKCB)* from the "Androgen Signaling" pathway were significantly down-regulated in the granulosa cells (**Table 3**; **Figure 1C**). As noted above, the *AR* transcript was down-regulated, however

not significantly. The four genes were down-regulated by 2-fold change, indicating a rapid chance in expression during the primordial-to-primary transition. Interestingly, no genes from the androgen signaling pathway was significantly up-regulated during the primordial to primary follicle transition. The Androgen Signaling Pathway and the molecular network associated with this pathway is illustrated in **Figure 2**.

Differentially Expressed Genes in "IGF1 Signaling" Pathway

We interrogated the presence of *IGF1*, *IGF2*, *IGF1R,* and *IGFR2* as well as the *IGFBP1-6* transcripts in human oocytes and granulosa cells from primordial and primary follicles (Ernst et al., 2017, 2018) and found that some were significantly expressed, whilst close to be significant across the triplicates of samples (**Table 4**). It is noteworthy that the expression levels of *IGF2* and *IGF1* in granulosa cells from primordial cells to primary follicles decreased, while *IGF1R* and *IGF2R* expression levels remained. In oocytes from primordial and primary follicles, *IGF2,* and *IGF1R* transcripts increased, while *IGF1* and *IGF2R* transcript were not significantly altered. Interestingly, expression of *IGFBP1-6* varied significantly, with *IGFBP-5* being highly expressed in all cells from both primordial and primary follicles. The *IGFBP3* transcript appears to be upregulated in oocytes from primordial and primary follicles, but down regulated from granulosa cells from primordial cells to primary follicles.

Although the "IGF1 signaling" pathway was not significantly enriched in granulosa cells from primordial (p = 4,25E-01) or primary follicles (p = 5,56E-01), it was selected for further analysis, as IGFs are important for ovarian physiology (Adashi et al., 1985, 1991; Mondschein et al., 1989; Armstrong et al., 1996; Baumgarten et al., 2014). The IGF Signaling Pathway from the IPA® analysis contains factors directly associated with the IGF system (e.g., IGF1 and IGF2 and their respective receptors, IGF1 receptor and IGF2 receptor, as well as six binding proteins, IGFBP1-6) as well as the signal tranducting factors requires to conduct the IGF signaling (Laviola et al., 2007; Kuijjer et al., 2013; Lodhia et al., 2015), including PKC, Caspase9, JAK2, PIK3C3, and PRKCI. Consequently, it is noteworthy that many of the signal transducing components assigned to IGF Signaling Pathways are also found in other Signal transducing pathways, such as EGFR signaling. The "IGF-1 Signaling" pathway in the granulosa cells from primordial follicles contained nine genes (*PRKCI, CASP9, PTPN11, SOS2, IGFBP3, SOCS2, JAK2, IGFBP2, GRB10)* (**Table 5**; **Figure 1B**), and from primary follicles, we noted four genes (*IGFBP4, NRAS, PIK3C3, PRKAG2* (**Table 6**; **Figure 1B**), suggesting a dynamic change of "IGF1 signaling"-related genes during the primordial to primary transition. During the primordial to primary follicle transition, the 'IGF1 Signaling' pathway was non-significantly downregulated (p = 5,64E-01). Interestingly, during the primordial to primary follicle transition, several members of the IGF1 Signaling family were significantly down- or up-regulated. Five genes (*PRKC1, CASP9, IGFBP3, SOC2, JAK2*) (**Figure 1C**) were significantly downregulated during the transition, and one gene (*PIK3C3*) (**Figure 1C**) was significantly up-regulated (**Table 7**).

TABLE 2 | "Androgen Signaling" pathway annotations—granulosa cells from primary follicles.

Gene name	Gene symbol	FPKM mean value	*p*-value
RNA Polymerase II Subunit I	*POLR2I*	1,712	0,042
ERCC Excision Repair 3, TFIIH Core Complex Helicase Subunit	*ERCC3*	1,563	0,190
G Protein Subunit Gamma 2	*GNG2*	2,731	0,185
G Protein Subunit Beta 5	*GNB5*	0,912	0,193
Protein Kinase AMP-Activated Non-Catalytic Subunit Gamma 2	*PRKAG2*	3,106	0,012
General Transcription Factor IIE Subunit 2	*GTF2E2*	3,597	0,194
G Protein Subunit Alpha 14	*GNA14*	4,808	0,075
G Protein Subunit Gamma 5	*GNG5*	1,989	0,119
G Protein Subunit Alpha L	*GNAL*	4,123	0,187

Androgens Signaling" pathway annotation of the nice transcripts identified in granulosa cells from primary follicles. FPKM mean values were calculated based on triplicate expression values of the same transcript using a one-sample t-test. The p-value is indicative of the consistency in expression pattern across triplicates.

IGF2 Protein Localizes to Human Oocytes and Granulosa Cells in Primordial and Primary Follicles

Transcriptomic data represents RNA profiling and thus, does not necessarily represents protein expression profiles. Human oocytes are loaded with maternal mRNA, of which many are packed into a protein complex preventing translation at this

TABLE 3 | Differently expressed genes annotated "Androgen Signaling" pathway.

Gene Name	Gene Symbol	GC from PDF mean FPKM value	*p*-value	GCs from PMF FPKM value	*p*-value	Significance, paired *t*-test	Fold-change down
Protein Kinase C Iota	*PRKCI*	4,140	0,027	1,999	0,410	0,226	2,071
RNA Polymerase II Subunit D	*POLR2D*	2,508	0,186	1,236	0,423	0,460	2,029
G Protein Subunit Beta 5	*GNB5*	2,043	0,211	0,912	0,193	0,426	2,242
Protein Kinase C Beta	*PRKCB*	2,157	0,112	1,239	0,236	0,010	1,741

Differently expressed genes identified by comparing transcriptomes of the granulosa cells from primordial follicles vs. granulosa cells from primary follicles. Four genes were significantly downregulated during the primordial to primary follicle transition. Significance: fold-change >2 and/or paired t-test significance ($p < 0.05$) between the two FPKM mean values.

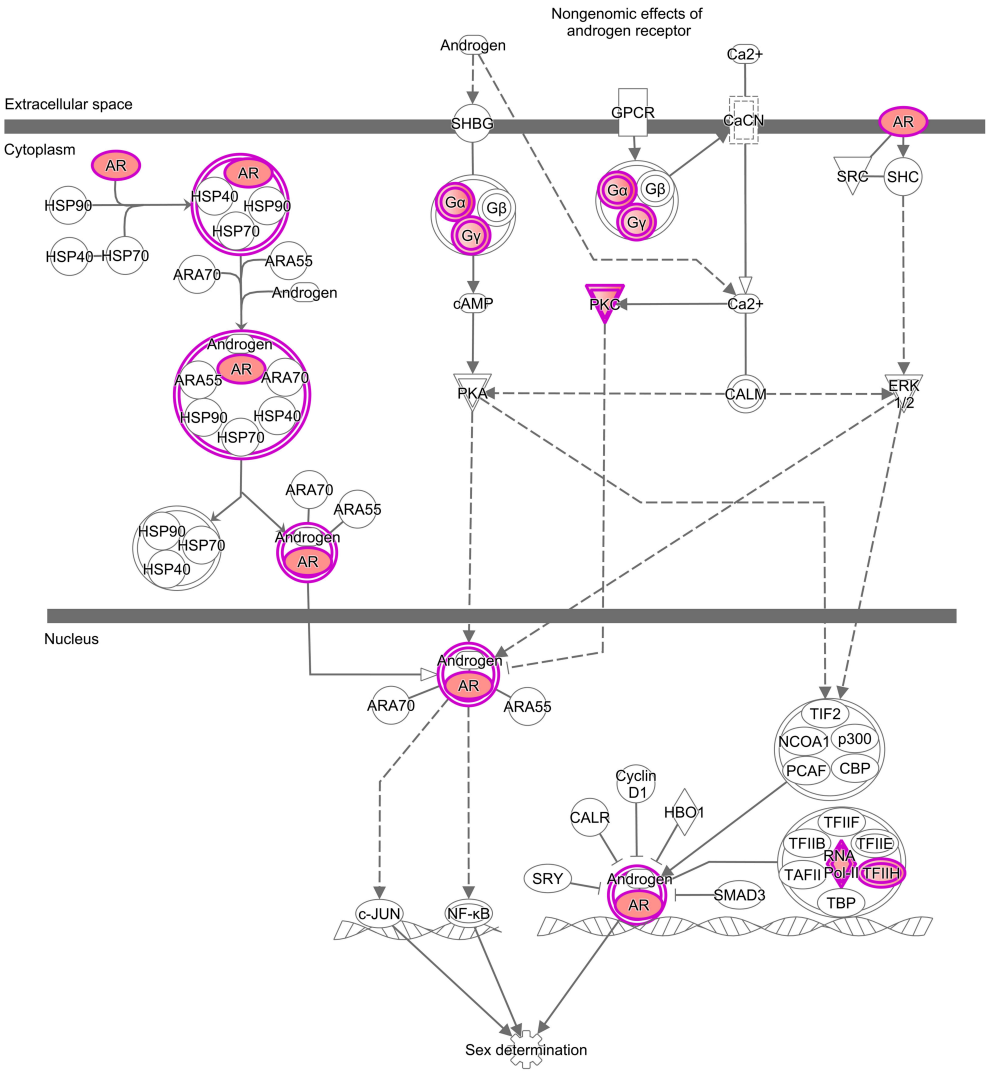

FIGURE 2 | Enrichments analysis and IPA® pathways highlighting trends in granulosa cells from primordial and primary follicles, respectively. Pathway analysis (IPA®) of the "Androgen Signaling" pathway in granulosa cells of the primordial follicle. Color intensities are based on FPKM values where high significance is most intensive in color (red).

stage. The IGF2 protein was selected for immunofluorescent staining since the *IGF2* gene was highly expressed in both oocytes and granulosa cells in primordial and primary follicles (Ernst et al., 2017, 2018) (**Table 4**). The immunofluorescence revealed a strong staining of the IGF2 protein in both oocytes and granulosa cells in primordial and primary follicles (**Figure 3**). The staining of IGF2 apeared as membranous and cytoplasmic staining in both oocytes and granulosa cells in primordial and primary follicles (**Figure 3**). The nuclear counter stain is Hoechst (blue) (**Figure 3**). Quantification of the IGF2 staining in primordial (pixel intensity = 16,1) and primary (pixel intensity = 20,7) follicles supports overall the RNA sequencing FPKM values noted for *IGF2* (**Table 4**), although distinction between cell compartments could not be precisely measured. As such, it is not possible to note of the upregulation of IGF2 is more strong in the oocytes compeared to the granulosa cells in the same follicels stages, although we observed that *IGF2* is uregulated on oocytes during the primordial to primary transition, in contrast to downregulation of *IGF2* in granulosa cells in the primordial to primary transition (**Table 4**).

Several Androgen-Responsive Genes Appear to Be Expressed During the Primordial to Primary Follicle Transition

To further reveal a potential effect of androgen signaling in primordial and primary follicles, we interrogated the presence of known androgen response genes (Romanuik et al., 2009) in the global transcriptomes of oocytes (Ernst et al., 2017) and granulosa cells (Ernst et al., 2018) from primordial and primary

TABLE 4 | Expression of *IGF1*, *IGF1R*, *IGF2*, *IGF2R,* and *IGFBP1-6* transcripts.

	Oocytes*				Granulosa cells*			
	Primordial follicles		Primary follicles		Primordial follicles		Primary follicles	
Gene names	**FPKM means**	***p*-value**	**FPKM means**	***p*-value**	**FPKM means**	***p*-value**	**FPKM means**	***p*-value**
IGF1	2,696	0,25	1,928	0,404	2,826	0,222	1,767	0,018
IGF1R	4,610	0,091	7,582	0,017	7,758	0,016	7,149	0,018
IGF2	6,031	0,049	8,340	0,025	4,654	0,101	1,631	0,379
IGF2R	1,987	0,231	1,572	0,198	4,683	0,203	3,157	0,184
IGFB1	0,935	0,423	0,307	0,301	0,489	0,353	0,608	0,423
IGFB2	1,236	0,147	2,168	0,094	3,217	0,030	2,445	0,221
IGFB3	0,834	0,423	3,323	0,012	3,356	0,067	0,784	0,423
IGFB4	1,026	0,122	0,896	0,191	1,523	0,225	1,547	0,103
IGFB5	5,071	0,052	6,283	0,007	7,116	0,005	5,733	0,052
IGFB6	–	–	–	–	1,439	0,303	0,056	0,423

*Gene names are followed by the mean FPKM and p-values for human oocytes and granulosa cells from primordial and primary follicels, as indicated. *Data extracted from Ernst et al. (2018) and Kuijjer et al. (2013).*

TABLE 5 | "IGF1 Signaling" pathway annotations—GCs from primordial follicles.

Gene name	Gene symbol	FPKM mean value	*p*-value
Protein Kinase C Iota	*PRKCI*	4,140	0,027
Caspase 9	*CASP9*	0,357	0,192
Protein Tyrosine Phosphatase, Non-Receptor Type 11	*PTPN11*	2,207	0,193
SOS Ras/Rho Guanine Nucleotide Exchange Factor 2	*SOS2*	2,635	0,006
Insulin Like Growth Factor Binding Protein 3	*IGFBP3*	3,356	0,067
Suppressor Of Cytokine Signaling 2	*SOCS2*	1,768	0,186
Janus Kinase 2	*JAK2*	5,792	0,022
Insulin Like Growth Factor Binding Protein 2	*IGFBP2*	3,217	0,030
Growth Factor Receptor Bound Protein 10	*GRB10*	2,420	0,191

"IGF1 Signaling" pathway annotation of the nine transcripts identified in granulosa cells from primordial follicles. FPKM mean values were calculated based on triplicate expression values of the same transcript using a one-sample t-test. The p-value is indicative of the consistency in expression pattern across triplicates.

TABLE 6 | "IGF1 Signaling" pathway annotations—granulosa cells from primary follicles.

Gene Name	Gene symbol	FPKM mean value	*p*-value
Insulin Like Growth Factor Binding Protein 4	*IGFBP4*	1,547	0,103
NRAS Proto-Oncogene, GTPase	*NRAS*	4,664	0,087
Phosphatidylinositol 3-Kinase Catalytic Subunit Type 3	*PIK3C3*	3,822	0,170
Protein Kinase AMP-Activated Non-Catalytic Subunit Gamma 2	*PRKAG2*	3,106	0,012

"IGF1 Signaling" pathway annotation of the four transcripts identified in granulosa cells from primary follicles. FPKM mean values were calculated based on triplicate expression values of the same transcript using a one-sample t-test. The p-value is indicative of the consistency in expression pattern across triplicates.

follicles. Of the known androgen-responsive genes (87 genes), 62 genes were found present in the transcriptome data (**Table 8**). Several of the androgen-responsive genes were very highly expressed (*ABHD2, ATP1A1, B2M, FDFT1, GOLPH3, NDRG1, ODC1, PAK2, RPL15, SOD1, TCP1, TPD52,* and *TSC22D1*), and several moderately expressed (such as *ACSL3, ADAM28, CNBD1, DHCR24, MANEA, PIK3R3, TMEFF2,* and *USP33*).

DISCUSSION

Ovarian follicles are subjected to to strict control of hormones and growth factors. In human granulosa cells, IGF1 is permissive for the positive feedback toward the FHS-induced expression of aromatase (CYP19A1) through AKT signaling (Baumgarten et al., 2014). This present study performed an *in silico* analysis of the transcriptomes representing granulosa cells from primordial and primary follicles, respectively. This provides a unique insight into the gene expression and perhaps actions of androgen-signaling and IGF-signaling in the two earliest stages of follicular development in the normal human ovary. Thus, we explored the potential of the earlist human follicles to be able to respond toward signals mediated by IGF- and androgen-signaling.

We applied strict filters in the bioinformatic management, and quality control to ensure the most precise outcome from the global transcriptome analysis. Therefore, the data presented must be evaluated with the fact that there is a fine balance between significant and non-significant outcomes. In some instances, variations between the data from the three patients is noted non-significant. Including more samples might even out this difference, and as many af of statistical analysis are close to a value

TABLE 7 | Differently expressed genes annotated "IGF1 Signaling" pathway.

Gene name	Gene Symbol	GC* from PDF mean FPKM value	*p*-value	GC* from PMF FPKM value	*p*-value	Significance, paired *t*-test	Fold-change down
SIGNIFICANTLY DOWN-REGULATED IN GRANULOSA CELLS DURING PRIMORDIAL TO PRIMARY TRANSITION							
Protein Kinase C Iota	*PRKCI*	4,140	0,027	1,999	0,410	0,226	2,071
Caspase 9	*CASP9*	0,357	0,192	0	0	Significant	∞
Insulin Like Growth Factor Binding Protein 3	*IGFBP3*	3,356	0,067	0,784	0,423	0,003	4,280
Suppressor Of Cytokine Signaling 2	*SOCS2*	1,768	0,186	0,300	0,307	0,318	5,894
Janus Kinase 2	*JAK2*	5,792	0,022	1,436	0,423	0,123	4,034
SIGNIFICANTLY UP-REGULATED IN GRANULOSA CELLS DURING PRIMORDIAL-PRIMARY TRANSITION							
Phosphatidylinositol 3-Kinase Catalytic Subunit Type 3	*PIK3C3*	3,254	0,198	3,822	0,170	0,033	0,851

*Differently expressed genes identified by comparing transcriptomes of the granulosa cells from primordial follicles vs. granulosa cells from primary follicles. Five genes were significantly downregulated, and one gene was significantly upregulated during the primordial to primary follicle transition. Significance: fold-change >2 and/or paired t-test significance ($p < 0.05$) between the two FPKM mean values. *Granulosa cells.*

for significance, it is most likely that most of the non-significant values indeed would be significant. The quantification of the IGF2 immunofluoresence on primordial and primary follicles aligned overall with the FPKM value, however, noteworthy, it is difficult to quantify immunofluorescent on slices performed on human follicles. Additionally, although maternally contributed mRNA are subjected to degradation, the turnover time for the corresponding protein may be differentially regulated and it is not known how much IGF2 protein that might be maternally supplied as well. Previous studies performed qPCR analysis to confirm the expression profiles of selected genes (Ernst et al., 2017, 2018) supporting that the FPKM values obtained reflects the intracellular levels. The analysis contains several DEG-lists based on both SSCEGs and non-SSCEGs. Therefore, caution in the analysis of fold of change for DEG transcripts is recommended. Importantly, this study interrogated the presence of transcripts, which do not necessarily reflect the corresponding protein product. Using single cell techniques, we are able to confirm the presence of proteins using immunohistochemistry. Interestingly, we found androgen signaling highly enriched in granulosa cells from primordial follicles and also enriched in granulosa cells from primary follicles, however less than in the granulosa cells from primordial follicles. Transcripts encoding for *AR* were significantly expressed in the granulosa cells from primordial follicles, and a non-significant downregulation of the *AR* gene expression in the granulosa cells during the primordial to primary follicle transition was detected, suggesting a dynamic expression of *AR* in the granulosa cells. This study is the first to show transcripts of *AR* expressed in the primordial follicle stage, which indicates an early responsiveness to androgens. Previously the *AR* transcript has been demonstrated in granulosa cells of rodent, primate and human from transitional follicles (oocyte, surrounded by one layer of mixed flattened and cuboidal granulosa cells) and onwards, but not in earlier follicular stages (Weil et al., 1999; Rice et al., 2007; Sen and Hammes, 2010). Interestingly, the androgen-responsive gene (*FDFT1*) encoding the Farnesyl diphosphate farnesyltransferase catalyzes the conversion of trans-farnesyl diphosphate to squalene, the first specific step in the cholesterol biosynthetic pathway, suggesting that already at the earliest stages of follicle development, the cells prepare to initiate steroidogenesis. The protein encoded by another androgen-responsive gene (*NDRG1*) appears to play a role in growth arrest and cell differentiation, possibly as a signaling protein shuttling between the cytoplasm and the nucleus. It is highly expressed during the primordial and primary transition, suggesting this candidate to be important for the activation of dormant oocytes. It is interesting that the androgen-responsive gene, the *SOD1* gene, encoding the superoxide dismutase-1 was highly expressed in both primordial and primary follicles. SOD1 is a major cytoplasmic antioxidant enzyme that metabolizes superoxide radicals to molecular oxygen and hydrogen peroxide, thus providing a defense against oxygen toxicity (Niwa et al., 2007). Intriguingly, the androgen-responsive gene, *PIK3R3,* encodes the phosphoinositide-3-Kinase Regulatory Subunit 3, a lipid kinases capable of phosphorylating the 3'OH of the inositol ring of phosphoinositide, and it has been demonstrated that IGF1R, INSR, and INSR substrate-1 (IRS1) bind to PIK3R3 *in vitro* (Dey et al., 1998). The study suggested that the interaction of PIK3R3 with IGFIR and INSR provides an alternative pathway for the activation of PI3-kinase.

This study interrogated the presence of the *AR* transcript through RNA sequencing during the human primordial to primary transition and suggests that at least parts of the AR responsive network, might be relevant during the first ovarian follicle activation step. Although a previous study did not detect the *AR* transcript in human primordial follicles (Suzuki et al., 1994; Rice et al., 2007), we believe this is attributable to technical limitations since that study used earlier version of mRNA preparations and RT-PCR analysis. The study further highlight the importance of interpretation of RT-PCR and point that its findings do not exclude the presence of a functionally active protein, and the possibility that androgens exert an effect from the earliest growing phase onwards (Rice et al., 2007). In human ovaries, AR was immunohistochemically localized to preantral, antral follicles, theca, and stroma (Chadha et al., 1994;

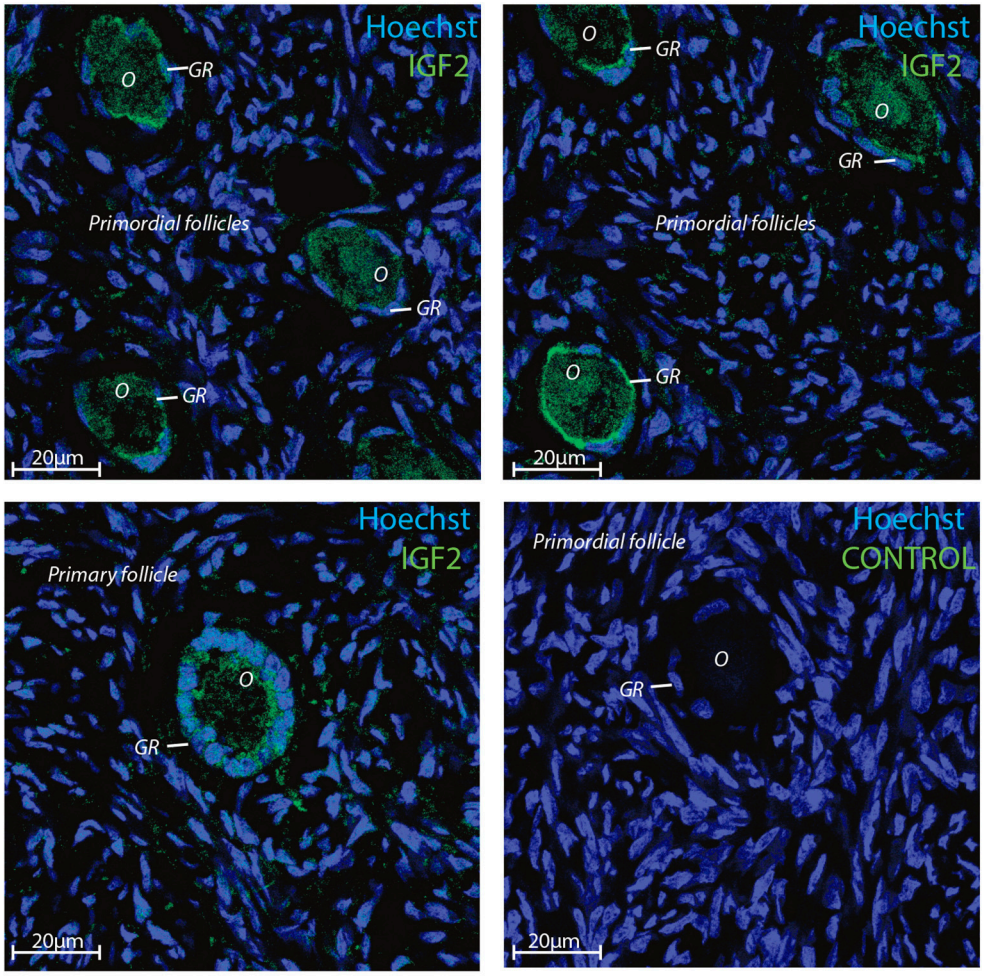

FIGURE 3 | Intra-ovarian distribution of IGF2 in human granulosa cells from primordial and primary follicles. Images show that IGF2 localized to oocytes and granulosa cells in primordial and primary follicles. A control without primary IGF2 antibody was included and reveals no staining. Hoechst staining identifies the nucleus of cells. Scale bars; 20 µm.

Takayama et al., 1996; Saunders et al., 2000). However, the stage of preantral follicle development could not be specified due to the inherent insensitivity of these techniques. Interestingly in this regard, a study cultured porcine primordial follicles in the absence or presence of testosterone, and found that testosterone increased the activation of primordial follicles (Magamage et al., 2011). The study further utilized cyproterone acetate, an AR antagonist, which inhibited the stimulatory effect of testosterone on primordial follicle activation. In addition, the results from Western blot and immunohistochemistry also showed that the AR was present in porcine primordial follicles. The results from porcine primordial follicles suggest to the possibility that human early follicles may also contain AR protein, however, this remains to be established through immunohistochemistry and protein analysis. In oocytes from primordial follicles, our group has recently demonstrated low, inconsisten expression of *AR*, and no detectable expression in the oocyte of primary follicles (Ernst et al., 2017). The mechanism of action of androgens is primarily the direct activation of gene transcription, by binding of the ligand-receptor complex to androgen-response elements in the nucleus, but androgens are also known to induce more rapid non-genomic pathways via cytosolic AR and the MAPK/ERK pathway (Kousteni et al., 2001), and influence the IGF-signaling (Vendola et al., 1999a). In the transcriptomic data from granulosa cells from primordial follicles (Ernst et al., 2018), "IGF1 signaling" and "ERK signaling" were, however not significantly enriched, which suggests that the possible androgen signaling mechanisms in the granulosa cells from primordial follicles is based on binding of androgens to nuclear AR, and the direct genomic transcriptional induction. This is in contrast to the results from oocytes from primordial and primary follicles, where the "IGF1 Signaling" and "ERK signaling" pathways were both enriched (Ernst et al., 2017), demonstrating that the non-genomic cytosolic pathway might be the molecular mechanism of action of the androgens in the oocyte-compartment. Androgen signaling has besides the above-mentioned pathways also been

linked to the canonical PI3K/PTEN/Akt pathway, which is known to regulate primordial follicle activation in human and rodent (Adhikari et al., 2012; Novella-Maestre et al., 2015). In neonatal mice, activation of the PI3K/PTEN/Akt pathway has been detected, with phosphorylation and translocation of FOXO3a, shortly after testosterone administration, as well as an increased percentage of growing follicles compared to controls (Yang et al., 2010). The link between androgen signaling and IGF1 signaling has been highly argued, as androgens were found to induce upregulation of IGF1 and IGF1R in oocytes of primordial follicles, which is positively correlated to follicular recruitment and activation (Vendola et al., 1999a). In the granulosa cells from primordial and primary follicles, we found that the "IGF1 Signaling" pathway as a group was not significantly enriched, but transcripts of several members of the IGF1 signaling family were detected including IGFBP3 and IGFBP2 in the primordial stage and IGFBP4 in the primary follicle stage. During the primordial to primary follicle transition IGFBP*3* was significantly down-regulated. We find this down-regulation of *IGFBP3* interesting, given IGFBP3's role as a modulator and antagonist of the IGF-IGFR interaction (Hu et al., 2017), which we speculate to be central in the fine-tuned regulation of IGF2-IGF1R interaction and thus downstream PI3K/PTEN/Akt activity in the activation of primordial follicles. Also, in the oocyte compartment, different interesting members of this pathway were detected including *IGF2* and *IGF1R*, both with a high expression (Ernst et al., 2017). Both the transcripts of *IGF1R* and *IGF2* were upregulated during the primordial to primary follicle transition in the oocyte, the latter of the two with a 2-fold increase. In contrast to the high expression of *IGF2* in oocytes from primordial and primary follicles, *IGF1* was only inconsistently expressed in a moderate level, which is consistent with previous studies on human ovarian tissue, showing that IGF2 seems more important than IGF1 in the normal ovarian physiology (Mazerbourg et al., 2003; Stubbs et al., 2013). However, our immunohistochemistry results clearly show that IGF2 protein is present in both oocytes and granulosa cell from primordial follicles, suggesting that it may also be maternally contributed as a protein. IGF1R is of particular interest, as it is a known upstream activator of the PI3K/PTEN/Akt pathway (Makker et al., 2014), which is known to be involved in the regulation of primordial follicles.

In the IGF signaling system, several other receptors besides IGF1R are also noteworthy; IGF2R and INSR. Transcripts of *IGF2R* and *INSR* were both detected in the oocytes, however the expression was low and inconsistent (Ernst et al., 2017). A higher expression of *IGF2R* was however detected in the whole follicle isolate compared to the oocyte only isolate, suggesting that *IGF2R* most likely is expressed in the granulosa cell compartment. Based on our collective results from the transcriptomic analysis of the primordial and primary granulosa cells and oocytes, and the existing literature, we pose the following hypothesis concerning the bidirectional communication in the primordial follicle activation: (1) Based on high *AR* expression, granulosa cells of primordial follicles may be androgen responsive through direct genomic action, (2) This responsiveness may induce transcription of paracrine factors, which in turn could stimulate the oocyte to express transcripts encoding IGF2 and IGF1R, (3) The regulation is the IGF signaling is tightly regulated, and the IGFBP1s are significant regulators of IGF signaling (Allard and Duan, 2018; Mazerbourg and Monget, 2018; Spitschak and Hoeflich, 2018). Therefore, the androgen responsiveness and its potential induction of *IGF2* and *IGF1R* transcription could be mediated through the activation of IGFBPs and IGF ligands in the grnaulosa cells during the primodial to primary transition, which through paracrine actions stimulate transcription of specific genes in the oocytes. In line with this, as mentioned above, androgen can mediate non-genomic signaling, which may also be relevant for IGF signaling. Activated AR in the cytoplasm can interact with several signaling molecules inclu ing the PI3K/Akt, Src, Ras-Raf-1, and PKC, which in turn converge on MAPK/ERK activation, leading to cell proliferation (Kamanga-Sollo et al., 2008). Cell signaling through androgen can also occur without ERK activation. Non-ERK pathways involve activation of mammalian target of rapamycin (mTOR) via the PI3K/Akt pathway or involvement of plasma membrane, G protein coupled receptors (GPCRs) and the sex hormone binding globulin receptor (SHBGR) that modulate intracellular Ca^{2+} concentration and cyclic adenosine monophosphate (cAMP) levels, respectively (Mellström and Naranjo, 2001; Heinlein and Chang, 2002). IGFBPs display higher binding affinities toward IGF than IGFR1/2, and IGFs are therefore regulated by IGFBPs (Firth and Baxter, 2002; Duan and Xu, 2005). During dormancy, granulosa cell-produced IGFBP3 could sequester IGF2 in the extracellular space, thus antagonizing ligand-receptor interaction. Upon IGFBP3-decrease in granulosa cells during the primordial to primary follicle transition, oocyte-derived IGF2 might be free to exert its local effect and to bind IGF1R on the oocyte thus stimulating growth in an autocrine manner, and at the same time bind to IGF2R on the granulosa cells to paracrinally stimulate cell growth, proliferation, differentiation, and/or survival. The scenario of IGF-mediated functions in ovarian physiology is intriguing and becomes very complex considering the pattern of *IGFBP* expression profiles (Mazerbourg and Monget, 2018). It has previously been reported that *IGFBP1* is expressed in granulosa cells of mature follicles (el-Roeiy et al., 1994; Kwon et al., 2010), and it is likely that the expression of *IGFBP1* increases during follicles development, as we note very low expression (if any) in both oocytes and granulosa cells from primordial and primary follicles. Previously, it was reported that *IGFBP2* decreases in the granulosa cells in an cAMP-dependent but FSH-independent manner, (Cataldo et al., 1993), suggesting perhaps an early role of this IGFBP in the early non-FSH responsive phase of follicle development. *IGFBP4* mRNA is expressed at low levels in both oocytes and granulosa cells from primordial and primary follicles, and is in line with a previous study that noted *IGFBP4* mRNA expression as decreasing during human follicle development (Kwon et al., 2010). While *IGFBP5* is higly expressed in all cells in both primordial and primary follicles, *IGPBP6* appears to be specific to granulosa cells in primordial follicles. Finally it is worthnoty that many IGF-independent functions have been reported for the IGFBPs (Allard and Duan, 2018), adding another layer of complexity to ovarian functions for this family, which hopefully will be addressed in future

TABLE 8 | Expression of androgen-responsive genes.

Oocytes*[a]				Granulosa cells*[a]			
Primordial follicles		Primary follicles		Primordial follicles		Primary follicles	
Gene names	FPKM means	Gene names	FPKM means	Gene names	FPKM means	Gene names	FPKM means
ABHD2	**4,865**	***ABHD2***	**5,290**	***ABHD2***	**4,541**	***ABHD2***	**2,969**
ACSL3	**1,950**	***ACSL3***	**5,552**	***ACSL3***	**4,267**	*ACSL3*	2,909
ADAM28	**2,591**	*ADAM28*	3,043	***ADAM28***	**1,944**	*ADAM28*	2,500
ADAMTS1	0,057			*ADAMTS1*	1,10	*ADAMTS1*	0,967
ARL6IP5	0,196			*ARL6IP5*	2,712	*ARL6IP5*	0,332
ATP1A1	**4,888**	***ATP1A1***	**4,012**	***ATP1A1***	**4,514**	***ATP1A1***	**5,862**
B2M	**4,032**	***B2M***	**3,058**	***B2M***	**5,220**	***B2M***	**5,339**
				BLVRB	0,818	*BLVRB*	0,507
C1orf21	1,566	*C1orf21*	1,480	***C1orf21***	**4,202**	*C1orf21*	1,250
CAMK2N1	**0,323**	*CAMK2N1*	0,097	*CAMK2N1*	1,014		
CAPNS1	0,760	*CAPNS1*	0,118	*CAPNS1*	2,776	*CAPNS1*	0,406
						C1orf216	1,325
CENPN	0,123	*CENPN*	0,158	*CENPN*	0,060	*CENPN*	0,107
CNBD1	2,910	*CNBD1*	3,304	***CNBD1***	**3,958**	*CNBD1*	2,523
DERA	0,044	*DERA*	2,082	*DERA*	**1,649**	*DERA*	0,0564
DHCR24	**1,975**	*DHCR24*	0,968	***DHCR24***	**4,669**	*DHCR24*	2,454
ENDOD1	2,238	***ENDOD1***	**2,638**	***ENDOD1***	**2,235**	***ENDOD1***	**3,211**
FDFT1	**7,041**	***FDFT1***	**8,865**	***FDFT1***	**9,266**	***FDFT1***	**6,836**
FKBP5	0,897	*FKBP5*	1,859	*FKBP5*	0,681	*FKBP5*	1,671
GOLPH3	**2,791**	***GOLPH3***	**4,881**	***GOLPH3***	**4,029**	*GOLPH3*	2,701
GOLPH3L	**3,261**	*GOLPH3L*	1,225	***GOLPH3L***	**5,083**	***GOLPH3L***	**5,045**
		HM13	**3,727**	*HM13*	2,325	*KCNMA1*	1,842
		HSP90B1	**7,722**	***HSP90B1***	**7,403**		
KCNMA1	0,113	*KCNMA1*	0,061	*KCNMA1*	0,482		
				KLK3	1,962		
				KRT8	0,432	***KRT8***	**0,1900**
LRIG1	**1,775**	*LRIG1*	0,061	*LRIG1*	1,993	*LRIG1*	0,565
MANEA	**1,140**	*MANEA*	0,115	*MANEA*	1,158	*MANEA*	1,100
NANS	**0,152**			*NANS*	**3,206**	*NANS*	0,565
NCAPD3	1,729	*NCAPD3*	1,709	*NCAPD3*	**1,806**	*NCAPD3*	1,691
NDRG1	**3,044**	***NDRG1***	**4,234**	***NDRG1***	**5,523**	***NDRG1***	**3,950**
NIPSNAP3A	**2,785**	*NIPSNAP3A*	0,710	***NIPSNAP3A***	**2,661**	***NIPSNAP3A***	**1,870**
NKX3-1	0,057	*NKX3-1*	0,922	*NKX3-1*	0,2813	*NKX3-1*	0,866
NTS	0,098	*NTS*	0,097				
NME7	2,056	*NUCB2*	1,031	*NME7*	4,846	*NME7*	2,7182
NUCB2	0,7986			*NUCB2*	**3,498**	*NUCB2*	1,549
ODC1	**5,9116**	***ODC1***	**7,978**	***ODC1***	**6,689**	***ODC1***	**5,0963**
OGDH	1,692	*OGDH*	1,891	***OGDH***	**3,741**	***OGDH***	**2,950**
PAK1IP1	0,057	***PAK1IP1***	**4,685**	***PAK1IP1***	**2,872**	*PAK1IP1*	1,316
PAK2	**5,683**	***PAK2***	**5,029**	***PAK2***	**5,677**	***PAK2***	**5,630**
PIK3R3	1,872	*PIK3R3*	1,392	*PIK3R3*	2,114	*PIK3R3*	0,839
		RHOU	1,422	*RHOU*	0,927	*RHOU*	1,221
PRKACB	**0,152**			*PRKACB*	1,579	*PRKACB*	1,081
				PPAP2A	1,581		
				RAB4A	**2,826**		
RPL15	**5,512**	***RPL15***	**5,607**	***RPL15***	**6,169**	***RPL15***	**6,514**
SEC61G	**1,681**	***SEC61G***	**1,677**	***SEC61G***	**3,222**	***SEC61G***	**2,213**
SF3B5	**1,828**	***SF3B5***	**1,887**	***SF3B5***	**3,095**	***SF3B5***	**1,855**

(Continued)

TABLE 8 | Continued

Oocytes*[a]				Granulosa cells*[a]			
Primordial follicles		Primary follicles		Primordial follicles		Primary follicles	
Gene names	FPKM means	Gene names	FPKM means	Gene names	FPKM means	Gene names	FPKM means
SLC41A1	1,760	*SLC41A1*	0,993	*SLC41A1*	1,450	*SLC41A1*	1,496
SLC45A3	0,044	*SLC45A3*	0,097	*SLC45A3*	0,772		
SOD1	**6,402**	*SOD1*	4,241	***SOD1***	**7,034**	***SOD1***	**5,333**
SORD	**0,074**	*SORD*	1,069	***SORD***	**0,399**	*SORD*	1,301
						STEAP4	0,3615
SVIP	**3,027**	***SVIP***	**2,562**	***SVIP***	**2,701**	*SVIP*	3,008
TAOK3	**0,222**	*TAOK3*	0,506	***TAOK3***	**3,437**	*TAOK3*	1,203
TCP1	**5,834**	***TCP1***	**4,781**	***TCP1***	**4,7636**		
TMEFF2	**2,853**	***TMEFF2***	**1,049**	***TMEFF2***	**6,087**	*TMEFF2*	1,324
TMPRSS2	0,057			*TMPRSS2*	0,985		
TPD52	**3,712**	***TPD52***	**3,582**	***TPD52***	**5,543**	***TPD52***	**4,387**
TPM1	1,786	***TPM1***	**3,533**	*TPM1*	1,759	*TPM1*	3,031
TSC22D1	**4,368**	***TSC22D1***	**3,411**	***TSC22D1***	**4,891**	***TSC22D1***	**3,186**
USP33	**2,439**	***USP33***	**3,777**	***USP33***	**5,667**	*USP33*	2,556

Gene names are followed by the mean FPKM values. Gene names and FPKM values in bold denotes SSCEGs.
**aData extracted from Ernst et al. (2018) and (Kuijjer et al., 2013).*

functional studies. Further studies are, however, needed to support this link between androgens and IGF-driven primordial follicle activation in the human ovary.

Androgens have received increased attention as a key-player in the early follicular development, as the hyperandrogenic microenvironment in the ovaries from women suffering from PCOS, is thought to be central in the anovulation phenotype (Franks and Hardy, 2010). Patients suffering from anovulatory PCOS is shown to have an increased percentage of growing follicles and stockpiling of the primary follicles compared to controls (Webber et al., 2003; Maciel et al., 2004). In a recent study, it was shown that oocytes from women suffering from hyperandrogenism have an increased expression of *IGF2* (Tian et al., 2017). In a future study comparing transcriptomic data from PCOS granulosa cells and oocytes, it would be interesting to investigate if also the *IGF1R* expression is increased in these patients. According to our hypothesis a potential pathogenic mechanism of PCOS could be that androgen-driven overexpression of *IGF1R*, would make the oocyte hypersensitive to growth factors such as IGF2, which is found in a high level, and thus trigger hyperactivity in the PI3K/PTEN/Akt pathway, resulting in a hyperactivation of primordial follicles.

MATERIALS AND METHODS

Tissue Collection and Follicle Isolation

Normal ovarian cortex tissue was donated from three women undergoing oophorectomy followed by cryopreservation before gonadotoxic treatment of non-gynecological cancer. The patients were aged 26, 34, and 34 years old, respectively. Written informed consent was obtained from all patients. The study was approved by Danish Scientific Ethical Committee (Approval number: KF299017 and J7KF/01/170/99) and the Danish Data Protection Agency. From the donated random selected tissue pieces 539 primordial follicles and 261 primary follicles were collected using the Laser Capture Microdissection (LCM) technique using Veritas™ Microdissection Instrument Model 704 (Arcturus XT™, Molecular Devices, Applied Biosystems, Life Technologies, Foster City, CA, U.S.A). The follicles and oocytes were isolated based on their morphological appearance.

LCM, library preparation, sequencing, bioinformatics management, and enrichment analysis was performed essentially as described previously (Ernst et al., 2017, 2018). Briefly, thee human cortical fragments (2 × 2 × 1 mm) were thawed and fixed by immersion into 4% paraformaldehyde (PFA) at 4°C for 4 h followed by dehydration and embedment in paraffin, and the embedding and sectioning was performed as previously described (Markholt et al., 2012). For the LCM isolation, whole follicles and oocytes were captured based on morphological appearance. Oocytes surrounded by 3–5 flattened pre-granulosa cells were defined as primordial follicles, whereas primary follicles were identified as an oocyte surrounded by one layer of cuboidal granulosa cells. During the laser capture, an outline surrounding the cells of interest (oocyte only or whole follicles isolates) was marked microscopically and subsequently cut using the ultraviolet laser. Membrane glass slides (Arcturus® PEN Membrane Glass Slides, Applied Biosystems, Life Technologies, Foster City, CA, U.S.A.), enabled to lift the cells onto a sterile cap (Arcturus® CapSure® HS LCM Caps, Applied Biosystems, Life Technologies, Foster City, CA, U.S.A.) using infrared pulses.

RNA extraction, Library preparation and sequencing, mapping, and statistical analysis as previously described (Ernst et al., 2017, 2018). Briefly, Total RNA was extracted from LCM-isolated cells using Arcturus® Paradise® Plus RNA

Extraction and Isolation Kit (#KIT0312I Arcturus Bioscience Inc., Mountain View, CA, U.S.A.), and subjected to linear amplification using the Ovation® RNA-Seq System V2 kit (NuGen Inc., San Carlos, CA, U.S.A.), and RNA-seq libraries were constructed from the output cDNA using Illumina TruSeq DNA Sample and Preparation kit (Illumina, San Diego, CA, USA), performed at AROS Applied Biotechnology, according to the manufacturer's protocol. BAM files were generated using Tophat (2.0.4), and Cufflinks (2.0.2) created a list of expressed transcripts. BWA (0.6.2) mapped all readings to the human reference genome (hg19). Expression of each gene in a given sample was normalized and transformed to a measurement of log2 [counts per million (CPM)]. Afterwards, fragments per kilobase of exon per million fragments mapped (FPKM) values were calculated on the basis of log2 (CPM) (R Core Team, 2012).

Output From Statistical Analysis for Enrichment Analysis

In silico extraction of granulosa cell transcriptomes was performed on global transcriptome data from patient triplicates of oocytes and oocytes with surrounding granulosa cells (follicle) for both the primordial and primary stage (Ernst et al., 2017, 2018) applying strict filters. The FPKM for all detected transcripts was quantified by performing a *t*-test on patient triplicate samples of same type. The level of consistency was based on *p*-values, with a low *p*-value noting a high degree of consistency in FPKM mean across patient triplicates. The cut-off in the level of consistency for all transcripts was set at $p < 0.2$ across triplicates for being included in all downstream analyses. Afterwards, we identified transcripts uniquely detected in the follicle isolates, and not in corresponding oocytes. All transcripts with a value >1.5 FPKM, was considered uniquely expressed in the follicle isolates and regarded as granulosa cell transcriptome contributions.

Extraction of transcripts encoding the androgen receptor and IGF-related molecules was performed from the lists generated (Ernst et al., 2018) and shows SSCEG and DEG in granulosa cells from primordial (**Tables 2**, **3**) and primary follicles (**Tables 2**, **5**), respectively.

The canonical AR and IGF1 Signaling Pathways were built using IPA® software (http://www.ingenuity.com).

Immunofluorescence Microscopy

Ovarian cortical tissue was sectioned in 5 μm slides and mounted on glass slides. Dehydration and antigen retrieval was performed as described elsewhere (Stubbs et al., 2005) followed by serum block (30 min), then primary antibody; anti-IGF2 rabbit polyclonal antibody (ab9574, Abcam, Cambridge, U.K.), (5 μg/ml) overnight at 4°C. This antibody was previously used and validated (Huang et al., 2010) and several other applications (http://www.abcam.com/igf2-antibody-ab9574-references.html). The sections were subsequently incubated in a 1:250 dilution of appropriate secondary antibody (donkey-anti-rabbit for IGF2) conjugated with Alexa Fluor 488 Dye (Life Technologies, Carlsbad, CA, U.S.A.). Sections were incubated in 1/3,500 Hoechst (Life Technologies, Carlsbad, CA, U.S.A.) followed by mounting with Dako Fluorescent Mounting Medium (Agilent Technologies, Santa Clara, CA, U.S.A) and analyzed using a LSM510 laser-scanning confocal microscope using a 63x C-Apochromat water immersion objective NA 1.2 (Carl Zeiss, Göttingen, Germany). Zen 2011 software (Carl Zeiss, Göttingen, Germany) was used for analysis and image capturing. The quantification of IGF2 immunofluorescence was done by as ImageJ (Jensen, 2013).

AUTHOR CONTRIBUTIONS

LS, EHE, and KL-H conceived the study. LS, EHE, and KL-H analyzed NGS and IPA® data. MA performed ICH and analyzed data. EE provided ovarian tissue from patients. LS, EHE, and KL-H wrote the manuscript. All authors approved the final manuscript.

FUNDING

EHE was supported by a Ph.D. scholarship from Health Faculty, Aarhus University. This work was further supported by The Independent Research Fund (DFF), Denmark (DFF−6120-00027 to KL-H), which supported LS and by grants from the Novo Nordisk Foundation (NNF16OC0022480 to KL-H (which supported MA), Fonden til Lægevidenskabens Fremme (to KL-H), Kong Christian Den Tiendes Fond (to KL-H), and Augustinus Fonden (to KL-H).

ACKNOWLEDGMENTS

We wish to thank the clinical, paramedical and laboratory team of the Fertility Clinic, Aarhus University Hospital and Lykke-Hartmann laboratory (AU) for help and scientific discussions. We thank Elisabeth Bruun for her help on immunofluorescence quantification.

REFERENCES

Adashi, E. Y., Resnick, C. E., D'Ercole, A. J.,Svoboda, M. E., and Van Wyk, J. J. (1985). Insulin-like growth factors as intraovarian regulators of granulosa cell growth and function. *Endocr. Rev.* 6, 400–420. doi: 10.1210/edrv-6-3-400

Adashi, E. Y., Resnick, C. E., Hernandez, E. R., Hurwitz, A., Roberts, C. T., Leroith, D., et al. (1991). Insulin-like growth factor I as an intraovarian regulator: basic and clinical implications. *Ann. N. Y. Acad. Sci.* 626, 161–168. doi: 10.1111/j.1749-6632.1991.tb37910.x

Adhikari, D., Gorre, N., Risal, S., Zhao, Z., Zhang, H., Shen, Y., et al. (2012). The safe use of a PTEN inhibitor for the activation of dormant mouse primordial follicles and generation of fertilizable eggs. *PLoS ONE* 7:e39034. doi: 10.1371/journal.pone.0039034

Allard, J. B., and Duan, C. (2018). IGF-binding proteins: why do they exist and why are there so many? *Front. Endocrinol.* 9:117. doi: 10.3389/fendo.2018.00117

Armstrong, D. G., Hogg, C. O., Campbell, B. K., and Webb, R. (1996). Insulin-like growth factor (IGF)-binding protein production by primary cultures of ovine granulosa and theca cells. Effects of IGF-I, gonadotropin, and follicle size. *Biol. Reprod.* 55, 1163–1171.

Baumgarten, S. C., Convissar, S. M., Fierro, M. A., Winston, N. J., Scoccia, B., Stocco, C., et al. (2014). IGF1R signaling is necessary for FSH-induced activation of AKT and differentiation of human Cumulus granulosa cells. *J. Clin. Endocrinol. Metab*. 99, 2995–3004. doi: 10.1210/jc.2014-1139

Becerra-Fernández, A., Perez-Lopez, G., Roman, M. M., Martin-Lazaro, J. F., Lucio Perez, M. J., Asenjo Araque, N., et al. (2014). Prevalence of hyperandrogenism and polycystic ovary syndrome in female to male transsexuals. *Endocrinol. Nutr*. 61, 351–358. doi: 10.1016/j.endonu.2014.01.010

Cataldo, N. A., Woodruff, T. K., and Giudice, L. C. (1993).Regulation of insulin-like growth factor binding protein production by human luteinizing granulosa cells cultured in defined medium. *J. Clin. Endocrinol. Metab*. 76, 207–215.

Chadha, S., Pache, T. D.,Huikeshoven, J. M., Brinkmann, A. O., and van der Kwast, T. H. (1994) Androgen receptor expression in human ovarian and uterine tissue of long-term androgen-treated transsexual women. *Hum. Pathol*. 25, 1198–1204. doi: 10.1016/0046-8177(94)90037-X

Dey, B. R., Furlanetto, R. W., and Nissley, S. P. (1998). Cloning of human p55 gamma, a regulatory subunit of phosphatidylinositol 3-kinase, by a yeast two-hybrid library screen with the insulin-like growth factor-I receptor. *Gene* 209, 175–183. doi: 10.1016/S0378-1119(98)00045-6

Duan, C., and Xu, Q. (2005). Roles of insulin-like growth factor (IGF) binding proteins in regulating IGF actions. *Gen. Comp. Endocrinol*. 142, 44–52. doi: 10.1016/j.ygcen.2004.12.022

el-Roeiy, A., Chen, X., Roberts, V. J., Shimasakai, S.,Ling, N., LeRoith, D., et al. (1994). Expression of the genes encoding the insulin-like growth factors (IGF-I and II), the IGF and insulin receptors, and IGF-binding proteins-1-6 and the localization of their gene products in normal and polycystic ovary syndrome ovaries. *J. Clin. Endocrinol. Metab*. 78, 1488–1496.

Eppig, J. J. (2001). Oocyte control of ovarian follicular development and function in mammals. *Reproduction* 122, 829–838. doi: 10.1530/rep.0.1220829

Ernst, E. H., Franks, S., Hardy, K., Villesen, P., and Lykke-Hartmann, K., (2018). Granulosa cells from human primordial and primary follicles show differential global gene expression profiles. *Hum. Reprod*. 33, 666–679. doi: 10.1093/humrep/dey011

Ernst, E. H., Grondahl, M. L., Grund, S., Hardy, K., Heuck, A. Sunde, L., et al. (2017). Dormancy and activation of human oocytes from primordial and primary follicles: molecular clues to oocyte regulation. *Hum. Reprod*. 32, 1684–1700. doi: 10.1093/humrep/dex238

Firth, S. M., and Baxter, R. C. (2002). Cellular actions of the insulin-like growth factor binding proteins. *Endocr. Rev*. 23, 824–854. doi: 10.1210/er.2001-0033

Franks, S. (1995). Polycystic ovary syndrome. *N. Engl. J. Med*. 333, 853–861. doi: 10.1056/NEJM199509283331307

Franks, S., and Hardy, K. (2010). Aberrant follicle development and anovulation in polycystic ovary syndrome. *Ann. Endocrinol.* 71, 228–230. doi: 10.1016/j.ando.2010.02.007

Gelmann, E. P. (2002). Molecular biology of the androgen receptor. *J. Clin. Oncol.* 20, 3001–3015. doi: 10.1200/JCO.2002.10.018

Gervasio, C. G., Bernuci, M. P. Silva-de-Sa, M. F., and Rosa E-Silva, A. C. (2014). The role of androgen hormones in early follicular development. *ISRN Obstet Gynecol*. 2014:818010. doi: 10.1155/2014/818010

Hague, W. M., Adams, J., Rodda, C., Brook, C. G.,de Bruyn, R., Grant, D. B., et al. (1990). The prevalence of polycystic ovaries in patients with congenital adrenal hyperplasia and their close relatives. *Clin. Endocrinol.* 33, 501–510. doi: 10.1111/j.1365-2265.1990.tb03887.x

Heinlein, C. A., and Chang, C. (2002). The roles of androgen receptors and androgen-binding proteins in nongenomic androgen actions. *Mol. Endocrinol*. 16, 2181–2187. doi: 10.1210/me.2002-0070

Hu, Q., Zhou, Y., Ying, K., and Ruan, W. (2017). IGFBP, a novel target of lung cancer? *Clin. Chim. Acta* 466, 172–177. doi: 10.1016/j.cca.2017.01.017

Huang, G. S., Brouwer-Visser, J., Ramirez, M. J., Kim, C. H.,Hebert, T. M., Lin, J., et al. (2010). Insulin-like growth factor 2 expression modulates Taxol resistance and is a candidate biomarker for reduced disease-free survival in ovarian cancer. *Clin. Cancer Res*. 16, 2999–3010. doi: 10.1158/1078-0432.CCR-09-3233

Jensen, E. C. (2013). Quantitative analysis of histological staining and fluorescence using Image. *J. Anat. Rec.* 296, 378–381. doi: 10.1002/ar.22641

Kamanga-Sollo, E., White, M. E., Hathaway, M. R., Chung, K. Y., Johnson, B. J., and Dayton, W. R. (2008). Roles of IGF-I and the estrogen, androgen and IGF-I receptors in estradiol-17beta- and trenbolone acetate-stimulated proliferation of cultured bovine satellite cells. *Domest Anim. Endocrinol.* 35, 88–97. doi: 10.1016/j.domaniend.2008.02.003

Knapczyk-Stwora, K., Grzesiak, M., Duda, M., Koziorowski, M., and Slomczynska, M. (2013). Effect of flutamide on folliculogenesis in the fetal porcine ovary–regulation by Kit ligand/c-Kit and IGF1/IGF1R systems. *Anim. Reprod Sci*. 142, 160–167. doi: 10.1016/j.anireprosci.2013.09.014

Kousteni, S., Bellido, T., Plotkin, L. I., O'Brien, C. A., Bodenner, L., Han, D. L., et al. (2001). Nongenotropic, sex-nonspecific signaling through the estrogen or androgen receptors: dissociation from transcriptional activity. *Cell* 104, 719–730. doi: 10.1016/S0092-8674(02)08100-X

Kuijjer, M. L., Peterse, E. F., van den Akker, B. E., Briaire-de Bruijn, I. H., Serra, M., Meza-Zepeda, L. A., et al. (2013). IR/IGF1R signaling as potential target for treatment of high-grade osteosarcoma. *BMC Cancer* 13:245. doi: 10.1186/1471-2407-13-245

Kwon, H., Choi, D. H., Bae, J. H.,Kim, J. H., and Kim, Y. S. (2010). mRNA expression pattern of insulin-like growth factor components of granulosa cells and cumulus cells in women with and without polycystic ovary syndrome according to oocyte maturity. *Fertil. Steril.* 94, 2417–2420. doi: 10.1016/j.fertnstert.2010.03.053

Laviola, L., Natalicchio, A., and Giorgino, F. (2007). The IGF-I signaling pathway. *Curr. Pharm. Des*. 13, 663–669. doi: 10.2174/138161207780249146

Lebbe, M., and Woodruff, T. K. (2013). Involvement of androgens in ovarian health and disease. *Mol. Hum. Reprod.* 19, 828–837. doi: 10.1093/molehr/gat065

Lodhia, K. A., Tienchaiananda, P., and, Haluska, P. (2015). Understanding the key to targeting the igf axis in cancer: a biomarker assessment. *Front. Oncol.* 5:142. doi: 10.3389/fonc.2015.00142

Maciel, G. A., Baracat, E. C., Benda, J. A., Markham, S. M., Hensinger, K., Chang, R. J., et al. (2004). Stockpiling of transitional and classic primary follicles in ovaries of women with polycystic ovary syndrome. *J. Clin. Endocrinol. Metab.* 89, 5321–5327. doi: 10.1210/jc.2004-0643

Magamage, M. P. S., Zengyo, M., Moniruzzaman, M., and Miyano, T. (2011). Testosterone induces activation of porcine primordial follicles *in vitro*. *Reprod. Med. Biol*. 10, 21–30. doi: 10.1007/s12522-010-0068-z

Makker, A., Goel, M. M., and Mahdi, A. A. (2014). PI3K/PTEN/Akt and TSC/mTOR signaling pathways, ovarian dysfunction, and infertility: an update. *J. Mol. Endocrinol*. 53, R103–R118. doi: 10.1530/JME-14-0220

Markholt, S., Grondahl, M. L., Ernst, E. H., Andersen, C. Y., Ernst, E., and Lykke-Hartmann, K. (2012). Global gene analysis of oocytes from early stages in human folliculogenesis shows high expression of novel genes in reproduction. *Mol. Hum. Reprod*. 18, 96–110. doi: 10.1093/molehr/gar083

Mazerbourg, S., and Monget, P. (2018). Insulin-like growth factor binding proteins and igfbp proteases: a dynamic system regulating the ovarian folliculogenesis. *Front Endocrinol.* 9:134. doi: 10.3389/fendo.2018.00134

Mazerbourg, S., Bondy, C. A., Zhou, J. and Monget, P. (2003). The insulin-like growth factor system: a key determinant role in the growth and selection of ovarian follicles? A comparative species study. *Reprod. Domest. Anim.* 38, 247–258. doi: 10.1046/j.1439-0531.2003.00440.x

Mellström, B., and Naranjo, J. R. (2001). Mechanisms of Ca(2+)-dependent transcription. *Curr. Opin. Neurobiol.* 11, 312–319. doi: 10.1016/S0959-4388(00)00213-0

Mondschein, J. S.,Canning, S. F., Miller, D. Q., and Hammond, J. M. (1989). Insulin-like growth factors (IGFs) as autocrine/paracrine regulators of granulosa cell differentiation and growth: studies with a neutralizing monoclonal antibody to IGF-I. *Biol. Reprod*. 41, 79–85. doi: 10.1095/biolreprod41.1.79

Niwa, J., Yamada, S., Ishigaki, S., Sone, J., Takahashi, M., Katsuno, M., et al. (2007). Disulfide bond mediates aggregation, toxicity, and ubiquitylation of familial amyotrophic lateral sclerosis-linked mutant SOD1. *J. Biol. Chem*. 282, 28087–28095. doi: 10.1074/jbc.M704465200

Novella-Maestre, E., Herraiz, S., Rodriguez-Iglesias, B., Diaz-Garcia, C., and Pellicer, A. (2015). Short-term pten inhibition improves *in vitro* activation of primordial follicles, preserves follicular viability, and restores amh levels in

cryopreserved ovarian tissue from cancer patients. *PLoS ONE* 10:e0127786. doi: 10.1371%2Fjournal.pone.0127786

Padmanabhan, V., and Veiga-Lopez, A. (2013). Sheep models of polycystic ovary syndrome phenotype. *Mol. Cell Endocrinol.* 373, 8–20. doi: 10.1016/j.mce.2012.10.005

R Core Team (2012). *R: A Language and Environment for Statistical Computing*. Vienna. Available online at: http://www.R-project.org/

Rice, S., Ojha, K., Whitehead, S., and Mason, H. (2007). Stage-specific expression of androgen receptor, follicle-stimulating hormone receptor, and anti-Mullerian hormone type II receptor in single, isolated, human preantral follicles: relevance to polycystic ovaries. *J. Clin. Endocrinol. Metab.* 92, 1034–1040. doi: 10.1210/jc.2006-1697

Romanuik, T. L., Wang, G., Holt, R. A., Jones, S. J., Marra, M. A., and Sadar, M. D. (2009). Identification of novel androgen-responsive genes by sequencing of LongSAGE libraries. *BMC Genomics*. 10:476. doi: 10.1186/1471-2164-10-476

Saunders, P. T., Millar, M. R., Williams, K., Macpherson, S., Harkiss, D., Anderson, R. A., et al. (2000). Differential expression of estrogen receptor-alpha and -beta and androgen receptor in the ovaries of marmosets and humans. *Biol. Reprod.* 63, 1098–1105. doi: 10.1095/biolreprod63.4.1098

Sen, A., and Hammes, S. R. (2010). Granulosa cell-specific androgen receptors are critical regulators of ovarian development and function. *Mol. Endocrinol.* 24, 1393–1403. doi: 10.1210/me.2010-0006

Spinder, T., Spijkstra, J. J., van den Tweel, J. G., Burger, C. W., van Kessel, H., Hompes, P. G., et al. (1989). The effects of long term testosterone administration on pulsatile luteinizing hormone secretion and on ovarian histology in eugonadal female to male transsexual subjects. *J. Clin. Endocrinol. Metab.* 69, 151–157. doi: 10.1210/jcem-69-1-151

Spitschak, M., and Hoeflich, A. (2018). Potential functions of IGFBP-2 for ovarian folliculogenesis and steroidogenesis. *Front Endocrinol.* 9:119. doi: 10.3389/fendo.2018.00119

Stubbs, S. A., Hardy, K., Da Silva-Buttkus, P., Stark, J., Webber, L. J., Flanagan, A. M., et al. (2005). Anti-mullerian hormone protein expression is reduced during the initial stages of follicle development in human polycystic ovaries. *J. Clin. Endocrinol. Metab.* 90, 5536–5543. doi: 10.1210/jc.2005-0907

Stubbs, S. A., Webber, L. J., Stark, J., Rice, S., Margara, R., Lavery, S., et al. (2013). Role of Insulin-like growth factors in initiation of follicle growth in normal and polycystic human ovaries. *J. Clin. Endocrinol. Metab.* 98, 3298–3305. doi: 10.1210/jc.2013-1378

Suzuki, T., Sasano, H., Kimura, N., Tamura, M.,Fukaya, T., Yajima, A., et al. (1994). Immunohistochemical distribution of progesterone, androgen and oestrogen receptors in the human ovary during the menstrual cycle: relationship to expression of steroidogenic enzymes. *Hum. Reprod.* 9, 1589–1595. doi: 10.1093/oxfordjournals.humrep.a138757

Takayama, K., Fukaya, T., Sasano, H., Funayama, Y.,Suzuki, T., Takaya, R., et al. (1996). Immunohistochemical study of steroidogenesis and cell proliferation in polycystic ovarian syndrome. *Hum. Reprod.* 11, 1387–1392. doi: 10.1093/oxfordjournals.humrep.a019405

Tian, S., Lin, X. H., Xiong, Y. M., Liu, M. E., Yu, T. T., Lv, M., et al. (2017). Prevalence of prediabetes risk in offspring born to mothers with hyperandrogenism. *EBioMedicine* 16, 275–283. doi: 10.1016/j.ebiom.2017.01.011

Vendola, K., Zhou, J., Wang, J., and Bondy, C. A. (1999a). Androgens promote insulin-like growth factor-I and insulin-like growth factor-I receptor gene expression in the primate ovary. *Hum. Reprod.* 14, 2328–2332.

Vendola, K., Zhou, J., Wang, J., Famuyiwa, O. A., Bievre, M., and Bondy, C. A. (1999b). Androgens promote oocyte insulin-like growth factor I expression and initiation of follicle development in the primate ovary. *Biol. Reprod.* 61, 353–357. doi: 10.1095/biolreprod61.2.353

Wandji, S. A., Srsen, V., Voss, A. K., Eppig, J. J., and Fortune, J. E. (1996). Initiation *in vitro* of growth of bovine primordial follicles. *Biol. Reprod.* 55, 942–948. doi: 10.1095/biolreprod55.5.942

Webber, L. J., Stubbs, S., Stark, J., Trew, G. H., Margara, R., Hardy, K., et al. (2003). Formation and early development of follicles in the polycystic ovar*y. Lancet* 362, 1017–1021. doi: 10.1016/S0140-6736(03)14410-8

Weil, S. J., Vendola, K., Zhou, J., Adesanya, O. O.,Wang, J., Okafor, J., et al. (1998). Androgen receptor gene expression in the primate ovary: cellular localization, regulation, and functional correlations. *J. Clin. Endocrinol. Metab.* 83, 2479–2485. doi: 10.1210/jcem.83.7.4917

Weil, S., Vendola, K., Zhou, J., and Bondy, C. A. (1999). Androgen and follicle-stimulating hormone interactions in primate ovarian follicle development. *J. Clin. Endocrinol. Metab.* 84, 2951–2956. doi: 10.1210/jcem.84.8.5929

Willis, D. S., Mason, H. D.,Watson, H., and Franks, S. (1998). Developmentally regulated responses of human granulosa cells to insulin-like growth factors (IGFs): IGF-I and IGF-II action mediated via the type-I IGF receptor. *J. Clin. Endocrinol. Metab.* 83, 1256–1259.

Yang, J. L., Zhang, C. P., Li, L., Huang, L.,Ji, S. Y., Lu, C. L., et al. (2010). Testosterone induces redistribution of forkhead box-3a and down-regulation of growth and differentiation factor 9 messenger ribonucleic acid expression at early stage of mouse folliculogenesis. *Endocrinology* 151, 774–782. doi: 10.1210/en.2009-0751

Conflict of Interest Statement: The authors declare that the research was conducted in the absence of any commercial or financial relationships that could be construed as a potential conflict of interest.

frontiers in Cell and Developmental Biology

REVIEW
published: 27 July 2018
doi: 10.3389/fcell.2018.00072

Molecular Basis of Human Sperm Capacitation

*Lis C. Puga Molina, Guillermina M. Luque, Paula A. Balestrini, Clara I. Marín-Briggiler, Ana Romarowski and Mariano G. Buffone**

Instituto de Biología y Medicina Experimental, Consejo Nacional de Investigaciones Científicas y Tecnológicas, Buenos Aires, Argentina

In the early 1950s, Austin and Chang independently described the changes that are required for the sperm to fertilize oocytes *in vivo*. These changes were originally grouped under name of "capacitation" and were the first step in the development of *in vitro* fertilization (IVF) in humans. Following these initial and fundamental findings, a remarkable number of observations led to characterization of the molecular steps behind this process. The discovery of certain sperm-specific molecules and the possibility to record ion currents through patch-clamp approaches helped to integrate the initial biochemical observation with the activity of ion channels. This is of particular importance in the male gamete due to the fact that sperm are transcriptionally inactive. Therefore, sperm must control all these changes that occur during their transit through the male and female reproductive tracts by complex signaling cascades that include post-translational modifications. This review is focused on the principal molecular mechanisms that govern human sperm capacitation with particular emphasis on comparing all the reported pieces of evidence with the mouse model.

Keywords: human sperm, capacitation, fertilization, hyperactivation, acrosomal exocytosis

OPEN ACCESS

Edited by:
Rafael A. Fissore, University of Massachusetts Amherst, United States

Reviewed by:
Christopher De Jonge, University of Minnesota Twin Cities, United States
Alexander Travis, Cornell University, United States

****Correspondence:***
Mariano G. Buffone
mgbuffone@ibyme.conicet.gov.ar

Specialty section:
This article was submitted to Signaling, a section of the journal Frontiers in Cell and Developmental Biology

Received: *20 February 2018*
Accepted: *19 June 2018*
Published: *27 July 2018*

Citation:
Puga Molina LC, Luque GM, Balestrini PA, Marín-Briggiler CI, Romarowski A and Buffone MG (2018) Molecular Basis of Human Sperm Capacitation. Front. Cell Dev. Biol. 6:72. doi: 10.3389/fcell.2018.00072

INTRODUCTION

In the early 1950s, two researchers, Austin and Chang, using rabbit as a model, independently described the changes that are required for sperm to fertilize oocytes *in vivo* (Austin, 1951; Chang, 1951). These changes were originally grouped under the name of "capacitation" (Austin, 1952) and were later modified to specify that sperm need to reside in the female reproductive tract to acquire this capacity (Austin and Bishop, 1958). These early important observations led to the development of *in vitro* fertilization (IVF). Initially, IVF experiments were performed either with sperm deposited in the oviduct (Austin, 1951; Chang, 1951) or collected from the uterus (Chang, 1959) due to the lack of appropriate conditions to fully support capacitation *in vitro*. A few years later, Yanagimachi and Chang used a medium with a defined chemical composition to capacitate hamster sperm and achieved the first successful IVF (Yanagimachi and Chang, 1963). In 1971, IVF was performed in mice using epididymal sperm and a chemically defined medium (Toyoda et al., 1971).

The remarkable initial discoveries of the fertilization process in mammals were achieved in non-human species such as rabbit, rat, and hamster. The possibility to capacitate mammalian sperm *in vitro* and fertilize the eggs led to the first attempts to capacitate human sperm (Norman et al., 1960; Edwards et al., 1966, 1969). Although little was known about the molecular aspects of human sperm capacitation, these were important steps for achieving the birth of Louise Brown by human IVF (Steptoe and Edwards, 1978).

During capacitation, sperm undergo a change in the motility pattern called hyperactivation (Yanagimachi, 1970) and become competent to undergo a physiological secretory event known as acrosome reaction (aka acrosomal exocytosis; AE). Experiments in mice demonstrated that hyperactivation is critical to fertilization because it facilitates the sperm release from the oviductal reservoir and the penetration through the cumulus oophorus and the extracellular matrix surrounding the egg, i.e., the *zona pellucida* (ZP) (Demott and Suarez, 1992). In addition, mammalian sperm must undergo AE in an orderly manner to penetrate the ZP (Yanagimachi, 1994; Buffone et al., 2009b). It is also proposed that only capacitated human sperm are able to do chemotactic swimming using progesterone gradients in close proximity to the egg (Guidobaldi et al., 2008; Teves et al., 2009; Gatica et al., 2013).

From a molecular point of view, sperm capacitation has been well studied *in vitro* in several species such as bovine, humans, rats, and hamsters, but without any doubt the best characterized model is the mouse. Most of the remarkable discoveries have been generally achieved in mice and later explored in other species. As a scientific tool, mice have helped to speed up the progress of research in all fields, and in sperm physiology, this is true due to several reasons: (i) the possibility to use transgenic tools to create knockout (KO) or transgenic sperm containing fluorescent proteins or molecular sensors; (ii) it is easy to perform assisted reproductive techniques such as intracytoplasmic sperm injection (ICSI), IVF, or embryo transfer; (iii) they are closely related to humans (∼99% of mouse genes have an equivalent in humans); (iv) their genome has been fully sequenced (published in 2002); (v) mice are small, have a short generation time, and have an accelerated lifespan; (vi) mice are cost effective because they are inexpensive and easy to look after; (vii) spermatogenesis in mice is comparable with humans (O'Bryan et al., 2006).

Despite the fact that differences might exist between species, mice serve as a *de facto* surrogate model for characterizing the capacitation of human sperm (De Jonge, 2017). However, there are certain aspects that are important to highlight before going deeper into molecular events associated with human sperm capacitation. These considerations not only include differences between both species, i.e., humans and mice, but also important aspects to consider when evaluating *in vitro* experiments. The most significant aspects, according to our opinion, are listed below:

a. Human sperm are highly pleomorphic in the sense that a large number of cells in the ejaculate display a great variety of morphological forms. In contrast, the proportion of mouse sperm with morphological variations is rather small.
b. Humans deposit the ejaculate in the vagina, in contrast to mice that ejaculate in the uterus (Kawano et al., 2014).
c. Human sperm are selected in the cervix, where only morphologically normal or slightly abnormal sperm can migrate through this channel. A cohort of sperm immediately pass into the cervical mucus, whereas the remaining sperm population becomes a part of the coagulum. Then, a second round of selection occurs in the uterotubal junction (UTJ). In contrast, mouse sperm are only selected in the UTJ by mechanisms that are not fully clarified but include ADAM3 and other proteins (Yamaguchi et al., 2009; Holtzmann et al., 2011; Okabe, 2013).
d. In general, the study of human sperm starts from a semen sample, whereas in mice, it starts from sperm recovered from the epididymis. In this condition, mouse sperm has not yet been exposed to high concentrations of HCO_3^-, cholesterol, Zn^{2+}, and seminal plasma proteins, among other components.
e. In humans, the semen is frequently manipulated to isolate the highly motile population of sperm. In contrast, virtually all studies use mouse sperm obtained from the cauda epididymis that have not been exposed to any selection procedure.
f. *In vitro* incubation under capacitating conditions for human sperm ranges from 3 to 24 h. As a result, a great variability of results is reported in the literature. In contrast, most studies in mouse sperm are performed using 1–1.5 h of incubation under capacitating conditions.
g. Based on non-human data, the oviductal epithelium is considered a sperm reservoir that regulates binding and release of sperm toward the site of fertilization. The role of oviductal epithelium and fluids on human sperm was generated *in vitro* by cell culture experiments. Hence, our knowledge about human sperm interaction with the oviduct is scarce in comparison with rodents.
h. The role of the uterus, the oviduct, and their secretions on human sperm capacitation is largely unknown due to practical and ethical limitations (De Jonge, 2017). A great number of molecules that are present in the female tract that have also been shown to modify sperm function are usually not included in the *in vitro* capacitation experiments (Luconi et al., 1995; Meizel et al., 1997; Edwards et al., 2007; Garbarino Azúa et al., 2017). In addition, uterine contractions facilitate the sperm transport mechanism that is essential for migration within the female reproductive tract.

For all these reasons (and many others that will be explained in the following sections), caution while transferring molecular and cellular concepts between species was proposed recently (Kaupp and Strünker, 2016). Alternatively, sperm from a given species should be studied using a vertical research strategy (Kaupp and Strünker, 2016).

We would also like to stress that, unless otherwise indicated, all data regarding human sperm function and regulation by electrophysiological processes are derived from *in vitro* experimentation and may not be reflective of what occurs during transit through the male and female reproductive tracts. The aim of this paper is to revisit the most important molecular events of human sperm capacitation.

SPERM PLASMA MEMBRANE AND SEMINAL PLASMA CHOLESTEROL

The sperm plasma membrane not only serves as the cell boundary but also presents a dynamic structure that has an impact on sperm capacitation and AE (Flesch and Gadella, 2000). During capacitation, several changes in the sperm membrane have been

described: increase in membrane fluidity, lateral movement of cholesterol to the apical region of the sperm head, and cholesterol efflux from the sperm plasma membrane to the extracellular environment (Martínez and Morros, 1996; Gadella, 2008). The approximate lipid content of mammalian sperm is composed of 70% phospholipids, 25% neutral lipids (cholesterol), and 5% glycoproteins (Mann and Lutwak-Mann, 1981), cholesterol being the main sterol in the cellular plasma membrane (∼90%) (Lalumière et al., 1976; Langlais et al., 1981; Zalata et al., 2010; Boerke et al., 2013). In addition, desmosterol, a cholesterol precursor, and sulfate derivatives were reported (∼10%) (Nimmo and Cross, 2003).

The cholesterol/phospholipid (C/PL) ratio in sperm varies between species (Davis, 1981), i.e., 0.20 in boar sperm, 0.36 in stallion sperm, about 0.40 in bovine sperm, 0.43 in ram sperm, and 0.83 in human sperm (Parks and Hammerstedt, 1985; Parks et al., 1987, 1992). Davis reported a correlation between the C/PL ratio in sperm and the time required to complete capacitation when comparing different mammalian species: the higher the C/PL ratio, the longer the incubation period for capacitation to be achieved (Davis, 1981; Ostermeier et al., 2018). Sperm of patients with unexplained infertility showed a higher C/PL ratio due to lower phospholipid content (Sugkraroek et al., 1991), and normospermic patients who failed in IVF had either an atypical high content of cholesterol or a slow efflux of cholesterol during *in vitro* incubation (Benoff et al., 1993).

Sperm cholesterol content is finely regulated within the male reproductive tract as the concentration of lipids in blood serum does not correlate with the seminal plasma levels (Grizard et al., 1995). Cholesterol is found in high abundance in seminal plasma (Grizard et al., 1995; Cross, 1996). Experiments in rabbit and bull sperm showed an inhibitory effect of seminal plasma on capacitation that could be reversed after re-incubation of the sperm in the oviduct (Chang, 1957). Incubation of human sperm in seminal plasma inhibited progesterone-induced AE, being the main inhibitor free cholesterol (Cross, 1996). Altogether, these early observations demonstrate the important regulatory role of seminal plasma sterols on the initiation and promotion of capacitation.

Cholesterol Efflux During Capacitation

It has been well demonstrated *in vitro* that capacitation is associated with removal of cholesterol from the plasma membrane (Visconti et al., 1999). Albumin is the most used cholesterol acceptor in *in vitro* experiments (Langlais et al., 1988; Suzuki and Yanagimachi, 1989; Leahy and Gadella, 2015), and it has been described to be in high abundance in the oviduct (Ehrenwald et al., 1990). The lipid transfer protein-I (LTP-I), a key protein in the human plasma metabolism of the high-density lipoprotein (HDL) (Albers et al., 1984; Tall, 1993), is present in the reproductive fluids and it also serves as a cholesterol acceptor (Ravnik et al., 1992).

Sterol-rich microdomains, known as lipid rafts, are organization centers involved in membrane protein distribution, activating receptors and signaling cascades. Markers for these rafts, such as the proteins caveolin-1, caveolin-2, flotilin-1 and flotilin-2, and the sphingolipids GM1 and GM3, have been described (Travis et al., 2001; Suzuki et al., 2017). A capacitation-associated movement, due to cholesterol efflux, of GM1 has been observed during capacitation (Selvaraj et al., 2007; Bruckbauer et al., 2010). GM1 binds decapacitating factors released during capacitation (Kawano et al., 2008) and can be used as a biomarker for lipid rafts, as it can be easily traced using cholera toxin (Selvaraj et al., 2006).

Lipocalin 2 is present in mouse oviduct and uterus and induces capacitation via raft aggregation in a PKA-dependent manner (Watanabe et al., 2014). Glycosylphosphatidylinositol-anchor proteins (GPI-APs) are also components of lipid rafts (Varma and Mayor, 1998), and their release is very important for male fertility (Kondoh et al., 2005; Ueda et al., 2007; Fujihara et al., 2013). Recent studies in mouse sperm described the importance of lipid raft movement in order for sperm to gain fertilization ability, using cholera toxin to track GM1 and (GPI)-anchored enhanced green fluorescent protein (EGFP-GPI) (Kondoh et al., 1999; Watanabe et al., 2017). Cholesterol efflux using methyl-β-cyclodextrin (M-β-CD) showed not only GM1 movement but also release of GPI-APs (Watanabe et al., 2017).

Phospholipid scrambling, one of the earliest capacitation events, is initiated by an increase in intracellular HCO_3^- followed by the activation of the cAMP/PKA pathway and may be essential to facilitate albumin-mediated cholesterol efflux (Gadella and Harrison, 2000; Harrison and Miller, 2000; Flesch et al., 2001).

Ravnik and coworkers proposed LTP-I as a capacitation inducer in human sperm, as it stimulates acrosomal loss and increases the penetration of hamster eggs by human sperm (Ravnik et al., 1995).

ACTIVATION OF cAMP-PKA PATHWAY

Human sperm capacitation can be mimicked *in vitro* in a chemically defined medium containing electrolytes (Na^+, K^+, Cl^-, HCO_3^-, Mg^{2+}, Ca^{2+}, and PO_4^{3-}), energy substrates (glucose, pyruvate, and lactate), and a cholesterol acceptor (usually serum albumin as previously described).

The activation of intracellular signaling pathways is dependent on the presence of the chemicals present in the capacitation medium. For instance, once human sperm are exposed to seminal plasma or the female reproductive tract, they encounter higher concentration of HCO_3^- (Okamura and Sugita, 1983; Okamura et al., 1985), which in turn stimulates the soluble adenylyl cyclase ADCY10 (Buck et al., 1999; Jaiswal and Conti, 2003). Activation of ADCY10 primarily by HCO_3^-, but also by Ca^{2+} leads to an increase in cyclic adenosine monophosphate (cAMP) synthesis in several mammalian species (Chen et al., 2000). The initial HCO_3^- entrance in mouse and human sperm occurs through NBC cotransporters (Demarco et al., 2003; Puga Molina et al., 2018). In addition, it was reported that inhibition of the cystic fibrosis transmembrane conductance regulator channel (CFTR) affects HCO_3^--entrance-dependent events (Puga Molina et al., 2017), such as phosphorylation in substrates of protein kinase A (PKA) and tyrosine phosphorylation (pY). In contrast, CFTR inhibition does not affect this pathway in mouse sperm (Wertheimer et al., 2008; Puga Molina et al., 2017).

In sperm as well as in other cells, intracellular cAMP levels are highly dynamic. Its concentration relies on the simultaneous action of both synthesis by ADCY10 and degradation by phosphodiesterases (PDE). In mammals, 11 PDE families have been described, with different substrate specificities and pharmacological sensitivities. In human sperm, inhibition of PDE4 enhanced sperm motility, whereas PDE1 inhibitors selectively stimulated the AE (Fisch et al., 1998). These observations suggest that molecules related to cAMP signaling such as cAMP targets, adenylyl cyclases, and PDE are compartmentalized and, as a consequence, participate in different sperm functions, some in the flagellum and others in the head (Buffone et al., 2014b).

The role of cAMP in sperm function is well described elsewhere (Buffone et al., 2014b), and some of its targets will be discussed in the following sections. One of the main targets of cAMP is PKA, which is essential in sperm biology (Burton and McKnight, 2007). PKA is an heterotetramer composed of two catalytic subunits (C) and two regulatory subunits (R). The active C subunit is dissociated as an active kinase when cAMP binds to R subunits. Using antibodies against PKA substrate consensus phosphorylation sites, it was shown in human sperm as well as in other species that PKA activity reaches maximum activity within 1 min of exposure to HCO_3^- (Battistone et al., 2013). Because PKA has multiple targets, phosphorylation of a given substrate may occur without affecting others by the action of A-kinase-anchoring proteins (AKAPs) (Carnegie et al., 2009). AKAPs anchor the R subunit of PKA, restricting its activity to discrete locations within the sperm (Carnegie et al., 2009; Scott and Pawson, 2009). Several reports have shown the presence and possible function of AKAPs such as AKAP3 and AKAP4 in human sperm (Carrera et al., 1996; Mandal et al., 1999; Harrison et al., 2000; Ficarro et al., 2003). In addition to PKA, cAMP can bind and regulate other targets such as the exchange protein directly activated by cAMP (EPAC). EPAC1 and EPAC2 are expressed in sperm from different species including human (Branham et al., 2006) and are localized to the sperm head. These enzymes play a major role in human sperm AE (Branham et al., 2006, 2009; Buffone et al., 2014a).

One of the best characterized events in sperm capacitation is the time-dependent increase in pY. The increase in sperm pY is downstream of a cAMP/PKA-dependent pathway in many species including humans (Visconti et al., 1995b; Osheroff et al., 1999; Battistone et al., 2013, 2014). Several reports have shown clear deficiencies in this process in infertile patients (Buffone et al., 2004, 2005, 2006, 2009a,c). Because PKA is a serine/threonine (Ser/Thr) protein kinase, a tyrosine kinase mediates the role of PKA in pY. The mechanism by which PKA activates pY in humans was reported to be mediated by proline-rich tyrosine kinase 2 (PYK2) (Battistone et al., 2014). On the contrary, sperm from *Pyk2*$^{-/-}$ mice have normal pY during capacitation, but in sperm from mice in which the tyrosine kinase FER was disrupted, pY was not increased (Alvau et al., 2016). FER has also been detected in human sperm (Matamoros-Volante et al., 2017), although its role during capacitation has not yet been established.

In summary, the cAMP/PKA signaling pathway is essential for human sperm capacitation and is activated by HCO_3^- and Ca^{2+} influx during the sperm transit from the epididymis to the oviduct. During this journey, sperm are exposed to large changes in HCO_3^-, Ca^{2+}, as well as H^+, Na^+, K^+ that ultimately impact on the membrane potential (Em) and the intracellular pH. These changes are regulated by the activation of the cAMP-PKA pathway and they will be explained in detail in the following sections.

EXTRACELLULAR AND INTRACELLULAR pH IN HUMAN SPERM

Regulation of intracellular pH (pHi) is fundamental for every cellular process. It is suggested that homeostasis of the pHi in mammals is mainly controlled by: (1) H^+ and (2) HCO_3^- transport. Particularly, sperm encounter a variety of dramatic changes in H^+ extracellular concentration during their transit from the epididymis to the site of fertilization in the female tract. Although extracellular pH (pHe) from epididymis is acidic (approx. 6.8) (Carr and Acott, 1989; Caflisch and DuBose, 1990; Rodriguez-Martinez et al., 1990), in humans, the pH of semen is approximately 7.2–8.4 (Owen and Katz, 2005), and in the human female, the reproductive tract is graduated, with lowest pH in the vagina (approx. pH 4.4), increasing toward the endocervix and uterus (approx. pH 7) (Macdonald and Lumley, 1970; Eggert-Kruse et al., 1993; Ng et al., 2017).

In addition to different H^+ concentrations, sperm encounter a variety of different ionic compositions such as HCO_3^-. In the porcine epididymis, the $[HCO_3^-]_e$ is approximately 2–4 mM (Okamura et al., 1985), whereas in rabbit, human, and porcine, seminal plasma is approximately 25 mM (Vishwakarma, 1962), and in the human and rabbit female tract, it is reported in the range of approximately 20–60 mM (Vishwakarma, 1962; Hamner et al., 1964; David et al., 1973).

In addition, it is postulated that pHe varies in the female tract according to the moment of ovulation. In the lumen of the *Macaca mulatta* (rhesus monkey) oviduct, pHe increases from approximately 7.2 to 7.6, whereas the $[HCO_3^-]_e$ increases from approximately 35 to 90 mM from the follicular phase to ovulation (Maas et al., 1977). These variations in $[H^+]_e$ and $[HCO_3^-]_e$ during the journey of the sperm and during ovulation in the female tract might be of great importance for the pHi regulation in sperm.

Alkalinization During Capacitation

During their transit through the female reproductive tract, sperm encounter an alkaline pH, higher HCO_3^- concentration, and albumin. All these factors contribute to the cytoplasmic alkalinization that occurs during mouse sperm capacitation (Zeng et al., 1996; Nishigaki et al., 2014). This event is widely associated with hyperactivated motility because the alkalinization of the cytoplasm is necessary for the activation of CatSper, and the activity of this channel is fundamental for the hyperactivation of the human sperm (see below).

In mouse sperm, it was shown that sperm alkalinization depends mainly on the Na^+/H^+ exchanger (NHE) activity (Wang et al., 2003b; Chávez et al., 2014) and also on the CFTR activity (Xu et al., 2007; Chávez et al., 2012). However, in humans,

the mechanism of the pH increase is thought to be different (Miller et al., 2016) as it is postulated that the main proton efflux depends mostly on Hv1 (Lishko et al., 2010).

The pHi of mammalian sperm, including humans, has been evaluated using different fluorescent indicators (Florman et al., 1989; Vredenburgh-Wilberg and Parrish, 1995; Brook et al., 1996; Hamamah et al., 1996; Cross and Razy-Faulkner, 1997), [^{31}P]-NMR (Smith et al., 1985; Robitaille et al., 1987), and also by the distribution of a radioactive amine (Gatti et al., 1993; Hamamah et al., 1996), resulting in pHi approximately 6.7–7.2. However, there are few reports showing an increase in pHi during capacitation in human sperm. By using the BCECF pH-sensitive fluorescent probe, Cross and Razy-Faulkner showed that 24-h capacitated sperm have higher pHi (7.08) compared with freshly ejaculated sperm (6.94). They also showed that when cholesterol loss is prevented, pHi is similar to that observed in ejaculated sperm (pHi approx. 6.7) (Cross and Razy-Faulkner, 1997). López-González et al. demonstrated by flow cytometry the existence of a subpopulation of capacitated sperm with more alkaline pH than those incubated in a noncapacitating medium (López-González et al., 2014). Because of the lack of *in vivo* experimentation, overall, the alkalization as a regulatory process during human sperm capacitation is still highly speculative.

Regulation of pHi

Although alkalinization has been demonstrated in human sperm *in vitro*, the molecular mechanisms related to this process have not yet been fully understood, and still remains much to be explored regarding the participation of different channels and transporters during capacitation. As mentioned before, ion transporters that regulate pHi can be divided into two groups: (1) H^+ transporters and (2) HCO_3^- transporters.

Voltage-Gated H^+ Channels (Hv1)

Hv1 is encoded by the *HVCN1* gene and mediates highly selective H^+ outward currents (Musset and Decoursey, 2012). Hv1 is the dominant proton conductance in human sperm; however, until now, the effect on Hv1 mutations in human fertility has not been reported. In contrast, mouse sperm do not have functional Hv1 (Lishko and Kirichok, 2010), and for this reason, $Hv1^{-/-}$ mice are fertile (Ramsey et al., 2009).

The Hv1 channel is present in the principal piece of the flagellum of human sperm as confirmed by immunoblotting and immunostaining (Lishko et al., 2010), and recently, a shorter variant (Hv1Sper) generated by proteolytic cleavage during spermatogenesis was reported (Berger et al., 2017).

Electrophysiological data have shown that Hv1 is an H^+-selective channel whose activity is potentiated by capacitation, anandamide, membrane depolarization, and alkaline extracellular pH (Lishko et al., 2010). Interestingly, this channel is inhibited by Zn^{2+} ($IC50 = 222 \pm 36$ nM) (Lishko et al., 2010; Qiu et al., 2016), which is present in high concentration in seminal plasma [in humans approx. 1.2–10.6 mM in seminal fluid vs. approx. 15.3 μM in serum (Owen and Katz, 2005)]. Hv1Sper is also inhibited by Zn^{2+}, but the loss of a fragment in Hv1 N-terminus tunes its sensitivity to pH. Hv1Sper variant can form heterodimers with Hv1. Hv1Sper-Hv1 tandem dimers display distinct pH and voltage dependence; however, the Hv1Sper/Hv1 ratio is independent of capacitation (Berger et al., 2017).

Although it has been proposed that Hv1 would be mainly responsible for pH control in human sperm, the participation of this channel on the rise of pHi during capacitation has not been reported yet.

Na^+/H^+ Exchangers (NHE)

The SLC9 gene family encodes 13 evolutionarily conserved NHE. The expression of three NHEs has been identified in rat, mouse and human sperm, such as NHE1, NHE5, and NHE10 (Woo et al., 2002; Wang et al., 2003a; Zhang et al., 2017). Furthermore, in mouse sperm, a new member of the NHE family (sperm-specific NHE; sNHE, *Slc9c1* gene) is expressed, whose localization is restricted to the principal piece (Wang et al., 2003a). sNHE-null males are infertile and have impaired sperm motility. As sNHE not only interacts but is also required for the sAC expression, it is postulated that this complex modulates pHi and HCO_3^- (Wang et al., 2007). Regarding the participation of pHi and HCO_3^- in sperm motility, it is worth knowing that the addition of NH_4^+ and cAMP analogs partially rescues the motility and fertility defects, suggesting that other important players may also be affected in this transgenic model (Wang et al., 2003a).

In human sperm, sNHE is mainly localized in the principal piece and its expression is downregulated in sperm from asthenozoospermic patients (Zhang et al., 2017). In addition, it has been reported that regulation of pHi in human sperm depends on the $[Na^+]_e$, and that ethyl-isopropyl amiloride (EIPA) affects this regulation within concentrations that inhibit NHE activity (Garcia and Meizel, 1999). Amiloride, another inhibitor of NHE, at 0.5 mM affects motility in human sperm, and the addition of nigericin, an ionophore that restores intracellular pH, partially rescues sperm motility (Peralta-Arias et al., 2015). As in mouse sperm, the ion transport-like region of the putative human sNHE is related to the membrane segments of voltage-gated ion channels (Wang et al., 2003a). For this reason, it is suggested that sNHE should play a central role in signaling (Kaupp and Strünker, 2016). Unfortunately, because sNHE is electroneutral, it is difficult to use traditional electrophysiological techniques to study its role in human sperm (Miller et al., 2015), and its role during capacitation still remains to be elucidated.

HCO_3^- Transporters

As HCO_3^- is a weak base, changes in $[HCO_3^-]_i$ can cause intracellular alkalinization. HCO_3^- transporters include the SLC26 and SLC4 families (Liu et al., 2012) and the CFTR (Anderson et al., 1991).

- **SLC4:** SLC4A1–5 and SLC4A7–11 family members include two groups: an Na^+-independent group and an Na^+-dependent group (Liu et al., 2012; Bernardino et al., 2013). Na^+-independent members include three anion exchangers, namely SLC4A1 (AE1), SLC4A2 (AE2), and SLC4A3 (AE3), which mediate electroneutral Cl^-/HCO_3^- exchange (Holappa et al., 1999; Medina et al., 2003). Although in human sperm,

the presence of SLC4A1 and SLC4A2 in the equatorial segment has been demonstrated (Parkkila et al., 1993), the participation of this family in the regulation of pHi is unknown. The Na^+-dependent members of the SLC4 family include five Na^+-coupled HCO_3^- transporters, also termed NBC. The NBC transporters are composed of two electrogenic Na^+/HCO_3^- cotransporters, NBC1 (SLC4A4, 2 HCO_3^-:1 Na^+) and NBC2 (SLC4A5, 2 HCO_3^-:1 Na^+), two electroneutral Na^+/HCO_3^- cotransporters, NBCn1 (SLC4A7; 2 HCO_3^-:1 Na^+) and NBCn2 (SLC4A10), and an electroneutral Na^+-driven Cl^-/HCO_3^- exchanger, NDCBE (SLC4A8 2 HCO_3^-:1 Na^+). The Na^+ dependence of "AE4" (SLC4A9) remains controversial (Liu et al., 2015); however, the latest evidence suggests that it is an electroneutral Cl^-/nonselective cation–HCO_3^- exchanger (Peña-Münzenmayer et al., 2016).

Na^+-coupled HCO_3^- transporters have been shown to play a role in the regulation of pHi during capacitation. Demarco et al. (2003) suggested that an electrogenic NBC is active in mouse sperm and is responsible for the initial HCO_3^- entrance during capacitation. In addition, in mouse sperm, Zeng et al. (1996) demonstrated that pHi is dependent on extracellular Na^+, HCO_3^-, and Cl^-. Jensen et al. (1999) showed the expression of the NBC1 in rat sperm. In humans, NBC2, NDCBE, and NBCn2 were detected in testis (Ishibashi et al., 1998; Damkier et al., 2007). It has recently been shown that NBC is involved in the initial HCO_3^- uptake in humans (Puga Molina et al., 2018).

- **SLC26:** In mouse and human sperm, elevation of pHi was shown to depend on CFTR activity (Xu et al., 2007; Puga Molina et al., 2017). It has also been shown that there is a physical interaction between CFTR and the SLC26A3, SLC26A6, and SLC26A8 exchangers in mouse, human, and guinea pig sperm (Chen et al., 2009; Chávez et al., 2012; Rode et al., 2012). This functional association between CFTR and the SLC26A3 and SLC26A6 modulates pHi in mouse sperm (Chávez et al., 2012).

  CFTR is a selective ion channel to Cl^- (Anderson et al., 1991; Bear et al., 1992; Tabcharani et al., 1993) and also transports other anions with different permeabilities ($pBr^- \geq pCl^- > pI^- > pHCO_3^-$) (Anderson et al., 1991). This ATP-gated channel is regulated by PKA, because its phosphorylation is mandatory for both the channel opening mechanism and the ATP association (Anderson et al., 1991; Tabcharani et al., 1991; Bergerz et al., 1993). The multiple potential sites of phosphorylation by PKA in the regulatory domain of CFTR (R) make the channel dependent on the cAMP concentration (Tabcharani et al., 1991; Bergerz et al., 1993; Sheppard and Welsh, 1999; Gadsby et al., 2006; Sorum et al., 2015). In addition, the interaction between CFTR and SLC26 is mediated by the R domain of the channel and the Sulfate Transporter and Anti-Sigma (STAS) domain of SLC26, which must be phosphorylated by PKA to favor interaction (Gray, 2004; Ko et al., 2004). In accordance to these results, it was reported by our group that PKA activity is essential for pHi regulation in human sperm (Puga Molina et al., 2017).

  CFTR protein is present in mature human and mouse sperm and is restricted to the mid-piece (Hernández-González et al., 2007; Xu et al., 2007) and the equatorial segment of the head (Xu et al., 2007).

  In humans, mutations in the CFTR gene that impair CFTR activity cause a severe disease called cystic fibrosis. It has been reported that patients with cystic fibrosis have deterioration in fertility in both women and men. The higher incidence of CFTR mutations in a male infertile subpopulation may indicate its participation in other fertilization-related events, such as sperm capacitation (Jakubiczka et al., 1999; Schulz et al., 2006). Supporting this hypothesis, human sperm treated with a specific inhibitor of CFTR decreases the percentage of sperm undergoing AE, hyperactivation, and penetration of ZP-free hamster eggs (Li et al., 2010). Regarding the SLC26 transporters that can interact in human sperm with CFTR, SLC26A6 is expressed in human efferent and epididymal ducts and colocalizes with CFTR (Kujala et al., 2007). SLC26A8 (TAT1) is expressed specifically in the male germ line, and it was shown to physically interact with CFTR *in vitro* and *in vivo* in mature sperm, activates CFTR, and, interestingly, is essential for the activation of the cAMP-PKA pathway in mouse sperm (Rode et al., 2012). Its role in human sperm has not been demonstrated but nonsense mutations in *SLC26A8* have been associated with asthenozoospermia (Dirami et al., 2013). In addition, in humans, mutations that impair SLC26A3 activity also cause subfertility and oligoasthenozoospermia (Hihnala et al., 2006; Höglund et al., 2006).

Carbonic Anhydrases (CAs)

Carbonic anhydrases (CAs) are metalloenzymes that catalyze the reversible hydration of carbon dioxide to HCO_3^- ($OH^- + CO_2 \leftrightarrow HCO_3^- + H^+$). CAs are encoded by five gene families: α, β, ɤ, δ, and ζ, but only 15 isoforms of the α family are found in primates (i.e., CAI-CAXIV, except CAXV) (Truppo et al., 2012). CAs are important in the regulation of pHi in bacteria, archaea, and eukarya. However, the role of these enzymes in sperm physiology is still not clear (Nishigaki et al., 2014). The expression of some CAs has been reported in human sperm, including CAI (Ali Akbar et al., 1998) and CAII (Ali Akbar et al., 1998), that were reported in the post-acrosomal region (Parkkila et al., 1991) and in the flagellum (José et al., 2015), and CAXIII (Lehtonen et al., 2004) localized in the flagellum of human sperm (José et al., 2015). The function of CAs is not yet fully understood, but the use of general blockers against these enzymes affects motility and increases the AE in capacitated human sperm (Wandernoth et al., 2010; José et al., 2015).

Albumin

Cross (1998) demonstrated that the cytoplasmic alkalinization in human sperm depends on the cholesterol removal during capacitation. Cross and Razy-Faulkner (1997) showed that sperm cells incubated with albumin saturated with cholesterol sulfate have a more acidic pHi than the capacitated control condition. Although the effects of cholesterol in pHi have been observed in platelets and fibroblasts (Poli de Figueiredo et al., 1991) and that cholesterol alters the activity of NHE and Cl^-/HCO_3^- exchangers in erythrocytes (Grunze et al., 1980), how this regulation occurs in human sperm remains largely unknown.

The proton-selective voltage-gated channel Hv1 can be activated by removing extracellular Zn^{2+} (Lishko and Kirichok, 2010; Lishko et al., 2010). It has been proposed that high concentrations of Zn^{2+} in the seminal plasma inhibit Hv1, and that in the female tract a decrease in Zn^{2+} due to dilution, absorption by the uterine epithelium, and chelation may render sperm free from Zn^{2+} in the fallopian tube (Gunn and Gould, 1958; Ehrenwald et al., 1990; Lu et al., 2008). Albumin is not only a cholesterol acceptor but it also chelates Zn^{2+} (Lu et al., 2008). Therefore, it is unclear whether the effect on pHi is due to the cholesterol efflux and/or the chelation of Zn^{2+}.

MEMBRANE POTENTIAL IN HUMAN SPERM

In any given cell, the metabolic state and specific ion channels and transporters determine the internal and the external ion concentration and the plasma membrane permeability that defines the Em. Sperm encounter different concentrations of extracellular K^+, Na^+, Cl^-, and HCO_3^- throughout their journey from the testis to the site of fertilization in the female tract. In the *ductus deferens*, the levels of K^+ (approx. 110 mM), Na^+ (approx. 30 mM), Cl^- (approx. 100 mM) (Hinton et al., 1981) (for humans), and HCO_3^- (approx. 2–4 mM) (Okamura et al., 1985) (for porcine) are different than in seminal plasma [K^+ (approx. 12–63 mM), Na^+ (approx. 102–143 mM), Cl^- (approx. 37–45 mM), and HCO_3^- (approx. 25 mM)] (Okamura et al., 1986; Owen and Katz, 2005), and than in human uterine tubal fluid [K^+ (approx. 4.5–21 mM), Na^+ (approx. 130–149 mM), Cl^- (approx. 118–132 mM), and HCO_3^- (approx. 20 a 60 mM)] (Lippes et al., 1972; David et al., 1973; Lopata et al., 1976; Borland et al., 1977; Aguilar and Reyley, 2005). Although Na^+ and HCO_3^- are higher in seminal plasma and in the female tract than in the *ductus deferens*, K^+ is lower and Cl^- varies reaching maximal concentration in the uterine tubal fluid. These ionic changes transduce variations not only in the Em but also in pH, as mentioned earlier.

In human sperm, it was demonstrated that the regulation of Em is related to male fertility due to the modulation of ion channels and transporters such as CatSper (sperm-specific Ca^{2+} channel) and Hv1 (Darszon et al., 1999; Lishko et al., 2012). It was reported that idiopathic and asthenozoospermic infertile men have more depolarized Em than fertile men (Calzada and Tellez, 1997), and that depolarization of Em is associated with low IVF success rate in subfertile men (Brown et al., 2016).

Hyperpolarization During Capacitation

Hyperpolarization of the Em occurs when there is an increase in the concentration of net negative charges in the intracellular compartment. Membrane hyperpolarization during capacitation has been demonstrated in murine, bovine, equine, and human sperm (Zeng et al., 1995; Hernández-González et al., 2007; Escoffier et al., 2012; López-González et al., 2014). Experiments in mouse sperm demonstrate that hyperpolarization is necessary and sufficient to prepare them for AE (De La Vega-Beltran et al., 2012).

Compared with mouse sperm, it was reported that changes in Em in human sperm are not as evident, probably due to the variability between donors and the small difference in Em values between capacitated and noncapacitated sperm. This could be because changes in the Em occur in a small fraction of human sperm population (López-González et al., 2014). Therefore, methods such as flow cytometry to distinguish membrane hyperpolarization are useful for studying this event. The reported values of resting Em in noncapacitated human sperm are approximately −40 mV (Linares-Hernández et al., 1998) and approximately −17.7 mV (Brown et al., 2016). In capacitated human sperm, these values shift to approximately −58 mV (Patrat et al., 2002) and approximately −22.7 mV (Brown et al., 2016). The differences between these values may be methodological: although Brown et al. inferred resting Em from reversal potential obtained by whole cell patch clamping, Linares-Hernández and Patrat used fluorimetry. In mouse sperm, the resting Em of noncapacitated sperm is approximately −35 to −45 mV, and after capacitation, this value changes to approximately −65 mV (Espinosa and Darszon, 1995; Zeng et al., 1995; Muñoz-Garay et al., 2001; Demarco et al., 2003; Hernández-González et al., 2006; Santi et al., 2010; De La Vega-Beltran et al., 2012).

Regulation of Em

It was reported that hyperpolarization of the plasma membrane occurs downstream of cAMP elevation in mouse and human sperm (Martínez-López et al., 2009; Escoffier et al., 2015; Puga Molina et al., 2017). In mouse sperm, it was suggested that cSrc is activated downstream of PKA and modulates the sperm-specific K^+ channel Slo3 (Stival et al., 2015). This possibility remains to be studied in human sperm where the PKA-dependent activation of CFTR also contributes to the regulation of Em (Puga Molina et al., 2017). In human sperm, then, it is postulated that hyperpolarization may occur as a result of either the increase of K^+ permeability and/or the reduction of Na^+ permeability (Santi et al., 2010).

K^+ Channels SLO1 and SLO3

In mammalian sperm, it has been shown that hyperpolarization associated with capacitation is inhibited using blockers such as Ba^{2+}, which inhibits the inward rectifying K^+ currents, and the sulfonylureas (tolbutamide and glibenclamide) that inhibit K^+ channels regulated by ATP (Muñoz-Garay et al., 2001; Acevedo et al., 2006). In addition, it has been reported that the physiological hyperpolarization induced during capacitation in mouse sperm does not depend on the reduction of Na^+ permeability, but on the increase in K^+ permeability (Chávez et al., 2013). Two members of the Slo family of K^+ channels were proposed to have a role in this phenomenon: Slo1, which is highly conserved and ubiquitously expressed, and sperm-specific Slo3, which is present only in mammals and has low sequence conservation (Santi et al., 2010; Miller et al., 2015). As K^+ currents in mouse sperm depends on the increase in pHi and Slo3 is activated by alkalinization of the cytoplasm, this channel was proposed to be a key player of Em changes in these species (Schreiber et al., 1998; Santi et al., 2010; Zeng et al., 2011). Taking

into account that male KO mice for SLO3 are infertile (Santi et al., 2010; Zeng et al., 2011), it is suggested that SLO3 would be the main channel that mediates hyperpolarization in this species.

In human sperm, the participation of K^+ channels is not as well established as it is in mouse sperm (Kaupp and Strünker, 2016). Human sperm K^+ current (KSper) is less sensitive to pH and more sensitive to $[Ca^{2+}]_i$ (Mannowetz et al., 2013), and is inhibited by progesterone (Mannowetz et al., 2013; Brenker et al., 2014). In human sperm, SLO1 was detected by Western blotting (Mannowetz et al., 2013), whereas SLO3 was detected by Western blotting and mass spectrometry (Brenker et al., 2014; López-González et al., 2014). From the biophysical and pharmacological properties that were described with respect to KSper, the currents seem to resemble SLO1 as it is a K^+ channel activated by Ca^{2+} (Mannowetz et al., 2013). However, recently, it was suggested that capacitated human sperm possess a different type of SLO channel (Mansell et al., 2014) or even a version of SLO3 that is sensitive to Ca^{2+} and weakly dependent on pH (Brenker et al., 2014). It was also proposed that *SLO3* is rapidly evolving in humans, and the variant allele C382R, which is present at a high frequency in the human population, has enhanced apparent Ca^{2+} and pH sensitivities (Geng et al., 2017).

Regarding the participation of SLO3 and SLO1 in male fertility, Brown and coworkers found in a recent study, where 81 subfertile patients undergoing IVF were investigated, that outward K^+ conductance from these patients was not significantly different from donor sperm. In approximately 10% of the patients, either a negligible outward conductance or an enhanced inward current causing depolarization of Em was observed. Interestingly, in this study, sperm from one patient with low fertilization rate at IVF had very low outward K^+ conductance and presented depolarized Em. However, no genetic abnormalities in *SLO1*, *SLO3*, or *LRCC52* genes were found in this patient (Brown et al., 2016).

Regarding the role of SLO1 and SLO3 during capacitation, López-González and coworkers have shown that human sperm capacitated in the presence of inhibitors of both SLO1 and SLO3 have a similar Em to that of sperm incubated in a noncapacitating medium (López-González et al., 2014). Therefore, further investigation is needed to establish the participation of SLO1 and SLO3 in the regulation of Em in human sperm.

Na^+ Transport

Previous evidence indicates that Na^+ participates in establishing the resting Em in mouse sperm (Demarco et al., 2003; Hernández-González et al., 2006). It was also observed in mouse sperm that in an Na^+-free medium, the addition of this cation induces a rapid depolarization of the Em, which is blocked by EIPA, an analog of amiloride (Escoffier et al., 2012). Both amiloride and EIPA are pharmacological inhibitors of the Na^+ epithelial channels (ENaC).

ENaC is an heteromultimeric channel composed of the combination of α, β, γ, or δ subunits (de la Rosa et al., 2000; Kellenberger and Schild, 2002). The activity of ENaC channels is closely associated with CFTR, as this channel negatively regulates ENaC (Kunzelmann, 2003; Guggino and Stanton, 2006; Berdiev et al., 2009). In humans, ENaC dysfunction can cause cystic fibrosis among other diseases (Fambrough and Benos, 1999; Snyder, 2002).

In mouse sperm, ENaC-α and ENaC-δ subunits were detected by Western blotting (Hernández-González et al., 2006). In addition, patch-clamp records in testicular sperm detected an amiloride-sensitive component that is in agreement with the presence of ENaC (Martínez-López et al., 2009). In humans, it was demonstrated the presence of the ENaC-δ subunit in the testis (Waldmann et al., 1995) of ENaC-α in the mid-piece of the sperm flagellum by immunocytochemistry and Western blotting (Kong et al., 2009) and the expression of ENaC-β by Western blotting in human sperm (Puga Molina et al., 2018). Interestingly, Kong and coworkers showed that the treatment of human sperm with EIPA improves sperm motility in both healthy donors and asthenozoospermic patients. Puga Molina and coworkers also showed that HCO_3^- produced a rapid membrane hyperpolarization mediated by CFTR-dependent closure of ENaC channels, which contribute to the regulation of Em during capacitation. In addition, the same authors showed that 1 μM amiloride produces hyperpolarization of the human sperm plasma membrane and decreases $[Na^+]i$ (Puga Molina et al., 2018).

As mentioned above, previous evidence indicates that mouse and human sperm display a HCO_3^- uptake through electrogenic Na^+/HCO_3^- cotransporters (NBC), resulting in a rapid hyperpolarization (Demarco et al., 2003; Puga Molina et al., 2018).

Na^+/K^+ ATPase

The Na^+/K^+ pump is an electrogenic transmembrane ATPase that catalyzes Na^+ and K^+ transport by using the energy derived from ATP hydrolysis (Skou, 1957). The proper function of Na^+/K^+ ATPase is of vital importance in every cell because it generates the electrochemical gradient for Na^+ and K^+ across the plasma membrane (Morth et al., 2007). Na^+/K^+ ATPase is an oligomer formed by two subunits: a catalytic α-subunit that contains the sites for binding of Na^+, K^+, ATP, and ouabain (an inhibitor of the pump) (Jorgensen et al., 2003), and a β-subunit that is required for guiding the α-subunit to the membrane and for occlusion of the K^+ ions (Lutsenko and Kaplan, 1993; Geering, 2001). There are several Na^+/K^+ ATPase isoenzymes due to the fact that there are 4 different α-subunits (α1, α2, α3, and α4) and 3 different β-subunits (β1, β2, and β3) (Blanco and Mercer, 1998). Each combination is cell- and tissue-specific and displays a particular pattern of expression (Jewell et al., 1992).

The α4-subunit is the most divergent (Woo et al., 2000; Clausen et al., 2016) and is specifically expressed in germ cells of rat, mouse, and human mature sperm (Woo et al., 2000; Sanchez et al., 2006; McDermott et al., 2012; Mcdermott et al., 2015). This isoform is more sensitive to ouabain (Blanco and Mercer, 1998; Sanchez et al., 2006) and is twofold more active than the Na^+/K^+ ATPase α1-subunit; which is also expressed in mature rat and human sperm (Shamraj and Lingrel, 1994; Wagoner et al., 2005; Sanchez et al., 2006). Jimenez and coworkers also reported that KO mice that lack α4 are completely sterile. This deletion hindered sperm motility and hyperactivation (Jimenez et al., 2012). Sperm from α4 null-mice showed a depolarized Em

due to high $[Na^+]_i$. The fact that the α1 was unable to compensate the absence of α4 demonstrates the absolute requirement of the α4 Na^+/K^+ ATPase subunit in mouse sperm fertility (Jimenez et al., 2012). Jimenez and coworkers suggested that the ion gradients maintained by α4 are important for controlling sperm cytoplasmic ion homeostasis because depolarization of the sperm plasma membrane and $[Na^+]$i levels are required for sperm motility during sperm capacitation (Jimenez et al., 2012).

It has been reported in rats that during capacitation, α4 Na^+/K^+ ATPase increases its activity, resulting in a rise in $[K^+]_i$, a decrease in $[Na^+]_i$, and consumption of ATP (Jimenez et al., 2012). In the same study, the authors showed a higher abundance of α4 in the plasma membrane after the occurrence of capacitation.

Human sperm treated with ouabain showed an $[Na^+]$i increase at concentrations that inhibit Na^+/K^+ ATPase α1 and α4 (Puga Molina et al., 2018) and a decrease in sperm motility at concentrations that selectively inhibited Na^+/K^+ ATPase α4 (Sanchez et al., 2006). McDermott and coworkers studied the function of human Na^+/K^+ ATPase α4 in transgenic mice and found higher levels of hyperactive motility compared to wild-type mice, without any alteration in Em or AE (Mcdermott et al., 2015). Therefore, α4 Na^+/K^+ ATPase is a very interesting target for male contraception due to its specific localization in sperm and its effects on motility, and its ability to regulate intracellular Na^+ and K^+.

CALCIUM REQUIREMENTS DURING CAPACITATION

Sperm functional changes that take place during capacitation depend on a combination of sequential and concomitant signaling processes (Visconti et al., 2011), which includes complex signaling cascades where intracellular Ca^{2+} plays a central role. There are some reports where Ca^{2+} levels were measured and showed an increase in intracellular Ca^{2+} concentration ($[Ca^{2+}]_i$) during mammalian sperm capacitation (Jai et al., 1978; Coronel and Lardy, 1987; White and Aitken, 1989; Ruknudin and Silver, 1990; Zhou et al., 1990; Baldi et al., 1991; Cohen et al., 2014; Luque et al., 2018). Moreover, the importance of this ion in the regulation of sperm motility, hyperactivation, and AE has been demonstrated through several pharmacological and genetic loss-of-function approaches (Suarez and Dai, 1995; Ho and Suarez, 2001; Darszon et al., 2011).

It has been described that Ca^{2+} can directly bind to membrane phospholipids and to numerous enzymes, modifying the membrane properties and enzymatic activity. This ion may also bind to calmodulin (CaM), and CaM antagonists have been shown to inhibit certain aspects of sperm function, as hyperactivated motility (Si and Olds-Clarke, 2000). Ca^{2+} binding to CaM causes conformational changes, and this complex modulates the activity of adenylyl cyclases (Gross et al., 1987), phosphatases (Tash et al., 1988; Rusnak and Mertz, 2000), phosphodiesterases (Wasco and Orr, 1984), and protein kinases (Hook and Means, 2001; Marín-Briggiler, 2005). Interestingly, testis specific ADCY10 is Ca^{2+}-dependent but CaM-independent (Jaiswal and Conti, 2003; Litvin et al., 2003), suggesting that Ca^{2+} regulates capacitation through multiple pathways. In particular, it has been shown in sperm of marine invertebrates that rises in $[Ca^{2+}]_i$ modulate the sperm swimming behavior by changing the flagellar beat pattern through Ca^{2+}-sensing proteins, calaxins (Mizuno et al., 2009, 2012). Dynein activity is inhibited within the axoneme by Ca^{2+}-bound calaxins, resulting in the high-amplitude asymmetric flagellar bending—typical of hyperactivated motility (Shiba et al., 2008).

As detailed above, one of the first events that triggers sperm capacitation is the activation of a cAMP pathway (Buffone et al., 2014b). At ejaculation, human sperm interact with higher HCO_3^- and Ca^{2+} concentrations present in the seminal fluid (Homonnai et al., 1978; Okamura et al., 1985). This causes an increase in cAMP levels by the opposing activities of the ADCY10 and PDE that stimulates PKA-dependent phosphorylation of proteins in Ser/Thr residues (Osheroff et al., 1999; Visconti et al., 2011; Battistone et al., 2013). Evidence in mouse and human sperm has shown that PKA-dependent phosphorylation is also regulated by the Src family kinase (SFK) inactivation of Ser/Thr phosphatases (Krapf et al., 2010; Battistone et al., 2013). Phosphorylation of PKA substrates leads to pY in sperm of all mammalian species studied (Visconti et al., 1995b; Leclerc et al., 1996; Galantino-Homer et al., 1997; Osheroff et al., 1999). Genetic loss-of-function experiments in mice demonstrated the essential role of proteins involved in the cAMP pathway in sperm capacitation and fertilization (Hess et al., 2005). On the other hand, mouse sperm exposed to the Ca^{2+} ionophore A23187 are able to develop hyperactivation, undergo AE, and acquire fertilizing ability even when the cAMP pathway is completely abolished (Tateno et al., 2013).

Ca^{2+} requirements during mammalian sperm capacitation have been widely studied in the murine and human models. Incubation of mouse sperm in the absence of added extracellular Ca^{2+} prevented the capacitation-associated increase in pY (Visconti et al., 1995a). However, the addition of EGTA to further lower the extracellular Ca^{2+} (medium without added Ca^{2+} still contains micromolar concentrations of this cation) promotes a strong increase in pY. A similar effect was also observed when adding CaM antagonists or calcineurin inhibitors (Navarrete et al., 2015). These results led the authors to propose that Ca^{2+} modulates mouse sperm cAMP and pY pathways in a biphasic manner, having both positive and negative roles, and that some of its effects are mediated by CaM (Navarrete et al., 2015). Recent studies have shown that in mouse sperm, the tyrosine kinase FER is involved in the capacitation-associated increase in pY (Alvau et al., 2016). Interestingly, human sperm display a different type of Ca^{2+} regulation during capacitation. Several reports have shown that extracellular Ca^{2+} negatively modulates phosphorylation on tyrosine residues, as human sperm incubated in a medium without added Ca^{2+} displayed increased pY compared to those incubated in complete medium (Carrera et al., 1996; Leclerc and Goupil, 2002; Marín-Briggiler et al., 2003; Baker et al., 2004; Battistone et al., 2014). The lack of added Ca^{2+} in the medium would lead to an increased tyrosine kinase activity through higher levels of ATP (Baker et al., 2004). In human sperm, lowering extracellular $[Ca^{2+}]$

was accompanied by a decrease in both ADCY10 activity and cAMP levels (Jaiswal and Conti, 2003; Torres-Flores et al., 2011), without affecting PDE1 activity (Lefièvre et al., 2002) and PKA-mediated phosphorylation (Battistone et al., 2014). Inhibition of CaM also increased pY with no changes in PKA-mediated phosphorylation, supporting the role of CaM in the increase in pY observed without adding Ca^{2+} to the medium (Battistone et al., 2014). As previously mentioned, PYK2 has been identified as the Ca^{2+}-dependent kinase involved in human sperm pY downstream PKA activation (Battistone et al., 2014).

Regarding Ca^{2+} requirements to maintain human sperm function *in vitro*, it has been reported that 0.22 mM Ca^{2+} is sufficient for the development of pY and hyperactivated motility, whereas more than 0.58 mM of this cation is necessary to maintain follicular fluid-induced AE and sperm–ZP interaction (Marín-Briggiler et al., 2003). Therefore, transit through the female tract affords sperm to be modified by changes in the ionic environment that are not available in *in vitro* models. Moreover, there is evidence indicating that Ca^{2+} ions can be replaced by Sr^{2+} in maintaining human sperm capacitation-related events (Marín-Briggiler et al., 1999). These results would indicate that at least *in vitro*, different sperm events have specific Ca^{2+} requirements. Such information can be used for the development of culture conditions that would allow the dissociation of these events of the fertilization process.

Calcium Transport Systems in Sperm

Some aspects of sperm physiology depend on the maintenance and regulation of $[Ca^{2+}]_i$, which involves a range of pumps and channels at the plasma membrane or intracellular stores that import, export, and/or sequester Ca^{2+} ions [reviewed by (Jimenez-Gonzalez et al., 2006; Clapham, 2007; Darszon et al., 2007, 2011; Correia et al., 2015)].

Two Ca^{2+} transport systems have been identified in mammalian sperm. The first one involves Ca^{2+} efflux through the plasma membrane Ca^{2+} ATPase (PMCA) and the Na^+/Ca^{2+}-exchanger (NCX), which pump Ca^{2+} out of the cell or into intracellular Ca^{2+} stores (Michelangeli et al., 2005). PMCA, localized in the principal piece of the flagellum of mouse sperm, is relevant for sperm function as its ablation alters sperm motility. Sperm from *PMCA4b* KO mice failed to develop hyperactivated motility and therefore are sterile (Okunade et al., 2004; Schuh et al., 2004). Mitochondrial abnormalities found in PMCA4-deficient sperm (Okunade et al., 2004) suggest Ca^{2+} overload due to defective Ca^{2+} extrusion. NCX is present in the plasma membrane of mammalian sperm (Babcock and Pfeiffer, 1987) and is thought to be of great importance for the regulation of Ca^{2+} homeostasis (Reddy et al., 2001; Su and Vacquier, 2002). Pharmacological inhibition of NCX provokes an increase in $[Ca^{2+}]_i$ and a significant reduction of human sperm motility (Krasznai et al., 2006).

The second Ca^{2+} transport system is related to Ca^{2+} influx and involves mainly the sperm-specific Ca^{2+} channel CatSper (see below). Other Ca^{2+} plasma membrane channels have also been identified in spermatogenic and sperm cells. Several voltage-gated Ca^{2+} (Ca_v) channel subunits have been detected in the head and flagellum of mammalian sperm, and their activity has been assessed in both germ cells and sperm (Arnoult et al., 1996, 1999; Serrano et al., 1999; Westenbroek and Babcock, 1999; Wennemuth et al., 2000; Sakata et al., 2002; Cohen et al., 2014). In particular, animals devoid of the α_{1E} subunit of the $Ca_v2.3$ channel show aberrant sperm motility (Sakata et al., 2002) and reduced litter sizes and IVF success, mainly due to impaired ability to undergo AE (Cohen et al., 2014). It has been suggested that the interaction of sperm $Ca_v2.3$ channel subunits with membrane G_{M1} regulates Ca^{2+} currents and the occurrence of AE (Cohen et al., 2014). In addition, T-type Ca_v3 channel subunits have been found in the head and flagellum of mouse and human sperm; however, drugs that inhibit these channels do not affect human sperm motility (Treviño et al., 2004). Cyclic nucleotide-gated channels (CNG), permeable to Ca^{2+}, have also been described in bovine testis and sperm and suggested to be involved in sperm motility (Wiesner et al., 1998). The A subunit was observed along the flagellum, whereas the short B subunit is restricted to the principal piece. Furthermore, there is evidence showing that CNG channels act as a Ca^{2+} entry pathway being more responsive to cGMP rather than to cAMP (Wiesner et al., 1998). The A3 and B1 subunits are present in the flagellum of mouse sperm, but the A3 null mice are fertile (Kaupp and Seifert, 2002), questioning the relevance of these channels in sperm physiology. Moreover, some members of the transient receptor potential channel (TRPC) family have been found in the flagella of mouse (transient receptor potential canonical; TRPC1 and C3) (Treviño et al., 2001) and human sperm (TRPC1, C3, C4, and C6), and their inhibition abolished human sperm motility (Castellano et al., 2003). More recently, store-operated channel proteins (ORAI) and their activators, i.e., STIM, have been shown to interact with TRPC and regulate sperm function (Darszon et al., 2012).

Sperm intracellular Ca^{2+} can be exchanged to or from internal stores localized in the acrosome, as well as in the neck (redundant nuclear envelope, RNE) by inositol triphosphate and ryanodine receptors (IP_3R and RyR, respectively) (Darszon et al., 2011; Visconti et al., 2011). In human sperm, the presence of the RyR was determined by several techniques and it was located mainly in the neck region and very rarely in the acrosome (Harper et al., 2004; Lefièvre et al., 2007), whereas the IP3 receptors were found in the neck region and in the acrosome (Dragileva et al., 1999; Kuroda et al., 1999; Rossato et al., 2001). In the acrosome, it was demonstrated that Ca^{2+} is mobilized through the IP-3-sensitive channel (De Blas et al., 2002; Branham et al., 2009; Lopez et al., 2012), and it is proposed that the Ca^{2+} influx by these channels is dependent on HCO_3^- and involves EPAC activity. It has been shown that Ca^{2+} release from the reservoirs is a necessary event for the AE (De Blas et al., 2005), and that hyperactivated motility depends on the mobilization of intracellular Ca^{2+} by IP_3R activation (Alasmari et al., 2013), and chemotaxis in response to progesterone needs Ca^{2+} mobilization from intracellular stores followed by the activation of TRPC (Teves et al., 2009). In addition, two Ca^{2+} pumps were identified and located in human sperm: sarcoplasmic-endoplasmic reticulum Ca^{2+} ATPase (SERCA) (Lawson et al., 2007) and secretory pathway Ca^{2+} ATPases (SPCA) (Harper et al., 2005). Both are

sensitive to thapsigargin at different concentrations (Thastrup et al., 1990; Rossato et al., 2001; Harper et al., 2005). SERCA 2 has been localized in the acrosome and mid-piece regions of mammalian species, including human, and it has been suggested to participate in Ca^{2+} sequestration in internal stores during sperm capacitation (Lawson et al., 2007).

CatSper Channel: Structure and Regulation

Despite a large body of evidence indicating the presence of multiple Ca^{2+} channels in human sperm, their activity has not been totally elucidated. The advent of sperm electrophysiology (Kirichok et al., 2006; Lishko et al., 2010) allowed the characterization of Ca^{2+} currents through CatSper channels. This channel complex is localized in the sperm flagellum and comprises four homologous α subunits (CatSper 1–4) (Navarro et al., 2008; Kirichok et al., 2011) and auxiliary subunits: CatSper β, CatSper ϫ, and CatSper δ (Liu et al., 2007; Wang et al., 2009; Chung et al., 2011). Deficiency of any subunit affects the expression of all the other subunits and is detrimental to male fertility (Qi et al., 2007). Recently two new auxiliary subunits have been described: CatSper ξ and CatSper ζ (Chung et al., 2017). Evidence from KO mice has shown that CatSper is essential for hyperactivation and fertilization (Ren et al., 2001; Quill et al., 2003). CatSper-KO sperm are unable to migrate efficiently *in vivo* (Ho et al., 2009; Chung et al., 2014) and penetrate the egg cumulus (Chung et al., 2017) and the ZP (Ren et al., 2001). However, a transient exposure to Ca^{2+} ionophore A23187 enables *in vitro* fertilization of these as well as other KO sterile mice models (Navarrete et al., 2016). In contrast to what occurs in wild-type sperm, CatSper1 KO undergoes PKA activation and a remarkable increase in pY even in nominal zero Ca^{2+} media, suggesting that CatSper transports the Ca^{2+} involved in the regulation of the cAMP-PKA-dependent pathway required for sperm capacitation (Navarrete et al., 2015). Moreover, evidence in the human has shown that point mutations within the CatSper1 gene as well as deletion of the CatSper2 gene are related to male infertility (Avidan et al., 2003; Zhang et al., 2007; Hildebrand et al., 2010). In a CatSper2-deficient infertile patient, no appreciable CatSper current was observed, which is caused by the complete lack of other CatSper complex members (Smith et al., 2013).

Recent groundbreaking work from Chung and coworkers using super-resolution microscopy (STORM) in the mouse model showed that CatSper distributes longitudinally following four backbone lines, which are localized in the plasma membrane of the principal piece, close to the fibrous sheath (Chung et al., 2014, 2017). Similarly, it has been reported that human CatSper ξ is arranged in four domains along the flagellum (Chung et al., 2017). Together with CatSper, other signaling molecules display a similar spatial distribution along the principal piece, which reveals a complex organization of signaling pathways in the sperm flagellum that focuses pY in time and space (Chung et al., 2014). In addition, a variation in subflagellar localization of CatSper domains in capacitated sperm has been described by 3D STORM (Chung et al., 2014). It has been reported that approximately 30% of sperm presented a quadrilateral CatSper1 domain organization and they were able to display hyperactivated motility and pY (Chung et al., 2014). This is consistent with the observations made by different groups that only a subpopulation of sperm achieved hyperactivation upon capacitation (Kulanand and Shivaji, 2001; Buffone et al., 2009a; Goodson et al., 2011). However, evidence in human sperm suggests that the development of hyperactivation does not directly depend on CatSper activation, but on the release of stored Ca^{2+} at the sperm neck (Alasmari et al., 2013). It has been proposed that CatSper channels would rather be involved in intracellular Ca^{2+} stores mobilization during sperm capacitation, affecting hyperactivated motility indirectly (Alasmari et al., 2013).

CatSper activity was directly recorded in 2006 using the patch-clamp method (Kirichok et al., 2006). Murine CatSper current ($I_{CatSper}$) is weakly voltage dependent (Kirichok et al., 2006), which can be attributed to heterogeneity in the arginine and lysine compositions of the putative voltage sensor domains from each CatSper α subunits. Mice devoid of any CatSper α subunits or the CatSper δ do not display the $I_{CatSper}$ and, as previously mentioned, are all infertile (Carlson et al., 2003, 2005; Kirichok et al., 2006; Liu et al., 2007; Qi et al., 2007; Wang et al., 2009; Chung et al., 2011). Human $I_{CatSper}$ was recorded in 2010 (Lishko and Kirichok, 2010; Lishko et al., 2010), and the comparison with mouse CatSper currents revealed important differences in this channel regulation and function. The human CatSper channel is slightly more voltage dependent in comparison to the mice one. Although intracellular alkalinization allows the opening of mice CatSper channels, this is not sufficient for human sperm (Kirichok et al., 2006; Lishko et al., 2010, 2011). The highly enriched histidine composition of the N-termini of both CatSper1 proteins is thought to be involved in the pH sensitivity of the channel, which made this difference totally unexpected.

In addition to voltage and pHi, mammalian CatSper is also controlled by numerous ligands present in the oviductal fluid as well as different synthetic chemicals (Kirichok et al., 2006; Lishko et al., 2010, 2011; Strünker et al., 2011; Brenker et al., 2012; Tavares et al., 2013). In humans but not mice, progesterone (Lishko et al., 2011; Strünker et al., 2011) activates CatSper via binding to the serine hydrolase ABHD2 (α/β hydrolase domain–containing protein 2) (Miller et al., 2016; Mannowetz et al., 2017). It has been shown that at rest the human CatSper channel is inhibited by the endocannabinoid 2-arachidonoylglycerol (2-AG); after progesterone binding, ABHD2 degrades 2-AG, relieving CatSper inhibition (Miller et al., 2016). The Ca^{2+} influx mediated by progesterone has been involved in sperm capacitation, chemotaxis, hyperactivation, and AE (Harper et al., 2003; Oren-Benaroya et al., 2008; Publicover et al., 2008), but the participation of CatSper has been unequivocally demonstrated in hyperactivation. Prostaglandins also activate the human CatSper channel, but independent of the ABHD2 mechanism (Miller et al., 2016). The prostaglandins-induced Ca^{2+} influx evokes AE and increases motility (Aitken and Kelly, 1985; Schaefer et al., 1998). Both progesterone and prostaglandin modulation is suggested to be restricted to human and primate sperm (Lishko et al., 2011) and do not involve classical nuclear receptors or G

protein-coupled receptors (GPCRs) (Lishko et al., 2011; Strünker et al., 2011).

More recently, patch-clamp recordings from human sperm revealed that the neurosteroid pregnenolone sulfate exerted similar effects as progesterone on CatSper currents (Mannowetz et al., 2017; Brenker et al., 2018). CatSper-deficient patients were described as infertile (Avidan et al., 2003; Zhang et al., 2007). Further studies showed that these sperm did not produce any progesterone (Smith et al., 2013) nor pregnenolone sulfate-activated currents (Brenker et al., 2018).

Nowadays, there are some controversies about the effects of testosterone, estrogen, and hydrocortisone on CatSper currents. Results from Mannowetz and coworkers revealed that they abolish CatSper activation by progesterone but these steroids do not activate CatSper themselves (Mannowetz et al., 2017). On the other hand, more recent evidence from Brenker et al. determined that testosterone, hydrocortisone, and estradiol are agonists that activate CatSper (Brenker et al., 2018). These differences might be due to different conditions and experimental approaches. Further studies are needed to understand this complex regulation.

The mechanism underlying the activation of the CatSper channel by various ligands remains largely unknown. There are reports that suggest the involvement of human ß-defensin 1, a small secretory peptide with antimicrobial activities, which interacts with the sperm chemokine receptor type 6 (CCR6), triggering Ca^{2+} mobilization (Com et al., 2003; Caballero-Campo et al., 2014; Diao et al., 2014). CCR6 colocalizes and interacts with CatSper in human sperm, and both CCR6 and CatSper are required for the Ca^{2+} entry/current induced by physiological ligands DEFB1, chemokine (C-C motif) ligand 20 (CCL20), and progesterone in human sperm (Diao et al., 2017). Environmental toxins, including some endocrine disruptors, have also been shown to induce the $[Ca^{2+}]_i$ increase through CatSper activation (Tavares et al., 2013; Schiffer et al., 2014). In addition, previous reports have shown that bovine serum albumin (BSA) induces $[Ca^{2+}]_i$ influx through CatSper channel activation (Xia and Ren, 2009), because this response is absent in CatSper1 KO sperm. Lishko and coworkers suggested that the modification in the lipid content of the sperm plasma membrane may induce CatSper gating (Lishko et al., 2012), as albumin was reported to induce a Ca^{2+} influx through CatSper in mouse sperm (Xia and Ren, 2009). This possibility remains to be elucidated.

The characterization of CatSper function and regulation encounters several difficulties due to: (i) the promiscuous nature

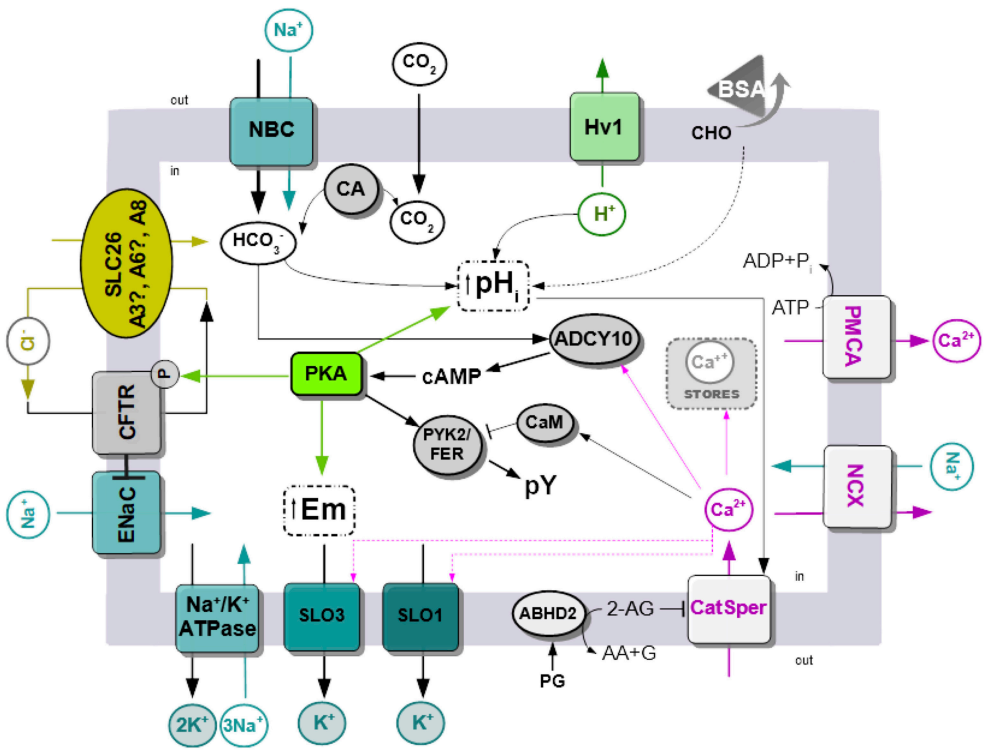

FIGURE 1 | Simplified model of signaling pathways an ion fluxes involved in human sperm capacitation. Na^+/K^+ ATPase, Na^+/K^+ pump ATPase; SLO1 and 3, sperm-specific K^+ channel 1 and 3; ENaC, epithelial Na^+ channels; CFTR, cystic fibrosis transmembrane conductance channel; SLC26, solute carrier 26, there is still no evidence of A3 and A6 is present in mature human sperm; Hv1, voltage-gated H^+ channels; BSA, bovine serum albumin; CHO, cholesterol; CA, carbonic anhydrase; PYK2/FER, proline-rich tyrosine kinase 2; ADCY10, atypical soluble adenylyl cyclase 10; EPAC, exchange protein activated by cAMP; CaM, calmodulin; CatSper, sperm-specific Ca^{2+} channel; NCX, Na^+/Ca^{2+}-exchanger; PMCA Plasma Membrane Ca^{2+} ATPase; PG, progesterone; ABDH2, α/β hydrolase domain–containing protein 2; 2-AG, 2-Arachidonoylglycerol; AA, arachidonic acid; G, glycerol.

of CatSper activation, (ii) the lack of specific antagonists, and (iii) so far, CatSper expression in heterologous systems has not been possible. Regarding the regulation of CatSper during capacitation, evidence in the mouse sperm suggests that SLO3 K^+ channels control Ca^{2+} entry through CatSper (Chávez et al., 2014). High concentrations of HCO_3^- trigger an initial change in the pHi, which activates SLO3 channels (Santi et al., 2010); the resulting membrane hyperpolarization raises pHi even more, probably through an NHE mechanism (Chávez et al., 2014). This intracellular alkalization activates the CatSper channel, which results in a very rapid $[Ca^{2+}]_i$ increase. On the other hand, Ca^{2+} rather than pHi controls KSper in human sperm (Mannowetz et al., 2013). Therefore, it was suggested that CatSper might be placed upstream SLO1/3 (Kaupp and Strünker, 2016). In this regard, a recent report indicated that certain patients show impaired K^+ conductance and abnormal resting Em, but normal resting $[Ca^{2+}]_i$ and progesterone-induced $[Ca^{2+}]_i$ responses similar to those of donor sperm, which suggest unaltered CatSper function (Brown et al., 2016). However, further studies are needed to determine the relationship among sperm ion channels and to establish the similarities and differences between mouse and human sperm.

FINAL REMARKS

This review is focused on the principal molecular mechanisms that govern human sperm capacitation with particular emphasis in comparing all the reported evidence with the mouse model.

The data presented in this review are summarized in **Figure 1**. Sperm are exposed to higher HCO_3^- concentration at the time of ejaculation and during their transit through the female reproductive tract. In addition, removal of sperm cholesterol from the plasma membrane to acceptors present in the uterus and fallopian tubes, such as albumin, results in biophysical modification of the plasma membrane. The best characterized change is the increase in membrane fluidity. The initial HCO_3^- transport through NBC cotransporters activates ADCY10 and that in turn produce an increase in cAMP concentration, leading to the activation of PKA. Phosphorylation by PKA is essential for CFTR activity, and together with other Cl^-/HCO_3^- cotransporters (SLC A3/6/8), it produces a sustained increase in HCO_3^-. Other possible sources of HCO_3^- may be related to the action of carbonic anhydrases. Activation of PKA led to protein tyrosine phosphorylation by mechanisms that are not completely elucidated, which involved the kinases PYK2/FERT. At the same time, upon contact with HCO_3^-, there is an increase in sperm intracellular pH. Human sperm alkalinization is also favored by the efflux of proton through Hv1 channels. Alkalinization and certain steroids present in the female reproductive tract such as progesterone activate CatSper channels and produce a sustained increase in $[Ca^{2+}]$i. The levels of $[Ca^{2+}]$i are also regulated by the action of exchangers and pumps such as NCX and PMCA. Activation of cAMP/PKA pathways also leads to hyperpolarization of the plasma membrane. The contribution of both the opening of K^+ channels (SLO1 and/or SLO3) and the closure of Na^+ channels, such as ENaC, was reported. In the last case, ENaC is inhibited by CFTR.

These complex molecular mechanisms built over the time using results from different groups do not take into account the following two important considerations:

i) In the mouse, the estrous (receptive period) lasts less than a day, and mating is timed to favor the encounter between sperm and eggs. However, in humans, the timing of when sperm encounter the egg is spread over a long period of time (2–3 days), and concomitantly, human sperm require long incubation time (more than 3 h) to undergo capacitation-related events. In this regard, it was recently demonstrated that the timing of human sperm capacitation (as evaluated with the novel Cap-score™) is reproducible within each individual but varies among men (Ostermeier et al., 2018). The Cap-Score™ was defined as the percentage of sperm having G_{M1} localization patterns consistent with capacitation and was shown to be a good indicator of male fertility (Cardona et al., 2017). The reasons for such variability are unknown but they may be related with the fact that human semen samples are not homogeneous. They are composed of different subpopulations of sperm with different functional features (Buffone et al., 2004).

ii) All the *in vitro* experiments conducted so far to study capacitation were performed in the absence of the periovulatory female reproductive tract. For example, the occurrence of AE was long enough to occur upon sperm binding to the ZP. However, recent evidence from different laboratories demonstrated *in vivo* that mouse sperm undergo AE prior to encountering the cumulus-oocyte complexes in the upper segments of the oviduct (Hino et al., 2016; La Spina et al., 2016; Muro et al., 2016). However, this is not the case for human sperm because *in vivo* experimentation using human sperm is virtually impossible nowadays for ethical consideration. Therefore, immediate translation of previous capacitation investigations from mouse to human is questionable and must be analyzed with caution. In addition, the high success rates of ICSI also had a negative impact on basic reproductive studies in both humans and mice. However, this is not the case for artificial insemination where pregnancy rates are really low. The understanding of molecular mechanisms underlying human sperm capacitation would help in the treatment of patients subjected to low-complexity assisted fertilization procedures, but also, it is essential to the development of alternative contraceptive strategies.

AUTHOR CONTRIBUTIONS

MB defined the topics. LP, GL, PB, CM-B, and MB wrote the paper. All authors discussed the results and implications and commented on the manuscript at all stages.

FUNDING

This work was supported by Agencia Nacional de Promoción Científica y Tecnológica (PICT 2015−2294).

ACKNOWLEDGMENTS

We would like to thank Fulbright Scholar Program and Rene Baron, Fortabat and Williams Foundations.

REFERENCES

Acevedo, J. J., Mendoza-Lujambio, I., de la Vega-Beltrán, J. L., Trevino, C. L., Felix, R., and Darszon, A. (2006). K ATP channels in mouse spermatogenic cells and sperm, and their role in capacitation. *Dev. Biol.* 289, 395–405. doi: 10.1016/j.ydbio.2005.11.002

Aguilar, J., and Reyley, M. (2005). The uterine tubal fluid: secretion, composition and biological effects. *Anim. Reprod.* 2, 91–105. doi: 10.1093/molehr/gaq056

Aitken, R. J., and Kelly, R. W. (1985). Analysis of the direct effects of prostaglandins on human sperm function. *J. Reprod. Fertil.* 73, 139–146. doi: 10.1530/jrf.0.0730139

Alasmari, W., Costello, S., Correia, J., Oxenham, S. K., Morris, J., Fernandes, L., et al. (2013). Ca2+ signals generated by CatSper and Ca2+ stores regulate different behaviors in human sperm. *J. Biol. Chem.* 288, 6248–6258. doi: 10.1074/jbc.M112.439356

Albers, J. J., Tollefson, J. H., Chen, C. H., and Steinmetz, A. (1984). Isolation and characterization of human plasma lipid transfer proteins. *Arteriosclerosis* 4, 49–58.

Ali Akbar, S., Nicolaides, K. H., and Brown, P. R. (1998). Carbonic anhydrase isoenzymes CAI and CAII in semen, decidua, chorionic villi and various fetal tissues. *Early Hum. Dev.* 51, 205–211. doi: 10.1016/S0378-3782(97)00119-9

Alvau, A., Battistone, M. A., Gervasi, M. G., Navarrete, F. A., Xu, X., Sánchez-Cárdenas, C., et al. (2016). The tyrosine kinase FER is responsible for the capacitation-associated increase in tyrosine phosphorylation in murine sperm. *Development* 143, 2325–2333. doi: 10.1242/dev.136499

Anderson, M. P., Gregory, R. J., Thompson, S., Souza, D. W., Paul, S., Mulligan, R. C., et al. (1991). Demonstration that CFTR is a chloride channel by alteration of its anion selectivity. *Science* 253, 202–205. doi: 10.1126/science.1712984

Arnoult, C., Kazam, I. G., Visconti, P. E., Kopf, G. S., Villaz, M., and Florman, H. M. (1999). Control of the low voltage-activated calcium channel of mouse sperm by egg ZP3 and by membrane hyperpolarization during capacitation. *Proc. Natl. Acad. Sci. U.S.A.* 96, 6757–6762. doi: 10.1073/pnas.96.12.6757

Arnoult, C., Zeng, Y., and Florman, H. M. (1996). ZP3-dependent activation of sperm cation channels regulates acrosomal secretion during mammalian fertilization. *J. Cell Biol.* 134, 637–645. doi: 10.1083/jcb.134.3.637

Austin, C. R. (1951). Observations on the penetration of the sperm in the mammalian egg. *Aust. J. Sci. Res.* 4, 581–596. doi: 10.1071/BI9510581

Austin, C. R. (1952). The capacitation of the mammalian sperm. *Nature* 170, 326. doi: 10.1038/170326a0

Austin, C. R., and Bishop, M. W. H. (1958). Capacitation of Mammalian Spermatozoa. *Nature* 181, 851–851. doi: 10.1038/181851a0

Avidan, N., Tamary, H., Dgany, O., Cattan, D., Pariente, A., Thulliez, M., et al. (2003). CATSPER2, a human autosomal nonsyndromic male infertility gene. *Eur. J. Hum. Genet.* 11, 497–502. doi: 10.1038/sj.ejhg.5200991

Babcock, D. F., and Pfeiffer, D. R. (1987). Independent elevation of cytosolic [Ca2+] and pH of mammalian sperm by voltage-dependent and pH-sensitive mechanisms. *J. Biol. Chem.* 262, 15041–15047.

Baker, M. A., Hetherington, L., Ecroyd, H., Roman, S. D., and Aitken, R. J. (2004). Analysis of the mechanism by which calcium negatively regulates the tyrosine phosphorylation cascade associated with sperm capacitation. *J. Cell Sci.* 117, 211–222. doi: 10.1242/jcs.00842

Baldi, E., Casano, R., Falsetti, C., Krausz, C., Maggi, M., and Forti, G. (1991). Intracellular calcium accumulation and responsiveness to progesterone in capacitating human spermatozoa. *J. Androl.* 12, 323–330.

Battistone, M. A., Alvau, A., Salicioni, A. M., Visconti, P. E., Da Ros, V. G., and Cuasnic,ú, P. S. (2014). Evidence for the involvement of proline-rich tyrosine kinase 2 in tyrosine phosphorylation downstream of protein kinase A activation during human sperm capacitation. *Mol. Hum. Reprod.* 20, 1054–1066. doi: 10.1093/molehr/gau073

Battistone, M. A., Da Ros, V. G., Salicioni, A. M., Navarrete, F. A., Krapf, D., Visconti, P. E., et al. (2013). Functional human sperm capacitation requires both bicarbonate-dependent PKA activation and down-regulation of Ser/Thr phosphatases by Src family kinases. *Mol. Hum. Reprod.* 19, 570–580. doi: 10.1093/molehr/gat033

Bear, C. E., Li, C. H., Kartner, N., Bridges, R. J., Jensen, T. J., Ramjeesingh, M., et al. (1992). Purification and functional reconstitution of the cystic fibrosis transmembrane conductance regulator (CFTR). *Cell* 68, 809–818. doi: 10.1016/0092-8674(92)90155-6

Benoff, S., Hurley, I., Cooper, G. W., Mandel, F. S., Hershlag, A., Scholl, G. M., et al. (1993). Fertilization potential *in vitro* is correlated with head-specific mannose-ligand receptor expression, acrosome status and membrane cholesterol content. *Hum. Reprod.* 8, 2155–2166. doi: 10.1093/oxfordjournals.humrep.a137997

Berdiev, B. K., Qadri, Y. J., and Benos, D. J. (2009). Assessment of the CFTR and ENaC association. *Mol. Biosyst.* 5, 123–127. doi: 10.1039/B810471A

Berger, T. K., Fußhöller, D. M., Goodwin, N., Bönigk, W., Müller, A., Dokani Khesroshahi, N., et al. (2017). Post-translational cleavage of Hv1 in human sperm tunes pH-and voltage-dependent gating. *J. Physiol.* 595, 1533–1546. doi: 10.1113/JP273189

Bergerz, H. A., Travis, S. M., and Welsh, M. J. (1993). Regulation of the cystic fibrosis transmembrane conductance regulator C1- channel by specific protein kinases and protein phosphatases. *J. Biol. Chem.* 268, 2037–2047.

Bernardino, R. L. L., Jesus, T. T. T., Martins, A. D. D., Sousa, M., Barros, A., Cavaco, J. E. E., et al. (2013). Molecular basis of bicarbonate membrane transport in the male reproductive tract. *Curr. Med. Chem.* 20, 4037–4049. doi: 10.2174/15672050113109990200

Blanco, G., and Mercer, R. W. (1998). Isozymes of the Na-K-ATPase: heterogeneity in structure, diversity in function. *Am. J. Physiol.* 275, F633–F650. doi: 10.1152/ajprenal.1998.275.5.F633

Boerke, A., Brouwers, J. F., Olkkonen, V. M., van de Lest, C. H. A., Sostaric, E., Schoevers, E. J., et al. (2013). Involvement of bicarbonate-induced radical signaling in oxysterol formation and sterol depletion of capacitating mammalian sperm during *in vitro* fertilization. *Biol. Reprod.* 88:21. doi: 10.1095/biolreprod.112.101253

Borland, R. M., Hazra, S., Biggers, J. D., and Lechene, C. P. (1977). The elemental composition of the environments of the gametes and preimplantation embryo during the initiation of pregnancy. *Biol. Reprod.* 16, 147–157. doi: 10.1095/biolreprod16.2.147

Branham, M. T., Bustos, M. A., De Blas, G. A., Rehmann, H., Zarelli, V. E. P., Treviño, C. L., et al. (2009). Epac activates the small G proteins Rap1 and Rab3A to achieve exocytosis. *J. Biol. Chem.* 284, 24825–24839. doi: 10.1074/jbc.M109.015362

Branham, M. T., Mayorga, L. S., and Tomes, C. N. (2006). Calcium-induced acrosomal exocytosis requires cAMP acting through a protein kinase A-independent, Epac-mediated pathway. *J. Biol. Chem.* 281, 8656–8666. doi: 10.1074/jbc.M508854200

Brenker, C., Goodwin, N., Weyand, I., Kashikar, N. D., Naruse, M., Krähling, M., et al. (2012). The CatSper channel: a polymodal chemosensor in human sperm. *EMBO J.* 31, 1654–1665. doi: 10.1038/emboj.2012.30

Brenker, C., Schiffer, C., Wagner, I. V., Tüttelmann, F., Röpke, A., Rennhack, A., et al. (2018). Action of steroids and plant triterpenoids on CatSper Ca 2+ channels in human sperm. *Proc. Natl. Acad. Sci. U.S.A.* 115, E344-E346. doi: 10.1073/pnas.1717929115

Brenker, C., Zhou, Y., Müller, A., Echeverry, F. A., Trötschel, C., Poetsch, A., et al. (2014). The Ca2+-activated K+ current of human sperm is mediated by Slo3. *Elife* 3:e01438. doi: 10.7554/eLife.01438

Brook, P. F., Lawry, J., Cooke, I. D., and Barratt, C. L. (1996). Measurement of intracellular pH in human spermatozoa by flow cytometry with the benzo[c]xanthene dye SNAFL-1: a novel, single excitation, dual emission, molecular probe. *Mol. Hum. Reprod.* 2, 18–25. doi: 10.1093/molehr/2.1.18

Brown, S. G., Publicover, S. J., Mansell, S. A., Lishko, P. V., Williams, H. L., Ramalingam, M., et al. (2016). Depolarization of sperm membrane potential is a common feature of men with subfertility and is associated with low fertilization rate at IVF. *Hum. Reprod.* 31, 1147–1157. doi: 10.1093/humrep/dew056

Bruckbauer, A., Dunne, P. D., James, P., Howes, E., Zhou, D., Jones, R., et al. (2010). Selective diffusion barriers separate membrane compartments. *Biophys. J.* 99, L1–L3. doi: 10.1016/j.bpj.2010.03.067

Buck, J., Sinclair, M. L., Schapal, L., Cann, M. J., and Levin, L. R. (1999). Cytosolic adenylyl cyclase defines a unique signaling molecule in mammals. *Proc. Natl. Acad. Sci. U.S.A.* 96, 79–84. doi: 10.1073/pnas.96.1.79

Buffone, M. G., Brugo-Olmedo, S., Calamera, J. C., Verstraeten, S. V., Urrutia, F., Grippo, L., et al. (2006). Decreased protein tyrosine phosphorylation and membrane fluidity in spermatozoa from infertile men with varicocele. *Mol. Reprod. Dev.* 73, 1591–1599. doi: 10.1002/mrd.20611

Buffone, M. G., Calamera, J. C., Verstraeten, S. V., and Doncel, G. F. (2005). Capacitation-associated protein tyrosine phosphorylation and membrane fluidity changes are impaired in the spermotozoa of asthenozoospermic patients. *Reproduction* 129, 697–705. doi: 10.1530/rep.1.00584

Buffone, M. G., Doncel, G. F., Calamera, J. C., and Verstraeten, S., V (2009a). Capacitation-associated changes in membrane fluidity in asthenozoospermic human spermatozoa. *Int. J. Androl.* 32, 360–375. doi:10.1111/j.1365-2605.2008.00874.x

Buffone, M. G., Doncel, G. F., Marín Briggiler, C. I., Vazquez-Levin, M. H., and Calamera, J. C. (2004). Human sperm subpopulations: relationship between functional quality and protein tyrosine phosphorylation. *Hum. Reprod.* 19, 139–146. doi: 10.1093/humrep/deh040

Buffone, M. G., Hirohashi, N., and Gerton, G. (2014a). Unresolved questions concerning mammalian sperm acrosomal exocytosis. *Biol. Reprod.* 90:112. doi: 10.1095/biolreprod.114.117911

Buffone, M. G., Rodriguez-Miranda, E., Storey, B. T., and Gerton, G. L. (2009b). Acrosomal exocytosis of mouse sperm progresses in a consistent direction in response to zona pellucida. *J. Cell. Physiol.* 220, 611–620. doi:10.1002/jcp.21781

Buffone, M. G., Verstraeten, S. V., Calamera, J. C., and Doncel, G. F. (2009c). High cholesterol content and decreased membrane fluidity in human spermatozoa are associated with protein tyrosine phosphorylation and functional deficiencies. *J. Androl.* 30, 552–558. doi: 10.2164/jandrol.108.006551

Buffone, M. G., Wertheimer, E. V., Visconti, P. E., and Krapf, D. (2014b). Central role of soluble adenylyl cyclase and cAMP in sperm physiology. *Biochim Biophys Acta* 4, 2610–2620. doi: 10.1016/j.bbadis.2014.07.013

Burton, K. A., and McKnight, G. S. (2007). PKA, germ cells, and fertility. *Physiology* 22, 40–46. doi: 10.1152/physiol.00034.2006

Caballero-Campo, P., Buffone, M. G., Benencia, F., Conejo-García, J. R., Rinaudo, P. F., and Gerton, G. L. (2014). A role for the chemokine receptor CCR6 in mammalian sperm motility and chemotaxis. *J. Cell. Physiol.* 229, 68–78. doi: 10.1002/jcp.24418

Caflisch, C. R., and DuBose, T. D. J. (1990). Direct evaluation of acidification by rat testis and epididymis: role of carbonic anhydrase. *Am. J. Physiol.* 258, E143–E150. doi: 10.1152/ajpendo.1990.258.1.E143

Calzada, L., and Tellez, J. (1997). Defective function of membrane potential (psi) on sperm of infertile men. *Arch. Androl.* 38, 151–155. doi: 10.3109/01485019708987892

Cardona, C., Neri, Q. V., Simpson, A. J., Moody, M. A., Ostermeier, G. C., Seaman, E. K., et al. (2017). Localization patterns of the ganglioside GM1 in human sperm are indicative of male fertility and independent of traditional semen measures. *Mol. Reprod. Dev.* 84, 423–435. doi: 10.1002/mrd.22803

Carlson, A. E., Quill, T. A., Westenbroek, R. E., Schuh, S. M., Hille, B., and Babcock, D. F. (2005). Identical phenotypes of CatSper1 and CatSper2 null sperm. *J. Biol. Chem.* 280, 32238–32244. doi: 10.1074/jbc.M501430200

Carlson, A. E., Westenbroek, R. E., Quill, T., Ren, D., Clapham, D. E., Hille, B., et al. (2003). CatSper1 required for evoked Ca2+ entry and control of flagellar function in sperm. *Proc. Natl. Acad. Sci. U.S.A.* 100, 14864–14868. doi: 10.1073/pnas.2536658100

Carnegie, G. K., Means, C. K., and Scott, J. D. (2009). A-kinase anchoring proteins: From protein complexes to physiology and disease. *IUBMB Life* 61, 394–406. doi: 10.1002/iub.168

Carr, D. W., and Acott, T. S. (1989). Intracellular pH regulates bovine sperm motility and protein phosphorylation. *Biol. Reprod.* 41, 907–920. doi: 10.1095/biolreprod41.5.907

Carrera, A., Moos, J., Ning, X. P., Gerton, G. L., Tesarik, J., Kopf, G. S., et al. (1996). Regulation of protein tyrosine phosphorylation in human sperm by a calcium/calmodulin-dependent mechanism: identification of a kinase anchor proteins as major substrates for tyrosine phosphorylation. *Dev. Biol.* 180, 284–296. doi: 10.1006/dbio.1996.0301

Castellano, L. E., Treviño, C. L., Rodríguez, D., Serrano, C. J., Pacheco, J., Tsutsumi, V., et al. (2003). Transient receptor potential (TRPC) channels in human sperm: Expression, cellular localization and involvement in the regulation of flagellar motility. *FEBS Lett.* 541, 69–74. doi: 10.1016/S0014-5793(03)00305-3

Chang, M. C. (1951). Fertilizing capacity of spermatozoa deposited into the fallopian tubes. *Nature* 168, 697–698. doi: 10.1038/168697b0

Chang, M. C. (1957). A detrimental effect of seminal plasma on the fertilizing capacity of sperm. *Nature* 179, 258–259. doi: 10.1038/179258a0

Chang, M. C. (1959). Fertilization of rabbit ova *in vitro*. *Nature* 184(Suppl. 7), 466–467. doi: 10.1038/184466a0

Chávez, J. C., De La Vega-Beltrá N. J. L., Escoffier, J., Visconti, P. E., Treviñ O, C. L., Darszon, A., et al. (2013). Ion permeabilities in mouse sperm reveal an external trigger for SLO3-dependent hyperpolarization. *PLoS ONE* 8:e60578. doi: 10.1371/journal.pone.0060578

Chávez, J. C., Ferreira, J. J., Butler, A., De La Vega Beltran, J. L., Trevino, C. L., Darszon, A., et al. (2014). SLO3 K+ Channels control calcium entry through CATSPER channels in sperm. *J. Biol. Chem.* 289, 32266–32275. doi: 10.1074/jbc.M114.607556

Chávez, J. C., Hernández-González, E. O., Wertheimer, E., Visconti, P. E., Darszon, A., and Treviño, C. L. (2012). Participation of the Cl–/HCO3– Exchangers SLC26A3 and SLC26A6, the Cl– Channel CFTR, and the Regulatory Factor SLC9A3R1 in Mouse Sperm Capacitation. *Biol. Reprod.* 86, 1–14. doi: 10.1095/biolreprod.111.094037

Chen, J.-H., Cai, Z., and Sheppard, D. N. (2009). Direct sensing of intracellular pH by the cystic fibrosis transmembrane conductance regulator (CFTR) Cl – channel. *J. Biol. Chem.* 284, 35495–35506. doi: 10.1074/jbc.M109.072678

Chen, Y., Cann, M. J., Litvin, T. N., Iourgenko, V., Sinclair, M. L., Levin, L. R., et al. (2000). Soluble adenylyl cyclase as an evolutionarily conserved bicarbonate sensor. *Science* 289, 625–628. doi: 10.1126/science.289.5479.625

Chung, J.-J. J., Shim, S.-H. H., Everley, R. A., Gygi, S. P., Zhuang, X., and Clapham, D. E. (2014). Structurally distinct Ca2+ signaling domains of sperm flagella orchestrate tyrosine phosphorylation and motility. *Cell* 157, 808–822. doi: 10.1016/j.cell.2014.02.056

Chung, J.-J., Miki, K., Kim, D., Shim, S.-H., Shi, H. F., Hwang, J. Y., et al. (2017). CatSperζ regulates the structural continuity of sperm Ca2+ signaling domains and is required for normal fertility. *Elife* 6:e23082. doi: 10.7554/eLife.23082

Chung, J.-J., Navarro, B., Krapivinsky, G., Krapivinsky, L., and Clapham, D. E. (2011). A novel gene required for male fertility and functional CATSPER channel formation in spermatozoa. *Nat. Commun.* 2:153. doi: 10.1038/ncomms1153

Clapham, D. E. (2007). Calcium signaling. *Cell* 131, 1047–1058. doi: 10.1016/j.cell.2007.11.028

Clausen, M. V., Nissen, P., and Poulsen, H. (2016). The α4 isoform of the Na^+, K^+ ATPase is tuned for changing extracellular environments. *FEBS J.* 283, 282–293. doi: 10.1111/febs.13567

Cohen, R., Buttke, D. E., Asano, A., Mukai, C., Nelson, J. L., Ren, D., et al. (2014). Lipid modulation of calcium flux through CaV2.3 regulates acrosome exocytosis and fertilization. *Dev. Cell* 28, 310–321. doi: 10.1016/j.devcel.2014.01.005

Com, E., Bourgeon, F., Evrard, B., Ganz, T., Colleu, D., Jégou, B., et al. (2003). Expression of antimicrobial defensins in the male reproductive tract of rats, mice, and humans. *Biol. Reprod.* 68, 95–104. doi: 10.1095/biolreprod.102.005389

Coronel, C. E., and Lardy, H. A. (1987). Characterization of Ca2+ uptake by guinea pig epididymal spermatozoa. *Biol. Reprod.* 37, 1097–1107. doi: 10.1095/biolreprod37.5.1097

Correia, J., Michelangeli, F., and Publicover, S. (2015). Regulation and roles of Ca2+ stores in human sperm. *Reproduction* 150, R56–R76. doi: 10.1530/REP-15-0102

Cross, N. L. (1996). Human seminal plasma prevents sperm from becoming acrosomally responsive to the agonist, progesterone: cholesterol is the major inhibitor. *Biol. Reprod.* 54, 138–145. doi: 10.1095/biolreprod54.1.138

Cross, N. L. (1998). Role of cholesterol in sperm capacitation. *Biol. Reprod.* 59, 7–11. doi: 10.1095/biolreprod59.1.7

Cross, N. L., and Razy-Faulkner, P. (1997). Control of human sperm intracellular pH by cholesterol and its relationship to the response of the acrosome to progesterone. *Biol. Reprod.* 56, 1169–1174. doi: 10.1095/biolreprod56.5.1169

Damkier, H. H., Nielsen, S., and Praetorius, J. (2007). Molecular expression of SLC4-derived Na+-dependent anion transporters in selected human tissues. *Am. J. Physiol. Regul. Integr. Comp. Physiol.* 293, R2136–R2146. doi: 10.1152/ajpregu.00356.2007

Darszon, A. I., Trevino, C. L., Wood, C., Galindo, B., Rodriguez-Miranda, E., Acevedo, J. J., et al. (2007). Ion channels in sperm motility and capacitation. *Soc. Reprod. Fertil. Suppl.* 65, 229–244.

Darszon, A., Labarca, P., Nishigaki, T., and Espinosa, F. (1999). Ion channels in sperm physiology. *Physiol. Rev.* 79, 481–510. doi: 10.1152/physrev.1999.79.2.481

Darszon, A., Nishigaki, T., Beltran, C., and Treviño, C. L. (2011). Calcium channels in the development, maturation, and function of spermatozoa. *Physiol. Rev.* 91, 1305–1355. doi: 10.1152/physrev.00028.2010

Darszon, A., Sánchez-Cárdenas, C., Orta, G., Sánchez-Tusie, A., a, Beltrán, C., López-González, I., et al. (2012). Are TRP channels involved in sperm development and function? *Cell Tissue Res.* 349, 749–764. doi: 10.1007/s00441-012-1397-5

David, A., Serr, D. M., and Czernobilsky, B. (1973). Chemical Composition of Human Oviduct Fluid**Presented in part at the VIIth World Congress on Fertility and Sterility, Tokyo, Japan, October 17–25, 1971. *Fertil. Steril.* 24, 435–439. doi: 10.1016/S0015-0282(16)39731-X

Davis, B. K. (1981). Timing of fertilization in mammals: sperm cholesterol/phospholipid ratio as a determinant of the capacitation interval. *Proc. Natl. Acad. Sci. U.S.A.* 78, 7560–7564. doi: 10.1073/pnas.78.12.7560

De Blas, G. A., Roggero, C. M., Tomes, C. N., and Mayorga, L. S. (2005). Dynamics of SNARE assembly and disassembly during sperm acrosomal exocytosis. *PLoS Biol.* 3:e323. doi: 10.1371/journal.pbio.0030323

De Blas, G., Michaut, M., Treviño, C. L., Tomes, C. N., Yunes, R., Darszon, A., et al. (2002). The intraacrosomal calcium pool plays a direct role in acrosomal exocytosis. *J. Biol. Chem.* 277, 49326–49331. doi: 10.1074/jbc.M208587200

De Jonge, C. (2017). Biological basis for human capacitation-revisited. *Hum. Reprod. Update* 23, 289–299. doi: 10.1093/humupd/dmw048

de la Rosa, D. A., Canessa, C. M., Fyfe, G. K., and Zhang, P. (2000). Structure and regulation of amiloride-sensitive sodium channels. *Annu. Rev. Physiol.* 62, 573–594. doi: 10.1146/annurev.physiol.62.1.573

De La Vega-Beltran, J. L., Sánchez-Cárdenas, C., Krapf, D., Hernandez-González, E. O., Wertheimer, E., Treviño, C. L., et al. (2012). Mouse sperm membrane potential hyperpolarization is necessary and sufficient to prepare sperm for the acrosome reaction. *J. Biol. Chem.* 287, 44384–44393. doi: 10.1074/jbc.M112.393488

Demarco, I. A., Espinosa, F., Edwards, J., Sosnik, J., de la Vega-Beltrán, J. L., Hockensmith, J. W., et al. (2003). Involvement of a Na+/HCO-3 cotransporter in mouse sperm capacitation. *J. Biol. Chem.* 278, 7001–7009. doi: 10.1074/jbc.M206284200

Demott, R. P., and Suarez, S. S. (1992). Hyperactivated sperm progress in the mouse oviduct. *Biol. Reprod.* 46, 779–785. doi: 10.1095/biolreprod46.5.779

Diao, R., Fok, K. L., Chen, H., Yu, M. K., Duan, Y., Chung, C. M., et al. (2014). Deficient human β-defensin 1 underlies male infertility associated with poor sperm motility and genital tract infection. *Sci. Transl. Med.* 6:249ra108. doi: 10.1126/scitranslmed.3009071

Diao, R., Wang, T., Fok, K. L., Li, X., Ruan, Y., Yu, M. K., et al. (2017). CCR6 is required for ligand-induced CatSper activation in human sperm. *Oncotarget* 8, 91445–91458. doi: 10.18632/oncotarget.20651

Dirami, T., Rode, B., Jollivet, M., Da Silva, N., Escalier, D., Gaitch, N., et al. (2013). Missense mutations in SLC26A8, encoding a sperm-specific activator of CFTR, are associated with human asthenozoospermia. *Am. J. Hum. Genet.* 92, 760–766. doi: 10.1016/j.ajhg.2013.03.016

Dragileva, E., Rubinstein, S., and Breitbart, H. (1999). Intracellular Ca2+-Mg2+-ATPase regulates calcium influx and acrosomal exocytosis in bull and ram spermatozoa. *Biol. Reprod.* 61, 1226–1234. doi: 10.1095/biolreprod61.5.1226

Edwards, R. G., Bavister, B. D., and Steptoe, P. C. (1969). Early stages of fertilization *in vitro* of human oocytes matured *in vitro*. *Nature* 221, 632–635. doi: 10.1038/221632a0

Edwards, R. G., Donahue, R. P., Baramki, T. A., and Jones, H. W. (1966). Preliminary attempts to fertilize human oocytes matured *in vitro*. *Am. J. Obstet. Gynecol.* 96, 192–200. doi: 10.1016/0002-9378(66)90315-2

Edwards, S. E., Buffone, M. G., Knee, G. R., Rossato, M., Bonanni, G., Masiero, S., et al. (2007). Effects of extracellular adenosine 5′-triphosphate on human sperm motility. *Reprod. Sci.* 14, 655–666. doi: 10.1177/1933719107306227

Eggert-Kruse, W., Köhler, A., Rohr, G., and Runnebaum, B. (1993). The pH as an important determinant of sperm-mucus interaction. *Fertil. Steril.* 59, 617–628. doi: 10.1016/S0015-0282(16)55810-5

Ehrenwald, E., Foote, R. H., and Parks, J. E. (1990). Bovine oviductal fluid components and their potential role in sperm cholesterol efflux. *Mol. Reprod. Dev.* 25, 195–204. doi: 10.1002/mrd.1080250213

Escoffier, J., Krapf, D., Navarrete, F., Darszon, A., and Visconti, P. E. (2012). Flow cytometry analysis reveals a decrease in intracellular sodium during sperm capacitation. *J. Cell Sci.* 125, 473–485. doi: 10.1242/jcs.093344

Escoffier, J., Navarrete, F., Haddad, D., Santi, C. M., Darszon, A., and Visconti, P. E. (2015). Flow cytometry analysis reveals that only a subpopulation of mouse sperm undergoes hyperpolarization during capacitation. *Biol. Reprod.* 92, 2–3. doi: 10.1095/biolreprod.114.127266

Espinosa, F., and Darszon, A. (1995). Mouse sperm membrane potential: changes induced by Ca 2+. *FEBS Lett.* 372, 119–125. doi: 10.1016/0014-5793(95)00962-9

Fambrough, D. M., and Benos, D. J. (eds.). (1999). *Amiloride-sensitive Sodium Channels: Physiology and Functional Diversity*, *Vol. 47, 1st Edn*. Cambridge, MA: Academic Press.

Ficarro, S., Chertihin, O., Westbrook, V. A., White, F., Jayes, F., Kalab, P., et al. (2003). Phosphoproteome analysis of capacitated human sperm: Evidence of tyrosine phosphorylation of a kinase-anchoring protein 3 and valosin-containing protein/p97 during capacitation. *J. Biol. Chem.* 278, 11579–11589. doi: 10.1074/jbc.M202325200

Fisch, J. D., Behr, B., and Conti, M. (1998). Enhancement of motility and acrosome reaction in human spermatozoa: Differential activation by type-specific phosphodiesterase inhibitors. *Hum. Reprod.* 13, 1248–1254. doi: 10.1093/humrep/13.5.1248

Flesch, F. M., Brouwers, J. F., Nievelstein, P. F., Verkleij, A. J., van Golde, L. M., Colenbrander, B., et al. (2001). Bicarbonate stimulated phospholipid scrambling induces cholesterol redistribution and enables cholesterol depletion in the sperm plasma membrane. *J. Cell Sci.* 114, 3543–3555.

Flesch, F. M., and Gadella, B. M. (2000). Dynamics of the mammalian sperm plasma membrane in the process of fertilization. *Biochim. Biophys. Acta* 1469, 197–235. doi: 10.1016/S0304-4157(00)00018-6

Florman, H. M., Tombes, R. M., First, N. L., and Babcock, D. F. (1989). An adhesion-associated agonist from the zona pellucida activates G protein-promoted elevations of internal Ca 2+ and pH that mediate mammalian sperm acrosomal exocytosis. *Dev. Biol.* 135, 133–146. doi: 10.1016/0012-1606(89)90164-4

Fujihara, Y., Tokuhiro, K., Muro, Y., Kondoh, G., Araki, Y., Ikawa, M., et al. (2013). Expression of TEX101, regulated by ACE, is essential for the production of fertile mouse spermatozoa. *Proc. Natl. Acad. Sci. U.S.A.* 110, 8111–8116. doi: 10.1073/pnas.1222166110

Gadella, B. M. (2008). Sperm membrane physiology and relevance for fertilization. *Anim. Reprod. Sci.* 107, 229–236. doi: 10.1016/j.anireprosci.2008.05.006

Gadella, B. M., and Harrison, R. A. (2000). The capacitating agent bicarbonate induces protein kinase A-dependent changes in phospholipid transbilayer behavior in the sperm plasma membrane. *Development* 127, 2407–2420.

Gadsby, D. C., Vergani, P., and Csanády, L. (2006). The ABC protein turned chloride channel whose failure causes cystic fibrosis. *Nature* 440, 477–483. doi: 10.1038/nature04712

Galantino-Homer, H. L., Visconti, P. E., and Kopf, G. S. (1997). Regulation of protein tyrosine phosphorylation during bovine sperm capacitation by a cyclic adenosine 3′5′-monophosphate-dependent pathway. *Biol. Reprod.* 56, 707–719.

Garbarino Azúa, D. J., Saucedo, L., Giordana, S., Magri, M. L., Buffone, M. G., Neuspiller, F., et al. (2017). Fibroblast growth factor 2 (FGF2) is present in human spermatozoa and is related with sperm motility. The use of recombinant FGF2 to improve motile sperm recovery. *Andrology* 5, 990–998. doi: 10.1111/andr.12398

Garcia, M. A., and Meizel, S. (1999). Regulation of intracellular pH in capacitated human spermatozoa by a Na+/H+ exchanger. *Mol. Reprod. Dev.* 52, 189–195.

Gatica, L. V., Guidobaldi, H. A., Montesinos, M. M., Teves, M. E., Moreno, A. I., Uñates, D. R., et al. (2013). Picomolar gradients of progesterone select functional human sperm even in subfertile samples. *Mol. Hum. Reprod.* 19, 559–569. doi: 10.1093/molehr/gat037

Gatti, J., Chevrier, C., Paquignon, M., and Dacheux, J.-L. (1993). External ionic conditions, internal pH and motility of ram and boar spermatozoa. *J. Reprod. Fertil.* 98, 439–449. doi: 10.1530/jrf.0.0980439

Geering, K. (2001). The functional role of beta subunits in oligomeric P-type ATPases. *J. Bioenerg. Biomembr.* 33, 425–438. doi: 10.1023/A:1010623724749

Geng, Y., Ferreira, J. J., Dzikunu, V., Butler, A., Lybaert, P., Yuan, P., et al. (2017). A genetic variant of the sperm-specific SLO3 K+ channel has altered pH and Ca2+ sensitivities. *J. Biol. Chem.* 292, 8978–8987. doi: 10.1074/jbc.M117.776013

Goodson, S. G., Zhang, Z., Tsuruta, J. K., Wang, W., and O'Brien, D. A. (2011). Classification of mouse sperm motility patterns using an automated multiclass support vector machines model. *Biol. Reprod.* 84, 1207–1215. doi: 10.1095/biolreprod.110.088989

Gray, M. A. (2004). Bicarbonate secretion: it takes two to tango. *Nat. Cell Biol.* 6, 292–294. doi: 10.1038/ncb0404-292

Grizard, G., Sion, B., Jouanel, P., Benoit, P., and Boucher, D. (1995). Cholesterol, phospholipids and markers of the function of the accessory sex glands in the semen of men with hypercholesterolaemia. *Int. J. Androl.* 18, 151–156. doi: 10.1111/j.1365-2605.1995.tb00404.x

Gross, M. K., Toscano, D. G., and Toscano, W. A. (1987). Calmodulin-mediated adenylate cyclase from mammalian sperm. *J. Biol. Chem.* 262, 8672–8676.

Grunze, M., Forst, B., and Deuticke, B. (1980). Dual effect of membrane cholesterol on simple and mediated transport processes in human erythrocytes. *Biochim. Biophys. Acta* 600, 860–869. doi: 10.1016/0005-2736(80)90489-7

Guggino, W. B., and Stanton, B. A. (2006). New insights into cystic fibrosis: molecular switches that regulate CFTR. *Nat. Rev. Mol. cell Biol.* 7, 426–436. doi: 10.1038/nrm1949

Guidobaldi, H. A., Teves, M. E., Uñates, D. R., Anastasía, A., and Giojalas, L. C. (2008). Progesterone from the cumulus cells is the sperm chemoattractant secreted by the rabbit oocyte cumulus complex. *PLoS ONE* 3:e3040. doi: 10.1371/journal.pone.0003040

Gunn, S. A., and Gould, T. C. (1958). Role of zinc in fertility and fecundity in the rat. *Am. J. Physiol. Content* 193, 505–508. doi: 10.1152/ajplegacy.1958.193.3.505

Hamamah, S., Magnoux, E., Royere, D., Barthelemy, C., Dacheux, J. L., and Gatti, J. L. (1996). Internal pH of human spermatozoa: effect of ions, human follicular fluid and progesterone. *Mol. Hum. Reprod.* 2, 219–224. doi: 10.1093/molehr/2.4.219

Hamner, C. E., Williams, W. L., Hamner, E., and Williams, W. L. (1964). Identification of sperm stimulating factor of rabbit oviduct fluid. *Exp. Biol. Med.* 117, 240–243. doi: 10.3181/00379727-117-29546

Harper, C., Wootton, L., Michelangeli, F., Lefièvre, L., Barratt, C., Publicover, S., et al. (2005). Secretory pathway Ca(2+)-ATPase (SPCA1) Ca(2)+ pumps, not SERCAs, regulate complex [Ca(2+)](i) signals in human spermatozoa. *J. Cell Sci.* 118, 1673–1685. doi: 10.1242/jcs.02297

Harper, C. V., Barratt, C. L. R., and Publicover, S. J. (2004). Stimulation of human spermatozoa with progesterone gradients to simulate approach to the oocyte. Induction of [Ca(2+)](i) oscillations and cyclical transitions in flagellar beating. *J. Biol. Chem.* 279, 46315–46325. doi: 10.1074/jbc.M401194200

Harper, C. V., Kirkman-Brown, J. C., Barratt, C. L. R., and Publicover, S. J. (2003). Encoding of progesterone stimulus intensity by intracellular [Ca2+] ([Ca2+]i) in human spermatozoa. *Biochem. J.* 372, 407–417. doi: 10.1042/bj20021560

Harrison, D. A., Carr, D. W., and Meizel, S. (2000). Involvement of protein kinase A and A kinase anchoring protein in the progesterone-initiated human sperm acrosome reaction. *Biol. Reprod.* 62, 811–820. doi: 10.1095/biolreprod62.3.811

Harrison, R. A. P., and Miller, N. G. A. (2000). cAMP-dependent protein kinase control of plasma membrane lipid architecture in boar sperm. *Mol. Reprod. Dev.* 55, 220–228.

Hernández-González, E. O., Sosnik, J., Edwards, J., Acevedo, J. J., Mendoza-Lujambio, I., López-González, I., et al. (2006). Sodium and epithelial sodium channels participate in the regulation of the capacitation-associated hyperpolarization in mouse sperm. *J. Biol. Chem.* 281, 5623–5633. doi: 10.1074/jbc.M508172200

Hernández-González, E. O., Treviño, C. L., Castellano, L. E., de la Vega-Beltrán, J. L., Ocampo, A. Y., Wertheimer, E., et al. (2007). Involvement of cystic fibrosis transmembrane conductance regulator in mouse sperm capacitation. *J. Biol. Chem.* 282, 24397–24406. doi: 10.1074/jbc.M701603200

Hess, K. C., Jones, B. H., Marquez, B., Chen, Y., Ord, T. S., Kamenetsky, M., et al. (2005). The "soluble" adenylyl cyclase in sperm mediates multiple signaling events required for fertilization. *Dev. Cell* 9, 249–259. doi: 10.1016/j.devcel.2005.06.007

Hihnala, S., Kujala, M., Toppari, J., Kere, J., Holmberg, C., and Höglund, P. (2006). Expression of SLC26A3, CFTR and NHE3 in the human male reproductive tract: role in male subfertility caused by congenital chloride diarrhoea. *Mol. Hum. Reprod.* 12, 107–111. doi: 10.1093/molehr/gal009

Hildebrand, M. S., Avenarius, M. R., Fellous, M., Zhang, Y., Meyer, N. C., Auer, J., et al. (2010). Genetic male infertility and mutation of CATSPER ion channels. *Eur. J. Hum. Genet.* 18, 1178–1184. doi: 10.1038/ejhg.2010.108

Hino, T., Muro, Y., Tamura-Nakano, M., Okabe, M., Tateno, H., and Yanagimachi, R. (2016). The behavior and acrosomal status of mouse spermatozoa *in vitro*, and within the oviduct during fertilization after natural mating. *Biol. Reprod.* 95, 50–50. doi: 10.1095/biolreprod.116.140400

Hinton, B. T., Pryor, J. P., Hirsh, A. V., and Setchell, B. P. (1981). The concentration of some inorganic ions and organic compounds in the luminal fluid of the human ductus deferens. *Int. J. Androl.* 4, 457–461. doi: 10.1111/j.1365-2605.1981.tb00730.x

Ho, H. C., and Suarez, S. S. (2001). Hyperactivation of mammalian spermatozoa: function and regulation. *Reproduction* 122, 519–526. doi: 10.1530/rep.0.1220519

Ho, K., Wolff, C. A., and Suarez, S. S. (2009). CatSper-null mutant spermatozoa are unable to ascend beyond the oviductal reservoir. *Reprod. Fertil. Dev.* 21, 345–350. doi: 10.1071/RD08183

Höglund, P., Hihnala, S., Kujala, M., Tiitinen, A., Dunkel, L., and Holmberg, C. (2006). Disruption of the SLC26A3-mediated anion transport is associated with male subfertility. *Fertil. Steril.* 85, 232–235. doi: 10.1016/j.fertnstert.2005.06.043

Holappa, K., Mustonen, M., Parvinen, M., Vihko, P., Rajaniemi, H., and Kellokumpu, S. (1999). Primary structure of a sperm cell anion exchanger and its messenger ribonucleic acid expression during spermatogenesis. *Biol. Reprod.* 61, 981–986. doi: 10.1095/biolreprod61.4.981

Holtzmann, I., Wolf, J. P., and Ziyyat, A. (2011). Réservoir spermatique chez la souris: implication des ADAMs. *Gynecol. Obstet. Fertil.* 39, 630–632. doi: 10.1016/j.gyobfe.2011.09.002

Homonnai, Z. T., Matzkin, H., Fainman, N., Paz, G., and Kraicer, P. F. (1978). The cation composition of the seminal plasma and prostatic fluid and its correlation to semen quality. *Fertil. Steril.* 29, 539–542. doi: 10.1016/S0015-0282(16)43281-4

Hook, S. S., and Means, A. R. (2001). Ca2+ /CaM-dependent kinases: from activation to function. *Annu. Rev. Pharmacol. Toxicol.* 41, 471–505. doi: 10.1146/annurev.pharmtox.41.1.471

Ishibashi, K., Sasaki, S., and Marumo, F. (1998). Molecular cloning of a new sodium bicarbonate cotransporter cDNA from human retina. *Biochem. Biophys. Res. Commun.* 246, 535–538. doi: 10.1006/bbrc.1998.8658

Jai, B., Singh, P. A. L., Babcock, D. F., and Lardy, H. A. (1978). Increased calcium-ion influx is a component of capacitation of spermatozoa. *Biochem J.* 549–556.

Jaiswal, B. S., and Conti, M. (2003). Calcium regulation of the soluble adenylyl cyclase expressed in mammalian spermatozoa. *Proc. Natl. Acad. Sci. U.S.A.* 100, 10676–10681. doi: 10.1073/pnas.1831008100

Jakubiczka, S., Bettecken, T., Stumm, M., Nickel, I., Müsebeck, J., Krebs, P., et al. (1999). Frequency of CFTR gene mutations in males participating in an ICSI programme. *Hum. Reprod.* 14, 1833–1834. doi: 10.1093/humrep/14.7.1833

Jensen, L. J., Schmitt, B. M., Berger, U. V., Nsumu, N. N., Boron, W. F., Hediger, M. A., et al. (1999). Localization of sodium bicarbonate cotransporter (NBC) protein and messenger ribonucleic acid in rat epididymis. *Biol. Reprod.* 60, 573–579. doi: 10.1095/biolreprod60.3.573

Jewell, E. A., Shamraj, O. I., and Lingrel, J. B. (1992). Isoforms of the alpha subunit of Na,K-ATPase and their significance. *Acta Physiol. Scand. Suppl.* 607, 161–169.

Jimenez-Gonzalez, C., Michelangeli, F., Harper, C. V., Barratt, C. L. R., and Publicover, S. J. (2006). Calcium signalling in human spermatozoa: a specialized "toolkit" of channels, transporters and stores. *Hum. Reprod. Update* 12, 253–267. doi: 10.1093/humupd/dmi050

Jimenez, T., Sanchez, G., and Blanco, G. (2012). Activity of the Na,K-ATPase a4 Isoform is regulated during sperm capacitation to support sperm motility. *J. Androl.* 33, 1047–1057. doi: 10.2164/jandrol.111.015545

Jorgensen, P. L., Håkansson, K. O., and Karlish, S. J. D. (2003). Structure and mechanism of Na,K-ATPase: functional sites and their interactions. *Annu. Rev. Physiol.* 65, 817–849. doi: 10.1146/annurev.physiol.65.092101.142558

José, O., Torres-Rodríguez, P., Forero-Quintero, L. S., Chávez, J. C., De la Vega-Beltrán, J. L., Carta, F., et al. (2015). Carbonic anhydrases and their functional differences in human and mouse sperm physiology. *Biochem. Biophys. Res. Commun.* 468, 713–718. doi: 10.1016/j.bbrc.2015.11.021

Kaupp, U. B., and Seifert, R. (2002). Cyclic nucleotide-gated ion channels. *Physiol. Rev.* 82, 769–824. doi: 10.1152/physrev.00008.2002

Kaupp, U. B., and Strünker, T. (2016). Signaling in sperm: more different than similar. *Trends Cell Biol.* 27, 101–109. doi: 10.1016/j.tcb.2016.10.002

Kawano, N., Araki, N., Yoshida, K., Hibino, T., Ohnami, N., Makino, M., et al. (2014). Seminal vesicle protein SVS2 is required for sperm survival in the uterus. *Proc. Natl. Acad. Sci. U.S.A.* 111, 4145–4150. doi: 10.1073/pnas.1320715111

Kawano, N., Yoshida, K., Iwamoto, T., and Yoshida, M. (2008). Ganglioside GM1 mediates decapacitation effects of SVS2 on murine spermatozoa. *Biol. Reprod.* 79, 1153–1159. doi: 10.1095/biolreprod.108.069054

Kellenberger, S., and Schild, L. (2002). Epithelial Sodium channel/degenerin family of ion channels: a variety of functions for a shared structure. *Physiol. Rev.* 82, 735–767. doi: 10.1152/physrev.00007.2002

Kirichok, Y., and Lishko, P., V (2011). Rediscovering sperm ion channels with the patch-clamp technique. *Mol. Hum. Reprod.* 17, 478–499. doi: 10.1093/molehr/gar044

Kirichok, Y., Navarro, B., and Clapham, D. E. (2006). Whole-cell patch-clamp measurements of spermatozoa reveal an alkaline-activated Ca2+ channel. *Nature* 439, 737–740. doi: 10.1038/nature04417

Ko, S. B. H., Zeng, W., Dorwart, M. R., Luo, X., Kim, K. H., Millen, L., et al. (2004). Gating of CFTR by the STAS domain of SLC26 transporters. *Nat. Cell Biol.* 6, 343–350. doi: 10.1038/ncb1115

Kondoh, G., Gao, X. H., Nakano, Y., Koike, H., Yamada, S., Okabe, M., et al. (1999). Tissue-inherent fate of GPI revealed by GPI-anchored GFP transgenesis. *FEBS Lett.* 458, 299–303. doi: 10.1016/S0014-5793(99)01172-2

Kondoh, G., Tojo, H., Nakatani, Y., Komazawa, N., Murata, C., Yamagata, K., et al. (2005). Angiotensin-converting enzyme is a GPI-anchored protein releasing factor crucial for fertilization. *Nat. Med.* 11, 160–166. doi: 10.1038/nm1179

Kong, X., Bin, M.a, H. G., Li, H. G., and Xiong, C. L. (2009). Blockade of epithelial sodium channels improves sperm motility in asthenospermia patients. *Int. J. Androl.* 32, 330–336. doi: 10.1111/j.1365-2605.2008.00864.x

Krapf, D., Arcelay, E., Wertheimer, E. V., Sanjay, A., Pilder, S. H., Salicioni, A. M., et al. (2010). Inhibition of Ser/Thr Phosphatases Induces Capacitation-associated Signaling in the Presence of Src Kinase Inhibitors. *J. Biol. Chem.* 285, 7977–7985. doi: 10.1074/jbc.M109.085845

Krasznai, Z., Krasznai, Z. T., Morisawa, M., Bazsán,é, Z. K., Hernádi, Z., Fazekas, Z., et al. (2006). Role of the Na+/Ca2+ exchanger in calcium homeostasis and human sperm motility regulation. *Cell Motil. Cytoskeleton* 63, 66–76. doi: 10.1002/cm.20108

Kujala, M., Hihnala, S., Tienari, J., Kaunisto, K., Hästbacka, J., Holmberg, C., et al. (2007). Expression of ion transport-associated proteins in human efferent and epididymal ducts. *Reproduction* 133, 775–784. doi: 10.1530/rep.1.00964

Kulanand, J., and Shivaji, S. (2001). Capacitation-associated changes in protein tyrosine phosphorylation, hyperactivation and acrosome reaction in hamster spermatozoa. *Andrologia* 33, 95–104. doi: 10.1046/j.1439-0272.2001.00410.x

Kunzelmann, K. (2003). ENaC is inhibited by an increase in the intracellular Cl-concentration mediated through activation of Cl-channels. *Pflügers Arch. Eur. J. Physiol.* 445, 504–512. doi: 10.1007/s00424-002-0958-y

Kuroda, Y., Kaneko, S., Yoshimura, Y., Nozawa, S., and Mikoshiba, K. (1999). Are there inositol 1, 4, 5-triphosphate (IP3) receptors in human sperm? *Life Sci.* 65, 135–143.

La Spina, F. A., Puga, L. C., Romarowski, A., Vitale, A. M., Falzone, T. L., Krapf, D., et al. (2016). Mouse sperm begin to undergo acrosomal exocytosis in the upper isthmus of the oviduct. *Dev. Biol.* 411, 172–182. doi: 10.1016/j.ydbio.2016.02.006

Lalumière, G., Bleau, G., Chapdelaine, A., and Roberts, K. D. (1976). Cholesteryl sulfate and sterol sulfatase in the human reproductive tract. *Steroids* 27, 247–260. doi: 10.1016/0039-128X(76)90101-X

Langlais, J., Kan, F. W. K., Granger, L., Raymond, L., Bleau, G., and Roberts, K. D. (1988). Identification of sterol acceptors that stimulate cholesterol efflux from human spermatozoa during *in vitro* capacitation. *Gamete Res.* 20, 185–201. doi: 10.1002/mrd.1120200209

Langlais, J., Zollinger, M., Plante, L., Chapdelaine, A., Bleau, G., and Roberts, K. D. (1981). Localization of cholesteryl sulfate in human spermatozoa in support of a hypothesis for the mechanism of capacitation. *Proc. Natl. Acad. Sci. U.S.A.* 78, 7266–7270. doi: 10.1073/pnas.78.12.7266

Lawson, C., Dorval, V., Goupil, S., and Leclerc, P. (2007). Identification and localisation of SERCA 2 isoforms in mammalian sperm. *Mol. Hum. Reprod.* 13, 307–316. doi: 10.1093/molehr/gam012

Leahy, T., and Gadella, B. M. (2015). New insights into the regulation of cholesterol efflux from the sperm membrane. *Asian J. Androl.* 17, 561–567. doi: 10.4103/1008-682X.153309

Leclerc, P., de Lamirande, E., and Gagnon, C. (1996). Cyclic adenosine 3′,5′monophosphate-dependent regulation of protein tyrosine phosphorylation in relation to human sperm capacitation and motility. *Biol. Reprod.* 55, 684–692.

Leclerc, P., and Goupil, S. (2002). Regulation of the human sperm tyrosine kinase c-yes. Activation by cyclic adenosine 3′, 5′-monophosphate and inhibition by Ca2+. *Biol. Reprod.* 67, 301–307. doi: 10.1095/biolreprod67.1.301

Lefièvre, L., Chen, Y., Conner, S. J., Scott, J. L., Publicover, S. J., Ford, W. C. L., et al. (2007). Human spermatozoa contain multiple targets for protein S-nitrosylation: an alternative mechanism of the modulation of sperm function by nitric oxide? *Proteomics* 7, 3066–3084. doi: 10.1002/pmic.200700254

Lefièvre, L., Jha, K. N., de Lamirande, E., Visconti, P., and Gagnon, C. (2002). Activation of protein kinase A during human sperm capacitation and acrosome reaction. *J. Androl.* 23, 709–716. doi: 10.1002/j.1939-4640.2002.tb02314.x

Lehtonen, J., Shen, B., Vihinen, M., Casini, A., Scozzafava, A., Supuran, C. T., et al. (2004). Characterization of CA XIII, a novel member of the carbonic anhydrase isozyme family. *J. Biol. Chem.* 279, 2719–2727. doi: 10.1074/jbc.M308984200

Li, C.-Y. Y., Jiang, L.-Y. Y., Chen, W.-Y. Y., Li, K., Sheng, H.-Q. Q., Ni, Y., et al. (2010). CFTR is essential for sperm fertilizing capacity and is correlated with sperm quality in humans. *Hum. Reprod.* 25, 317–327. doi: 10.1093/humrep/dep406

Linares-Hernández, L., Guzmán-Grenfell, A. M., Hicks-Gomez, J. J., and González-Martínez, M. T. (1998). Voltage-dependent calcium influx in human sperm assessed by simultaneous optical detection of intracellular calcium and membrane potential. *Biochim. Biophys. Acta - Biomembr.* 1372, 1–12. doi: 10.1016/S0005-2736(98)00035-2

Lippes, J., Enders, R. G., Pragay, D. A., and Bartholomew, W. R. (1972). The collection and analysis of human fallopian tubal fluid. *Contraception* 5, 85–103. doi: 10.1016/0010-7824(72)90021-2

Lishko, P. V., Botchkina, I. L., Fedorenko, A., and Kirichok, Y. (2010). Acid extrusion from human spermatozoa is mediated by flagellar voltage-gated proton channel. *Cell* 140, 327–337. doi: 10.1016/j.cell.2009.12.053

Lishko, P. V., Botchkina, I. L., and Kirichok, Y. (2011). Progesterone activates the principal Ca2+ channel of human sperm. *Nature* 471, 387–391. doi: 10.1038/nature09767

Lishko, P. V., and Kirichok, Y. (2010). The role of Hv1 and CatSper channels in sperm activation. *J. Physiol.* 588, 4667–4672. doi: 10.1113/jphysiol.2010.194142

Lishko, P. V., Kirichok, Y., Ren, D., Navarro, B., Chung, J.-J., Clapham, D. E., et al. (2012). The control of male fertility by spermatozoan ion channels. *Annu. Rev. Physiol.* 74, 453–457. doi: 10.1146/annurev-physiol-020911-153258

Litvin, T. N., Kamenetsky, M., Zarifyan, A., Buck, J., and Levin, L. R. (2003). Kinetic properties of "soluble" adenylyl cyclase: synergism between calcium and bicarbonate. *J. Biol. Chem.* 278, 15922–15926. doi: 10.1074/jbc.M212475200

Liu, J., Xia, J., Cho, K.-H., Clapham, D. E., and Ren, D. (2007). CatSperbeta, a novel transmembrane protein in the CatSper channel complex. *J. Biol. Chem.* 282, 18945–18952. doi: 10.1074/jbc.M701083200

Liu, Y., Wang, D.-K., and Chen, L.-M. (2012). The physiology of bicarbonate transporters in mammalian reproduction. *Biol. Reprod.* 86, 99. doi: 10.1095/biolreprod.111.096826

Liu, Y., Yang, J., and Chen, L. M. (2015). Structure and function of SLC4 family HCO3- transporters. *Front. Physiol.* 6:355. doi: 10.3389/fphys.2015.00355

Lopata, A., Patullo, M. J., Chang, A., and James, B. (1976). A method for collecting motile spermatozoa from human semen. *Fertil. Steril.* 27, 677–684. doi: 10.1016/S0015-0282(16)41899-6

López-González, I., Torres-Rodríguez, P., Sánchez-Carranza, O., Solís-López, A., Santi, C. M., Darszon, A. I., et al. (2014). Membrane hyperpolarization during human sperm capacitation. *Mol. Hum. Reprod.* 20, 619–629. doi: 10.1093/molehr/gau029

Lopez, C. I., Pelletán, L. E., Suhaiman, L., De Blas, G. A., Vitale, N., Mayorga, L. S., et al. (2012). Diacylglycerol stimulates acrosomal exocytosis by feeding into a PKC- and PLD1-dependent positive loop that continuously supplies phosphatidylinositol 4,5-bisphosphate. *Biochim. Biophys. Acta* 1821, 1186–1199. doi: 10.1016/j.bbalip.2012.05.001

Luque, G. M., Dalotto-Moreno, T., Martín-Hidalgo, D., Ritagliati, C., Puga Molina, L. C., Romarowski, A., et al. (2018). Only a subpopulation of mouse sperm displays a rapid increase in intracellular calcium during capacitation. *J. Cell Physiol.* doi: 10.1002/jcp.26883. [Epub ahead of print].

Lu, J., Stewart, A. J., Sadler, P. J., Pinheiro, T. J. T., and Blindauer, C. A. (2008). Albumin as a zinc carrier: properties of its high-affinity zinc-binding site. *Biochem. Soc. Trans.* 36, 1317–1321. doi: 10.1042/BST0361317

Luconi, M., Bonaccorsi, L., Krausz, C., Gervasi, G., Forti, G., and Baldi, E. (1995). Stimulation of protein tyrosine phosphorylation by platelet-activating factor and progesterone in human spermatozoa. *Mol. Cell. Endocrinol.* 108, 35–42. doi: 10.1016/0303-7207(95)92576-A

Lutsenko, S., and Kaplan, J. H. (1993). An essential role for the extracellular domain of the sodium-potassium-ATPase.beta.-subunit in cation occlusion. *Biochemistry* 32, 6737–6743. doi: 10.1021/bi00077a029

Macdonald, R. R., and Lumley, I. B. (1970). Endocervical pH measured *in vivo* through the normal menstrual cycle. *Obstet. Gynecol.* 35, 202–206.

Mandal, A., Naaby-Hansen, S., Wolkowicz, M. J., Klotz, K., Shetty, J., Retief, J. D., et al. (1999). FSP95, a testis-specific 95-kilodalton fibrous sheath antigen that undergoes tyrosine phosphorylation in capacitated human spermatozoa. *Biol. Reprod.* 61, 1184–1197. doi: 10.1095/biolreprod61.5.1184

Mann, T., and Lutwak-Mann, C. (1981). "Biochemistry of seminal plasma and male accessory fluids; application to andrological problems," in *Male Reproductive Function and Semen* (London: Springer), 269–336.

Mannowetz, N., Miller, M. R., and Lishko, P. V. (2017). Regulation of the sperm calcium channel CatSper by endogenous steroids and plant triterpenoids. *Proc. Natl. Acad. Sci. U.S.A.* 114, 5743–5748. doi: 10.1073/pnas.1700367114

Mannowetz, N., Naidoo, N. M., Choo, S.-A. S., Smith, J. F., Lishko, P. V., Sara Choo, S.-A., et al. (2013). Slo1 is the principal potassium channel of human spermatozoa. *Elife* 2:e01009. doi: 10.7554/eLife.01009.001

Mansell, S. A., Publicover, S. J., Barratt, C. L. R., and Wilson, S. M. (2014). Patch clamp studies of human sperm under physiological ionic conditions reveal three functionally and pharmacologically distinct cation channels. *Mol. Hum. Reprod.* 20, 392–408. doi: 10.1093/molehr/gau003

Marín-Briggiler, C. I. (2005). Evidence of the presence of calcium/calmodulin-dependent protein kinase IV in human sperm and its involvement in motility regulation. *J. Cell Sci.* 118, 2013–2022. doi: 10.1242/jcs.02326

Marín-Briggiler, C. I., Gonzalez-Echeverría, F., Buffone, M. G., Calamera, J. C., Tezón, J. G., and Vazquez-Levin, M. H. (2003). Calcium requirements for human sperm function *in vitro*. *Fertil. Steril.* 79, 1396–1403. doi: 10.1016/S0015-0282(03)00267-X

Marín-Briggiler, C. I., Vazquez-Levin, M. H., Gonzalez-Echeverría, F., Blaquier, J. A., Tezón, J. G., and Miranda, P., V (1999). Strontium supports human sperm capacitation but not follicular fluid-induced acrosome reaction. *Biol. Reprod.* 61, 673–680. doi: 10.1095/biolreprod61.3.673

Martínez-López, P., Santi, C. M., Treviño, C. L., Ocampo-Gutiérrez, A. Y., Acevedo, J. J., Alisio, A., et al. (2009). Mouse sperm K + currents stimulated by pH and cAMP possibly coded by Slo3 channels. *Biochem. Biophys. Res. Commun.* 381, 204–209. doi: 10.1016/j.bbrc.2009.02.008

Martínez, P., and Morros, A. (1996). Membrane lipid dynamics during human sperm capacitation. *Front. Biosci.* 1, d103–d117.

Maas, D. H., Storey, B. T., and Mastroianni, L. Jr. (1977). Hydrogen ion and carbon dioxide content of the oviductal fluid of the rhesus monkey (*Macaca mulatta*). *Fertil Steril.* 28, 981–985.

Matamoros-Volante, A., Moreno-Irusta, A., Torres-Rodriguez, P., Giojalas, L., Gervasi, M. G., Visconti, P. E., et al. (2017). Semi-automatized segmentation method using image-based flow cytometry to study sperm physiology: the case of capacitation-induced tyrosine phosphorylation. *MHR Basic Sci. Reprod. Med.* 24:gax062. doi: 10.1093/molehr/gax062

McDermott, J. P., Sánchez, G., Chennathukuzhi, V., and Blanco, G. (2012). Green fluorescence protein driven by the Na,K-ATPase α4 isoform promoter is expressed only in male germ cells of mouse testis. *J. Assist. Reprod. Genet.* 29, 1313–1325. doi: 10.1007/s10815-012-9876-x

Mcdermott, J., Sánchez, G., Nangia, A. K., and Blanco, G. (2015). Role of human Na,K-ATPase alpha 4 in sperm function, derived from studies in transgenic mice. *Mol. Reprod. Dev.* 82, 167–181. doi: 10.1002/mrd.22454

Medina, J. F., Recalde, S., Prieto, J., Lecanda, J., Saez, E., Funk, C. D., et al. (2003). Anion exchanger 2 is essential for spermiogenesis in mice. *Proc. Natl. Acad. Sci. U.S.A.* 100, 15847–15852. doi: 10.1073/pnas.2536127100

Meizel, S., Turner, K. O., and Nuccitelli, R. (1997). Progesterone triggers a wave of increased free calcium during the human sperm acrosome reaction. *Dev. Biol.* 182, 67–75. doi: 10.1006/dbio.1997.8477

Michelangeli, F., Ogunbayo, O. A., and Wootton, L. L. (2005). A plethora of interacting organellar Ca2+ stores. *Curr. Opin. Cell Biol.* 17, 135–140. doi: 10.1016/j.ceb.2005.01.005

Miller, M. R., Mannowetz, N., Iavarone, A. T., Safavi, R., Gracheva, E. O., Smith, J. F., et al. (2016). Unconventional endocannabinoid signaling governs sperm activation via sex hormone progesterone. *Science* 352, 555–559. doi: 10.1126/science.aad6887

Miller, M. R., Mansell, S. A., Meyers, S. A., and Lishko, P. V. (2015). Flagellar ion channels of sperm: similarities and differences between species. *Cell Calcium* 58, 105–113. doi: 10.1016/j.ceca.2014.10.009

Mizuno, K., Padma, P., Konno, A., Satouh, Y., Ogawa, K., and Inaba, K. (2009). A novel neuronal calcium sensor family protein, calaxin, is a potential Ca(2+)-dependent regulator for the outer arm dynein of metazoan cilia and flagella. *Biol. cell* 101, 91–103. doi: 10.1042/BC20080032

Mizuno, K., Shiba, K., Okai, M., Takahashi, Y., Shitaka, Y., Oiwa, K., et al. (2012). Calaxin drives sperm chemotaxis by Ca^{2+}-mediated direct modulation of a dynein motor. *Proc. Natl. Acad. Sci. U.S.A.* 109, 20497–20502. doi: 10.1073/pnas.1217018109

Morth, J. P., Pedersen, B. P., Toustrup-Jensen, M. S., Sørensen, T. L.-M., Petersen, J., Andersen, J. P., et al. (2007). Crystal structure of the sodium–potassium pump. *Nature* 450, 1043–1049. doi: 10.1038/nature06419

Muñoz-Garay, C., José, L., Delgado, R., Labarca, P., Felix, R., and Darszon, A. (2001). Inwardly rectifying K+ channels in spermatogenic cells: functional expression and implication in sperm capacitation. *Dev. Biol.* 234, 261–274. doi: 10.1006/dbio.2001.0196

Muro, Y., Hasuwa, H., Isotani, A., Miyata, H., Yamagata, K., Ikawa, M., et al. (2016). Behavior of mouse spermatozoa in the female reproductive tract from soon after mating to the beginning of fertilization. *Biol. Reprod.* 94, 80–80. doi: 10.1095/biolreprod.115.135368

Musset, B., and Decoursey, T. (2012). Biophysical properties of the voltage-gated proton channel HV1. *Wiley Interdiscip. Rev. Membr. Transp. Signal.* 1, 605–620. doi: 10.1002/wmts.55

Navarrete, F. A., Alvau, A., Lee, H. C., Levin, L. R., Buck, J., Leon, P. M.-D., et al. (2016). Transient exposure to calcium ionophore enables *in vitro* fertilization in sterile mouse models. *Sci. Rep.* 6:33589. doi: 10.1038/srep33589

Navarrete, F. A., García-Vázquez, F. A., Alvau, A., Escoffier, J., Krapf, D., Sánchez-Cárdenas, C., et al. (2015). Biphasic role of calcium in mouse sperm capacitation signaling pathways. *J. Cell. Physiol.* 230, 1758–1769. doi: 10.1002/jcp.24873

Navarro, B., Kirichok, Y., Chung, J.-J., and Clapham, D. E. (2008). Ion channels that control fertility in mammalian spermatozoa. *Int. J. Dev. Biol.* 52, 607–613. doi: 10.1387/ijdb.072554bn

Ng, K. Y. B., Mingels, R., Morgan, H., Macklon, N., and Cheong, Y. (2017). *In vivo* oxygen, temperature and pH dynamics in the female reproductive tract and their importance in human conception: a systematic review. *Hum. Reprod. Update* 24, 15–34. doi: 10.1093/humupd/dmx028

Nimmo, M. R., and Cross, N. L. (2003). Structural features of sterols required to inhibit human sperm capacitation1. *Biol. Reprod.* 68, 1308–1317. doi: 10.1095/biolreprod.102.008607

Nishigaki, T., José, O., González-Cota, A. L., Romero, F., Treviño, C. L., and Darszon, A. (2014). Intracellular pH in sperm physiology. *Biochem. Biophys. Res. Commun.* 450, 1149–1158. doi: 10.1016/j.bbrc.2014.05.100

Norman, C., Goldberg, E., Porterfielid, I. D., and Johnson, C. E. (1960). Prolonged survival of human sperm in chemically defined media at room temperatures. *Nature* 188, 760–760. doi: 10.1038/188760a0

O'Bryan, M. K., De Kretser, D., Ivell, R., Skakkebæk, N. E., Almstrup, K., and Leffers, H. (2006). Mouse models for genes involved in impaired spermatogenesis. *Int. J. Androl.* 29, 76–89. doi: 10.1111/j.1365-2605.2005.00614.x

Okamura, N., and Sugita, Y. (1983). Activation of spermatozoan adenylate cyclase by a low molecular weight factor in porcine seminal plasma. *J. Biol. Chem.* 258, 13056–13062.

Okamura, N., Tajima, Y., Ishikawa, H., Yoshii, S., Koiso, K., and Sugita, Y. (1986). Lowered levels of bicarbonate in seminal plasma cause the poor sperm motility in human infertile patients. *Fertil. Steril.* 45, 265–272. doi: 10.1016/S0015-0282(16)49166-1

Okamura, N., Tajima, Y., Soejima, A., Masuda, H., and Sugita, Y. (1985). Sodium bicarbonate in seminal plasma stimulates the motility of mammalian spermatozoa through direct activation of adenylate cyclase. *J. Biol. Chem.* 260, 9699–9705.

Okunade, G. W., Miller, M. L., Pyne, G. J., Sutliff, R. L., O'Connor, K. T., Neumann, J. C., et al. (2004). Targeted ablation of plasma membrane Ca2+-ATPase (PMCA) 1 and 4 indicates a major housekeeping function for PMCA1 and a critical role in hyperactivated sperm motility and male fertility for PMCA4. *J. Biol. Chem.* 279, 33742–33750. doi: 10.1074/jbc.M404628200

Oren-Benaroya, R., Orvieto, R., Gakamsky, A., Pinchasov, M., and Eisenbach, M. (2008). The sperm chemoattractant secreted from human cumulus cells is progesterone. *Hum. Reprod.* 23, 2339–2345. doi: 10.1093/humrep/den265

Osheroff, J. E., Visconti, P. E., Valenzuela, J. P., Travis, a, J., Alvarez, J., and Kopf, G. S. (1999). Regulation of human sperm capacitation by a cholesterol efflux-stimulated signal transduction pathway leading to protein kinase A-mediated up-regulation of protein tyrosine phosphorylation. *Mol. Hum. Reprod.* 5, 1017–1026. doi: 10.1093/molehr/5.11.1017

Ostermeier, G. C., Cardona, C., Moody, M. A., Simpson, A. J., Mendoza, R., Seaman, E., et al. (2018). Timing of sperm capacitation varies reproducibly among men. *Mol. Reprod. Dev.* 85, 387–396. doi: 10.1002/mrd.22972

Okabe, M. (2013). The cell biology of mammalian fertilization. *Development* 140, 4471–4479. doi: 10.1242/dev.090613

Owen, D. H., and Katz, D. F. (2005). A review of the physical and chemical properties of human semen and the formulation of a semen simulant. *J. Androl.* 26, 459–469. doi: 10.2164/jandrol.04104

Parkkila, S., Kaunisto, K., Kellokumpu, S., and Rajaniemi, H. (1991). A high activity carbonic anhydrase isoenzyme (CA II) is present in mammalian spermatozoa. *Histochemistry* 95, 477–482. doi: 10.1007/BF00315743

Parkkila, S., Rajaniemi, H., and Kellokumpu, S. (1993). Polarized expression of a band 3-related protein in mammalian sperm cells. *Biol. Reprod.* 49, 326–331. doi: 10.1095/biolreprod49.2.326

Parks, J. E., Arion, J. W., and Foote, R. H. (1987). Lipids of plasma membrane and outer acrosomal membrane from bovine spermatozoa. *Biol. Reprod.* 37, 1249–1258. doi: 10.1095/biolreprod37.5.1249

Parks, J. E., and Hammerstedt, R. H. (1985). Development changes occurring in the lipids of ram epididymal spermatozoa plasma membrane. *Biol. Reprod.* 32, 653–668. doi: 10.1095/biolreprod32.3.653

Parks, J. E., and Lynch, D., V (1992). Lipid composition and thermotropic phase behavior of boar, bull, stallion, and rooster sperm membranes. *Cryobiology* 29, 255–266. doi: 10.1016/0011-2240(92)90024-V

Patrat, C., Serres, C., and Jouannet, P. (2002). Progesterone induces hyperpolarization after a transient depolarization phase in human spermatozoa. *Biol. Reprod.* 66, 1775–1780. doi: 10.1095/biolreprod66.6.1775

Peña-Münzenmayer, G., George, A. T., Shull, G. E., Melvin, J. E., and Catalán, M. A. (2016). Ae4 (Slc4a9) is an electroneutral monovalent cation-dependent Cl – /HCO 3 – exchanger. *J. Gen. Physiol.* 147, 423–436. doi: 10.1085/jgp.201611571

Peralta-Arias, R. D., Vívenes, C. Y., Camejo, M. I., Piñero, S., Proverbio, T., Martínez, E., et al. (2015). ATPases, ion exchangers and human sperm motility. *Reprod.* 149, 475–484. doi: 10.1530/REP-14-0471

Poli de Figueiredo, C. E., Ng, L. L., Davis, J. E., Lucio-Cazana, F. J., Ellory, J. C., and Hendry, B. M. (1991). Modulation of Na-H antiporter activity in human lymphoblasts by altered membrane cholesterol. *Am. J. Physiol.* 261, C1138–C1142. doi: 10.1152/ajpcell.1991.261.6.C1138

Publicover, S. J., Giojalas, L. C., Teves, M. E., de Oliveira, G. S. M. M., Garcia, A. A. M., Barratt, C. L. R., et al. (2008). Ca2+ signalling in the control of motility and guidance in mammalian sperm. *Front. Biosci.* 13, 5623–5637. doi: 10.2741/3105

Puga Molina, L. C., Pinto, N. A., Torres, N. I., Gonzalez-Cota, A. L., Luque, G. M., Balestrini, P. A., et al. (2018). CFTR/ENaC dependent regulation of membrane potential during human sperm capacitation is initiated by bicarbonate uptake through NBC. *J. Biol. Chem.* 293, 9924–9936. doi: 10.1074/jbc.RA118.003166

Puga Molina, L. C., Pinto, N. A., Torres Rodríguez, P., Romarowski, A., Vicens Sanchez, A., Visconti, P. E., et al. (2017). Essential role of CFTR in PKA-dependent phosphorylation, alkalinization, and hyperpolarization during human sperm capacitation. *J. Cell. Physiol.* 232, 1404–1414. doi: 10.1002/jcp.25634

Qi, H., Moran, M. M., Navarro, B., Chong, J. A., Krapivinsky, G., Krapivinsky, L., et al. (2007). All four CatSper ion channel proteins are required for male fertility and sperm cell hyperactivated motility. *Proc. Natl. Acad. Sci. U.S.A.* 104, 1219–1223. doi: 10.1073/pnas.0610286104

Qiu, F., Chamberlin, A., Watkins, B. M., Ionescu, A., Perez, M. E., Barro-Soria, R., et al. (2016). Molecular mechanism of Zn 2+ inhibition of a voltage-gated proton channel. *Proc. Natl. Acad. Sci. U.S.A.* 113, E5962–E5971. doi: 10.1073/pnas.1604082113

Quill, T., a, Sugden, S., a, Rossi, K. L., Doolittle, L. K., Hammer, R. E., and Garbers, D. L. (2003). Hyperactivated sperm motility driven by CatSper2 is required for fertilization. *Proc. Natl. Acad. Sci. U.S.A.* 100, 14869–14874. doi: 10.1073/pnas.2136654100

Ramsey, I. S., Ruchti, E., Kaczmarek, J. S., and Clapham, D. E. (2009). Hv1 proton channels are required for high-level NADPH oxidase-dependent superoxide production during the phagocyte respiratory burst. *Proc. Natl. Acad. Sci. U.S.A.* 106, 7642–7647. doi: 10.1073/pnas.0902761106

Ravnik, S. E., Albers, J. J., and Muller, C. H. (1995). Stimulation of human sperm capacitation by purified lipid transfer protein. *J. Exp. Zool.* 272, 78–83. doi: 10.1002/jez.1402720110

Ravnik, S. E., Zarutskie, P. W., and Muller, C. H. (1992). Purification and characterization of a human follicular fluid lipid transfer protein that stimulates human sperm capacitation. *Biol. Reprod.* 47, 1126–1133. doi: 10.1095/biolreprod47.6.1126

Reddy, P. R., Patni, A., Sharma, A., Gupta, S., and Tiwary, A. K. (2001). Effect of 2′,4′-dichlorobenzamil hydrochloride, a Na+-Ca2+ exchange inhibitor, on human spermatozoa. *Eur. J. Pharmacol.* 418, 153–155. doi: 10.1016/S0014-2999(01)00892-5

Ren, D., Navarro, B., Perez, G., Jackson, A. C., Hsu, S., Shi, Q., et al. (2001). A sperm ion channel required for sperm motility and male fertility. *Nature* 413, 603–609. doi: 10.1038/35098027

Robitaille, P. M. L., Robitaille, P. A., Martin, P. A., and Brown, G. G. (1987). Phosphorus-31 nuclear magnetic resonance studies of spermatozoa from the boar, ram, goat and bull. *Comp. Biochem. Physiol. B Biochem.* 87, 285–296. doi: 10.1016/0305-0491(87)90141-6

Rode, B., Dirami, T., Bakouh, N., Rizk-Rabin, M., Norez, C., Lhuillier, P., et al. (2012). The testis anion transporter TAT1 (SLC26A8) physically and functionally interacts with the cystic fibrosis transmembrane conductance regulator channel: a potential role during sperm capacitation. *Hum. Mol. Genet.* 21, 1287–1298. doi: 10.1093/hmg/ddr558

Rodriguez-Martinez, H., Ekstedt, E., Einarsson, S., Rodríguez-Martínez, H., Ekstedt, E., and Einarsson, S. (1990). Acidification of epididymal fluid in the boar. *Int. J. Androl.* 13, 238–243. doi: 10.1111/j.1365-2605.1990.tb00982.x

Rossato, M., Virgilio, F., Di Rizzuto, R., Galeazzi, C., and Foresta, C. (2001). Intracellular calcium store depletion and acrosome reaction in human spermatozoa: role of calcium and plasma membrane potential. *Mol. Hum. Reprod.* 7, 119–128. doi: 10.1093/molehr/7.2.119

Ruknudin, A., and Silver, I. A. (1990). Ca2+ uptake during capacitation of mouse spermatozoa and the effect of an anion transport inhibitor on Ca2+ uptake. *Mol. Reprod. Dev.* 26, 63–68. doi: 10.1002/mrd.1080260110

Rusnak, F., and Mertz, P. (2000). Calcineurin: form and function. *Physiol. Rev.* 80, 1483–1521. doi: 10.1152/physrev.2000.80.4.1483

Sakata, Y., Saegusa, H., Zong, S., Osanai, M., Murakoshi, T., Shimizu, Y., et al. (2002). Ca(v)2.3 (alpha1E) Ca2+ channel participates in the control of sperm function. *FEBS Lett.* 516, 229–233. doi: 10.1016/S0014-5793(02)02529-2

Sanchez, G., Nguyen, A.-N. T. N. T., Timmerberg, B., Tash, J. S., and Blanco, G. (2006). The Na,K-ATPase α4 isoform from humans has distinct enzymatic properties and is important for sperm motility. *Mol. Hum. Reprod.* 12, 565–576. doi: 10.1093/molehr/gal062

Santi, C. M., Martínez-López, P., de la Vega-Beltrán, J. L., Butler, A., Alisio, A., Darszon, A., et al. (2010). The SLO3 sperm-specific potassium channel plays a vital role in male fertility. *FEBS Lett.* 584, 1041–1046. doi: 10.1016/j.febslet.2010.02.005

Schaefer, M., Hofmann, T., Schultz, G., and Gudermann, T. (1998). A new prostaglandin E receptor mediates calcium influx and acrosome reaction in human spermatozoa. *Proc. Natl. Acad. Sci. U.S.A.* 95, 3008–3013. doi: 10.1073/pnas.95.6.3008

Schiffer, C., Muller, A., Egeberg, D. L., Alvarez, L., Brenker, C., Rehfeld, A., et al. (2014). Direct action of endocrine disrupting chemicals on human sperm. *EMBO Rep.* 15, 758–765. doi: 10.15252/embr.201438869

Schreiber, M., Wei, A., Yuan, A., Gaut, J., Saito, M., and Salkoff, L. (1998). Slo3, a Novel pH-sensitive K+ Channel from Mammalian Spermatocytes. *J. Biol. Chem.* 273, 3509–3516. doi: 10.1074/jbc.273.6.3509

Schuh, K., Cartwright, E. J., Jankevics, E., Bundschu, K., Liebermann, J., Williams, J. C., et al. (2004). Plasma membrane Ca2+ ATPase 4 Is required for sperm motility and male fertility. *J. Biol. Chem.* 279, 28220–28226. doi: 10.1074/jbc.M312599200

Schulz, S., Jakubiczka, S., Kropf, S., Nickel, I., Muschke, P., and Kleinstein, J. (2006). Increased frequency of cystic fibrosis transmembrane conductance regulator gene mutations in infertile males. *Fertil. Steril.* 85, 135–138. doi: 10.1016/j.fertnstert.2005.07.1282

Scott, J. D., and Pawson, T. (2009). Cell signaling in space and time: Where proteins come together and when they're apart. *Science* 326, 1220–1224. doi: 10.1126/science.1175668

Selvaraj, V., Asano, A., Buttke, D. E., McElwee, J. L., Nelson, J. L., Wolff, C. A., et al. (2006). Segregation of micron-scale membrane sub-domains in live murine sperm. *J. Cell. Physiol.* 206, 636–646. doi: 10.1002/jcp.20504

Selvaraj, V., Buttke, D. E., Asano, A., McElwee, J. L., Wolff, C. A., Nelson, J. L., et al. (2007). GM1 dynamics as a marker for membrane changes associated with the process of capacitation in murine and bovine spermatozoa. *J. Androl.* 28, 588–599. doi: 10.2164/jandrol.106.002279

Serrano, C. J., Treviño, C. L., Felix, R., and Darszon, A. (1999). Voltage-dependent Ca(2+) channel subunit expression and immunolocalization in mouse spermatogenic cells and sperm. *FEBS Lett.* 462, 171–176. doi: 10.1016/S0014-5793(99)01518-5

Shamraj, O., and Lingrel, J. (1994). A putative fourth Na+, K (+)-ATPase alpha-subunit gene is expressed in testis. *Proc. Natl. Acad. Sci. U.S.A.* 91, 12952–12956. doi: 10.1073/pnas.91.26.12952

Sheppard, D. N., and Welsh, M. J. (1999). Structure and function of the CFTR chloride channel. *Physiol. Rev.* 79, S23–S45. doi: 10.1152/physrev.1999.79.1.S23

Shiba, K., Baba, S. A., Inoue, T., and Yoshida, M. (2008). Ca2+ bursts occur around a local minimal concentration of attractant and trigger sperm chemotactic response. *Proc. Natl. Acad. Sci. U.S.A.* 105, 19312–19317. doi: 10.1073/pnas.0808580105

Si, Y., and Olds-Clarke, P. (2000). Evidence for the involvement of calmodulin in mouse sperm capacitation. *Biol. Reprod.* 62, 1231–1239. doi: 10.1095/biolreprod62.5.1231

Skou, J. C. (1957). The influence of some cations on an adenosine triphosphatase from peripheral nerves. *Biochim. Biophys. Acta* 23, 394–401. doi: 10.1016/0006-3002(57)90343-8

Smith, J. F., Syritsyna, O., Fellous, M., Serres, C., Mannowetz, N., Kirichok, Y., et al. (2013). Disruption of the principal, progesterone-activated sperm Ca2+ channel in a CatSper2-deficient infertile patient. *Proc. Natl. Acad. Sci. U.S.A.* 110, 6823–6828. doi: 10.1073/pnas.1216588110

Smith, M. B., Babcock, D. F., and Lardy, H. A. (1985). A 31P NMR study of the epididymis and epididymal sperm of the bull and hamster. *Biol. Reprod.* 33, 1029–1040. doi: 10.1095/biolreprod33.5.1029

Snyder, P. M. (2002). The epithelial Na+ channel: cell surface insertion and retrieval in Na+ homeostasis and hypertension. *Endocr. Rev.* 23, 258–275. doi: 10.1210/edrv.23.2.0458

Sorum, B., Czégé, D., and Csanády, L. (2015). Timing of CFTR Pore Opening and Structure of Its Transition State. *Cell* 163, 724–733. doi: 10.1016/j.cell.2015.09.052

Steptoe, P. C., and Edwards, R. G. (1978). Birth after the reimplantation of a human embryo. *Lancet* 2:366.

Stival, C., La Spina, F. A., Baró Graf, C., Arcelay, E., Arranz, S. E., Ferreira, J. J., et al. (2015). Src kinase is the connecting player between Protein Kinase A (PKA) activation and hyperpolarization through SLO3 potassium channel regulation in mouse sperm. *J. Biol. Chem.* 290, 18855–18864. doi: 10.1074/jbc.M115.640326

Strünker, T., Goodwin, N., Brenker, C., Kashikar, N. D., Weyand, I., Seifert, R., et al. (2011). The CatSper channel mediates progesterone-induced Ca2+ influx in human sperm. *Nature* 471, 382–386. doi: 10.1038/nature09769

Su, Y.-H., and Vacquier, V. D. (2002). A flagellar K(+)-dependent Na(+)/Ca(2+) exchanger keeps Ca(2+) low in sea urchin spermatozoa. *Proc. Natl. Acad. Sci. U.S.A.* 99, 6743–6748. doi: 10.1073/pnas.102186699

Suarez, S. S., and Dai, X. (1995). Intracellular calcium reaches different levels of elevation in hyperactivated and acrosome-reacted hamster sperm. *Mol. Reprod. Dev.* 42, 325–333. doi: 10.1002/mrd.1080420310

Sugkraroek, P., Kates, M., Leader, A., and Tanphaichitr, N. (1991). Levels of cholesterol and phospholipids in freshly ejaculated sperm and Percoll-gradient-pelletted sperm from fertile and unexplained infertile men. *Fertil. Steril.* 55, 820–827. doi: 10.1016/S0015-0282(16)54255-1

Suzuki, F., and Yanagimachi, R. (1989). Changes in the distribution of intramembranous particles and filipin-reactive membrane sterols during *in vitro* capacitation of golden hamster spermatozoa. *Gamete Res.* 23, 335–347. doi: 10.1002/mrd.1120230310

Suzuki, K. G. N., Ando, H., Komura, N., Fujiwara, T. K., Kiso, M., and Kusumi, A. (2017). Development of new ganglioside probes and unraveling of raft domain structure by single-molecule imaging. *Biochim. Biophys. Acta* 1861, 2494–2506. doi: 10.1016/j.bbagen.2017.07.012

Tabcharani, J. A., Chang, X.-B., Riordan, J. R., and Hanrahan, J. W. (1991). Phosphorylation-regulated CI– channel in CHO cells stably expressing the cystic fibrosis gene. *Nature* 352, 628–631. doi: 10.1038/352628a0

Tabcharani, J. A., Rommens, J. M., Hou, Y. X., Chang, X. B., Tsui, L. C., Riordan, J. R., et al. (1993). Multi-ion pore behaviour in the CFTR chloride channel. *Nature* 366, 79–82. doi: 10.1038/366079a0

Tall, A. R. (1993). Plasma cholesteryl ester transfer protein. *J. Lipid Res.* 34, 1255–1274.

Tash, J. S., Krinks, M., Patel, J., Means, R. L., Klee, C. B., and Means, A. R. (1988). Identification, characterization, and functional correlation of calmodulin-dependent protein phosphatase in sperm. *J. Cell Biol.* 106, 1625–1633. doi: 10.1083/jcb.106.5.1625

Tateno, H., Krapf, D., Hino, T., Sánchez-Cárdenas, C., Darszon, A., Yanagimachi, R., et al. (2013). Ca2+ ionophore A23187 can make mouse spermatozoa capable of fertilizing *in vitro* without activation of cAMP-dependent phosphorylation pathways. *Proc. Natl. Acad. Sci. U.S.A.* 110, 18543–18548. doi: 10.1073/pnas.1317113110

Tavares, R. S., Mansell, S., Barratt, C. L. R., Wilson, S. M., Publicover, S. J., and Ramalho-Santos, J. (2013). p,p'-DDE activates CatSper and compromises human sperm function at environmentally relevant concentrations. *Hum. Reprod.* 28, 3167–3177. doi: 10.1093/humrep/det372

Teves, M. E., Guidobaldi, H. A., Uñates, D. R., Sanchez, R., Miska, W., Publicover, S. J., et al. (2009). Molecular mechanism for human sperm chemotaxis mediated by progesterone. *PLoS ONE* 4:e8211. doi: 10.1371/journal.pone.0008211

Thastrup, O., Cullen, P. J., Drøbak, B. K., Hanley, M. R., and Dawson, A. P. (1990). Thapsigargin, a tumor promoter, discharges intracellular Ca2+ stores by specific inhibition of the endoplasmic reticulum Ca2(+)-ATPase. *Proc. Natl. Acad. Sci. U.S.A.* 87, 2466–2470. doi: 10.1073/pnas.87.7.2466

Torres-Flores, V. V., Picazo-Juárez, G., Hernández-Rueda, Y., Darszon, A., González-Martínez, M. T., and Gonzlez-Martínez, M. T. (2011). Sodium influx induced by external calcium chelation decreases human sperm motility. *Hum. Reprod.* 26, 2626–2635. doi: 10.1093/humrep/der237

Toyoda, Y., Yokoyama, M., and Hosi, T. (1971). Studies on the fertilization of mouse eggs *in vitro*. I. *In vitro* fertilization of eggs by fresh epididymal sperm. *Jpn. J. Anim. Reprod.* 16, 147–151. doi: 10.1262/jrd1955.16.152

Travis, A. J., Merdiushev, T., Vargas, L. a, Jones, B. H., Purdon, M., a, Nipper, R. W., et al. (2001). Expression and localization of caveolin-1, and the presence of membrane rafts, in mouse and Guinea pig spermatozoa. *Dev. Biol.* 240, 599–610. doi: 10.1006/dbio.2001.0475

Treviño, C. L., Felix, R., Castellano, L. E., Gutiérrez, C., Rodríguez, D., Pacheco, J., et al. (2004). Expression and differential cell distribution of low-threshold Ca2+channels in mammalian male germ cells and sperm. *FEBS Lett.* 563, 87–92. doi: 10.1016/S0014-5793(04)00257-1

Treviño, C. L., Serrano, C. J., Beltrán, C., Felix, R., and Darszon, A. (2001). Identification of mouse trp homologs and lipid rafts from spermatogenic cells and sperm. *FEBS Lett.* 509, 119–125. doi: 10.1016/S0014-5793(01)03134-9

Truppo, E., Supuran, C. T., Sandomenico, A., Vullo, D., Innocenti, A., Di Fiore, A., et al. (2012). Carbonic anhydrase VII is S-glutathionylated without loss of catalytic activity and affinity for sulfonamide inhibitors. *Bioorganic Med. Chem. Lett.* 22, 1560–1564. doi: 10.1016/j.bmcl.2011.12.134

Ueda, Y., Yamaguchi, R., Ikawa, M., Okabe, M., Morii, E., Maeda, Y., et al. (2007). PGAP1 knock-out mice show otocephaly and male infertility. *J. Biol. Chem.* 282, 30373–30380. doi: 10.1074/jbc.M705601200

Varma, R., and Mayor, S. (1998). GPI-anchored proteins are organized in submicron domains at the cell surface. *Nature* 394, 798–801. doi: 10.1038/29563

Visconti, P. E., Bailey, J. L., Moore, G. D., Pan, D., Olds-Clarke, P., and Kopf, G. S. (1995a). Capacitation of mouse spermatozoa. I. Correlation between the capacitation state and protein tyrosine phosphorylation. *Development* 121, 1129–1137.

Visconti, P. E., Krapf, D., de la Vega-Beltrán, J. L., Acevedo, J. J., and Darszon, A. (2011). Ion channels, phosphorylation and mammalian sperm capacitation. *Asian J. Androl.* 13, 395–405. doi: 10.1038/aja.2010.69

Visconti, P. E., Moore, G. D., Bailey, J. L., Leclerc, P., Connors, S. A., Pan, D., et al. (1995b). Capacitation of mouse spermatozoa. II. Protein tyrosine phosphorylation and capacitation are regulated by a cAMP-dependent pathway. *Development* 121, 1139–1150.

Visconti, P. E., Ning, X. P., Fornés, M. W., Alvarez, J. G., Stein, P., Connors, S. A., et al. (1999). Cholesterol efflux-mediated signal transduction in mammalian sperm: cholesterol release signals an increase in protein tyrosine phosphorylation during mouse sperm capacitation. *Dev. Biol.* 214, 429–443. doi: 10.1006/dbio.1999.9428

Vishwakarma, P. (1962). The pH and bicarbonate-ion content of the oviduct and uterine fluids. *Fertil. Steril.* 13, 481–485. doi: 10.1016/S0015-0282(16)34633-7

Vredenburgh-Wilberg, W. L., and Parrish, J. J. (1995). Intracellular pH of bovine sperm increases during capacitation. *Mol. Reprod. Dev.* 40, 490–502. doi: 10.1002/mrd.1080400413

Wagoner, K., Sanchez, G., Nguyen, A.-N., Enders, G. C., and Blanco, G. (2005). Different expression and activity of the alpha1 and alpha4 isoforms of the Na,K-ATPase during rat male germ cell ontogeny. *Reproduction* 130, 627–641. doi: 10.1530/rep.1.00806

Waldmann, R., Champigny, G., Bassilana, F., Voilley, N., and Lazdunski, M. (1995). Molecular cloning and functional expression of a novel amiloride-sensitive Na+ channel. *J. Biol. Chem.* 270, 27411–27414. doi: 10.1074/jbc.270.46.27411

Wandernoth, P. M., Raubuch, M., Mannowetz, N., Becker, H. M., Deitmer, J. W., Sly, W. S., et al. (2010). Role of carbonic anhydrase IV in the bicarbonate-mediated activation of murine and human sperm. *PLoS ONE* 5:e15061. doi: 10.1371/journal.pone.0015061

Wang, D., Hu, J., Bobulescu, I. A., Quill, T. A., McLeroy, P., Moe, O. W., et al. (2007). A sperm-specific Na+/H+ exchanger (sNHE) is critical for expression and *in vivo* bicarbonate regulation of the soluble adenylyl cyclase (sAC). *Proc. Natl. Acad. Sci. U.S.A.* 104, 9325–9330. doi: 10.1073/pnas.0611296104

Wang, D., King, S. M., Quill, T. A., Doolittle, L. K., and Garbers, D. L. (2003a). A new sperm-specific Na+/H+ Exchanger required for sperm motility and fertility. *Nat. Cell Biol.* 5, 1117–1122. doi: 10.1038/ncb1072

Wang, H., Liu, J., Cho, K.-H., and Ren, D. (2009). A novel, single, transmembrane protein CATSPERG is associated with CATSPER1 channel protein. *Biol. Reprod.* 81, 539–544. doi: 10.1095/biolreprod.109.077107

Wang, X. F., Zhou, C. X., Shi, Q. X., Yuan, Y. Y., Yu, M. K., Ajonuma, L. C., et al. (2003b). Involvement of CFTR in uterine bicarbonate secretion and the fertilizing capacity of sperm. *Nat. Cell Biol.* 5, 902–906. doi: 10.1038/ncb1047

Wasco, W. M., and Orr, G. A. (1984). Function of calmodulin in mammalian sperm: presence of a calmodulin-dependent cyclic nucleotide phosphodiesterase associated with demembranated rat caudal epididymal sperm. *Biochem. Biophys. Res. Commun.* 118, 636–642. doi: 10.1016/0006-291X(84)91350-0

Watanabe, H., Takeda, R., Hirota, K., and Kondoh, G. (2017). Lipid raft dynamics linked to sperm competency for fertilization in mice. *Genes Cells* 22, 493–500. doi: 10.1111/gtc.12491

Watanabe, H., Takeo, T., Tojo, H., Sakoh, K., Berger, T., Nakagata, N., et al. (2014). Lipocalin 2 binds to membrane phosphatidylethanolamine to induce lipid raft movement in a PKA-dependent manner and modulates sperm maturation. *Development* 141, 2157–2164. doi: 10.1242/dev.105148

Wennemuth, G., Westenbroek, R. E., Xu, T., Hille, B., and Babcock, D. F. (2000). CaV2.2 and CaV2.3 (N- and R-type) Ca2+ channels in depolarization-evoked entry of Ca2+ into mouse sperm. *J. Biol. Chem.* 275, 21210–21217. doi: 10.1074/jbc.M002068200

Wertheimer, E. V., Salicioni, A. M., Liu, W., Trevino, C. L., Chávez, J. C., Hernández-González, E. O., et al. (2008). Chloride is essential for capacitation and for the capacitation-associated increase in tyrosine phosphorylation. *J. Biol. Chem.* 283, 35539–35550. doi: 10.1074/jbc.M804586200

Westenbroek, R. E., and Babcock, D. F. (1999). Discrete regional distributions suggest diverse functional roles of calcium channel alpha1 subunits in sperm. *Dev. Biol.* 207, 457–469. doi: 10.1006/dbio.1998.9172

White, D. R., and Aitken, R. J. (1989). Relationship Between Calcium, Cyclic AMP, ATP, and lntracellular pH and the Capacity of Hamster Spermatozoa to Express Hyperactivated Motility. *Gamete Res.* 177, 163–177. doi: 10.1002/mrd.1120220205

Wiesner, B., Weiner, J., Middendorff, R., Hagen, V., Kaupp, U. B., and Weyand, I. (1998). Cyclic nucleotide-gated channels on the flagellum control Ca2+ entry into sperm. *J. Cell Biol.* 142, 473–484. doi: 10.1083/jcb.142.2.473

Woo, A. L., James, P. F., and Lingrel, J. B. (2000). Sperm motility is dependent on a unique isoform of the Na,K-ATPase. *J. Biol. Chem.* 275, 20693–20699. doi: 10.1074/jbc.M002323200

Woo, A. L., James, P. F., and Lingrel, J. B. (2002). Roles of the Na,K-ATPase α4 isoform and the Na+/H+ exchanger in sperm motility. *Mol. Reprod. Dev.* 62, 348–356. doi: 10.1002/mrd.90002

Xia, J., and Ren, D. (2009). The BSA-induced Ca2+ influx during sperm capacitation is CATSPER channel-dependent. *Reprod. Biol. Endocrinol.* 7, 119. doi: 10.1186/1477-7827-7-119

Xu, W. M., Shi, Q. X., Chen, W. Y., Zhou, C. X., Ni, Y., Rowlands, D. K., et al. (2007). Cystic fibrosis transmembrane conductance regulator is vital to sperm fertilizing capacity and male fertility. *Proc. Natl. Acad. Sci. U.S.A.* 104, 9816–9821. doi: 10.1073/pnas.0609253104

Yamaguchi, R., Muro, Y., Isotani, A., Tokuhiro, K., Takumi, K., Adham, I., et al. (2009). Disruption of ADAM3 impairs the migration of sperm into oviduct in mouse. *Biol. Reprod.* 81, 142–146. doi: 10.1095/biolreprod.108.074021

Yanagimachi, R. (1970). The movement of golden hamster spermatozoa before and after capacitation. *J. Reprod. Fertil.* 23, 193–196. doi: 10.1530/jrf.0.0230193

Yanagimachi, R. (1994). *Mammalian Fertilization*. eds J. D. Neill and E. Knobil (New York, NY: Raven Press).

Yanagimachi, R., and Chang, M. C. (1963). Fertilization of hamster eggs *in vitro*. *Nature* 200, 281–282. doi: 10.1038/200281b0

Zalata, A., Hassan, A., Christophe, A., Comhaire, F., and Mostafa, T. (2010). Cholesterol and desmosterol in two sperm populations separated on Sil-Select gradient. *Int. J. Androl.* 33, 528–535. doi: 10.1111/j.1365-2605.2009.00961.x

Zeng, X. H., Yang, C., Kim, S. T., Lingle, C. J., and Xia, X. M. (2011). Deletion of the *Slo3* gene abolishes alkalization-activated K^+ current in mouse spermatozoa. *Proc. Natl. Acad. Sci. U.S.A.* 108, 5879–5884. doi: 10.1073/pnas.1100240108

Zeng, Y., Clark, E. N., and Florman, H. M. (1995). Sperm membrane potential: hyperpolarization during capacitation regulates zona pellucida-dependent acrosomal secretion. *Dev. Biol.* 171, 554–563. doi: 10.1006/dbio.1995.1304

Zeng, Y., Oberdorf, J. A., and Florman, H. M. (1996). pH regulation in mouse sperm: identification of Na^+-, Cl^--, and HCO_3^--dependent and arylaminobenzoate-dependent regulatory mechanisms and characterization of their roles in sperm capacitation. *Dev. Biol.* 173, 510–520. doi: 10.1006/dbio.1996.0044

Zhang, Y., Malekpour, M., Al-Madani, N., Kahrizi, K., Zanganeh, M., Mohseni, M., et al. (2007). Sensorineural deafness and male infertility: a contiguous gene deletion syndrome. *J. Med. Genet.* 44, 233–240. doi: 10.1136/jmg.2006.045765

Zhang, Z., Yang, Y., Wu, H., Zhang, H. H., Zhang, H. H., Mao, J., et al. (2017). Sodium-Hydrogen-Exchanger expression in human sperm and its relationship with semen parameters. *J. Assist. Reprod. Genet.* 34, 795–801. doi: 10.1007/s10815-017-0898-2

Zhou, R., Shi, B., Chou, K. C. K., Oswalt, M. D., and Haug, A. (1990). Changes in intracellular calcium of porcine sperm during *in vitro* incubation with seminal plasma and a capacitating medium. *Biochem. Biophys. Res. Commun.* 172, 47–53. doi: 10.1016/S0006-291X(05)80171-8

Conflict of Interest Statement: The authors declare that the research was conducted in the absence of any commercial or financial relationships that could be construed as a potential conflict of interest.

frontiers in Cell and Developmental Biology

ORIGINAL RESEARCH
published: 24 July 2018
doi: 10.3389/fcell.2018.00078

Transcriptome Analysis of Long Non-coding RNAs and Genes Encoding Paraspeckle Proteins During Human Ovarian Follicle Development

Emil H. Ernst[1], *Julie Nielsen*[1†], *Malene B. Ipsen*[1†], *Palle Villesen*[2,3] *and Karin Lykke-Hartmann*[1,3,4*]

[1] Department of Biomedicine, Aarhus University, Aarhus, Denmark, [2] Bioinformatic Research Centre, Aarhus University, Aarhus, Denmark, [3] Department of Clinical Medicine, Aarhus University, Aarhus, Denmark, [4] Department of Clinical Genetics, Aarhus University Hospital, Aarhus, Denmark

OPEN ACCESS

Edited by:
Eugene V. Makeyev,
King's College London,
United Kingdom

Reviewed by:
Hongmin Qin,
Texas A&M University, United States
Xavier Roca,
Nanyang Technological University,
Singapore

***Correspondence:**
Karin Lykke-Hartmann
kly@biomed.au.dk

[†] These authors have contributed equally to this work.

Specialty section:
This article was submitted to Cell Growth and Division, a section of the journal Frontiers in Cell and Developmental Biology

Received: 14 March 2018
Accepted: 02 July 2018
Published: 24 July 2018

Citation:
Ernst EH, Nielsen J, Ipsen MB, Villesen P and Lykke-Hartmann K (2018) Transcriptome Analysis of Long Non-coding RNAs and Genes Encoding Paraspeckle Proteins During Human Ovarian Follicle Development. Front. Cell Dev. Biol. 6:78. doi: 10.3389/fcell.2018.00078

Emerging evidence indicated that many long non-coding (lnc)RNAs function in multiple biological processes and dysregulation of their expression can cause diseases. Most regulatory lncRNAs interact with biological macromolecules such as DNA, RNA, and protein. LncRNAs regulate gene expression through epigenetic modification, transcription, and posttranscription, through DNA methylation, histone modification, and chromatin remodeling. Interestingly, differential lncRNA expression profiles in human oocytes and cumulus cells was recently assessed, however, lncRNAs in human follicle development has not previously been described. In this study, transcriptome dynamics in human primordial, primary and small antral follicles were interrogated and revealed information of lncRNA genes. It is known that some lncRNAs form a complex with paraspeckle proteins and therefore, we extended our transcriptional analysis to include genes encoding paraspeckle proteins. Primordial, primary follicles and small antral follicles was isolated using laser capture micro-dissection from ovarian tissue donated by three women having ovarian tissue cryopreserved before chemotherapy. After RN sequencing, a bioinformatic class comparison was performed and primordial, primary and small antral follicles were found to express several lncRNA and genes encoding paraspeckle proteins. Of particular interest, we detected the lncRNAs *XIST*, *NEAT1, NEAT2 (MALAT1),* and *GAS5*. Moreover, we noted a high expression of *FUS*, *TAF15,* and *EWS* components of the paraspeckles, proteins that belong to the FET (previously TET) family of RNA-binding proteins and are implicated in central cellular processes such as regulation of gene expression, maintenance of genomic integrity, and mRNA/microRNA processing. We also interrogated the intra-ovarian localization of the FUS, TAF15, and EWS proteins using immunofluorescence. The presence and the dynamics of genes that encode lncRNA and paraspeckle proteins may suggest that these may mediate functions in the cyclic recruitment and differentiation of human follicles and could participate in biological processes known to be associated with lncRNAs and paraspeckle proteins, such as gene expression control, scaffold formation and epigenetic control through

human follicle development. This comprehensive transcriptome analysis of lncRNAs and genes encoding paraspeckle proteins expressed in human follicles could potentially provide biomarkers of oocyte quality for the development of non-invasive tests to identify embryos with high developmental potential.

Keywords: human follicle, lncRNA, paraspeckle, fertility, treatment

INTRODUCTION

The nuclei of mammalian cells are highly organized and composed of distinct subnuclear structures termed nuclear bodies (Naganuma and Hirose, 2013; Yamazaki and Hirose, 2015). Paraspeckles are mammalian-specific sub-nuclear bodies built on long, non-protein-coding RNA (lncRNA), *NEAT1* (nuclear-enriched abundant transcript 1), which assembles various protein components, including RNA-binding proteins of the DBHS (Drosophila behavior and human splicing) family. Paraspeckles have been proposed to control of several biological processes, such as stress responses, gene expression, and cellular differentiation. Human follicle development represents a continuous cyclic process throughout the reproductive lifespan of a woman and encompasses both cell growth and differentiation. Paraspeckles are among the most recently identified nuclear bodies and were first described in 2002 (Fox et al., 2002; Bond and Fox, 2009). The generation of paraspeckle sub-nuclear compartments has been extensively described (Naganuma and Hirose, 2013; Yamazaki and Hirose, 2015). Paraspeckles are sensitive to RNAse treatment, suggesting that their structures depend on RNAs for maintenance (Fox et al., 2002, 2005). Later the lncRNA *NEAT1* was shown to be essential for paraspeckle formation, as a knockdown of the *NEAT1* lncRNA function caused a disintegration of paraspeckles (Chen and Carmichael, 2009; Clemson et al., 2009; Sasaki et al., 2009; Sunwoo et al., 2009). Paraspeckle formation proceeds in conjunction with *NEAT1* lncRNA biogenesis and involves the cooperation of multiple paraspeckle-localized RNA-binding proteins (Naganuma and Hirose, 2013; Yamazaki and Hirose, 2015). Currently about 40 proteins are known to assemble in paraspeckles (Naganuma et al., 2012). Paraspeckle proteins include DBHS (Drosophila melanogaster behavior, human splicing) proteins, PSPC1 (paraspeckle component 1), NONO (non-POU domain-containing octamer-binding), and SFPQ [splicing factor, proline- and glutamine-rich (also known as PSF (PTB-associated splicing factor)], RNA binding motif (RBM) 14, and CPSF6 (cleavage and polyadenylation specific factor 6) [Reviewed in (Yamazaki and Hirose, 2015)]. Many paraspeckle proteins are RNA binding proteins that contain an RNA recognition motif (RRM), a KH (hnRNP K homology) domain, a RGG (glycine-arginine-rich) box, or a zinc finger motif as the RNA-binding domain. The paraspeckle proteins NONO, SFPQ, RBM14, EWS, FUS, TAF15, and TDP-43 are RNA binding proteins that mediate transcription and RNA processing (Auboeuf et al., 2005).

The paraspeckle-localized FET family of RNA-binding proteins (Bertolotti et al., 1996) consists of FUS (TLS) (Crozat et al., 1993), EWS (Delattre et al., 1992), and TAF15 (TAFII68, TAF2N, RBP56) (Crozat et al., 1993). The proteins are structurally similar and contain a number of evolutionary conserved areas such as the RRM motif, the SYGQ-rich domain, a G rich domain, a RanBP2-type zinc finger motif, and the C-terminal RGG domain (Morohoshi et al., 1998; Guipaud et al., 2006; Nguyen et al., 2011; Chau et al., 2016). The FUS, EWS, and TAF15 proteins bind RNA as well as DNA and have both unique and overlapping functions. The human FET proteins are associated with transcription (Law et al., 2006), RNA splicing, microRNA (miRNA) processing, RNA transport, and the signaling and maintenance of genomic integrity (Schwartz et al., 2015).

Several paraspeckle proteins are disease-related. For instance, NONO, SFPQ, CPSF6, EWS, FUS, TAF15, DAZAP1, RBM3, SS18L1, WT1, BCL6, BCL11A, ZNF4444, and HNRNPH1 are implicated in various types of cancer (reviewed in Yamazaki and Hirose, 2015). Some paraspeckle proteins, such as TDP-13, FUS, EWS, TAF15, HNRNPA1, SS18L1, and SFPQ have been associated with neuro-degenerative diseases, such as amyotrophic lateral sclerosis (ALS) and frontotemporal dementia (FTD) (Svetoni et al., 2016).

Paraspeckles have been described as nuclear sponges sequestering transcription factors and/or RNA-binding proteins such as lncRNAs. They are dynamic structures changing in size in response to ever changing cellular challenges/environment (Yamazaki and Hirose, 2015).

In addition to *NEAT1*, a number of lncRNAs localize to different subcellular compartments (Chen and Carmichael, 2010). *MALAT1* (*NEAT2* in human) is transcribed downstream of the *NEAT1* gene and is found specifically associated with splicing speckles (Hutchinson et al., 2007). Moreover, lncRNA have also been implicated in stem cell pluripotency and in differentiation in mice (Dinger et al., 2008). Furthermore, roles for ncRNAs in cell fate decision have been explored (Ambasudhan et al., 2011; Yoo et al., 2011; Kurian et al., 2013).

Interestingly, lncRNAs have been shown to act as chromatin modifiers (Mercer et al., 2009) and potent regulators of histone methylation (Yamazaki and Hirose, 2015), including chromatin structure modeling and the integrity of subcellular compartments (Chen and Carmichael, 2010; Wang and Chang, 2011; Wang et al., 2011; Wapinski and Chang, 2011; Yan et al., 2012; Backofen and Vogel, 2014; Joh et al., 2014; Peschansky and Wahlestedt, 2014; Liu and Pan, 2015). A previous study showed that some human lncRNAs were bound to the polycomb repressive complex 2 (PRC2) and other chromatin-modifying complexes (Khalil et al., 2009).

Several lncRNA, including *Xist*, *Tsix,* and *Xite* contribute to X chromosome inactivation, the process of ensuring dosage

regulation of X chromosome-expressed genes (Chow and Heard, 2009; Leeb et al., 2009) in a complex and highly controlled manner (Zhao et al., 2008). Furthermore, *Xist* transcription is required for maintenance of X-chromosome inactivation (Penny et al., 1996). Interestingly, another lncRNA, *RepA*, the reassembling part of the 5′UTR sequence of *Xist*, was found to associate indirectly with PRC2 (Zhao et al., 2008). The recruitment of PRC2 by *RepA* happens in competition with lncRNA *Tsix*, which acts as an antisense toward *Xist*, and the binding of *RepA* to PRC2 is inhibited by *Tsix*, and thus competes with *RepA* (Zhao et al., 2008).

In support of the developmental roles of lncRNA and paraspeckles, *Neat1* knockout (KO) mice fail to become pregnant despite normal ovulation, which was found to be a caused by corpus luteum dysfunction and concomitant low progesterone (Nakagawa et al., 2014).

The developmental capacity of the matured oocyte for generating viable offspring is determined throughout follicle development in the ovary. The integrity of the oocytes is essential in maintaining the reproductive potential of the female. Pre-ovulatory oocyte maturation is a complex process resulting from multiple interactions between the oocyte and the surrounding follicular cells (Carabatsos et al., 2000; Adhikari and Liu, 2009; Binelli and Murphy, 2010; Reddy et al., 2010; Bonnet et al., 2013). The transition from primordial to primary follicle is a key first step event in follicle development, in which the primordial follicle is believed to have escaped the resting phase and has entered the follicular growth phase (Zuccotti et al., 2011). Subsequently, the cohort of follicles must remain activated in order to enter the secondary follicle stage, and a few continue to mature to the tertiary and antral follicle stages (McGee and Hsueh, 2000). Tertiary and antral follicles are characterized by the presence of a cavity known as the antrum, and have both granulosa and theca cells present. Tertiary follicles have an extensive network of gap junctions that permits the transfer of nutrients and regulatory signals between the oocyte and the granulosa cells (Espey, 1994). Only a small fraction of the ovarian follicles present in a fetal ovary will reach ovulation (Markström et al., 2002). Identifying the factors controlling follicle development may provide a basis for the fundamental mechanisms that regulate follicle activation and could potentially lead to new therapeutics in female reproduction as well as improvements in reproductive health and productivity in women of advanced maternal age (Baird et al., 2005). As paraspeckles and the regulatory molecules sequestered within them have been shown to be of importance in development, gene expression, and epigenetic control, these nuclear structures may prove essential in human fertility and infertility.

So far, only limited reports of the potential regulatory impact of short ncRNA in follicle development exist and our knowledge of the involvement of lncRNAs in human follicle development is almost non-existent (Wilhelmm and Bernard, 2016).

Therefore, in this study, the presence of lncRNAs were interrogated bioinformatically using RNA sequencing data representative of selected stages in human follicle development. We previously developed a method for isolating pure populations of oocytes from human primordial, intermediate and primary follicles using laser capture micro-dissection microscopy (Markholt et al., 2012). From these transcriptome data (Ernst et al., 2017, 2018), *in silico* extraction of data for lncRNAs. We identified the presence of the paraspeckle forming lncRNAs *NEAT1* and *NEAT2* as well as several other lncRNAs, such as *XIST*. As the discovery of *NEAT1* and *NEAT2* in early ovarian follicles suggested the presence of paraspeckle proteins, we further asked if genes encoding these proteins would also be present during human ovarian follicle development. We found the transcripts encoding the well-characterized FUS, EWS, and TAF15 highly expressed during early ovarian follicle development. We further employed immunohistochemistry in human ovary tissue to explore the presence and intraovarian localization of FUS, EWS, and TAF15 proteins to be present.

In summary, we identified the presence of several lncRNAs and genes encoding paraspeckle proteins not previously reported for human ovarian follicle development. This may hint that the functions of lncRNAs and paraspeckle proteins could indeed be relevant to oocyte physiology and development.

MATERIALS AND METHODS

Procurement of Human Ovarian Cortex and Isolation of Oocytes and Supportive Somatic Cells

We procured human ovarian cortex tissue from the Danish Cryopreservation Programme offering cryopreservation as means of fertility preservation prior to gonadotoxic chemotherapy (Rosendahl et al., 2011). Oocyte samples were obtained from ovarian cortical tissue procured from three patients who underwent unilateral oophorectomy prior to gonadotoxic treatment for a malignant disease (unrelated to any ovarian malignancies). Patients were normo-ovulatory, with normal reproductive hormones, and not received ovarian stimulation with exogenous gonadotropins. All methods were carried out in accordance with relevant guidelines and regulations, and The Central Denmark Region Committees on Biomedical Research Ethics and the Danish Data Protection Agency approved the study. Written informed consent was obtained from all participants before inclusion. Patients consented to the research conducted. In subjects undergoing oophorectomy, a small piece of the ovarian cortex is used for evaluating the ovarian reserve, and for research purposes (Danish Scientific Ethical Committee Approval Number: KF 299017 and J/KF/01/170/99) (Schmidt et al., 2003).

Laser Capture Micro-Dissection (LCM)

The LCM procedure to isolate staged oocytes and follicles was performed as previously described (Markholt et al., 2012; Ernst et al., 2017, 2018). Briefly, the ovarian cortical fragments, which had a size of 2 × 2 × 1 mm, were thawed and fixed by direct immersion into 4% paraformaldehyde (PFA) at 4°C for 4 h followed by dehydration and embedding in paraffin. Paraffin blocks were stored at −80°C until use. The blocks were cut into 15 μm thick sections on a microtome (Leica Microsystems, Wetzlar, Germany). Diethylpyrocarbonate

(DEPC)-treated water was used in the microtome bath to avoid RNA degradation. The sections were mounted on RNase-free membrane glass slides (Molecular Devices, Sunnyvale, CA, USA) and immediately processed. Consecutively, the slides were de-paraffinized, stained, and dehydrated immediately before micro-dissection: Xylene (VWR—Bieog Berntsen, Herlev, Denmark) (5 min), 99.9% ethanol (Merck, Darmstadt, Germany) (5 min), 99.9% ethanol (5 min), 96% ethanol (5 min), 70% ethanol (5 min), DEPC-treated water (5 min), hematoxylin (Merck, Darmstadt, Germany) (5 min), DEPC-treated water (immersion), 70% ethanol (30 s), 96% ethanol (30 s), 99.9% ethanol (30 s), 99.9% ethanol (30 s), xylene (1 min), and xylene (5 min). All solutions were prepared with DEPC-treated water. LCM was performed using the Veritas™ Microdissection Instrument Model 704 (ArcturusXT™, Molecular Devices, Applied Biosystems®, Life Technologies, Foster City, CA, U.S.A.). The cells were isolated based on morphological appearance. Primordial oocytes were defined as an oocyte surrounded by 3–5 flattened pre-granulosa cells, and primary oocytes were defined as an oocyte surrounded by one layer of cuboidal granulosa cells. Antral follicles were defined as a follicle with an antral cavity. For the antral follicle to be eligible for isolation, we should be able to morphologically differentiate between the oocyte, the mural granulosa cells and the theca cell layer. In the antral stage the large size of the different compartments enabled us to isolate each compartment individually. An outline surrounding the cell(s) of interest was marked and subsequently cut using the ultraviolet laser. Following this the use of membrane glass slides (Arcturus® PEN Membrane Glass Slides, Applied Biosystems, Life Technologies, Foster City, CA, U.S.A.) enabled us to lift the isolate onto a sterile cap (Arcturus® CapSure® HS LCM Caps, Applied Biosystems, Life Technologies, Foster City, CA, U.S.A.) using infrared pulses. Isolated cells were inspected on the cap to ensure that no contamination from surrounding unwanted cells was present. From each of the three patients, several isolations were made (**Table 1**, **Figure 1**). RNA isolation, library preparation and

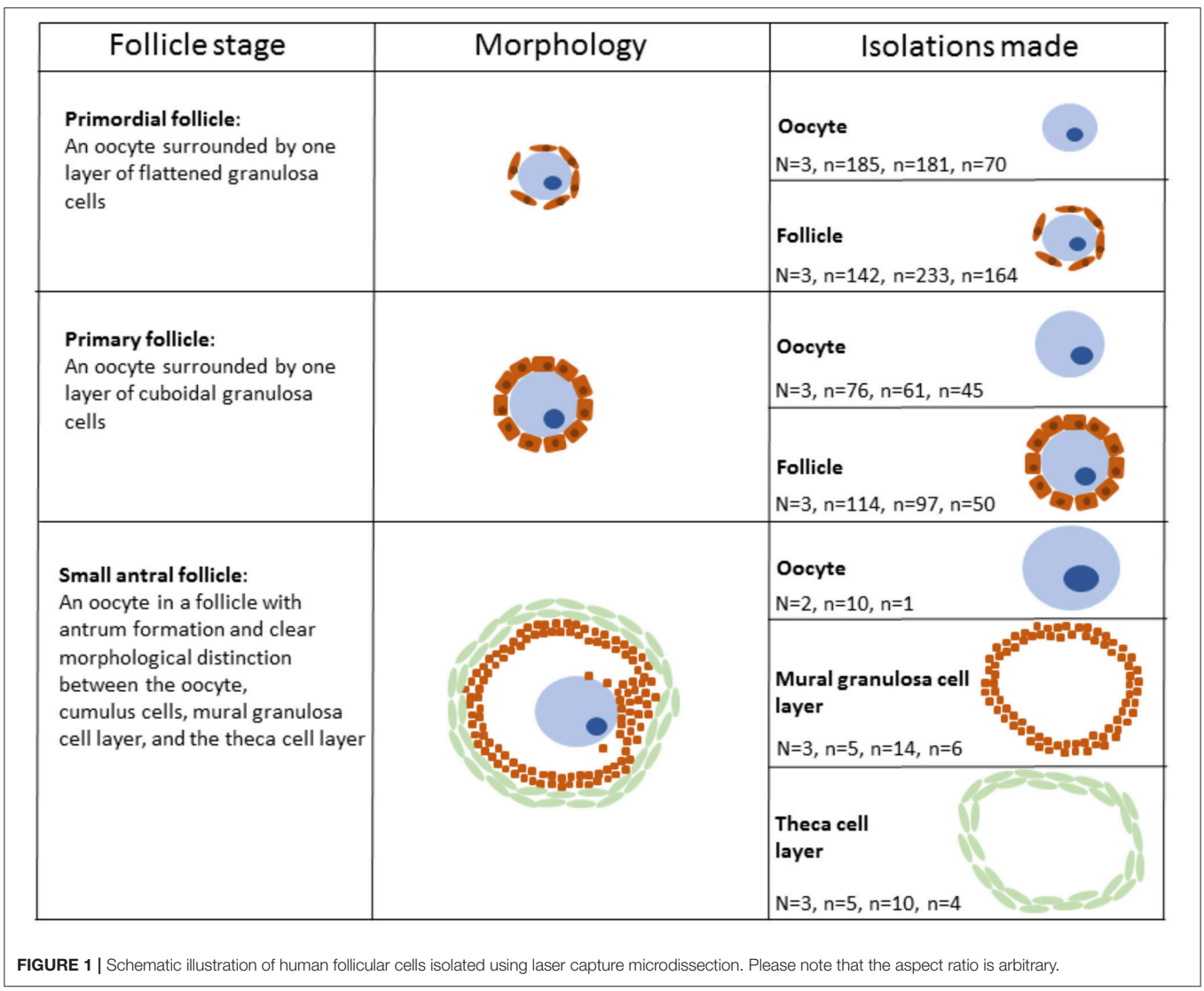

FIGURE 1 | Schematic illustration of human follicular cells isolated using laser capture microdissection. Please note that the aspect ratio is arbitrary.

TABLE 1 | Numbers of oocytes, follicles, and other somatic cells analyzed in RNA–seq. in three different patients.

Cell type and Follicular Stages	No. of laser-collected cells from three patients respectively
Oocytes from primordial follicles	$N = 3$, $n = 185$, $n = 181$, $n = 70$
Primordial follicles	$N = 3$, $n = 142$, $n = 233$, $n = 164$
Oocytes from primary follicles	$N = 3$, $n = 76$, $n = 61$, $n = 45$
Primary follicles	$N = 3$, $n = 114$, $n = 97$, $n = 50$
Mural granulosa cell layers from small antral follicles	$N = 3$, $n = 5$, $n = 14$, $n = 6$
Theca cell layers from small antral follicles	$N = 3$, $n = 5$, $n = 10$, $n = 4$
Oocytes from small antral follicles*1	$N = 2$, $n = 10$, $n = 1$

*1 *Based on duplicate samples.*

sequencing, mapping and statistical analysis and bioinformatics were performed as described (Ernst et al., 2017, 2018).

Library Preparation and Sequencing

RNA was extracted from the LCM-derived samples, converted to cDNA and subjected to linear amplification [Ovation® RNA-Seq System V2 kit (NuGen Inc., San Carlos, CA, U.S.A.)]. RNA-seq libraries (constructed from the output cDNA using Illumina TruSeq DNA Sample and Preparation kit (Illumina, San Diego, CA, USA, according to AROS Applied Biotechnology, now Eurofins (https://www.eurofinsgenomics.eu/). Integrity of libraries was verified on library yield via KAPA qPCR measurement, and Agilent Bioanalyzer 2100 peak size with a RNA 6000 Nano Lab Chip (Agilent Technologies, Santa Clare, CA, U.S.A.) during different library preparation stages. Sequencing was performed on an Illumina HiSeq2000 platform (Illumina Inc., San Diego, CA, U.S.A.) with 5 random samples per lane (AROS Applied Biotechnology).

Mapping and Statistical Analysis

Using Tophat (2.0.4), and Cufflinks (2.0.2) BAM files were generated to create a list of expressed transcripts in the samples. BWA (0.6.2) was subsequently used to map all readings to the human reference genome (hg19) using the transcript list as a filter so only readings mapping to RefSeq exons [incl. non-coding RNA, and mitochondrial RNA) overlapping with expressed transcripts were used. Expression of each gene in a given sample was normalized and transformed to a measurement of log2 (counts per million (CPM)]. On the basis of log2 (CPM), fragments per kilobase of exon per million fragments mapped (FPKM) values were calculated, and further filtered using custom analysis in R [R Development Core Team. R: A language and environment for statistical computing. R Foundation for Statistical Computing, Vienna, Austria. URL http://www.R-project.org] (R Core Team, 2012).

Output From Statistical Analysis

The mean FPKM value for all ncRNA transcripts was calculated using a one-sample *t*-test on FPKM values for each identified transcript from patient triplicates (two for oocytes from small antral follicles) (Resource Data) (http://users-birc.au.dk/biopv/published_data/ernst_et_al_ncRNAs_2018/).

Cell Specific Consistently Expressed Genes (CSCEG) were defined as one-sample *t*-test *p*-value < 0.05 [(Resource Data), in gray]. *In silico* merging of transcriptomes from three patients was performed to account for biological variance. The transcripts in the CSCEG list were ranked based on *p*-value, with low *p*-value indicating a high degree of consistency in FPKM gene expression level between patients for the given isolate type. Full lists of ncRNAs detected in human follicle development is availiable (**Supplementary Table 1**).

Furthermore, we generated a list of all known paraspeckle proteins based on annotated protein-coding RNAs detected (**Table 2**) and non-coding RNAs (**Table 3**). Some of these data (oocytes and granulosa cells from primordial and primary follicles) has previously been published with a different focus in a global expression profile study (Ernst et al., 2017, 2018).

Immunofluorescence Microscopy

Human ovarian cortical tissue was cut in 5 μm sections and mounted on glass slides. Dehydration and antigen retrieval was performed as described elsewhere (Stubbs et al., 2005) followed by serum block (30 min), then the primary antibody; (1/200) anti-TAFII68 Rabbit pAb (Bethyl Laboratories, #IHC-00094), (1/500) anti-FUS Rabbit pAb (Bethyl Laboratories, #A300-302A), or (1/200) anti-EWS Rabbit pAb (Bethyl Laboratories, #IHC-00086) overnight at 4°C. The sections were then incubated in a 1:700 dilution of secondary antibody (Donkey-anti-Rabbit) conjugated with Alexa Fluor 488 Dye (Life Technologies). Finally, sections were incubated in 1/7500 Hoechst (Life Technologies) followed by mounting with Dako Fluorescent Mounting Medium (Agilent Technologies, Santa Clara, CA, U.S.A.) and analyzed using a LSM510 laser-scanning confocal microscope using a 63x C-Apochromat water immersion objective NA 1.2 (Carl Zeiss, Göttingen, Germany) and ZEN 2011 software (Carl Zeiss, Göttingen, Germany).

RESULTS

Laser-Isolation of Oocytes and Somatic Cells During Human Follicle Development

Specific isolates of oocytes and follicles (oocytes with surrounding somatic granulosa cells) from the primordial and primary stage, respectively, as well as oocytes, mural granulosa cells, and theca cells from small antral follicles were collected via Laser Capture Microdissection (LCM). Each stage was isolated on the basis of stringent morphological criteria (Gougeon, 1996) (**Figure 1).** Primordial follicles were defined as an oocyte surrounded by one layer of flattened granulosa cells (**Figure 1**) and primary follicles were defined as an oocyte surrounded by a single layer of cubic granulosa cells (**Figure 1**). Small antral follicles were defined based on the presence of a follicular antrum with a clear distinction between the oocyte, the mural granulosa cells and the theca cell layer (**Figure 1**) The samples (1,473 isolates) of cells from primordial, primary, and small antral follicles were pooled into 20 samples (**Table 1**, **Figure 1**). These 20 samples were then subjected to RNA

TABLE 2 | Expression of paraspeckle-protein encoding mRNAs in human follicle development.

Ensemble	Symbol	Oocytes from primordial follicles, FPKM mean	*t*-test (*p*-value)	Primordial follicles, FPKM mean	*t*-test (p-value)
PRIMORDIAL FOLLICLES					
ENSG00000126705	AHDC1	ND	ND	0.195	0.423
ENSG00000011243	AKAP8L	2.094	0.366	0.347	0.423
ENSG00000140488	CELF6	ND	ND	ND	ND
ENSG00000099622	CIRBP	1.826	0.053	2.486	0.059
ENSG00000111605	CPSF6	3.718	0.033	4.289	0.064
ENSG00000149532	CPSF7	2.089	0.351	2.739	0.003
ENSG00000071626	DAZAP1	1.817	0.408	1.368	0.192
ENSG00000064195	DLX3	ND	ND	ND	ND
ENSG00000182944	**EWS/EWSR1**[*1]	5.765	0.073	6.132	0.173
ENSG00000119812	FAM98A	1.727	0.235	2.013	0.188
ENSG00000182263	FIGN	0.284	0.187	2.842	0.184
ENSG00000089280	**FUS**[*1]	3.150	0.149	3.150	0.146
ENSG00000139675	HNRNPA1L2	0.029	0.423	0.060	0.423
ENSG00000169813	HNRNPF	2.550	0.028	3.836	0.085
ENSG00000169045	HNRNPH1	3.410	0.017	6.310	0.002
ENSG00000096746	HNRNPH3	3.177	0.171	3.178	0.199
ENSG00000165119	HNRNPK	5.365	0.068	5.511	0.060
ENSG00000125944	HNRNPR	4.346	0.107	3.778	0.127
ENSG00000105323	HNRNPUL1	4.041	0.005	6.086	0.007
ENSG00000176624	MEX3C*1	1.365	0.204	3.570	0.160
ENSG00000147140	NONO*1	2.160	0.189	4.367	0.089
ENSG00000167005	NUDT21	4.365	0.155	5.401	0.065
ENSG00000121390	PSPC1	1.709	0.274	3.114	0.189
ENSG00000102317	RBM3	0.475	0.238	0.586	0.423
ENSG00000268489	RBM3	ND	ND	ND	ND
ENSG00000173914	RBM4B	1.878	0.359	1.489	0.400
ENSG00000076053	RBM7	1.519	0.330	1.191	0.222
ENSG00000244462	RBM12	4.391	0.106	4.400	0.112
ENSG00000239306	RBM14	1.072	0.207	1.164	0.394
ENSG00000147274	RBMX	4.218	0.117	3.981	0.122
ENSG00000020633	RUNX3	ND	ND	0.054	0.423
ENSG00000116560	SFPQ	4.459	0.025	5.770	0.071
ENSG00000188529	SRSF10	1.465	0.373	3.245	0.109
ENSG00000184402	SS18L1	0.083	0.423	1.002	0.213
ENSG00000172660	**TAF15**[*1]	1.303	0.172	2.055	0.226
ENSG00000143569	UBAP2L	7.856	0.006	7.315	0.006
ENSG00000188177	ZC3H6	6.564	0.002	2.015	0.365

Ensemble	Symbol[*1]	Oocytes from primary follicles		Primary follicles	
		FPKM mean	*t*-test (*p*-value)	FPKM mean	*t*-test (*p*-value)
PRIMARY FOLLICLES					
ENSG00000198026	ZNF335	ND	ND	1.216	0.423
ENSG00000120948	TARDBP	5.408	0.131	4.119	0.112
ENSG00000126705	*AHDC1*	0.883	0.423	ND	ND
ENSG00000011243	*AKAP8L*	ND	ND	ND	ND
ENSG00000140488	*CELF6*	1.933	0.186	4.296	0.196
ENSG00000099622	*CIRBP*	2.339	0.359	1.864	0.423
ENSG00000111605	*CPSF6*	1.331	0.246	3.621	0.189

(Continued)

TABLE 2 | Continued

Ensemble	Symbol*1	Oocytes from primary follicles		Primary follicles	
		FPKM mean	*t*-test (*p*-value)	FPKM mean	t-test (p-value)
PRIMARY FOLLICLES					
ENSG00000149532	*CPSF7*	0.208	0.423	1.386	0.399
ENSG00000071626	*DAZAP1*	ND	ND	ND	ND
ENSG00000064195	*DLX3*	4.564	0.087	5.184	0.185
ENSG00000182944	***EWS/EWSR1****2,3	0.835	0.423	1.826	0.409
ENSG00000119812	*FAM98A*	2.007	0.423	1.189	0.401
ENSG00000182263	*FIGN*	2.666	0.066	2.451	0.268
ENSG00000089280	***FUS****2,3	0.158	0.204	0.439	0.423
ENSG00000139675	*HNRNPA1L2*	3.494	0.280	3.308	0.147
ENSG00000169813	*HNRNPF*	2.572	0.176	4.849	0.118
ENSG00000169045	*HNRNPH1*	6.586	0.022	2.636	0.287
ENSG00000096746	*HNRNPH3*	4.526	0.097	3.360	0.217
ENSG00000165119	*HNRNPK*	0.554	0.244	3.590	0.195
ENSG00000125944	*HNRNPR*	2.285	0.110	2.451	0.185
ENSG00000105323	*HNRNPUL1*	1.790	0.336	3.198	0.184
ENSG00000176624	*MEX3C**1	3.151	0.046	3.493	0.167
ENSG00000147140	*NONO**1	4.165	0.201	5.300	0.047
ENSG00000167005	*NUDT21*	1.994	0.312	3.174	0.199
ENSG00000121390	*PSPC1*	1.712	0.133	1.077	0.374
ENSG00000102317	*RBM3*	ND	ND	ND	ND
ENSG00000268489	*RBM3*	2.873	0.253	1.890	0.409
ENSG00000173914	*RBM4B*	0.654	0.423	0.161	0.259
ENSG00000076053	*RBM7*	5.893	0.057	5.262	0.177
ENSG00000244462	*RBM12*	0.952	0.423	0.716	0.353
ENSG00000239306	*RBM14*	4.337	0.019	3.784	0.175
ENSG00000147274	*RBMX*	ND	ND	ND	ND
ENSG00000020633	*RUNX3*	5.408	0.027	4.258	0.206
ENSG00000116560	*SFPQ*	3.097	0.160	4.403	0.176
ENSG00000188529	*SRSF10*	0.564	0.423	0.5280	0.374
ENSG00000184402	*SS18L1*	0.411	0.423	2.030	0.306
ENSG00000172660	***TAF15****1	7.527	0.013	7.630	0.002
ENSG00000143569	*UBAP2L*	4.010	0.184	2.057	0.411
ENSG00000188177	*ZC3H6*	ND	ND	0.911	0.423
ENSG00000198026	*ZNF335*	1.576	0.378	2.515	0.393
ENSG00000120948	*TARDBP*	ND	ND	ND	ND

Ensemble	Symbol	Mural garnulosa cell layer		Theca cell layer	
		FPKM mean	*t*-test (*p*-value)	FPKM mean	*t*-test (*p*-value)
SMALL ANTRAL FOLLICLES					
ENSG00000126705	*AHDC1*	1.967	0.333	0.955	0.134
ENSG00000011243	*AKAP8L*	1.100	0.132	2.477	0.103
ENSG00000140488	*CELF6*	ND	ND	0.181	0.423
ENSG00000099622	*CIRBP*	3.468	0.017	4.523	0.021
ENSG00000111605	*CPSF6*	4.481	0.022	3.007	0.039
ENSG00000149532	*CPSF7*	4.775	0.001	1.925	0.075
ENSG00000071626	*DAZAP1*	1.899	0.063	1.419	0.045
ENSG00000064195	*DLX3*	ND	ND	ND	ND
ENSG00000182944	***EWS/EWSR1***	8.561	0.001	6.354	0.009

(Continued)

TABLE 2 | Continued

Ensemble	Symbol	Mural garnulosa cell layer		Theca cell layer	
		FPKM mean	*t*-test (*p*-value)	FPKM mean	*t*-test (*p*-value)
SMALL ANTRAL FOLLICLES					
ENSG00000119812	*FAM98A*	3.164	0.057	4.066	0.025
ENSG00000182263	*FIGN*	3.326	0.018	3.210	0.023
ENSG00000089280	***FUS***	4.624	0.003	3.323	0.077
ENSG00000139675	*HNRNPA1L2*	1.234	0.136	1.193	0.263
ENSG00000169813	*HNRNPF*	3.712	0.004	4.046	0.001
ENSG00000169045	*HNRNPH1*	6.458	0.011	6.056	0.004
ENSG00000096746	*HNRNPH3*	4.316	0.033	3.635	0.014
ENSG00000165119	*HNRNPK*	5.862	0.004	5.249	1.7237E-05
ENSG00000125944	*HNRNPR*	5.096	0.011	4.504	0.014
ENSG00000105323	*HNRNPUL1*	6.769	0.002	5.058	0.049
ENSG00000176624	*MEX3C*	5.705	0.006	2.639	0.036
ENSG00000147140	*NONO*	6.395	0.002	5.664	0.027
ENSG00000167005	*NUDT21*	5.327	0.015	3.735	0.131
ENSG00000121390	*PSPC1*	2.929	0.086	4.015	0.003
ENSG00000102317	*RBM3*	3.057	0.104	4.013	0.033
ENSG00000268489	*RBM3*	ND	ND	ND	ND
ENSG00000173914	*RBM4B*	2.125	0.140	1.097	0.078
ENSG00000076053	*RBM7*	1.148	0.190	0.728	0.200
ENSG00000244462	*RBM12*	5.530	0.028	4.575	0.017
ENSG00000239306	*RBM14*	0.882	0.028	1.247	0.192
ENSG00000147274	*RBMX*	5.781	0.011	4.702	0.017
ENSG00000020633	*RUNX3*	ND	ND	ND	ND
ENSG00000116560	*SFPQ*	6.759	0.009	5.362	0.014
ENSG00000188529	*SRSF10*	3.181	0.149	3.040	0.054
ENSG00000184402	*SS18L1*	0.916	0.317	0.856	0.212
ENSG00000172660	***TAF15***	3.400	0.060	3.245	0.001
ENSG00000143569	*UBAP2L*	6.232	0.001	5.205	0.032
ENSG00000188177	*ZC3H6*	2.827	0.066	2.762	0.195
ENSG00000198026	*ZNF335*	0.811	0.110	0.143	0.245
ENSG00000120948	*TARDBP*	4.411	0.028	3.083	0.097

Ensemble	Symbol	Oocytes from small antral follicles	
		FPKM mean	*t*-test (*p*-value)
ENSG00000126705	*AHDC1*	0.416	0.5
ENSG00000011243	*AKAP8L*	ND	ND
ENSG00000140488	*CELF6*	ND	ND
ENSG00000099622	*CIRBP*	2.916	0.444
ENSG00000111605	*CPSF6*	0.871	0.272
ENSG00000149532	*CPSF7*	2.361	0.429
ENSG00000071626	*DAZAP1*	0.294	0.5
ENSG00000064195	*DLX3*	ND	ND
ENSG00000182944	***EWS/EWSR1***	8.638	0.149
ENSG00000119812	*FAM98A*	0.307	0.320
ENSG00000182263	*FIGN*	0.238	0.5
ENSG00000089280	***FUS***	4.790	0.253
ENSG00000139675	*HNRNPA1L2*	0.190	0.5
ENSG00000169813	*HNRNPF*	5.995	0.232

(Continued)

TABLE 2 | Continued

Ensemble	Symbol	Oocytes from small antral follicles	
		FPKM mean	*t*-test (*p*-value)
ENSG00000169045	*HNRNPH1*	4.243	0.050
ENSG00000096746	*HNRNPH3*	4.087	0.375
ENSG00000165119	*HNRNPK*	3.696	0.359
ENSG00000125944	*HNRNPR*	6.266	0.169
ENSG00000105323	*HNRNPUL1*	2.232	0.424
ENSG00000176624	*MEX3C*	3.173	0.5
ENSG00000147140	*NONO*	3.516	0.381
ENSG00000167005	*NUDT21*	3.383	0.452
ENSG00000121390	*PSPC1*	2.223	0.5
ENSG00000102317	*RBM3*	0.069	0.5
ENSG00000268489	*RBM3*	ND	ND
ENSG00000173914	*RBM4B*	2.100	0.5
ENSG00000076053	*RBM7*	ND	ND
ENSG00000244462	*RBM12*	4.552	0.436
ENSG00000239306	*RBM14*	0.069	0.5
ENSG00000147274	*RBMX*	3.804	0.258
ENSG00000020633	*RUNX3*	ND	ND
ENSG00000116560	*SFPQ*	5.167	0.116
ENSG00000188529	*SRSF10*	3.538	0.5
ENSG00000184402	*SS18L1*	ND	ND
ENSG00000172660	*TAF15*	2.933	0.442
ENSG00000143569	*UBAP2L*	3.791	0.457
ENSG00000188177	*ZC3H6*	4.146	0.189
ENSG00000198026	*ZNF335*	0.069	0.5
ENSG00000120948	*TARDBP*	5.918	0.025

[1] Genes alphabetically sorted.
*[2] Genes presented in Heatmap (**Figure 2**).*
*[3] Transcripts in bold are used in immunofluorescence (**Figures 3–5**).*

sequencing using the IlluminaHiSeq2000 sequencing platform (Illumina Inc., San Diego, CA, U.S.A.) at an external sequencing facility (AROS Applied Biotechnology, Aarhus, Denmark). We previously validated the expression pattern for various RNAs in the present RNA seq. dataset using RT-qPCR (Ernst et al., 2017, 2018). The RNA sequencing yielded on average 35.3 million reads per sample (range: 31.8–39.6 million reads) and was mapped to the human genome (hg19) (average number of reads mapped: 31.7 million, range: 29.4–34.0). Gene expression was calculated as FPKM by a custom R script (Ernst et al., 2017, 2018).

Transcriptional Profiles of Genes Encoding Paraspeckle Proteins Across Different Follicle Stages

The expression of 39 genes encoding paraspeckle proteins (Naganuma et al., 2012) was interrogated during human follicle development (**Table 2**). The highest expression of paraspeckle genes in the primordial follicle stage, based on FPKM values, were *EWS*, *HNRNPK*, *ZC3H6*, *UBAP2L*, and *TARDBP* (**Table 2**). Several other genes encoding paraspeckle proteins were present (e.g., *MEX3C*, *FUS*, *TAF15*, *CPSF6*, *NUDT21*, *RBM12*, *RBMX*, *DLX3*).

Interestingly, the expression of *ZC3H6* appears to be downregulated from primordial to primary follicles, indicating a specific function associated with the primordial follicle. The *EXSR1* gene expression remains high and upregulated in small antral follicles. *NONO* was noted to be upregulated as follicle development advances, with the highest expression detected in the somatic cells in the small antral follicle (**Table 2**).

A heatmap of FPKM data for selected genes encoding paraspeckle genes was generated to show the expression for the two different cell-stages in isolates - and the correlation between cell-specific isolates (**Figure 2**).

Intra-ovarian Distribution of Paraspeckle Proteins TAF15, EWS, and FUS

The gene products of *TAF15*, *EWS,* and *FUS* were selected for immunofluorescent staining (IMF) (bold in **Table 2**) to reveal their localization in human ovarian sections.

The TAF15 translational product was expressed in both oocytes and follicles from primordial, primary, and small antral stages, with a particular high expression in oocytes

TABLE 3 | Long non-coding RNAs ($p < 0.05$) in human follicle development.

Oocytes from primordial follicles			Primordial follicle		
Symbol*1	**FPKM mean**	***t*-test (*p*-value)**	**Symbol**	**FPKM mean**	***t*-test (*p*-value)**
PRIMORDIAL FOLLICLES					
ADCY10P1	0.763	0.046	BDNF-AS	2.395	0.017
LINC00485	2.7643	0.046	FGD5-AS1	3.335	0.013
LINC00924	0.171	0.015	GLG1	2.640	0.007
LINC01128	5.889	0.009	LINC00221	3.800	0.012
LINC01511	6.533	0.019	LINC00485	2.770	0.007
LOC100129434	6.859	0.0036	LINC00707	4.801	0.041
LOC100507557	3.783	0.005	LINC01483	2.976	0.040
LOC101927487	4.044	0.036	LOC100129434	6.765	0.012
LOC101928137	2.656	0.029	LOC100506885	3.548	0.028
LOC101929128	4.250	0.023	LOC100507156	2.776	0.013
LOC101929567	4.773	0.014	LOC100507557	2.443	0.018
LOC101929612	3.972	0.005	LOC101926943	1.428	0.008
LOC102467226	0.335	0.016	LOC101927487	3.216	0.035
LOC284798	2.494	0.002	LOC101928137	1.999	0.012
MALAT1	7.954	0.006	LOC101929567	3.513	0.033
MIR3609	5.490	0.012	LOC101929612	3.197	0.005
MIR99AHG	0.262	0.016	LOC440300	1.490	0.041
NPY6R	0.211	0.013	LOC643201	4.491	0.034
OIP5-AS1	4.190	0.029	MALAT1	8.992	0.026
RN7SK	11.285	0.005	MGC32805	0.219	0.039
RN7SL2	8.794	0.012	MIR4426	0.622	0.018
RPS3A	1.279	0.021	OIP5-AS1	5.527	0.033
UGDH-AS1	6.637	0.013	RN7SK	11.227	0.001
XIST	5.393	0.026	RN7SL2	8.9514	0.001
			RPL13AP5	2.322	0.002
			RPL21P28	0.582	0.012
			RPS3A	1.118	0.043
			SCARNA7	5.888	0.039
			SLC8A1-AS1	5.409	0.007
			SYN2	4.108	0.043
			TUNAR	3.893	0.047
			UBXN8	2.491	0.050
			UGDH-AS1	6.382	0.006
			XIST	8.236	0.003
			ZFAS1	4.296	0.014
			ZNF252P	3.537	0.038
Oocytes from primary follciles			**Primary follicle**		
Symbol	**FPKM mean**	***t*-test (*p*-value)**	**Symbol**	**FPKM mean**	***t*-test (*p*-value)**
PRIMARY FOLLICLES					
BCAR4	4.563	0.008	CEACAM22P	0.182	0.033
LINC00485	1.902	0.002	GLG1	1.270	0.046
LINC00665	4.298	0.046	KIZ	4.874	0.014
LINC01511	4.625	0.016	LINC01511	5.425	0.028
LOC100129434	6.444	0.011	LOC100129434	5.792	0.047
LOC100506885	2.187	0.039	LOC100507557	1.854	0.041
LOC101926943	1.548	0.044	LOC101927487	3.822	0.007

(Continued)

TABLE 3 | Continued

Oocytes from primary follciles			Primary follicle		
Symbol	**FPKM mean**	***t*-test (*p*-value)**	**Symbol**	**FPKM mean**	***t*-test (*p*-value)**
PRIMARY FOLLICLES					
LOC101927337	2.226	0.014	LOC101929567	4.053	0.049
LOC101929491	0.330	0.004	LOC101929612	3.456	0.010
LOC101929567	4.287	0.008	MALAT1	9.345	0.016
LOC101929612	3.152	0.016	NEXN-AS1	0.534	0.046
LOC102546299	2.551	0.001	OIP5-AS1	5.950	0.017
MALAT1	9.614	0.001	RN7SK	11.308	0.004
MEG3	0.220	0.024	RN7SL2	8.743	0.001
MIR3609	3.887	0.012	RPL13AP5	2.877	0.003
MIR4426	0.595	0.020	RPL21P28	0.868	0.008
RN7SK	11.845	0.001	RPL21P28	2.165	0.032
RN7SL2	9.110	0.004	SNORD89	1.513	0.034
RPL13AP5	1.418	0.011	UGDH-AS1	6.216	0.016
RPL21P28	0.916	0.047	XIST	7.610	0.030
RPS3A	0.894	0.007	ZFAS1	5.249	0.005
SCARNA7	5.424	0.009			
UGDH-AS1	6.397	0.003			
XIST	6.751	0.014			
ZNF518A	2.983	0.018			
Mural granulosa cell			**Theca cells**		
Symbol	**FPKM mean**	***t*-test (*p*-value)**	**Symbol**	**FPKM mean**	***t*-test (*p*-value)**
SMALL ANTRAL					
ANP32AP1	0.683	0.009	ANKRD36B	2.277	0.020
CASP8AP2	3.530	0.034	BCYRN1	2.661	0.034
CROCCP2	1.453	0.006	BDNF-AS	2.317	0.033
EBLN3	3.812	0.002	CD27-AS1	2.007	0.041
FGD5-AS1	4.032	0.019	CLEC2D	1.283	0.027
GOLGA6L5P	1.750	0.015	CSNK1A1	2.753	0.001
H3F3AP4	2.121	0.027	CTBP1-AS2	2.457	0.028
LINC00657	5.467	0.009	FGD5-AS1	3.506	0.045
LINC01128	4.413	0.018	FLJ42627	0.239	0.000
LINC01420	2.152	0.012	H3F3AP4	2.185	0.014
LOC100129434	3.831	0.025	HCG18	3.976	0.035
LOC100131564	2.425	0.024	HERC2P3	0.111	0.017
LOC100507557	1.904	0.028	LINC00485	1.467	0.049
LOC101927027	1.875	0.003	LINC00657	4.740	0.009
LOC101929124	3.0195	0.010	LINC01128	3.643	0.020
LOC101929612	3.418	0.007	LINC01133	0.111	0.017
LOC102477328	0.135	0.020	LOC100129434	4.893	0.008
LOC150776	3.000	0.002	LOC101929612	3.455	0.001
LOC643201	3.740	0.013	LOC102724699	0.420	0.021
LOC646762	2.431	0.008	MAGI2-AS3	2.791	0.020
LOC728554	1.619	0.023	MALAT1	10.73	0.000
MALAT1	9.495	0.006	MEG3	7.602	0.001
MIR3609	5.033	0.001	MIR3609	4.974	0.009
MIR99AHG	3.823	0.014	MIR4426	0.504	0.043
OIP5-AS1	5.926	0.003	MIR99AHG	5.083	0.008
PCBP1-AS1	2.541	0.029	NCBP2-AS2	0.824	0.001

(Continued)

TABLE 3 | Continued

Mural granulosa cell			Theca cells		
Symbol	**FPKM mean**	***t*-test (*p*-value)**	**Symbol**	**FPKM mean**	***t*-test (*p*-value)**
SMALL ANTRAL					
PIGBOS1	1.804	0.011	NEXN-AS1	0.735	0.025
PKI55	4.600	0.000	NKAPP1	3.545	0.032
RN7SK	10.395	0.002	OIP5-AS1	4.636	0.039
RN7SL2	8.088	0.004	PCBP1-AS1	4.558	0.009
RPL13AP5	2.509	0.006	PDIA3P1	0.450	0.016
RPL21P28	2.293	0.012	PGM5P2	1.302	0.028
RPL21P28	0.589	0.026	PKI55	4.791	0.024
RPL34P6	0.405	0.013	PTOV1-AS1	2.060	0.001
RPS3A	2.326	0.001	RN7SK	10.57	0.005
SCAND2P	1.312	0.014	RN7SL2	8.740	0.006
SCARNA7	5.104	0.016	RNU4-2	4.075	0.007
SNHG17	3.099	0.018	RPL13AP5	2.816	0.011
TMEM120A	3.042	0.002	RPL21P28	2.840	0.006
TUG1	6.0234	0.003	RPL21P28	1.081	0.017
UGDH-AS1	3.874	0.031	RPL34P6	0.844	0.019
XIST	8.056	0.004	RPS3A	1.846	0.010
ZFAS1	5.124	0.005	SCARNA7	5.588	0.026
ZNF761	4.206	0.017	SDHAP2	2.223	0.001
ZNF826P	0.990	0.018	SH3BP5-AS1	2.069	0.008
			SNORA23	0.659	0.007
			SNORA79	1.713	0.039
			SNORD89	2.354	0.017
			SPON1	3.979	0.030
			THUMPD3-AS1	0.829	0.049
			TMEM120A	1.996	0.042
			TUG1	6.154	0.008
			UBXN8	4.509	0.006
			UGDH-AS1	4.596	0.000
			XIST	8.474	0.001
			ZFAS1	4.881	0.013
			ZNF252P	1.822	0.012
			ZNF518A	2.901	0.020
			ZSCAN26	3.800	0.007
Oocyte from small antral follicle					
Symbol	**FPKM mean**	***t*-test (*p*-value)**			
LOC100653061	5.033	0.033			
MALAT1	7.219	0.027			
OIP5-AS1	0.842	0.007			
PMS2CL	0.481	0.008			
RN7SK	10.140	0.021			
ROR1-AS1	0.481	0.008			

[1] Genes alphabetically sorted.
*[2] Presented in heat map (**Figure 2**).*

from primordial follicles, as well as in primordial follicles (**Table 2).** We interrogated the TAF15 protein using a specific antibody toward TAF15. This showed detection of the TAF15 protein in both oocyte and granulosa cells of primordial (**Figure 3A),** primary **(Figure 3B**), secondary (**Figure 3C**), as well as small pre-antral/early antral follicles (**Figures 3D–F)**. As the TAF15 protein appears detectable in both oocytes and the surrounding somatic cells are in line with the RNA sequencing

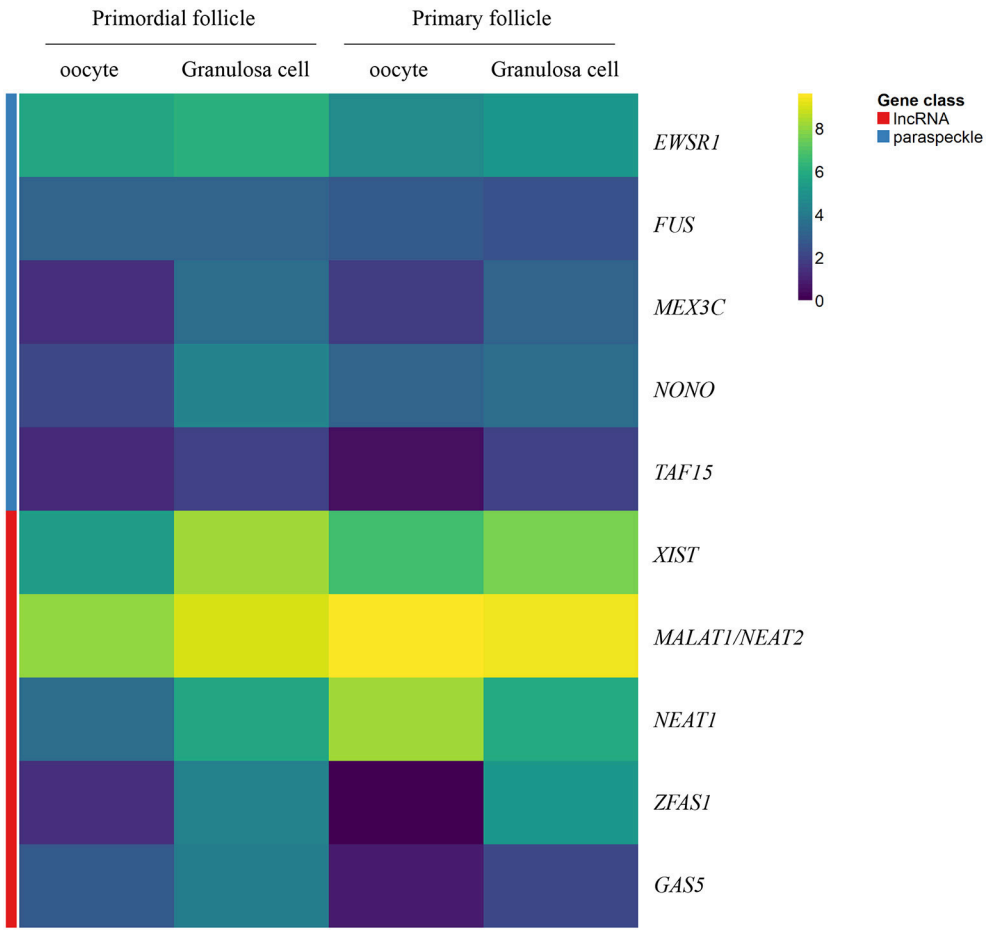

FIGURE 2 | Heatmap representation of selected genes encoding paraspeckle proteins and lncRNA genes. Heatmap of gene expression in oocytes and granulosa cells during the primordial-to-primary follicle transition. The heatmap includes the paraspeckle-encoding genes (blue bar) *MEX3C, NONO*, FUS, *EWS, TAF15* transcripts, and the lncRNAs (red bar) *NEAT1*, *MALAT1* (*NEAT2*), *XIST*, *ZFAS1*, *GAS5*. Color code reflects average FPKM values.

data, gene expression and its translational product appears coupled.

The IMF of EWS showed that EWS is present in both oocytes and the surrounding granulosa cells, and in primordial and primary follicles (**Figures 4A–C**). The *EWS* transcript was found highly expressed in these early stages of follicle development, and thus the RNA expression appears coupled to its translational protein product.

The *FUS* transcript was also highly expressed during early follicle development (**Table 2**), and as we interrogated its protein using IMF, found that the FUS protein was detectable in primordial follicles, (**Figure 5A**), primary follicles (**Figures 5B, C**), as well as in late pre-antral/early antral follicles (**Figure 5C**).

All samples were compared to a no-antibody control, which did not detect any signal (**Figure 5D**).

We detected nuclear localization of TAF15, EWS and FUS, with evidence of speckle-like structures in an infrequent manner distributed throughout the cells.

Non-coding RNAs

ncRNA genes produce functional RNA molecules rather than encoding proteins (Eddy, 2001). The groups of ncRNA are diverse and include, for instance, short and long ncRNAs as well as micro (mi)RNA, snoRNA, scaRNA, SRP RNA, and antisense RNA. The presence of ncRNAs during human follicle development was analyzed in transcriptomes representative for oocytes and follicles from primordial and primary follicles as well as oocytes, mural granulosa cell layers, and theca cell layers of small antral follicles [**Figure 1**, **Table 1,** (Resource Data)]. Genes encoding ncRNAs was identified using the Ensembl gene annotation version GRCh37.p13.

Long ncRNAs

Most ncRNAs longer than 200 nucleotides are referred to as 'long non-coding RNAs' (lncRNAs). Although the estimated number of different types of human lncRNAs has ranged from 5,400 to 53,000 (Palazzo and Lee, 2015), these ncRNAs appear to comprise functions for the control of various levels of gene expression in physiology and development, including chromatin

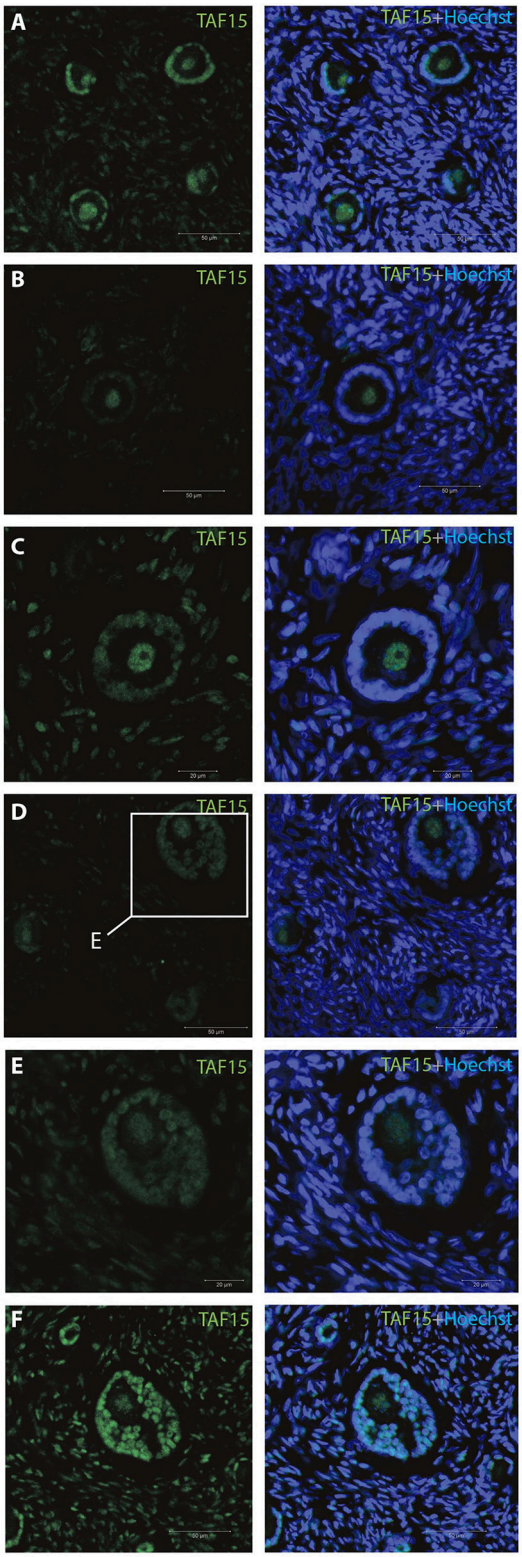

FIGURE 3 | Intra-ovarian distribution of TAF15 in human primordial and primary follicles. This showed detection of the TAF15 protein in both oocyte and granulosa cells of **(A)** primordial, **(B)** primary, and **(C)** secondary, as well as **(D–F)** small pre-antral/early antral follicles. Hoechst staining identifies the nucleus of cells. Scale bars; 30 μm.

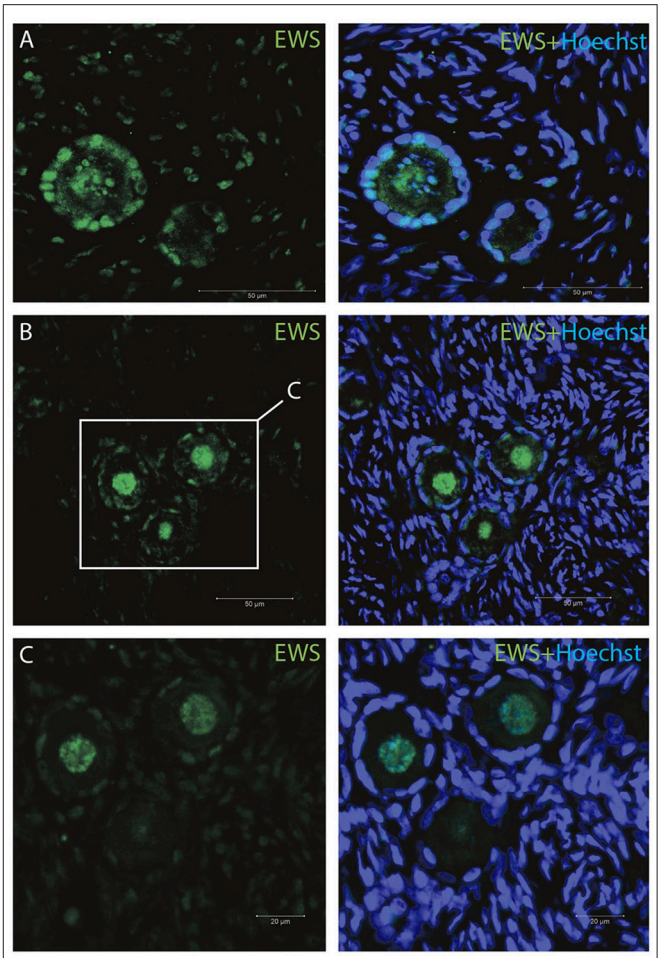

FIGURE 4 | Intra-ovarian distribution of EWS in human primordial and primary follicles **(A-C)**. EWS is present in both oocytes and the surrounding granulosa cells in primordial and primary follicles. Hoechst staining identifies the nucleus of cells. Scale bars; 30 μm.

architecture/epigenetic memory, transcription, RNA splicing, editing, translation, and turnover (Mattick and Makunin, 2006). In this study the presence of lncRNAs was interrogated (**Table 3**).

Interestingly, we detected the lncRNA *XIST* during human follicle development in both oocytes and follicle samples (**Table 3**). It should be noted, however, that *XIST* in the oocytes from small antral follicles did not display a cell-specific consistently expressed expression pattern but was noted used a less stringent *p*-value (Resource Data), which was likewise observed for *TSIX* (**Table 3**). The fact that a less stringent *p*-value was needed to detect this transcript in the oocytes from small antral follicles was expected, as these oocytes were rarely found in the ovarian biopsies, and thus these oocyte samples are less represented (**Table 1**, **Figure 1**).

MALAT1 (NEAT2) was detected throughout all the included stages (Resource Data), indicating the need for this paraspeckle-forming protein during human follicle development. Interestingly, several lncRNAs with no biological

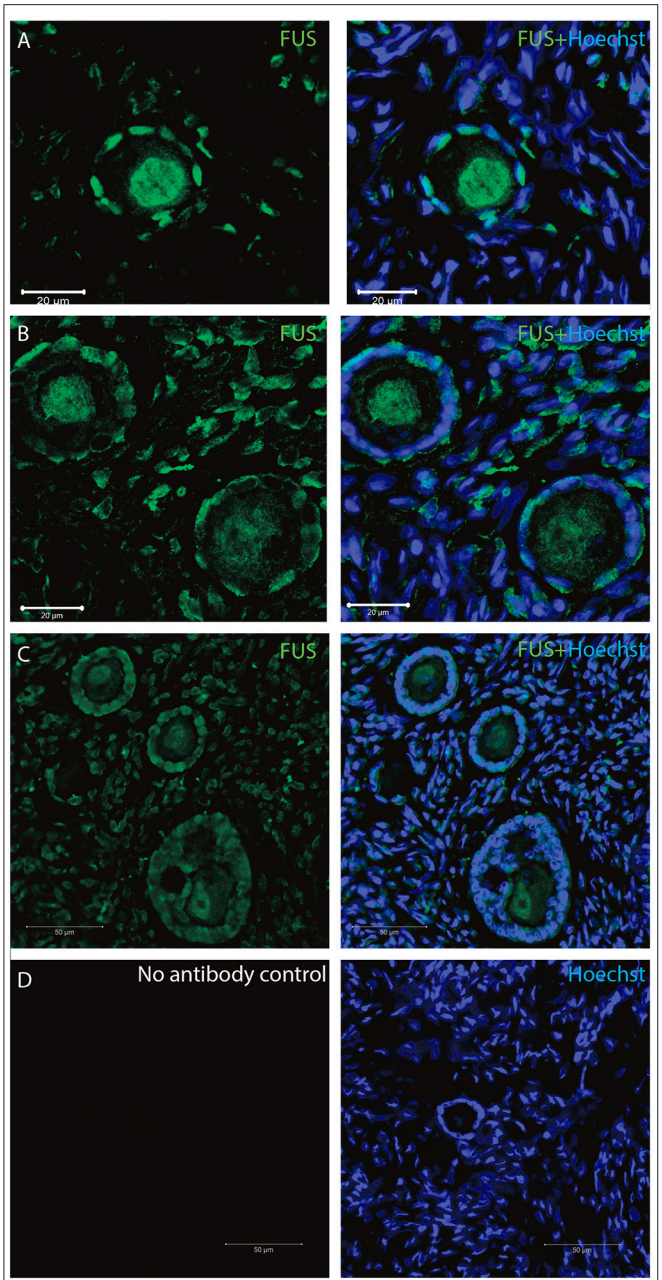

FIGURE 5 | Intra-ovarian distribution of FUS in human primordial, and primary follicles. The FUS protein was detectable in **(A)** primordial follicles, **(B,C)** primary follicles **(C)** late pre-antral/early antral follicles. All samples were compared to a **(D)** no-antibody control. Hoechst staining identifies the nucleus of cells. Scale bars; 30 μm.

functions annotated were noted (Resource Data). While the expression of several lncRNA genes (*OIP5-AS1*, *RN7SK*, *RN7SL2*) was present in all samples tested, others appeared to be cell- and stage-specifically (*GLG1*, *KIZ*, *BCAR4*, *EBLN3*) expressed (Resource Data).

The lncRNA *ZFAS1* appears to be restricted to somatic cells, e.g., the mural granuloma cell layer and the theca cell layer in the small antral follicle (Resource Data). Interestingly, the *ROR1-AS1* seems to be specific to the oocyte from small antral follicles (Resource Data). We found lncRNA Growth Arrest Specific 5 (*GAS5*) expressed in oocytes from primordial follicles, as well as a high expression in primordial follicles, somewhat lower in primary follicles, and in turn high in the mural granulosa cell layer and the theca cell layer from small antral follicles (Resource Data).

A heatmap of FPKM data for selected lncRNA genes was generated to show the expression for the two different cell-stages (primordial versus primary) in isolates - and the correlation between cell-specific (oocyte versus granulosa cell) isolates (**Figure 2**).

DISCUSSION

Extensive efforts to gain deeper understanding of RNA biology have yielded evidence of the diverse structural and regulatory roles in protecting chromosome integrity, maintaining genomic architecture, X chromosome inactivation, imprinting, transcription, translation and epigenetic regulation (Khorkova et al., 2015). Bioinformatics analysis of chromatin marks in intergenic DNA regions and of expressed sequence tags (ESTs) predicts the existence of more than 5,000 long noncoding RNA (lncRNA) genes in the human genome (Gomez et al., 2013). Some studies have found the number of lncRNAs to exceed that of protein-coding genes (Bouckenheimer et al., 2016; Hon et al., 2017). In our transcriptome study of lncRNA, we applied a strict filter to only consider transcript that were consistently expressed in our samples. This was applied as a major limiting factor is the number of patients included in the study. In oocytes and granulosa cells from primordial and primary follicles, 20, 33, and 20 and 19 lncRNAs were noted expressed (using a cut of value of 1 FPKM). Interestingly comparing this to the number of protein coding transcripts in the same stages (oocytes and granulosa cells from primordial and primary follicles showed 1099, 1695, and 1046 and 815, SSCEG, respectively (Ernst et al., 2017, 2018), it is noteworthy that few lncRNAs compared to the protein coding transcript are present during these early stages in human follicle development.

Strict filters in the bioinformatic management was applied to this study to ensure the most precise outcome from the global transcriptome analysis. Previous studies validated selected candidates by qPCR analysis (Ernst et al., 2017, 2018). Moreover, the analysis contains several DEG-lists based on both SSCEGs and non-SSCEGs and caution in the analysis of fold of change for DEG transcripts is recommended. Importantly, this study analyzed the presence of transcripts, and whether a gene is translated or its protein product present, is unknown. Using single cell techniques, we confirmed the presence of selected paraspeckle proteins using immunohistochemistry.

In a few well-studied cases, such as *AIR*, *XIST*, and *HOTAIR*, these lncRNAs have been shown to operate at the transcriptional level by binding to proteins in histone-modifying

complexes and targeting them to particular genes (Nagano et al., 2008; Chu et al., 2011; Jeon and Lee, 2011; Wang and Chang, 2011). A role for lncRNAs in human follicle development has not previously been described (Wilhelmm and Bernard, 2016) although their potential involvement has been suggested (Zhao and Rajkovic, 2008; Bouckenheimer et al., 2016). Differential lncRNA expression profiles in human oocytes and cumulus cells was recently analyzed (Bouckenheimer et al., 2018), which determined the lncRNA expression profiles of human MII oocytes (*BCAR4*, *C3orf56, TUNAR, OOEP-AS1*, *CASC18*, and *LINC01118*) and cumulus cells (*NEAT1*, *MALAT1*, *ANXA2P2, MEG3*, *IL6STP1*, and *VIM-AS1*).

The presence of the paraspeckle-forming *NEAT1* and *MALAT1* (*NEAT2*) indicates that paraspeckles are actively formed and present during human follicle development. Paraspeckle formation is initiated by transcription of the *NEAT1* chromosomal locus and proceeds in conjunction with *NEAT1* lncRNA biogenesis and a subsequent assembly step involving >39 paraspeckle proteins (PSPs). Interestingly, a study has shown that subunits of SWItch/Sucrose NonFermentable (SWI/SNF) chromatin-remodeling complexes were identified as paraspeckle components that interact with PSPs and *NEAT1* lncRNA (Kawaguchi et al., 2015). In particular, it was shown by electron microscopy that SWI/SNF complexes were enriched in paraspeckle subdomains depleted of chromatin. Interestingly, and consistent with this, it was found that the arginine methyltransferase CARM1 (coactivator-associated arginine methyltransferase 1) promotes the nuclear export of mRNAs that contain inverted Alu elements in their 3' untranslated region by methylating the paraspeckle component p54(nrb), which reduces the binding of p54(nrb) to the inverted Alu elements. It also down-regulated the synthesis of NEAT1. This in turn inhibited paraspeckle formation (Elbarbary and Maquat, 2015).

The lncRNA *XIST* was present at high levels throughout the stages tested during human follicle development. To ensure X-linked gene dosage compensation between females (XX) and males (XY), one X chromosome randomly undergoes X chromosome inactivation (XCI) in female cells (Lyon, 1961). The human *XIST* (Brown et al., 1991a,b) and mouse *Xist* (Borsani et al., 1991; Brockdorff et al., 1991) lncRNAs accumulate over the X chromosome. X chromosomal inactivation is tightly regulated throughout development with *XIST* as a key regulator involved in the establishment of several layers of repressive epigenetic modifications. These reported functions of *XIST* are consistent with our observation that this gene is highly transcribed during human follicle development and reveals that *XIST* lncRNA is present already from the dormant primordial stage of human follicle development. The functional role of *XIST* during early follicle development remains to be elucidated, and this may include early marks of maternal imprinting and dosage regulation.

The lncRNA *ZFAS1* appears specific to somatic cells during human follicle development. *ZFAS1* has been described as being upregulated in different cancer types (Askarian-Amiri et al., 2011; Li et al., 2015; Nie et al., 2016; Thorenoor et al., 2016) and is involved in cell apoptosis and cell cycle control. It was recently shown that the action of *ZFAS1* occurred through interaction with EZH2 and LSD1/CoREST in order to repress the underlying targets KLF2 and NKD2 transcription (Nie et al., 2016). The epigenetic dysregulation of central granulosa cell factors such as FOXL2 are involved in the development of granulosa cell tumors (Xu et al., 2016), which is possible through EZH2 interaction. Furthermore, prominent roles for FOXL2 include control of primordial follicle activation (Schmidt et al., 2004).

It remains to be tested if lncRNA *ZFAS1* functions to regulate transcriptional control in follicle development, and this may have an effect on granulosa cell proliferation and cell cycle control in the human follicle.

We identified the potential tumor suppressor lncRNA growth arrest specific 5 (*GAS5*), expressed particularly in the primordial stage, as well as in primary follicles and in mural granulosa cell layers and the theca cell layers. Part of the *GAS5* RNA structure mimics the glucocorticoid response element, enabling it to bind the DNA binding domain of the glucocorticoid receptor, thus inhibiting glucocorticoid induced transcription. *GAS5* is further thought to regulate transcriptional activity of the androgen receptor. In line with this, *GAS5* lncRNA has been found to repress the AR/androgen complex from binding to target through sequestering, thus repressing transcription (Wang and Lee, 2009). Of further interest, *GAS5* lncRNA has been found to supress the AKT/mTOR signaling pathway in prostate cancer cells (Yacqub-Usman et al., 2015). As previous studies have shown that activated AKT/mTOR signaling increases primordial follicle activation (Makker et al., 2014), we suggest that *GAS5* expression in the primordial follicle may be involved in primordial follicle dormancy and survival. Recently, the GAS5 was found to promote proliferation and survival of female germline stem cells *in vitro* (Wang et al., 2018). The functional involvement of *GAS5* in normal and aberrant human follicle development remains to be determined.

Increasing evidence supports a central role for ncRNA in numerous aspects of chromatin function (Názer and Lei, 2014). Interestingly, it has long been appreciated that ncRNAs are central components of the dosage compensation machinery, and recent work has elucidated how various ncRNAs contribute to Polycomb Group (PcG) and chromatin insulator activities (reviewed in Názer and Lei, 2014). The PcG proteins are required for the adequate development of multicellular organisms, functioning to preserve pluripotency and/or cellular identity. Their main function however is to repress the expression of genes that would otherwise promote differentiation into other cell types (reviewed in Simon and Kingston, 2013).

The precise role of lncRNAs in chromatin modifications during human follicle development remains to be elucidated. However, our data suggests that several distinct lncRNAs are present and that they probably have separate functions in order to secure follicle integrity and development.

We found the protein-coding *MEX3C* gene present during human follicle development. However, the role of the gene product, MEX3C, is unknown. The MEX3BM isoform and the E3 ubiquitin ligase DZIP3 are bought together with

their substrates (Ataxin-1 and Snurportin-1) by the lncRNA *HOTAIR*, accelerating their degradation (Khorkova et al., 2015), thus lncRNA-mediated regulation also affects protein stability (reviewed in Khorkova et al., 2015). Furthermore, proteasomal inhibition causes upregulation of paraspeckle-associated lncRNA *NEAT1*, which in turn protects fibroblasts from cell death triggered by proteasome inhibition (Khorkova et al., 2015). Interestingly, it was found that a MEX3 homolog is required for differentiation during planarian stem cell lineage development (Zhu et al., 2015). In this study it was shown that MEX3-1 was required for generating differentiated cells of multiple lineages, while restricting the size of the stem cell compartment. This indicates that MEX3-1 functions as a cell fate regulator (Zhu et al., 2015).The presence of the *MEX3C* transcript during human follicle development has not been functionally addressed, and future studies should reveal whether MEX3C has a pivotal role in cell commitment and/or differentiation in the selection of the dominant follicle.

The upregulated expression profile of *NONO* during follicle development suggests that this protein is under tight control. NONO deficiency led to upregulation of PSPC1, which replaces NONO in a stable complex with SFPQ (Li et al., 2014). The knockdown of PSPC1 in a *Nono*-deficient background led to severe radio-sensitivity and delayed resolution of double stranded break (DSB) repair foci. From this it can be concluded that NONO or related proteins are critical for DSB repair (Li et al., 2014). The complex of NONO with SFPQ and PSPC1 served a multipurpose scaffold, including frequently identified engagement at almost every step of gene regulation, and including, but not limited to, transcriptional regulation, RNA processing and transport, and DNA repair (Knott et al., 2016). Interestingly, a report has investigated the inner cell mass marker OCT4 and its gene expression patterns, as well as CpG sites methylation profiles during embryonic stem (ES) cell differentiation into neurons (Park et al., 2013). It was found that NONO binds to the CpG island of the *Oct4* promoter and positively regulates *Oct4* gene expression in ES cells (Park et al., 2013), thus indicating a role in cell lineage during early development. The future role of NONO during human follicle development and how this might participate in regulating gene expression and/or DNA repair will be important steps toward the understanding of the capacity of the human ovarian follicles.

Several lines of evidence suggest paraspeckle proteins to be essential in cell fate determination, which is highly relevant for early developmental processes (Yamazaki and Hirose, 2015).

FUS, EWS, and TAF15 are structurally similar multifunctional proteins that were initially discovered in the process of characterization of fusion oncogenes in human sarcomas and leukemias. As they are implicated in numerous central cellular processes such as gene regulation, genomic integrity maintenance and mRNA/microRNA processing, it is therefore not surprising to find them in many cellular contexts and in different cell types and tissues. The expression profile of the FET proteins were characterized in both the human (Andersson et al., 2008) and porcine (Blechingberg et al., 2012b) developing brain. The FET proteins are expressed in most human tissues and are localized mainly in the cell nucleus (Andersson et al., 2008), but are also found in the cytoplasm (Zinszner et al., 1997; Belyanskaya et al., 2001; Jobert et al., 2009). This is supported by the fact that the functions of hnRNPs include nucleocytoplasmic shuttling (Bedford and Clarke, 2009; Yu, 2011). Interestingly, FUS, EWS, and TAF15 has previously revealed a cell-specific expression pattern (Andersson et al., 2008), and processes such a heat shock and/or oxidative stress induce the re-localization of these proteins to stress granules (Andersson et al., 2008; Blechingberg et al., 2012a). The fact that we observed infrequent staining in nuclear and cytoplasmic localizations supports the activity of these FET proteins.

The FET proteins also frequently exhibit gene translocation in human cancers (Paronetto, 2013; Campos-Melo et al., 2014). Emerging evidence demonstrates their physical interactions with DNA Damage Response proteins (Kai, 2016) and thus suggests their involvement in the maintenance of genome stability. Interestingly, it was recently proposed that FET proteins are involved in the maintenance of lifespan, cellular stress resistance, and neuronal integrity (Therrien et al., 2016).

It has been shown that FUS interact directly with *NEAT1* lncRNA, reducing the expression of FUS, and subsequently causing cell apoptosis. In combination with miR-548ar-3p, this regulates breast cancer cell apoptosis (Ke et al., 2016).

CONCLUSION

We identified the presence of lncRNAs as well as the genes encoding the paraspeckle proteins, offering insights into how their transcripts are expressed during human follicle development. The study is descriptive in nature. As a proof of concept, we probed for the intracellular presence and localization of three selected paraspeckle proteins. It remains to be determined for several other proteins encoding by genes noted, as well as lncRNAs. In particular, our study indicates that they may be involved in cellular processes such as cell differentiation and cell integrity. This could be accomplished by their ability to control gene expression, epigenetics and mRNA turnover during follicle development.

AUTHOR CONTRIBUTIONS

EE and KL-H conceived the study. PV performed bioinformatics analysis. EE, JN, and MI performed IMF. EE and KL-H analyzed RNA sequencing data and wrote the manuscript. All authors approved the final manuscript.

FUNDING

EE was supported by a Ph.D. scholarship from Health Faculty, Aarhus University. This work was further supported by grants from Kong Christian Den Tiendes Fond (to EE and KL-H), Th. Maigaards Eft. Fru Lily Benthine Lunds Fond and Fonden til Lægevidenskabens Fremme (to KL-H). KL-H was further

supported by a grant from the Novo Nordisk Foundation (NNF16OC0022480 to KL-H).

ACKNOWLEDGMENTS

The authors wish to thank the clinical, paramedical and laboratory team of the Fertility Clinic, Aarhus University Hospital. We thank Lykke-Hartmann laboratory (AU) for scientific discussions. Anders Heuck is also thanked for excellent laboratory work.

SUPPLEMENTARY MATERIAL

The Supplementary Material for this article can be found online at: https://www.frontiersin.org/articles/10.3389/fcell.2018.00078/full#supplementary-material

Supplementary Table 1 | Full lists of ncRNAs detected in human follicle development [oocytes from primordial follicles (tab 1), primordial follicles (tab 2), oocytes from primary follicles (tab 3), mural granulosa cell layers from small antral follicles (tab 4), theca cell layers from small antral follicles (tab 5), oocytes from small antral follicles (tab 6)]. Cell specific consistently expressed genes (CSCEG) (one-sample *t*-test *p*-value < 0.05 in gray).

REFERENCES

Adhikari, D., and Liu, K. (2009). Molecular mechanisms underlying the activation of mammalian primordial follicles. *Endocr. Rev.* 30, 438–464. doi: 10.1210/er.2008-0048

Ambasudhan, R., Talantova, M., Coleman, R., Yuan, X., Zhu, S., Lipton, S. A., et al. (2011). Direct reprogramming of adult human fibroblasts to functional neurons under defined conditions. *Cell Stem Cell* 9, 113–118. doi: 10.1016/j.stem.2011.07.002

Andersson, M. K., Ståhlberg, A., Arvidsson, Y., Olofsson, A., Semb, H., Stenman, G., et al. (2008). The multifunctional FUS, EWS and TAF15 proto-oncoproteins show cell type-specific expression patterns and involvement in cell spreading and stress response. *BMC Cell Biol.* 9:37. doi: 10.1186/1471-2121-9-37

Askarian-Amiri, M. E., Crawford, J., French, J. D., Smart, C. E., Smith, M. A., Clark, M. B., et al. (2011). SNORD-host RNA Zfas1 is a regulator of mammary development and a potential marker for breast cancer. *RNA* 17, 878–891. doi: 10.1261/rna.2528811

Auboeuf, D., Dowhan, D. H., Dutertre, M., Martin, N., Berget, S. M., and O'Malley, B. W. (2005). A subset of nuclear receptor coregulators act as coupling proteins during synthesis and maturation of RNA transcripts. *Mol. Cell. Biol.* 25, 5307–5316. doi: 10.1128/MCB.25.13.5307-5316.2005

Backofen, R., and Vogel, T. (2014). Biological and bioinformatical approaches to study crosstalk of long-non-coding RNAs and chromatin-modifying proteins. *Cell Tissue Res.* 356, 507–526. doi: 10.1007/s00441-014-1885-x

Baird, D. T., Collins, J., Egozcue, J., Evers, L. H., Gianaroli, L., Leridon, H., et al. (2005). Fertility and ageing. *Hum. Reprod. Update* 11, 261–276. doi: 10.1093/humupd/dmi006

Bedford, M. T., and Clarke, S. G. (2009). Protein arginine methylation in mammals: who, what, and why. *Mol. Cell.* 33, 1–13. doi: 10.1016/j.molcel.2008.12.013

Belyanskaya, L. L., Gehrig, P. M., and Gehring, H. (2001). Exposure on cell surface and extensive arginine methylation of ewing sarcoma (EWS) protein. *J. Biol. Chem.* 276, 18681–18687. doi: 10.1074/jbc.M011446200

Bertolotti, A., Lutz, Y., Heard, D. J., Chambon, P., and Tora, L. (1996). hTAF(II)68, a novel RNA/ssDNA-binding protein with homology to the pro-oncoproteins TLS/FUS and EWS is associated with both TFIID and RNA polymerase II. *EMBO J.* 15, 5022–5031.

Binelli, M., and Murphy, B. D. (2010). Coordinated regulation of follicle development by germ and somatic cells. *Reprod. Fertil. Dev.* 22, 1–12. doi: 10.1071/RD09218

Blechingberg, J., Luo, Y., Bolund, L., Damgaard, C. K., and Nielsen, A. L. (2012a). Gene expression responses to FUS, EWS, and TAF15 reduction and stress granule sequestration analyses identifies FET-protein non-redundant functions. *PLoS ONE* 7:e46251. doi: 10.1371/journal.pone.0046251

Blechingberg, J., Holm, I. E., and Nielsen, A. L. (2012b). Characterization and expression analysis in the developing embryonic brain of the porcine FET family: FUS, EWS, and TAF15. *Gene* 493, 27–35. doi: 10.1016/j.gene.2011.11.038

Bond, C. S., and Fox, A. H. (2009). Paraspeckles: nuclear bodies built on long noncoding RNA. *J. Cell Biol.* 186, 637–644. doi: 10.1083/jcb.200906113

Bonnet, A., Cabau, C., Bouchez, O., Sarry, J., Marsaud, N., Foissac, S., et al. (2013). An overview of gene expression dynamics during early ovarian folliculogenesis: specificity of follicular compartments and bi-directional dialog. *BMC Genomics* 14:904. doi: 10.1186/1471-2164-14-904

Borsani, G., Tonlorenzi, R., Simmler, M. C., Dandolo, L., Arnaud, D., Capra, V., et al. (1991). Characterization of a murine gene expressed from the inactive X chromosome. *Nature* 351, 325–329. doi: 10.1038/351325a0

Bouckenheimer, J., Assou, S., Riquier, S., Hou, C., Philippe, N., Sansac, C., et al. (2016). Long non-coding RNAs in human early embryonic development and their potential in ART. *Hum. Reprod. Update* 23, 19–40. doi: 10.1093/humupd/dmw035

Bouckenheimer, J., Fauque, P., Lecellier, C. H., Bruno, C., Commes, T., Lemaître, J. M., et al. (2018). Differential long non-coding RNA expression profiles in human oocytes and cumulus cells. *Sci. Rep.* 8:2202. doi: 10.1038/s41598-018-20727-0

Brockdorff, N., Ashworth, A., Kay, G. F., Cooper, P., Smith, S., McCabe, V. M., et al. (1991). Conservation of position and exclusive expression of mouse Xist from the inactive X chromosome. *Nature* 351, 329–331. doi: 10.1038/351329a0

Brown, C. J., Ballabio, A., Rupert, J. L., Lafreniere, R. G., Grompe, M., Tonlorenzi, R., et al. (1991a). A gene from the region of the human X inactivation centre is expressed exclusively from the inactive X chromosome. *Nature* 349, 38–44. doi: 10.1038/349038a0

Brown, C. J., Lafreniere, R. G., Powers, V. E., Sebastio, G., Ballabio, A., Pettigrew, A. L., et al. (1991b). Localization of the X inactivation centre on the human X chromosome in Xq13. *Nature* 349, 82–84. doi: 10.1038/349082a0

Campos-Melo, D., Droppelmann, C. A., Volkening, K., and Strong, M. J. (2014). RNA-binding proteins as molecular links between cancer and neurodegeneration. *Biogerontology* 15, 587–610. doi: 10.1007/s10522-014-9531-2

Carabatsos, M. J., Sellitto, C., Goodenough, D. A., and Albertini, D. F. (2000). Oocyte-granulosa cell heterologous gap junctions are required for the coordination of nuclear and cytoplasmic meiotic competence. *Dev. Biol.* 226, 167–179. doi: 10.1006/dbio.2000.9863

Chau, B. L., Ng, K. P., Li, K. K., and Lee, K. A. (2016). RGG boxes within the TET/FET family of RNA-binding proteins are functionally distinct. *Transcription* 7, 141–151. doi: 10.1080/21541264.2016.1183071

Chen, L. L., and Carmichael, G. G. (2009). Altered nuclear retention of mRNAs containing inverted repeats in human embryonic stem cells: functional role of a nuclear noncoding RNA. *Mol. Cell* 35, 467–478. doi: 10.1016/j.molcel.2009.06.027

Chen, L. L., and Carmichael, G. G. (2010). Decoding the function of nuclear long non-coding RNAs. *Curr. Opin. Cell Biol.* 22, 357–364. doi: 10.1016/j.ceb.2010.03.003

Chow, J., and Heard, E. (2009). X inactivation and the complexities of silencing a sex chromosome. *Curr. Opin. Cell Biol.* 21, 359–366. doi: 10.1016/j.ceb.2009.04.012

Chu, C., Qu, K., Zhong, F. L., Artandi, S. E., and Chang, H. Y. (2011). Genomic maps of long noncoding RNA occupancy reveal principles of RNA-chromatin interactions. *Mol. Cell* 44, 667–678. doi: 10.1016/j.molcel.2011.08.027

Clemson, C. M., Hutchinson, J. N., Sara, S. A., Ensminger, A. W., Fox, A. H., Chess, A., et al. (2009). An architectural role for a nuclear noncoding RNA: NEAT1 RNA is essential for the structure of paraspeckles. *Mol. Cell* 33, 717–726. doi: 10.1016/j.molcel.2009.01.026

Crozat, A., Aman, P., Mandahl, N., and Ron, D. (1993). Fusion of CHOP to a novel RNA-binding protein in human myxoid liposarcoma. *Nature* 363, 640–644. doi: 10.1038/363640a0

Delattre, O., Zucman, J., Plougastel, B., Desmaze, C., Melot, T., Peter, M., et al. (1992). Gene fusion with an ETS DNA-binding domain caused by chromosome translocation in human tumours. *Nature* 359, 162–165. doi: 10.1038/359162a0

Dinger, M. E., Amaral, P. P., Mercer, T. R., Pang, K. C., Bruce, S. J., Gardiner, B. B., et al. (2008). Long noncoding RNAs in mouse embryonic stem cell pluripotency and differentiation. *Genome Res.* 18, 1433–1445. doi: 10.1101/gr.078378.108

Eddy, S. R. (2001). Non-coding RNA genes and the modern RNA world. *Nat. Rev. Genet.* 2, 919–929. doi: 10.1038/35103511

Elbarbary, R. A., and Maquat, L. E. (2015). CARMing down the SINEs of anarchy: two paths to freedom from paraspeckle detention. *Genes Dev.* 29, 687–689. doi: 10.1101/gad.261438.115

Ernst, E. H., Grøndahl, M. L., Grund, S., Hardy, K., Heuck, A., Sunde, L., et al. (2017). Dormancy and activation of human oocytes from primordial and primary follicles: molecular clues to oocyte regulation. *Hum. Reprod.* 32, 1684–1700. doi: 10.1093/humrep/dex238

Ernst, E. H., Franks, S., Hardy, K., Villesen, P., and Lykke-Hartmann, K. (2018). Granulosa cells from human primordial and primary follicles show differential global gene expression profiles. *Hum Reprod.* 33, 666–679. doi: 10.1093/humrep/dey011

Espey, L. L. (1994). Current status of the hypothesis that mammalian ovulation is comparable to an inflammatory reaction. *Biol. Reprod.* 50, 233–238. doi: 10.1095/biolreprod50.2.233

Fox, A. H., Lam, Y. W., Leung, A. K., Lyon, C. E., Andersen, J., Mann, M., et al. (2002). Paraspeckles: a novel nuclear domain. *Curr. Biol.* 12, 13–25. doi: 10.1016/S0960-9822(01)00632-7

Fox, A. H., Bond, C. S., and Lamond, A. I. (2005). P54nrb forms a heterodimer with PSP1 that localizes to paraspeckles in an RNA-dependent manner. *Mol. Biol. Cell.* 16, 5304–5315. doi: 10.1091/mbc.e05-06-0587

Gomez, J. A., Wapinski, O. L., Yang, Y. W., Bureau, J. F., Gopinath, S., Monack, D. M., et al. (2013). The NeST long ncRNA controls microbial susceptibility and epigenetic activation of the interferon-gamma locus. *Cell* 152, 743–754. doi: 10.1016/j.cell.2013.01.015

Gougeon, A. (1996). Regulation of ovarian follicular development in primates: facts and hypotheses. *Endocr. Rev.* 17, 121–155. doi: 10.1210/edrv-17-2-121

Guipaud, O., Guillonneau, F., Labas, V., Praseuth, D., Rossier, J., Lopez, B., et al. (2006). An *in vitro* enzymatic assay coupled to proteomics analysis reveals a new DNA processing activity for Ewing sarcoma and TAF(II)68 proteins. *Proteomics* 6, 5962–5972. doi: 10.1002/pmic.200600259

Hon, C. C., Ramilowski, J. A., Harshbarger, J., Bertin, N., Rackham, O. J., Gough, J., et al. (2017). An atlas of human long non-coding RNAs with accurate 5' ends. *Nature* 543, 199–204. doi: 10.1038/nature21374

Hutchinson, J. N., Ensminger, A. W., Clemson, C. M., Lynch, C. R., Lawrence, J. B., and Chess, A. (2007). A screen for nuclear transcripts identifies two linked noncoding RNAs associated with SC35 splicing domains. *BMC Genomics* 8:39. doi: 10.1186/1471-2164-8-39

Jeon, Y., and Lee, J. T. (2011). YY1 tethers Xist RNA to the inactive X nucleation center. *Cell* 146, 119–133. doi: 10.1016/j.cell.2011.06.026

Jobert, L., Argentini, M., and Tora, L. (2009). PRMT1 mediated methylation of TAF15 is required for its positive gene regulatory function. *Exp. Cell Res.* 315, 1273–1286. doi: 10.1016/j.yexcr.2008.12.008

Joh, R. I., Palmieri, C. M., Hill, I. T., and Motamedi, M. (2014). Regulation of histone methylation by noncoding RNAs. *Biochim. Biophys. Acta* 1839, 1385–1394. doi: 10.1016/j.bbagrm.2014.06.006

Kai, M. (2016). Roles of RNA-Binding Proteins in DNA Damage Response. *Int. J. Mol. Sci.* 17:310. doi: 10.3390/ijms17030310

Kawaguchi, T., Tanigawa, A., Naganuma, T., Ohkawa, Y., Souquere, S., Pierron, G., et al. (2015). SWI/SNF chromatin-remodeling complexes function in noncoding RNA-dependent assembly of nuclear bodies. *Proc. Natl. Acad. Sci. U.S.A.* 112, 4304–4309. doi: 10.1073/pnas.1423819112

Ke, H., Zhao, L., Feng, X., Xu, H., Zou, L., Yang, Q., et al. (2016). NEAT1 is required for survival of breast cancer cells through FUS, and miR-548. *Gene Regul Syst Bio.* 10(Suppl. 1), 11–7. doi: 10.4137/GRSB.S29414

Khalil, A. M., Guttman, M., Huarte, M., Garber, M., Raj, A., Rivea Morales, D., et al. (2009). Many human large intergenic noncoding RNAs associate with chromatin-modifying complexes and affect gene expression. *Proc. Natl. Acad. Sci. U.S.A.* 106, 11667–11672. doi: 10.1073/pnas.0904715106

Khorkova, O., Hsiao, J., and Wahlestedt, C. (2015). Basic biology and therapeutic implications of lncRNA. *Adv. Drug Deliv. Rev.* 87, 15–24. doi: 10.1016/j.addr.2015.05.012

Knott, G. J., Bond, C. S., and Fox, A. H. (2016). The DBHS proteins SFPQ, NONO and PSPC1: a multipurpose molecular scaffold. *Nucleic Acids Res.* 44, 3989–4004. doi: 10.1093/nar/gkw271

Kurian, L., Sancho-Martinez, I., Nivet, E., Aguirre, A., Moon, K., Pendaries, C., et al. (2013). Conversion of human fibroblasts to angioblast-like progenitor cells. *Nat. Methods* 10, 77–83. doi: 10.1038/nmeth.2255

Law, W. J., Cann, K. L., and Hicks, G. G. (2006). TLS, EWS and TAF15: a model for transcriptional integration of gene expression. *Brief. Funct. Genomic. Proteomic* 5, 8–14. doi: 10.1093/bfgp/ell015

Leeb, M., Steffen, P. A., and Wutz, A. (2009). X chromosome inactivation sparked by non-coding RNAs. *RNA Biol.* 6, 94–99. doi: 10.4161/rna.6.2.7716

Li, S., Li, Z., Shu, F. J., Xiong, H., Phillips, A. C., and Dynan, W. S. (2014). Double-strand break repair deficiency in NONO knockout murine embryonic fibroblasts and compensation by spontaneous upregulation of the PSPC1 paralog. *Nucleic Acids Res.* 42, 9771–9780. doi: 10.1093/nar/gku650

Li, T., Xie, J., Shen, C., Cheng, D., Shi, Y., Wu, Z., et al. (2015). Amplification of Long Noncoding RNA ZFAS1 Promotes Metastasis in Hepatocellular Carcinoma. *Cancer Res.* 75, 3181–3191. doi: 10.1158/0008-5472.CAN-14-3721

Liu, N., and Pan, T. (2015). RNA epigenetics. *Transl. Res.* 165, 28–35. doi: 10.1016/j.trsl.2014.04.003

Lyon, M. F. (1961). Gene action in the X-chromosome of the mouse (Mus musculus L.). *Nature* 190, 372–373. doi: 10.1038/190372a0

Makker, A., Goel, M. M., and Mahdi, A. A. (2014). PI3K/PTEN/Akt and TSC/mTOR signaling pathways, ovarian dysfunction, and infertility: an update. *J. Mol. Endocrinol.* 53, R103–R118. doi: 10.1530/JME-14-0220

Markholt, S., Grøndahl, M. L., Ernst, E. H., Andersen, C. Y., Ernst, E., and Lykke-Hartmann, K. (2012). Global gene analysis of oocytes from early stages in human folliculogenesis shows high expression of novel genes in reproduction. *Mol. Hum. Reprod.* 18, 96–110. doi: 10.1093/molehr/gar083

Markström, E., Svensson, E., Shao, R., Svanberg, B., and Billig, H. (2002). Survival factors regulating ovarian apoptosis – dependence on follicle differentiation. *Reproduction* 123, 23–30. doi: 10.1530/rep.0.1230023

Mattick, J. S., and Makunin, I. V. (2006). Non-coding RNA. *Hum Mol Genet.* 15, R17–R29. doi: 10.1093/hmg/ddl046

McGee, E. A., and Hsueh, A. J. (2000). Initial and cyclic recruitment of ovarian follicles. *Endocr. Rev.* 21, 200–214. doi: 10.1210/er.21.2.200

Mercer, T. R., Dinger, M. E., and Mattick, J. S. (2009). Long non-coding RNAs: insights into functions. *Nat. Rev. Genet.* 10, 155–159. doi: 10.1038/nrg2521

Morohoshi, F., Ootsuka, Y., Arai, K., Ichikawa, H., Mitani, S., Munakata, N., et al. (1998). Genomic structure of the human RBP56/hTAFII68 and FUS/TLS genes. *Gene* 221, 191–198. doi: 10.1016/S0378-1119(98)00463-6

Nagano, T., Mitchell, J. A., Sanz, L. A., Pauler, F. M., Ferguson-Smith, A. C., Feil, R., et al. (2008). The Air noncoding RNA epigenetically silences transcription by targeting G9a to chromatin. *Science* 322, 1717–1720. doi: 10.1126/science.1163802

Naganuma, T., and Hirose, T. (2013). Paraspeckle formation during the biogenesis of long non-coding RNAs. *RNA Biol.* 10, 456–461. doi: 10.4161/rna.23547

Naganuma, T., Nakagawa, S., Tanigawa, A., Sasaki, Y. F., Goshima, N., and Hirose, T. (2012). Alternative 3′-end processing of long noncoding RNA initiates construction of nuclear paraspeckles. *EMBO J.* 31, 4020–4034. doi: 10.1038/emboj.2012.251

Nakagawa, S., Shimada, M., Yanaka, K., Mito, M., Arai, T., Takahashi, E., et al. (2014). The lncRNA Neat1 is required for corpus luteum formation and the establishment of pregnancy in a subpopulation of mice. *Development* 141, 4618–4627. doi: 10.1242/dev.110544

Názer, E., and Lei, E. P. (2014). Modulation of chromatin modifying complexes by noncoding RNAs in trans. *Curr. Opin. Genet. Dev.* 25, 68–73. doi: 10.1016/j.gde.2013.11.019

Nguyen, C. D., Mansfield, R. E., Leung, W., Vaz, P. M., Loughlin, F. E., Grant, R. P., et al. (2011). Characterization of a family of RanBP2-type zinc fingers that can recognize single-stranded RNA. *J. Mol. Biol.* 407, 273–283. doi: 10.1016/j.jmb.2010.12.041

Nie, F., Yu, X., Huang, M., Wang, Y., Xie, M., Ma, H., et al. (2016). Long noncoding RNA ZFAS1 promotes gastric cancer cells proliferation

by epigenetically repressing KLF2 and NKD2 expression. *Oncotarget* 8, 38227–38238. doi: 10.18632/oncotarget.9611

Palazzo, A. F., and Lee, E. S. (2015). Non-coding RNA: what is functional and what is junk? *Front. Genet.* 6:2. doi: 10.3389/fgene.2015.00002

Park, Y., Lee, J. M., Hwang, M. Y., Son, G. H., and Geum, D. (2013). NonO binds to the CpG island of oct4 promoter and functions as a transcriptional activator of oct4 gene expression. *Mol. Cells* 35, 61–69. doi: 10.1007/s10059-013-2273-1

Paronetto, M. P. (2013). Ewing sarcoma protein: a key player in human cancer. *Int. J. Cell Biol.* 2013:642853. doi: 10.1155/2013/642853

Penny, G. D., Kay, G. F., Sheardown, S. A., Rastan, S., and Brockdorff, N. (1996). Requirement for Xist in X chromosome inactivation. *Nature* 379, 131–137. doi: 10.1038/379131a0

Peschansky, V. J., and Wahlestedt, C. (2014). Non-coding RNAs as direct and indirect modulators of epigenetic regulation. *Epigenetics* 9, 3–12. doi: 10.4161/epi.27473

R Core Team (2012). *R: A Language and Environment for STATISTICAL COMPUTING*. R Vienna: Foundation for Statistical Computing. Available online at: http://www.R-project.org/.

Reddy, P., Zheng, W., and Liu, K. (2010). Mechanisms maintaining the dormancy and survival of mammalian primordial follicles. *Trends Endocrinol. Metab.* 21, 96–103. doi: 10.1016/j.tem.2009.10.001

Rosendahl, M., Schmidt, K. T., Ernst, E., Rasmussen, P. E., Loft, A., Byskov, A. G., et al. (2011). Cryopreservation of ovarian tissue for a decade in Denmark: a view of the technique. *Reprod. Biomed. Online* 22, 162–171. doi: 10.1016/j.rbmo.2010.10.015

Sasaki, Y. T., Ideue, T., Sano, M., Mituyama, T., and Hirose, T. (2009). MENepsilon/beta noncoding RNAs are essential for structural integrity of nuclear paraspeckles. *Proc. Natl. Acad. Sci. U.S.A.* 106, 2525–2530. doi: 10.1073/pnas.0807899106

Schmidt, K. L., Byskov, A. G., Nyboe Andersen, A., Müller, J., and Yding Andersen, C. (2003). Density and distribution of primordial follicles in single pieces of cortex from 21 patients and in individual pieces of cortex from three entire human ovaries. *Hum. Reprod.* 18, 1158–1164. doi: 10.1093/humrep/deg246

Schmidt, D., Ovitt, C. E., Anlag, K., Fehsenfeld, S., Gredsted, L., Treier, A. C., et al. (2004). The murine winged-helix transcription factor Foxl2 is required for granulosa cell differentiation and ovary maintenance. *Development* 131, 933–942. doi: 10.1242/dev.00969

Schwartz, J. C., Cech, T. R., and Parker, R. R. (2015). Biochemical properties and biological functions of FET proteins. *Annu. Rev. Biochem.* 84, 355–379. doi: 10.1146/annurev-biochem-060614-034325

Simon, J. A., and Kingston, R. E. (2013). Occupying chromatin: Polycomb mechanisms for getting to genomic targets, stopping transcriptional traffic, and staying put. *Mol. Cell.* 49, 808–824. doi: 10.1016/j.molcel.2013.02.013

Stubbs, S. A., Hardy, K., Da Silva-Buttkus, P., Stark, J., Webber, L. J., Flanagan, A. M., et al. (2005). Anti-mullerian hormone protein expression is reduced during the initial stages of follicle development in human polycystic ovaries. *J. Clin. Endocrinol. Metab.* 90, 5536–5543. doi: 10.1210/jc.2005-0907

Sunwoo, H., Dinger, M. E., Wilusz, J. E., Amaral, P. P., Mattick, J. S., and Spector, D. L. (2009). MEN epsilon/beta nuclear-retained non-coding RNAs are up-regulated upon muscle differentiation and are essential components of paraspeckles. *Genome Res.* 19, 347–359. doi: 10.1101/gr.087775.108

Svetoni, F., Frisone, P., and Paronetto, M. P. (2016). Role of FET proteins in neurodegenerative disorders. *RNA Biol.* 13, 1089–1102. doi: 10.1080/15476286.2016.1211225

Therrien, M., Rouleau, G. A., Dion, P. A., and Parker, J. A. (2016). FET proteins regulate lifespan and neuronal integrity. *Sci. Rep.* 6:25159. doi: 10.1038/srep25159

Thorenoor, N., Faltejskova-Vychytilova, P., Hombach, S., Mlcochova, J., Kretz, M., Svoboda, M., et al. (2016). Long non-coding RNA ZFAS1 interacts with CDK1 and is involved in p53-dependent cell cycle control and apoptosis in colorectal cancer. *Oncotarget* 7, 622–637. doi: 10.18632/oncotarget.5807

Wang, K. C., and Chang, H. Y. (2011). Molecular mechanisms of long noncoding RNAs. *Mol. Cell.* 43, 904–914. doi: 10.1016/j.molcel.2011.08.018

Wang, Y., and Lee, C. G. (2009). MicroRNA and cancer–focus on apoptosis. *J. Cell. Mol. Med.* 13, 12–23. doi: 10.1111/j.1582-4934.2008.00510.x

Wang, X., Song, X., Glass, C. K., and Rosenfeld, M. G. (2011). The long arm of long noncoding RNAs: roles as sensors regulating gene transcriptional programs. *Cold Spring Harb. Perspect. Biol.* 3:a003756. doi: 10.1101/cshperspect.a003756

Wang, J., Gong, X., Tian, G. G., Hou, C., Zhu, X., Pei, X., et al. (2018). Long noncoding RNA growth arrest-specific 5 promotes proliferation and survival of female germline stem cells *in vitro*. *Gene* 653, 14–21. doi: 10.1016/j.gene.2018.02.021

Wapinski, O., and Chang, H. Y. (2011). Long noncoding RNAs and human disease. *Trends Cell Biol.* 21, 354–361. doi: 10.1016/j.tcb.2011.04.001

Wilhelmm, D., and Bernard, P. (2016). Non-coding RNAs and the Reproductive System. *Adv Exp Med Biol.* 886, V–Vi. doi: 10.1007/978-94-017-7417-8

Xu, Y., Li, X., Wang, H., Xie, P., Yan, X., Bai, Y., et al. (2016). Hypermethylation of CDH13, DKK3 and FOXL2 promoters and the expression of EZH2 in ovary granulosa cell tumors. *Mol. Med. Rep.* 14, 2739–2745. doi: 10.3892/mmr.2016.5521

Yacqub-Usman, K., Pickard, M. R., and Williams, G. T. (2015). Reciprocal regulation of GAS5 lncRNA levels and mTOR inhibitor action in prostate cancer cells. *Prostate* 75, 693–705. doi: 10.1002/pros.22952

Yamazaki, T., and Hirose, T. (2015). The building process of the functional paraspeckle with long non-coding RNAs. *Front. Biosci.* 7, 1–41. doi: 10.2741/e715

Yan, B., Wang, Z. H., and Guo, J. T. (2012). The research strategies for probing the function of long noncoding RNAs. *Genomics* 99, 76–80. doi: 10.1016/j.ygeno.2011.12.002

Yoo, A. S., Sun, A. X., Li, L., Shcheglovitov, A., Portmann, T., Li, Y., et al. (2011). MicroRNA-mediated conversion of human fibroblasts to neurons. *Nature* 476, 228–231. doi: 10.1038/nature10323

Yu, M. C. (2011). The role of protein arginine methylation in mRNP dynamics. *Mol. Biol. Int.* 2011:163827. doi: 10.4061/2011/163827

Zhao, H., and Rajkovic, A. (2008). MicroRNAs and mammalian ovarian development. *Semin. Reprod. Med.* 26, 461–468. doi: 10.1055/s-0028-1096126

Zhao, J., Sun, B. K., Erwin, J. A., Song, J. J., and Lee, J. T. (2008). Polycomb proteins targeted by a short repeat RNA to the mouse X chromosome. *Science* 322, 750–756. doi: 10.1126/science.1163045

Zhu, S. J., Hallows, S. E., Currie, K. W., Xu, C., and Pearson, B. J. (2015). A mex3 homolog is required for differentiation during planarian stem cell lineage development. *eLife* 4:e07025. doi: 10.7554/eLife.07025

Zinszner, H., Sok, J., Immanuel, D., Yin, Y., and Ron, D. (1997). TLS (FUS) binds RNA in vivo and engages in nucleo-cytoplasmic shuttling. *J Cell Sci.* 110 (Pt 15), 1741–1750.

Zuccotti, M., Merico, V., Cecconi, S., Redi, C. A., and Garagna, S. (2011). What does it take to make a developmentally competent mammalian egg? *Hum. Reprod. Update* 17, 525–540. doi: 10.1093/humupd/dmr009

Conflict of Interest Statement: The authors declare that the research was conducted in the absence of any commercial or financial relationships that could be construed as a potential conflict of interest.

frontiers in Cell and Developmental Biology

REVIEW
published: 26 June 2018
doi: 10.3389/fcell.2018.00063

Ion Channel Function During Oocyte Maturation and Fertilization

Ingrid Carvacho[1], Matthias Piesche[2], Thorsten J. Maier[3] and Khaled Machaca[4]*

[1] Department of Biology and Chemistry, Faculty of Basic Sciences, Universidad Católica del Maule, Talca, Chile, [2] Biomedical Research Laboratories, Medicine Faculty, Universidad Católica del Maule, Talca, Chile, [3] Department of Anesthesiology, Intensive Care Medicine and Pain Therapy, Goethe-University Hospital, Frankfurt, Germany, [4] Department of Physiology and Biophysics, Weill Cornell-Medicine-Qatar, Education City, Qatar Foundation, Doha, Qatar

The proper maturation of both male and female gametes is essential for supporting fertilization and the early embryonic divisions. In the ovary, immature fully-grown oocytes that are arrested in prophase I of meiosis I are not able to support fertilization. Acquiring fertilization competence requires resumption of meiosis which encompasses the remodeling of multiple signaling pathways and the reorganization of cellular organelles. Collectively, this differentiation endows the egg with the ability to activate at fertilization and to promote the egg-to-embryo transition. Oocyte maturation is associated with changes in the electrical properties of the plasma membrane and alterations in the function and distribution of ion channels. Therefore, variations on the pattern of expression, distribution, and function of ion channels and transporters during oocyte maturation are fundamental to reproductive success. Ion channels and transporters are important in regulating membrane potential, but also in the case of calcium (Ca^{2+}), they play a critical role in modulating intracellular signaling pathways. In the context of fertilization, Ca^{2+} has been shown to be the universal activator of development at fertilization, playing a central role in early events associated with egg activation and the egg-to-embryo transition. These early events include the block of polyspermy, the completion of meiosis and the transition to the embryonic mitotic divisions. In this review, we discuss the role of ion channels during oocyte maturation, fertilization and early embryonic development. We will describe how ion channel studies in *Xenopus* oocytes, an extensively studied model of oocyte maturation, translate into a greater understanding of the role of ion channels in mammalian oocyte physiology.

Keywords: ion currents, fertilization, patch-clamp, membrane potential, oocyte maturation, Ca^{2+} signaling

OPEN ACCESS

Edited by:
Karin Lykke-Hartmann, Aarhus University, Denmark

Reviewed by:
Rajprasad Loganathan, Johns Hopkins University, United States
Andrew Burgess, Anzac Research Institute, Australia

****Correspondence:***
Ingrid Carvacho
icarvacho@ucm.cl;
ingridcarvacho@gmail.com

Specialty section:
This article was submitted to Cell Growth and Division, a section of the journal Frontiers in Cell and Developmental Biology

Received: *14 February 2018*
Accepted: *04 June 2018*
Published: *26 June 2018*

Citation:
Carvacho I, Piesche M, Maier TJ and Machaca K (2018) Ion Channel Function During Oocyte Maturation and Fertilization. Front. Cell Dev. Biol. 6:63. doi: 10.3389/fcell.2018.00063

INTRODUCTION

Historically, the studies of gamete maturation and fertilization have been intimately associated with the regulation of ionic currents in these cells. Some of the earliest discoveries in ion channel biology have been driven by the desire to understand the mechanisms governing fertilization. The calcium (Ca^{2+})-release theory of egg activation, which was conceived based on early experiments in the late 1920s and into the 1930s (Tyler, 1941) has withstood the test of time. Indeed, both single and repetitive Ca^{2+} transient(s), propagating as a Ca^{2+} release wave across the egg is recognized as the trigger for egg activation at fertilization in all species tested to date (Stricker, 1999; Machaca, 2007; Kashir et al., 2013). Further improvements in our understanding of the electrical properties of

both oocyte and the egg, have shed light on important processes involved in fertilization including the block to polyspermy. Initial electrophysiology studies determined the essential role of plasma membrane (PM) depolarization to the establishment of a fast block to polyspermy in sea urchin and *Xenopus* oocytes, among other species (Jaffe, 1976; Cross and Elinson, 1980; Jaffe and Cross, 1984).

Oocyte maturation in vertebrates is initiated following the release of the extended meiotic arrest that vertebrate oocytes experience during their growth and development. Oocytes arrest at the prophase stage of meiosis I with the nuclear envelope still intact. During this stage, oocytes grow and accumulate macromolecular components required for fertilization and early embryonic development. Upon hormonal stimulation, oocytes exit this extended meiotic arrest and undergo a complex differentiation pathway that encompasses both a reductionist nuclear division (meiosis) and a comprehensive cytoplasmic reorganization. This prepares the oocyte for the egg-to-embryo transition following fertilization (Smith, 1989; Miyazaki, 1995; Hassold and Hunt, 2001). An important aspect of oocyte maturation is the remodeling of the Ca^{2+} signaling machinery to allow the egg to activate properly at fertilization (Machaca, 2007; Nader et al., 2013). The induction of oocyte maturation ultimately culminates through multiple steps in the activation of maturation promoting factor (MPF). MPF is composed of cyclin dependent kinase 1 (Cdk1), in complex with cyclin B (B-Cdk1), and the associated nuclear kinase Greatwall, also known as microtubule associate threonine like kinase (Gwl/MASTL). MPF is the master regulator of both meitotic and mitotic M-phase (Kishimoto, 2015). Oocyte maturation is complete when oocyte reaches a second arrest in metaphase of meiosis II at which stage they become fertilization-competent and are typically referred to as "eggs" (Smith, 1989; Bement and Capco, 1990). The arrest at metaphase II requires cytostatic factor (CSF) which inhibits the anaphase promoting complex (APC) and prevents progression to Anaphase II (Tunquist and Maller, 2003). The APC is an ubiquitin ligase that tags cyclin B and other regulatory proteins which results in the loss of Cdk1 activity triggering exit from metaphase arrest and allowing progression to anaphase (Schmidt et al., 2005; Inoue et al., 2007; Nishiyama et al., 2007). The activity of ion channels and transporters and their remodeling during oocyte maturation is ultimately governed by this complex signaling cascade. Therefore, oocyte maturation is a cellular differentiation program that prepares the egg for fertilization and for the egg-to-embryo transition processes where ionic conductances play essential roles.

In mammals, fertilization results in the release of a sperm specific phospholipase [phospholipase ζ (PLCζ)] into the egg cytoplasm upon sperm-egg fusion. It has been proposed that PLCζ hydrolyzes not only PM phosphoinositol 4,5 bisphosphate (PIP_2) but mainly intracellular PIP_2 (Yu et al., 2012; Swann and Lai, 2016), generating inositol triphosphate ($InsP_3$) and diacylglycerol (DAG). $InsP_3$ binds to the IP_3 receptor (IP_3R) on the endoplasmic reticulum (ER) and triggers the release of Ca^{2+} which mediates egg activation (Saunders et al., 2002). The ultimate role of PLCζ as the trigger for the Ca^{2+} oscillations in mammals was recently elucidated through the generation of a mice lacking *Plcz1* (*Plcz1*$^{-}$). Wild type eggs that were injected with *Plcz1*$^{-}$ sperm were unable to mount Ca^{2+} oscillations. Similar results were observed in experiments of *in-vitro* fertilization (IVF) using *Plcz1*$^{-}$ sperm. Surprisingly, *Plcz1*$^{-}$ mice are fertile, yet they do exhibit subfertility phenotype, suggesting a redundant system for egg activation to assure reproduction in animals (Hachem et al., 2017). The fertilization Ca^{2+} signal takes the form of multiple oscillations that encode egg activation events, including pro-nucleus formation and the transition to embryonic development (Ducibella et al., 2002). In frogs, sea urchin and starfish, fertilization is also associated with a change of resting membrane potential, referred to as the "fertilization potential" which was compared to the action potential in neurons early on. The egg membrane potential undergoes a transient positive shift at fertilization that acts as an electrical polyspermy blockade. The effect of membrane potential depolarization on the polyspermy block was confirmed by holding the membrane potential of an unfertilized egg at positive potentials which prevented fertilization (Jaffe and Cross, 1984). In 2014, a detailed analysis of published data challenged the evidence of the fast block of polyspermy in sea urchin, proposing that a particular organization of the cytoskeleton could determine monospermic fertilization (Dale, 2014). However, the time scale of the electrical fast block would argue against it.

In contrast, hamster eggs showed transients hyperpolarization in response to fertilization (Miyazaki and Igusa, 1981), while mice eggs only showed very small hyperpolarization (3–4 mV), questioning the existence of electrical block to polyspermy in this species (Igusa et al., 1983). It has rather been proposed that the block to polyspermy in mammals is based on the hardening of the *zona pellucida* (ZP). This process is mediated by the protein ovastacin whose function is to cleave *zona pellucida* 2 (ZP2), rendering the ZP resistance to protease digestion and inhibiting sperm binding (Burkart et al., 2012). Notwithstanding, transgenic mice containing a non-cleavable ZP2 and female mice null for ovastacin are both fertile, suggesting an additional mechanism or a combination of different strategies to avoid polyspermy (Bianchi and Wright, 2016).

In this review, we discuss the role of ionic currents at the PM primarily during oocyte maturation and fertilization. These conductances encompass transporters in addition to Cl^{-} channels, K^{+} channels, Ca^{2+} channels, and other channels that are important in mediating fertilization and egg activation. Therefore, it is important to understand the regulation of these conductances as their remodeling contributes to define the competence of the egg to fertilization and undergo the egg-to-embryo transition. Interestingly, the activity of ion channels during the processes of oocyte maturation and fertilization is not limited to channels localizing to the PM but also includes intracellular channels. As a case in point, the role of changes in the IP_3 Receptor (IP_3R) activity and localization observed during *Xenopus* oocyte maturation in preparing the egg for fertilization will be discussed.

The role that ionic currents play in the regulation of oocyte maturation is increasingly being recognized. Hence, it is important to elucidate the molecular mechanisms governing their remodeling during maturation and activity at fertilization.

Furthermore, comparative studies from different species, as would be discussed herein between *Xenopus* and mammals, provide important insights into the mechanisms governing the regulation of ion channels in gametes.

INITIAL MEASUREMENTS OF ION CHANNEL ACTIVITY IN REPRODUCTION

The electrical properties of eggs particularly at fertilization have been of interest to embryologists since membrane potential changes were first recorded in neurons and muscle cells (Hille, 2001). It is now well established that the membrane potential is maintained by differences in ion concentrations between the intra and extra cellular media. The resulting generation of an electrical potential difference across the PM can be measured through electrophysiology. Intracellular voltage and current polarity are defined in relation to the "ground" (zero voltage) reference electrode in the extracellular medium (Ypey and DeFelice, 2000). Original assessments of the egg's membrane potential using standard electrophysiological approaches were performed in eggs from marine species. Although initial attempts using capillary microelectrodes failed, the implementation of intracellular microelectrodes allowed the measurement of resting potential and ion fluxes through the membrane of star fish eggs (Tyler et al., 1956). Invariably, the membrane potential in the resting state or "resting potential" (RP), in all living cells has a negative value expressed as a difference using the bath as the "ground" reference (for example, a neuron RP ranges from −70 to −90 mV). Ion channels transport ions down their concentration gradient, from areas of high to low abundance, generating ion currents that determine, and regulate membrane potential (Hille, 2001; Tosti et al., 2013).

Using an intracellular microelectrode and a conventional extracellular ringer, the RP of mouse eggs was shown to vary depending on the mouse strain (∼ −14 to −20 mV). The membrane showed permeability to K^+ and Na^+, however, one needs to consider the possibility that these conductances may be affected by damage to the eggs by the electrode impalement procedure (Powers and Tupper, 1974; Hagiwara and Jaffe, 1979). The development of the patch-clamp technique changed the landscape relating to accuracy in data acquisition, allowing the mouse egg's RP and ion channel activity to be measured with minimal damage to the cell (Hamill et al., 1981). Conventional voltage-clamp and patch-clamp measurements indicate that in mouse eggs, the RP ranges between ∼ −30 and −50 mV depending on the composition of the extracellular media (Igusa et al., 1983; Peres, 1986; Bernhardt et al., 2015). Using the same methodology, Maeno described a fundamental difference between the action potential of a nerve or muscle cell and the ones measured from oocytes and eggs from the toad. During egg activation, changes in membrane potential were caused by an increased permeability to Cl^- ions, whereas action potentials of neurons and muscle cells were driven by changes in Na^+ and K^+ conductances (Maeno, 1959). Electrophysiology is the most direct approach to study ion channels and allows direct characterization of these proteins in oocytes and eggs. Below, we describe the properties of ion channels that have been implicated in oocyte maturation and fertilization.

XENOPUS VS. MAMMALIAN OOCYTES: COMPARISON OF ION CHANNEL EXPRESSION AND FUNCTION

The fluxes of ions during oocyte maturation and at fertilization are mediated by ion channels, transporters and pumps. Most of them localize at the PM; however, intra and intercellular channels are also fundamental players supporting cellular processes. Ca^{2+} is the main signal underlying oocyte maturation and egg activation. Transport of Ca^{2+} through ion channels have been recognized as critical step, for example, to assure egg activation. In this section ion channels expressed in *Xenopus* and mammalian oocytes and eggs will be reviewed. Due to the fundamental role of Ca^{2+} in reproduction, we will focus on Ca^{2+} channels and Ca^{2+} modulated channels.

Ca^{2+} Signaling

Ca^{2+} is a universal second messenger that is fundamental to cellular signaling and homeostasis (Berridge, 2005; Clapham, 2007). The ionic nature of Ca^{2+} makes it unique among second messengers. Agonist activation of particular receptor types triggers the transport of Ca^{2+} into the signaling compartment (the cytoplasm) through channels, transporters and/or pumps. Cells support Ca^{2+} signaling by maintaining low cytoplasmic Ca^{2+} levels at rest (∼100 nM). During the rising phase of a Ca^{2+} signal, Ca^{2+} flows into the cytoplasm either from the endoplasmic reticulum (ER) which concentrates Ca^{2+} at 250–600 μM, or from the extracellular space, where Ca^{2+} concentrations are typically 1–2 mM (Clapham, 1995; Demaurex and Frieden, 2003). ER localized non-selective cation channels, typically IP_3 Receptors (IP_3R) or Ryanodine Receptors (RyR), mediate Ca^{2+} release from the ER. Both IP_3Rs, and RyRs have been detected in rodent oocytes (Miyazaki et al., 1992; Kline and Kline, 1994). *Xenopus* oocytes, in contrast, express only a single isoform of Ca^{2+} release channels, the type 1 IP_3R (Parys et al., 1992; Parys and Bezprozvanny, 1995). Both mammals and *Xenopus* eggs require IP_3-dependent Ca^{2+} release from the ER for egg activation at fertilization (Larabell and Nuccitelli, 1992; Miyazaki et al., 1992, 1993; Swann, 1992; Nuccitelli et al., 1993; Kline and Kline, 1994; Jones et al., 1995; Runft et al., 2002).

Ca^{2+} is the universal signal for egg activation at fertilization in all sexually reproducing species tested (Stricker, 1999; Whitaker, 2006). Thus, different species have evolved elaborate strategies to safeguard reproductive isolation. These include preventing the fusion of gametes from divergent species even if they are evolutionarily similar (Vieira and Miller, 2006). The versatility and diversity of Ca^{2+} in mediating a plethora of physiological responses make it an ideal second messenger to induce egg activation at fertilization. Ca^{2+} is able to signal across broad spatial (from the nm to cm scales) and temporal (μsec to h) ranges (Berridge et al., 2000). Ca^{2+} mediates cellular responses ranging from the rapid and localized like neurotransmitter

release, to the slow and spatially spread out, such as the activation of development at fertilization.

Immature fully-grown vertebrate oocytes in the ovary are unable to support the egg-to-embryo transition. Eggs acquire the ability to be activated at fertilization during oocyte maturation. A major component of acquiring this competence is the remodeling of the Ca^{2+} signaling machinery, primarily the modulation of Ca^{2+} channels and transporters function during oocyte maturation. This has been best studied in *Xenopus* (Machaca, 2007) and mammalian oocytes, and will be reviewed briefly below.

Ca^{2+} Release

The frog egg is an exemplary model for the study of Ca^{2+} dependent egg activation processes including block to polyspermy and the release of metaphase II arrest to complete meiosis (Stricker, 1999; Runft et al., 2002; Whitaker, 2006). Immediately after sperm fusion, the Ca^{2+} transient activates Ca^{2+}-activated Cl^- channels (CaCC), resulting in membrane depolarization and the so called "fast electrical block to polyspermy" (Machaca et al., 2001). This is followed by cortical granule fusion which is also a Ca^{2+}-dependent event. The cortical granule reaction results in modification of the egg extracellular matrix and a more permanent block to polyspermy (Grey et al., 1974; Wolf, 1974). Polyspermy block in mammals is hypothesized to occur through a similar Ca^{2+} evoked cortical granule release process (Abbott and Ducibella, 2001), in addition to other mechanisms.

Following the establishment of the polyspermy block, Ca^{2+} signaling then induces the egg to exit from metaphase II. The exit occurs by activating Ca^{2+}-calmodulin-dependent protein kinase II (CaMKII) to start the egg activation processes (Lorca et al., 1993). CaMKII phosphorylates Emi2, an essential component of CSF (Schmidt et al., 2006). Emi2 is a direct inhibitor of APC. CaMKII-mediated degradation of Emi2 releases the oocyte from CSF-mediated metaphase II arrest, allowing anaphase II to proceed (Liu and Maller, 2005; Rauh et al., 2005; Tung et al., 2005). This activates the APC, leading to ubiquitination and degradation of Cyclin B. Degradation of Cyclin B, in turn, downregulates MPF activity and allows meiosis to reach completion (Morin et al., 1994). The fertilization-induced Ca^{2+} signal also activates the Ca^{2+}-dependent phosphatase, calcineurin, which reinforces APC activation and the degradation of Cyclin B (Mochida and Hunt, 2007; Nishiyama et al., 2007). The Ca^{2+} transient induced by fertilization encodes sequential cellular rearrangements that are critical for egg activation.

IP_3 Receptor

IP_3 receptors (IP_3R) are tetrameric channels with the structure of each subunit consisting of six transmembrane domains, a p-loop and a large cytoplasmic domain representing the bulk of the protein. They are non-selective cation channels that are Ca^{2+}-permeant. Given the large Ca^{2+} gradient established across the ER membrane, IP_3R gating results in Ca^{2+} release from intracellular ER Ca^{2+} stores (Parys and Bezprozvanny, 1995; Foskett et al., 2007). The IP_3R has three isoforms, type 1, 2, and 3. All three isoforms are expressed in mammalian oocytes and eggs, with the type I isoform being the most dominant (Wakai et al., 2011). The IP_3R is modulated by Ca^{2+} and IP_3 and requires the binding of both for the conduction path to open (Taylor and Tovey, 2010). In most vertebrates, the IP_3R is responsible for the fertilization-induced Ca^{2+} transient. In mammals, an initial first large Ca^{2+} transient is observed upon fertilization, similar to event observed in frog eggs. Unique to mammals however, are the multiple Ca^{2+} oscillations that follow this large transient, and last for several hours (Kline and Kline, 1992; Mohri et al., 2001). The phosphorylation of the IP_3R was proposed to modulate Ca^{2+} fluxes from the ER. Initial theories proposed that phosphorylation impacted the activity of the IP_3R during oocyte maturation by promoting Ca^{2+} transport at fertilization (Fujiwara et al., 1993; Mehlmann and Kline, 1994; Terasaki et al., 2001; Machaca, 2004; Zhang et al., 2015); (**Table 1**). In mouse IP_3R, several serine/threonine residues have been identified as targets for phosphorylation during oocyte maturation (Westendorf et al., 1994). Cell cycle kinases such as mitogen-activated protein kinase (MAPK), extracellular signal-regulated kinase (ERK) and Cdk1 have been shown to phosphorylate the receptor (Bai et al., 2006; Lee et al., 2006; Zhang et al., 2015). Kinase motifs include the Cdk1 consensus sites [S^{421}, T^{799}, S^{2147}] (Nigg, 1991; Malathi et al., 2003; Wakai et al., 2012) and the ERK site [S^{436}] (Bai et al., 2006; Lee et al., 2006). In addition, several other kinases have been reported to phosphorylate the IP_3R including protein kinase A (PKA, [S^{1589}, S^{1755}, and T^{930}] Ferris et al., 1991; Haun et al., 2012; Xu and Yang, 2017), protein kinase G (PKG, same sites as PKA), protein kinase C (PKC, Vanderheyden et al., 2009) and protein kinase B (PKB or Akt, [S^{2681}] Vanderheyden et al., 2009. Other kinases such as CaMKII and Rho kinases also mediate phosphorylation of the IP_3R (Vanderheyden et al., 2009). Originally, it was suggested that phosphorylation modulates the function of the IP_3R by sensitizing its release of Ca^{2+} at fertilization (Fujiwara et al., 1993; Mehlmann and Kline, 1994; Terasaki et al., 2001; Machaca, 2004; Zhang et al., 2015) (**Table 1**). In *Xenopus*, this sensitization was thought to be due to an increased affinity of the IP_3R for IP_3 (Machaca, 2004; Ullah et al., 2007). However, phosphorylation of the IP_3R does not ultimately result in an increased affinity for IP_3 (Sun et al., 2009). High constitutive PKA activity in the oocyte is required to maintain meiotic arrest, resulting in basal phosphorylation of IP_3R PKA sites. This phosphorylation is unaltered during maturation (Sun et al., 2009). The IP_3R is also phosphorylated at additional sites that match the MAPK and/or the Cdk1. Activation of MAPK or Cdk1 is required for sensitizing IP_3-dependent Ca^{2+} release during oocyte maturation (Sun et al., 2009). The MAPK/Cdk1 consensus phosphorylation sites altered during oocyte maturation are T931, T1136, and T1145 (Sun et al., 2009). Surprisingly though, phosphorylation of the IP_3R on at least one of those residues decreased its affinity to IP_3 rather than the expected increase in affinity (Haun et al., 2012). This observation argues against phosphorylation being the primary driver of the increased sensitivity of the IP_3R for IP_3 observed during maturation. As it turns out, the mechanism is much more complex and elegant. The ER suffers dramatic remodeling that is dependent on the kinase cascades activated during maturation, in the process of "geometric sensitization" (Sun et al., 2011).

TABLE 1 | Channel expression and function in *Xenopus* and mouse oocytes and eggs.

Channel	*Xenopus*	Mouse
INTRACELLULAR		
IP_3R1	Oocytes and eggs showed responses to IP_3. IP_3R in mature eggs is more sensitive to IP_3 than it is in oocytes (Terasaki et al., 2001; Machaca, 2004; Sun et al., 2009, 2011)	Expressed at GV oocytes and MII eggs. Increases activity during oocyte maturation (Mehlmann and Kline, 1994)
PLASMA MEMBRANE (PM)		
CRAC (ORAI+STIM)	Inactivates during oocyte maturation (Machaca and Haun, 2000, 2002; Yu et al., 2009, 2010)	Inactivates during oocyte maturation (Cheon et al., 2013; Lee et al., 2013). *Orai* and *Stim* KO animals are fertile (Bernhardt et al., 2017)
T type Ca^{2+} channel	Not reported	Expressed in GV and MII. KO animals are fertile (Chen et al., 2003; Bernhardt et al., 2015)
TRPV3	Not reported	Expressed at MI oocytes and MII eggs. KO animals are fertile (Cheng et al., 2010; Carvacho et al., 2013)
TRPM7	Not reported	TRPM7-like currents are expressed at GV, MII and in 2-cell embryos (Carvacho et al., 2016)
Ca^{2+} activated chloride channels (CaCC)	Expressed in eggs. Responsible for fast electrical block to polyspermy (Cross and Elinson, 1980), regulates resting membrane potential (Kuruma and Hartzell, 2000), and length of microvilli (Courjaret et al., 2016)	Expressed in embryos (Li et al., 2007)
Swell-activated Cl^- channels	Not reported	Functionally expressed in MII eggs and embryos (Kolajova et al., 2001)
Voltage activated K^+ channels	Expressed in eggs (Tokimasa and North, 1996)	Reported in MII eggs (Day et al., 1993)
Connexins (Cx37 and Cx43)	Not reported	Cx37 KO animals are infertile (Simon et al., 1997) Ovaries lacking Cx43 contain oocytes that cannot be fertilized (Ackert et al., 2001)

The ER remodeling results in the formation of large patches of convoluted membranes highly enriched with IP_3Rs orienting in close apposition to each other (Sun et al., 2011). IP_3Rs within these ER patches exhibit a significantly enhanced sensitivity to IP_3 compared to IP_3Rs within the adjacent ER, despite the fact that IP_3Rs exchange freely between the patches and adjacent ER (Sun et al., 2011). Thus, the sensitization of IP_3Rs during oocyte maturation is due to ER remodeling, and the enhanced Ca^{2+}-induced Ca^{2+} release evoked by the close apposition of IP_3Rs (geometric sensitization) (Sun et al., 2011).

Another Ca^{2+} transport protein, the PM Ca^{2+}-ATPase (PMCA), is also modulated during oocyte maturation. In *Xenopus* oocytes, PMCA localizes to the PM where it contributes to Ca^{2+} extrusion. This activity supports the return of cytoplasmic Ca^{2+} concentration to baseline levels following a Ca^{2+} transient at fertilization (El Jouni et al., 2005, 2008). During oocyte maturation, the PMCA is removed from the PM through an internalization process that places them in an intracellular vesicular pool (El Jouni et al., 2005, 2008). PMCA internalization during meiosis is dependent on its N-terminal cytoplasmic domain and on MPF activation (El Jouni et al., 2008). Furthermore, several lines of evidence argue that PMCA internalization goes through a lipid-raft endocytic pathway (El Jouni et al., 2008).

Calcium Channels

Store-Operated Ca^{2+} Entry, SOCE

Ca^{2+} influx into cells is mediated by a diverse population of Ca^{2+} transport proteins exhibiting significant diversity in their gating and activation mechanisms. Ca^{2+} channels at the PM can be gated by voltage, ligand, second messengers, store depletion, or physically through protein-protein interactions. In vertebrate oocytes the predominant Ca^{2+} influx pathway appears to be through store-operated Ca^{2+} entry (SOCE). SOCE is directly regulated by the level of Ca^{2+} in intracellular ER stores (Kline and Kline, 1992; Hartzell, 1996; Machaca and Haun, 2000, 2002). Emptying of intracellular ER stores can be triggered using thapsigargin, an irreversible inhibitor of the sarcoplasmic reticulum/ER Ca-ATPase (SERCA). The pathway through which Ca^{2+} exits the ER into the cytoplasm following thapsigargin treatment has not yet been identified. Thapsigargin-induced depletion of the ER Ca^{2+} store activates the influx of extracellular Ca^{2+} into the cytoplasm of unfertilized eggs (Kline and Kline, 1992). When ER Ca^{2+} stores have been significantly depleted by the persistent presence of thapsigargin, sperm are no longer capable of triggering Ca^{2+} oscillations (Kline and Kline, 1992). Evidence that Ca^{2+} influx is essential for the maintenance of oscillations triggered by sperm was demonstrated by addition of BAPTA to the extracellular media. BAPTA is a membrane impermeable Ca^{2+} chelator which prevented the generation of oscillations by the sperm (Kline and Kline, 1992). Additionally, the frequency of Ca^{2+} oscillations can be modulated by changing the external concentration of Ca^{2+} (Shiina et al., 1993). Thus, extracellular Ca^{2+} is an important source to support Ca^{2+} oscillations.

SOCE or Ca^{2+} release-activated Ca^{2+} channels (CRAC), were first described in immune cells where they have been shown to be critical for their activation. Accordingly, defects in SOCE in

humans are associated with severe immunodeficiencies (Bogeski et al., 2010). SOCE is mediated through the interactions of ER Ca^{2+} sensors, stromal interaction molecule (STIM), with ORAI ion channels at the PM. STIM proteins cluster in the ER following store depletion, localizing to ER-PM junctions where they physically recruit and interact with ORAI proteins to gate their pore open (Lewis, 1999). ORAIs are 4 pass transmembrane proteins that form highly Ca^{2+}-selective channels (Prakriya et al., 2006; Vig et al., 2006). STIM has two homologs: STIM 1 and 2; and ORAI has three family members, ORAI1, 2 and 3 (Shim et al., 2015).

During *Xenopus* oocyte maturation, SOCE is completely inactivated (Machaca and Haun, 2000). This inactivation is essential for the remodeling of Ca^{2+} signaling pathways to enable the generation of the specialized fertilization-specific Ca^{2+} transient that encodes the egg-to-embryo transition (Machaca, 2007; Nader et al., 2013) (**Table 1**). As discussed above, this Ca^{2+} signal at fertilization is the spark that induces egg activation (Fontanilla and Nuccitelli, 1998). *Xenopus* oocyte SOCE downregulation may represent a safety mechanism to prevent premature activation due to spontaneous Ca^{2+} influx. *Xenopus* eggs are ovulated in pond water of uncontrolled ionic content. Indeed, all ionic currents across the egg PM tend to be downregulated, with the exception of the Ca^{2+}-activated Cl channels which are required for the block to polyspermy as discussed below (Nader et al., 2013).

The mechanisms governing SOCE inhibition during *Xenopus* oocyte maturation have been studied in detail. The activation of MPF is required for SOCE inhibition during maturation (Machaca and Haun, 2002). This results in the internalization of ORAI1 into a Rab5-positive endosomal compartment through a caveolin and dynamin-dependent endocytic pathway (Yu et al., 2009, 2010). STIM1 does maintain its ability to interact with ORAI1 in *Xenopus* eggs, however, in mature eggs; ER store depletion does not lead to STIM1 clustering. Clustering is a pre-requisite for STIM stabilization in the cortical ER (Yu et al., 2009). Although stim1 is phosphorylated during oocyte maturation, this phosphorylation does not modulate STIM1 function or its inhibition during meiosis. Mutant STIM proteins that cannot be phosphorylated are unable to rescue SOCE downregulation in *Xenopus* eggs, even when co-expressed with an *Orai1* mutant that cannot be internalized (Yu et al., 2009; 2010).

Expression of SOCE components in mammals has been shown at the mRNA levels as well as by immunocytochemistry and western blotting in mouse oocytes (Gomez-Fernandez et al., 2009; Cheon et al., 2013) and porcine eggs (Koh et al., 2009; Wang et al., 2012). However, in some cases, the specificity of the antibodies used requires additional confirmation. Further, the function of SOCE during mouse fertilization remains controversial and may play a minor role. In a MII egg study, STIM1 was found to form discrete patches co-localizing with an ER marker prior to fertilization. This organization changed following Ca^{2+} depletion showing high co-localization with ORAI1. Thus, a role for SOCE in Ca^{2+} signaling during fertilization was suggested (Gomez-Fernandez et al., 2009, 2012). However, the size of the large STIM patches observed in these studies was not consistent with the patch size noted in other cells. In addition, specific inhibitors of SOCE did not disrupt Ca^{2+} oscillations induced by fertilization (Miao et al., 2012; Carvacho et al., 2013). Finally, experiments tracking the expression of exogenously-tagged STIM1 and ORAI1 proteins found that SOCE downregulation during oocyte maturation was mainly due to reorganization of STIM and an internalization of ORAI1 (Cheon et al., 2013; Lee et al., 2013) (**Table 1** and **Figure 1**).

One of the main issues regarding the functional expression of CRAC channels in mouse eggs is the lack of electrophysiological evidence. CRAC channels have a small unitary conductance such that at physiological concentration of Ca^{2+} (2 mM) the single channel conductance of CRAC channels is $\leq$ 9 fS, and at 20 mM Ca^{2+} it is 18–24 fS (McNally and Prakriya, 2012). Given the magnitude of the expected whole-cell current and

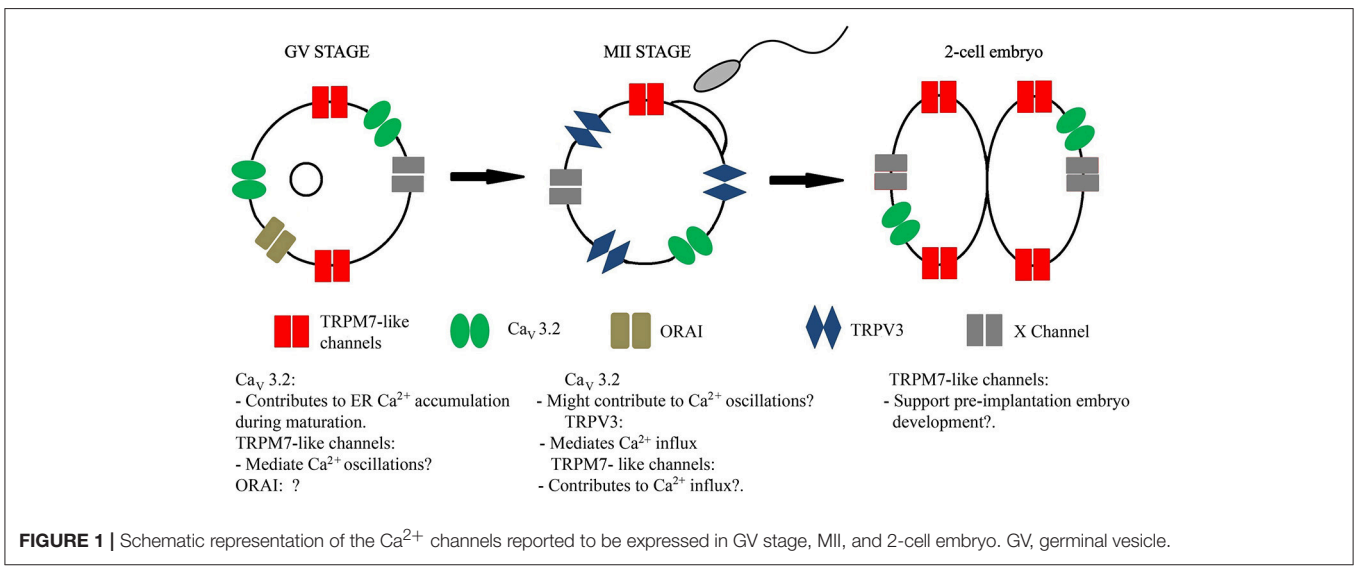

FIGURE 1 | Schematic representation of the Ca^{2+} channels reported to be expressed in GV stage, MII, and 2-cell embryo. GV, germinal vesicle.

the background currents in eggs, detection of CRAC channels activity would be technically challenging. Additionally, protocols to empty intracellular Ca^{2+} stores weaken the stability of the patch-clamp seal during electrophysiological measurements. Final confirmation that the function of STIM1 and ORAI1 are not required for fertilization and the egg-to-embryo transition came from the generation of oocyte-specific knockout mouse line for *Stim1/2* and the study of the global KO for *Orai1* (Vig et al., 2008). These lines showed no fertility defects and the eggs showed a normal pattern of Ca^{2+} oscillations at fertilization (Bernhardt et al., 2017).

There are reports that SOCE in some cell types can be mediated by interaction between STIM1 and members of the Transient Receptor Potential (TRP) channel family, particularly from the TRP canonical (TRPC) subfamily (Zeng et al., 2008; Yuan et al., 2009). TRPCs channels have been proposed to interact with STIM1 and act as store-operated channels. TRPC can form complexes with ORAI, however, it has been shown that ORAI channels are functional in absence of TRPCs (Birnbaumer, 2015). Additionally, the heptaKO females for TRPCs (C1–C7) channels are fertile (Birnbaumer, 2015) and eggs from these animals showed normal Ca^{2+} oscillations (Bernhardt et al., 2017). These evidences rule out a role for TRPCs in Ca^{2+} influx. The fact that a *Stim 1/2* KO mouse is fertile argues that SOCE is not essential for fertilization in this species or that there are redundant ionic pathways in the eggs able to refill the stores sufficiently even in the absence of SOCE. The latter scenario seems more attractive especially that SOCE is detectable by Ca^{2+} imaging in mouse eggs despite the fact that it is downregulated during oocyte maturation (Cheon et al., 2013; Lee et al., 2013). Despite the strong evidence against a role for STIM and ORAI at fertilization, their overexpression in mouse oocyte has been shown to disrupt early embryonic development (Lee et al., 2013). Thus, the regulation of Ca^{2+} influx during fertilization is critical for normal egg-to-embryo transition.

In pig eggs, the evidence that STIM1 plays a role in refilling intracellular Ca^{2+} stores and fertilization is more direct: knockdown of *Stim1*, using RNAi, abolished thapsigargin-induced Ca^{2+} influx (Koh et al., 2009), sperm-induced Ca^{2+} oscillations and affected embryo development (Lee et al., 2012). Manipulating the expression of *Orai1* also had consequences on store-operated Ca^{2+} influx. Overexpression of *Orai1* disrupted the oscillations triggered by fertilization. Downregulation of *Orai*1 abolished Ca^{2+} oscillations and diminished the rate of blastocyst formation (Wang et al., 2012; Machaty et al., 2017). Using FRET (Fluorescence Resonance Energy Transfer) it was shown that mVenus-*Stim1* and mTurquoise2-*Orai*, constructs that were injected in eggs, interacted following a cyclic pattern in response to store depletion during sperm-induced Ca^{2+} oscillations (Zhang et al., 2018). This interaction suggests a role for SOCE during fertilization in pigs. Overexpression of proteins that accumulate at the PM or in its vicinity can cause non-specific effects on the function of channels. Therefore, electrophysiological detection of native CRAC current in these eggs will be necessary to confirm its functional expression and clarify its role in the early stage of development.

Voltage Gated Ca^{2+} Channels, Ca_V Channels

Voltage-gated Ca^{2+} (Ca_V) channels are transmembrane proteins that are organized in four domains (I–IV) with each domain having six transmembrane segments (S1–S6). Ca_V channels can be classified into two groups according to the voltage changes required for activation: high-voltage activated (HVA) channels and low-voltage activated (LVA). Ca_v 1.1–1.4 (L-type current) and Ca_v2.1–2.3 (P/Q, N, and R type) belong to the HVA group, while Ca_v3.1–3.3 (T-type current) to the LVA group. Between other functions, voltage-gated Ca^{2+} channels are responsible for initiation of synaptic transmission, hormone secretion, and excitation-contraction coupling (Hille, 2001; Catterall, 2011; Ramirez et al., 2017).

In 1977, using the voltage-clamp technique, an inward Ca^{2+}current was described in mouse eggs. The recordings were done in 20 mM external Ca^{2+} and the inward current increased in response to depolarizing steps. The peak current was measured at ~ -15 mV and it showed a dramatic reduction at temperatures below 20° C. Replacement of external Ca^{2+} by Sr^{2+} or Ba^{2+} retained the biophysical characteristics of the channel. Sea urchin and tunicate eggs also showed an inward Ca^{2+}current but with different inactivation time and permeability ratio than the one recorded in mouse eggs (Okamoto et al., 1977). In mouse eggs, using an improved set-up, the maximal current was at ~ -30 mV and its reversal potential was $\sim +50$ mV (Peres, 1987). Similar characteristics were found using the patch-clamp technique (Kang et al., 2007; Bernhardt et al., 2015). Additional recordings of mouse ovarian oocytes using single-glass microelectrodes showed inward currents carried by monovalent cations. These currents were blocked by Ca^{2+} channel antagonists and were insensitive to tetrodotoxin (TTX), confirming the functional presence of Ca^{2+} channels before ovulation (Yoshida, 1983). After fertilization, the voltage-gated Ca^{2+} channel varies in magnitude but not in kinetics or selectivity (Yamashita, 1982; Day et al., 1998; Kang et al., 2007). Voltage-gated Ca^{2+} channels were also described in hamster (Georgiou et al., 1984) and bovine eggs (Tosti et al., 2000). Comparable voltage-gated channels were recorded in ascidians and mollusks (Gallo et al., 2013; Tosti et al., 2013). Later, biophysical characterizations of the Ca_V current in mouse eggs assigned it molecularly as a T-type 3.2, voltage-gated Ca^{2+} channel (Kang et al., 2007) (**Table 1**). Surprisingly, even when the T-type current is prominent in mouse eggs (peak reaches $\sim$1.5 nA in MII eggs, in 2 mM Ca^{2+}), mice null for this channel, *Cacna1h*$^{-/-}$ (Chen et al., 2003), showed only marginal subfertility (Bernhardt et al., 2015). These results suggest that the function of this channel may be to support Ca^{2+} influx during the germinal vesicle arrest (GV; **Figure 1**) and during maturation. Ca_V channels would then contribute to fill the intracellular ER Ca^{2+} stores (**Figure 1**) and maintain Ca^{2+} homeostasis in preparation for fertilization (Bernhardt et al., 2015).

Native Ca_V channels of an unspecified type are expressed in *Xenopus* oocyte. The conductance was smaller than most conductances recorded in these cells (Dascal et al., 1986). Their function remains unknown.

Transient Receptor Potential (TRP) Channels

The TRP channels are a family of cationic non-selective channels that are known as cellular sensors. TRP channels are modulated by common second messengers such as PIP_2 and intracellular Ca^{2+} but also respond to more general stimuli such as temperature, pH and osmolarity, among others. TRP channels are tetramers where each subunit includes six transmembrane domains (S1–S6) and a p-loop that defines the channel pore (Wu et al., 2010).

TRP channels expression in mouse eggs have been recently validated, despite the fact that a temperature-dependent, outward current was reported in mouse eggs nearly 40 years ago (Okamoto et al., 1977). Confirmation of expression and function of TRP channels in mature eggs was accomplished using patch-clamp and Ca^{2+} imaging (Carvacho et al., 2013). The first TRP channel reported in eggs was TRPV3 channel. TRPV3 is a member of the vanilloid subfamily of the TRP family which is highly expressed in skin. TRPV3 is activated by stimuli such as temperature and plant-derivatives compounds (e.g., carvacrol and eugenol). Other traditional Ca^{2+} channel blockers such as 2-aminoethoxydiphenyl borate (2-APB) are also modulators of TRPV3 (Peier et al., 2002; Smith et al., 2002; Xu et al., 2002; Hu et al., 2004; Lee et al., 2016). TRPV3, similar to many other members of the TRP family can act downstream of G-protein coupled receptor activation (Yang and Zhu, 2014). In mouse eggs a combination of electrophysiological recording and using the agonist 2-APB showed that TRPV3 current is detectable in WT eggs but not in those from *TprV3*$^{-/-}$ animals (Carvacho et al., 2013). The current developed progressively during oocyte maturation, reaching the highest level in eggs at the MII stage. TRPV3 can mediate Ca^{2+} influx (**Figure 1**) which causes an intracellular Ca^{2+} rise capable of promoting parthenogenesis in ovulated eggs. Parthenogenesis and Ca^{2+} oscillations can be triggered artificially by incubation of the ovulated eggs in a strontium-containing media (Whittingham and Siracusa, 1978). TRPV3 channels are responsible for the influx of strontium (Sr^{2+}) into eggs. Incubation of mouse eggs in Sr^{2+} containing media has been used for years to induce artificial activation. Sr^{2+}-induced egg activation is a procedure that is widely used for animal cloning (Wakayama et al., 1998). Despite the expression of TRPV3 current in MII eggs, *TrpV3*$^{-/-}$ females are fertile (Cheng et al., 2010; Carvacho et al., 2013). These studies suggest the function of an additional channel mediating Ca^{2+} influx, or as discussed above, the concerted function of multiple redundant pathways to ensure proper egg activation. Consistently, a recent study showed the presence of the *TrpV3* transcript in human oocytes. The TRPV3 agonists 2-APB and carvacrol were shown to promote egg activation suggesting functional expression of channels, despite the fact that Sr^{2+} fails to induce activation in human eggs (Lu et al., 2018). One explanation to these results could be that human TRPV3 channels display a different sequence of ion selectivity than mouse TRPV3. Alternatively, the level of localization of TRPV3 at the PM could be too low to allow sufficient Sr^{2+} to induce intracellular Ca^{2+} release. Direct assessments of functional expression of TRPV3 channels in human oocytes would help to solve differences between mouse and human eggs.

Recently, another member of the TRP channels family, TRPM7, was found to be expressed in mouse eggs. TRPM7 belongs to the subfamily of melastatin and exhibits a ubiquitous tissue distribution. *Trpm7*$^{-/-}$ global knock-out is embryonic lethal. Embryos *Trpm7*$^{fl/fl}$ (Cre-ER) derived from a tamoxifen-inducible (Cre-ER) transgenic line bred to *Trpm7*$^{fl/fl}$ died earlier than E14.5 (Jin et al., 2008, 2012). One possible interpretation of these results is that TRPM7 is expressed in eggs and/or embryos. Accordingly, a monovalent cationic outward current with the characteristics of a TRP channel was recorded in mouse TRPV3 KO eggs using whole cell patch clamp. The channel responds to TRPM7 agonists and blockers. TRPM7-like current was also detected in 2-cell stage embryos (**Table 1** and **Figure 1**). The chemical suppression of the channel hours after fertilization reduced progression to the blastocyst stage, in agreement with a possible role of TRPM7 in pre-implantation embryo development (Carvacho et al., 2016). Using the same blocker (NS8593), Williams's group showed that eggs treated with NS8593 and fertilized *in-vitro* display impaired Ca^{2+} oscillations (Bernhardt et al., 2017). Future studies following the generation of an oocyte-specific KO for TRPM7 will provide more specific answers about the contribution of TRPM7 during fertilization and/or pre-implantation embryo development.

Expression of TRP channels have been reported in *Xenopus* oocytes. In contrast to mouse oocytes, *Xenopus* TRP channels seem to be inactive. TRPC1 protein was detected by western blot and immunolocalization, and it was suggested to underlie SOCE in *Xenopus* oocytes (Bobanovic et al., 1999). However, the function of the TRPC1 protein as channel is debatable (Wu et al., 2010). Using RT-PCR and western blot, a *Xenopus* homolog of TRPV5/6, xTRPV6, was found in *Xenopus* oocytes (Courjaret et al., 2013). xTRPV6 channel is not active at PM, although it has been suggested that its functional expression is modulated by interacting with TRPC1 (Schindl et al., 2012; Courjaret et al., 2013).

Chloride Channels

Ca^{2+}-Activated Cl^- Channels

The *Xenopus* egg is ∼1.2 mm in diameter allowing ample membrane area for sperm entry. The slow fusion of cortical granules induced by the fertilization-specific Ca^{2+} signal and the time required for the released enzymes to modify the egg extracellular matrix are too long to prevent additional sperm from entering the egg after the first sperm-egg fusion event. Therefore, *Xenopus* eggs have evolved a fast electrical block to polyspermy that is dependent on the Ca^{2+}-dependent gating of Ca^{2+}-activated Cl^- channels (CaCC) (**Table 1**). CaCC depolarize the cell membrane thus preventing additional sperm from fusing with the egg (Cross and Elinson, 1980; Jaffe et al., 1983). Interestingly, early studies have shown that simply incubating eggs in media with high Cl^- or replacing Cl^- with other anions such as I^- or Br^- lead to polyspermy (Bataillon, 1919; Grey et al., 1982). In retrospect, the effects of these ion substitutions on polyspermy are expected. CaCC induces

membrane depolarization by conducting Cl^- out of the cell, thus a high extracellular Cl^- will inhibit Cl^- efflux and membrane depolarization, promoting polyspermy.

CaCC-mediated currents are the predominant currents in *Xenopus* oocytes and are required to maintain the oocyte resting membrane potential (Kuruma and Hartzell, 2000). CaCC are encoded by TMEM16A also known as Anoctamin 1 or Ano1 (Schroeder et al., 2008; Yang et al., 2008). In *Xenopus* oocytes, CaCC interact with ERM proteins to regulate the length of microvilli and the membrane surface area (Courjaret et al., 2016; **Table 1**). CaCC are activated in response to the sperm-induced Ca^{2+} release at fertilization. CaCC activation and membrane depolarization can be replicated in the egg using different Ca^{2+} sources. Functional assays include pricking the egg and injecting Ca^{2+} or IP_3 directly on the egg. Another alternative is treating the egg with Ca^{2+} ionophores (Wolf, 1974; Cross, 1981; Busa et al., 1985; Machaca et al., 2001).

CaCCs are also expressed in mouse embryos (**Table 1**). The trophic factor platelet activating factor, PAF (1-*o*-alkyl-2-acetyl-*sn*-glycerol-3-phosphocoline) has been shown to cause activation of a protein G coupled receptor, phospholipase C and phosphatidylinositol 3-kinase (PIK3). PAF induces transient increases in intracellular Ca^{2+}, Ca^{2+} influx, and an anion-driven outward current. The outward current was blocked by niflumic acid (NFA), a selective inhibitor of CaCCs, confirming the identity of the channel. Treatment of 1-cell stage embryos with NFA significantly reduced development to blastocyst stage (Li et al., 2007, 2009), arguing a role for CaCC in early mammalian embryonic development.

Swell-Activated Cl^- Channels and Transporters

The cell volume regulation is a process that is highly controlled during embryo development. The cell volume regulation is mediated by the activity of swell-activated Cl^- channels, which are expressed and active in mouse eggs. Early mouse embryos express chloride channels that are permeable to organic osmolytes and whose expression was shown to be cell-cycle dependent (Kolajova et al., 2001) (**Table 1**). Mouse zygotes can recover from swelling by activating these channels to release intracellular osmolytes out of the cell. Swell-activated channels are active during meiotic maturation and until the 8-cell or morula stage (Seguin and Baltz, 1997; Kolajova et al., 2001). Nevertheless, later studies showed that regulation of cell volume in pre-implantation embryos is a more complex phenomenon that involves more than one type of channels. These include the Na^+/H^+ (NHE1) and the HCO_3^-/Cl^- (AE2) exchangers (Baltz and Zhou, 2012). Remarkably, these exchangers are inactive during meiotic maturation and are activated after fertilization. Other proteins involved in cell volume regulation after ovulation include the GLTY1 glycine transporter (Steeves et al., 2003) and the betaine and proline SIT1 transporter. SIT1 transporter regulates the accumulation of the organic osmolyte betaine after fertilization and it is mostly active in the 1- and 2-cell stages, whereas GLTY1 seems to be functionally active until the 4-cell stage (Baltz and Zhou, 2012).

Potassium Channels

Ca^{2+} Activated Potassium Channels ($K_{(Ca)}$)

Ca^{2+}-activated potassium channels ($K_{(Ca)}$) are tetramers and each subunit has six or seven transmembrane domains. They are divided in three groups depending of their unitary conductance: Big conductance (BK), intermediate conductance (IK) and small conductance (SK). $K_{(Ca)}$ channels are ubiquitously expressed in nearly every vertebrate excitable cell (Hille, 2001).

Fertilization in hamster eggs is marked by hyperpolarization spikes (Miyazaki and Igusa, 1981) that were related with the activity of $K_{(Ca)}$ channels (Miyazaki and Igusa, 1982). The periodic hyperpolarizing pulses during fertilization reach to −70 to −80 mV from a resting potential of −30 mV. They were abolished by injection of the Ca^{2+} chelator EGTA into eggs, suggesting $K_{(Ca)}$ channels function (Georgiou et al., 1983; Igusa et al., 1983). The hyperpolarization responses after fertilization in mouse eggs are Ca^{2+} independent smaller in magnitude than those observed in hamster eggs. Thus, a different pool of channels activity during fertilization between the two species is suggested (Igusa et al., 1983).

Unfertilized human eggs showed hyperpolarization and increased basal current, following an injection of sperm factor, thimerosal (Homa and Swann, 1994), or in response to the Ca^{2+} ionophore A23187. Application of the ionophore in unfertilized eggs activated a bell-shaped current that was blocked by iberiotoxin, a selective blocker of BK channels. In agreement with $K_{(Ca)}$ current, preloading oocytes with EGTA inhibited the current triggered by microinjection of IP_3. Therefore, the mechanism of hyperpolarization in human eggs seems to be similar to hamster eggs (Gianaroli et al., 1994; Dale et al., 1996).

Voltage-Gated Potassium Channels (K_V)

In mouse eggs, a large conductance voltage-activated K^+ current was reported in unfertilized eggs. This current is not modulated by cytosolic Ca^{2+} and its activity is linked to the cell cycle, being high in M/G1 and low in S/G2 (Day et al., 1993; **Table 1**).

Endogenous voltage-activated K^+ currents, sensitive to Barium blockade, have been reported in *Xenopus* oocyte. However, their function and molecular identity remains elusive (Tokimasa and North, 1996).

Intercellular Channels: Connexins

Gap junctions are structures composed by intercellular channels which link the cytoplasm of adjacent cells and allow the exchange of metabolites, nutrients and signaling molecules. Gap junctions are aggregates of connexins (six) organized as large channels (connexons) between cells. In order to develop and mature, primordial oocytes need to establish direct cytoplasmic communication with the granulosa cells through gap junctions. In mice, the connexin responsible for the intercellular communication between oocytes and granulosa cells is connexin 37 (Cx37). The disruption of the gene encoding for Cx37 results in female infertility characterized by oocytes that fail to acquire meiotic competence and showed inappropriate formation of the *corpora lutea*. Ultimately, Cx37 KO females showed anovulation (Simon et al., 1997). Connexin 43 (Cx43) mediates interactions between granulosa cells and may be present in a minor fraction

(if any) on the surface of oocytes. The absence of Cx43 in mice ovaries cause impaired postnatal folliculogenesis with failure to develop multiple layers of granulosa cells. Ovary-specific deletion of Cx43 gene generated oocytes that were morphologically abnormal and meiotically incompetent, therefore, cannot be fertilized (Ackert et al., 2001; Kidder and Mhawi, 2002). Connexin 26 (Cx26) has been linked to the implantation process, however, in mice, the specific deletion of the gene encoding Cx26 in the uterine epithelium did not shown any obvious impairment of implantation (Winterhager and Kidder, 2015). In human cumulus cells, the addition of endothelin-1 has been shown to downregulate Cx26, blocking the resumption of meiosis and promoting the germinal-vesicle stage (Cui et al., 2018).

CONCLUSIONS

From the brief overview of the regulation and function of ionic conductances during fertilization, the egg-to-embryo transition and early embryogenesis, it is clear that channels play a fundamental role in mediating these processes. In *Xenopus* oocytes, the regulation of various ion channels at the PM and the ER membrane have been well characterized and their relative contribution to fertilization are fairly well defined. In contrast, there remains much to be learned about mammalian systems. For example, here, we have revisited the channels responsible for the electrical blockade to polyspermy, well-characterized in *Xenopus* but controversial in mammalian oocytes. Currently, the scientific evidence shows that for mammalian eggs, the blockade of polyspermy must be a combination of mechanisms, including changes in the membrane potential, reorganization of proteins expressed at the PM and even intracellular re-arrangements (Bianchi and Wright, 2016).

Current evidence collectively argue that Ca^{2+} influx is critical to maintain Ca^{2+} oscillations which are required for egg activation (Kline and Kline, 1992). However, the molecular identity of the channel(s) supporting Ca^{2+} influx during oocyte maturation and fertilization remains a puzzle that needs to be solved. In this regard, it is interesting to notice that current knowledge argue against a fundamental role for TRP channels during oocyte maturation and fertilization in *Xenopus* oocyte (see **Table 1**). In contrast, in mammals, members of the TRP channel family have been suggested to mediate Ca^{2+} influx during egg-to-embryo transition. Four main channels have been proposed to support Ca^{2+} influx in the egg: ORAI1, TRPV3, Ca_v and TRPM7-like channels. Results obtained using genetically modified animals, argue against an essential role for ORAI, Ca_v and TRPV3 at fertilization. Assessment of the role of a TRPM7-like channel awaits the generation of an oocyte-specific KO for TRPM7. Additionally, the possibility of a redundant system needs to be addressed. Orchestrated functioning of channels to promote Ca^{2+} influx might be the way to assure egg activation. Fertilization is an essential process in the evolution and maintenance of any sexually reproducing species. Therefore, it is likely that mammals have evolved multiple redundant mechanisms to assure Ca^{2+} influx at fertilization. These need to be sufficient to refill the stores and maintain the Ca^{2+} oscillations for extended periods of time. Current evidence argues that the egg is agnostic regarding the specific molecular pathway that mediates Ca^{2+} influx as long as it is able to maintain Ca^{2+} oscillations. It should be noted, however, that this Ca^{2+} influx needs to be balanced since overexpression of channels mediating Ca^{2+} influx such as ORAI1 disrupts early embryonic development (Lee et al., 2013). In this regard, the generation of genetically modified animals where a combination of channels are KO would be an interesting model to study Ca^{2+} signaling in oocyte physiology.

Ca^{2+} signals are fundamental to activate eggs at fertilization and to support pre-implantation embryo development. Ca^{2+} also plays a role in completion but not in the initiation of meiosis. Ca^{2+} signaling depends on Ca^{2+} influx and Ca^{2+} release from intracellular reservoirs such as the ER. In most cells, including gametes, Ca^{2+} influx and Ca^{2+} release are mediated by ion channels, in addition to other proteins. **Figure 1** summarizes the current model for functional Ca^{2+} channels activity at the PM of mouse oocytes, eggs and early embryos. At the GV stage, spontaneous Ca^{2+} oscillations might be controlled by TRPM7-like and Ca_V channels (Carvacho et al., 2016). In ovulated eggs, TRPV3 contributes to Ca^{2+} influx (Carvacho et al., 2013). Additionally, Ca_V channels have been proposed to play a role in fertilization-triggered Ca^{2+} oscillations. However, the contribution of Ca_v channels must be negligible, since no major differences in Ca^{2+} oscillations were observed between *Cacna1h*$^{-/-}$ and *Cacna1h*$^{-/+}$ eggs (Bernhardt et al., 2015). After fertilization, pharmacological blockade of TRPM7-like channels suggest a fundamental role of the protein supporting Ca^{2+} oscillations and pre-implantation development (Carvacho et al., 2016; Bernhardt et al., 2017) (**Figure 1**). It was suggested that STIM and ORAI might mediate Ca^{2+} influx following store depletion in mouse GV oocytes. Mice lacking *Stim1/2* and *Orai1* did not show any difference in ER Ca^{2+} stores in comparison to WT oocytes (Bernhardt et al., 2017). Nevertheless, the expression of native ORAI proteins has been shown by western blot (Cheon et al., 2013), therefore, ORAI in GV oocytes has been added to the model. Besides the aforementioned channels, we cannot rule out possible contributions of yet unknown channels, thus, this possibility is also indicated (**channel X**, **Figure 1**). Furthermore, one needs to interpret the KO studies with caution as they do not replicate the normal physiological state despite the fact that currently they provide the best tool available to directly assess the role of such channels. The KO of a channel in the oocyte is likely to remodel the expression and/or activity of other channels and/or transporters during oocyte growth and development using a feedback mechanism to ensure appropriate ionic and cellular homeostasis. As such phenotypes observed from mouse KO studies may not reflect the normal physiological state, despite the fact that they would conclusively define the absolute requirement for a particular gene. In that context, current data collectively argue that Ca^{2+} influx at fertilization in mammals is not mediated by rather multiple redundant pathways.

Studying ion channels in gametes remains technically challenging compared to somatic cells. Due to specialized biology of the gametes, researchers face difficulties in manipulating

expression and controlling maternal effects. Different model systems are more amenable to certain experimental approaches than others. For example, given the large size of the oocyte, the *Xenopus* system is ideally suited for expression, imaging and biochemical analysis. However, these advantages create a challenge to visualize changes that occur deep in the oocyte. In that context, mammalian oocytes are more advantageous but are of limited use for detailed biochemical analysis. Therefore, a comparative approach building on knowledge from different systems is useful, as long as one remain cognizant of the need of individual species to evolve distinct mechanisms to maintain reproductive isolation.

AUTHOR CONTRIBUTIONS

IC and KM wrote the first draft of the manuscript. MP designed the figure. IC, MP, TM, and KM critically revised the manuscript. IC and KM prepared the manuscript for submission. IC, MP, TM, and KM approved the final version to be published.

ACKNOWLEDGMENTS

We would like to thank Dr. Rafael A. Fissore for discussion and helpful suggestion to the manuscript. We thank Dr. Stephanie C. Stotz for critical revision of the manuscript.

REFERENCES

Abbott, A. L., and Ducibella, T. (2001). Calcium and the control of mammalian cortical granule exocytosis. *Front. Biosci.* 6, D792–D806. doi: 10.2741/Abbott

Ackert, C. L., Gittens, J. E., O'Brien, M. J., Eppig, J. J., and Kidder, G. M. (2001). Intercellular communication via connexin43 gap junctions is required for ovarian folliculogenesis in the mouse. *Dev. Biol.* 233, 258–270. doi: 10.1006/dbio.2001.0216

Bai, G. R., Yang, L. H., Huang, X. Y., and Sun, F. Z. (2006). Inositol 1,4,5-trisphosphate receptor type 1 phosphorylation and regulation by extracellular signal-regulated kinase. *Biochem. Biophys. Res. Commun.* 348, 1319–1327. doi: 10.1016/j.bbrc.2006.07.208

Baltz, J. M., and Zhou, C. (2012). Cell volume regulation in mammalian oocytes and preimplantation embryos. *Mol. Reprod. Dev.* 79, 821–831. doi: 10.1002/mrd.22117

Bataillon, E. (1919). Analyze de l'activation par la technique des oeufs nus et la polyspermie experimentale chez les batraciens. *Ann. Sci. Nat. Zool.* 10, 1–38.

Bement, W. M., and Capco, D. G. (1990). Transformation of the amphibian oocyte into the egg: structural and biochemical events. *J. Electron Microsc. Tech.* 16, 202–234. doi: 10.1002/jemt.1060160303

Bernhardt, M. L., Padilla-Banks, E., Stein, P., Zhang, Y., and Williams, C. J. (2017). Store-operated Ca($^{2+}$) entry is not required for fertilization-induced Ca(2+) signaling in mouse eggs. *Cell Calcium* 65, 63–72. doi: 10.1016/j.ceca.2017.02.004

Bernhardt, M. L., Zhang, Y., Erxleben, C. F., Padilla-Banks, E., McDonough, C. E., Miao, Y. L., et al. (2015). CaV3.2 T-type channels mediate Ca(2)(+) entry during oocyte maturation and following fertilization. *J. Cell Sci.* 128, 4442–4452. doi: 10.1242/jcs.180026

Berridge, M. J. (2005). Unlocking the secrets of cell signaling. *Annu. Rev. Physiol.* 67, 1–21. doi: 10.1146/annurev.physiol.67.040103.152647

Berridge, M. J., Lipp, P., and Bootman, M. D. (2000). The versatility and universality of calcium signalling. *Nat. Rev. Mol. Cell Biol.* 1, 11–21. doi: 10.1038/35036035

Bianchi, E., and Wright, G. J. (2016). Sperm meets egg: the genetics of mammalian fertilization. *Annu. Rev. Genet.* 50, 93–111. doi: 10.1146/annurev-genet-121415-121834

Birnbaumer, L. (2015). From GTP and G proteins to TRPC channels: a personal account. *J. Mol. Med.* 93, 941–953. doi: 10.1007/s00109-015-1328-5

Bobanovic, L. K., Laine, M., Petersen, C. C., Bennett, D. L., Berridge, M. J., Lipp, P., et al. (1999). Molecular cloning and immunolocalization of a novel vertebrate trp homologue from *Xenopus*. *Biochem. J.* 340 (Pt 3), 593–599.

Bogeski, I., Al-Ansary, D., Qu, B., Niemeyer, B. A., Hoth, M., and Peinelt, C. (2010). Pharmacology of ORAI channels as a tool to understand their physiological functions. *Expert Rev. Clin. Pharmacol.* 3, 291–303. doi: 10.1586/ecp.10.23

Burkart, A. D., Xiong, B., Baibakov, B., Jiménez-Movilla, M., and Dean, J. (2012). Ovastacin, a cortical granule protease, cleaves ZP2 in the zona pellucida to prevent polyspermy. *J. Cell Biol.* 197, 37–44. doi: 10.1083/jcb.201112094

Busa, W. B., Ferguson, J. E., Joseph, S. K., Williamson, J. R., and Nuccitelli, R. (1985). Activation of frog (*Xenopus laevis*) eggs by inositol trisphosphate. I. Characterization of Ca^{2+} release from intracellular stores. *J. Cell Biol.* 101, 677–682. doi: 10.1083/jcb.101.2.677

Carvacho, I., Ardestani, G., Lee, H. C., McGarvey, K., Fissore, R. A., and Lykke-Hartmann, K. (2016). TRPM7-like channels are functionally expressed in oocytes and modulate post-fertilization embryo development in mouse. *Sci. Rep.* 6:34236. doi: 10.1038/srep34236

Carvacho, I., Lee, H. C., Fissore, R. A., and Clapham, D. E. (2013). TRPV3 channels mediate strontium-induced mouse-egg activation. *Cell Rep.* 5, 1375–1386. doi: 10.1016/j.celrep.2013.11.007

Catterall, W. A. (2011). Voltage-gated calcium channels. *Cold Spring Harb. Perspect. Biol.* 3:a003947. doi: 10.1101/cshperspect.a003947

Chen, C. C., Lamping, K. G., Nuno, D. W., Barresi, R., Prouty, S. J., Lavoie, J. L., et al. (2003). Abnormal coronary function in mice deficient in alpha1H T-type Ca^{2+} channels. *Science* 302, 1416–1418. doi: 10.1126/science.1089268

Cheng, X., Jin, J., Hu, L., Shen, D., Dong, X. P., Samie, M. A., et al. (2010). TRP channel regulates EGFR signaling in hair morphogenesis and skin barrier formation. *Cell* 141, 331–343. doi: 10.1016/j.cell.2010.03.013

Cheon, B., Lee, H. C., Wakai, T., and Fissore, R. A. (2013). Ca^{2+} influx and the store-operated Ca^{2+} entry pathway undergo regulation during mouse oocyte maturation. *Mol. Biol. Cell* 24, 1396–1410. doi: 10.1091/mbc.e13-01-0065

Clapham, D. E. (1995). Calcium signaling. *Cell* 80, 259–268. doi: 10.1016/0092-8674(95)90408-5

Clapham, D. E. (2007). Calcium signaling. *Cell* 131, 1047–1058. doi: 10.1016/j.cell.2007.11.028

Courjaret, R., Hodeify, R., Hubrack, S., Ibrahim, A., Dib, M., Daas, S., et al. (2016). The Ca2+-activated Cl- channel Ano1 controls microvilli length and membrane surface area in the oocyte. *J. Cell Sci.* 129, 2548–2558. doi: 10.1242/jcs.188367

Courjaret, R., Hubrack, S., Daalis, A., Dib, M., and Machaca, K. (2013). The *Xenopus* TRPV6 homolog encodes a Mg(2+) -permeant channel that is inhibited by interaction with TRPC1. *J. Cell. Physiol.* 228, 2386–2398. doi: 10.1002/jcp.24411

Cross, N. L. (1981). Initiation of the activation potential by an increase in intracellular calcium in eggs of the frog, Rana pipiens. *Dev. Biol.* 85, 380–384. doi: 10.1016/0012-1606(81)90269-4

Cross, N. L., and Elinson, R. P. (1980). A fast block to polyspermy in frogs mediated by changes in the membrane potential. *Dev. Biol.* 75, 187–198. doi: 10.1016/0012-1606(80)90154-2

Cui, L., Shen, J., Fang, L., Mao, X., Wang, H., and Ye, Y. (2018). Endothelin-1 promotes human germinal vesicle-stage oocyte maturation by downregulating connexin-26 expression in cumulus cells. *Mol. Hum. Reprod.* 24, 27–36. doi: 10.1093/molehr/gax058

Dale, B. (2014). Is the idea of a fast block to polyspermy based on artifact? *Biochem. Biophys. Res. Commun.* 450, 1159–1165. doi: 10.1016/j.bbrc.2014.03.157

Dale, B., Fortunato, A., Monfrecola, V., and Tosti, E. (1996). A soluble sperm factor gates Ca($^{2+}$)-activated K^+ channels in human oocytes. *J. Assist. Reprod. Genet.* 13, 573–577. doi: 10.1007/BF02066611

Dascal, N., Snutch, T. P., Lübbert, H., Davidson, N., and Lester, H. A. (1986). Expression and modulation of voltage-gated calcium channels after RNA injection in *Xenopus* oocytes. *Science* 231, 1147–1150. doi: 10.1126/science.2418503

Day, M. L., Johnson, M. H., and Cook, D. I. (1998). Cell cycle regulation of a T-type calcium current in early mouse embryos. *Pflugers Arch.* 436, 834–842. doi: 10.1007/s004240050712

Day, M. L., Pickering, S. J., Johnson, M. H., and Cook, D. I. (1993). Cell-cycle control of a large-conductance K^+ channel in mouse early embryos. *Nature* 365, 560–562. doi: 10.1038/365560a0

Demaurex, N., and Frieden, M. (2003). Measurements of the free luminal ER $Ca(^{2+})$ concentration with targeted "cameleon" fluorescent proteins. *Cell Calcium* 34, 109–119. doi: 10.1016/S0143-4160(03)00081-2

Ducibella, T., Huneau, D., Angelichio, E., Xu, Z., Schultz, R. M., Kopf, G. S., et al. (2002). Egg-to-embryo transition is driven by differential responses to $Ca(^{2+})$ oscillation number. *Dev. Biol.* 250, 280–291. doi: 10.1006/dbio.2002.0788

El Jouni, W., Haun, S., and Machaca, K. (2008). Internalization of plasma membrane Ca^{2+}-ATPase during *Xenopus* oocyte maturation. *Dev. Biol.* 324, 99–107. doi: 10.1016/j.ydbio.2008.09.007

El Jouni, W., Jang, B., Haun, S., and Machaca, K. (2005). Calcium signaling differentiation during *Xenopus* oocyte maturation. *Dev. Biol.* 288, 514–525. doi: 10.1016/j.ydbio.2005.10.034

Ferris, C. D., Cameron, A. M., Bredt, D. S., Huganir, R. L., and Snyder, S. H. (1991). Inositol 1,4,5-trisphosphate receptor is phosphorylated by cyclic AMP-dependent protein kinase at serines 1755 and 1589. *Biochem. Biophys. Res. Commun.* 175, 192–198. doi: 10.1016/S0006-291X(05)81219-7

Fontanilla, R. A., and Nuccitelli, R. (1998). Characterization of the sperm-induced calcium wave in *Xenopus* eggs using confocal microscopy. *Biophys. J.* 75, 2079–2087. doi: 10.1016/S0006-3495(98)77650-7

Foskett, J. K., White, C., Cheung, K. H., and Mak, D. O. (2007). Inositol trisphosphate receptor Ca^{2+} release channels. *Physiol. Rev.* 87, 593–658. doi: 10.1152/physrev.00035.2006

Fujiwara, T., Nakada, K., Shirakawa, H., and Miyazaki, S. (1993). Development of inositol trisphosphate-induced calcium release mechanism during maturation of hamster oocytes. *Dev. Biol.* 156, 69–79. doi: 10.1006/dbio.1993.1059

Gallo, A., Russo, G. L., and Tosti, E. (2013). T-type Ca^{2+} current activity during oocyte growth and maturation in the ascidian *Styela plicata*. *PLoS ONE* 8:e54604. doi: 10.1371/journal.pone.0054604

Georgiou, P., Bountra, C., Bland, K. P., and House, C. R. (1983). Calcium-evoked opening of potassium channels in hamster eggs. *Q. J. Exp. Physiol.* 68, 687–700. doi: 10.1113/expphysiol.1983.sp002758

Georgiou, P., Bountra, C., Bland, K. P., and House, C. R. (1984). Calcium action potentials in unfertilized eggs of mice and hamsters. *Q. J. Exp. Physiol.* 69, 365–380. doi: 10.1113/expphysiol.1984.sp002812

Gianaroli, L., Tosti, E., Magli, C., Iaccarino, M., Ferraretti, A. P., and Dale, B. (1994). Fertilization current in the human oocyte. *Mol. Reprod. Dev.* 38, 209–214. doi: 10.1002/mrd.1080380212

Gómez-Fernández, C., López-Guerrero, A. M., Pozo-Guisado, E., Álvarez, I. S., and Martín-Romero, F. J. (2012). Calcium signaling in mouse oocyte maturation: the roles of STIM1, ORAI1 and SOCE. *Mol. Hum. Reprod.* 18, 194–203. doi: 10.1093/molehr/gar071

Gomez-Fernandez, C., Pozo-Guisado, E., Ganan-Parra, M., Perianes, M. J., Alvarez, I. S., and Martin-Romero, F. J. (2009). Relocalization of STIM1 in mouse oocytes at fertilization: early involvement of store-operated calcium entry. *Reproduction* 138, 211–221. doi: 10.1530/REP-09-0126

Grey, R. D., Bastiani, M. J., Webb, D. J., and Schertel, E. R. (1982). An electrical block is required to prevent polyspermy in eggs fertilized by natural mating of *Xenopus laevis*. *Dev. Biol.* 89, 475–484. doi: 10.1016/0012-1606(82)90335-9

Grey, R. D., Wolf, D. P., and Hedrick, J. L. (1974). Formation and structure of the fertilization envelope in *Xenopus laevis*. *Dev. Biol.* 36, 44–61. doi: 10.1016/0012-1606(74)90189-4

Hachem, A., Godwin, J., Ruas, M., Lee, H. C., Ferrer Buitrago, M., Ardestani, G., et al. (2017). PLCzeta is the physiological trigger of the $Ca(^{2+})$ oscillations that induce embryogenesis in mammals but conception can occur in its absence. *Development* 144, 2914–2924. doi: 10.1242/dev.150227

Hagiwara, S., and Jaffe, L. A. (1979). Electrical properties of egg cell membranes. *Annu. Rev. Biophys. Bioeng.* 8, 385–416. doi: 10.1146/annurev.bb.08.060179.002125

Hamill, O. P., Marty, A., Neher, E., Sakmann, B., and Sigworth, F. J. (1981). Improved patch-clamp techniques for high-resolution current recording from cells and cell-free membrane patches. *Pflugers Arch.* 391, 85–100. doi: 10.1007/BF00656997

Hartzell, H. C. (1996). Activation of different Cl currents in *Xenopus* oocytes by Ca liberated from stores and by capacitative Ca influx. *J. Gen. Physiol.* 108, 157–175. doi: 10.1085/jgp.108.3.157

Hassold, T., and Hunt, P. (2001). To err (meiotically) is human: the genesis of human aneuploidy. *Nat. Rev. Genet.* 2, 280–291. doi: 10.1038/35066065

Haun, S., Sun, L., Hubrack, S., Yule, D., and Machaca, K. (2012). Phosphorylation of the rat $Ins(1,4,5)P_3$ receptor at T930 within the coupling domain decreases its affinity to $Ins(1,4,5)P_3$. *Channels* 6, 379–384. doi: 10.4161/chan.21170

Hille, B. (2001). *Ion Channels of Excitable Membranes.* Sunderland, MA: Sinauer Associates, Inc.

Homa, S. T., and Swann, K. (1994). A cytosolic sperm factor triggers calcium oscillations and membrane hyperpolarizations in human oocytes. *Hum. Reprod.* 9, 2356–2361. doi: 10.1093/oxfordjournals.humrep.a138452

Hu, H. Z., Gu, Q., Wang, C., Colton, C. K., Tang, J., Kinoshita-Kawada, M., et al. (2004). 2-aminoethoxydiphenyl borate is a common activator of TRPV1, TRPV2, and TRPV3. *J. Biol. Chem.* 279, 35741–35748. doi: 10.1074/jbc.M404164200

Igusa, Y., Miyazaki, S., and Yamashita, N. (1983). Periodic hyperpolarizing responses in hamster and mouse eggs fertilized with mouse sperm. *J. Physiol.* 340, 633–647. doi: 10.1113/jphysiol.1983.sp014784

Inoue, D., Ohe, M., Kanemori, Y., Nobui, T., and Sagata, N. (2007). A direct link of the Mos-MAPK pathway to Erp1/Emi2 in meiotic arrest of *Xenopus laevis* eggs. *Nature* 446, 1100–1104. doi: 10.1038/nature05688

Jaffe, L. A. (1976). Fast block to polyspermy in sea urchin eggs is electrically mediated. *Nature* 261, 68–71. doi: 10.1038/261068a0

Jaffe, L. A., and Cross, N. L. (1984). Electrical properties of vertebrate oocyte membranes. *Biol. Reprod.* 30, 50–54. doi: 10.1095/biolreprod30.1.50

Jaffe, L. A., Cross, N. L., and Picheral, B. (1983). Studies of the voltage-dependent polyspermy block using cross-species fertilization of Amphibians. *Dev. Biol.* 98, 319–326. doi: 10.1016/0012-1606(83)90362-7

Jin, J., Desai, B. N., Navarro, B., Donovan, A., Andrews, N. C., and Clapham, D. E. (2008). Deletion of Trpm7 disrupts embryonic development and thymopoiesis without altering Mg^{2+} homeostasis. *Science* 322, 756–760. doi: 10.1126/science.1163493

Jin, J., Wu, L. J., Jun, J., Cheng, X., Xu, H., Andrews, N. C., et al. (2012). The channel kinase, TRPM7, is required for early embryonic development. *Proc. Natl. Acad. Sci. U.S.A.* 109, E225–233. doi: 10.1073/pnas.1120033109

Jones, K. T., Carroll, J., and Whittingham, D. G. (1995). Ionomycin, thapsigargin, ryanodine, and sperm induced Ca^{2+} release increase during meiotic maturation of mouse oocytes. *J. Biol. Chem.* 270, 6671–6677. doi: 10.1074/jbc.270.12.6671

Kang, D., Hur, C. G., Park, J. Y., Han, J., and Hong, S. G. (2007). Acetylcholine increases Ca^{2+} influx by activation of CaMKII in mouse oocytes. *Biochem. Biophys. Res. Commun.* 360, 476–482. doi: 10.1016/j.bbrc.2007.06.083

Kashir, J., Deguchi, R., Jones, C., Coward, K., and Stricker, S. A. (2013). Comparative biology of sperm factors and fertilization-induced calcium signals across the animal kingdom. *Mol. Reprod. Dev.* 80, 787–815. doi: 10.1002/mrd.22222

Kidder, G. M., and Mhawi, A. A. (2002). Gap junctions and ovarian folliculogenesis. *Reproduction* 123, 613–620. doi: 10.1530/rep.0.1230613

Kishimoto, T. (2015). Entry into mitosis: a solution to the decades-long enigma of MPF. *Chromosoma* 124, 417–428. doi: 10.1007/s00412-015-0508-y

Kline, D., and Kline, J. T. (1992). Thapsigargin activates a calcium influx pathway in the unfertilized mouse egg and suppresses repetitive calcium transients in the fertilized egg. *J. Biol. Chem.* 267, 17624–17630.

Kline, J. T., and Kline, D. (1994). Regulation of intracellular calcium in the mouse egg: evidence for inositol trisphosphate-induced calcium release, but not calcium-induced calcium release. *Biol. Reprod.* 50, 193–203. doi: 10.1095/biolreprod50.1.193

Koh, S., Lee, K., Wang, C., Cabot, R. A., and Machaty, Z. (2009). STIM1 regulates store-operated Ca^{2+} entry in oocytes. *Dev. Biol.* 330, 368–376. doi: 10.1016/j.ydbio.2009.04.007

Kolajova, M., Hammer, M. A., Collins, J. L., and Baltz, J. M. (2001). Developmentally regulated cell cycle dependence of swelling-activated anion channel activity in the mouse embryo. *Development* 128, 3427–3434.

Kuruma, A., and Hartzell, H. C. (2000). Bimodal control of a Ca^{2+} -activated Cl^{-} channel by different Ca^{2+} signals. *J. Gen. Physiol.* 115, 59–80. doi: 10.1085/jgp.115.1.59

Larabell, C., and Nuccitelli, R. (1992). Inositol lipid hydrolysis contributes to the Ca^{2+} wave in the activating egg of *Xenopus laevis*. *Dev. Biol.* 153, 347–355. doi: 10.1016/0012-1606(92)90119-2

Lee, B., Palermo, G., and Machaca, K. (2013). Downregulation of store-operated Ca^{2+} entry during mammalian meiosis is required for the egg-to-embryo transition. *J. Cell Sci.* 126(Pt 7), 1672–1681. doi: 10.1242/jcs.121335

Lee, B., Vermassen, E., Yoon, S. Y., Vanderheyden, V., Ito, J., Alfandari, D., et al. (2006). Phosphorylation of IP3R1 and the regulation of $[Ca^{2+}]$i responses at fertilization: a role for the MAP kinase pathway. *Development* 133, 4355–4365. doi: 10.1242/dev.02624

Lee, H. C., Yoon, S. Y., Lykke-Hartmann, K., Fissore, R. A., and Carvacho, I. (2016). TRPV3 channels mediate Ca^{2+} influx induced by 2-APB in mouse eggs. *Cell Calcium* 59, 21–31. doi: 10.1016/j.ceca.2015.12.001

Lee, K., Wang, C., and Machaty, Z. (2012). STIM1 is required for Ca^{2+} signaling during mammalian fertilization. *Dev. Biol.* 367, 154–162. doi: 10.1016/j.ydbio.2012.04.028

Lewis, R. S. (1999). Store-operated calcium channels. *Adv. Second Messenger Phosphoprotein Res.* 33, 279–307. doi: 10.1016/S1040-7952(99)80014-7

Li, Y., Day, M. L., and O'Neill, C. (2007). Autocrine activation of ion currents in the two-cell mouse embryo. *Exp. Cell Res.* 313, 2786–2794. doi: 10.1016/j.yexcr.2007.05.022

Li, Y., O'Neill, C., and Day, M. L. (2009). Activation of a chloride channel by a trophic ligand is required for development of the mouse preimplantation embryo *in vitro*. *Biol. Reprod.* 81, 759–767. doi: 10.1095/biolreprod.108.074567

Liu, J., and Maller, J. L. (2005). Calcium elevation at fertilization coordinates phosphorylation of XErp1/Emi2 by Plx1 and CaMK II to release metaphase arrest by cytostatic factor. *Curr. Biol.* 15, 1458–1468. doi: 10.1016/j.cub.2005.07.030

Lorca, T., Cruzalegui, F. H., Fesquet, D., Cavadore, J. C., Mery, J., Means, A., et al. (1993). Calmodulin-dependent protein kinase II mediates inactivation of MPF and CSF upon fertilization of *Xenopus* eggs. *Nature* 366, 270–273. doi: 10.1038/366270a0

Lu, Y., Reddy, R., Ferrer Buitrago, M., Vander Jeught, M., Neupane, J., De Vos, W. H., et al. (2018). Strontium fails to induce Ca^{2+} release and activation in human oocytes despite the presence of functional TRPV3 channels. *Human Reproduction Open* 2018, 1–11. doi: 10.1093/hropen/hoy005

Machaca, K. (2004). Increased sensitivity and clustering of elementary Ca^{2+} release events during oocyte maturation. *Dev. Biol.* 275 170–182. doi: 10.1016/j.ydbio.2004.08.004

Machaca, K. (2007). Ca^{2+} signaling differentiation during oocyte maturation. *J. Cell. Physiol.* 213, 331–340. doi: 10.1002/jcp.21194

Machaca, K., and Haun, S. (2000). Store-operated calcium entry inactivates at the germinal vesicle breakdown stage of *Xenopus* meiosis. *J. Biol. Chem.* 275, 38710–38715. doi: 10.1074/jbc.M007887200

Machaca, K., and Haun, S. (2002). Induction of maturation-promoting factor during *Xenopus* oocyte maturation uncouples Ca^{2+} store depletion from store-operated Ca^{2+} entry. *J. Cell Biol.* 156, 75–85. doi: 10.1083/jcb.200110059

Machaca, K., Qu, Z., Kuruma, A., Hartzell, H. C., and McCarty, N. (2001). "The endogenous calcium-activated Cl channel in *Xenopus* oocytes: a physiologically and biophysically rich model system," in *Calcium Activates Chloride Channels,* ed C. M. Fuller (San Diego, CA: Academic Press), 3–39.

Machaty, Z., Wang, C., Lee, K., and Zhang, L. (2017). Fertility: store-operated $Ca(^{2+})$ entry in germ cells: role in egg activation. *Adv. Exp. Med. Biol.* 993, 577–593. doi: 10.1007/978-3-319-57732-6_29

Maeno, T. (1959). Electrical characteristics and activation potential of Bufo eggs. *J. Gen. Physiol.* 43, 139–157. doi: 10.1085/jgp.43.1.139

Malathi, K., Kohyama, S., Ho, M., Soghoian, D., Li, X., Silane, M., et al. (2003). Inositol 1,4,5-trisphosphate receptor (type 1) phosphorylation and modulation by Cdc2. *J. Cell. Biochem.* 90, 1186–1196. doi: 10.1002/jcb.10720

McNally, B. A., and Prakriya, M. (2012). Permeation, selectivity and gating in store-operated CRAC channels. *J. Physiol.* 590, 4179–4191. doi: 10.1113/jphysiol.2012.233098

Mehlmann, L., and Kline, D. (1994). Regulation of intracellular calcium in the mouse egg: calcium release in response to sperm or inositol trisphosphate is enhanced after meiotic maturation. *Biol. Reprod.* 51, 1088–1098. doi: 10.1095/biolreprod51.6.1088

Miao, Y. L., Stein, P., Jefferson, W. N., Padilla-Banks, E., and Williams, C. J. (2012). Calcium influx-mediated signaling is required for complete mouse egg activation. *Proc. Natl. Acad. Sci. U.S.A.* 109, 4169–4174. doi: 10.1073/pnas.1112333109

Miyazaki, S. (1995). Calcium signalling during mammalian fertilization. *Ciba Found. Symp.* 188, 235–247; discussion: 247–251.

Miyazaki, S., and Igusa, Y. (1981). Fertilization potential in golden hamster eggs consists of recurring hyperpolarizations. *Nature* 290, 702–704. doi: 10.1038/290702a0

Miyazaki, S., and Igusa, Y. (1982). Ca-mediated activation of a K current at fertilization of golden hamster eggs. *Proc. Natl. Acad. Sci. U.S.A.* 79, 931–935. doi: 10.1073/pnas.79.3.931

Miyazaki, S., Shirakawa, H., Nakada, K., and Honda, Y. (1993). Essential role of the inositol 1,4,5-trisphosphate receptor/Ca^{2+} release channel in Ca^{2+} waves and Ca^{2+} oscillations at fertilization of mammalian eggs. *Dev. Biol.* 158, 62–78. doi: 10.1006/dbio.1993.1168

Miyazaki, S., Yuzaki, M., Nakada, K., Shirakawa, H., Nakanishi, S., Nakade, S., et al. (1992). Block of Ca^{2+} wave and Ca^{2+} oscillation by antibody to the inositol 1,4,5-trisphosphate receptor in fertilized hamster eggs. *Science* 257, 251–255. doi: 10.1126/science.1321497

Mochida, S., and Hunt, T. (2007). Calcineurin is required to release *Xenopus* egg extracts from meiotic M phase. *Nature* 449, 336–340. doi: 10.1038/nature06121

Mohri, T., Shirakawa, H., Oda, S., Sato, M. S., Mikoshiba, K., and Miyazaki, S. (2001). Analysis of $Mn(^{2+})/Ca(^{2+})$ influx and release during $Ca(^{2+})$ oscillations in mouse eggs injected with sperm extract. *Cell Calcium* 29, 311–325. doi: 10.1054/ceca.2000.0196

Morin, N., Abrieu, A., Lorca, T., Martin, F., and Doree, M. (1994). The proteolysis-dependent metaphase to anaphase transition: calcium/calmodulin-dependent protein kinase II mediates onset of anaphase in extracts prepared from unfertilized *Xenopus* eggs. *EMBO J.* 13, 4343–4352.

Nader, N., Kulkarni, R. P., Dib, M., and Machaca, K. (2013). How to make a good egg!: the need for remodeling of oocyte $Ca(^{2+})$ signaling to mediate the egg-to-embryo transition. *Cell Calcium* 53, 41–54. doi: 10.1016/j.ceca.2012.11.015

Nigg, E. A. (1991). The substrates of the cdc2 kinase. *Semin. Cell Biol.* 2, 261–270.

Nishiyama, T., Yoshizaki, N., Kishimoto, T., and Ohsumi, K. (2007). Transient activation of calcineurin is essential to initiate embryonic development in *Xenopus laevis*. *Nature* 449, 341–345. doi: 10.1038/nature06136

Nuccitelli, R., Yim, D. L., and Smart, T. (1993). The sperm-induced Ca2+ wave following fertilization of the *Xenopus* egg requires the production of Ins(1, 4, 5)P3. *Dev. Biol.* 158, 200–212. doi: 10.1006/dbio.1993.1179

Okamoto, H., Takahashi, K., and Yamashita, N. (1977). Ionic currents through the membrane of the mammalian oocyte and their comparison with those in the tunicate and sea urchin. *J. Physiol.* 267, 465–495. doi: 10.1113/jphysiol.1977.sp011822

Parys, J. B., and Bezprozvanny, I. (1995). The inositol trisphosphate receptor of *Xenopus* oocytes. *Cell Calcium* 18, 353–363. doi: 10.1016/0143-4160(95)90051-9

Parys, J. B., Sernett, S. W., DeLisle, S., Snyder, P. M., Welsh, M. J., and Campbell, K. P. (1992). Isolation, characterization, and localization of the inositol 1,4,5-trisphosphate receptor protein in *Xenopus laevis* oocytes. *J. Biol. Chem.* 267, 18776–18782.

Peier, A. M., Reeve, A. J., Andersson, D. A., Moqrich, A., Earley, T. J., Hergarden, A. C., et al. (2002). A heat-sensitive TRP channel expressed in keratinocytes. *Science* 296, 2046–2049. doi: 10.1126/science.1073140

Peres, A. (1986). Resting membrane potential and inward current properties of mouse ovarian oocytes and eggs. *Pflugers Arch.* 407, 534–540. doi: 10.1007/BF00657512

Peres, A. (1987). The calcium current of mouse egg measured in physiological calcium and temperature conditions. *J. Physiol.* 391, 573–588. doi: 10.1113/jphysiol.1987.sp016757

Powers, R. D., and Tupper, J. T. (1974). Some electrophysiological and permeability properties of the mouse egg. *Dev. Biol.* 38, 320–331. doi: 10.1016/0012-1606(74)90010-4

Prakriya, M., Feske, S., Gwack, Y., Srikanth, S., Rao, A., and Hogan, P. G. (2006). Orai1 is an essential pore subunit of the CRAC channel. *Nature* 443, 230–233. doi: 10.1038/nature05122

Ramirez, D., Gonzalez, W., Fissore, R. A., and Carvacho, I. (2017). Conotoxins as tools to understand the physiological function of voltage-gated calcium (CaV) channels. *Mar. Drugs* 15:313. doi: 10.3390/md15100313

Rauh, N. R., Schmidt, A., Bormann, J., Nigg, E. A., and Mayer, T. U. (2005). Calcium triggers exit from meiosis II by targeting the APC/C inhibitor XErp1 for degradation. *Nature* 437, 1048–1052. doi: 10.1038/nature04093

Runft, L. L., Jaffe, L. A., and Mehlmann, L. M. (2002). Egg activation at fertilization: where it all begins. *Dev. Biol.* 245, 237–254. doi: 10.1006/dbio.2002.0600

Saunders, C. M., Larman, M. G., Parrington, J., Cox, L. J., Royse, J., Blayney, L. M., et al. (2002). PLC zeta: a sperm-specific trigger of $Ca^{(2+)}$ oscillations in eggs and embryo development. *Development* 129, 3533–3544.

Schindl, R., Fritsch, R., Jardin, I., Frischauf, I., Kahr, H., Muik, M., et al. (2012). Canonical transient receptor potential (TRPC) 1 acts as a negative regulator for vanilloid TRPV6-mediated Ca^{2+} influx. *J. Biol. Chem.* 287, 35612–35620. doi: 10.1074/jbc.M112.400952

Schmidt, A., Duncan, P. I., Rauh, N. R., Sauer, G., Fry, A. M., Nigg, E. A., et al. (2005). *Xenopus* polo-like kinase Plx1 regulates XErp1, a novel inhibitor of APC/C activity. *Genes Dev.* 19, 502–513. doi: 10.1101/gad.320705

Schmidt, A., Rauh, N. R., Nigg, E. A., and Mayer, T. U. (2006). Cytostatic factor: an activity that puts the cell cycle on hold. *J. Cell Sci.* 119(Pt 7), 1213–1218. doi: 10.1242/jcs.02919

Schroeder, B. C., Cheng, T., Jan, Y. N., and Jan, L. Y. (2008). Expression cloning of TMEM16A as a calcium-activated chloride channel subunit. *Cell* 134, 1019–1029. doi: 10.1016/j.cell.2008.09.003

Seguin, D. G., and Baltz, J. M. (1997). Cell volume regulation by the mouse zygote: mechanism of recovery from a volume increase. *Am. J. Physiol.* 272(6 Pt 1), C1854–C1861. doi: 10.1152/ajpcell.1997.272.6.C1854

Shiina, Y., Kaneda, M., Matsuyama, K., Tanaka, K., Hiroi, M., and Doi, K. (1993). Role of the extracellular Ca^{2+} on the intracellular Ca^{2+} changes in fertilized and activated mouse oocytes. *J. Reprod. Fertil.* 97, 143–150. doi: 10.1530/jrf.0.0970143

Shim, A. H., Tirado-Lee, L., and Prakriya, M. (2015). Structural and functional mechanisms of CRAC channel regulation. *J. Mol. Biol.* 427, 77–93. doi: 10.1016/j.jmb.2014.09.021

Simon, A. M., Goodenough, D. A., Li, E., and Paul, D. L. (1997). Female infertility in mice lacking connexin 37. *Nature* 385, 525–529. doi: 10.1038/385525a0

Smith, G. D., Gunthorpe, M. J., Kelsell, R. E., Hayes, P. D., Reilly, P., Facer, P., et al. (2002). TRPV3 is a temperature-sensitive vanilloid receptor-like protein. *Nature* 418, 186–190. doi: 10.1038/nature00894

Smith, L. D. (1989). The induction of oocyte maturation: transmembrane signaling events and regulation of the cell cycle. *Development* 107, 685–699.

Steeves, C. L., Hammer, M. A., Walker, G. B., Rae, D., Stewart, N. A., and Baltz, J. M. (2003). The glycine neurotransmitter transporter GLYT1 is an organic osmolyte transporter regulating cell volume in cleavage-stage embryos. *Proc. Natl. Acad. Sci. U.S.A.* 100, 13982–13987. doi: 10.1073/pnas.2334537100

Stricker, S. A. (1999). Comparative biology of calcium signaling during fertilization and egg activation in animals. *Dev. Biol.* 211, 157–176. doi: 10.1006/dbio.1999.9340

Sun, L., Haun, S., Jones, R. C., Edmondson, R. D., and Machaca, K. (2009). Kinase-dependent regulation of IP3-dependent Ca^{2+} release during oocyte maturation. *J. Biol. Chem.* 284, 20184–20196. doi: 10.1074/jbc.M109.004515

Sun, L., Yu, F., Ullah, A., Hubrack, S., Daalis, A., Jung, P., et al. (2011). Endoplasmic reticulum remodeling tunes IP3-dependent Ca^{2+} release sensitivity *PLoS ONE* 6:e27928. doi: 10.1371/journal.pone.0027928

Swann, K. (1992). Different triggers for calcium oscillations in mouse eggs involve a ryanodine-sensitive calcium store. *Biochem. J.* 287(Pt 1), 79–84. doi: 10.1042/bj2870079

Swann, K., and Lai, F. A. (2016). The sperm phospholipase C-zeta and Ca^{2+} signalling at fertilization in mammals. *Biochem. Soc. Trans.* 44, 267–272. doi: 10.1042/BST20150221

Taylor, C. W., and Tovey, S. C. (2010). IP(3) receptors: toward understanding their activation. *Cold Spring Harb. Perspect. Biol.* 2:a004010. doi: 10.1101/cshperspect.a004010

Terasaki, M., Runft, L. L., and Hand, A. R. (2001). Changes in organization of the endoplasmic reticulum during *Xenopus* oocyte maturation and activation. *Mol. Biol. Cell* 12, 1103–1116. doi: 10.1091/mbc.12.4.1103

Tokimasa, T., and North, R. A. (1996). Effects of barium, lanthanum and gadolinium on endogenous chloride and potassium currents in *Xenopus* oocytes. *J. Physiol.* 496(Pt 3), 677–686. doi: 10.1113/jphysiol.1996.sp021718

Tosti, E., Boni, R., and Cuomo, A. (2000). $Ca^{(2+)}$ current activity decreases during meiotic progression in bovine oocytes. *Am. J. Physiol. Cell Physiol.* 279, C1795–C1800. doi: 10.1152/ajpcell.2000.279.6.C1795

Tosti, E., Boni, R., Gallo, A., and Silvestre, F. (2013). Ion currents modulating oocyte maturation in animals. *Syst. Biol. Reprod. Med.* 59, 61–68. doi: 10.3109/19396368.2012.758790

Tung, J. J., Hansen, D. V., Ban, K. H., Loktev, A. V., Summers, M. K., Adler, J. R. III, et al. (2005). A role for the anaphase-promoting complex inhibitor Emi2/XErp1, a homolog of early mitotic inhibitor 1, in cytostatic factor arrest of *Xenopus* eggs. *Proc. Natl. Acad. Sci. U.S.A* 102, 4318–4323. doi: 10.1073/pnas.0501108102

Tunquist, B. J., and Maller, J. L. (2003). Under arrest: cytostatic factor (CSF)-mediated metaphase arrest in vertebrate eggs. *Genes Dev.* 17, 683–710. doi: 10.1101/gad.1071303

Tyler, A. (1941). Artificial parthenogenesis. *Biol. Rev.* 16, 291–336. doi: 10.1111/j.1469-185X.1941.tb01105.x

Tyler, A., Monroy, A., Kao, C. Y., and Grundfest, H. (1956). Membrane potential and resistance of the starfish egg before and after fertilization. *Biol. Bull.* 111, 153–177. doi: 10.2307/1539191

Ullah, G., Jung, P., and Machaca, K. (2007). Modeling $Ca^{(2+)}$ signaling differentiation during oocyte maturation. *Cell Calcium* 42, 556–564. doi: 10.1016/j.ceca.2007.01.010

Vanderheyden, V., Devogelaere, B., Missiaen, L., De Smedt, H., Bultynck, G., and Parys, J. B. (2009). Regulation of inositol 1,4,5-trisphosphate-induced Ca^{2+} release by reversible phosphorylation and dephosphorylation. *Biochim. Biophys. Acta* 1793, 959–970. doi: 10.1016/j.bbamcr.2008.12.003

Vieira, A., and Miller, D. J. (2006). Gamete interaction: is it species-specific? *Mol. Reprod. Dev.* 73, 1422–1429. doi: 10.1002/mrd.20542

Vig, M., Beck, A., Billingsley, J. M., Lis, A., Parvez, S., Peinelt, C., et al. (2006). CRACM1 multimers form the ion-selective pore of the CRAC channel. *Curr. Biol.* 16, 2073–2079. doi: 10.1016/j.cub.2006.08.085

Vig, M., DeHaven, W. I., Bird, G. S., Billingsley, J. M., Wang, H., Rao, P. E., et al. (2008). Defective mast cell effector functions in mice lacking the CRACM1 pore subunit of store-operated calcium release-activated calcium channels. *Nat. Immunol.* 9, 89–96. doi: 10.1038/ni1550

Wakai, T., Vanderheyden, V., and Fissore, R. A. (2011). Ca^{2+} signaling during mammalian fertilization: requirements, players, and adaptations. *Cold Spring Harb. Perspect. Biol.* 3:a006767. doi: 10.1101/cshperspect.a006767

Wakai, T., Vanderheyden, V., Yoon, S. Y., Cheon, B., Zhang, N., Parys, J. B., et al. (2012). Regulation of inositol 1,4,5-trisphosphate receptor function during mouse oocyte maturation. *J. Cell. Physiol.* 227, 705–717. doi: 10.1002/jcp.22778

Wakayama, T., Perry, A. C., Zuccotti, M., Johnson, K. R., and Yanagimachi, R. (1998). Full-term development of mice from enucleated oocytes injected with cumulus cell nuclei. *Nature* 394, 369–374. doi: 10.1038/28615

Wang, C., Lee, K., Gajdocsi, E., Papp, A. B., and Machaty, Z. (2012). Orai1 mediates store-operated Ca^{2+} entry during fertilization in mammalian oocytes. *Dev. Biol.* 365, 414–423. doi: 10.1016/j.ydbio.2012.03.007

Westendorf, J. M., Rao, P. N., and Gerace, L. (1994). Cloning of cDNAs for M-phase phosphoproteins recognized by the MPM2 monoclonal antibody and determination of the phosphorylated epitope. *Proc. Natl. Acad. Sci. U.S.A.* 91, 714–718. doi: 10.1073/pnas.91.2.714

Whitaker, M. (2006). Calcium at fertilization and in early development. *Physiol. Rev.* 86, 25–88. doi: 10.1152/physrev.00023.2005

Whittingham, D. G., and Siracusa, G. (1978). The involvement of calcium in the activation of mammalian oocytes. *Exp. Cell Res.* 113, 311–317. doi: 10.1016/0014-4827(78)90371-3

Winterhager, E., and Kidder, G. M. (2015). Gap junction connexins in female reproductive organs: implications for women's reproductive health. *Hum. Reprod. Update* 21, 340–352. doi: 10.1093/humupd/dmv007

Wolf, D. P. (1974). The cortical granule reaction in living eggs of the toad, *Xenopus laevis*. *Dev. Biol.* 36, 62–71. doi: 10.1016/0012-1606(74)90190-0

Wu, L. J., Sweet, T. B., and Clapham, D. E. (2010). International Union of Basic and Clinical Pharmacology. LXXVI. Current progress in the mammalian TRP ion channel family. *Pharmacol. Rev.* 62, 381–404. doi: 10.1124/pr.110.002725

Xu, H., Ramsey, I. S., Kotecha, S. A., Moran, M. M., Chong, J. A., Lawson, D., et al. (2002). TRPV3 is a calcium-permeable temperature-sensitive cation channel. *Nature* 418, 181–186. doi: 10.1038/nature00882

Xu, Y. R., and Yang, W. X. (2017). Calcium influx and sperm-evoked calcium responses during oocyte maturation and egg activation. *Oncotarget* 8, 89375–89390. doi: 10.18632/oncotarget.19679

Yamashita, N. (1982). Enhancement of ionic currents through voltage-gated channels in the mouse oocyte after fertilization. *J. Physiol.* 329, 263–280. doi: 10.1113/jphysiol.1982.sp014302

Yang, P., and Zhu, M. X. (2014). Trpv3. *Handb. Exp. Pharmacol.* 222, 273–291. doi: 10.1007/978-3-642-54215-2_11

Yang, Y. D., Cho, H., Koo, J. Y., Tak, M. H., Cho, Y., Shim, W. S., et al. (2008). TMEM16A confers receptor-activated calcium-dependent chloride conductance. *Nature* 455, 1210–1215. doi: 10.1038/nature07313

Yoshida, S. (1983). Permeation of divalent and monovalent cations through the ovarian oocyte membrane of the mouse. *J. Physiol.* 339, 631–642. doi: 10.1113/jphysiol.1983.sp014739

Ypey, D. L., and DeFelice, L. J. (2000). *The Patch-Clamp Technique Explained and Exercised with the use of Simple Electrical Equivalent Circuits*. Available online at: http://mdc.custhelp.com/euf/assets/images/KB864_ModelCells.pdf

Yu, F., Sun, L., and Machaca, K. (2009). Orai1 internalization and STIM1 clustering inhibition modulate SOCE inactivation during meiosis. *Proc. Natl. Acad. Sci. U.S.A.* 106, 17401–17406. doi: 10.1073/pnas.0904651106

Yu, F., Sun, L., and Machaca, K. (2010). Constitutive recycling of the store-operated Ca^{2+} channel Orai1 and its internalization during meiosis. *J. Cell Biol.* 191, 523–535. doi: 10.1083/jcb.201006022

Yu, Y., Nomikos, M., Theodoridou, M., Nounesis, G., Lai, F. A., and Swann, K. (2012). PLCzeta causes $Ca^{(2+)}$ oscillations in mouse eggs by targeting intracellular and not plasma membrane PI(4,5)P(2). *Mol. Biol. Cell* 23, 371–380. doi: 10.1091/mbc.e11-08-0687

Yuan, J. P., Kim, M. S., Zeng, W., Shin, D. M., Huang, G., Worley, P. F., et al. (2009). TRPC channels as STIM1-regulated SOCs. *Channels* 3, 221–225. doi: 10.4161/chan.3.4.9198

Zeng, W., Yuan, J. P., Kim, M. S., Choi, Y. J., Huang, G. N., Worley, P. F., et al. (2008). STIM1 gates TRPC channels, but not Orai1, by electrostatic interaction. *Mol. Cell* 32, 439–448. doi: 10.1016/j.molcel.2008.09.020

Zhang, L., Chao, C. H., Jaeger, L. A., Papp, A. B., and Machaty, Z. (2018). Calcium oscillations in fertilized pig oocytes are associated with repetitive interactions between STIM1 and ORAI1. *Biol. Reprod.* 98, 510–519. doi: 10.1093/biolre/ioy016

Zhang, N., Yoon, S. Y., Parys, J. B., and Fissore, R. A. (2015). Effect of M-phase kinase phosphorylations on type 1 inositol 1,4,5-trisphosphate receptor-mediated Ca^{2+} responses in mouse eggs. *Cell Calcium* 58, 476–488. doi: 10.1016/j.ceca.2015.07.004

Conflict of Interest Statement: The authors declare that the research was conducted in the absence of any commercial or financial relationships that could be construed as a potential conflict of interest.

frontiers in Cell and Developmental Biology

ORIGINAL RESEARCH
published: 11 June 2018
doi: 10.3389/fcell.2018.00060

Changes in Protein O-GlcNAcylation During Mouse Epididymal Sperm Maturation

Darya A. Tourzani[1], *Bidur Paudel*[1], *Patricia V. Miranda*[2], *Pablo E. Visconti*[1]* and *María G. Gervasi*[1]*

[1] Department of Veterinary and Animal Sciences, Integrated Sciences Building, University of Massachusetts, Amherst, MA, United States, [2] Instituto de Agrobiotecnología Rosario S.A. (INDEAR), Rosario, Argentina

After leaving the testis, sperm undergo two sequential maturational processes before acquiring fertilizing capacity: sperm maturation in the male epididymis, and sperm capacitation in the female reproductive tract. During their transit through the epididymis, sperm experience several maturational changes; the acquisition of motility is one of them. The molecular basis of the regulation of this process is still not fully understood. Sperm are both transcriptionally and translationally silent, therefore post-translational modifications are essential to regulate their function. The post-translational modification by the addition of O-linked β-N-acetylglucosamine (O-GlcNAc) can act as a counterpart of phosphorylation in different cellular processes. Therefore, our work was aimed to characterize the O-GlcNAcylation system in the male reproductive tract and the occurrence of this phenomenon during sperm maturation. Our results indicate that O-GlcNAc transferase (OGT), the enzyme responsible for O-GlcNAcylation, is present in the testis, epididymis and immature caput sperm. Its presence is significantly reduced in mature cauda sperm. Consistently, caput sperm display high levels of O-GlcNAcylation when compared to mature cauda sperm, where it is mostly absent. Our results indicate that the modulation of O-GlcNAcylation takes place during sperm maturation and suggest a role for this post-translational modification in this process.

Keywords: sperm maturation, O-GlcNAcylation, O-GlcNAc transferase, spermatozoa, epididymis

OPEN ACCESS

Edited by:
Karin Lykke-Hartmann, Aarhus University, Denmark

Reviewed by:
John A. Hanover, National Institutes of Health (NIH), United States
Gilda Cobellis, Università degli Studi della Campania "Luigi Vanvitelli" Caserta, Italy

***Correspondence:**
Pablo E. Visconti
pvisconti@vasci.umass.edu
María G. Gervasi
mariagracia@vasci.umass.edu

Specialty section:
This article was submitted to Signaling, a section of the journal Frontiers in Cell and Developmental Biology

Received: *08 February 2018*
Accepted: *22 May 2018*
Published: *11 June 2018*

Citation:
Tourzani DA, Paudel B, Miranda PV, Visconti PE and Gervasi MG (2018) Changes in Protein O-GlcNAcylation During Mouse Epididymal Sperm Maturation. Front. Cell Dev. Biol. 6:60. doi: 10.3389/fcell.2018.00060

INTRODUCTION

Mammalian fertilization is a complex process in which a spermatozoon fuses with an MII-arrested oocyte to form a new individual (Yanagimachi, 1994). The dynamic interactions that occur during fertilization depend on the proper function of gametes. Sperm are produced in the testis and released into the epididymis, where they undergo a post-testicular maturational process known as maturation (Eddy, 2006; Gervasi and Visconti, 2017 and references therein). The epididymis is an organ formed by a convoluted tubule that extends from the testis to the *vas deferens*. The mouse epididymis is anatomically organized into four regions known as initial segment, caput, corpus and cauda (Breton et al., 2016; Domeniconi et al., 2016). During epididymal maturation sperm migrate from the initial segment toward the cauda region, where they are stored until ejaculation occurs. It is known that immature caput sperm are immotile and unable to fertilize (Gervasi and Visconti, 2017).

Conversely, mature cauda sperm are progressively motile and acquire their fertilization competence after a process of capacitation in the female reproductive tract (Gervasi and Visconti, 2016). The acquisition of progressive motility during epididymal maturation has been linked to inactivation of both, the glycogen synthase kinase 3 (GSK3) and the serine/threonine protein phosphatase 1 gamma (PP1γ) (Vijayaraghavan et al., 1996; Somanath et al., 2004; Bhattacharjee et al., 2018). The Wnt signaling pathway has been recently proposed as a new molecular player involved in sperm maturation (Koch et al., 2015). In addition, the regulation of lipid mediators from the endocannabinoid system has been related to sperm acquisition of motility during maturation. A gradient of the endocannabinoid 2-arachidonoylglycerol (2-AG) in the epididymis prevents activation of motility in caput sperm through activation of cannabinoid receptor 1 (CB1) (Ricci et al., 2007; Cobellis et al., 2010). In human sperm, 2-AG inhibits the sperm calcium channel (CatSper), and its degradation allows calcium influx and activation of sperm motility (Miller et al., 2016). Despite the advances in this field of study, the mechanisms by which immature sperm acquire progressive motility and the ability to capacitate when incubated in proper conditions remain largely unknown.

The unique nature of sperm cells being transcriptionally and translationally silent (Diez-Sanchez et al., 2003) has led researchers to investigate post-translational modifications as key regulators of sperm function. Phosphorylation events, either in serine/threonine or in tyrosine residues, have been related to both, sperm maturation and capacitation (Buffone et al., 2014; Dacheux and Dacheux, 2014). Incubation of cauda sperm in a capacitation media supplemented with HCO_3^- and BSA induces a rapid activation of protein kinase A (PKA) which phosphorylates several substrates in serine/threonine residues (Visconti et al., 1997; Wertheimer et al., 2013). This massive phosphorylation event is followed by an increase of protein phosphorylation in tyrosine residues that leads to acquisition of fertilization competence (Visconti et al., 1995a,b). Interestingly, tyrosine phosphorylation is not attainable in immature caput sperm regardless of the supporting media (Visconti et al., 1995a) even after the addition of permeable cAMP agonists.

In recent years, the addition of O-linked β-N-Acetylglucosamine (O-GlcNAc) to proteins in serine or threonine residues has been described as a new post-translational modification in various cellular types (Yang and Qian, 2017). Contrary to phosphorylation, mediated by several families of kinases and phosphatases, the turnover of O-GlcNAc is tightly regulated by only two well-conserved enzymes: uridine diphospho-N-acetylglucosamine:polypeptide β-N-acetylglucosaminyl transferase (O-GlcNAc transferase, OGT) and β-D-N-acetylglucosaminidase (O-GlcNAcase, OGA) (Hu et al., 2010). OGT is the enzyme that transfers O-GlcNAc from the donor substrate UDP-glucosamine to serine/threonine residues of proteins, and OGA is the enzyme that hydrolyzes this modification (Hart et al., 2007). It has been shown by generation of a knock-out mouse line that OGT is required for mouse embryonic development (Shafi et al., 2000), and by conditional mutagenesis, that OGT is essential for somatic cell function (O'Donnell et al., 2004). Generation of an OGA conditional knock-out model indicated that this enzyme is critical to maintain metabolic homeostasis and, animals lacking OGA died shortly after birth (Keembiyehetty et al., 2015). The interplay between O-GlcNAcylation and protein phosphorylation has been proposed as a mechanism that regulates cellular homeostasis with several levels of complexity (Hart et al., 2007; Mishra et al., 2011; Yang and Qian, 2017). In addition, it has been shown that OGT forms functional complexes with PP1γ in the brain (Wells et al., 2004). Considering that PP1γ activity is regulated during epididymal maturation (Vijayaraghavan et al., 1996), the interplay between O-GlcNAcylation and phosphorylation could be part of the mechanism by which caput sperm acquire progressive motility during their transit through the epididymis. There is still no evidence of the presence of this post-translational modification in sperm. Therefore, the aim of this work was first to characterize the O-GlcNAc system in male reproductive tissues; and second, to investigate the extent by which this post-translational modification is regulated in sperm during epididymal maturation. We report here that both, the transferase and the post-translational modification, are present in testis, epididymis, and sperm cells. The levels of O-GlcNAc were found to decrease in sperm during epididymal maturation. In addition, OGT and O-GlcNAcylated proteins also showed differences in their localization when sperm recovered from the caput and the cauda regions were compared. Altogether, these results indicate that sperm O-GlcNAcylation is regulated during mouse sperm maturation and suggest a functional role for this post-translational modification.

RESULTS

Characterization of O-GlcNAcylation in Mouse Testis

The protein OGT (Uniprot ref # Q8CGY8, IUPAC EC 2.4.1.255) is encoded by the gene Ogt (ID: 108155). We used RT-PCR to compare the mRNA levels of the transferase OGT present in testis with the ones expressed in other tissues. OGT mRNA was found to be expressed in adult mouse brain, liver, kidney, heart, and testis (**Figure 1A**). The RT-PCR analyses at various postnatal ages indicated that OGT expression levels did not variate between testes that present cells at diverse gametogenic stages (**Figure 1B**). Because other testicular cell types could be expressing OGT, *In-situ* hybridization experiments were performed to complement the RT-PCR results. *In-situ* hybridization results indicated that OGT transcripts are present in all germ cell types in the adult male testis (**Figure 1C**). As a negative control, mouse testes were incubated with a sense probe and no staining was observed (**Figure 1D**).

The next step was to determine the presence of the protein OGT and of the post-translational modification O-GlcNAcylation in testis by Western blotting and immunofluorescence. Our results showed that both, a ∼110 KDa band corresponding to OGT (**Figure 2A**), and a band corresponding to an O-GlcNAcylated protein (**Figure 2B**) were present in mouse testis extracts. OGT was found in all germ

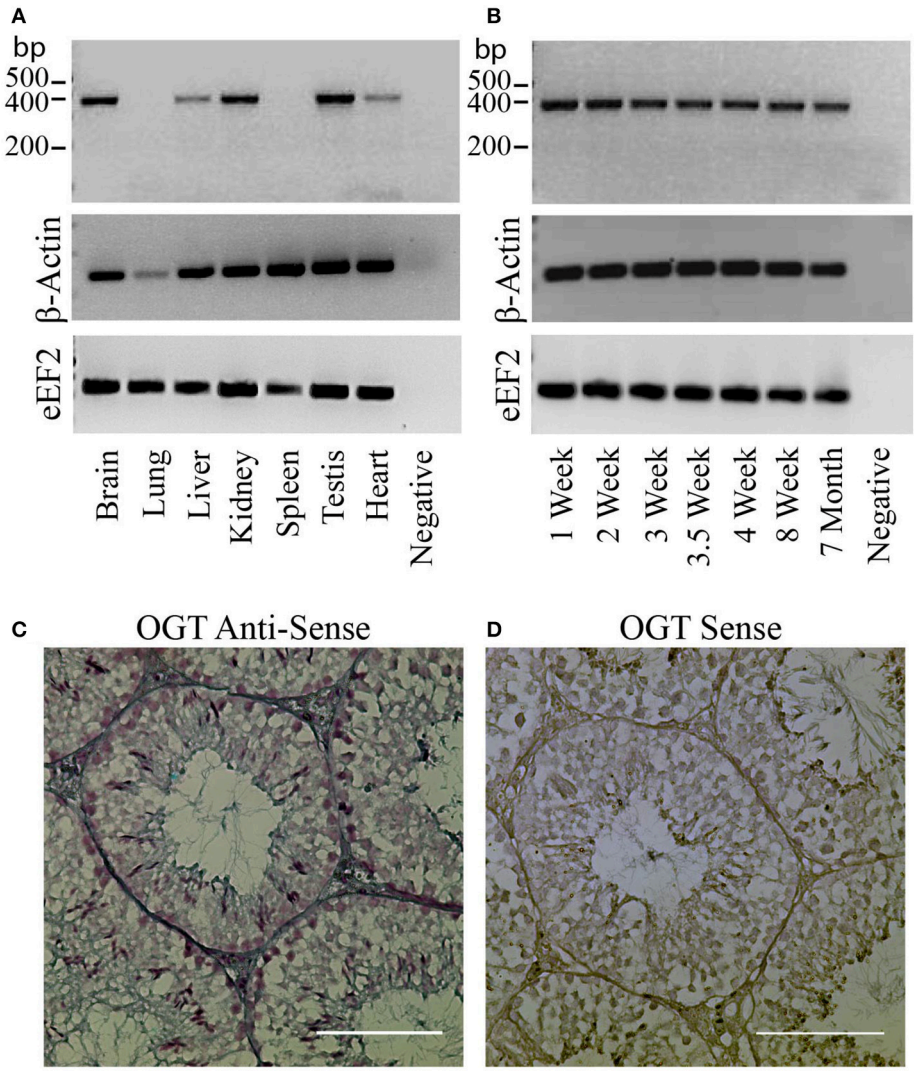

FIGURE 1 | OGT expression in mouse testis. **(A)** Analysis of OGT mRNA expression by RT-PCR in various adult mouse tissues: brain, lung, liver, kidney, spleen, testis, and heart. β-actin and eEF2 were used as loading control. $N = 3$ **(B)** Analysis of OGT mRNA expression by RT-PCR during post-natal testis development: 1 week-, 2 week-, 3 week-, 3.5 week-, 4 week-, 8 week-, and 7 month-old mice. β -actin and eEF2 were used as loading control. $N = 3$. **(C)** *In-situ* hybridization of OGT (anti-sense probe) in adult mouse testis. **(D)** Sense OGT probe used as negative control. Images are representative of three independent experiments. Scale bar = 100 μm.

cell types during spermatogenesis (**Figure 2C**). In addition, the localization of O-GlcNAcylated proteins was also observed in all germ cell types within the testis with high intensity in the sperm flagella (**Figure 2D**). These results indicate that OGT is present in mouse testis, and that O-GlcNAcylation of testicular proteins occurs during all the phases of spermatogenesis. Negative controls showed some levels of unspecific fluorescence in the connective tissue with undetectable unspecific signal within the seminiferous tubules (**Figures 2C,D** lower panel).

O-GlcNAcylation in Mouse Epididymal Sperm

After leaving the testis, sperm undergo maturation as part of their transit from the caput to the cauda epididymis. Similar to testicular sperm, OGT is present in caput sperm. However, the amount of OGT was significantly decreased in cauda sperm (**Figures 3A,B**). Besides the predicted ∼110 KDa protein detected by the anti-OGT antibody, a second band at ∼60 KDa was recognized. This could be a product of OGT degradation. In addition, caput sperm contained high levels of O-GlcNAcylated proteins and this post-translational modification was significantly reduced in cauda spermatozoa (**Figures 3C,D**). Similar differences in protein O-GlcNAcylation between caput and cauda sperm were found when an alternative specific O-GlcNAc antibody (clone RL2) was used for immunodetection (**Supplementary Figure 1A**).

Contrary to cauda sperm collection resulting in almost pure sperm populations, caput sperm suspensions typically

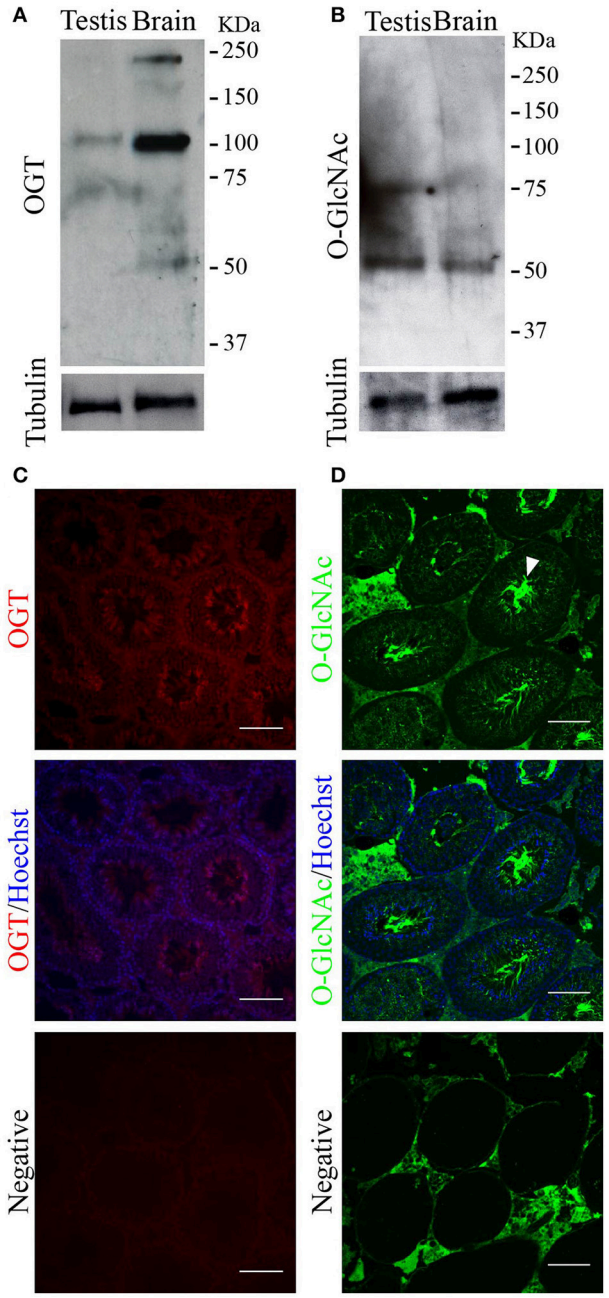

FIGURE 2 | OGT and O-GlcNAcylated proteins in mouse testis. **(A)** Western blotting analysis of OGT in adult testis. Rat brain was used as positive control. Membrane stripping and re-probing with anti-tubulin antibody was used as loading control. $N = 4$ **(B)** Western blotting analysis of O-GlcNAcylated proteins (anti-O-GlcNAc antibody, clone CTD110.6) in adult testis. Rat brain was used as positive control. Membrane stripping and re-probing with anti-tubulin antibody was used as loading control. $N = 4$ **(C)** Immunofluorescence analysis indicating OGT localization in adult testis (upper panel). OGT signal merged with Hoechst nuclear staining (medium panel). Negative control was performed by incubation with secondary antibody alone (lower panel). $N = 3$ **(D)** Immunofluorescence analysis indicating O-GlcNAc (anti-O-GlcNAc antibody, clone CTD110.6) localization in adult testis. Arrowhead indicates the sperm flagella. O-GlcNAc staining merged with Hoechst nuclear staining (medium panel). Negative control was performed by incubation with secondary antibody alone (lower panel). Images are representative of three independent experiments. Scale bar = 100 μm.

contain other cell types and debris. Therefore, to assure that the OGT and O-GlcNAc signals were of sperm origin, each of the sperm samples obtained from caput and cauda were purified using a Percoll wash as explained in the methods section. Western blotting of Percoll-washed sperm also indicated higher levels of OGT (**Figures 3E,F**) and O-GlcNAc modification (**Figures 3G,H**) in sperm from caput epididymis when compared to those from cauda.

O-GlcNAc modifications occur in serine/threonine amino acids and have been postulated to block phosphorylation of these residues and consequently counteract phosphorylation pathways (Hu et al., 2010). Contrary to cauda sperm, caput sperm are not capable to undergo capacitation-induced increase in tyrosine phosphorylation (Visconti et al., 1995a). Our current observations confirmed those findings (**Figures 3I,J**). Although O-GlcNAc does not occur on tyrosine residues, tyrosine phosphorylation during cauda sperm capacitation is downstream of phosphorylation cascades involving PKA, a serine/threonine kinase. Interestingly, PKA-dependent phosphorylation was also blocked in caput epididymal sperm (**Figures 3K,L**). Currently, because of the complex protein pattern of both PKA-dependent phosphorylation and O-GlcNAcylation, it is not possible to know the extent by which these post-translational modifications occur in the same proteins and residues.

Next, the localization of O-GlcNAcylated proteins in sperm recovered from caput and cauda epididymis was evaluated by immunofluorescence. Caput sperm presented O-GlcNAcylated proteins in the head and throughout the flagellum (**Figure 4A**), while in cauda sperm the signal was absent or restricted to the head region (**Figure 4B**). The different patterns found for O-GlcNAcylated proteins (head, flagellum or absent) were quantified, and the results indicated a significant difference between caput and cauda sperm (**Figure 4C**). The differential localization of O-GlcNAcylated proteins in caput and cauda sperm was also detected by immunofluorescence using the alternative O-GlcNAc specific antibody clone RL2 (**Supplementary Figures 1B,C**). These results are in agreement with the Western analyses, shown in **Figure 3**, and indicate that the levels of O-GlcNAcylation in sperm decrease during epididymal maturation.

As OGT is the only known enzyme that catalyzes the addition of O-GlcNAc to proteins, the localization of OGT was also evaluated. Coincidently with O-GlcNAc localization, OGT was found mainly localized to the flagellum of caput sperm (**Figure 4D**), while it was absent or restricted to the head of cauda sperm (**Figure 4E**). The differences in localization of OGT between caput and cauda sperm were quantified and the results show that a high percentage of cauda sperm have undetectable levels of OGT (**Figure 4F**). Overall, our results point to a decrease in the levels of protein O-GlcNAcylation during sperm maturation which is consistent with the loss of OGT during this process.

OGT and O-GlcNAcylated Proteins in Mouse Epididymis

Sperm maturation occurs in the male epididymis. Therefore, we investigated OGT and O-GlcNAc localization in the mouse epididymis by immunofluorescence. Caput epididymis presented

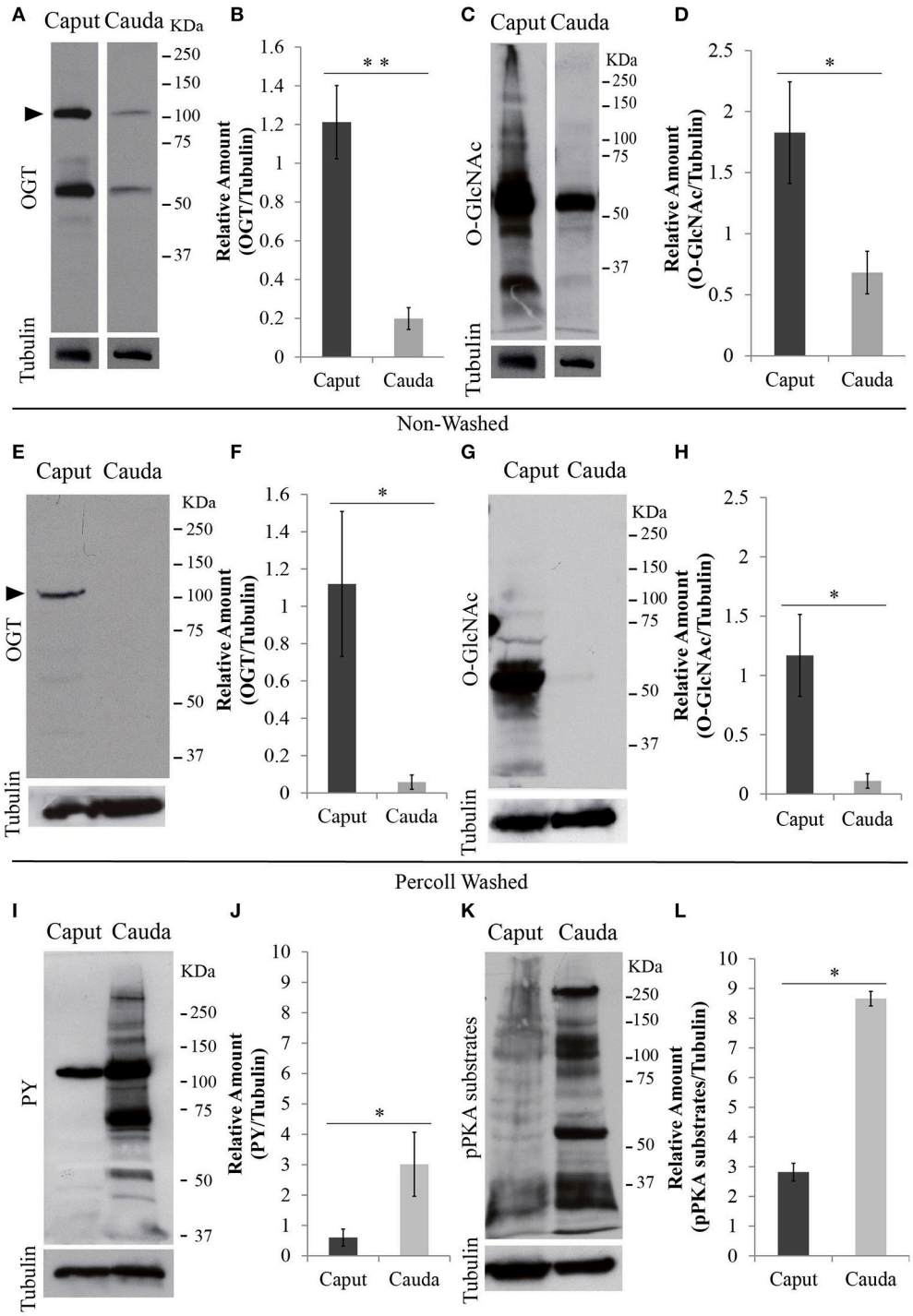

FIGURE 3 | Protein analyses of OGT and post-translational modifications in epididymal sperm. Sperm were collected from caput or cauda epididymis and proteins were extracted and separated by SDS-PAGE. **(A)** Western blotting of OGT from unwashed collection of caput and cauda sperm. Membranes were stripped and re-probed with anti-tubulin antibody to evaluate equal loading. $N = 4$ **(B)** Graph indicating the optical densitometry ratio between OGT and tubulin. Statistical significance between groups is indicated, $^{**}p < 0.01$. **(C)** Western blotting of O-GlcNAcylated proteins (anti-O-GlcNAc antibody, clone CTD110.6) from unwashed collection of caput and cauda sperm. Membranes were stripped and re-probed with anti-tubulin antibody to evaluate equal loading.

(Continued)

FIGURE 3 | $N = 4$ **(D)** Graph indicating the optical densitometry ratio between O-GlcNAcylated proteins and tubulin. Statistical significance between groups is indicated, $^*p < 0.05$. **(E)** Western blotting of OGT from Percoll-washed caput and cauda sperm. Membrane stripping and re-probing with tubulin antibody was used as loading control. $N = 3$. **(F)** Graph indicating the optical densitometry ratio between OGT and tubulin. Statistical significance between groups is indicated, $^*p < 0.05$. **(G)** Western blotting of O-GlcNAcylated proteins (anti-O-GlcNAc antibody, clone CTD110.6) in Percoll-washed caput and cauda sperm. Membranes were stripped and re-probed with anti-tubulin antibody to evaluate equal loading. $N = 3$. **(H)** Graph indicating the optical densitometry ratio between O-GlcNAcylated proteins and tubulin. Statistical significance between groups is indicated, $^*p < 0.05$. **(I)** Western blotting of tyrosine phosphorylation (PY) after 60-min-capacitation of unwashed caput and cauda sperm. Membranes were stripped and re-probed with anti-tubulin antibody to evaluate equal loading. $N = 4$ **(J)** Graph indicating the optical densitometry ratio between PY and tubulin. Statistical significance between groups is indicated, $^*p < 0.05$. **(K)** Western blotting of phosphorylated protein kinase A substrates (pPKA substrates) after 60-min-capacitation of unwashed caput and cauda sperm. Membranes were stripped and re-probed with anti-tubulin antibody to evaluate equal loading. $N = 4$ **(L)** Graph indicating the optical densitometry ratio between p-PKA and tubulin. Statistical significance between groups is indicated, $^*p < 0.05$.

high levels of OGT in the luminal epithelium and in the center of the tubules where the sperm cells are located (**Figure 5A**). In the cauda epididymal epithelium, low levels of OGT staining were found. Similar to the results shown above, OGT was lost in cauda spermatozoa (**Figure 5B**). When O-GlcNAc was evaluated in caput epididymis, this post-translational modification was absent from the epithelium and only localized to the center of the tubules where the sperm are located (**Figure 5C**). In contrast, the cauda epididymis showed O-GlcNAcylated proteins in the epithelium, suggesting that this pathway remains partially active in these cells. No O-GlcNAcylation signal was detected in cauda sperm (**Figure 5D**). Negative controls displayed some unspecific background in the connective tissue but neither in sperm nor in the epididymal epithelium. Altogether, these data indicate that there is a differential localization of OGT and the occurrence of O-GlcNAcylation between caput and cauda epididymis. In addition, these results support our findings indicating that O-GlcNAc is regulated in sperm during epididymal maturation.

DISCUSSION

Several post-translational modifications have been shown to change in sperm during epididymal transit (Gervasi and Visconti, 2017). Being transcriptionally and translationally inactive, these changes are particularly relevant in sperm. The proteome is limited by a fixed number of genes, but protein functionality can be amplified by post-translational modifications that regulate cellular processes (Walsh et al., 2005). Phosphorylation, acetylation, methylation, and ubiquitylation can be found amongst the most widely studied protein modifications. In the last decades, O-GlcNAcylation of proteins in serine or threonine residues has emerged as a novel mechanism for protein regulation (Torres and Hart, 1984; Holt and Hart, 1986). This post-translational modification involves a unique glycosylation event in which a single O-linked β-N-acetylglucosamine (O-GlcNAc) moiety is actively transferred from the donor UDP-GlcNAc to a hydroxyl group of the recipient amino acid (Hart et al., 2007; Yang and Qian, 2017). OGT is the enzyme responsible for the transfer of O-GlcNAc to proteins (Haltiwanger et al., 1992), and OGA is the enzyme responsible for O-GlcNAc hydrolisys (Gao et al., 2001). The occurrence of O-GlcNAcylation in sperm and the male reproductive tract has not been previously reported. In the present work, we studied this novel system and evaluated its association to sperm maturation.

RT-PCR expression analyses indicated that OGT transcripts are found in the testis as well as in other mouse tissues. These results are in agreement with the OGT expression analysis conducted by Shafi and coworkers (Shafi et al., 2000). In addition, we found that the OGT mRNA and protein are present in all phases of spermatogenesis, and that O-GlcNAcylated proteins in the mouse testis are found in all germ cell types from spermatogonia to testicular sperm. These levels of O-GlcNAcylation suggest that this post-translational modification is functional during spermatogenesis.

During epididymal maturation, sperm undergo a series of changes at the molecular level that induce their ability to move progressively and the potential to become fertilization-competent after capacitation (Gervasi and Visconti, 2017). The molecular basis of sperm maturation is largely unknown. However, the inactivation of PP1γ is required for the acquisition of progressive motility in sperm (Vijayaraghavan et al., 1996, 2007). Interestingly, in the brain, the catalytic subunit of PP1γ forms functional complexes with OGT (Wells et al., 2004). Considering that PP1γ and OGT target serine/threonine sites of proteins, the reported elevated activity of PP1γ in caput sperm is consistent with the increased O-GlcNAcylation of proteins found.

Due to the impossibility of reproducing sperm maturation in *in vitro* models, the study of this process relies on the comparison between sperm recovered from caput and cauda regions. It has been proposed that in caput sperm PP1γ remains active by indirect action of GSK3 (Vijayaraghavan et al., 1996) and, that during epididymal maturation, GSK3 is inactivated by phosphorylation in serine residues. The latter is indicated by the increase in phosphorylated GSK3 in cauda sperm when compared with caput (Somanath et al., 2004). Several protein kinases have been proposed to phosphorylate and inactivate GSK3, Akt being one of them (Vadnais et al., 2013). In addition, it has been shown that Akt undergoes O-GlcNAcylation in other cell types (Vosseller et al., 2002), and that this post-translational modification decreases Akt activity (Wang et al., 2012). Interestingly, we found decreased levels of O-GlcNAcylated proteins in mature cauda sperm. One possible mechanism for the acquisition of sperm motility in cauda sperm is an increase of Akt activity due to decreased Akt O-GlcNAcylation. Further experiments are needed to test this hypothesis.

After gaining basal motility, when mature cauda sperm are exposed to capacitation conditions, a cascade of signaling events that leads to acquisition of sperm fertilization ability is

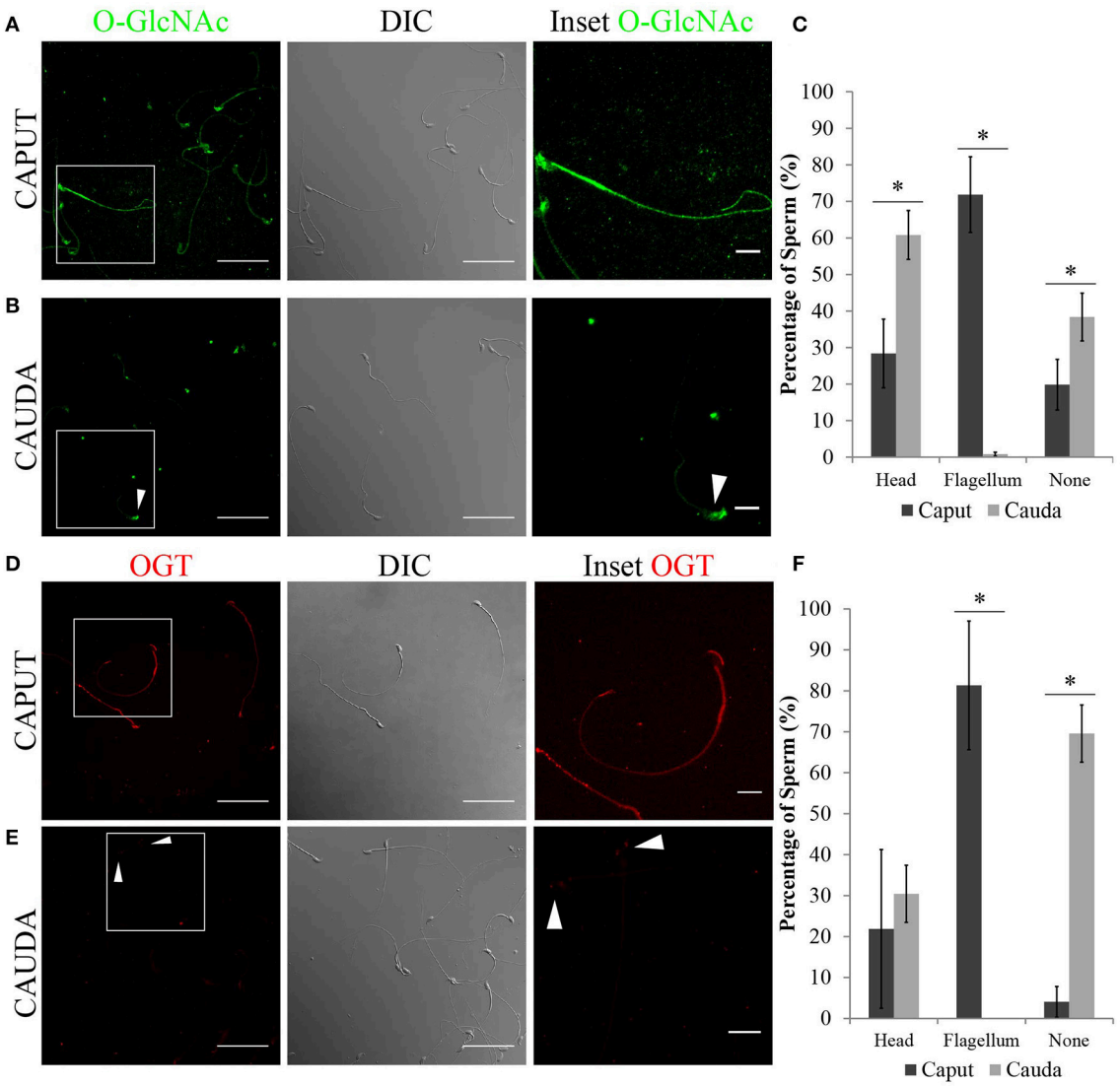

FIGURE 4 | Localization of O-GlcNAcylated proteins and OGT in epididymal sperm by immunofluorescence. **(A)** Localization of O-GlcNAcylated proteins (O-GlcNAc, green) in sperm recovered from the caput region (left panel), scale bar 50 μm. DIC image of the same field of view (middle panel). O-GlcNAc inset (right panel), scale bar = 10 μm. **(B)** Localization of O-GlcNAcylated proteins (O-GlcNAc, green) in sperm recovered from the cauda region (left panel), scale bar = 50 μm. DIC image of the same field of view (middle panel). O-GlcNAc inset (right panel), scale bar = 10 μm. Arrowhead indicates the sperm head. **(C)** Quantification of O-GlcNAc immunofluorescences shown in **(A,B)**. A total of 425 caput and 671 cauda sperm from six independent experiments were counted. Statistical significance between groups is indicated, $^{*}p < 0.05$. **(D)** Localization of OGT (red) in sperm recovered from the caput region (right panel), scale bar = 50 μm. DIC image of the same field of view (middle panel). OGT inset (right panel), scale bar = 10 μm. **(E)** Localization of OGT (red) in sperm recovered from the cauda region (left panel), scale bar = 50 μm. DIC image of the same field of view (middle panel). OGT inset (right panel), scale bar = 10 μm. Arrowheads indicate the sperm head. **(F)** Quantification of OGT immunofluorescences shown in **(D,E)**. A total of 350 caput and 915 cauda sperm from four independent experiments were counted. Statistical significance between groups is indicated, $^{*}p < 0.05$.

activated (Gervasi and Visconti, 2016). Fast activation of PKA and phosphorylation of PKA substrates is followed by a later increase in tyrosine phosphorylation (Visconti, 2009). Contrary to mature cauda sperm, immature caput sperm are unable to undergo phosphorylation on tyrosine residues when incubated in conditions that support capacitation (Visconti et al., 1995a). In the present work, we confirmed that immature caput sperm are not able to display an increase in tyrosine phosphorylation. In addition, we found that PKA-dependent phosphorylation is also decreased in caput sperm when compared to mature sperm. PKA phosphorylates its substrates in serine/threonine residues; therefore, there is a possible competition for these sites between PKA and OGT. Localization of the catalytic subunit of PKA to the sperm flagellum in mature sperm (Wertheimer et al., 2013) coincides with the localization of OGT found in immature caput sperm. Then, OGT could be targeting PKA substrates and

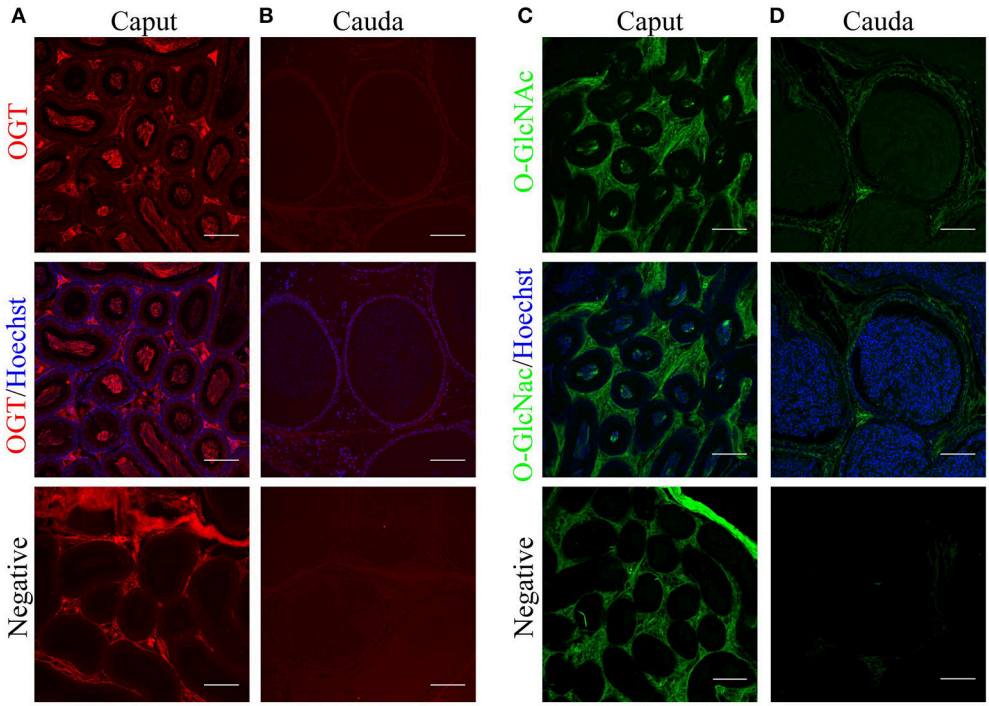

FIGURE 5 | Localization of O-GlcNAcylated proteins and OGT in mouse epididymal tissue by immunofluorescence. **(A)** Localization of OGT (red) in caput epididymal sections (upper panel). OGT signal was merged with Hoechst nuclear staining (medium panel). Negative control was performed by incubation with secondary antibody alone (lower panel). **(B)** Localization of OGT (red) in cauda epididymal sections (upper panel). OGT signal merged with Hoechst nuclear staining (medium panel). Negative control was performed by incubation with secondary antibody alone (lower panel). **(C)** Localization of O-GlcNAcylated proteins (anti-O-GlcNAc antibody clone CTD110.6, green) in caput epididymal sections (upper panel). O-GlcNAc signal merged with Hoechst nuclear staining (medium panel). Negative control was performed by incubation with secondary antibody alone (lower panel). **(D)** Localization of O-GlcNAcylated proteins (anti-O-GlcNAc antibody clone CTD110.6, green) in cauda epididymal sections (upper panel). O-GlcNAc signal merged with Hoechst nuclear staining (medium panel). Negative control was performed by incubation with secondary antibody alone (lower panel). Images are representative of three independent experiments. Scale bars = 100 μm.

preventing their phosphorylation by catalyzing O-GlcNAcylation of the available amino acid residues. In this sense, caput OGT induces O-GlcNAcylation of proteins in caput sperm, and therefore might be preventing phosphorylation of PKA substrates and the activation of the sperm capacitation pathway that triggers the acquisition of fertilization competence. Consistent with this hypothesis, we found the OGT enzyme is mostly absent from cauda sperm, and the levels of O-GlcNAcylated proteins were greatly reduced. This would increase the availability of sites for PKA phosphorylation and activation of the capacitation pathway when sperm are exposed to the proper stimuli.

Differential gene expression and luminal concentrations of ions and endocannabinoids in the different regions of the segmented epididymis are essential to coordinate sperm maturation (Cobellis et al., 2010; Belleannée et al., 2012a,b; Björkgren et al., 2015). Therefore, the differential expression of the O-GlcNAc transferase OGT found between caput and cauda luminal epithelium is consistent with a functional difference of these epididymal regions. The mechanisms by which OGT is lost from sperm during epididymal transit is still unknown. Most reports indicate that proteins are incorporated to sperm during maturation (reviewed in Gervasi and Visconti, 2017), however the protein dicarbonyl L-xylulose reductase (DCXR) has been reported to be selectively removed from bovine sperm during maturation (Akintayo et al., 2015). Our data suggest that OGT is lost from the sperm flagellum during transit through the epididymis, and further investigations are necessary to determine whether it is due to the specific degradation of this transferase.

Protein O-GlcNAcylation is regulated by the fine-tuned activity of the enzymes OGT and OGA (Hart et al., 2007). The lack of either of these enzymes disrupts cell homeostasis and function (Shafi et al., 2000; O'Donnell et al., 2004; Keembiyehetty et al., 2015). Therefore, in addition to OGT, it is important to take into consideration the possible modulation of OGA during sperm maturation. Future investigations regarding OGA are required to fulfill this need.

The present study introduces O-GlcNAcylation as a novel molecular player that participates in epididymal sperm maturation. The drastic changes in O-GlcNAcylation of spermatic proteins during maturation could be part of the still unknown molecular mechanisms that regulate the acquisition of fertilization competence. A model illustrating the incorporation of OGT and O-GlcNAc to the established pathways is presented in **Figure 6**. Our work raises further questions related to sperm maturation. More work is needed to investigate the possible

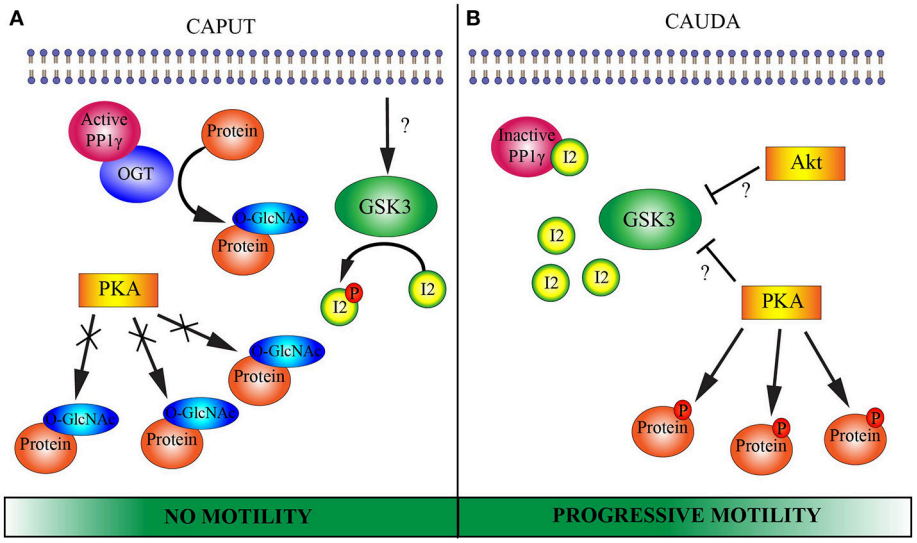

FIGURE 6 | Proposed model of putative molecular pathways involved in epididymal sperm maturation**. (A)** CAPUT: Glycogen synthase kinase 3 (GSK3) is active and phosphorylates protein inhibitor 2 (I2). Once phosphorylated, I2 is not able to bind to and inactivate the serine/threonine phosphatase PP1γ. OGT potentially interacts with PP1γ which would remove phosphates from serine/threonine residues and render them available for OGT. OGT catalyzes O-GlcNAcylation in serine/threonine residues of several proteins. This O-GlcNAcylation potentially blocks phosphorylation sites for protein kinase A (PKA). Caput sperm lack motility. **(B)** CAUDA: GSK3 is phosphorylated on serine residues and rendered inactive by an unidentified serine/threonine kinase. Among the proposed kinases involved in GSK3 phosphorylation and inactivation are PKA and RAC-alpha protein kinase (Akt). Due to GSK3 inactivation, protein I2 can no longer undergo phosphorylation and consequently binds to PP1γ, inactivating its catalytic activity. OGT is absent from cauda sperm and O-GlcNAcylation of proteins is lost. Then, serine/threonine sites are available for phosphorylation by PKA. Together, inactivation of PP1γ leads to the ability of the sperm cell to move progressively and PKA can phosphorylate its substrates when exposed to an appropriate medium. Note that the Wnt and 2-AG pathways mentioned in the introduction have been excluded from the schematic model with the goal of simplifying the understanding of the molecular pathways.

interaction between OGT and PP1γ in immature sperm, and its connection to the acquisition of sperm motility.

METHODS

Animals

Mouse sperm samples were collected from male CD1 retired breeders (Charles River Laboratories, Wilmington, MA, USA). Animal care and use of experimental animals was conducted in accordance with specific guidelines and standards dictated by the Office of Laboratory Animal Welfare (OLAW) and approved by the Institutional Animal Use and Care Committee (IACUC), University of Massachusetts-Amherst (Protocol #201 6-0026).

Media

The non-capacitation medium used for sperm was Hepes-based, modified Toyoda-Yokoyama-Hosi (m-TYH) medium, consisting of (in millimolar): 119.37 NaCl, 4.78 KCl, 1.19 KH_2PO_4, 1.19 $MgSO_4$, 5.56 glucose, 1.71 $CaCl_2$, 20 HEPES, 0.51 Na-pyruvate, 10 μg/mL gentamicin, 0.0006 % phenol red at pH 7.2 to pH 7.4. Capacitating m-TYH was prepared by supplementing non-capacitation media with 25 mM $NaHCO_3$ and 5 mg/mL of bovine serum albumin (BSA, Sigma cat # A0281, St. Louis, MO) to the m-TYH at pH 7.2 to 7.4.

Sperm Sample Collection

Caput epididymis sperm were obtained by squeezing the tissue in non-capacitating m-TYH media approximately 10–15 times. Cauda epididymis sperm were obtained by the "swim-out" method using the same non-capacitating m-TYH media. Briefly, cauda epididymides were dissected, and three incisions were made with fine scissors prior placing the tissue into 1 ml of m-TYH media. Sperm were allowed to swim-out for 10 min at 37°C, and then the epididymides were removed from the sperm suspension. In experiments in which phosphorylation by PKA and tyrosine phosphorylation was investigated, sperm were incubated for 60 min in capacitation media. Otherwise, sperm were used directly after recovery from tissue for further analysis.

Sperm Purification

Caput and cauda epididymal sperm were purified by modification of a method previously described (Vadnais et al., 2013). Briefly, samples were centrifuged at 600 × g for 20 min in a 35% Percoll (Sigma, cat # P1644, St. Louis, MO) in PBS column. After centrifugation, purified sperm found in the pellet were resuspended in PBS and centrifuged at 800 × g for 10 min at room temperature. The sperm pellets were resuspended in m-TYH and processed for Western blotting.

Reverse-Transcriptase-PCR (RT-PCR)

Tissues from adult male mice were collected: brain, lung, liver, spleen, kidney, heart, and testis (1-week to 8-month old);

then homogenized and total RNA was extracted using High Pure RNA Isolation Kit (Roche, Indianapolis, IN). Total RNA concentration was validated and measured using a Nanodrop Spectrophotometer (BioDrop, Cambridge, UK). cDNA was synthesized from RNA samples using iScript^{TM} cDNA Synthesis Kit (Bio-Rad, Hercules, CA) in 20 μL reaction volume. Starting amount of total RNA used was 500 ng. Reverse transcriptase PCR was performed with the following oligonucleotide primers: *OGT* (anti-sense: 5′-TAATACGACTCACTATAGGGTGTC ACCTGCTGCTACCAAG- 3′); *OGT* (sense: 5′-TAATACG ACTCACTATAGGGTTAGCTGAGTTGGCACATCG-3′); β-Actin (anti-sense: 5′-GACGATGCTCCCCGGGCTGTATTC-3′); β-Actin (sense: 5′- TCTCTTGCTCTGGGCCTCGTCACC-3′); eEF2 (sense: 5′-GCGTGCCAAGAAAGTAGAGG-3′); and eEF2 (anti-sense: 5′-GGGATGGTAAGTGGATGGTG-3′) (Integrated DNA Technologies). Amplifications were performed using Taq DNA polymerase enzyme master mix (Affimetrix, Santa Clara, CA). For OGT and β-Actin PCR were performed as follows: 98°C for 1 min (initial denaturation) and 35 cycles at 95°C for 30 s, 56°C for 30 s, 72°C for 30 s and 72°C for 2 min. For eEF2 PCR was performed as follows: 95°C for 2 min (initial denaturation) and 35 cycles at 95°C for 30 s, 55.2°C for 30 s, 72°C for 30 s and 72°C for 2 min. PCR products were separated on a 2% (w/v) agarose gel, stained with ethidium bromide and detected under UV light.

Tissue Collection and Preparation for Immunofluorescence

Mouse testis and epididymal tissue were dissected and fixed in 4% paraformaldehyde (EMS, Hatfield, PA) in PBS overnight at 4°C. Then, progressive dehydration was performed by incubation in increasing concentrations of methanol (25, 50, 75, and 100%), and tissues were left overnight in 100% methanol at −20°C. The following day, the tissues were incubated in 100% xylene for 1 h at room temperature, proceeded by a second replicate incubation of xylene and then an overnight incubation in paraffin at 37°C. Blocks of paraffin-embedded tissue were then prepared and left to harden at room temperature before storage at 4°C. Tissues were sectioned at 7–9 μm-thick slices, lifted onto Superfrost Plus positively charged glass slides (Fisherbrand, Waltham, MA) and left to dry at 37°C overnight before being stored at −20°C. Rehydration was performed by first incubation with 100% xylene for 15 min at room temperature, followed by a second 100% xylene incubation, followed by incubation in decreasing ethanol concentrations in (100, 95, and 70%).

In-Situ Hybridization

Mouse testis sections were prepared and rehydrated as described above. Sections were then permeabilized with Proteinase-K for 13 min. After slides were washed three times for 5 min with PBS-T (0.1% Tween-20 in PBS prepared with DEPC-Water), fixation with 4% paraformaldehyde and 0.2% glutaraldehyde for 20 min at room temperature was performed. Then, slides were washed for 5 min with PBS-T. Sections were then incubated with pre-heated hybridization buffer (50% Formamide, 1% SDS, 5X SSC (3M NaCl, 0.3M $Na_2.Citrate_2.H_2O$), 5μg/mL Heparin, 50 μg/mL Yeast tRNA) and placed into an air-tight incubation chamber for 1 h at 65°C. Followed, by incubation with hybridization buffer and 600 ng/μL of OGT sense or anti-sense probe in an air-tight incubation chamber for 16 h at 65°C. Slides were then incubated twice with a di-formamide solution (2% 5X SSC, 0.1% Tween-20) for 30 min at 65°C. Sections were then washed three times for 5 min at room temperature with 5 mg/mL of Levamisole in PBS-T, proceeded another three times for 15 min at room temperature with the same media. Sections were then blocked with fetal goat serum in 10% BM blocking reagent for 30 min at room temperature, preceded with anti-digoxigenin block (1:500) for 1 h at room temperature. Another set of washes with 5 mg/mL of Levamisole in PBS-T were performed as described before washing with NTMT media (0.1% Tween-20, 5 M NaCl, 1 M MgCl, 1 M Tris at pH 9.5) for 5 min at room temperature. Slides were then stained with BM-purple-AP substrate (Roche, Indianapolis, IN) until desired staining was achieved. Once stained, slides were washed with 0.5 M EDTA three times for 5 min at room temperature. Then, fixation with 4% paraformaldehyde and 0.2% glutaraldehyde for 20 min at room temperature was performed, followed by washes with increasing ethanol concentrations (70, 90, and 100%) before a final xylene wash for 10 min at room temperature. Slides were then mounted with Cytoseal-60 (Richard-Allan Scientific, San Diego, CA). Brightfield images were taken using a 20X objective (Nikon, PlanApo, NA 0.75) in an inverted microscope (Nikon Eclipse T300) equipped with a RGB illumination system and an Andor Zyla camera.

Whole Testis Protein Extraction

Whole testis samples were collected and homogenized in ice-cold RIPA buffer (50 mM Tris-Cl pH 7.4, 150 mM NaCl, 10% glycerol, 0.1% SDS, 1% Triton X-100, 0.5% deoxycholate) supplemented with 1X protease cocktail inhibitors (Roche, Indianapolis, IN), 20 mM β-glycerophosphate, 10 mM Na_3VO_4. Samples were then placed on ice and vortexed every 5 min for 30 min, followed by centrifugation at 10,000 × g for 5 min at 4°C. After centrifugation, supernatant was transferred to fresh tubes and protein determination was done by the Bradford method (Bradford, 1976). 100 μg of protein were re-suspended in SDS-sample buffer (Laemmli, 1970), supplemented with 5% β-mercaptoethanol, boiled for 4 min and loaded in 8% SDS/PAGE. Analysis of proteins by Western blotting was performed as mentioned below.

SDS/PAGE and Western Blotting

After collection, sperm were capacitated for 60 min in full capacitation m-TYH media (3.0×10^6 sperm per treatment). After capacitation, sperm were centrifuged at 12,100 × g for 2 min, washed in 600 μl of cold PBS, centrifuged at 12,100 × g for 3 min and re-suspended in SDS-sample buffer (Laemmli, 1970). Samples were supplemented with 5% β-mercaptoethanol and boiled for 4 min before loading into 8% SDS/PAGE gels. Proteins were then transferred to PVDF membranes, and blockage of nonspecific binding and incubation with primary antibodies were done as follows. For OGT and O-GlcNAc, PVDF membranes were incubated in 5% bovine serum albumin (BSA, Sigma cat # A7906, St. Louis, MO) in Tris-buffered saline with 0.01%

Tween-20 (TBS-T) for 1 h at room temperature; Western blotting was carried out using the following dilution of O-GlcNAc monoclonal antibody (clone CTD110.6) 1:2,000 (Cell Signaling, cat # 9875, Danvers, MA), O-GlcNAc monoclonal antibody (clone RL2) 1:1,000 (ThermoFisher, cat # MA1-072, Rockford, IL), and OGT polyclonal antibody 1:1,000 (Cell Signaling, cat # 5368, Danvers, MA) in 1% BSA/TBS-T overnight at 4°C with slow rocking. For phosphorylated PKA substrates, PVDF membranes were blocked with 5% milk in TBS-T for 1 h at room temperature; Western blotting was carried out by using a dilution of anti-pPKA monoclonal antibody 1:10,000 (Cell Signaling, cat # 9624, Danvers, MA) in 1% BSA/TBS-T overnight at 4°C with slow rocking. For Tyrosine phosphorylated proteins, PVDF membranes were blocked with 20% fish gelatin (Sigma cat # G7765, St. Louis, MO) for 1 h at room temperature; Western blotting was carried out by using a dilution of anti-pY antibody 1:10,000 (Millipore, cat # 05-321, Burlington, MA) overnight at 4°C with slow rocking.

In all cases, after three washes with TBS-T, incubation with the corresponding HRP-conjugated anti-mouse or anti-rabbit secondary antibody (1:10,000, Jackson Immunoresearch Laboratories, West Grover, PA) in TBS-T was conducted for 1 h at room temperature. Equal protein loading was determined by stripping membranes and re-probing with anti-tubulin antibody (1:5,000, clone E7, Hybridoma Bank, University of Iowa). Membranes were developed by using an enhanced chemiluminescence detection kit (ECLprime, GE Healthcare, Pittsburg, PA).

Immunofluorescence

For mouse testis and epididymal tissue, samples were dehydrated, sectioned and rehydrated as described above for *in-situ* hybridization. Prior to staining, sections were treated with 1 % BSA in PBS-T blocking solution at 4°C overnight, followed by incubation with either O-GlcNAc clone CTD110.6 (1:100) or OGT antibody (1:100) in 1% BSA in T-PBS for 3 h in humidifier chamber at room temperature. Sections were then washed with PBS-T and incubated with the corresponding Alexa Fluo555-conjugated secondary antibody (1:1,000) diluted in 1% BSA in PBS-T for 3 h at room temperature; these solutions also contained Hoechst 33258 (1 μg/μl) for nuclear staining. After that, sections were washed three times for 5 min with PBS-T, and mounted using VectaShield (H-1000, Vector Laboratories, Burlingame, CA). Images were taken using a 20 × objective (Nikon, Plan Apo, NA 0.8) in a Nikon confocal Microscope.

For immunolocalization studies in epididymal sperm, samples were obtained as described above, and fixed in 4% paraformaldehyde (EMS, Hatfield, MA) in PBS for 10 min at room temperature. Sperm samples were centrifuged at 800 × g for 5 min, washed with PBS, and air-dried on Poly-L-Lysine-coated glass slides. Sperm were then permeabilized with 0.5% Triton X-100 in PBS for 5 min at room temperature and washed three times for 5 min with PBS and blocked with 10% BSA in PBS-T for 1 h at room temperature. After blocking, sperm were incubated with either O-GlcNAc antibody clone CTD110.6 (1:100), O-GlcNAc antibody clone RL2 (1:100) or OGT antibody (1:100) in 1% BSA in T-PBS over-night in humidifier chamber at 4°C. Following the incubation, sperm were washed with PBS-T and incubated with the corresponding Alexa Fluo555-conjugated secondary antibody (1:1,000) diluted in 1% BSA in PBS-T for 1 h at room temperature; these solutions also contained Alexa Fluo488-conjugated PNA (1:100) for staining of the mouse sperm acrosome and Hoechst 33258 (1 μg/μl) for nuclear staining. After that, samples were washed three times for 5 min with PBS-T and mounted as described above. Negative controls were run in parallel by incubation with secondary antibody alone. Images were taken using a 60 × objective (Nikon, PlanApo, NA 1.49) in a fluorescence microscope (Nikon Eclipse T300). Differential interference contrast (DIC) images were taken in parallel and served as control for sperm morphology.

Statistical Analysis

The software Infostat 2011 (www.infostat.com.ar) was used for the statistical analyses. Homogeneity of variances and normality were tested. Optical densitometry data comply with the parametric test requirements, then comparison between groups was performed by analysis of variance (ANOVA). When the ANOVA tests were significantly different between groups ($P < 0.05$), multiple comparisons were performed by Tukey's test. Immunofluorescence patterns frequency data were evaluated by non-parametric Kruskal-Wallis analyses. *P*-values $P < 0.01$ or $P < 0.05$ were considered significant as indicated in the Figure legends.

AUTHOR CONTRIBUTIONS

MG, PV and PM designed research. DT and BP performed research. DT and MG analyzed data. DT, PV and MG wrote the initial draft.

ACKNOWLEDGMENTS

We thank Dr. Ana María Salicioni for critical reading and editing of this manuscript. This study was supported by NIH R01 grant HD38082 to PV, and by the Lalor Foundation Postdoctoral Grant to MG. Confocal images were taken at the Light Microscopy Facility and Nikon Center of Excellence at the Institute for Applied Life Sciences, University of Massachusetts-Amherst, which is supported by the Massachusetts Life Sciences Center.

SUPPLEMENTARY MATERIAL

The Supplementary Material for this article can be found online at: https://www.frontiersin.org/articles/10.3389/fcell.2018.00060/full#supplementary-material

Supplemental Figure 1 | Protein analysis of post-translational modification using O-GlcNAc antibody clone RL2 in epididymal sperm. Protein extracts of sperm collected from caput or cauda epididymis were separated by SDS-PAGE. **(A)** Western blotting of O-GlcNAcylated proteins (antibody Anti-O-GlcNAc clone RL2) from unwashed collection of caput and cauda sperm. Membranes were stripped and re-probed with anti-tubulin antibody to evaluate equal loading. $N = 3$. **(B)** Localization of O-GlcNAcylated proteins (O-GlcNAc clone RL2, green) in sperm recovered from the caput region (middle panel), scale bar 50 μm. DIC image of the same field of view (left panel). O-GlcNAc clone RL2 inset (right panel), scale bar 10 μm. **(C)** Localization of O-GlcNAcylated proteins (O-GlcNAc clone RL2, green) in sperm recovered from the cauda region (middle panel), scale bar 50 μm. DIC image of the same field of view (left panel). O-GlcNAc clone RL2 inset (right panel), scale bar 10 μm. Arrowhead indicates sperm head.

REFERENCES

Akintayo, A., Légaré, C., and Sullivan, R. (2015). Dicarbonyl L-Xylulose Reductase (DCXR), a "moonlighting protein" in the bovine epididymis. *PLoS ONE* 10:e0120869. doi: 10.1371/journal.pone.0120869

Belleannée, C., Calvo, E., Thimon, V., Cyr, D. G., Légaré, C., Garneau, L., et al. (2012a). Role of microRNAs in controlling gene expression in different segments of the human epididymis. *PLoS ONE* 7:e34996. doi: 10.1371/journal.pone.0034996

Belleannée, C., Thimon, V., and Sullivan, R. (2012b). Region-specific gene expression in the epididymis. *Cell Tissue Res.* 349, 717–731. doi: 10.1007/s00441-012-1381-0

Bhattacharjee, R., Goswami, S., Dey, S., Gangoda, M., Brothag, C., Eisa, A., et al. (2018). Isoform specific requirement for GSK3alpha in sperm for male fertility. *Biol. Reprod.* doi: 10.1093/biolre/ioy020. [Epub ahead of print].

Björkgren, I., Gylling, H., Turunen, H., Huhtaniemi, I., Strauss, L., Poutanen, M., et al. (2015). Imbalanced lipid homeostasis in the conditional Dicer1 knockout mouse epididymis causes instability of the sperm membrane. *FASEB J.* 29, 433–442. doi: 10.1096/fj.14-259382

Bradford, M. M. (1976). A rapid and sensitive method for the quantitation of microgram quantities of protein utilizing the principle of protein-dye binding. *Anal. Biochem.* 72, 248–254. doi: 10.1016/0003-2697(76)90527-3

Breton, S., Ruan, Y. C., Park, Y. J., and Kim, B. (2016). Regulation of epithelial function, differentiation, and remodeling in the epididymis. *Asian J. Androl.* 18, 3–9. doi: 10.4103/1008-682X.165946

Buffone, M. G., Wertheimer, E. V., Visconti, P. E., and Krapf, D. (2014). Central role of soluble adenylyl cyclase and cAMP in sperm physiology. *Biochim. Biophys. Acta* 1842, 2610–2620. doi: 10.1016/j.bbadis.2014.07.013

Cobellis, G., Ricci, G., Cacciola, G., Orlando, P., Petrosino, S., Cascio, M. G., et al. (2010). A gradient of 2-arachidonoylglycerol regulates mouse epididymal sperm cell start-up. *Biol. Reprod.* 82, 451–458. doi: 10.1095/biolreprod.109.079210

Dacheux, J. L., and Dacheux, F. (2014). New insights into epididymal function in relation to sperm maturation. *Reproduction* 147, 27–42. doi: 10.1530/REP-13-0420

Diez-Sanchez, C., Ruiz-Pesini, E., Montoya, J., Perez-Martos, A., Enriquez, J. A., and Lopez-Perez, M. J. (2003). Mitochondria from ejaculated human spermatozoa do not synthesize proteins. *FEBS Lett.* 553, 205–208. doi: 10.1016/S0014-5793(03)01013-5

Domeniconi, R. F., Souza, A. C., Xu, B., Washington, A. M., and Hinton, B. T. (2016). Is the epididymis a series of organs placed side by side? *Biol. Reprod.* 95:10. doi: 10.1095/biolreprod.116.138768

Eddy, E. M. (2006). "The Spermatozoon," in *Knobil and Neill's Physiology of Reproduction*, Vol. 1, ed J. D. Neill (St. Louis, MO; San Diego, CA; London, UK: Elsevier), 3–54.

Gao, Y., Wells, L., Comer, F. I., Parker, G. J., and Hart, G. W. (2001). Dynamic O-Glycosylation of nuclear and cytosolic proteins: cloning and charaterization of a neutral, cytosolic β-N-Acetylglucosaminidase from human brain. *J. Biol. Chem.* 276, 9839–9845. doi: 10.1074/jbc.M010420200

Gervasi, M. G., and Visconti, P. E. (2016). Chang's meaning of capacitation: a molecular perspective. *Mol. Reprod. Dev.* 83, 860–874. doi: 10.1002/mrd.22663

Gervasi, M. G., and Visconti, P. E. (2017). Molecular changes and signaling events occurring in spermatozoa during epididymal maturation. *Andrology* 5, 204–218. doi: 10.1111/andr.12320.

Haltiwanger, R. S., Blomberg, M. A., and Hart, G. W. (1992). Glycosylation of nuclear and cytoplasmic proteins. Purification and characterization of a uridine diphospho-N-acetylglucosamine:polypeptide beta-N-acetylglucosaminyltransferase. *J. Biol. Chem.* 267, 9005–9013.

Hart, G. W., Housley, M. P., and Slawson, C. (2007). Cycling of O-linked beta-N-acetylglucosamine on nucleocytoplasmic proteins. *Nature* 446, 1017–1022. doi: 10.1038/nature05815

Holt, G. D., and Hart, G. W. (1986). The subcellular distribution of terminal N-acetylglucosamine moieties. Localization of a novel protein-saccharide linkage, O-linked GlcNAc. *J. Biol. Chem.* 261, 8049–8057.

Hu, P., Shimoji, S., and Hart, G. W. (2010). Site-specific interplay between O-GlcNAcylation and phosphorylation in cellular regulation. *FEBS Lett.* 584, 2526–2538. doi: 10.1016/j.febslet.2010.04.044

Keembiyehetty, C., Love, D. C., Harwood, K. R., Gavrilova, O., Comly, M. E., and Hanover, J. A. (2015). Conditional knockout reveals a requirement for O-GlcNAcase in metabolic homeostasis. *J. Biol. Chem.* 290, 7097–7113. doi: 10.1074/jbc.M114.617779

Koch, S., Acebron, S. P., Herbst, J., Hatiboglu, G., and Niehrs, C. (2015). Post-transcriptional Wnt signaling governs epididymal sperm maturation. *Cell* 163, 1225–1236. doi: 10.1016/j.cell.2015.10.029.

Laemmli, U. K. (1970). Cleavage of structural proteins during the assembly of the head of bacteriophage T4. *Nature* 227, 680–685.

Miller, M. R., Mannowetz, N., Iavarone, A. T., Safavi, R., Gracheva, E. O., Smith, J. F., et al. (2016). Unconventional endocannabinoid signaling governs sperm activation via the sex hormone progesterone. *Science* 352, 555–559. doi: 10.1126/science.aad6887

Mishra, S., Ande, S. R., and Salter, N. W. (2011). O-GlcNAc modification: why so intimately associated with phosphorylation? *Cell Commun. Signal.* 9:1. doi: 10.1186/1478-811X-9-1.

O'Donnell, N., Zachara, N. E., Hart, G. W., and Marth, J. D. (2004). Ogt-dependent X-chromosome-linked protein glycosylation is a requisite modification in somatic cell function and embryo viability. *Mol. Cell. Biol.* 24, 1680–1690. doi: 10.1128/MCB.24.4.1680-1690.2004

Ricci, G., Cacciola, G., Altucci, L., Meccariello, R., Pierantoni, R., Fasano, S., et al. (2007). Endocannabinoid control of sperm motility: the role of epididymus. *Gen. Comp. Endocrinol.* 153, 320–322. doi: 10.1016/j.ygcen.2007.02.003

Shafi, R., Iyer, S. P., Ellies, L. G., O'Donnell, N., Marek, K. W., Chui, D., et al. (2000). The O-GlcNAc transferase gene resides on the X chromosome and is essential for embryonic stem cell viability and mouse ontogeny. *Proc. Natl. Acad. Sci. U.S.A.* 97, 5735–5739. doi: 10.1073/pnas.100471497

Somanath, P. R., Jack, S. L., and Vijayaraghavan, S. (2004). Changes in sperm glycogen synthase kinase-3 serine phosphorylation and activity accompany motility initiation and stimulation. *J. Androl.* 25, 605–617. doi: 10.1002/j.1939-4640.2004.tb02831.x

Torres, C. R., and Hart, G. W. (1984). Topography and polypeptide distribution of terminal N-acetylglucosamine residues on the surfaces of intact lymphocytes. Evidence for O-linked GlcNAc. *J. Biol. Chem.* 259, 3308–3317.

Vadnais, M. L., Aghajanian, H. K., Lin, A., and Gerton, G. L. (2013). Signaling in sperm: toward a molecular understanding of the acquisition of sperm motility in the mouse epididymis. *Biol. Reprod.* 89:127. doi: 10.1095/biolreprod.113.110163

Vijayaraghavan, S., Chakrabarti, R., and Myers, K. (2007). Regulation of sperm function by protein phosphatase PP1gamma2. *Soc. Reprod. Fertil. Suppl.* 63, 111–121.

Vijayaraghavan, S., Stephens, D. T., Trautman, K., Smith, G. D., Khatra, B., da Cruz e Silva, E. F., et al. (1996). Sperm motility development in the epididymis is associated with decreased glycogen synthase kinase-3 and protein phosphatase 1 activity. *Biol. Reprod.* 54, 709–718.

Visconti, P. E. (2009). Understanding the molecular basis of sperm capacitation through kinase design. *Proc. Natl. Acad. Sci. U.S.A.* 106, 667–668. doi: 10.1073/pnas.0811895106

Visconti, P. E., Bailey, J. L., Moore, G. D., Pan, D., Olds-Clarke, P., and Kopf, G. S. (1995a). Capacitation of mouse spermatozoa. I. Correlation between the capacitation state and protein tyrosine phosphorylation. *Development* 121, 1129–1137.

Visconti, P. E., Johnson, L. R., Oyaski, M., Fornés, M., Moss, S. B., Gerton, G. L., et al. (1997). Regulation, localization, and anchoring of protein kinase A subunits during mouse sperm capacitation. *Dev. Biol.* 192, 351–363. doi: 10.1006/dbio.1997.8768

Visconti, P. E., Moore, G. D., Bailey, J. L., Leclerc, P., Connors, S. A., Pan, D., et al. (1995b). Capacitation of mouse spermatozoa. II. Protein tyrosine phosphorylation and capacitation are regulated by a cAMP-dependent pathway. *Development* 121, 1139–1150.

Vosseller, K., Wells, L., Lane, M. D., and Hart, G. W. (2002). Elevated nucleocytoplasmic glycosylation by O-GlcNAc results in insulin resistance

associated with defects in Akt activation in 3T3-L1 adipocytes. *Proc. Natl. Acad. Sci. U.S.A.* 99, 5313–5318. doi: 10.1073/pnas.072072399

Walsh, C. T., Garneau-Tsodikova, S., and Gatto, G. J. Jr. (2005). Protein posttranslational modifications: the chemistry of proteome diversifications. *Angew. Chem. Int. Ed. Engl.* 44, 7342–7372. doi: 10.1002/anie.200501023

Wang, S., Huang, X., Sun, D., Xin, X., Pan, Q., Peng, S., et al. (2012). Extensive crosstalk between O-GlcNAcylation and phosphorylation regulates Akt signaling. *PLoS ONE* 7:e37427. doi: 10.1371/journal.pone.0037427

Wells, L., Kreppel, L. K., Comer, F. I., Wadzinski, B. E., and Hart, G. W. (2004). O-GlcNAc transferase is in a functional complex with protein phosphatase 1 catalytic subunits. *J. Biol. Chem.* 279, 38466–38470. doi: 10.1074/jbc.M406481200

Wertheimer, E., Krapf, D., de la Vega-Beltran, J. L., Sánchez-Cárdenas, C., Navarrete, F., Haddad, D., et al. (2013). Compartmentalization of distinct cAMP signaling pathways in mammalian sperm. *J. Biol. Chem.* 288, 35307–35320. doi: 10.1074/jbc.M113.489476

Yanagimachi, R. (1994). "Mammalian Fertilization," in *The Phyisiology of Reproduction*, Vol. 1, eds E. Knobil and J. D. Neill (New York, NY: Raven Press), 189–317.

Yang, X., and Qian, K. (2017). Protein O-GlcNAcylation: emerging mechanisms and functions. *Nat. Rev. Mol. Cell Biol.* 18, 452–465. doi: 10.1038/nrm.2017.22

Conflict of Interest Statement: The authors declare that the research was conducted in the absence of any commercial or financial relationships that could be construed as a potential conflict of interest.

frontiers in Cell and Developmental Biology

ORIGINAL RESEARCH
published: 03 April 2018
doi: 10.3389/fcell.2018.00036

PLCζ Induced Ca^{2+} Oscillations in Mouse Eggs Involve a Positive Feedback Cycle of Ca^{2+} Induced $InsP_3$ Formation From Cytoplasmic PIP_2

*Jessica R. Sanders[1], Bethany Ashley[2], Anna Moon[2], Thomas E. Woolley[3] and Karl Swann[2]**

[1] School of Medicine, Cardiff University, Cardiff, United Kingdom, [2] School of Biosciences, Cardiff University, Cardiff, United Kingdom, [3] School of Mathematics, Cardiff University, Cardiff, United Kingdom

OPEN ACCESS

Edited by:
Rafael A. Fissore, University of Massachusetts Amherst, United States

Reviewed by:
Carmen Williams, National Institute of Environmental Health Sciences (NIH), United States
Takuya Wakai, Okayama University, Japan

***Correspondence:**
Karl Swann
swannk1@cardiff.ac.uk

Specialty section:
This article was submitted to Cell Growth and Division, a section of the journal Frontiers in Cell and Developmental Biology

Received: *01 December 2017*
Accepted: *15 March 2018*
Published: *03 April 2018*

Citation:
Sanders JR, Ashley B, Moon A, Woolley TE and Swann K (2018) PLCζ Induced Ca^{2+} Oscillations in Mouse Eggs Involve a Positive Feedback Cycle of Ca^{2+} Induced $InsP_3$ Formation From Cytoplasmic PIP_2. Front. Cell Dev. Biol. 6:36. doi: 10.3389/fcell.2018.00036

Egg activation at fertilization in mammalian eggs is caused by a series of transient increases in the cytosolic free Ca^{2+} concentration, referred to as Ca^{2+} oscillations. It is widely accepted that these Ca^{2+} oscillations are initiated by a sperm derived phospholipase C isoform, PLCζ that hydrolyses its substrate PIP_2 to produce the Ca^{2+} releasing messenger $InsP_3$. However, it is not clear whether PLCζ induced $InsP_3$ formation is periodic or monotonic, and whether the PIP_2 source for generating $InsP_3$ from PLCζ is in the plasma membrane or the cytoplasm. In this study we have uncaged $InsP_3$ at different points of the Ca^{2+} oscillation cycle to show that PLCζ causes Ca^{2+} oscillations by a mechanism which requires Ca^{2+} induced $InsP_3$ formation. In contrast, incubation in Sr^{2+} media, which also induces Ca^{2+} oscillations in mouse eggs, sensitizes $InsP_3$-induced Ca^{2+} release. We also show that the cytosolic level Ca^{2+} is a key factor in setting the frequency of Ca^{2+} oscillations since low concentrations of the Ca^{2+} pump inhibitor, thapsigargin, accelerates the frequency of PLCζ induced Ca^{2+} oscillations in eggs, even in Ca^{2+} free media. Given that Ca^{2+} induced $InsP_3$ formation causes a rapid wave during each Ca^{2+} rise, we use a mathematical model to show that $InsP_3$ generation, and hence PLCζ's substate PIP_2, has to be finely distributed throughout the egg cytoplasm. Evidence for PIP_2 distribution in vesicles throughout the egg cytoplasm is provided with a rhodamine-peptide probe, PBP10. The apparent level of PIP_2 in such vesicles could be reduced by incubating eggs in the drug propranolol which also reversibly inhibited PLCζ induced, but not Sr^{2+} induced, Ca^{2+} oscillations. These data suggest that the cytosolic Ca^{2+} level, rather than Ca^{2+} store content, is a key variable in setting the pace of PLCζ induced Ca^{2+} oscillations in eggs, and they imply that $InsP_3$ oscillates in synchrony with Ca^{2+} oscillations. Furthermore, they support the hypothesis that PLCζ and sperm induced Ca^{2+} oscillations in eggs requires the hydrolysis of PIP_2 from finely spaced cytoplasmic vesicles.

Keywords: Ca^{2+} oscillations, phospholipase C, strontium, inositol trisphosphate, egg, phosphatidyl inositol bisphosphate

INTRODUCTION

The fertilization of a mammalian egg involves a series of low frequency Ca^{2+} oscillations that last for many hours. Such Ca^{2+} oscillations play the key role in egg activation and the subsequent development of the embryo (Stricker, 1999). The first Ca^{2+} increase takes ∼10 s to travel as a wave across the egg from the point of sperm entry (Miyazaki et al., 1986; Deguchi et al., 2000). However, all the subsequent Ca^{2+} transients have a rising phase of about 1 s which is due to a fast Ca^{2+} wave (>50 μm/s) that crosses the egg from apparently random points in the egg cortex (Deguchi et al., 2000). Each Ca^{2+} increase during the oscillations is due to release from internal Ca^{2+} stores via inositol 1,4,5-trisphophate receptors (IP3R) which are exclusively of type 1 IP3R in mammalian eggs (Miyazaki, 1988; Miyazaki et al., 1993). The sperm stimulates the Ca^{2+} oscillations via inositol 1,4,5-trisphosphate ($InsP_3$) production, and all the reproducible studies suggest that this is principally due to the introduction of a sperm specific phospholipase Czeta (PLCζ) into the egg after gamete fusion (Saunders et al., 2002). Injection of PLCζ protein or cRNA causes prolonged Ca^{2+} oscillations that mimic those seen at fertilization in eggs of mice, rat, humans, cows, and pigs (Cox et al., 2002; Saunders et al., 2002; Fujimoto et al., 2004; Kouchi et al., 2004; Kurokawa et al., 2005; Bedford-Guaus et al., 2008; Ito et al., 2008; Ross et al., 2008; Yoon et al., 2012; Sato et al., 2013). PLCζ is distinctive compared to most mammalian PLC isozymes in that it is stimulated by low levels of Ca^{2+} such that it is maximally sensitive to Ca^{2+} around the resting levels in eggs (Nomikos et al., 2005). PLCζ is expected to diffuse across the egg in about 10 min following sperm-egg fusion, hence the fast Ca^{2+} waves seen after the initial Ca^{2+} transient are propagated within a cytoplasm in which PLCζ has probably dispersed throughout the egg.

There are two classes of model to explain how $InsP_3$ causes Ca^{2+} oscillations in cells, both which have been proposed for fertilizing mammalian eggs (Dupont and Goldbeter, 1994; Politi et al., 2006). There are some models that propose Ca^{2+} dependent sensitization, and then de-sensitization, of the IP3R is necessary to generate each Ca^{2+} transient (Politi et al., 2006). This class of models supports the finding that mouse and hamster eggs can be stimulated to oscillate by sustained injection of $InsP_3$, or by injection of the IP3R agonist adenophostin (Swann et al., 1989; Brind et al., 2000; Jones and Nixon, 2000). On the other hand there are other models in which Ca^{2+} dependent production of $InsP_3$ generates each Ca^{2+} transient, and in which $InsP_3$ is predicted to oscillate alongside Ca^{2+} (Politi et al., 2006). This second class of model is supported by the detection of $InsP_3$ oscillations in mouse eggs injected with PLCζ, albeit at high levels of PLCζ (Shirakawa et al., 2006). However, it is not clear if any oscillatory changes in $InsP_3$ oscillations are necessary for generating Ca^{2+} increases. Either classes of model have to incorporate the observation that the Ca^{2+} oscillations have a dependence upon Ca^{2+} influx. So for example, if fertilizing hamster or mouse eggs are incubated in Ca^{2+} free media the oscillations run down and stop (Igusa and Miyazaki, 1983; Lawrence and Cuthbertson, 1995; McGuinness et al., 1996). It has been suggested that the Ca^{2+} store content is critical in setting the timing of Ca^{2+} oscillations in mouse eggs. This is supported by evidence that the SERCA inhibitor thapsigargin can also be used to block sperm and PLCζ induced Ca^{2+} oscillations by depleting Ca^{2+} stores content (Kline and Kline, 1992b). However, changes in cytosolic Ca^{2+} may also play a role in the timing of oscillations since cytosolic Ca^{2+} can regulate both IP3Rs and PLCζ activity.

Sustained Ca^{2+} oscillations in mouse eggs can also be triggered by incubation in media containing Sr^{2+} instead of Ca^{2+} (Kline and Kline, 1992a; Bos-Mikich et al., 1995). Sr^{2+}-induced Ca^{2+} oscillations resemble those seen at fertilization, and they are as effective as fertilization or PLCζ in triggering development to the blastocyst stage (Yu et al., 2008). The oscillations are dependent upon Sr^{2+} influx into the egg and the presence of functional IP3Rs (Zhang et al., 2005). However, it is not clear how Sr^{2+} causes Ca^{2+} oscillations. One study suggested that the effect of Sr^{2+} requires $InsP_3$ production (Zhang et al., 2005). However, unlike fertilization, there is no Sr^{2+} induced downregulation of IP3Rs and this suggests that Sr^{2+} does not cause any substantial $InsP_3$ generation (Jellerette et al., 2000). *In vitro* preparations of IP3Rs receptors can be stimulated to open by Sr^{2+} ions (Marshall and Taylor, 1994), so a direct effect of Sr^{2+} on IP3Rs is also likely, but any changes in InP_3 sensitivity in eggs have yet to be shown.

As well as its high sensitivity to Ca^{2+}, another unusual characteristic of PLCζ is that it does not localize to the plasma membrane (Yu et al., 2012). The substrate for PLCζ, phosphatidylinositol 4,5-bisphophate (PIP_2), can be detected in the plasma membrane of mouse eggs using the PH domain of PLCδ1 (Halet et al., 2002), but the depletion of such PIP_2 from the plasma membrane does not affect the generation of Ca^{2+} oscillations in response to PLCζ or fertilization (Yu et al., 2012). In contrast to somatic cells, mouse eggs have been shown to contain PIP_2 in intracellular vesicles (Yu et al., 2012). These vesicles were detected using PIP_2 antibodies and were found to be dispersed throughout the cytoplasm of mouse eggs (Yu et al., 2012). PLCζ can also be detected on small cytoplasmic vesicles using immunostaining (Yu et al., 2012). The significance of this type of intracellular localization of PLCζ and PIP_2 has not been made clear.

Here we report experiments that analyse the mechanism of PLCζ induced Ca^{2+} oscillations in mouse eggs. We use photo-release of caged $InsP_3$ to show that PLCζ causes Ca^{2+} oscillations via a positive feedback cycle of Ca^{2+} release and Ca^{2+} induced $InsP_3$ production. In contrast the Sr^{2+} induced Ca^{2+} oscillations in mouse eggs involve a sensitization of $InsP_3$ induced Ca^{2+} release. We go on to show that the cytosolic Ca^{2+} is more likely to be important for setting the pace of oscillations in eggs than Ca^{2+} store content. In addition, we present simulations to show that the restricted diffusion of $InsP_3$ in cytoplasm implies that the source of $InsP_3$ generation, PIP_2, needs to be dispersed through the egg interior to account for PLCζ induced rapid Ca^{2+} waves. Finally, we provide further evidence that PIP_2 is present on intracellular vesicles in eggs and that this is required for PLCζ and sperm induced Ca^{2+} oscillations in eggs.

MATERIALS AND METHODS

Handling and Microinjection of Mouse Eggs

MF1 mice between 6 and 8 weeks of age were injected with pregnant mare's serum gonadotrophin (PMSG, Intervet) followed by human chorionic gonadotrophin (hCG, Invervet) ∼50 h later (Fowler and Edwards, 1957). Eggs were collected from these mice 15 h after HCG injection, from the dissected ovaries. All animal handling and procedures were carried out under a UK Home Office License and approved by the Animal Ethics Committee at Cardiff University. Once collected, the eggs were kept at 37°C in M2 media (Sigma Aldrich). All Ca^{2+} dyes and intracellular probes were introduced into the cytosol of the eggs using a high pressure microinjection system with the eggs maintained in M2 media throughout (Swann, 2013). For *in vitro* fertilization sperm was collected from the epididymis of F1 C57/CBA hybrid male mice. The sperm were isolated in T6 media containing 16 mg/ml bovine serum albumin (BSA, Sigma Aldrich) and left to capacitate for 2–3 h before adding to eggs (Yu et al., 2012).

Measurements and Analysis of Intracellular Ca^{2+} and $InsP_3$ Uncaging

In all experiments cytosolic Ca^{2+} was measured using fluorescent Ca^{2+} indictor Oregon Green BAPTA dextran (OGBD) (Life Technologies). OGBD was diluted in a KCl HEPES buffer (120 mM KCl, 20 mM HEPES at pH 7.4) so that the injection solution contained 0.33 or 0.5 mM OGBD. The OGBD mix was microinjected into eggs using high pressure pulses. In those eggs that were stimulated by adenophostin this was microinjected into eggs along with the OGBD. In this case instead of mixing the OGBD with KCL HEPES it was mixed with KCL HEPES containing 5 μM adenophostin in the same quantities. Where PLCζ cRNA was used this was microinjected alongside OGBD in the same way at a concentration of 0.02 μg/μl. For imaging, eggs were then transferred to a glass-bottomed dish, containing HKSOM media, on an epifluorescence imaging system (Nikon TiU) attached to a cooled CCD camera as described previously (Swann, 2013). Ca^{2+} dynamics were measured using the time-lapse imaging mode of Micromanager software (https://micro-manager.org/) where an image was captured every 10 s. Where IVF was performed, or drugs were later added to the eggs, the zona pellucidas were removed from the eggs using acid Tyrodes treatment prior to imaging. For those experiments that required $InsP_3$ stimulation, NPE-caged-$InsP_3$ (1 mM in the pipette) from ThermoFisher Scienific was microinjected prior to imaging at the same time as the injection of fluorescent dye (OGBD). In order to photo-release $InsP_3$ the eggs were exposed to an electronically gated UV LED light source (365 nm, Optoled Lite, Cairn Research Ltd) that was positioned just above the dish containing the eggs. The duration of the UV pulse was controlled by a time gated TTL pulse that was delivered in between two successive fluorescence acquisitions. All data measuring Ca^{2+} dynamics were recorded as .tif files using the Micromanger software on the epifluorescence system.

Media, Chemicals, and Drugs

M2 media was purchased from Sigma Aldrich as a working solution. HKSOM was made up to pH 7.4, in cell culture grade water as follows: 95 mM NaCl, 0.35 mM KH2PO4, 0.2 MgSO4, 2.5 mM KCl, 4 mM $NaHCO_3$, 20 mM HEPES, 0.01 mM EDTA, 0.2 mM Na Pyruvate, 1 mM L-glutamine, 0.2 mM glucose, 10 mM Na Lactate 1.7 mM $CaCl_2$, 0.063 g/l Benzylpenicllin, and 10 mg/l phenol red. Ca^{2+} free media was made in the same way as HKSOM however $CaCl_2$ was not added and the media was supplemented with 100 μM EGTA. Sr^{2+} containing media was made in the same way as HKSOM however, instead of adding 1.7 mM $CaCl_2$, 10 mM $SrCl_2$ was added instead.

All drugs and chemicals used, unless otherwise mentioned, were purchased from Sigma Aldrich. Propranolol was used at a working concentration of 300 μM in HKSOM media. A stock of 300 mM propranolol was made up in DMSO which was then diluted 1:100 in HKSOM media. Then 100 μl of this solution was pipetted into the imaging dish containing 900 μl of standard HKSOM. Propranolol was removed by washing out this media and replacing it with fresh HKSOM media using a perfusion system that passed 10 ml of clean HKSOM through the dish containing the eggs to ensure sufficient wash out. In a similar way a stock of 5 mM thapsigarin in DMSO was diluted 1:1,000 to a concentration of 5 μM in HKSOM and then 100 μl of this thapsigargin solution was added to the imaging dish containing 900 μl of HKSOM to give a working concentration of 500 nM of thapsigargin.

Confocal Imaging

In those eggs that were microinjected with PBP10, a solution of 1 mM PBP10 (Tocris Biosciences, UK) was made up in KCl HEPES and ∼4–10 pl of this solution was microinjected into each egg. Following PBP10 microinjection, eggs were imaged on a Leica SP2 Confocal (Leica, Wetzler, Germany) microscope using a Helium-Neon laser (543 nm) at 30% intensity. Eggs were imaged in M2 media using a x63 oil objective and a pinhole aperture of 91 nm. Images were acquired with a line averaging of 8 and a resolution of 1,058 × 1,058 pixels. For each egg a single z-stack image of (1 μm depth) was captured of an equatorial slice through the egg. All images were exported as .tif files and analyzed using Image J (https://imagej.nih.gov/ij/).

Data Analysis

Quantitative data measuring the Ca^{2+} dynamics of the eggs on the widefield imaging system was extracted from .tif stacks using Image J (https://imagej.nih.gov/ij/). Background fluorescence was first subtracted from the egg fluorescence value. These fluorescence values were then normalized by dividing each fluorescence value in the egg by the baseline fluorescence value at the start of the imaging run to provide a relative change in fluorescence (F/F0) that could be plotted against time. These traces were produced and analyzed using SigmaPlot 12. The Confocal images were also analyzed using Image J software. PIP_2 positive vesicle size and distribution was calculated using the particle analysis function on Image J and a nearest neighbor distance (Nnd) plugin in Image J. A bandpass filter function was applied to the images (large objects were filtered down to

40 pixels and small ones enlarged to 3 pixels). The threshold was altered to between 2 and 5% so only the fluorescence of the vesicles inside the image of the egg were included in the analysis. The particle analysis function was applied and configured so it recorded area, integrated intensity and coordinates for each fluorescent vesicle in the egg. These areas were used to work out the radius and diameter of the vesicles. The coordinates were fed into a nearest distance neighbor plugin (https://icme.hpc.msstate.edu/mediawiki/index.php/Nearest_Neighbor_Distances_Calculation_with_ImageJ) to give the mean distance between the vesicles. The total fluorescence of the vesicles was calculated by adding all the integrated intensity readings for a single egg which was carried out using the measure tool in ImageJ and background fluorescence values were subtracted. Statistical analysis was carried out using SigmaPlot 12. If not stated otherwise the data is presented as the mean and standard errors of the mean. Shapiro–Wilk tests for normality and tests for equal variances were conducted prior to carrying out group comparison tests. If the data passed both these tests a Student's *T-test* was conducted. If the data failed either or both of these tests a Mann-Whitney *U-test* was conducted instead.

Mathematical Method of Ca^{2+} Waves

The model and associated parameter values are based on the work of (Politi et al., 2006; Theodoridou et al., 2013). The reaction-diffusion equations define the interactions between free cytosolic calcium, u; stored calcium, v; and IP3, p,

$$\frac{\mathrm{d}u}{\mathrm{d}t} = d\nabla^2 u + A - D\frac{u^{ed}}{u^{ed}+u_d^{ed}}\left(1-\frac{p^{es}}{p^{es}+p_s^{es}}\right) + K(u,v,p), \tag{1}$$

$$\frac{\mathrm{d}v}{\mathrm{d}t} = d\nabla^2 v - K(u,v,p)S(x,y,L_0), \tag{2}$$

$$\frac{\mathrm{d}p}{\mathrm{d}t} = d\nabla^2 p + \epsilon + PLC\frac{u^{ep}}{u^{ep}+u_p^{ep}}S(x,y,L) - rp, \tag{3}$$

$$K(u,v,p) = -B\frac{u^{eb}}{u^{eb}+u_b^{eb}} + C\frac{v^{ec}}{v^{ec}+v_c^{ec}}\frac{p^{epc}}{p^{epc}+p_c^{epc}}\frac{u^{epa}}{u^{epa}+u_{pa}^{epa}}\left(1-\frac{u^{epi}}{u^{epi}+u_{pi}^{epi}}\right) - Ev. \tag{4}$$

$$S(x,y,L) = \begin{cases} 1 \text{ if } \left(\frac{x}{L} - \lfloor\frac{x}{L}\rfloor\right) < \frac{L_{on}}{L} \text{ and } \left(\frac{y}{L} - \lfloor\frac{y}{L}\rfloor\right) < \frac{L_{on}}{L}, \\ 0 \text{ Otherwise.} \end{cases} \tag{5}$$

The equations represent interactions in which free Ca^{2+} acts as a self-inhibitor but, along with $InsP_3$ and stored Ca^{2+}, stimulates the release of stored Ca^{2+}, creating a system that can produce oscillations in the concentrations of calcium and $InsP_3$. Critically, all species are able to diffuse with the same diffusion coefficient, d.

The actions of the stored Ca^{2+} and the $InsP_3$ only occur in discrete regions. This spatial discreteness is controlled by the repeating function $S(x,y,L)$. Essentially, the function $S(x,y,L)$ creates a regular grid of squares of size $L_{on} \times L_{on}$ in which the specified kinetics are active. We are then able to alter the wavelength, or separation distance, L, between these active regions.

The equations were simulated using a finite element Runge-Kutta method on a two-dimensional disk of diameter 70 μm, which was discretised into 6,550 elements. The 2D assumption is considered valid because any dilution effects of going to three dimensions are off set equally by an increase in the third dimension production. The two-dimensional simulations can be thought of a single slice through a cell and it offers speed, clarity and insight. Finally, the boundary was specified to have a zero-flux condition, meaning that no substances were able to leak out of the domain. This is a simplification considered valid since it is known that PLCζ induced Ca^{2+} spikes can be generated in mouse eggs where no membrane Ca^{2+} fluxes occur (Miao et al., 2012). The equations are accompanied by the parameter values specified in **Table 1**, where all unit dimensions are chosen to make u, v, and p have units of μMol, space is in μm and time is in seconds. The initial conditions for all populations were at steady state except for a small perturbation of a two-dimensional Gaussian profile at the point (20,20), in the free Ca^{2+} population.

TABLE 1 | Parameter values for Equations (1)–(5).

Parameter	Value	Definition
A	0.25	Calcium source
B	200	Strength of calcium induced calcium degradation
C	3,125	Calcium release depending on all forms of calcium and IP_3
D	7.5	Strength of IP_3 blocking calcium degradation
E	0.00125	Calcium leakage
PLC	100	Strength of calcium induced IP_3 release
ϵ	0.001	IP_3 source
r	10	IP_3 degradation
d	10	Diffusion rate
u_d	0.5	Calcium degradation sensitivity to calcium
ed	2	Hill coefficient
p_s	0.1	Calcium degradiation sensitivity to IP_3
es	3	Hill coefficient
u_p	0.025	IP_3 production sensitivity to calcium
ep	4	Hill coefficient
u_b	2.25	Calcium degradation sensitivity to calcium
eb	2	Hill coefficient
v_c	9	Calcium release sensitivity to stored calcium
ec	2	Hill coefficient
u_{pa}	0.45	Calcium release sensitivity to cytosolic calcium
epa	4	Hill coefficient
u_{pi}	1	Calcium release sensitivity to cytosolic calcium
epi	5	Hill coefficient
p_c	0.1	Calcium release sensitivity to IP_3
epc	2	Hill coefficient
L_0	1.5	Calcium store spacing

All unit dimensions have been chosen to make u, v, and p have units of μMol, space is in μm and time is in seconds.

RESULTS

PLCζ and Sr^{2+} Trigger Ca^{2+} Oscillations in Eggs via Different Mechanisms

We investigated the mechanism generating Ca^{2+} oscillations by using photo-release of caged $InsP_3$ that was microinjected into mouse eggs. In initial experiments we uncaged $InsP_3$ in unfertilized (control) mouse eggs that were not undergoing any Ca^{2+} oscillations. **Figure 1A** shows that UV pulses of light from 50 ms through to 2 s generated Ca^{2+} increases with the amplitudes that were larger with longer duration pulses. With the protocol we used there was adequate amounts of caged $InsP_3$ for multiple releases of $InsP_3$ even with longer duration pulses of UV light as illustrated by **Figure 1B** which shows that 3 s pulses could generate repeated large rises in Ca^{2+} in control eggs. We then tested the effects of triggering such pulses during Ca^{2+} oscillations induced by either Sr^{2+} media or by PLCζ injection. **Figure 1C** shows that when a 100 ms pulse was used in eggs injected with PLCζ the uncaging of $InsP_3$ caused no Ca^{2+} increase. In contrast, **Figure 1D** shows Ca^{2+} oscillations occurring in response to Sr^{2+} media and in such eggs there was a rapid and large Ca^{2+} transient every time a pulse of just 100 ms was used to uncage $InsP_3$. Since the response to 100 ms pulses of UV were minimal in control eggs (**Figure 1A**) these data show that Sr^{2+} media sensitizes eggs to $InsP_3$ induced Ca^{2+} release and that, in contrast, IP3R are not sensitized to $InsP_3$ by PLCζ injection.

The two classes of model for Ca^{2+} oscillations, those that involve the dynamic properties of IP3Rs and those that involve $InsP_3$ production oscillations, can be distinguished in a definitive manner by examining the response to a sudden pulse of $InsP_3$ (Sneyd et al., 2006). Models that are dependent upon IP3R kinetics alone respond to a pulse of $InsP_3$ by showing a transient increase in the frequency of Ca^{2+} oscillations (Sneyd et al., 2006). In contrast, models that depend on Ca^{2+} induced $InsP_3$ production, and imply $InsP_3$ oscillations, respond to a sudden increase in $InsP_3$ by showing an interruption of the oscillations which leads to a resetting of the phase of oscillations

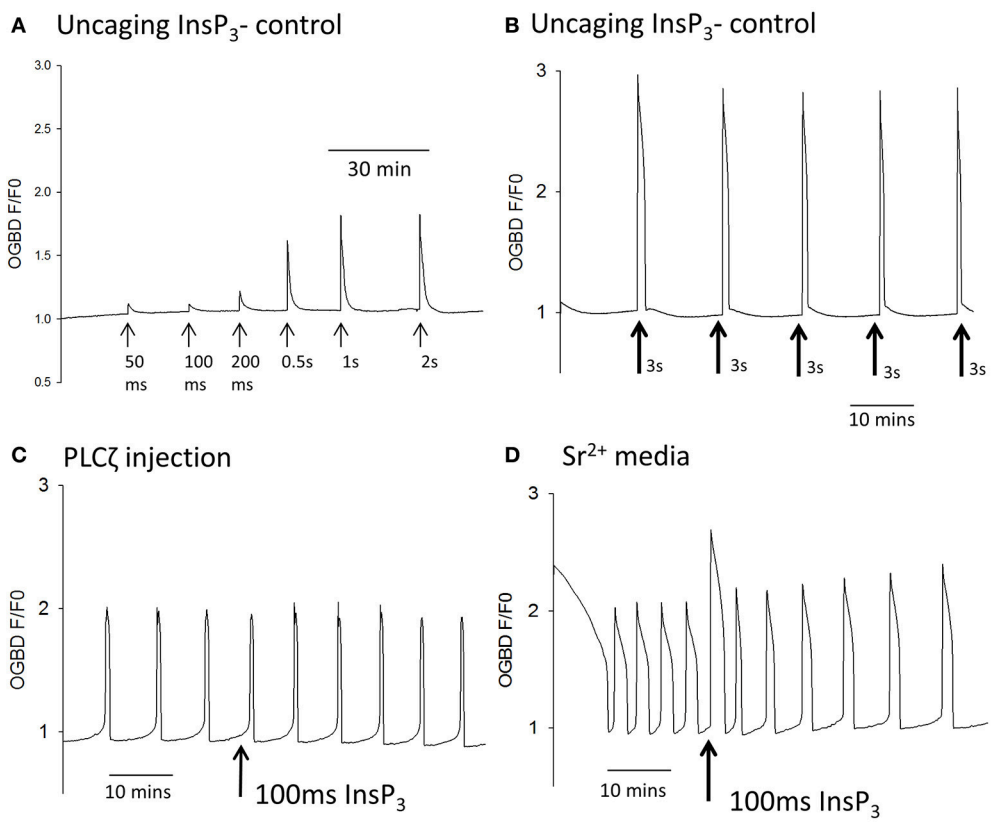

FIGURE 1 | Ca^{2+} oscillations and uncaging pulses of $InsP_3$. In **(A)** an example trace is shown of Ca^{2+} increases (as measured by OGBD fluorescence) in an egg in response to different amounts of $InsP_3$. Eggs were injected with caged $InsP_3$ and exposed to varying durations of UV light pulse (from 50 ms to 2 s) to photo-release the $InsP_3$ (trace typical of $n = 21$ eggs). In this and all other traces shown, the pulses were applied at points indicated by the arrows. In **(B)** an example trace is shown of changes in cytosolic Ca^{2+} in an egg in response to the "uncaging" of caged InsP3 using long duration UV pulses of 3 s. Arrows indicate where pulses of UV light were applied (typical of $n = 7$ eggs). In **(C)** an example trace is shown of changes in cytosolic Ca^{2+} in an egg stimulated following the microinjection of mouse derived PLCζ cRNA (0.02 μg/μl) and caged $InsP_3$. The arrow indicates where a 100 ms pulse of UV light was applied ($n = 14$ eggs). In all 14/14 such recordings there was no sudden increase in Ca^{2+} even when the pulse was applied during the pacemaker rising phase of Ca^{2+}. In **(D)** an example trace is shown with changes in cytosolic Ca^{2+} in an egg stimulated by media containing 10 mM Sr^{2+}. The arrow indicates where a 100 ms pulse of UV light was applied to uncage $InsP_3$ ($n = 32$ eggs). In all 32/32 cases there was a rapid Ca^{2+} increase that started with the very next OGBD fluorescence measurement after the UV pulse (<10 s).

(Sneyd et al., 2006). We tested the effect of using large uncaging pulses of $InsP_3$ on Sr^{2+} induced, or PLCζ induced, Ca^{2+} oscillations in mouse eggs. **Figure 2A** shows that during Sr^{2+} induced oscillations a 3 s uncaging pulse of $InsP_3$ caused a large increase in Ca^{2+} followed by a significant increase in the frequency of Ca^{2+} oscillations. In contrast, with PLCζ induced Ca^{2+} oscillations, **Figure 2B** shows that the same 3 s uncaging pulse of $InsP_3$ did not cause any increase in frequency, but interrupted the periodicity of oscillations leading to a delay before the next Ca^{2+} increase. To confirm that this phenomenon was phase resetting, we plotted the shift in phase (PS) caused by uncaging of $InsP_3$ against the time delay (dt) of the $InsP_3$ pulse from the subsequent Ca^{2+} spike (see **Figure 2C**). Each of these values was divided by the time period T in order to take into account the different frequency of Ca^{2+} oscillations in each egg. With phase resetting this plot should give a line from 1 to 1 on each axis, and **Figure 2D** shows that the data from 23 PLCζ injected eggs exposed to uncaging pulses of $InsP_3$ fit closely on such a line. These data clearly show that a pulse of $InsP_3$ causes phase resetting of Ca^{2+} oscillations in mouse eggs, which is completely different from that seen with Sr^{2+} induced oscillations. Hence, overall the data suggest that PLCζ and Sr^{2+} media trigger Ca^{2+} oscillations in mouse eggs via fundamentally different mechanisms. Sr^{2+} stimulates IP3Rs to make them effectively more sensitive to $InsP_3$, and that PLCζ induced Ca^{2+} oscillations involve Ca^{2+} stimulated $InsP_3$ production where $InsP_3$ acts as a dynamic variable that should oscillate in synchrony with Ca^{2+} oscillations.

Cytosolic Ca^{2+} vs. Ca^{2+} Stores and the Frequency of Ca^{2+} Oscillations

Since Ca^{2+} release and $InsP_3$ formation are predicted to form part of a positive feedback loop we decided to re-investigate some observation previously made on Ca^{2+} oscillations in eggs. One finding made in hamster and mouse eggs is that both sperm (and PLCζ)-triggered Ca^{2+} oscillations "run down" and can cease entirely in Ca^{2+} free media (Igusa and Miyazaki, 1983; Lawrence and Cuthbertson, 1995). This phenomena has been explained in terms of Ca^{2+} store depletion but the level of cytosolic Ca^{2+} and its effect on $InsP_3$ production could also be important. We re-examined the role of Ca^{2+} stores and resting Ca^{2+} using the SERCA inhibitor thapsigarin. Previous studies used high concentrations (>10 μM) of thapsigargin to completely block Ca^{2+} oscillations in eggs (Kline and Kline,

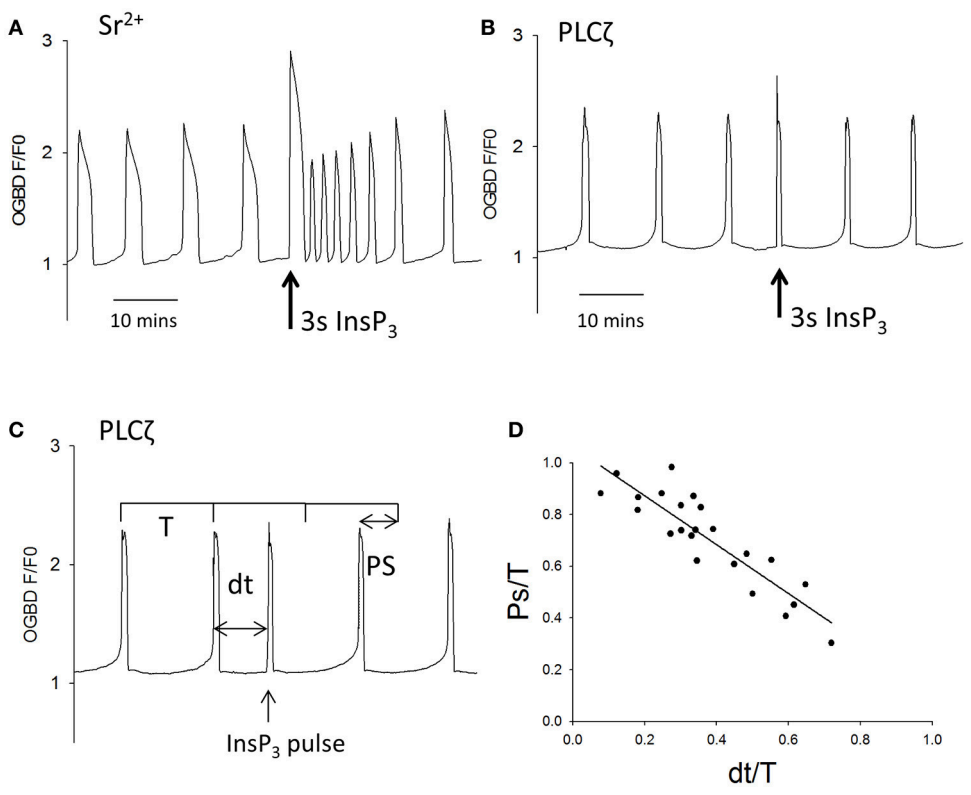

FIGURE 2 | The effect of large pulses of $InsP_3$ on PLCζ or Sr^{2+} triggered Ca^{2+} oscillations. **(A)** shows an example of the way eggs responded a large uncaging pulse of $InsP_3$ (3 s UV light at the arrow) by an increase in the frequency of Sr^{2+} triggered Ca^{2+} oscillations ($n = 20$ eggs). There was a significant increase in frequency of Ca^{2+} spikes from 3.45 (±0.27 sem) in 20 min to 5.05 (±0.35 sem) in 20 min ($p < 0.001$). In **(B)** a similar experiment is shown but with PLCζ induced Ca^{2+} oscillations. The sample trace in **(B)** shows that a 3 s uncaging pulse of $InsP_3$ (at the arrow) caused an immediate Ca^{2+} increase but no increase in frequency ($n = 23$ eggs). We analyzed the ability of such pulses to reset the phase of oscillations by measuring then phase shift (PS) and comparing it to time delay (dt) at which the $InsP_3$ pulse was applied. **(C)** Illustrates how these values were measured on an actual sample trace. Each value was divided by the time-period (T) for the oscillations in order to normalize the values between different eggs. **(D)** Shows a plot of these values for all 23 eggs tested.

1992b). To investigate the role of Ca^{2+} store content we used much lower concentrations of thapsigargin which caused only a small elevation of cytosolic Ca^{2+}. **Figures 3A,B** show that the addition of 500 nM thapsigargin to mouse eggs caused a small and prolonged increase in resting cytosolic Ca^{2+} in normal media and Ca^{2+} free media, which is consistent with a slight inhibition

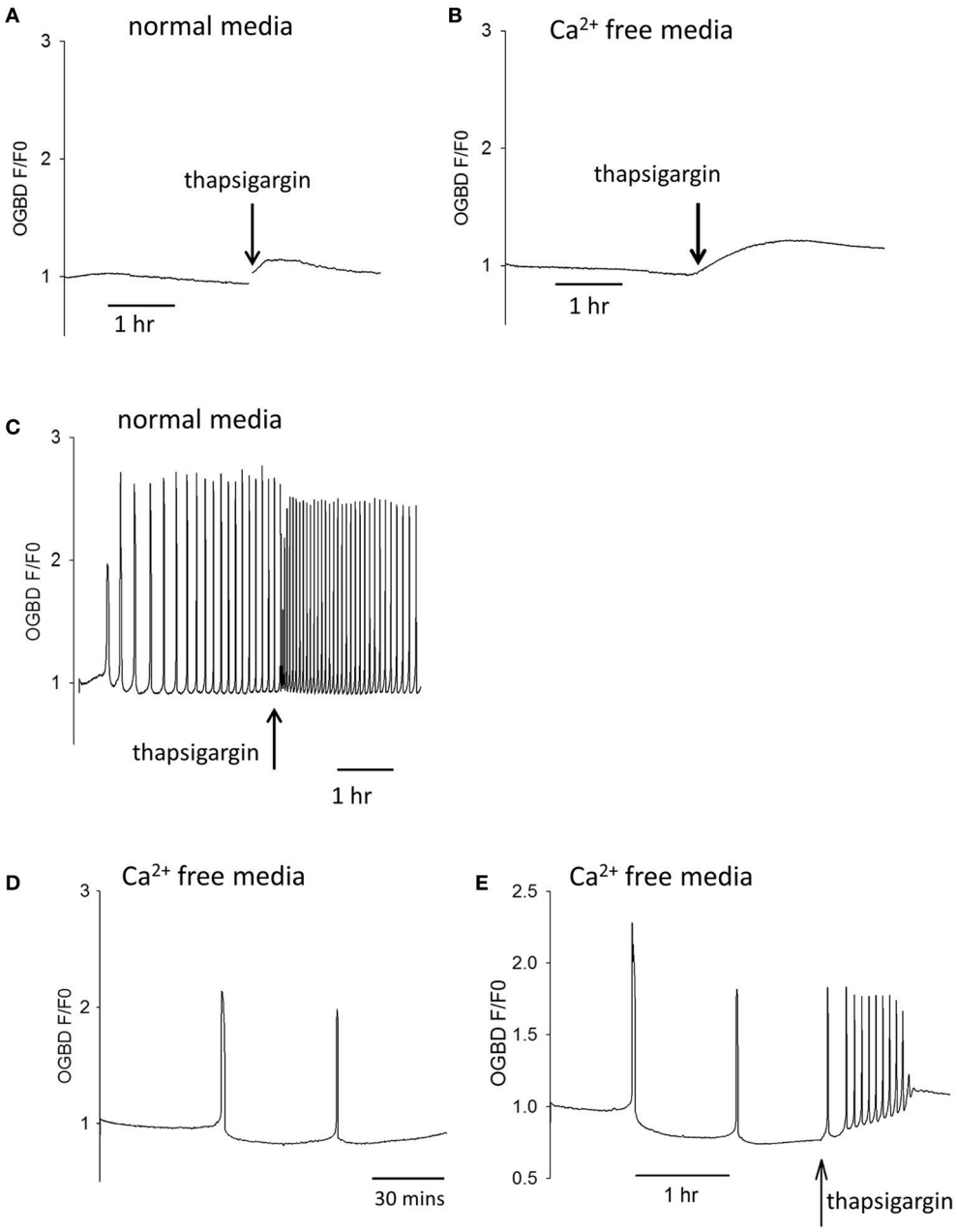

FIGURE 3 | Cytosolic Ca^{2+} and the frequency of Ca^{2+} oscillations. In **(A)** an example is shown of a trace showing changes in cytosolic Ca^{2+} in an egg incubated in normal HKSOM media following the addition of 500 nM thapsigargin (typical of $n = 12$ eggs). The increase in Ca^{2+} was from 0.936 ± 0.013 SEM to 1.07 ± 0.0197 SEM which is a significant ($P < 0.01$). In **(B)** a similar example is shown of the addition 500 nM thapsigargin to an egg in Ca^{2+} free media (containing 100 μM EGTA), which was typical of $n = 12$ eggs. The increase in basal Ca^{2+} was from 0.908 ± 0.0134 SEM up to 1.29 ± 0.0168 SEM which was significant ($P < 0.001$). In **(C)** an example of one of 6 eggs is shown where the same low concentration of thapsigargin increased the frequency of Ca^{2+} oscillations by 1.72-fold (±0.07 SEM). In **(D)** a trace is shown from an egg that was injected with PLCζ RNA and then placed in Ca^{2+} free media. The mean number of Ca^{2+} spikes in such experiments was 1.56 ($n = 18$ eggs, ±0.31 SEM) Ca^{2+} spikes in 10,000 s (2 h 47 min) h. The Ca^{2+} levels decreased to 0.84 ± 0.029 SEM which was significantly less than the starting level ($P < 0.001$). In **(E)** is shown an example of an egg that had been injected with PLCζ RNA and then placed in Ca^{2+} free media as in **(C).** However, in these experiments 500 nM thapsigarin was added after >2 h. In 16/17 such treated eggs there was an increase in the frequency of Ca^{2+} oscillations. There were an average of 1.77 spikes (±0.18 SEM) before adding thapsigarin but a mean of 7.11 spikes (±1.3 SEM) after thapsigarin addition. The resting Ca^{2+} level increased from 0.84 ± 0.029 SEM, before adding thapsigargin to 1.076 ± 0.017 sem in eggs where it stabilized. This is a signicant increase in Ca^{2+} concentration ($P < 0.001$).

of SERCA pumps. When the same concentration of thapsigargin was added to eggs undergoing Ca^{2+} oscillations in response to PLCζ there was a marked acceleration of Ca^{2+} oscillations, and a reduction in the amplitude of Ca^{2+} spikes (**Figure 3C**). Similar to previous reports, we found that the pattern of PLCζ induced Ca^{2+} oscillations show a run down in Ca^{2+} free media (containing EGTA). We noted that this was associated with a decline in the fluorescence of OGBD, suggesting that resting Ca^{2+} levels were also undergoing a decline (**Figure 3D**). When low concentrations of thapsigargin (500 nM) were added to PLCζ injected eggs in Ca^{2+} free media there was a restoration of Ca^{2+} oscillations (**Figure 3E**). It is noteworthy that in **Figure 3E** the eggs were in Ca^{2+} free media and yet the addition of thapsigargin, which would cause further Ca^{2+} store depletion, actually leads to a restoration of Ca^{2+} oscillations. Nevertheless, the restoration of Ca^{2+} oscillations was associated with a rise in the "basal" Ca^{2+} level (**Figure 3E**). These data are consistent with the idea that cytosolic Ca^{2+} plays a key role in triggering each Ca^{2+} rise, and that Ca^{2+} stores are not significantly depleted in mouse eggs by incubation in Ca^{2+} free media.

PLCζ Induced Ca^{2+} Oscillations and Intracellular PIP_2

Previous studies of fertilizing mouse and hamster eggs show that most Ca^{2+} waves cross the egg in about 1 s, and propagate through the cytoplasm at speeds in excess of 50 μm/s. This matches the rising phase of (all but the initial) Ca^{2+} transients in mouse eggs which is ~1 s after fertilization or after PLCζ protein injection (Deguchi et al., 2000). Since data in **Figure 2** implies that the upstroke of each Ca^{2+} rise involves an $InsP_3$ and Ca^{2+} positive feedback loop, then it is necessary for both molecules to be sufficiently diffusible. The Ca^{2+} stores (the endoplasmic reticulum) are spread across the egg. However, this may not be the case with PIP_2 that is the precursor to $InsP_3$. In most cells PIP_2 is in the plasma membrane, and if this is used in Ca^{2+} waves in eggs then $InsP_3$ diffusion range might constrain the ability to generate fast Ca^{2+} waves. Recently, the diffusion coefficient of $InsP_3$ in intact cells has been shown to be $<10\ \mu m^2/s$ which means that $InsP_3$ may only diffuse $<5\ \mu m$ in 1 s (Dickinson et al., 2016). We have previously presented models of Ca^{2+} oscillations based upon Ca^{2+} induced $InsP_3$ formation and $InsP_3$ induced opening of Ca^{2+} release channels (Theodoridou et al., 2013). We have now simulated the Ca^{2+} waves in mouse eggs using a similar set of equations in a two-dimensional model of the Ca^{2+} wave. **Figure 4** shows that with the source of Ca^{2+} stimulated $InsP_3$ production at the periphery (plasma membrane) it is not possible to generate a Ca^{2+} wave through the egg cytoplasm, and only a concentric pattern of Ca^{2+} release occurs. We previously presented evidence for PIP_2 being present in intracellular vesicles spread throughout the cytoplasm in mouse eggs (Yu et al., 2012). These could provide a source of $InsP_3$ that might carry a Ca^{2+} wave through the cytoplasm if they are sufficiently dispersed. In **Figure 4** we show simulations based upon Ca^{2+} induced $InsP_3$ generation where the PIP_2 is dispersed on vesicles at different distances apart (from 2 to 4 μm). Our simulations show that when the PIP_2 vesicles are within 2 or 3 μm of each other a

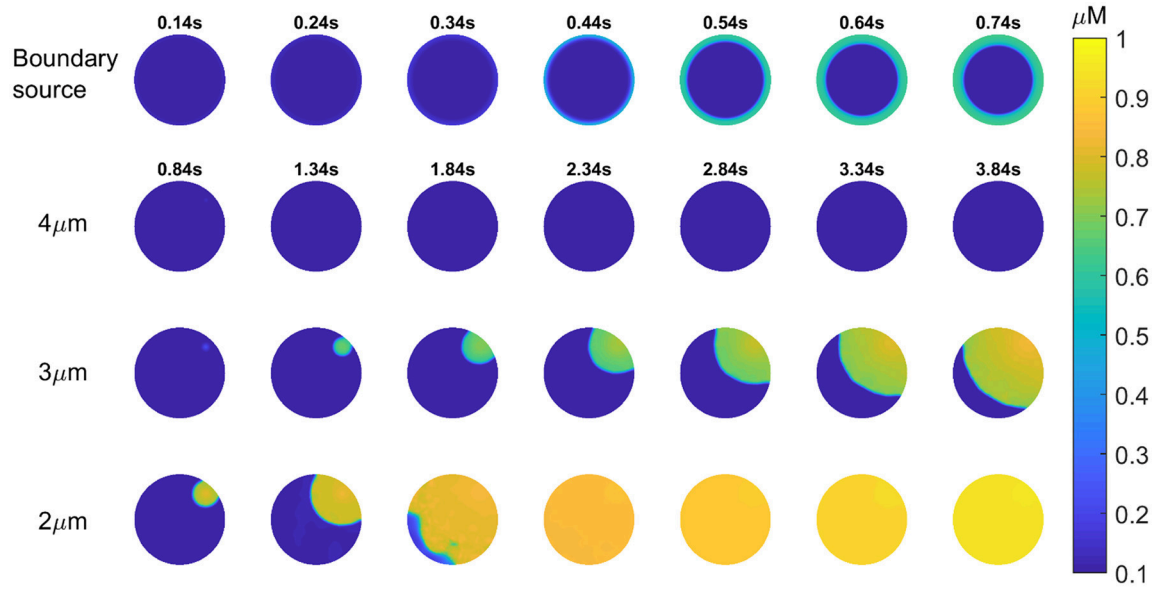

FIGURE 4 | Simulation of $InsP_3$ induced Ca^{2+} release in eggs**.** Images are shown for a 2-dimensional simulation of the propagation of a Ca^{2+} wave in a mouse egg using a mechanism based upon Ca^{2+} induced $InsP_3$ formation. Images for each time series is shown in each of the rows. For the first row the only source of PIP_2 for making $InsP_3$ is at the boundary (the plasma membrane) and this does not cause a wave at all. The times for each image (in seconds) in the top row is indicated by numbers above each image. In the next three rows the source of Ca^{2+} induced $InsP_3$ formation is spaced at different distances. The time intervals for each image is indicated in the second row and it is then the same for each image going down in each column. In the first row the distance for the PIP_2 is 4 μm, and again no Ca^{2+} wave can be generated. With a PIP_2 source spaced at 3 or 2 μm we found that a Ca^{2+} wave can be generated. With a 2 μm separation a wave occurs that crosses the "egg" in ~1 s.

rapid Ca^{2+} can be generated, but that once the PIP_2 is more than 3 μm the Ca^{2+} increase fails to occur. These results suggests that PIP_2 needs to be present on vesicles spaced <3 μm apart in the cytoplasm in order to propagate a rapid Ca^{2+} wave of the type seen in fertilizing and PLCζ injected eggs.

Previous evidence for the existence of PIP_2 within the cytoplasm of eggs came from studies using antibodies to PIP_2 (Yu et al., 2012). Gelsolin is a protein that has been shown to bind to PIP_2, and contains a short peptide sequence responsible for PIP_2 binding (Cunningham et al., 2001). We injected mouse eggs with PBP-10, which is a probe in which rhodamine is coupled to a gelsolin peptide that binds PIP_2. **Figure 5A** shows a mouse egg injected with PBP-10. After >1 h the fluorescence of PBP-10 could be predominantly seen in many small vesicles throughout the egg cytoplasm, with the occasional larger aggregate. This supports the hypothesis that PIP_2 is localized in vesicles within mouse eggs (Yu et al., 2012). Further examination of these vesicles using particle analysis indicates that they are distributed throughout the whole egg cytoplasm. Interestingly, following nearest neighbor analysis, we found that these vesicles were ~2 μm apart (**Figures 5A,D**). This suggests that these PIP_2 containing vesicles are within the correct distance predicted to produce the rapid rising phase of 1 s for each wave as predicted by our mathematical modeling.

We have previously sought to modify the level of PIP_2 in mouse eggs using various phosphatases, but without success.

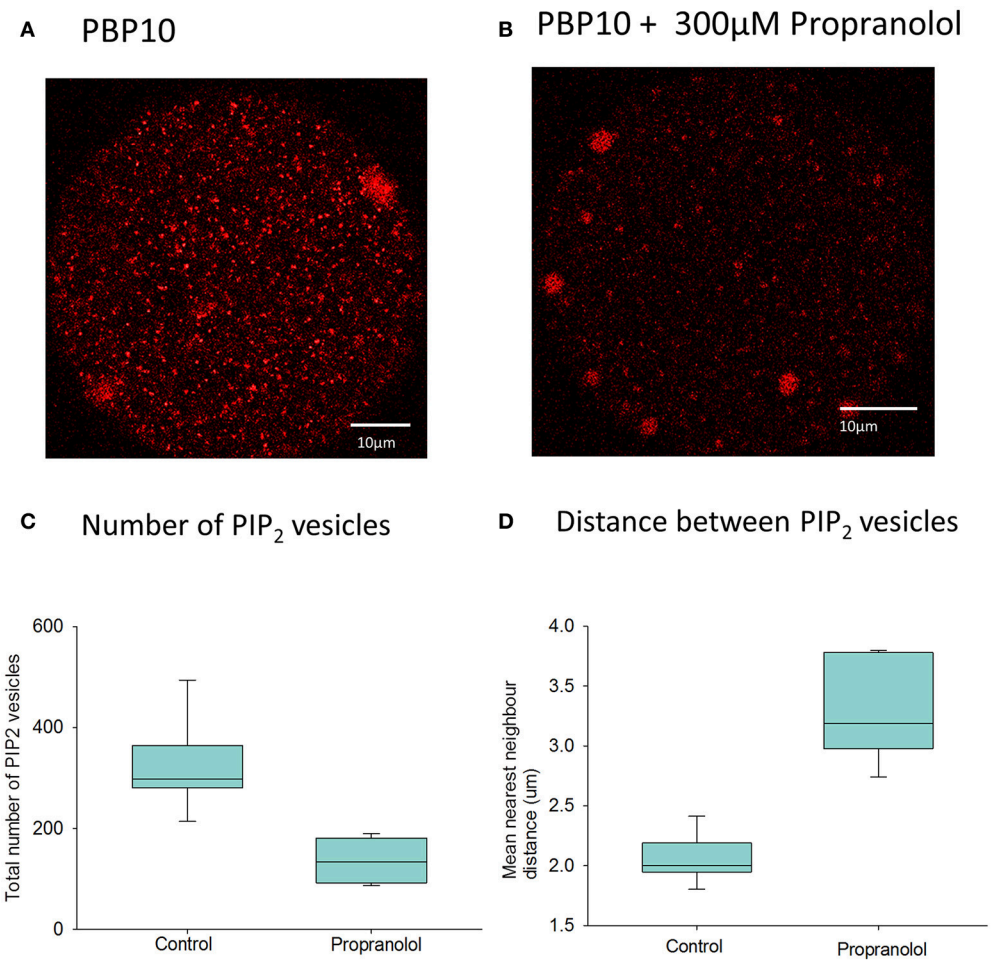

FIGURE 5 | PIP_2 distribution in mouse eggs using PBP10. In **(A)** an example is shown of the distribution of fluorescence of PBP10 in a mouse egg 1.5 h after injection of PBP10 ($n = 21$). Scale bars are 10 μm. **(A)** nearest neighbor analysis indicated that the mean vesicle distance for all 21 control eggs is 2.2 μm. In **(B)** an example is shown of an egg injected with PBP10 where and incubated in media with 300 μM propranolol ($n = 13$). In **(C)** particle analysis ($n = 14$ eggs) indicates that the mean vesicle diameter is 0.89 μm and the mean number of vesicles present per egg is 298.9. **(C)** Shows a plot of the total number of PIP_2 positive vesicles present in eggs following injection of PBP10 using particle analysis. Results are shown for both eggs incubated in standard M2 media (control) (mean number of vesicles = 324, $n = 7$) and those incubated in M2 containing 300 μM propranolol during imaging (mean number of vesicles= 131, $n = 7$). There is a significant reduction in the number of PBP10 vesicles following propranolol treatment compared to control media ($p = < 0.001$, Student's *T-test*). **(D)** shows a plot of the mean nearest neighbor distances of PIP_2 positive vesicles present in eggs. The results are shown for parallel groups of eggs incubated in standard M2 media (control) (mean distance = 2.0 μm, $n = 7$) and for those incubated in M2 containing 300 μM propranolol during imaging, (mean distance = 3.3 μm, $n = 7$). A Mann–Whitney *U-test* showed a significant increase in the distance between the PBP10 vesicles following propranolol treatment compared to control media ($p = < 0.001$).

Internal membranes in somatic cells do not in general contain much PIP_2, but one organelle where PIP_2 and DAG have been reported in some cells is the Golgi apparatus. In mature mammalian eggs, like mitotic cells, the Golgi is fragmented into small vesicles (Moreno et al., 2002; Axelsson and Warren, 2004). It has been shown that propranolol blocks DAG synthesis in Golgi membranes and leads to a loss of Golgi structure (Asp et al., 2009). We applied propranolol to mouse eggs injected with PBP10 and found a marked loss of staining (**Figure 5B**). Further particle analysis showed that the mean number of these PIP_2 vesicles was significantly reduced following the addition of propranolol (**Figure 5C**). Furthermore, the distance of these vesicles from each other was significantly increased in those eggs treated with propranolol (**Figure 5D**). The overall total fluorescence of the vesicles was seen to reduce by approximately half from a mean of 5.77×10^4 RFU ($n = 7$) in control eggs to a mean of 2.93×10^4 RFU ($n = 7$) in those eggs treated with propranolol. This difference was significant following a Student's *T-test* ($p = 0.006$). This implies that propranolol is affecting PIP_2 levels in cytoplasmic vesicles.

Since proproanolol appears to reduce PIP_2 inside eggs, we investigated the effect of propranolol on Ca^{2+} oscillations. **Figure 6A** shows that propranolol addition to eggs undergoing Ca^{2+} oscillations in response to fertilization by IVF were rapidly blocked. **Figure 6B** shows the same effect of propranolol on those eggs stimulated by PLCζ cRNA. The inhibition by propranolol was associated with a slight decline in Ca^{2+} levels and the inhibition was reversed upon removal of propranolol (**Figure 6C**). However, whilst it blocked sperm and PLCζ induced responses, propranolol did not block Ca^{2+} oscillations induced in eggs by Sr^{2+} media, or by injection of the IP3R agonist adenophostin (**Figures 6D,E**). These data show that the inhibitory effects of propranolol are both reversible and specific to PLCζ and sperm induced Ca^{2+} oscillations. They support the proposal that PIP_2 in vesicles in the cytoplasm of mouse eggs is important for the generation of PLCζ induced Ca^{2+} oscillations.

DISCUSSION

The Ca^{2+} oscillations seen in mammalian eggs at fertilization have distinct characteristics compared with those seen in somatic cell types (Dupont and Goldbeter, 1994; Politi et al., 2006). The oscillations at fertilization are low frequency, and long lasting, but they have a very rapid rising phase that occurs throughout the whole cytoplasm of a very large cell, in less than a second. Considerable evidence suggests that PLCζ is the primary stimulus for these Ca^{2+} oscillations (Saunders et al., 2002). The current data shows that PLCζ induced Ca^{2+} oscillations are driven by Ca^{2+} induced $InsP_3$ formation. In contrast, we show that Sr^{2+} media sensitizes eggs to $InsP_3$ induced Ca^{2+} release. Hence, there are at least two different mechanisms for generating Ca^{2+} oscillations in mouse eggs. Our data also implies that the substrate of PLCζ, PIP_2, needs to be localized in a finely distributed source within the egg in order to generate fast Ca^{2+} wave, and we present evidence that such vesicular PIP_2 is required for PLCζ induced Ca^{2+} oscillations.

There are two fundamentally different classes of models for $InsP_3$ induced Ca^{2+} oscillations in cells. One relies on the properties of $InsP_3$ receptor and implies that stimulation involves an elevated but monotonic or constant elevation of $InsP_3$ levels. The other involves a positive feedback model of $InsP_3$ induced Ca^{2+} release and Ca^{2+} induced $InsP_3$ formation. It is possible to determine which one of these two model types applies by studying the Ca^{2+} responses after triggering a large pulsed release of $InsP_3$ (Sneyd et al., 2006). The IP3R based models respond to a pulse of $InsP_3$ by temporarily increasing the frequency of Ca^{2+} oscillations, whereas the Ca^{2+}-induced $InsP_3$ formation models show an interruption in the series of Ca^{2+} transients with a resetting of the phase of the oscillations (Sneyd et al., 2006). We previously presented preliminary evidence for an interruption in the series transients with sperm or PLCζ induced Ca^{2+} oscillations responding to a pulse of $InsP_3$ (Swann and Yu, 2008). We now show that the response of PLCζ induced Ca^{2+} oscillations to a sudden large pulse of $InsP_3$ is clearly characterized by a resetting of the phase of oscillations. This means that $InsP_3$ has to be a dynamic variable in the oscillation cycle and that it will undergo oscillations in close phase with the oscillations in Ca^{2+}. Small oscillations in $InsP_3$ have been recorded previously in response to high frequency Ca^{2+} oscillations achieved with high concentrations of PLCζ (Shirakawa et al., 2006). The sensitivity of such indicators may be limited since we can now assert that $InsP_3$ oscillations should occur with all the PLCζ induced Ca^{2+} oscillations and, most significantly, that increased $InsP_3$ production plays a causal role in generating each Ca^{2+} rise. We have also shown here that Sr^{2+} works via an entirely different mechanism in mouse eggs. The increase in frequency of Ca^{2+} oscillations caused by uncaging $InsP_3$ indicates that Sr^{2+} induced oscillations rely on the properties of the IP3R. This is supported by the finding that Sr^{2+} media sensitized mouse eggs to $InsP_3$ pulses, which is consistent with the idea that Sr^{2+} stimulates the opening of $InsP_3$ receptor. These data overall show that mouse eggs have more than one mechanism for generating Ca^{2+} oscillations and that in some cases Ca^{2+} oscillations can appear to be similar in form, but be generated by different mechanisms.

It is well-established that Ca^{2+} free media leads to a reduction or abolishment of Ca^{2+} oscillations in response to fertilization or PLCζ injection in mammalian eggs (Igusa and Miyazaki, 1983; Lawrence and Cuthbertson, 1995). It has been assumed that this reflects the loss or some reduction of Ca^{2+} in the endoplasmic reticulum (Kline and Kline, 1992b). However, our data suggest that a reduction in resting, or interspike, cytosolic Ca^{2+} levels also occurs during incubation in Ca^{2+} free media. The reduction in cytosolic Ca^{2+} is apparent with the Ca^{2+} dye we used because it is dextran linked and hence is only within the cytosolic compartment, and because the K_d for OGBD and Ca^{2+} is around 250 nm. The reduction in resting Ca^{2+} level appears to cause the inhibition of Ca^{2+} oscillations, rather than a loss of Ca^{2+} store content, because low concentrations of thapsigargin, which will only reduce Ca^{2+} stores content further, actually restores Ca^{2+} oscillations in Ca^{2+} free media.

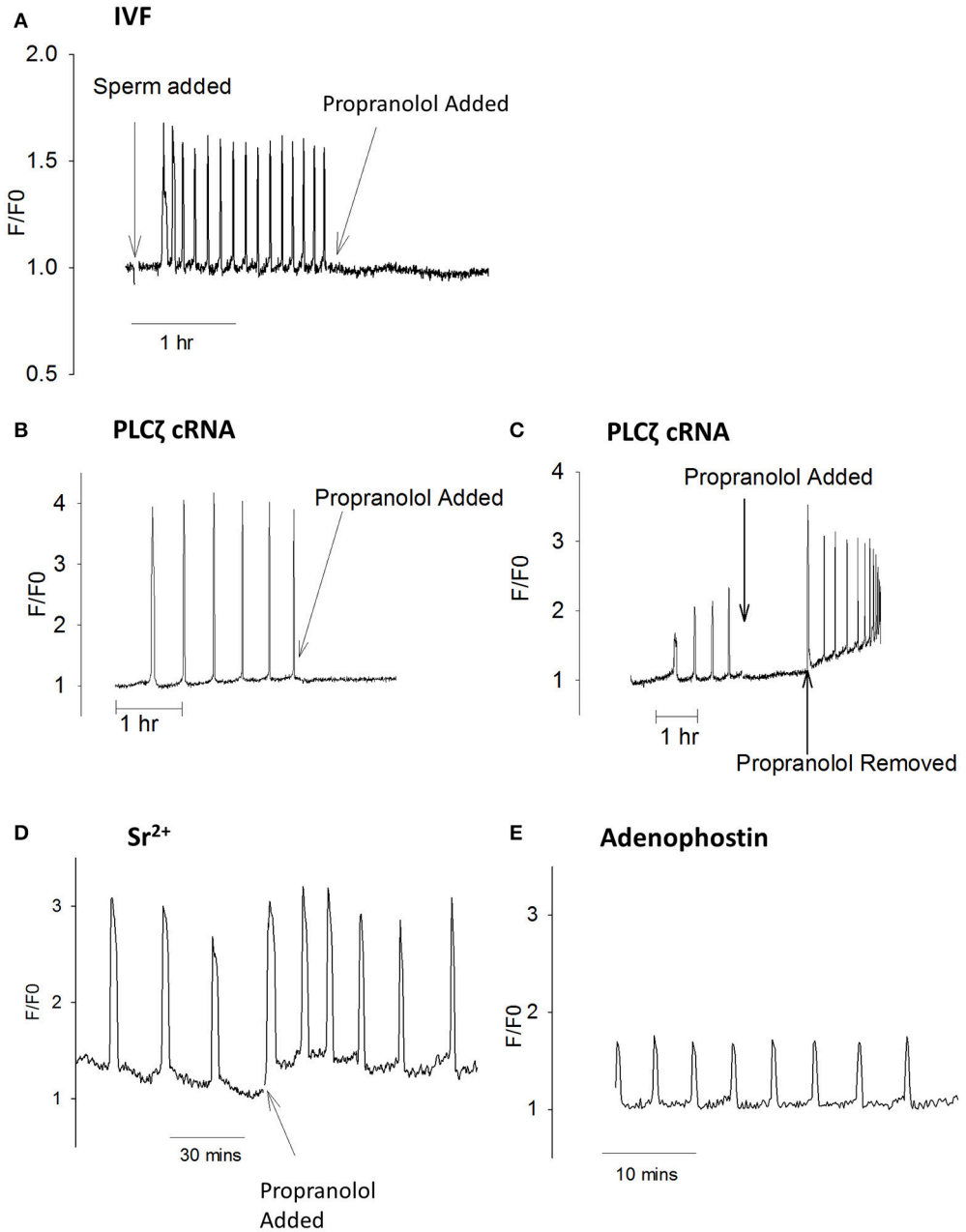

FIGURE 6 | Ca^{2+} oscillations blocked by propranolol. In **(A)** an example is shown of a mouse egg undergoing Ca^{2+} oscillations at fertilization where the addition of 300 μM propranolol inhibited subsequent oscillations ($n = 13$ eggs). Before addition of propranolol the mean frequency was 12.2 ± 1.14 spikes/h with all eggs oscillating. After adding propranolol there were 0.8 ± 0.23 spikes /h (a significant difference from before propranolol, $p = < 0.0001$). 6/13 eggs stopped oscillating immediately, 4/13 eggs had one Ca^{2+} spike, and 3/13 has 2 spikes in an hour. **(B)** shows PLCζ cRNA (pipette concentration = 0.02 μg/μl) induced Ca^{2+} oscillations inhibited by propranolol ($n = 21$ eggs). Before propranolol all eggs oscillated with 4.3 ± 0.46 spikes/h. After addition of propranolol there were 0.95 ± 0.25 spikes/h (a significant difference $p < 0.0001$). With propranolol, 10/21 eggs stopped Ca^{2+} oscillations, 6/21 showed a single spike, and 5/21 had >1 Ca^{2+} spike. In **(C)** an example is shown of an egg where PLCζ induced Ca^{2+} oscillations were blocked by the addition of propranolol but then oscillations were restored when propranolol was washed out (typical of $n = 8$ eggs). Before propranolol, all eggs oscillated with 6.7 ± 1.3 spikes/h. After propranolol this decreased to 1.33 ± 0.29 spikes/h, with all oscillations stopping after 2 spikes. When propranolol was removed there were 10 ± 0.55 spikes in 30 min. Adding propranol and then removing it both caused significant changes in the number of Ca^{2+} spikes ($p < 0.001$). **(D)** shows an example of an egg undergoing Ca^{2+} oscillations in response to Sr^{2+} media where propranolol was subsequently added ($n = 10$ eggs). Before propranolol all eggs oscillated with 4.1 ± 0.29 spikes/h. After adding propranolol all eggs continues to oscillate with 3.9 ± 0.66 Ca^{2+} spikes/h (not significantly different). In **(E)** an example is shown of an egg undergoing Ca^{2+} oscillations in response to microinjection of 5 μM adenophostin in media that contained 300 μM propranolol form the start of the experiment ($n = 8$ eggs). In propranolol there were 5.5 ± 0.51 Ca^{2+} spikes 30 min, compared with 10.4 ± 0.71 spikes/30 min ($n = 11$) for eggs in media with HKSOM. This is significantly different (unpaired *t-test*, $p = < 0.0001$).

The restoration of such Ca^{2+} oscillations by thapsigargin in our experiments was clearly associated with a rise in the basal Ca^{2+} level. PLCζ induced Ca^{2+} oscillations eventually stopped in Ca^{2+} free media with thapsigargin and this could be because Ca^{2+} stores eventually became depleted. However, the earlier rise in cytosolic Ca^{2+} seems to be a stimulatory factor because low concentrations of thapsigarin, which raise basal Ca^{2+}, could also increase the frequency Ca^{2+} oscillations in normal media. This was associated a reduction in the amplitude of Ca^{2+} spikes, presumably because Ca^{2+} store content is reduced. Low concentrations of thapsigargin have also previously been found to stimulate Ca^{2+} oscillations in immature mouse oocytes (Igusa and Miyazaki, 1983; Lawrence and Cuthbertson, 1995). Hence, these data together imply that cytosolic Ca^{2+} level, rather than Ca^{2+} store content is the more significant factor setting the frequency and occurrence of physiological Ca^{2+} oscillations.

These data are consistent with recent studies measuring free Ca^{2+} inside the endoplasmic reticulum in mouse eggs (Wakai et al., 2013). It was shown that a reduction in ER Ca^{2+} occurs following each Ca^{2+} spike, but that there is no correlation between when a Ca^{2+} transient is initiated and the level of Ca^{2+} in the ER (Wakai et al., 2013). Whilst it is obvious that some Ca^{2+} store refilling will occur in the intervals between Ca^{2+} spikes, it is not likely that this sets of the pace of the low frequency Ca^{2+} oscillations characteristic of mammalian eggs. We suggest that the pacemaker that determines when the next Ca^{2+} transient occurs after PLCζ injection is more likely to be the rise in cytosolic Ca^{2+}. A gradual rise in cytosolic Ca^{2+} between spikes is evident in the PLCζ induced Ca^{2+} oscillations in all the traces in this paper. This gradual Ca^{2+} increase could promote a gradual rise in $InsP_3$ that will eventually lead to a positive feedback loop and a regenerative Ca^{2+} wave.

Although the Ca^{2+} oscillations triggered by fertilization in mammalian eggs are of low frequency, each of the waves of Ca^{2+} release that causes the upstroke of a Ca^{2+} increase crosses the egg remarkably quickly. Previous analysis of the wave dynamics of Ca^{2+} release in mammalian eggs have suggested that the rising phase of each Ca^{2+} oscillation is ∼1 s. This correlates with the speed of the Ca^{2+} wave that crosses the egg at a speed of >50 μm/s. This is significant because the diffusion coefficient of $InsP_3$ in intact cells has been estimated to be no more that 10 $\mu m^2/s$ (Dickinson et al., 2016). In models where $InsP_3$ is elevated at a constant level during Ca^{2+} oscillations the restricted diffusion of $InsP_3$ is not an issue because it will reach a steady state concentration across the egg. However, our data shows that Ca^{2+} and $InsP_3$ act together in a positive feedback loop to cause each propagating Ca^{2+} wave. In this case the diffusion of $InsP_3$ could be a rate limiting step. If all the $InsP_3$ is generated in the plasma membrane then our simulations show that a Ca^{2+} induced $InsP_3$ production model cannot generate Ca^{2+} waves through the egg cytoplasm. If we simulate the $InsP_3$ production from discrete sites within the egg cytoplasm then rapid Ca^{2+} waves of some type can be generated, but full waves can only be seen when the sites of $InsP_3$ generation are within 3 μm of each other. This suggests that in order to explain both the fast Ca^{2+} waves and the basic mechanism of sperm or PLCζ induced oscillations in mammalian eggs, the PIP_2 substrate has to be dispersed in sites throughout the egg cytoplasm. This conclusion is similar to that previously suggested for ascidian oocyte at fertilization which also show rapid Ca^{2+} waves and oscillations (Dupont and Dumollard, 2004).

We previously reported evidence for a vesicular source of PIP_2 in mouse eggs using immunostaining (Yu et al., 2012). The vesicular staining with PIP_2 antibodies closely mimics the distribution of PLCζ also probed with antibodies (Yu et al., 2012). We now report a similar pattern of vesicular staining using another probe (PBP10) which based upon the PIP_2 binding region of gelsolin (Cunningham et al., 2001). This probe has the advantage that it is microinjected into eggs that can then be imaged whilst still alive and so does not require the fixation and permeabilization procedures associated with immunostaining. It gives a very different pattern of staining from another commonly used probe for PIP_2 which is the GFP-PH domain which localizes predominantly to the plasma membrane in mouse eggs (Halet et al., 2002). However, the PH domain of PLCδ1 that is used for the localization of PIP_2 in such a probe may also bind cholesterol so may be influenced by factors other than PIP_2 (Rissanen et al., 2017). It is entirely possible that PBP10 is also influenced by factors other than PIP_2, but it is noteworthy that the PBP10 staining gives a vesicular localization pattern that closely resembles that seen with the PIP_2 antibodies. The fact that two very different methods for localization PIP_2 in eggs, immunostaining with a monoclonal antibody and a fluorescently tagged peptide, show such a distinctive and similar pattern of localization provides good evidence that PIP_2 is indeed localized within vesicles in the cytoplasm in of mouse eggs. Using the live cell probe, PBP10, we were able to estimate that the apparently PIP_2 containing vesicles we see in eggs are within about 2 μm of each other. This distance closely correlates with the estimate of how close PIP2 vesicles need to be in order to propagate a Ca^{2+} wave across the egg within ∼1 s. Hence, our data provide a coherent view of PLCζ induced Ca^{2+} release in eggs in which Ca^{2+} induced $InsP_3$ formation from closely spaced vesicles containing PIP_2 accounts for the upstroke of each Ca^{2+} rise.

The precise nature of the PIP_2 containing vesicles that appear to exist in mouse eggs is unclear. We have tested a number of antibodies and other probes for specific organelles in eggs and found that many either localize to the endoplasmic reticulum or else show only a limited overlap in staining with the PIP_2 or PLCζ positive vesicles. The identification of PBP10 positive vesicles is further complicated by our finding that its pattern of localization does not persist after fixation and membrane permeabilization (Sanders and Swann, unpublished). In somatic cells, non-plasma membrane PIP_2 has been found in the Golgi apparatus (De Matteis et al., 2005). Mature mouse egg are unusual compared with somatic cells in that they are arrested in meiosis, which is similar to the mitotic phase of the cell cycle. During mitosis the Golgi fragments to form small vesicles known as the Golgi haze (Axelsson and Warren, 2004), and the Golgi in mouse eggs has been shown to be fragmented into small vesicles (Moreno et al., 2002). The structure of the Golgi and its associated vesicles is maintained by the presence of diacyglycerol (DAG) (Asp et al., 2009). The drug propranolol disrupts Golgi resident proteins and lipids by inhibiting DAG production and as a result, it

also disrupts Golgi-ER trafficking (Asp et al., 2009). Interestingly propranolol was found to block Ca^{2+} oscillations triggered by PLCζ and fertilization. This effect was specific in that the same concentration of propranolol did not effect oscillations when added to other Ca^{2+} releasing agents such as Sr^{2+} media which causes a pattern of oscillations most similar to fertilization. The small effect on adenosphostin induced Ca^{2+} oscillations is unlikely to be sufficient to explain the effects of propranolol because it was only a 2-fold decrease in oscillations compared the cessation of oscillations after propranolol in most eggs that were fertilized or injected with PLCζ. It is also noteworthy that the Ca^{2+} levels remained low in propranolol treated eggs, and that its effects were reversible. In mouse eggs we found that propranolol also decreased the number of the PIP_2 containing vesicles and the mean distance between vesicles, therefore presumably, the availability of the vesicular PIP_2 to propagate a Ca^{2+} wave. This effect could be because propranolol disrupts the structure of the vesicles or because trafficking between the Golgi and the ER is inhibited. Whatever the actual mechanism, the loss of PIP_2 after treatment with propranolol supports our hypothesis that these vesicles are required for generating Ca^{2+} oscillations in eggs in response to sperm or PLCζ. Since there is evidence for intracellular PIP_2 on organelles in frog and sea urchin eggs, which also show Ca^{2+} waves at fertilization, it is attractive to speculate that intracellular PIP_2 is an important feature that allows eggs to generate the Ca^{2+} signal needed for egg activation.

AUTHOR CONTRIBUTIONS

JS: Performed some of the Ca^{2+} measurements and the PIP_2 imaging experiments, analyzed data, and co-wrote the manuscript; BA and AM: Performed Ca^{2+} measurement experiments on eggs and analyzed data; TW: Produced and analyzed the mathematical simulation; KS: Conceived the study, directed experiments and co-wrote the manuscript. All authors approved the final manuscript.

ACKNOWLEDGMENTS

The authors wish to thank the School of Medicine for funding JS for her postgraduate studies, and Michail Nomikos for providing us with the PLCζ RNA used in this study.

REFERENCES

Asp, L., Kartberg, F., Fernandez-Rodriguez, J., Smedh, M., Elsner, M., Laporte, F., et al. (2009). Early stages of Golgi vesicle and tubule formation require diacylglycerol. *Mol. Biol. Cell* 20, 780–790. doi: 10.1091/mbc.E08-03-0256

Axelsson, M. A., and Warren, G. (2004). Rapid, endoplasmic reticulum-independent diffusion of the mitotic Golgi haze. *Mol. Biol. Cell* 15, 1843–1852. doi: 10.1091/mbc.E03-07-0459

Bedford-Guaus, S. J., Yoon, S. Y., Fissore, R. A., Choi, Y. H., and Hinrichs, K. (2008). Microinjection of mouse phospholipase C zeta complementary RNA into mare oocytes induces long-lasting intracellular calcium oscillations and embryonic development. *Reprod. Fertil. Dev* 20, 875–883. doi: 10.1071/RD08115

Bos-Mikich, A., Swann, K., and Whittingham, D. G. (1995). Calcium oscillations and protein synthesis inhibition synergistically activate mouse oocytes. *Mol. Reprod. Dev.* 41, 84–90. doi: 10.1002/mrd.1080410113

Brind, S., Swann, K., and Carroll, J. (2000). Inositol 1,4,5-trisphosphate receptors are downregulated in mouse oocytes in response to sperm or adenophostin A but not to increases in intracellular Ca^{2+} or egg activation. *Dev. Biol.* 223, 251–265. doi: 10.1006/dbio.2000.9728

Cox, L. J., Larman, M. G., Saunders, C. M., Hashimoto, K., Swann, K., and Lai, F. A. (2002). Sperm phospholipase C zeta from humans and cynomolgus monkeys triggers Ca^{2+} oscillations, activation and development of mouse oocytes. *Reproduction* 124, 611–623. doi: 10.1530/rep.0.1240611

Cunningham, C. C., Vegners, R., Bucki, R., Funaki, M., Korde, N., Hartwig, J., et al. (2001). Cell permeant polyphosphoinositide-binding peptides that block cell motility and actin assembly. *J. Biol. Chem.* 276, 43390–43399. doi: 10.1074/jbc.M105289200

Deguchi, R., Shirakawa, H., Oda, S., Mohri, T., and Miyazaki, S. (2000). Spatiotemporal analysis of Ca^{2+} waves in relation to the sperm entry site and animal-vegetal axis during Ca^{2+} oscillations in fertilized mouse eggs. *Dev. Biol.* 218, 299–313. doi: 10.1006/dbio.1999.9573

De Matteis, M. A., Di Campli, A., and Godi, A. (2005). The role of the phosphoinositides at the Golgi complex. *Biochim. Biophys. Acta* 1744, 396–405. doi: 10.1016/j.bbamcr.2005.04.013

Dickinson, G. D., Ellefsen, K. L., Dawson, S. P., Pearson, J. E., and Parker, I. (2016). Hindered cytoplasmic diffusion of inositol trisphosphate restricts its cellular range of action. *Sci. Signal.* 9:ra108. doi: 10.1126/scisignal.aag1625

Dupont, G., and Dumollard, R. (2004). Simulation of calcium waves in ascidian eggs: insights into the origin of the pacemaker sites and the possible nature of the sperm factor. *J. Cell. Sci.* 117, 4313–4323. doi: 10.1242/jcs.01278

Dupont, G., and Goldbeter, A. (1994). Properties of intracellular Ca^{2+} waves generated by a model based on Ca^{2+}-induced Ca^{2+} release. *Biophys. J.* 67, 2191–2204. doi: 10.1016/S0006-3495(94)80705-2

Fowler, R. E., and Edwards, R. G. (1957). Induction of super ovulation and pregnancy in mature mice by gonadotrophins. *J. Endocrinol.* 15, 374–384.

Fujimoto, S., Yoshida, N., Fukui, T., Amanai, M., Isobe, T., Itagaki, C., et al. (2004). Mammalian phospholipase C zeta induces oocyte activation from the sperm perinuclear matrix. *Dev. Biol.* 274, 370–383. doi: 10.1016/j.ydbio.2004.07.025

Halet, G., Tunwell, R., Balla, T., Swann, K., and Carroll, J. (2002). The dynamics of plasma membrane PtdIns(4,5)P(2) at fertilization of mouse eggs. *J. Cell. Sci.* 115, 2139–2149.

Igusa, Y., and Miyazaki, S. (1983). Effects of altered extracellular and intracellular calcium concentration on hyperpolarizing responses of the hamster egg. *J. Physiol.* 340, 611–632. doi: 10.1113/jphysiol.1983.sp014783

Ito, M., Shikano, T., Oda, S., Horiguchi, T., Tanimoto, S., Awaji, T., et al. (2008). Difference in Ca^{2+} oscillation-inducing activity and nuclear translocation ability of PLCZ1, an egg-activating sperm factor candidate, between mouse, rat, human, and medaka fish. *Biol. Reprod.* 78, 1081–1090. doi: 10.1095/biolreprod.108.067801

Jellerette, T., He, C. L., Wu, H., Parys, J. B., and Fissore, R. A. (2000). Down-regulation of the inositol 1,4,5-trisphosphate receptor in mouse eggs following fertilization or parthenogenetic activation. *Dev. Biol.* 223, 238–250. doi: 10.1006/dbio.2000.9675

Jones, K. T., and Nixon, V. L. (2000). Sperm-induced Ca^{2+} oscillations in mouse oocytes and eggs can be mimicked by photolysis of caged inositol 1,4,5-trisphosphate: evidence to support a continuous low level production of inositol 1,4,5-trisphosphate during mammalian fertilization. *Dev. Biol.* 225, 1–12. doi: 10.1006/dbio.2000.9826

Kline, D., and Kline, J. T. (1992a). Repetitive calcium transients and the role of calcium in exocytosis and cell cycle activation in the mouse egg. *Dev. Biol* 149, 80–89.

Kline, D., and Kline, J. T. (1992b). Thapsigargin activates a calcium influx pathway in the unfertilized mouse egg and suppresses repetitive calcium transients in the fertilized egg. *J. Biol. Chem.* 267, 17624–17630.

Kouchi, Z., Fukami, K., Shikano, T., Oda, S., Nakamura, Y., Takenawa, T., et al. (2004). Recombinant phospholipase Czeta has high Ca^{2+} sensitivity and induces Ca^{2+} oscillations in mouse eggs. *J. Biol. Chem.* 279, 10408–10412. doi: 10.1074/jbc.M313801200

Kurokawa, M., Sato, K., Wu, H., He, C., Malcuit, C., Black, S., et al. (2005). Functional, biochemical, and chromatographic characterization of the complete [Ca^{2+}]i oscillation-inducing activity of porcine sperm. *Dev. Biol.* 285, 376–392. doi: 10.1016/j.ydbio.2005.06.029

Lawrence, Y. M., and Cuthbertson, K. S. (1995). Thapsigargin induces cytoplasmic free Ca^{2+} oscillations in mouse oocytes. *Cell Calcium* 17, 154–164. doi: 10.1016/0143-4160(95)90084-5

Marshall, I. C., and Taylor, C. W. (1994). Two calcium-binding sites mediate the interconversion of liver inositol 1,4,5-trisphosphate receptors between three conformational states. *Biochem. J.* 301(Pt 2), 591–598. doi: 10.1042/bj3010591

McGuinness, O. M., Moreton, R. B., Johnson, M. H., and Berridge, M. J. (1996). A direct measurement of increased divalent cation influx in fertilised mouse oocytes. *Development* 122, 2199–2206.

Miao, Y. L., Stein, P., Jefferson, W. N., Padilla-Banks, E., and Williams, C. J. (2012). Calcium influx-mediated signaling is required for complete mouse egg activation. *Proc. Natl. Acad. Sci. U.S.A.* 109, 4169–4174. doi: 10.1073/pnas.1112333109

Miyazaki, S. (1988). Inositol 1,4,5-trisphosphate-induced calcium release and guanine nucleotide-binding protein-mediated periodic calcium rises in golden hamster eggs. *J. Cell Biol.* 106, 345–353. doi: 10.1083/jcb.106.2.345

Miyazaki, S., Hashimoto, N., Yoshimoto, Y., Kishimoto, T., Igusa, Y., and Hiramoto, Y. (1986). Temporal and spatial dynamics of the periodic increase in intracellular free calcium at fertilization of golden hamster eggs. *Dev. Biol.* 118, 259–267. doi: 10.1016/0012-1606(86)90093-X

Miyazaki, S., Shirakawa, H., Nakada, K., and Honda, Y. (1993). Essential role of the inositol 1,4,5-trisphosphate receptor/Ca^{2+} release channel in Ca^{2+} waves and Ca^{2+} oscillations at fertilization of mammalian eggs. *Dev. Biol.* 158, 62–78. doi: 10.1006/dbio.1993.1168

Moreno, R. D., Schatten, G., and Ramalho-Santos, J. (2002). Golgi apparatus dynamics during mouse oocyte *in vitro* maturation: effect of the membrane trafficking inhibitor brefeldin A. *Biol. Reprod.* 66, 1259–1266. doi: 10.1095/biolreprod66.5.1259

Nomikos, M., Blayney, L. M., Larman, M. G., Campbell, K., Rossbach, A., Saunders, C. M., et al. (2005). Role of phospholipase C-zeta domains in Ca^{2+}-dependent phosphatidylinositol 4,5-bisphosphate hydrolysis and cytoplasmic Ca^{2+} oscillations. *J. Biol. Chem.* 280, 31011–31018. doi: 10.1074/jbc.M500629200

Politi, A., Gaspers, L. D., Thomas, A. P., and Höfer, T. (2006). Models of IP3 and Ca^{2+} oscillations: frequency encoding and identification of underlying feedbacks. *Biophys. J.* 90, 3120–3133. doi: 10.1529/biophysj.105.072249

Rissanen, S., Salmela, L., Vattulainen, I., and Róg, T. (2017). PI(4,5)P2 binds to phospholipase C delta 1 in a cholesterol concentration dependent manner. perspective on implications to PI(4,5)P2-binding proteins. *Biophys. J.* 112, 137a—138a. doi: 10.1016/j.bpj.2016.11.762

Ross, P. J., Beyhan, Z., Iager, A. E., Yoon, S. Y., Malcuit, C., Schellander, K., et al. (2008). Parthenogenetic activation of bovine oocytes using bovine and murine phospholipase C zeta. *BMC Dev. Biol.* 8:16. doi: 10.1186/1471-213X-8-16

Sato, K., Wakai, T., Seita, Y., Takizawa, A., Fissore, R. A., Ito, J. et al. (2013). Molecular characteristics of horse phospholipase C zeta (PLCzeta). *Anim. Sci. J.* 84, 359–368. doi: 10.1111/asj.12044

Saunders, C. M., Larman, M. G., Parrington, J., Cox, L. J., Royse, J., Lai, F. A., et al. (2002). PLCζ: a sperm-specific trigger of Ca^{2+} oscillations in eggs and embryo development. *Development* 129, 3533–3544.

Shirakawa, H., Ito, M., Sato, M., Umezawa, Y., and Miyazaki, S. (2006). Measurement of intracellular IP3 during Ca^{2+} oscillations in mouse eggs with GFP-based FRET probe. *Biochem. Biophys. Res. Commun.* 345, 781–788. doi: 10.1016/j.bbrc.2006.04.133

Sneyd, J., Tsaneva-Atanasova, K., Reznikov, V., Bai, Y., Sanderson, M. J., and Yule, D. I. (2006). A method for determining the dependence of calcium oscillations on inositol trisphosphate oscillations. *Proc. Natl. Acad. Sci. U.S.A.* 103, 1675–1680. doi: 10.1073/pnas.0506135103

Stricker, S. A. (1999). Comparative biology of calcium signaling during fertilization and egg activation in animals. *Dev. Biol.* 211, 157–176. doi: 10.1006/dbio.1999.9340

Swann, K. (2013). Measuring Ca^{2+} oscillations in mammalian eggs. *Methods Mol. Biol.* 957, 231–248. doi: 10.1007/978-1-62703-191-2_16

Swann, K., Igusa, Y., and Miyazaki, S. (1989). Evidence for an inhibitory effect of protein kinase C on G-protein-mediated repetitive calcium transients in hamster eggs. *EMBO J.* 8, 3711–3718.

Swann, K., and Yu, Y. (2008). The dynamics of calcium oscillations that activate mammalian eggs. *Int. J. Dev. Biol.* 52, 585–594. doi: 10.1387/ijdb.072530ks

Theodoridou, M., Nomikos, M., Parthimos, D., Gonzalez-Garcia, J. R., Elgmati, K., Calver, B. L. et al. (2013). Chimeras of sperm PLCzeta reveal disparate protein domain functions in the generation of intracellular Ca2+ oscillations in mammalian eggs at fertilization. *Mol. Hum. Reprod.* 19, 852–864. doi: 10.1093/molehr/gat070

Wakai, T., Zhang, N., Vangheluwe, P., and Fissore, R. A. (2013). Regulation of endoplasmic reticulum Ca^{2+} oscillations in mammalian eggs. *J. Cell Biol.* 126, 5714–24. doi: 10.1242/jcs.136549

Yoon, S.-Y., Eum, J. H., Lee, J. E., Lee, H. C., Kim, Y. S., Han, J. E. et al. (2012). Recombinant human phospholipase C zeta 1 induces intracellular calcium oscillations and oocyte activation in mouse and human oocytes. *Hum. Reprod.* 27, 1768–80. doi: 10.1093/humrep/des092

Yu, Y., Nomikos, M., Theodoridou, M., Nounesis, G., Lai, F. A., and Swann, K. (2012). PLCζ causes Ca^{2+} oscillations in mouse eggs by targeting intracellular and not plasma membrane PI(4,5)P2. *Mol. Biol. Cell* 23, 371–80. doi: 10.1091/mbc.E11-08-0687

Yu, Y., Saunders, C. M., Lai, F. A., and Swann, K. (2008). Preimplantation development of mouse oocytes activated by different levels of human phospholipase C zeta. *Hum. Reprod.* 23, 365–73. doi: 10.1093/humrep/dem350

Zhang, D., Pan, L., Yang, L. H., He, X. K., Huang, X. Y., and Sun, F. Z. (2005). Strontium promotes calcium oscillations in mouse meiotic oocytes and early embryos through InsP3 receptors, and requires activation of phospholipase and the synergistic action of InsP3. *Hum. Reprod.* 20, 3053–3061. doi: 10.1093/humrep/dei215

Conflict of Interest Statement: The authors declare that the research was conducted in the absence of any commercial or financial relationships that could be construed as a potential conflict of interest.

frontiers in Cell and Developmental Biology

ORIGINAL RESEARCH
published: 06 February 2018
doi: 10.3389/fcell.2018.00005

Central and Peripheral Nervous System Progenitors Derived from Human Pluripotent Stem Cells Reveal a Unique Temporal and Cell-Type Specific Expression of PMCAs

Muwan Chen[1,2], *Sofie H. Laursen*[1,2], *Mette Habekost*[1,2], *Camilla H. Knudsen*[1,2], *Susanne H. Buchholdt*[1,2], *Jinrong Huang*[3,4], *Fengping Xu*[3,4,5,6], *Xin Liu*[3,5], *Lars Bolund*[2,3,4,5], *Yonglun Luo*[2,3,4,5], *Poul Nissen*[1,7], *Fabia Febbraro*[1,8] and *Mark Denham*[1,2]*

[1] Danish Research Institute of Translational Neuroscience, Nordic EMBL Partnership for Molecular Medicine, Aarhus University, Aarhus, Denmark, [2] Department of Biomedicine, Aarhus University, Aarhus, Denmark, [3] Beijing Genomics Institute, Shenzhen, China, [4] Lars Bolund Institute of Regenerative Medicine, Beijing Genomics Institute-Qingdao, Qingdao, China, [5] China National GeneBank, Beijing Genomics Institute, Shenzhen, China, [6] Laboratory of Genomics and Molecular Biomedicine, Department of Biology, University of Copenhagen, Copenhagen, Denmark, [7] Department of Molecular Biology and Genetics, Aarhus University, Aarhus, Denmark, [8] Department of Health Science and Technology, Aalborg University, Aalborg, Denmark

OPEN ACCESS

Edited by:
Rafael A. Fissore, University of Massachusetts Amherst, United States

Reviewed by:
Shang Li, Duke Medical School, National University of Singapore, Singapore
Song-Hai Shi, Memorial Sloan Kettering Cancer Center, United States

***Correspondence:**
Mark Denham
mden@dandrite.au.dk

Specialty section:
This article was submitted to Cell Growth and Division, a section of the journal Frontiers in Cell and Developmental Biology

Received: *16 November 2017*
Accepted: *19 January 2018*
Published: *06 February 2018*

Citation:
Chen M, Laursen SH, Habekost M, Knudsen CH, Buchholdt SH, Huang J, Xu F, Liu X, Bolund L, Luo Y, Nissen P, Febbraro F and Denham M (2018) Central and Peripheral Nervous System Progenitors Derived from Human Pluripotent Stem Cells Reveal a Unique Temporal and Cell-Type Specific Expression of PMCAs. Front. Cell Dev. Biol. 6:5. doi: 10.3389/fcell.2018.00005

The P-type ATPases family consists of ion and lipid transporters. Their unique diversity in function and expression is critical for normal development. In this study we investigated human pluripotent stem cells (hPSC) and different neural progenitor states to characterize the expression of the plasma membrane calcium ATPases (PMCAs) during human neural development and in mature mesencephalic dopaminergic (mesDA) neurons. Our RNA sequencing data identified a dynamic change in ATPase expression correlating with the differentiation time of the neural progenitors, which was independent of the neuronal progenitor type. Expression of ATP2B1 and ATP2B4 were the most abundantly expressed, in accordance with their main role in Ca^{2+} regulation and we observed all of the PMCAs to have a subcellular punctate localization. Interestingly in hPSCs ATP2B1 and ATP2B3 were highly expressed in a cell cycle specific manner and ATP2B2 and ATP2B4 were highly expressed in a hPSC sub-population. In neural rosettes a strong apical PMCA expression was identified in the luminal region. Lastly, we confirmed all PMCAs to be expressed in mesDA neurons, however at varying levels. Our results reveal that PMCA expression dynamically changes during stem cell differentiation and highlights the diverging needs of cell populations to regulate and properly integrate Ca^{2+} changes, which can ultimately correspond to changes in specific stem cell transcription states.

Keywords: plasma membrane calcium ATPase, human pluripotent stem cells, neural stem cells, neuromesodermal progenitors, mesencephalic dopaminergic neurons

INTRODUCTION

Cytosolic Ca^{2+} is an abundant intracellular second messenger involved in many cellular processes. A diverse array of proteins are able to bind to Ca^{2+} each with a varying range in affinity, from which the calcium binding can alter the protein's shape and charge, resulting in a potential functional change and alteration in cellular signaling. As such, of particular importance are the Ca^{2+} P-type

ATPases, the plasma membrane calcium ATPases (PMCAs) and the sarco/endoplasmic reticulum Ca2+ ATPase (SERCAs), which reside in different compartments of the cell and along with other Ca^{2+} transporting system contribute to the regulation of the intracellular Ca^{2+} concentration.

The PMCA's ability to extrude and regulate Ca^{2+} levels is critical for cellular function and in turn the precise regulation of PMCA expression is also essential. The C-terminal of the PMCA is the main regulatory site of its pump and contains a calmodulin (CaM) binding domain and phosphorylation sites (Penniston and Enyedi, 1998; Brini and Carafoli, 2011; Tidow et al., 2012). Increased intracellular Ca^{2+} results in CaM stimulating pump activity by bending the C-terminal regulatory domain away from the active site of the pump releasing it from the auto-inhibitory state (Brini and Carafoli, 2011; Tidow et al., 2012). Phosphorylation in the regulatory C-terminal is executed by both Protein Kinase A (PKA) and Protein Kinase C (PKC); PKA stimulate Ca^{2+} extrusion, whereas PKC inhibits (James et al., 1989; Enyedi et al., 1997). PKC conducts its inhibitory effect by phosphorylation of the CaM binding domain, creating a barrier for CaM interaction and hereby inhibiting CaM stimulation (Enyedi et al., 1997). PMCA regulation of Ca^{2+} is therefore crucial in fine-tuning the levels of Ca^{2+} in the cytoplasm with sequence variability, splice variants, and cell type specific expression seen between the different PMCA isoforms all having varying effects on the multitude of affected signaling pathways.

Regulation of signaling pathways by Ca^{2+} occurs at the earliest stages of development where it plays a critical role in fertilization and hPSC maintenance (Deguchi et al., 2000; Todorova et al., 2009). Furthermore, Ca^{2+} has been interconnected with several neural properties such as synaptic transmission and long-term potentiation and dysregulation of intracellular calcium due to altered PMCA expression has been shown to affect neural differentiation through their involvement in Fgf and Wnt signaling (Brini et al., 2014; Abdul-Wajid et al., 2015; Boczek et al., 2015). Different PMCA genes maintain different expression profiles. In humans ATP2B1 and ATP2B4 are expressed throughout the body, whereas the two other isoforms, ATP2B2 and ATP2B3, exhibit neural and muscular tissue specific expression (Stauffer et al., 1995). Mutations in ATP2B1 is embryonic lethal and mutations in ATP2B2-4 have been correlated with different neuronal deficits: hearing loss, congenital ataxias, and familial spastic paraplegia, respectively (Okunade et al., 2004; Ficarella et al., 2007; Zanni et al., 2012; Ho et al., 2015). These studies highlight the important role of the various PMCAs in Ca^{2+} handling across the diverse cell types, therefore identifying their cell type specific expression during development is crucial for understanding cell type specific Ca^{2+} regulation.

The precise localization and neural specific expression of PMCAs during the development of the human nervous system is poorly understood. To address this we used hPSCs to generated neural stem cells (NSCs) of the central and peripheral nervous system and investigated the main neural progenitor states for the presence of PMCAs using RNA sequencing (RNA-seq) and immunofluorescent labeling. Our results uncovered a dynamic change in ATPase expression that correlates directly with the stage of differentiation. Furthermore, PMCA expression was not only altered between stem cell states, but also in addition showed unique cell cycle specific changes. Lastly due to the importance of Ca^{2+} regulation in Parkinson's disease (PD) we differentiated the NSC further and generated mesencephalic dopaminergic (mesDA) neurons to characterize the presence of PMCA proteins (Schöndorf et al., 2014). These data have important implications for understanding the role of Ca^{2+} in development and potentially how disease states, which disrupted Ca^{2+} homeostasis, can result in global cellular dysfunction.

MATERIALS AND METHODS

Human Pluripotent Stem Cell Culture

H9 (WA-09, WiCell) and iPSC-CCD (reprogrammed from human Foreskin fibroblasts, ATCC) cell lines were cultured as previously described (Denham and Dottori, 2011). Briefly, hESCs and hPSCs were cultured on irradiated human foreskin fibroblasts (HFF) in KSR media consisting of DMEM/nutrient mixture F-12, supplemented with β-mercaptoethanol 0.1 mM, non-essential amino acids (NEAA) 1%, glutamine 2 mM, penicillin 25 U/ml, streptomycin 25 μg/ml, and knockout serum replacement 20% (all from Life Technologies), supplemented with FGF2 (10 ng/ml; Peprotech) and Activin A (10 ng/ml; R&D systems). All cells were cultured at 37°C 5% CO_2. Colonies were mechanically dissected every 7 days and transferred to freshly prepared HFF. Media was changed every second day.

Neural Stem Cell Differentiation

hESCs or hPSCs were mechanically dissected into pieces ∼0.5 mm in diameter and transferred to laminin-coated organ culture plates in N2B27 medium containing 1:1 mix of neurobasal medium with DMEM/F12 medium, supplemented with insulin/transferrin/selenium 1%, N2 1%, retinol-free B27 1%, glucose 0.3%, penicillin 25 U/ml, and streptomycin 25 μg/ml (all from Life Technologies) for 11 days. Cultures were grown on laminin for the first 4 days after which they were dissected into 0.5 mm pieces and cultured in suspension in low-attachment 96-well plates (Corning) in N2B27 medium. For neural epithelial progenitors (NEP) specification SB431542 (SB; 10 μM, Tocris) was added to the media and cells were collected at day 4. To further specify the cells to rostral neural stem cell (NSC), NEP were generated and then further cultured to day11 in the absence of SB and supplemented with FGF2 (20 ng/ml; Peprotech). For neuromesodermal progenitors (NMP) induction, NEP induction was performed as above and cultures were additionally supplemented with GSK3β inhibitor CHIR99021 (CHIR; 3 μM, Stemgent) from days 0 to 4. For neural crest stem cells (NCSCs) specification NMP induction was performed and from days 4 to 11 cultures were supplemented with FGF2 (20 ng/ml; Peprotech) and BMP2 (50 ng/ml; Peprotech). For caudal NSC specification NMP induction was performed and from days 4 to 11 cultures were supplemented with FGF2 (20 ng/ml; Peprotech).

Mesencephalic Dopaminergic Neuron Differentiation

Generation of mesDA neurons was achieved by modification of previous described protocols (Denham et al., 2012; Kirkeby et al., 2012). Briefly, from day 0 to day 9 cells were grown in N2B27 media with 10 μM SB431542, 0.7 μM CHIR99021, 0.1 μM LDN-193189 (Stemgent), and 400 nM SAG (Millipore), day 4 to day 9 basal media change to ½ N2B27. At day 9 to day 11, the media was changed to ½ N2B27 without small molecules. From Day 11 the cells were grown in Neurobasal media supplemented with B27 1%, Pen/Strep 25 U/mL, Glutamax 0.5%, 200 μM Ascorbic Acid (AA) (Sigma-Aldrich) and grown on culture plate coated with polyornithine, fibronectin, and laminin (all from Sigma). From day 14, 2.5 μM DAPT (Tocris bioscience) was added into the culture media. The media was changed every second day and samples were collected on day 45.

Immunolabeling

Cell monolayers and neurospheres were fixed in 4% PFA for 20 min at 4°C and then washed briefly in PBS. Neurospheres were embedded in Tissue-Tek OCT compound (Labtek), cut at 10 μm on a cryostat, and sections were placed on superfrost slides. Sections or culture dishes were blocked for 1 h at room temperature (RT) in blocking solution. The following primary antibodies were used: goat anti-Sox10 (1:100, R&D systems), goat anti-Sox2 (1:100, R&D), mouse anti-Sox2 (1:100 R&D), mouse anti-Oct4 (1:100, Santa Cruz), mouse anti-Nanog (1:100, eBioscience), mouse anti-ßIII-tubulin (1:1,000, Millipore), goat anti-FOXA2/HNF3Beta (1:500, Santa Cruz), mouse anti- Tyrosine hydroxylase (TH, 1:2000, Millipore), rabbit anti-ATP2B1 (1:1,000, SWANT) (Stauffer et al., 1995, 1997), goat anti-ATP2B2 (1:200, S-18 sc-22073, Santa Cruz) (Sahly et al., 2012), rabbit anti-ATP2B3 (1:1000, SWANT) (Stauffer et al., 1995, 1997), and goat anti-ATP2B4 (1:200, Y-20 sc-22080, Santa Cruz) (Patel et al., 2013). Antibodies were diluted in blocking solution incubated on sections and cultures overnight at 4°C. Following three 10-min washes in PBT, the corresponding Alexa Fluor-647, Alexa Fluor-488 or Alexa Fluor-594 donkey secondary antibodies were applied for 1 h at RT (1:400, Jackson ImmunoResearch). Nuclei were counterstained with 49,6-diamidino-2-phenylindole (DAPI; 1 μg/ml, Sigma). Slides were mounted in PVA-DABCO for viewing under a fluorescent microscope (ZEISS ApoTome), and images captured using the ZEN software. Confocal microscopy was performed using a ZEISS LSM 780 Confocal Microscope. The images were reconstructed as an intensity projection over the Z-axis using ZEN software.

RNA Sequencing

RNA sequencing was performed in collaboration with BGI-Research, Shenzhen, China. Briefly, total RNA was first assessed with Agilent 2100 Bioanaylzer and treated with DNase I. Magnetic beads with Oligo dT were used to isolate mRNA. The mRNA was then fragmented into short fragments with fragmentation buffer and complement DNA (cDNA) was synthesized using the mRNA fragments as templates. Short fragments were purified with EB buffer for end reparation and single nucleotide A (adenine) addition. After that, the short fragments were linked to adapters. After agarose gel electrophoresis, the suitable fragments were selected for the PCR amplification as templates. During the QC steps, Agilent 2100 Bioanaylzer and ABI StepOnePlus Real-Time PCR System were used for quantification and qualification of the sample library. Finally, the library was sequenced using Ion proton platform. Raw data from the Ion proton was subjected to data QC. Raw reads were filtered into clean reads and aligned to the reference gene with TMAP to calculate distribution of reads on reference genes and perform coverage analysis. At the same time, the clean reads were aligned to ref genome (hg19) with TopHat for a series of subsequent analysis. Finally, gene expression level and differential expression analysis was performed.

Statistical Analysis

One-way ANOVAs and post-hoc analyses were performed for statistical analyses on RPKM values using GraphPad Prism 6. To generate Heatmaps, RPKM values were log2 transformed and mean centered and graphed using R studio with heatmap.2. Principal components were calculated by singular value decomposition of the centered and scaled data matrix using the prcomp function in R stats package.

RESULTS

Profiling of ATPase Expression in Human Embryonic Stem Cells and in Early Neural Stem Cell States by RNA Sequencing

We first set out to characterize ATPase transcripts in hESCs and hESC-neural derivatives, including early NSCs of the central and peripheral nervous system. To generate CNS and PNS progenitors we implemented our previously described protocol (Denham et al., 2012, 2015). Day 4 NEPs along with the subsequent day 11 rostral NSCs were derived (**Figure 1A**). Additionally NMPs were generated and by further differentiating the day 4 NMPs in two distinct ways, caudal neural progenitors (day11; CNPs) and day 11 NCSCs were derived (**Figure 1A**). With these 6 distinct time points we set out to validate the gene expression of these populations by RNA-seq analysis (undifferentiated hESC and the five NSC states: NEP, NMP, rostral NSC, caudal NSC, and NCSC). Firstly we examined the gene expression of known markers indicative of the various stem cell states. As expected we identified *POU5F1* (previously known as *OCT4*) and *NANOG* as highly expressed in the undifferentiated hESCs and down-regulated in all of the neural populations: *SOX2* was maintained throughout all progenitor states (**Figure 1B**). Furthermore, day 4 NEP expressed transcripts indicative of anterior identity, such as *OTX2*, *SIX3,* and *LHX2*. Rostral NSCs expressed high levels of *SOX1*, *OTX2 FOXG1*, *SIX3,* and *LHX2*. NMPs as previously described are known to co-express *T* and *Sox2* (Tzouanacou et al., 2009; Gouti et al., 2014; Turner et al., 2014; Denham et al., 2015). In accordance with this we detected both high levels of *T* and *SOX2* in NMPs and we also detected *NKX1-2* and *FOXB1* (**Figure 1B**; Turner et al., 2014). Caudal neural markers were also detected such

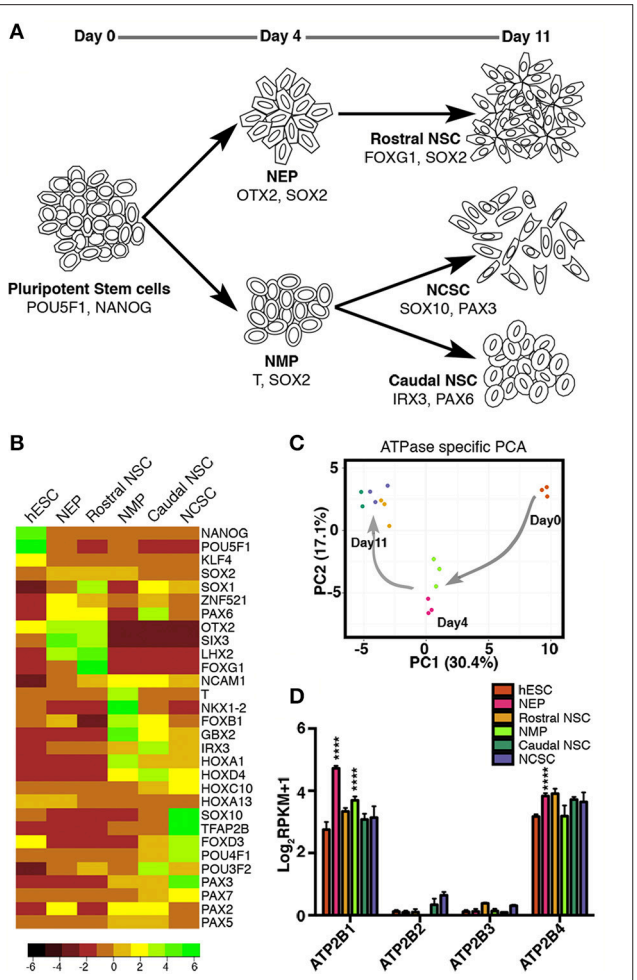

FIGURE 1 | RNAseq profiling of ATPase expression in human embryonic stem cells and in early neural stem cell states. **(A)** Overview of protocol for deriving neural epithelial progenitors (NEP), and neuromesodermal progenitors (NMP) on day 4; rostral neural stem cells (NSC), neural crest stem cells (NCSCs) and caudal NSC on day 11. **(B)** Gene expression of known markers indicative of the various stem cell states. **(C)** Principal component analysis of expression of ATPases during early neural progenitor states. **(D)** RNAseq profiling of ATP2B1-4 expression (in RPKM values) in human embryonic stem cells and in early neural stem cell states (****$p < 0.001$). Not all significant differences are indicated. Legend shown in **(D)** also represents colored dots in **(C)**.

as *HOXA1* in the NMP state. Caudal NSCs expressed *IRX3* and *HOXD4,* additional *HOX* genes were also expressed with the most caudal representing the lumbar regions of the spinal cord (**Figure 1B**; Figure S1). NCSCs expressed the crest marker *SOX10*, *TFAP2B*, *FOXD3*, *PAX3,* and *POU4F1* (previously known as *BRN3A*).

To explore the variation in expression of ATPases during early neural progenitor states we performed a principal component analysis on all ATPases. Strikingly we observed that principal component 1 (PC1), which had the highest percentage of variance (30.4%) separated the stem cell states based on the time of differentiation, whereas the PC2 could separate only some of the stem cell states at each time point (**Figure 1C**). These results indicated that a dynamic change in ATPase expression occurs between the distinct progenitor states, progressively changing as the neural progenitors developed toward more committed progenitors.

Based on these results we further sought to examine the P-type ATPase PMCA members (*ATP2B1-4*; **Figure 1D**). *ATP2B1-4* were all examined between each of the stem cell states. *ATP2B1* and *ATP2B4* had higher amount of transcripts across all of the stem cell populations (**Figure 1D**). Interestingly the *ATP2B1* expression significantly increased ($p < 0.0001$) when differentiated from the pluripotent state to both NEP and NMP day4 progenitor states. In the NEP group *ATP2B4* expression was also significantly increased compared to the pluripotent state ($p < 0.0001$; **Figure 1D**). *ATP2B2* and *ATP2B3* were also detected, in all groups, except for in the NMP group where *ATP2B2* was undetected (**Figure 1D**).

PMCA Expression in Human Pluripotent Stem Cells

We next investigated whether the expression of PMCAs, as indicated by RNAseq analysis (**Figure 1D**), were translated into detectable protein levels and to subsequently determine the cell subtype specific expression. ATP2B1-4 were all detected in pluripotent stem cells and showed a punctate localization pattern within the cells (**Figure 2**). ATP2B1 was ubiquitously expressed and interestingly vastly higher amounts were seen in dividing cells that also maintained expression of POU5F1 (**Figure 2**, arrow head). To further validate the pluripotent status of these cells NANOG expression was analyzed and, indeed, high ATP2B1 expressing cells also co-expressed NANOG (Figure S2).

In contrast, ATP2B2 expression was more restricted to a subpopulation of the hPSCs that could be identified also by an atypical morphology, consisting of a larger cytoplasm to nuclear ratio. Despite this morphology, POU5F1 and NANOG were both expressed in the ATP2B2 positive cells within the pluripotent culture. Notably however these cells were frequently located closer to the edges of the colony.

ATP2B3 showed a similar ubiquitous expression pattern to ATP2B1 and higher expression in dividing cells. However, interestingly, not all dividing cells expressed higher levels of ATP2B3, potentially representing a discrete stage during mitosis (**Figure 2**). Furthermore, ATP2B3 positive cells expressed POU5F1 and NANOG (**Figure 2**, Figure S2). Lastly we identified ATP2B4 positive cells that corresponded with a population close to the edge of the colony, with all positive cells having a large cytoplasm similar to ATP2B2 (**Figure 2**). Moreover, these cells also still expressed POU5F1 and NANOG.

Based on our analysis of hPSCs, all PMCAs were expressed in pluripotent, POU5F1 and NANOG positive, cells. The expression of PMCAs varied, however, with respect to cell morphology and cell cycle stage, with the most notable change being ATP2B1 and ATP2B3 expression being highest during cell division, a point at which cell differentiation can occur. Overall, precise regulation of Ca^{2+} by PMCAs could be required during mitosis in hPSCs.

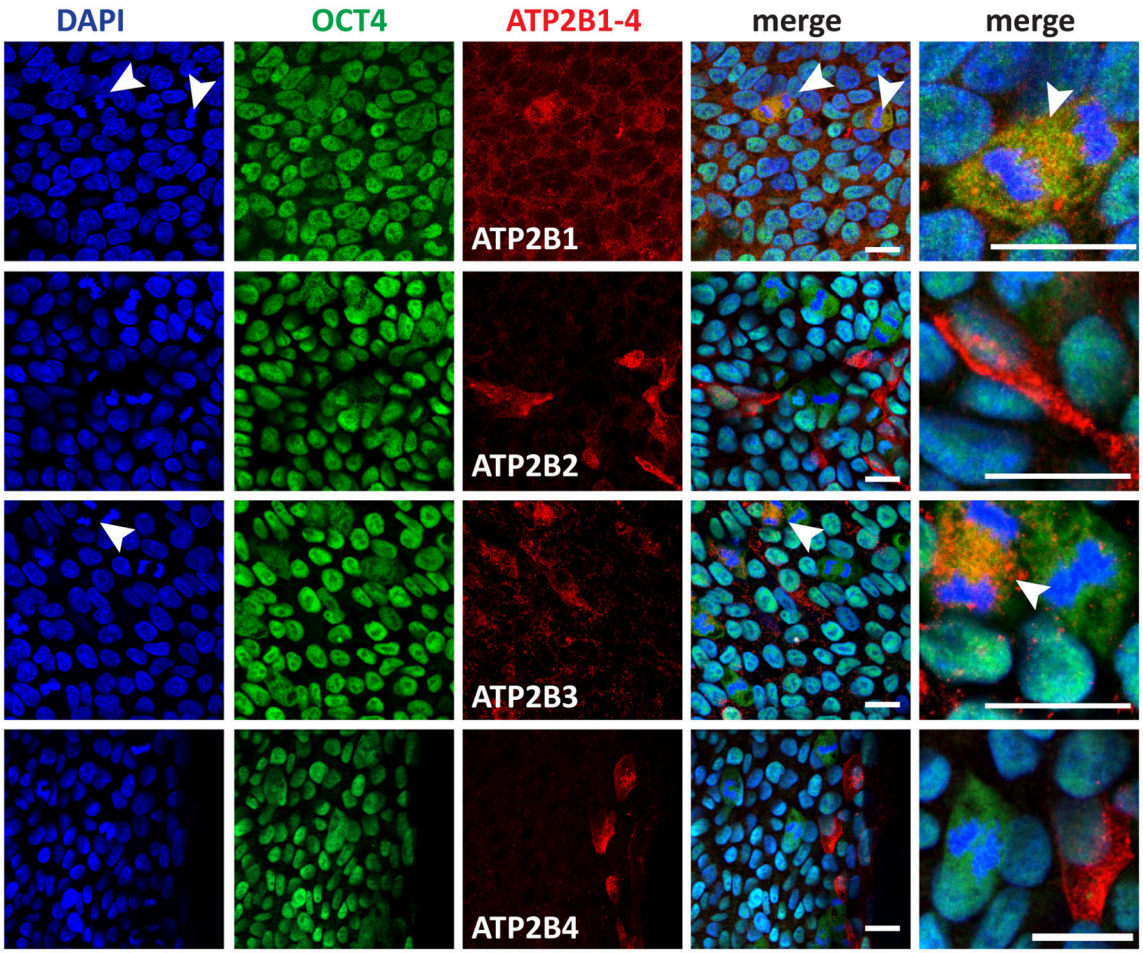

FIGURE 2 | Immunocytochemistry analysis of ATP2B1-4 and POU5F1 expression in human pluripotent stem cells. Arrow heads point to the dividing cells. Scale bars = 20 μm.

Furthermore, ATP2B2 and ATP2B4 were highly expressed in cells with morphologies indicative of a metastable differentiation state.

PMCA Expression in Early Neural Stem Cells

Differentiation of pluripotent stem cells toward a neuroectoderm fate coincides with transient increases in intracellular Ca^{2+}. Based on our RNAseq data we identified a significant change in expression between pluripotent and day 4 time points for ATP2B1 (**Figure 1D**). Additionally, the higher expression of PMCAs in morphologically larger hPSCs and during cell division indicates a changing cellular state with varying requirements for Ca^{2+} regulation. We therefore further investigated the PMCA protein expression and localization during neural development. NEPs and NMPs were examined, which represent progenitors of the same differentiation time point but with vastly different potential (**Figures 3A,B**). PMCA expression in NEPs and NMPs were indiscernible from each other, both populations showing ubiquitous expression throughout the cultures for ATP2B1. In contrast to the RNAseq data, ATP2B2 was detected in both groups and it was mainly detected in dividing cells and also found in discrete sub-populations of cells, which SOX2 could not discriminate. In both groups ATP2B3 was ubiquitously expressed but at lower levels consistent with the RNAseq analysis. The ATP2B4 was strongly expressed in cell membranes of a sub-population of cells, however SOX2 expression could also not separate this population.

PMCA Expression in Central and Peripheral Neural Stem Cells

We further characterized the PMCA expression at later differentiation states, the Rostral NSCs, Caudal NSCs and NCSCs (**Figures 4A–C**). In accordance with the RNAseq data and consistent with the early stem cell states all PMCA genes were detected within all groups. Interestingly in all three groups ATP2B1 expression was apically localized to the luminal regions of the neural rosettes, which also co-stained for SOX2. Furthermore, ATP2B2 within the Rostral NSCs was also apically localized to the luminal

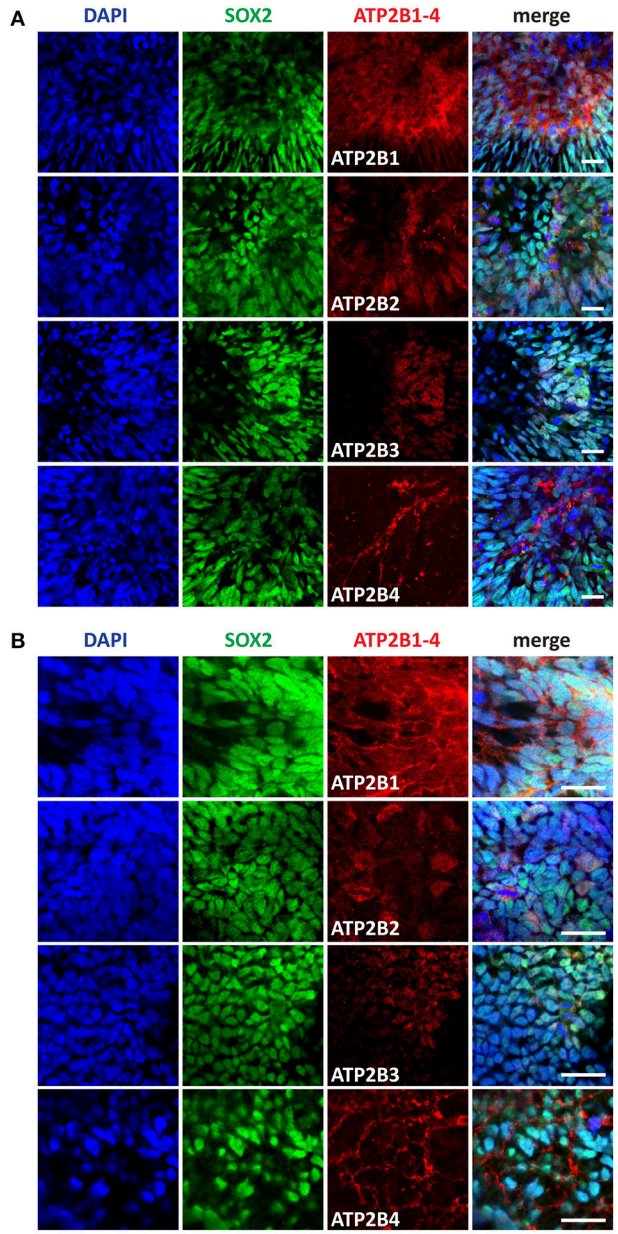

FIGURE 3 | Immunocytochemistry analysis of ATP2B1-4 and SOX2 expression in **(A)** neural epithelial progenitors (NEP) and in **(B)** neuromesodermal progenitors (NMP) on day 4. Scale bars = 20 μm.

region of the rosettes and within the NCSCs ATP2B2 was selectively localized to the SOX2 positive cells. ATP2B4 expression was higher at the edges of the spheres except for the Caudal NSC groups, which showed a more ubiquitous expression.

PMCA Expression in Mesencephalic Dopaminergic Neurons

Having identified the changing expression between the maturation states of the NSC we lastly sought to characterize the expression of PMCAs in mature neurons. We therefore investigated PMCA expression in mesDA neurons. mesDA neurons were differentiated *in vitro* for 45 days following our previously established protocol (**Figure 5A**). We first validated the protocol by staining differentiated cell populations with FOXA2 and Tyrosine Hydroxylase (TH), markers indicative of mesDA neurons, and identified neurons positive for both markers (**Figure 5B**). ATP2B1 was highly expressed and localized to the soma and the axons of the dopaminergic neurons. ATP2B2 and ATP2B3 were also expressed throughout the TH+ neurons, whilst ATP2B4 was detected weakly in the mesDA neurons (**Figure 5**).

DISCUSSION

Calcium acts as a major second messenger system within cells and as such it is involved in the regulation of numerous signaling pathways. During development stem cell fate is dictated by the precise temporal and spatial activation of signaling events, which requires specific ligand-receptor interactions and can rely on cytoplasmic calcium for transcriptional regulation (Lee et al., 2009; Thrasivoulou et al., 2013). This study has identified the expression changes of PMCAs that occur during early human stem cell states of the developing nervous system. In particular we have characterized the expression of PMCAs within: hPSCs, NEPs, NMPs, Rostral NSCs, Caudal NSCs, and NCSCs. Strikingly we observed a dynamic change in ATPase expression that coincided with the advanced differentiation states of NSC, which was independent of the differentiation of the NSCs (**Figure 1C**). We identified *ATP2B1* and *ATP2B4* as the most abundantly expressed, consistent with previous reports in other cell types and with ATP2B1 regarded as providing a housekeeping function for Ca^{2+} homeostasis (Okunade et al., 2004). Furthermore, *ATP2B1* expression significantly increased when differentiating from a pluripotent state to either a NMP or NEP, indicated a change in the transcriptional regulation of *ATP2B1* when transitioning to neural ectoderm. In contrast to *ATP2B1* and *ATP2B4*, the RPKM values of *ATP2B2* and *ATP2B3* were lower and *ATP2B2* was undetected in NMP. Despite the absence of detected transcripts, ATP2B2 proteins could be detected in NMPs, which was a sub-population of mainly dividing cells (**Figure 1D**). The depth of sequencing and the fact that ATP2B2 was only observed in a small subpopulation is the likely reason for the discrepancies between the sequencing and immunostaining results. Moreover, the differences between the RNAseq data and immunostaining results reflects the known divergence in transcript production and half-life to that of protein synthesis and turnover (Maier et al., 2009). Furthermore, our immunostaining also revealed a subcellular punctate localization for all the PMCAs, which suggests that the localization rather than the abundant of PMCAs are important for normal cellular function. The punctate localization of the PMCAs is likely formed to produce specific signaling complexes, which has been reported previously for ATP2B1-4, and the C-terminal tail of ATP2B4 has been shown to act as a signaling peptide involved in controlling its cellular

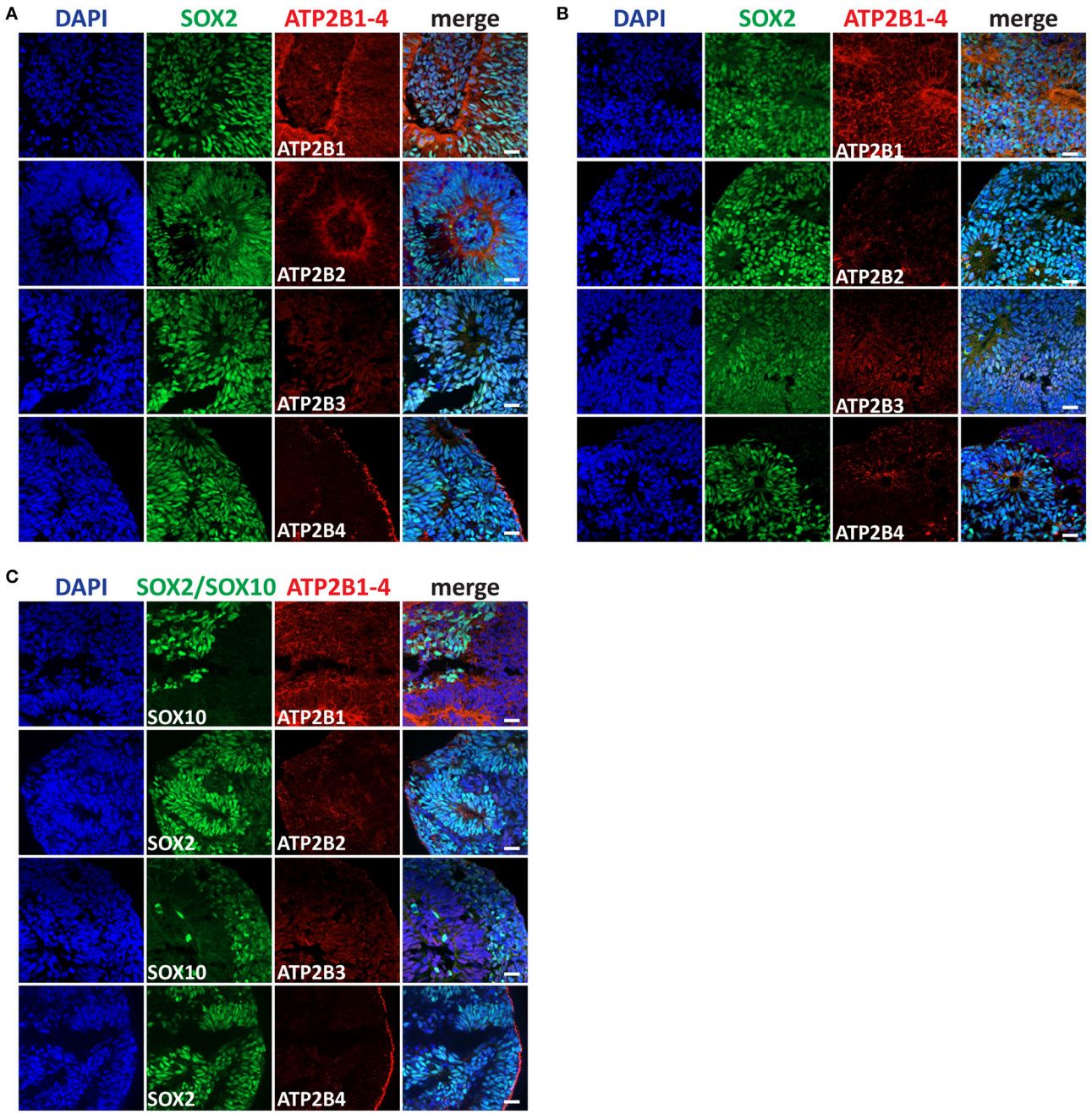

FIGURE 4 | Immunocytochemistry analysis of ATP2B1-4 and SOX2 or SOX10 expression in **(A)** rostral neural stem cells (NSC), in **(B)** caudal NSC, and in **(C)** neural crest stem cells (NCSCs) on day 11. Scale bars = 20 μm.

localization (Marcos et al., 2009; Kenyon et al., 2010; Antalffy et al., 2013).

In contrast to mouse embryonic stem cells, which have been shown to only express *ATP2B1* and *ATP2B4,* we identified a transient pluripotent state with an atypical morphology that express ATP2B2 and still expressed POU5F1 and NANOG (**Figure 2**, Figure S2; Yanagida et al., 2004). These ATP2B2 expressing pluripotent stem cells may represent a primed state of hPSCs committed to differentiate but not yet having down-regulated all pluripotency genes (Kalkan et al., 2017; Liu et al., 2017; Smith, 2017).

Interestingly, in pluripotent cultures, ATP2B1 and ATP2B3 were highly expressed in cells undergoing mitosis. Both ionic current and PMCA activity have been shown to fluctuate during mitosis in the development of simpler eukaryotes

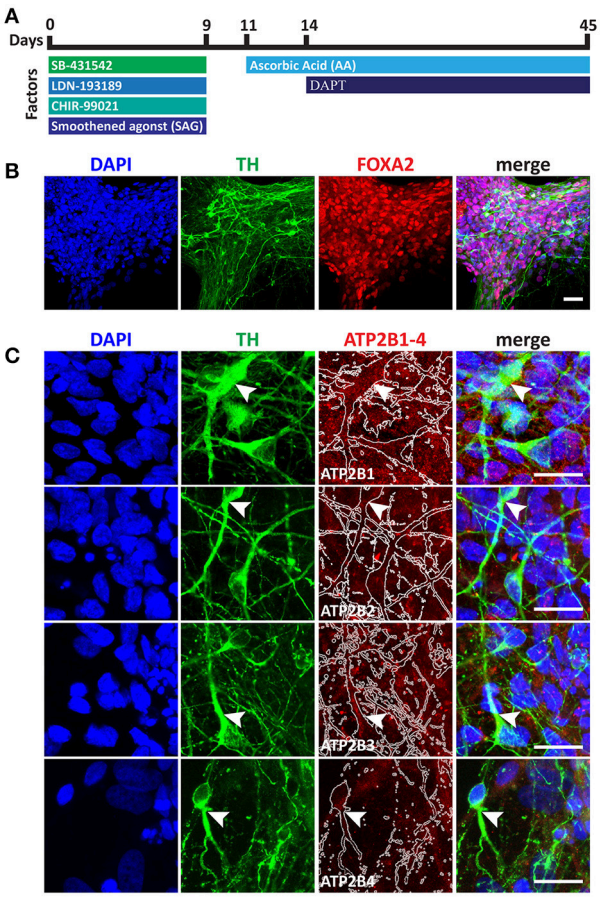

FIGURE 5 | Immunocytochemistry analysis of ATP2B1-4 expression in mesencephalic dopaminergic neurons. **(A)** Overview protocol for making mesDA *in vitro* for 45 days. **(B)** Immunostaining of mesDA with double positive of FOXA2 and Tyrosine Hydroxylase (TH) markers indicates the efficient protocol. **(C)** Immunostaining of ATP2B1-4 and TH expression. Arrow heads point to the TH positive staining with ATP2B1-4 staining and white lines in ATP2B1-4 panels outlines TH positive staining. Scale bars = 20 μm.

(Zivkovic et al., 1991). Moreover, prevention of Ca^{2+} surges prior to or during mitosis result in inhibition of mitosis entry and exit, respectively (Steinhardt and Alderton, 1988). Thus, regulation of Ca^{2+} surges seems to be essential for cell division. Interestingly we could observe increased ATP2B1 and ATP2B3 in a period close to or during the anaphase-telophase transition, a stage which is dependent on a sustained increased Ca^{2+} level (Tombes and Borisy, 1989). Furthermore, nuclear Ca^{2+} can operate in an independent manner within the nucleus to that of the cytoplasm through the regulation of its own Ca^{2+} stores, with nuclear $InsP_3$ being capable of regulating nuclear Ca^{2+} levels (Leite et al., 2003). In accordance with this, the cell cycle specific expression of PMCAs likely represents an altered requirement of cytoplasmic calcium regulation during nuclear envelope break down in cytokinesis (Stehno-Bittel et al., 1995).

Previous studies have identified ATP2B2 and ATP2B3 to be predominantly expressed in neuronal tissues (Stauffer et al., 1995; Strehler and Zacharias, 2001). Consistent with that we detected all PMCA isoforms in both NEPs and NMPs. Interestingly, at later stages in neural development we found ATP2B1 to be apically localized to the luminal regions of the neural rosettes. Active Ca^{2+} secretion to the lumen of the neural rosettes could be required for the generation of a specific lumen environment that promote neural tube closure (Abdul-Wajid et al., 2015; Suzuki et al., 2017). Furthermore, we identified ATP2B4 to be highly expressed at the edges of the neurospheres in the Rostral NSC and NCSC groups, however we could not identify a specific protein marker that could define this population. Nevertheless, an explanation for this could be that PMCA expression can be altered by changes in physical environmental rather than cell identity (Antalffy et al., 2013).

Dopamine release by mesDA neurons is dependent on precise Ca^{2+} fluctuations (Sgobio et al., 2014). We found that mesDA neurons expressed all four PMCAs. Alterations therefore in PMCA expression in mesDA neurons could contribute to mesDA neurons increased sensitivity to Ca^{2+} and hence to the PD pathogenesis. In support of this, impairment of Ca^{2+} homeostasis has been observed in iPSC-derived mesDA neurons from patients with heterozygous mutations for GBA1 (Schöndorf et al., 2014). These neurons showed an increase in basal Ca^{2+} levels and increased vulnerability to Ca^{2+} mediated endoplasmic reticulum (ER) stress. In addition, in PMCA overexpressing rats a neuroprotective function of PMCAs has been shown by its ability to decrease vulnerability to MPTP treatment (Brendel et al., 2014). Hence, strategies to regulate PMCA activity could serve as a neural protective mechanism in mesDA neurons by providing additional support for intracellular Ca^{2+} regulation.

CONCLUSION

In summary, we have identified a dynamic change in the expression of P-type ATPases between distinct progenitor types. The transcriptional mechanisms that regulate these changes is still unknown and the functional significance of progenitor cell types requiring distinct P-type ATPase expression has yet to be elucidated, however it may reflect cell type specialization requirements. Most significantly we identified a novel expression timing of ATP2B1 and ATP2B3 during cell division of hPSCs and expression of ATP2B2 was observed in a subpopulation of hPSCs. Neural rosettes were identified as having a distinct apical localization of ATP2B1 to their luminal side. Lastly, we identified ATP2B1-4 were all expressed in mesDA neurons. Overall these results contribute to our understanding of the respective roles of the PMCA isoforms in neural development and their potential use as drug target for disease therapies.

AUTHOR CONTRIBUTIONS

MD and PN: conceived the project and MD: designed the experiments; MC, SL, FF, CK, SB, JH, FX, and XL: performed the experiments; YL and LB: contributed RNA sequencing instrumentation and expertise in analysis; SL, MH, MC, and MD: analyzed data; MD, SL, and MC: wrote the manuscript; All authors reviewed the manuscript.

FUNDING

This paper was supported by the following grants: Innovation Fund Denmark. Lundbeck Foundation.

ACKNOWLEDGMENTS

MD and YL are partners of BrainStem—Stem Cell Center of Excellence in Neurology, funded by Innovation Fund Denmark. MC is supported by a postdoctoral fellowship from the Lundbeck Foundation (R209-2015-3100).

SUPPLEMENTARY MATERIAL

The Supplementary Material for this article can be found online at: https://www.frontiersin.org/articles/10.3389/fcell.2018.00005/full#supplementary-material

REFERENCES

Abdul-Wajid, S., Morales-Diaz, H., Khairallah, S. M., and Smith, W. C. (2015). T-type calcium channel regulation of neural tube closure and EphrinA/EPHA expression. *Cell Rep.* 13, 829–839. doi: 10.1016/j.celrep.2015.09.035

Antalffy, G., Pászty, K., Varga, K., Hegedus, L., Enyedi, Á., and Padányi, R. (2013). A C-terminal di-leucine motif controls plasma membrane expression of PMCA4b. *Biochim. Biophys. Acta* 1833, 2561–2572. doi: 10.1016/j.bbamcr.2013.06.021

Boczek, T., Ferenc, B., Lisek, M., and Zylinska, L. (2015). Regulation of GAP43/calmodulin complex formation via calcineurin-dependent mechanism in differentiated PC12 cells with altered PMCA isoforms composition. *Mol. Cell. Biochem.* 407, 251–262. doi: 10.1007/s11010-015-2473-4

Brendel, A., Renziehausen, J., Behl, C., and Hajieva, P. (2014). Downregulation of PMCA2 increases the vulnerability of midbrain neurons to mitochondrial complex I inhibition. *Neurotoxicology* 40, 43–51. doi: 10.1016/j.neuro.2013.11.003

Brini, M., Calì, T., Ottolini, D., and Carafoli, E. (2014). Neuronal calcium signaling: function and dysfunction. *Cell. Mol. Life Sci.* 71, 2787–2814. doi: 10.1007/s00018-013-1550-7

Brini, M., and Carafoli, E. (2011). The plasma membrane Ca^{2+} ATPase and the plasma membrane sodium calcium exchanger cooperate in the regulation of cell calcium. *Cold Spring Harb. Perspect. Biol.* 3:a004168. doi: 10.1101/cshperspect.a004168

Deguchi, R., Shirakawa, H., Oda, S., Mohri, T., and Miyazaki, S. (2000). Spatiotemporal analysis of $Ca^{(2+)}$ waves in relation to the sperm entry site and animal-vegetal axis during $Ca^{(2+)}$ oscillations in fertilized mouse eggs. *Dev. Biol.* 218, 299–313. doi: 10.1006/dbio.1999.9573

Denham, M., Bye, C., Leung, J., Conley, B. J., Thompson, L. H., and Dottori, M. (2012). Glycogen synthase kinase 3β and activin/nodal inhibition in human embryonic stem cells induces a pre-neuroepithelial state that is required for specification to a floor plate cell lineage. *Stem Cells* 30, 2400–2411. doi: 10.1002/stem.1204

Denham, M., and Dottori, M. (2011). Neural differentiation of induced pluripotent stem cells. *Methods Mol. Biol.* 793, 99–110. doi: 10.1007/978-1-61779-328-8_7

Denham, M., Hasegawa, K., Menheniott, T., Rollo, B., Zhang, D., Hough, S., et al. (2015). Multipotent caudal neural progenitors derived from human pluripotent stem cells that give rise to lineages of the central and peripheral nervous system. *Stem Cells* 33, 1759–1770. doi: 10.1002/stem.1991

Enyedi, A., Elwess, N. L., Filoteo, A. G., Verma, A. K., Paszty, K., and Penniston, J. T. (1997). Protein kinase C phosphorylates the "a" forms of plasma membrane Ca^{2+} pump isoforms 2 and 3 and prevents binding of calmodulin. *J. Biol. Chem.* 272, 27525–27528. doi: 10.1074/jbc.272.44.27525

Ficarella, R., Di Leva, F., Bortolozzi, M., Ortolano, S., Donaudy, F., Petrillo, M., et al. (2007). A functional study of plasma-membrane calcium-pump isoform 2 mutants causing digenic deafness. *Proc. Natl. Acad. Sci. U.S.A.* 104, 1516–1521. doi: 10.1073/pnas.0609775104

Gouti, M., Tsakiridis, A., Wymeersch, F. J., Huang, Y., Kleinjung, J., Wilson, V., et al. (2014). *In vitro* generation of neuromesodermal progenitors reveals distinct roles for wnt signalling in the specification of spinal cord and paraxial mesoderm identity. *PLoS Biol.* 12:e1001937. doi: 10.1371/journal.pbio.1001937

Ho, P. W.-L., Pang, S. Y.-Y., Li, M., Tse, Z. H.-M., Kung, M. H.-W., Sham, P.-C., et al. (2015). PMCA4 (ATP2B4) mutation in familial spastic paraplegia causes delay in intracellular calcium extrusion. *Brain Behav.* 5:e00321. doi: 10.1002/brb3.321

James, P. H., Pruschy, M., Vorherr, T. E., Penniston, J. T., and Carafoli, E. (1989). Primary structure of the cAMP-dependent phosphorylation site of the plasma membrane calcium pump. *Biochemistry* 28, 4253–4258. doi: 10.1021/bi00436a020

Kalkan, T., Olova, N., Roode, M., Mulas, C., Lee, H. J., Nett, I., et al. (2017). Tracking the embryonic stem cell transition from ground state pluripotency. *Development* 144, 1221–1234. doi: 10.1242/dev.142711

Kenyon, K. A., Bushong, E. A., Mauer, A. S., Strehler, E. E., Weinberg, R. J., and Burette, A. C. (2010). Cellular and subcellular localization of the neuron-specific plasma membrane calcium ATPase PMCA1a in the rat brain. *J. Comp. Neurol.* 518, 3169–3183. doi: 10.1002/cne.22409

Kirkeby, A., Grealish, S., Wolf, D. A., Nelander, J., Wood, J., Lundblad, M., et al. (2012). Generation of regionally specified neural progenitors and functional neurons from human embryonic stem cells under defined conditions. *Cell Rep.* 1, 703–714. doi: 10.1016/j.celrep.2012.04.009

Lee, K. W., Moreau, M., Néant, I., Bibonne, A., and Leclerc, C. (2009). FGF-activated calcium channels control neural gene expression in Xenopus. *Biochim. Biophys. Acta* 1793, 1033–1040. doi: 10.1016/j.bbamcr.2008.12.007

Leite, M. F., Thrower, E. C., Echevarria, W., Koulen, P., Hirata, K., Bennett, A. M., et al. (2003). Nuclear and cytosolic calcium are regulated independently. *Proc. Natl. Acad. Sci. U.S.A.* 100, 2975–2980. doi: 10.1073/pnas.0536590100

Liu, X., Nefzger, C. M., Rossello, F. J., Chen, J., Knaupp, A. S., Firas, J., et al. (2017). Comprehensive characterization of distinct states of human naive pluripotency generated by reprogramming. *Nat. Methods* 14, 1055–1062. doi: 10.1038/nmeth.4436

Maier, T., Güell, M., and Serrano, L. (2009). Correlation of mRNA and protein in complex biological samples. *FEBS Lett.* 583, 3966–3973. doi: 10.1016/j.febslet.2009.10.036

Marcos, D., Sepulveda, M. R., Berrocal, M., and Mata, A. M. (2009). Ontogeny of ATP hydrolysis and isoform expression of the plasma membrane Ca^{2+}−ATPase in mouse brain. *BMC Neurosci.* 10:112. doi: 10.1186/1471-2202-10-112

Okunade, G. W., Miller, M. L., Pyne, G. J., Sutliff, R. L., O'Connor, K. T., Neumann, J. C., et al. (2004). Targeted ablation of plasma membrane Ca^{2+}−ATPase (PMCA) 1 and 4 indicates a major housekeeping function for PMCA1 and a critical role in hyperactivated sperm motility and male fertility for PMCA4. *J. Biol. Chem.* 279, 33742–33750. doi: 10.1074/jbc.M404628200

Patel, R., Al-Dossary, A. A., Stabley, D. L., Barone, C., Galileo, D. S., Strehler, E. E., et al. (2013). Plasma membrane Ca^{2+}−ATPase 4 in murine epididymis: secretion of splice variants in the luminal fluid and a role in sperm maturation. *Biol. Reprod.* 89, 6. doi: 10.1095/biolreprod.113.108712

Penniston, J. T., and Enyedi, A. (1998). Modulation of the plasma membrane Ca^{2+} pump. *J. Membr. Biol.* 165, 101–109. doi: 10.1007/s002329900424

Sahly, I., Dufour, E., Schietroma, C., Michel, V., Bahloul, A., Perfettini, I., et al. (2012). Localization of usher 1 proteins to the photoreceptor calyceal processes, which are absent from mice. *J. Cell Biol.* 199, 381–399. doi: 10.1083/jcb.201202012

Schöndorf, D. C., Aureli, M., McAllister, F. E., Hindley, C. J., Mayer, F., Schmid, B., et al. (2014). iPSC-derived neurons from GBA1-associated Parkinson's disease patients show autophagic defects and impaired calcium homeostasis. *Nat. Commun.* 5:4028. doi: 10.1038/ncomms5028

Sgobio, C., Kupferschmidt, D. A., Cui, G., Sun, L., Li, Z., Cai, H., et al. (2014). Optogenetic measurement of presynaptic calcium transients using conditional

genetically encoded calcium indicator expression in dopaminergic neurons. *PLoS ONE* 9:e111749. doi: 10.1371/journal.pone.0111749

Smith, A. (2017). Formative pluripotency: the executive phase in a developmental continuum. *Development* 144, 365–373. doi: 10.1242/dev.142679

Stauffer, T. P., Guerini, D., and Carafoli, E. (1995). Tissue distribution of the four gene products of the plasma membrane Ca pump. *J. Biol. Chem*. 270, 12184–12190. doi: 10.1074/jbc.270.20.12184

Stauffer, T. P., Guerini, D., Celio, M. R., and Carafoli, E. (1997). Immunolocalization of the plasma membrane Ca^{2+} pump isoforms in the rat brain. *Brain Res*. 748, 21–29. doi: 10.1016/S0006-8993(96)01282-6

Stehno-Bittel, L., Lückhoff, A., and Clapham, D. E. (1995). Calcium release from the nucleus by InsP3 receptor channels. *Neuron* 14, 163–167. doi: 10.1016/0896-6273(95)90250-3

Steinhardt, R. A., and Alderton, J. (1988). Intracellular free calcium rise triggers nuclear envelope breakdown in the sea urchin embryo. *Nature* 332, 364–366. doi: 10.1038/332364a0

Strehler, E. E., and Zacharias, D. A. (2001). Role of alternative splicing in generating isoform diversity among plasma membrane calcium pumps. *Physiol. Rev*. 81, 21–50. doi: 10.1152/physrev.2001.81.1.21

Suzuki, M., Sato, M., Koyama, H., Hara, Y., Hayashi, K., Yasue, N., et al. (2017). Distinct intracellular Ca^{2+} dynamics regulate apical constriction and differentially contribute to neural tube closure. *Development* 144, 1307–1316. doi: 10.1242/dev.141952

Thrasivoulou, C., Millar, M., and Ahmed, A. (2013). Activation of intracellular calcium by multiple Wnt ligands and translocation of β-catenin into the nucleus: a convergent model of Wnt/$Ca^{2+}$and Wnt/β-catenin pathways. *J. Biol. Chem*. 288, 35651–35659. doi: 10.1074/jbc.M112.437913

Tidow, H., Poulsen, L. R., Andreeva, A., Knudsen, M., Hein, K. L., Wiuf, C., et al. (2012). A bimodular mechanism of calcium control in eukaryotes. *Nature* 491, 468–472. doi: 10.1038/nature11539

Todorova, M. G., Fuentes, E., Soria, B., Nadal, A., and Quesada, I. (2009). Lysophosphatidic acid induces Ca^{2+} mobilization and c-Myc expression in mouse embryonic stem cells via the phospholipase C pathway. *Cell. Signal*. 21, 523–528. doi: 10.1016/j.cellsig.2008.12.005

Tombes, R. M., and Borisy, G. G. (1989). Intracellular free calcium and mitosis in mammalian cells: anaphase onset is calcium modulated, but is not triggered by a brief transient. *J. Cell Biol*. 109, 627–636. doi: 10.1083/jcb.109.2.627

Turner, D. A., Hayward, P. C., Baillie-Johnson, P., Rué, P., Broome, R., Faunes, F., et al. (2014). Wnt/β-catenin and FGF signalling direct the specification and maintenance of a neuromesodermal axial progenitor in ensembles of mouse embryonic stem cells. *Development* 141, 4243–4253. doi: 10.1242/dev.112979

Tzouanacou, E., Wegener, A., Wymeersch, F. J., Wilson, V., and Nicolas, J. F. (2009). Redefining the progression of lineage segregations during mammalian embryogenesis by clonal analysis. *Dev. Cell* 17, 365–376. doi: 10.1016/j.devcel.2009.08.002

Yanagida, E., Shoji, S., Hirayama, Y., Yoshikawa, F., Otsu, K., Uematsu, H., et al. (2004). Functional expression of Ca2+ signaling pathways in mouse embryonic stem cells. *Cell Calcium* 36, 135–146. doi: 10.1016/j.ceca.2004.01.022

Zanni, G., Cali, T., Kalscheuer, V. M., Ottolini, D., Barresi, S., Lebrun, N., et al. (2012). Mutation of plasma membrane Ca^{2+} ATPase isoform 3 in a family with X-linked congenital cerebellar ataxia impairs Ca^{2+} homeostasis. *Proc. Natl. Acad. Sci. U.S.A*. 109, 14514–14519. doi: 10.1073/pnas.1207488109

Zivkovic, D., Créton, R., and Dohmen, R. (1991). Cell cycle-related fluctuations in transcellular ionic currents and plasma membrane Ca2+/Mg2+ ATPase activity during early cleavages of *Lymnaea stagnalis* embryos. *Roux's Arch. Dev. Biol*. 200, 120–131. doi: 10.1007/BF00190231

Conflict of Interest Statement: The authors declare that the research was conducted in the absence of any commercial or financial relationships that could be construed as a potential conflict of interest.

frontiers in Cell and Developmental Biology

REVIEW
published: 09 January 2018
doi: 10.3389/fcell.2017.00121

Nuclear Envelope-Associated Chromosome Dynamics during Meiotic Prophase I

Xinhua Zeng, Keqi Li, Rong Yuan, Hongfei Gao, Junling Luo, Fang Liu, Yuhua Wu, Gang Wu and Xiaohong Yan**

Oil Crops Research Institute of the Chinese Academy of Agricultural Sciences, Key Laboratory of Biology and Genetic Improvement of Oil Crops, Ministry of Agriculture, Wuhan, China

Chromosome dynamics during meiotic prophase I are associated with a series of major events such as chromosomal reorganization and condensation, pairing/synapsis and recombination of the homologs, and chromosome movements at the nuclear envelope (NE). The NE is the barrier separating the nucleus from the cytoplasm and thus plays a central role in NE-associated chromosomal movements during meiosis. Previous studies have shown in various species that NE-linked chromosome dynamics are actually driven by the cytoskeleton. The linker of nucleoskeleton and cytoskeleton (LINC) complexes are important constituents of the NE that facilitate in the transfer of cytoskeletal forces across the NE to individual chromosomes. The LINCs consist of the inner and outer NE proteins Sad1/UNC-84 (SUN), and Klarsicht/Anc-1/Syne (KASH) domain proteins. Meiosis-specific adaptations of the LINC components and unique modifications of the NE are required during chromosomal movements. Nonetheless, the actual role of the NE in chromosomic dynamic movements in plants remains elusive. This review summarizes the findings of recent studies on meiosis-specific constituents and modifications of the NE and corresponding nucleoplasmic/cytoplasmic adaptors being involved in NE-associated movement of meiotic chromosomes, as well as describes the potential molecular network of transferring cytoplasm-derived forces into meiotic chromosomes in model organisms. It helps to gain a better understanding of the NE-associated meiotic chromosomal movements in plants.

Keywords: nuclear envelope, chromosome dynamics, meiosis prophase I, SUN proteins, KASH proteins, meiotic modification, cytoplasmic adaptors, nucleoplasmic adaptors

OPEN ACCESS

Edited by:
Rafael A. Fissore, University of Massachusetts Amherst, United States

Reviewed by:
Kim S. McKim, Rutgers University, The State University of New Jersey, United States
Song-Tao Liu, University of Toledo, United States

****Correspondence:***
Gang Wu
wugang@caas.cn
Xiaohong Yan
yanxiaohong@caas.cn

Specialty section:
This article was submitted to Cell Growth and Division, a section of the journal Frontiers in Cell and Developmental Biology

Received: *20 September 2017*
Accepted: *21 December 2017*
Published: *09 January 2018*

Citation:
Zeng X, Li K, Yuan R, Gao H, Luo J, Liu F, Wu Y, Wu G and Yan X (2018) Nuclear Envelope-Associated Chromosome Dynamics during Meiotic Prophase I. Front. Cell Dev. Biol. 5:121. doi: 10.3389/fcell.2017.00121

INTRODUCTION

Meiosis has the following characteristics, one round of DNA replication and two rounds of chromosome separation (Roeder, 1997). Prophase I is the longest and most complex phase of meiosis, which is vital to ensure the faithful completion of meiosis. A series of chromosome dynamics-associated events such as chromosomal reorganization and condensation, establishment of meiotic-specific chromosome structure, homologous chromosome pairing, and dynamic chromosome movements is closely integrated and finely spatiotemporally controlled during meiotic prophase I (Padmore et al., 1991; Dawe et al., 1994; Hunter and Kleckner, 2001; Blat et al., 2002; Borner, 2006; Golubovskaya et al., 2006; Kleckner, 2006; Zickler, 2006; Tiang et al., 2012). During meiosis, telomeres attach to the nuclear envelope (NE), which in turn drives

chromosome movement (Tiang et al., 2012). The NE is a highly conserved eukaryotic structure that protects DNA from enzymatic degradation (Stewart et al., 2007; Wilson and Dawson, 2011). Recent studies have shown that the NE fulfills distinct functions by regulating sets of the proteins that are embedded in the NE. Furthermore, the NE is a crucial determinant for reproduction and fertility; its particular components, the Klarsicht/ANC-1/Syne-1 homology (KASH) proteins and Sad-1/UNC-84 homology (SUN) proteins, play a key role in meiotic chromosome movements (Razafsky and Hodzic, 2009; Kracklauer et al., 2013; Subramanian and Hochwagen, 2014). Nonetheless, the precise role of the NE in chromosome dynamics remains elusive. Here, we review recent studies on meiosis-specific constituents and modifications involving the NE and related nucleoplasmic/cytoplasmic adaptors, as well as propose a molecular network of cytoplasm-derived forces that influence NE-linked meiotic chromosomal movements.

AN OVERVIEW OF THE NE STRUCTURE

In eukaryotes, the nucleus is a characteristic feature of eukaryotic cells that is enclosed by the NE. **Figure 1** shows the structure of the NE during interphase. The NE is a highly conserved eukaryotic double membrane that separates and protects the genetic material of cells (Stewart et al., 2007; Wilson and Dawson, 2011). The general structure of the NE consists of the inner nuclear membrane (INM), outer nuclear membrane (ONM), and the perinuclear space (PNS), which is about 50 nm in thickness and situated between the INM and ONM (**Figure 1**). The double nuclear membranes are connected by nuclear pore complexes (NPCs) and linkers of nucleoskeleton and cytoskeleton (LINC) complexes (**Figure 1**; Crisp et al., 2006). NPCs serve as the fusion site of the INM and ONM and form transport channels for macromolecules that move to and from the nucleus and cytoplasm. LINCs stabilize the structure of the NE, play important roles in cell division, and establish cellular polarity, fertilization, cellular migration, and differentiation by connecting the INM and ONM (Crisp et al., 2006; Rothballer et al., 2013; Sosa et al., 2013). However, despite these junctions, the ONM and INM are still divergent. The ONM is a specialized extension of the endoplasmic reticulum (ER), which is studded with ribosomes that facilitate protein synthesis (Park and Craig, 2010). The ONM also binds cytoskeletal components such as microtubules (MTs), as well as acts as a nucleation center of MTs during cell division (Han and Dawe, 2011; Masoud et al., 2013). A series of proteins in the INM interact with various nuclear constituents, including chromosomes and the nucleoskeleton, to ensure the link between the NE and the corresponding nuclear materials (Starr, 2009; Bickmore and van Steensel, 2013). The nuclear lamina as a protein network juxtaposed to the INM nucleoplasmic side. However, currently understanding of the nuclear lamina in plants is limited. An INM-linked dense meshwork was founded in plants by electron microscopy, that is similar to animal laminae (Ciska and de la Espina, 2014).

Recent studies have shown that the NE is not only a physical nucleocytoplasmic barrier, but also a multifunctional platform (Fransz and de Jong, 2011; Gross and Bhattacharya, 2011). The NE thus allows specific proteins to be embedded in the ONM and INM, respectively, thereby establishing specific cytoplasm-facing and nucleoplasm-facing functions. A collection of specific integral membrane proteins in the NE include nuclear pore complexes (NPCs), SUN proteins (Razafsky and Hodzic, 2009; Starr and Fridolfsson, 2010) in the INM, and KASH proteins (Wilhelmsen et al., 2006; Rothballer and Kutay, 2013) in the ONM. SUN proteins and KASH proteins form LINC complexes (Crisp et al., 2006). Thus, animal NE proteins transport nucleocytoplasmic macromolecules, are involved in chromosomal dynamics, regulate transcription, and induce aging and nuclear migration (Gruenbaum et al., 2005; Andres and Gonzalez, 2009; Hetzer and Wente, 2009; Starr, 2009). Furthermore, certain NE components play a key role in chromosome pairing and synapsis of homologs during meiosis (Subramanian and Hochwagen, 2014). The LINC complex is an important NE component that has been implicated in the directed movement of meiotic chromosomes within the nucleus (Razafsky and Hodzic, 2009; Kracklauer et al., 2013).

CHROMOSOME DYNAMICS IN MEIOSIS

DNA is replicated once, but chromosomes are segregated twice during meiosis (Roeder, 1997). Meiotic divisions are subdivided into meiosis I and meiosis II. Homologous chromosomes are separated in meiosis I, and sister chromatids are segregated from each other in meiosis II. A series of coordinated processes are required during the two meiotic divisions. Prophase I, metaphase I, anaphase I, and telophase I occur in meiosis I. Prophase I as the longest and most complex phase and is further subdivided into five distinguished stages according to the degree of chromatin condensation. The stages in succession are leptotene, zygotene, pachytene, diplotene, and diakinesis (Baarends and Grootegoed, 2003; Wijnker and Schnittger, 2013).

Chromosome dynamics including reorganization and condensation of chromosomes, homologous chromosome pairing, chromosome movements, and establishment of meiosis-specific chromosome structure occur during prophase I of meiosis (Tiang et al., 2012). Homologous chromosome pairing (Dawe et al., 1994) is tightly associated with the process of meiotic recombination (Tiang et al., 2012). Meiosis involves unique chromosome dynamic processes such as pairing/ synapsis and recombination of homologs that occur during meiotic prophase I, as have been extensively characterized in model systems involving *Saccharomyces cerevisiae*, *Schizosaccharomyces pombe*, and *C. elegans* (Hiraoka and Dernburg, 2009; Koszul and Kleckner, 2009). These meiosis-specific events are closely integrated and finely controlled temporally and spatially (Padmore et al., 1991; Hunter and Kleckner, 2001; Blat et al., 2002; Borner, 2006; Kleckner, 2006; Zickler, 2006). Synapsis and recombination ensure the establishment of chiasmata that hold homologous chromosomes together, thereby facilitating correct segregation (Tiang et al., 2012).

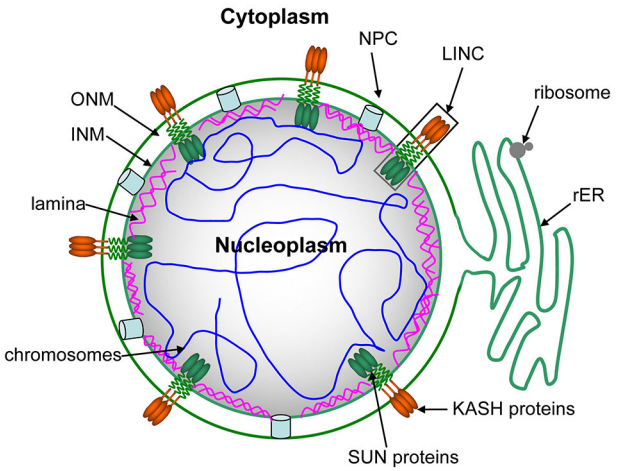

FIGURE 1 | The interphase structure of the NE. The NE consists of the inner nuclear membrane (INM), outer nuclear membrane (ONM) and the perinuclear space (PNS). The NE is embedded with nuclear pore complexes (NPCs), SUN proteins in the INM and KASH proteins in the ONM. LINC complexes are made of SUN proteins and KASH proteins, transferring cytoplasm-derived forces inti the chromosomes in the nucleoplasm. The ONM facing the cytoplasm is connected with the rough endoplasmic reticulum (rER). The nuclear lamina is a protein network that is situated close to the INM nucleoplasmic side. In plants, little is known about the nuclear lamina. However, electron microscopy has revealed there is an INM-associated dense meshwork, similar to the animal lamina.

TELOMERE MOVEMENTS AT THE NE DURING MEIOSIS

Telomeres are blocks of highly conserved repetitive DNA sequences at chromosome ends that protect chromosomes from nucleolytic degradation and fusion. The behavior of centromeres and telomeres largely controlls chromosomal dynamics of prophase I (Siderakis and Tarsounas, 2007). Previous studies have shown in various species that the cytoskeleton induces chromosomal movements using telomere-NE attachments (Bhalla and Dernburg, 2008; Koszul and Kleckner, 2009; Sheehan and Pawlowski, 2009; Woglar and Jantsch, 2014). During meiosis prophase I, telomere positions undergo dynamic changes, including telomeric attachment, clustering, dispersal, and redistribution across the nuclear periphery (**Figure 2**). During meiotic interphase, telomeres are distributed across the nucleolus instead of the NE. Prior to pairing, telomeres attach to the NE at the onset of leptotene stage. As leptotene proceeds, telomeres are attached to the NE and are stably linked to it. These tethered telomeres move within the INM and gather at a certain region, creating a characteristic flower-like structure, known as the bouquet of telomeres (Bass et al., 2000; Golubovskaya et al., 2002; Harper et al., 2004; Richards et al., 2012). Telomere clustering starts at the late leptotene stage, always overlaps with the zygotene stage, and usually persists until pachytene (Bass, 2003). The telomere bouquet always appears during the zygotene stage, after which telomeres are then scattered again. Despite telomere clustering may be observed at the early pachytene stage, if homologous chromosomes are completely paired at the end of pachytene, telomeres are dispersed evenly across the NE again while additional nuclear deformations and rotations occur.

The characteristic telomere-guided chromosome movements are an evolutionarily highly conserved hallmark of meiotic prophase I (Scherthan et al., 1996; Koszul and Kleckner, 2009). The telomere "bouquet" stage has been observed in all organisms studied regardless of whether they have big (maize) or small (fission yeast) genomes (Scherthan, 2001), except *C. elegans* and *Drosophila*, which both employ non-canonical methods of homology searching (Mckee, 2004).

FUNCTIONAL SIGNIFICANCE OF THE TELOMERE BOUQUET

Bouquet formation of telomeres feature chromosomal movements within the NE, which might facilitate homologous chromosome pairing and synapsis (Scherthan, 2001; Lee et al., 2012). Several lines of evidence show that one of the most likely functions of the bouquet is to warrant the efficient initiation of pairing and synapsis of between homologous chromosomes (Tabata, 1962; Carlton and Cande, 2002; Moens et al., 2011). Mutants with defects in bouquet generation always show defects in chromosome pairing, which suggests the possible role of the bouquet in chromosome pairing (Harper et al., 2004; Klutstein and Cooper, 2014). Several mutants, for example, *plural abnormalities of meiosis 1* (*pam 1*) (Golubovskaya et al., 2002), *desynaptic 1* (*dsy1*) (Bass et al., 2003), and *poor homologous synapsis1* (*phs1*) (Pawlowski et al., 2004) exhibit significant defects in homologous pairing in maize. Correspondingly, clusters of telomeres persist in pairing-defective *spo11* mutants of *Sordaria* and *S. cerevisiae* (Trelles-Sticken et al., 1999). Therefore, it seems likely that the bouquet physically brings homologous chromosomes into close proximity at a certain region of the NE, supporting homologous chromosome pairing and synapsis, double-strand break (DSB) repair, and recombination (Scherthan et al., 1996; Bass et al., 2000), thereby preventing and dissolving heterologous associations of non-homologous chromosomes (Zickler and Kleckner, 1998; Moens et al., 2011). However, the actual function of the meiotic bouquet is still not entirely clear.

LINC COMPLEXES

It has been shown in several species that the cytoskeleton induces dynamic motility of chromosomes via telomere-NE attachments (Bhalla and Dernburg, 2008; Koszul and Kleckner, 2009; Sheehan and Pawlowski, 2009; Woglar and Jantsch, 2014). The NE is the barrier separating the nucleus from the cytoplasm that plays a central role in the NE-associated chromosomal movements. Significantly, NE-linked chromosome dynamics are actually driven by the cytoskeleton during meiotic progression (Trelles-Sticken et al., 1999; Conrad et al., 2008; Koszul et al., 2008; Lee et al., 2012). The implication here is that there must be mechanisms that transmit cytoskeletal forces across the NE to individual chromosomes. The special double-layer-membrane

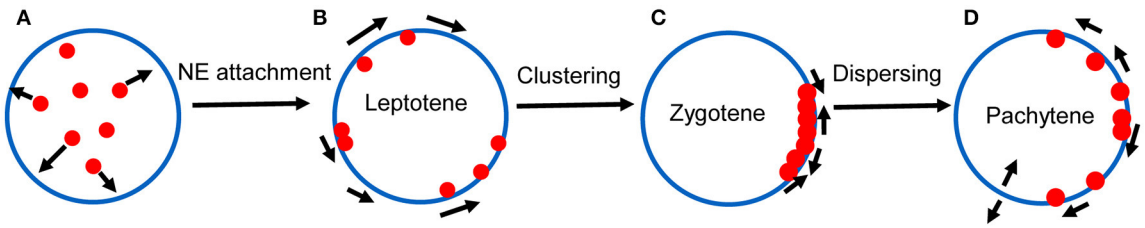

FIGURE 2 | Telomere movement at the NE during meiotic prophase. The four different movement classes are indicated as **(A–D)**. Red dots indicate the positions of the telomeres relative to the NE. The relative direction of telomeric movements is indicated by black arrows. **(A)** Telomeres scattering in the nucleus move to the NE at the onset of leptotene stage. **(B)** Telomeres are tethered to the NE and stably connected to it at the late leptotene stage. The telomere clustering starts in the late leptotene stage, always overlaps with the zygotene stage and usually persists until pachytene. **(C)** The tightest clustering of telomeres is usually observed at the zygotene stage. **(D)** At pachytene, telomeres are motile and scattered over the NE again, while additional nuclear deformations and rotations occur (black arrows). For further information please see the Scherthan (2007).

structure of the NE raises the question of how can various regions of chromosomes, telomeres in particular, be physically connected to the cytoskeleton during meiosis. Because the NE remains intact during the process of synapsis, there has to be a molecular machinery spanning both the INM and ONM and interacting with chromatin and other cytoskeletal components, respectively. The LINC complexes consist of SUN domain family proteins in the INM and KASH domain homology proteins in the ONM (Burke and Roux, 2009; Razafsky and Hodzic, 2009; Starr and Fridolfsson, 2010).

The LINC complexes span the INM and ONM and form the bridge between the nucleoskeleton and the cytoskeleton through the SUN-KASH domain interaction in the NE lumen (Razafsky and Hodzic, 2009; Starr and Fridolfsson, 2010; Kim et al., 2015). In this way, mechanical forces from the cytoskeleton are directly transduced to the NE and then into chromosomes. A chain of interactions from the cytoskeletal elements to the nucleoskeleton as follows, various components of the cytoskeleton interact with the cytoplasmic domains of KASH proteins, which in turn induces SUN proteins in the INM to interact with KASH proteins at their C-termini in the PNS and with specific nuclear contents at the N-termini in the nucleoplasm (Haque et al., 2006; Bone et al., 2014). The LINC complexes are responsible for the transfer of this force across the nuclear envelope and enable a direct communication and connection between nuclear and cytoplasmic content.

SUN DOMAIN PROTEINS

Molecular Characteristics of Sun Proteins

SUN proteins as important INM-integral components of LINC complexes that exhibit highly conserved structure and function (Starr, 2009). SUN proteins comprise an N-terminal region and a C-terminal region that are separated by one or more transmembrane domains (TMDs) (Tzur et al., 2006; Worman and Gundersen, 2006). The N-termini of SUN proteins are variable and directly or indirectly interact with lamins, which are the components of the nucleoskeleton (Lee et al., 2002; Crisp et al., 2006; Haque et al., 2006; Bone et al., 2014) and tether chromosomes to the nuclear periphery (Bupp et al., 2007; King et al., 2008; Morimoto et al., 2012; Link et al., 2014). The C-terminal region contains the well-conserved SUN domain, which extends into the PNS that interacts with KASH proteins. Most SUN proteins have coiled-coil domains (CCDs) at their N-termini, which facilitate in domain trimerization (Sosa et al., 2012; Zhou et al., 2012b).

Two divergent classes of SUN proteins have been identified by homology searching in plants: classical SUN proteins which contain SUN domains at the C-terminus (Murphy et al., 2010), and a second group of SUN proteins, with SUN domains in the center of the SUN protein, and thus designated as mid-SUN proteins (Murphy et al., 2010). The function of mid-SUN proteins is far less well-understood than the Cter-SUNs. Mid-SUN proteins differ from Cter-SUN proteins in both structure and localization. Mid-SUN proteins frequently contain three TMDs and plant mid-SUN proteins usually contain a conserved PM3-associated domain (PAD) (Murphy et al., 2010; Graumann et al., 2014). In addition, mid-SUN proteins are located in both the NE and the ER (Murphy et al., 2010; Graumann et al., 2014).

Members and Functions of Sun Proteins

SUN domain proteins have been identified in various species (**Table 1**). Three *Arabidopsis* SUN proteins (AtSUN3, AtSUN4, and AtSUN5) and three maize SUN proteins (ZmSUN3, ZmSUN4, and ZmSUN5) belong to the mid-SUN group (Murphy et al., 2010; Murphy and Bass, 2012; Graumann et al., 2014). The presence of several SUN protein members in a single organism (often at least five in humans) and their ability to form multimers implicate these are involved in a wide range of important cellular functions. Reports have shown that SUN proteins are implicated in interactions with lamins, nuclear positioning, spindle architecture, apoptosis, centrosome linkage to the nucleus, and maintenance of even spacing between the INM and ONM (**Table 1**). In addition, SUN proteins are required in a number of systems to attach telomeres or pairing centers to the NE during meiosis (Chikashige et al., 2006; Ding et al., 2007; Penkner et al., 2007; Conrad et al., 2008; Koszul et al., 2008). For example, SUN1, SUN2, Sad1, and Mps3 tether chromosomes to the nuclear periphery by interacting with telomere-binding proteins (Bupp et al., 2007; King et al., 2008; Morimoto et al., 2012; Link et al., 2014). The SUN protein trimer can usually bind three KASH domains of KASH homology proteins in the PNS (Sosa et al., 2012; Zhou et al., 2012a). In maize, ZmSUN2 produces a unique belt-like structure at the NE that undergoes

TABLE 1 | Members and functions of the SUN protein family.

Members	Functions	References
Mammals		
SUN1 SUN2	Movement and attachment of telomere in meiosis; nuclear anchorage and migration; integrity of the NE; recruit KASH proteins	Hodzic et al., 2004; Padmakumar et al., 2004; Crisp et al., 2006; Haque et al., 2006; Ding et al., 2007; Zhang et al., 2009; Morimoto et al., 2012
SUN3	Links the nucleus to posterior manchette during sperm head formation	Göb et al., 2010
SPAG4	Not at the NE, function unknown	Shao et al., 1999
SPAG4L	Not at the NE; Links the acrosomic vesicle to the spermatid nucleus; involved in acrosome biogenesis	Frohnert et al., 2011
Drosophila		
Klaroid	Nuclear anchorage during Drosophila oogenesis.; nuclear migration	Patterson et al., 2004; Yu et al., 2006; Kracklauer et al., 2007
SPAG4/Giacomo	Not at the NE; involved in centriolar-nuclear attachment during spermatogenesis	Malone et al., 2003
C. elegans		
UNC-84	Nuclear positioning; nuclear anchorage and migration	Starr et al., 2001; Starr and Han, 2002
SUN-1/matefin	Links the centrosome to nucleus; homologous chromosome pairing and synapsis in meiosis; apoptosis	Malone et al., 2003; Tzur et al., 2006; Penkner et al., 2009; Sato et al., 2009
S. pombe		
Sad1	Spindle architecture; meiotic chromosome pairing and synapsis	Shimanuki et al., 1997; Miki et al., 2004; Chikashige et al., 2006; Ding et al., 2007
S. cerevisiae		
Mps3	Linkage to the NE of SPB; SPB duplication; telomere attachment to and clustering within the NE	Jaspersen et al., 2006; Conrad et al., 2008; Wanat et al., 2008; Horigome et al., 2011
Arabidopsis		
AtSUN1 AtSUN2	Recruit KASH proteins to the NE; nuclear elongation and movement; meiotic recombination and synapsis	Graumann et al., 2010; Oda and Fukuda, 2011; Zhou et al., 2012a, 2015a,b; Tamura et al., 2013; Varas et al., 2015
AtSUN3, AtSUN4, AtSUN5	Mid-SUN proteins; seed development and involved in nuclear morphology	Graumann, 2014; Zhou et al., 2015b
Maize		
ZmSUN1 ZmSUN2	Involved in meiotic telomere dynamics	Murphy et al., 2014
ZmSUN3 ZmSUN4 ZmSUN5	Mid-SUN proteins; ZmSUN3 plays a role in meiosis; ZmSUN4/ZmSUN5: unknown functions	Murphy et al., 2010; Murphy and Bass, 2012
Dictyostelium		
Sun-1	Centrosome attachment; genome stability	Xiong et al., 2008

remarkable dynamic changes during meiosis (Murphy et al., 2014). Accordingly, AtSUN1 and AtSUN2 have been localized to meiotic prophase I-specific regions (Varas et al., 2015). In maize, ZmSUN3 as a mid-SUN protein, has been supposed to play an important role in meiotic divisions (Murphy and Bass, 2012). Of the five identified SUN proteins of mammals, SUN1 and SUN2 proteins have been demonstrated to be the only ones that are also expressed in meiotic cells, thereby indicating dual somatic and meiotic functions (Schmitt et al., 2007; Chi et al., 2009; Yu et al., 2011). To date, studies involving SUN1- and SUN1/SUN2-deficient mice have revealed that although SUN2 functions in part similarly to SUN1 in meiosis, SUN2 can not effectively compensate for the loss of SUN1 in meiosis (Schmitt et al., 2007; Chi et al., 2009; Lei et al., 2009). However, a single mutation for either *SUN1* or *SUN2* genes has no effect on reproduction or meiosis in *A. thaliana* (Varas et al., 2015). Several groups have then hypothesized that SUN1 and SUN2 assemble heteromultimeric complexes (Wang et al., 2006; Lu et al., 2008). Taking into account that in mice, SUN2 protein shares its localization with SUN1 protein and meiotic KASH5 protein, it is then speculated that during normal meiosis SUN1 and SUN2 form heterotrimers which interact with KASH5 protein to assemble meiotic LINCs. In the absence of SUN1, LINCs may only consist of SUN2 and KASH5, still attaching telomeres of chromosomes to the NE, yet in a less effective way than complete SUN1/SUN2-KASH5 complexes. And then this could explain the partial redundancy between SUN1 and SUN2 in mice. Further research is required to determine how these SUN family members coordinate in the near future.

KASH DOMAIN PROTEINS

Molecular Characteristics of KASH Proteins

Four criteria were employed to define KASH proteins (Starr, 2011). First, KASH proteins are positioned at the ONM. Second, the C-terminal KASH domain is essential for interaction between KASH and SUN proteins. Third, the KASH domains ensure

their localization to the ONM (Crisp et al., 2006). Fourth, N-terminal domains of KASH proteins are not highly conserved and are linked to the cytoskeleton. The KASH domain usually includes a hydrophobic transmembrane domain and a sequence of 6–30 amino acids in the PNS. The perinuclear 6- to 30-amino acid domain of KASH proteins is usually highly conserved, for example, 13 of 20 residues are identical between *C. elegans* ANC-1 and human Syne/Nesprin-1/-2. The terminal region of the perinuclear sequence of the KASH domain consists of a highly conserved four-amino acid motif PPPX in most animals; however, specifically, the penultimate proline appears to be widely conserved across kingdoms, which is essential in mediating SUN-KASH interaction (Lenne et al., 2000; Razafsky and Hodzic, 2009; Starr and Fridolfsson, 2010; Sosa et al., 2012). Apart from the PPPX motif, the last C-terminal four amino acids of plant KASH proteins are usually XVPT (X represents V/A/L/P) (Zhou et al., 2012a; Zhou and Meier, 2013). Similar to SUN proteins, KASH domain proteins can also form multimers (Djinovic-Carugo et al., 2002; Mislow et al., 2002). The SUN-KASH complexe usually comprise SUN protein trimers and KASH protein trimers. SUN-KASH interactions occur when the KASH domain fits into a hydrophobic pocket that is assembled by three SUN proteins.

Members and Functions of KASH Proteins

To date, KASH domain proteins have been identified in various species (**Table 2**). These KASH proteins are involved in different processes, such as nuclear migration, linkage to the nucleus, attaching nuclei to actin filaments and so on (**Table 2**).

The less similarity between KASH domains is very weak, suggesting that many KASH proteins have yet to be discovered. For example, *C. elegans* ZYG-12 and *S. cerevisiae* Csm4 poorly aligns with other KASH domains, but these fit the criteria for KASH proteins (Starr and Fischer, 2005; Conrad et al., 2008; Koszul et al., 2008). Tryptophan–proline–proline (WPP)-interacting proteins (WIP)1-3 and SUN-interacting NE 1-2 proteins (SINE 1-2) are plant-specific KASH proteins that share a low degree of similarity with metazoan KASH proteins (Graumann et al., 2010; Oda and Fukuda, 2011; Zhou et al., 2012a, 2014; Zhou and Meier, 2013). These proteins reside in the ONM via SUN-KASH interactions, fulfilling the criteria for KASH proteins mentioned. AtTIK is a novel *Arabidopsis* KASH domain protein that has been identified using a split-ubiquitin-based membrane yeast two-hybrid screen (Graumann et al., 2014).

TABLE 2 | Members and functions of the KASH protein family.

Members	Functions	References
Mammals		
Syne-1 (Nesprin-1) Syne-2 (Nesprin-2)	Attach nuclei to actin filaments; nuclear migration and nucleokinesis	Apel et al., 2000; Zhang et al., 2007, 2009
Nesprin-3	A versatile connector between the nucleus and the cytoskeleton	Ketema and Sonnenberg, 2011
Nesprin-4	Binding kinesin; cell polarization	Roux et al., 2009
KASH 5	Dynein-driven telomere dynamics in meiosis	Morimoto et al., 2012
Drosophila		
Klarsicht	Anchoring microtubules to the NE; nuclear migration and centrosome attachment	Mosleybishop et al., 1999; Patterson et al., 2004; Elhananytamir et al., 2012
MSP-300	Nuclear anchorage	Yu et al., 2006
C. elegans		
KDP-1	Cell- cycle progression	Mcgee et al., 2009
ANC-1	Nuclear anchorage	Starr and Han, 2002
UNC-83	Nuclear migration	Starr et al., 2001; Meyerzon et al., 2009
ZYG-12	Links centrosomes to nuclei; meiotic chromosome paring and synapsis	Malone et al., 2003; Sato et al., 2009; Zhou et al., 2009
S. pombe		
Kms1	Meiotic dynein-driven chromosome movement and pairing	Miki et al., 2004; Chikashige et al., 2006
Kms2	Meiotic and mitotic chromosome movements	Miki et al., 2004; Chikashige et al., 2006; King et al., 2008
S. cerevisiae		
Csm4	Meiotic actin-driven chromosome movements and pairing	Conrad et al., 2008; Koszul et al., 2008
Dictyostelium		
Interaptin	Function unknown	Rivero et al., 1998
Arabidopsis		
WIP1-3	Anchors WIT1-2 to the NE; anchoring RanGAP to the NE	Yu et al., 2011; Zhou et al., 2012b, 2015b
SINE1	Actin-dependent nuclear positioning	Zhou et al., 2014
SINE2	Contributes to innate immunity against an oomycete pathogen	Zhou et al., 2014
AtTIK	Function unknown	Graumann et al., 2014

Among these reported KASH proteins, only mammalian KASH5, *C. elegans* ZYG-12, and yeast Kms1, Kms2, and Csm4 have been confirmed to be involved in meiosis (**Table 2**).

Meiosis-Specific Adaptations Involving the NE

Although the NE has a highly conserved basic structure in eukaryotes, it also undergoes meiosis-specific adjustment to facilitate chromosome dynamics. The nuclear lamina is a protein network that is juxtaposed to the INM nucleoplasmic side. It is mainly composed of lamin proteins. In animals, the nuclear lamina undergoes significant modifications in lamin B1 (B-type lamin) and lamin C2 (A-type lamin isoform) during meiosis, and lamin C2 is exclusively expressed in meiotic cells. This implicates that NE is modified to adapt to the requirements of meiosis (Furukawa et al., 1994; Alsheimer and Benavente, 1996). Current understanding of the functions of the nuclear lamina is limited in plants. It has been postulated that the nuclear matrix component protein (NMCP) family members are likely the best appropriate candidates for plant lamins (Ciska and de la Espina, 2014). Fluorescence resonance energy transfer experiments have shown that the N-termini of AtSUN1 and AtSUN2 co-localize with CRWN1, which is a member of the NMCP family in *Arabidopsis* (Graumann, 2014). However, its physical co-localization does not demonstrate that AtSUN1 and AtSUN2 directly or indirectly interact with CRWN1. Investigations on meiosis-specific adjustments with respect to components and functions of the nuclear lamina in plants are limited.

LINC complexes are important components of the NE that also undergo remarkable adaptations to the requirements of meiosis. SUN proteins and KASH proteins are encoded by various genes that are differentially expressed in various cell types and tissues (Roux et al., 2009; Göb et al., 2010, 2011; Frohnert et al., 2011; Kracklauer et al., 2013; Duong et al., 2014). LINC complexes generally exhibit features that involve specific cellular processes. Meiotic chromosomal movements within the NE are driven by cytoskeletal forces that span the double NE and are transferred to the chromosomes via specific LINC complexes (Kracklauer et al., 2013; Yamamoto, 2014). Unique reconstruction of the NE structure and formation of meiosis-specific LINC complexes are required during telomere attachment, movements, clustering, and reposition (Hiraoka and Dernburg, 2009). The meiosis-specific LINC complexes are modulated with respect to their constituent proteins and interaction partners (**Table 3**). LINC complexes are species-specific. In mice, meiosis-specific LINC complexes are composed of SUN1 and/or SUN2, and KASH5, which promote chromosome pairing and synapsis (Ding et al., 2007; Schmitt et al., 2007; Morimoto et al., 2012). The SUN protein Sad1 directly interacts with a KASH protein Kms1, assembling a functional meiotic LINC complex in *S. pombe* (Miki et al., 2004). The KASH domain protein ZYG-12 as a SUN1-interacting meiotic LINC component in *C. elegans* (Malone et al., 2003). The *Zea mays* SUN protein, ZmSUN3 is necessary for homologous chromosome synapsis, recombination, and chromosome segregation (Murphy et al., 2010; Murphy and Bass, 2012). However, the real meiotic KASH partner of ZmSUN3 remains elusive. In *Arabidopsis*, AtSUN1 and AtSUN2 are both associated with meiosis (Duroc et al., 2014; Varas et al., 2015). At the same time, the *Arabidopsis* genome encodes four KASH proteins, three WIP proteins (AtWIP1, AtWIP2, and AtWIP3) and one AtTIK protein, which all interact with AtSUN1 (Zhou et al., 2012a; Graumann et al., 2014). However, their definitive meiosis-specific functions remain unclear.

Kinase-Associated Meiosis-Specific Modifications of the NE

The meiosis-specific functions of the ubiquitously expressed SUN proteins indicate that SUN proteins undergo post-translational modifications to mediate their meiotic functions. The Polo-like family of Ser/Thr kinase (PLK) of *C. elegans* co-localizes with PCs during meiosis, bringing about aggregation of SUN-1/ZYG-12 within the NE, thereby mediating dynein-driven chromosomal motions (Harper et al., 2011; Labella et al., 2011; Wynne et al., 2012; Rog and Dernburg, 2015). Phosphorylation modifications of the SUN1 nucleoplasmic domain through checkpoint protein kinase (CHK) family members CHK-2 and PLK-2 influence SUN1 motions within the INM during meiosis in *C. elegans* (Penkner et al., 2009; Sato et al., 2009; Labella et al., 2011). A recent study has shown that CHK-2 is a master regulator of meiosis in *C. elegans*, which first phosphorylates PC-binding zinc finger proteins HIM-8 and ZIMs, which in turn recruits PLK-2 to PCs (Kim et al., 2015).

Cyclin-dependent kinases (CDKs) are another group of highly conserved serine/threonine protein kinases that have been detected in various species from yeast to humans and play key roles in regulating the cell cycle and the cell division. During mammalian meiotic prophase I, CDK2 plays a critical role in meiosis-associated telomeric dynamics and meiosis-specific modifications of the NE components (Ashley et al., 2001; Berthet et al., 2003; Ortega et al., 2003; Viera et al., 2009, 2015). In

TABLE 3 | Constituents of meiotic-specific LINC complexes in various organisms.

	S. *pombe*	*S. cerevisiae*	*C. elegans*	Mice	*Arabidopsis*	Maize
SUN domain proteins	Sad1	Mps3	Metafin/SUN-1	SUN1, SUN2	AtSUN1, AtSUN2	ZmSUN1, ZmSUN2, ZmSUN3
KASH domain proteins	Kms1, Kms2	Csm4	ZYG-12	KASH5	AtWIP1-3	U

U, Unidentified.

mice, CDK2 mediates the accurate dynamic distribution of SUN1 protein via phosphorylation of SUN1 protein. SUN1 persists at the NE as a cap from the leptotene to pachytene phases in the absence of CDK2 in mice. CDK2 also affects the assembly of the meiosis-specific nuclear lamina. In the absence of CDK2, the distribution of lamin C2, a meiosis-specific isoform of lamin A and LAP2 (lamin-associated protein) are severely impaired, with a complete lack of LAP2 (Viera et al., 2015). However, the possible pathways to determine altered distribution of lamin C2 in meiosis are unknown.

Meiosis-Specific Adaptors between Telomeres/PCs and LINC

Telomeres link chromosomes to the NE through the LINCs. From yeast to humans, telomeres (or pairing centers in the worm) are always anchored to the NE by specific adaptors in the meiosis prophase I. The linkers connecting telomeres to LINCs are mainly composed telomere-binding proteins. In *S. pombe*, the linker between LINCs and telomeres is mediated by telomeric proteins Taz-1 and Rap-1, and the meiosis-specific proteins, Bouquet1-4 (Bqt1-4) (Chikashige et al., 2006, 2009). In *C. elegans*, chromosomes are connected to the NE through chromosome-specific pairing centers (PCs), instead of telomeres. Accordingly, LINCs tether chromosomes to the NE through PC-specific proteins, ZIM-1, ZIM-2, ZIM-3, and HIM-8 (Phillips et al., 2005; Phillips and Dernburg, 2006; Penkner et al., 2007; Sato et al., 2009; Baudrimont et al., 2010). During meiosis in *S. cerevisiae*, Ndj1 as a meiosis-specific adaptor connects LINCs to telomeres (Conrad et al., 2007, 2008). In mammals, telomere repeat-binding bouquet formation protein 1/2 (TERB1/2) and membrane-anchored junction protein (MAJIN) form a complex, TERB1/2-MAJIN, which serves as a meiosis-specific link between telomeres and LINCs (Daniel et al., 2014; Shibuya et al., 2014, 2015). In addition, meiotic LINCs of mammals are able to interact with meiosis-specific laminae. It is unknown whether meiosis-specific lamina proteins have an effect on telomere connection with LINCs. Currently, how telomeres are modified to mediate telomeric attachment to the NE during meiosis in plants remains unclear.

Meiosis-Specific Adaptors between the Cytoskeleton and the LINC

Anchoring linkers bridging LINCs and the cytoskeleton are responsible for transferring cytoskeletal forces to the NE, which then mediates meiotic chromosome movements along the NE during prophase I stages that comprise cytoskeleton or associated motor proteins (Koszul and Kleckner, 2009; Kracklauer et al., 2013). The LINC-complex is bound to the actin cytoskeleton via the atypical KASH protein Csm4 and actin in *S. cerevisiae* (Conrad et al., 2007, 2008). The LINC-complex is connected to microtubules (MTs) in the cytoplasm through Kms1 (KASH protein) and dynein light chain-family protein Dlc1 in *S. pombe* (Miki et al., 2002), KASH5, and dynein in mammals (Morimoto et al., 2012; Rothballer and Kutay, 2013), ZYG-12 KASH protein and dynein motors in *C. elegans* (Sato et al., 2009; Wynne et al., 2012), KASH proteins AtWIP-1, AtWIP-2 and a kinesin1-like

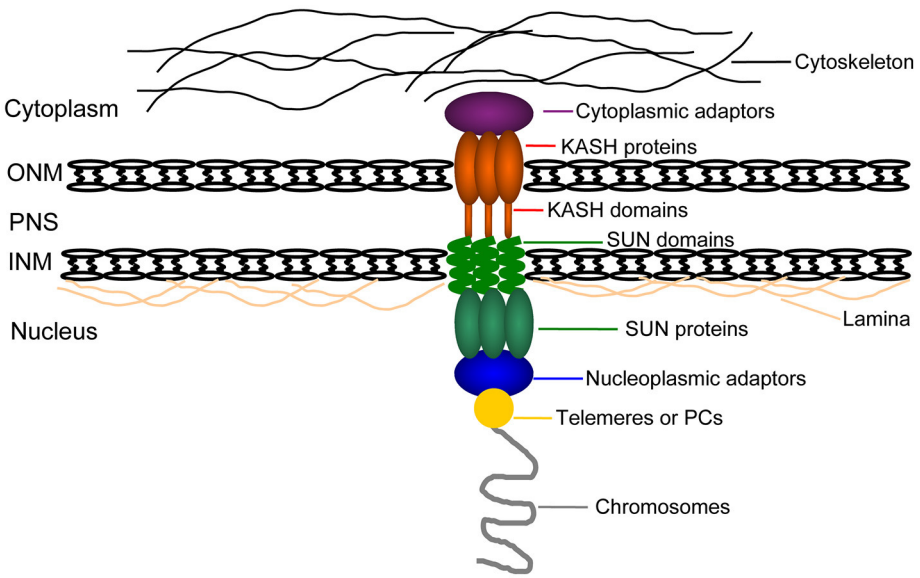

FIGURE 3 | A schematic representation of the link transferring cytoplasm forces into meiotic chromosomes. Telomeres or PCs (gold circle) connect to the NE through nucleoplasmic adaptors (schematized with a blue oval) and the nucleoplasmic domains (in green ovals) of SUN-domain proteins spanning the INM (in green; shown as a trimer). KASH domain proteins span the ONM (in red; shown as a trimer). Then SUN domains (in green helix) can interact with KASH domains (in red stub) in the PNS. Cytoplasmic adaptors (in purple) connect the cytoplasmic domains (in red ovals) of KASH proteins to the cytoskeleton (in black lines). The nucleoplasmic domains of SUN proteins can also interact with lamins (in orange). Cytoskeleton, cytoplasmic adaptors, SUN-KASH protein bridges, nucleoplasmic adaptors and telomeres/PCS form the central link that spans the nuclear envelope, transferring cytoplasm-derived forced into chromosomes. NE, nuclear envelope; INM, inner nuclear membrane; ONM, outer nuclear membrane; PNS, the perinuclear space.

protein AtPSS1 in *Arabidopsis* (Duroc et al., 2014; Wang et al., 2014).

An Integrated Mechanical System Transferring Cytoplasm Forces into Meiotic Chromosomes

The mechanisms responsible for dynamic chromosome movements have been partially deciphered in model organisms (**Figure 3**). The LINC complex couples the microtubule network and chromosomes. Nucleoplasmic adaptors tether telomeres or PCs (in *C. elegans*) to LINCs. Cytoplasmic adaptors connect cytoskeleton or cytoskeleton-associated proteins to LINC. The network between the cytoskeleton and chromosomes is telomeres/PCs-nucleoplasmic adaptors-NE-cytoplasmic adaptors-cytoskeleton. The molecular link system by which these forces are implemented differs in constituents in various organisms, telomeres-Taz1/Rap1/Bqt(1-4)-Sad1-Kms1/2-dynein (Dlc1)-MTs in *S. pombe*; PCs-ZIM(1-3)/HIM8-SUN1-ZYG12-Dynein-MTs in *C. elegans*; telomeres-Ndj1-Mps3-Csm4-actin-actin cable in *S. cerevisiae*; telomeres-TERB1/2/MAJIN-SUN1/SUN2-KASH5-dynein-MTs in mice; and telomeres-?-AtSUN1/AtSUN2-AtWIP1/2-kinesin (AtPSS1)-MTs in *Arabidopsis*. Whether and how NMCP family proteins and modification of SUN proteins are involved in the above molecular link system in plants remain unclear.

CONCLUSIONS AND FUTURE PERSPECTIVES

Telomere-led chromosomal dynamics within the NE and mediated by LINCs are pivotal for meiosis and thus fertility. The NE as a regulatory platform is finely modified with respect to its constituents in meiosis. Meiosis-specific adaptations of the LINC components, cytoplasmic linkers, and nucleoplasmic linkers contribute to these movements. Our current knowledge of the LINC network can serve as a starting point for future studies in plants. KASH proteins are not well conserved and thus warrant identification of additional novel family members. There are still a number of issues concerning the meiotic adaptions of the NE that need to be addressed. How are ubiquitously expressed NE components regulated during meiosis? Are plant NMCP family proteins involved in telomeric attachment to the NE, similar to the lamina proteins? Are there more adaptor molecules participating in the LINC network?

AUTHORS CONTRIBUTIONS

XY and XZ wrote the manuscript. RY, KL, HG, and JL contributed to the preparation of this manuscript. FL, YW, and GW organized and reviewed the manuscript. All authors have read and approved the final manuscript.

ACKNOWLEDGMENTS

The Natural Science Foundation of Hubei Province (grant numbers 2013CFB423 and 2014CFB320), the National Natural Science Foundation of China (grant numbers 31400243 and 31201152), the National Grand Project of Science and Technology (2018ZX08012001 and 2018ZX0801104B), Breeding special grants of seven major crops (2017YFD0102000), and the Major Research Project of CAAS Science and Technology Innovation Program supported this study.

REFERENCES

Alsheimer, M., and Benavente, R. (1996). Change of karyoskeleton during mammalian spermatogenesis: expression pattern of nuclear lamin C2 and its regulation. *Exp. Cell Res.* 228, 181–188. doi: 10.1006/excr.1996.0315

Andrés, V., and González, J. M. (2009). Role of A-type lamins in signaling, transcription, and chromatin organization. *J. Cell Biol.* 187, 945–957. doi: 10.1083/jcb.200904124

Apel, E. D., Lewis, R. M., Grady, R. M., and Sanes, J. R. (2000). Syne-1, a dystrophin- and Klarsicht-related protein associated with synaptic nuclei at the neuromuscular junction. *J. Biol. Chem.* 275, 31986–31995. doi: 10.1074/jbc.M004775200

Ashley, T., Walpita, D., and De Rooij, D. G. (2001). Localization of two mammalian cyclin dependent kinases during mammalian meiosis. *J. Cell Sci.* 114, 685–693.

Baarends, W. M., and Grootegoed, J. A. (2003). Chromatin dynamics in the male meiotic prophase. *Cytogenet. Genome Res.* 103, 225–234. doi: 10.1159/000076808

Bass, H. W. (2003). Telomere dynamics unique to meiotic prophase: formation and significance of the bouquet. *Cell. Mol. Life Sci.* 60, 2319–2324. doi: 10.1007/s00018-003-3312-4

Bass, H. W., Bordoli, S. J., and Foss, E. M. (2003). The desynaptic (dy) and desynaptic1 (dsy1) mutations in maize (*Zea mays* L) cause distinct telomere-misplacement phenotypes during meiotic prophase. *J. Exp. Bot.* 54, 39–46. doi: 10.1093/jxb/erg032

Bass, H. W., Riera-Lizarazu, O., Ananiev, E. V., Bordoli, S. J., Rines, H. W., Phillips, R. L., et al. (2000). Evidence for the coincident initiation of homolog pairing and synapsis during the telomere-clustering (bouquet) stage of meiotic prophase. *J. Cell Sci.* 113(Pt 6), 1033–1042.

Baudrimont, A., Penkner, A., Woglar, A., Machacek, T., Wegrostek, C., Gloggnitzer, J., et al. (2010). Leptotene/zygotene chromosome movement via the SUN/KASH protein bridge in *Caenorhabditis elegans*. *PLoS Genet.* 6:e1001219. doi: 10.1371/journal.pgen.1001219

Berthet, C., Aleem, E., Coppola, V., Tessarollo, L., and Kaldis, L. (2003). *Cdk2* knockout mice are viable. *Curr. Biol.* 13, 1775–1785. doi: 10.1016/j.cub.2003.09.024

Bhalla, N., and Dernburg, A. F. (2008). Prelude to a division. *Cell Dev. Biol.* 24, 397–424. doi: 10.1146/annurev.cellbio.23.090506.123245

Bickmore, W. A., and van Steensel, B. (2013). Genome architecture: domain organization of interphase chromosomes. *Cell* 152, 1270–1284. doi: 10.1016/j.cell.2013.02.001

Blat, Y., Protacio, R. U., Hunter, N., and Kleckner, N. (2002). Physical and functional interactions among basic chromosome organizational features govern early steps of meiotic chiasma formation. *Cell* 111, 791–802. doi: 10.1016/S0092-8674(02)01167-4

Bone, C. R., Tapley, E. C., Gorjánácz, M., and Starr, D. A. (2014). The *Caenorhabditis elegans* SUN protein UNC-84 interacts with lamin to transfer forces from the cytoplasm to the nucleoskeleton during nuclear migration. *Mol. Biol. Cell* 25, 2853–2865. doi: 10.1091/mbc.E14-05-0971

Börner, G. V. (2006). Balancing the checks: surveillance of chromosomal exchange during meiosis. *Biochem. Soc. Trans.* 34, 554–556. doi: 10.1042/BST0340554

Bupp, J. M., Martin, A. E., Stensrud, E. S., and Jaspersen, S. L. (2007). Telomere anchoring at the nuclear periphery requires the budding yeast Sad1-UNC-84

domain protein Mps3. *J. Cell Biol.* 179, 845–854. doi: 10.1083/jcb.200706040

Burke, B., and Roux, K. J. (2009). Nuclei take a position: managing nuclear location. *Dev. Cell*. 17, 587–597. doi: 10.1016/j.devcel.2009.10.018

Carlton, P. M., and Cande, W. Z. (2002). Telomeres act autonomously in maize to organize the meiotic bouquet from a semipolarized chromosome orientation. *J. Cell Biol.* 157, 231–242. doi: 10.1083/jcb.200110126

Chi, Y. H., Cheng, L. I., Myers, T., Ward, J. M., Williams, E., Su, Q., et al. (2009). Requirement for Sun1 in the expression of meiotic reproductive genes and piRNA. *Development* 136, 965–973. doi: 10.1242/dev.029868

Chikashige, Y., Tsutsumi, C., Yamane, M., Okamasa, K., Haraguchi, T., and Hiraoka, Y. (2006). Meiotic proteins bqt1 and bqt2 tether telomeres to form the bouquet arrangement of chromosomes. *Cell* 125, 59–69. doi: 10.1016/j.cell.2006.01.048

Chikashige, Y., Yamane, M., Okamasa, K., Tsutsumi, C., Kojidani, T., Sato, M., et al. (2009). Membrane proteins Bqt3 and−4 anchor telomeres to the nuclear envelope to ensure chromosomal bouquet formation. *J. Cell Biol.* 187, 413–427. doi: 10.1083/jcb.200902122

Ciska, M., and de la Espina, M. D. S. (2014). The intriguing plant nuclear lamina. *Front. Plant Sci.* 5:166. doi: 10.3389/fpls.2014.00166

Conrad, M. N., Lee, C. Y., Chao, G., Shinohara, M., Kosaka, H., Shinohara, A., et al. (2008). Rapid telomere movement in meiotic prophase is promoted by NDJ1, MPS3, and CSM4 and is modulated by recombination. *Cell* 133, 1175–1187. doi: 10.1016/j.cell.2008.04.047

Conrad, M. N., Lee, C. Y., Wilkerson, J. L., and Dresser, M. E. (2007). MPS3 mediates meiotic bouquet formation in *Saccharomyces cerevisiae*. *Proc. Natl. Acad. Sci. U.S.A.* 104, 8863–8868. doi: 10.1073/pnas.0606165104

Crisp, M., Liu, Q., Roux, K., Rattner, J. B., Shanahan, C., Burke, B., et al. (2006). Coupling of the nucleus and cytoplasm: role of the LINC complex. *J. Cell Biol.* 172, 41–53. doi: 10.1083/jcb.200509124

Daniel, K., Tränkner, D., Wojtasz, L., Shibuya, H., Watanabe, Y., Alsheimer, M., et al. (2014). Mouse CCDC79 (TERB1) is a meiosis-specific telomere associated protein. *BMC Cell Biol.* 15:17. doi: 10.1186/1471-2121-15-17

Dawe, R. K., Sedat, J. W., Agard, D. A., and Cande, W. Z. (1994). Meiotic chromosome pairing in maize is associated with a novel chromatin organization. *Cell* 76, 901–912. doi: 10.1016/0092-8674(94)90364-6

Ding, X., Xu, R., Yu, J., Xu, T., Zhuang, Y., and Han, M. (2007). SUN1 is required for telomere attachment to nuclear envelope and gametogenesis in mice. *Dev. Cell* 12, 863–872. doi: 10.1016/j.devcel.2007.03.018

Djinovic-Carugo, K., Gautel, M., Ylänne, J., and Young, P. (2002). The spectrin repeat: a structural platform for cytoskeletal protein assemblies. *FEBS Lett*. 513, 119–123. doi: 10.1016/S0014-5793(01)03304-X

Duong, N. T., Morris, G. E., Lam, L. T., Zhang, Q., Sewry, C. A., Shanahan, C. M., et al. (2014). Nesprins: tissue-specific expression of epsilon and other short isoforms. *PLoS ONE*. 9:e94380. doi: 10.1371/journal.pone.0094380

Duroc, Y., Lemhemdi, A., Larchevêque, C., Hurel, A., Cuacos, M., Cromer, L., et al. (2014). The kinesin AtPSS1 promotes synapsis and is required for proper crossover distribution in meiosis. *PLoS Genet.* 10:e1004674. doi: 10.1371/journal.pgen.1004674

Elhananytamir, H., Yu, Y. V., Shnayder, M., Jain, A., Welte, M., and Volk, T. (2012). Organelle positioning in muscles requires cooperation between two KASH proteins and microtubules. *J. Cell Biol.* 198, 833–846. doi: 10.1083/jcb.201204102

Fransz, P., and de Jong, H. (2011). From nucleosome to chromosome: a dynamic organization of genetic information. *Plant J.* 66, 4–17. doi: 10.1111/j.1365-313X.2011.04526.x

Frohnert, C., Schweizer, S., and Hoyer-Fender, S. (2011). SPAG4L/SPAG4L-2 are testis-specific SUN domain proteins restricted to the apical nuclear envelope of round spermatids facing the acrosome. *Mol. Hum. Reprod.* 17, 207–218. doi: 10.1093/molehr/gaq099

Furukawa, K., Inagaki, H., and Hotta, Y. (1994). Identification and cloning of an mRNA coding for a germ cell-specific A-type lamin in mice. *Exp. Cell Res.* 212, 426–430. doi: 10.1006/excr.1994.1164

Göb, E., Meyernatus, E., Benavente, R., and Alsheimer, M. (2011). Expression of individual mammalian Sun1 isoforms depends on the cell type. *Commun. Integr. Biol.* 4, 440–442. doi: 10.4161/cib.15369

Göb, E., Schmitt, J., Benavente, R., and Alsheimer, M. (2010). Mammalian sperm head formation involves different polarization of two novel LINC complexes. *PLoS ONE* 5:e12072. doi: 10.1371/journal.pone.0012072

Golubovskaya, I. N., Hamant, O., Timofejeva, L., Wang, C. J., Braun, D., Meeley, R., et al. (2006). Alleles of afd1 dissect REC8 functions during meiotic prophase I. *J. Cell Sci.* 119, 3306–3315. doi: 10.1242/jcs.03054

Golubovskaya, I. N., Harper, L. C., Pawlowski, W. P., Schichnes, D., and Cande, W. Z. (2002). The pam1 gene is required for meiotic bouquet formation and efficient homologous synapsis in maize (*Zea mays L.*). *Genetics* 162, 1979–1993.

Graumann, K. (2014). Evidence for LINC1-SUN associations at the plant nuclear periphery. *PLoS ONE* 9:e93406. doi: 10.1371/journal.pone.0093406

Graumann, K., Runions, J., and Evans, D. E. (2010). Characterization of SUN-domain proteins at the higher plant nuclear envelope. *Plant J.* 61, 134–144. doi: 10.1111/j.1365-313X.2009.04038.x

Graumann, K., Vanrobays, E., Tutois, S., Probst, A. V., Evans, D. E., and Tatout, C. (2014). Characterization of two distinct subfamilies of SUN-domain proteins in Arabidopsis and their interactions with the novel KASH-domain protein AtTIK. *J. Exp. Bot.* 65, 6499–6512. doi: 10.1093/jxb/eru368

Gross, J., and Bhattacharya, D. (2011). Endosymbiont or host: who drove mitochondrial and plastid evolution? *Biol. Direct*. 6:12. doi: 10.1186/1745-6150-6-12

Gruenbaum, Y., Margalit, A., Goldman, R. D., Shumaker, D. K., and Wilson, K. L. (2005). The nuclear lamina comes of age. *Nat. Rev. Mol. Cell Biol.* 6, 21–31. doi: 10.1038/nrm1550

Han, Z., and Dawe, R. K. (2011). Mechanisms of plant spindle formation. *Chromosome Res.* 19, 335–344. doi: 10.1007/s10577-011-9190-y

Haque, F., Lloyd, D. J., Smallwood, D. T., Dent, C. L., Shanahan, C. M., Fry, A. M., et al. (2006). SUN1 interacts with nuclear lamin A and cytoplasmic nesprins to provide a physical connection between the nuclear lamina and the cytoskeleton. *Mol. Cell. Biol.* 26, 3738–3751. doi: 10.1128/MCB.26.10.3738-3751.2006

Harper, L., Golubovskaya, I., and Cande, W. Z. (2004). A bouquet of chromosomes. *J. Cell Sci*. 117, 4025–4032. doi: 10.1242/jcs.01363

Harper, N. C., Rillo, R., Jover-Gil, S., Assaf, Z. J., Bhalla, N., and Dernburg, A. F. (2011). Pairing centers recruit a Polo-like kinase to orchestrate meiotic chromosome dynamics in *C. elegans*. *Dev. Cell* 21, 934–947. doi: 10.1016/j.devcel.2011.09.001

Hetzer, M. W., and Wente, S. R. (2009). Border control at the nucleus: biogenesis and organization of the nuclear membrane and pore complexes. *Dev. Cell* 17, 606–616. doi: 10.1016/j.devcel.2009.10.007

Hiraoka, Y., and Dernburg, A. F. (2009). The SUN rises on meiotic chromosome dynamics. *Dev. Cell* 17, 598–605. doi: 10.1016/j.devcel.2009.10.014

Hodzic, D. M., Yeater, D. B., Bengtsson, L., Otto, H., and Stahl, P. D. (2004). Sun2 is a novel mammalian inner nuclear membrane protein. *J. Biol. Chem.* 279, 25805–25812. doi: 10.1074/jbc.M313157200

Horigome, C., Okada, T., Shimazu, K., Gasser, S. M., and Mizuta, K. (2011). Ribosome biogenesis factors bind a nuclear envelope SUN domain protein to cluster yeast telomeres. *EMBO J.* 30, 3799–3811. doi: 10.1038/emboj.2011.267

Hunter, N., and Kleckner, N. (2001). The single-end invasion: an asymmetric intermediate at the double-strand break to double-holliday junction transition of meiotic recombination. *Cell* 106, 59–70. doi: 10.1016/S0092-8674(01)00430-5

Jaspersen, S. L., Martin, A. E., Glazko, G., Giddings, T. H. Jr., Morgan, G., Mushegian, A., et al. (2006). The Sad1-UNC-84 homology domain in Mps3 interacts with Mps2 to connect the spindle pole body with the nuclear envelope. *J. Cell Biol.* 174, 665–675. doi: 10.1083/jcb.200601062

Ketema, M., and Sonnenberg, A. (2011). Nesprin-3: a versatile connector between the nucleus and the cytoskeleton. *Biochem. Soc. Trans*. 39, 1719–1724. doi: 10.1042/BST20110669

Kim, D. I., Birendra, K. C., and Roux, K. J. (2015). Making the LINC: SUN and KASH protein interactions. *Biol. Chem.* 396, 295–310. doi: 10.1515/hsz-2014-0267

King, M. C., Drivas, T. G., and Blobel, G. (2008). A network of nuclear envelope membrane proteins linking centromeres to microtubules. *Cell* 134, 427–438. doi: 10.1016/j.cell.2008.06.022

Kleckner, N. (2006). Chiasma formation: chromatin/axis interplay and the role(s) of the synaptonemal complex. *Chromosoma* 115, 175–194. doi: 10.1007/s00412-006-0055-7

Klutstein, M., and Cooper, J. P. (2014). The chromosomal courtship dance-homolog pairing in early meiosis. *Curr. Opin. Cell Biol.* 26, 123–131. doi: 10.1016/j.ceb.2013.12.004

Koszul, R., and Kleckner, N. (2009). Dynamic chromosome movements during meiosis: a way to eliminate unwanted connections? *Trends Cell Biol.* 19, 716–724. doi: 10.1016/j.tcb.2009.09.007

Koszul, R., Kim, K. P., Prentiss, M., Kleckner, N., and Kameoka, S. (2008). Meiotic chromosomes move by linkage to dynamic actin cables with transduction of force through the nuclear envelope. *Cell* 133, 1188–1201. doi: 10.1016/j.cell.2008.04.050

Kracklauer, M. P., Banks, S. M., Xie, X., Wu, Y., and Fischer, J. A. (2007). Drosophila klaroid encodes a SUN domain protein required for Klarsicht localization to the nuclear envelope and nuclear migration in the eye. *Fly* 1, 75–85. doi: 10.4161/fly.4254

Kracklauer, M. P., Link, J., and Alsheimer, M. (2013). LINCing the nuclear envelope to gametogenesis. *Curr. Top. Dev. Biol.* 102, 127–157. doi: 10.1016/B978-0-12-416024-8.00005-2

Labella, S., Woglar, A., Jantsch, V., and Zetka, M. (2011). Polo kinases establish links between meiotic chromosomes and cytoskeletal forces essential for homolog pairing. *Dev. Cell* 21, 948–958. doi: 10.1016/j.devcel.2011.07.011

Lee, C. Y., Conrad, M. N., and Dresser, M. E. (2012). Meiotic chromosome pairing is promoted by telomere-led chromosome movements independent of bouquet formation. *PLoS Genet.* 8:e1002730. doi: 10.1371/journal.pgen.1002730

Lee, K. K., Starr, D., Cohen, M., Liu, J., Han, M., Wilson, K. L., et al. (2002). Lamin-dependent localization of UNC-84, a protein required for nuclear migration in *Caenorhabditis elegans*. *Mol. Biol. Cell* 13, 892–901. doi: 10.1091/mbc.01-06-0294

Lei, K., Zhang, X., Ding, X., Guo, X., Chen, M., Zhu, B., et al. (2009). SUN1 and SUN2 play critical but partially redundant roles in anchoring nuclei in skeletal muscle cells in mice. *Proc. Natl. Acad. Sci. U.S.A.* 106, 10207–10212. doi: 10.1073/pnas.0812037106

Lenne, P. F., Raae, A. J., Altmann, S. M., Saraste, M., and Hörber, J. K. (2000). States and transitions during forced unfolding of a single spectrin repeat. *FEBS Lett.* 476, 124–128. doi: 10.1016/S0014-5793(00)01704-X

Link, J., Leubner, M., Schmitt, J., Göb, E., Benavente, R., Jeang, K. T., et al. (2014). Analysis of meiosis in SUN1 deficient mice reveals a distinct role of SUN2 in mammalian meiotic LINC complex formation and function. *PLoS Genet.* 10:e1004099. doi: 10.1371/journal.pgen.1004099

Lu, W., Gotzmann, J., Sironi, L., Jaeger, V. M., Schneider, M., Luke, Y., et al. (2008). Sun1 forms immobile macromolecular assemblies at the nuclear envelope. *Biochim. Biophys. Acta* 1783, 2415–2426. doi: 10.1016/j.bbamcr.2008.09.001

Malone, C. J., Misner, L., Le Bot, N., Tsai, M. C., Campbell, J. M., Ahringer, J., et al. (2003). The *C. elegans* hook protein, ZYG-12, mediates the essential attachment between the centrosome and nucleus. *Cell* 115, 825–836. doi: 10.1016/S0092-8674(03)00985-1

Masoud, K., Herzog, E., Chaboute, M. E., and Schmit, A. C. (2013). Microtubule nucleation and establishment of the mitotic spindle in vascular plant cells. *Plant J.* 75, 245–257. doi: 10.1111/tpj.12179

Mcgee, M. D., Stagljar, I., and Starr, D. A. (2009). KDP-1 is a nuclear envelope KASH protein required for cell-cycle progression. *J. Cell Sci.* 122, 2895–2905. doi: 10.1242/jcs.051607

Mckee, B. D. (2004). Homologous pairing and chromosome dynamics in meiosis and mitosis. *Biochim. Biophys. Acta* 1677, 165–180. doi: 10.1016/j.bbaexp.2003.11.017

Meyerzon, M., Fridolfsson, H. N., Ly, N., Mcnally, F. J., and Starr, D. A. (2009). UNC-83 is a nuclear-specific cargo adaptor for kinesin-1-mediated nuclear migration. *Development* 136, 2725–2733. doi: 10.1242/dev.038596

Miki, F., Kurabayashi, A., Tange, Y., Okazaki, K., Shimanuki, M., and Niwa, O. (2004). Two-hybrid search for proteins that interact with Sad1 and Kms1, two membrane-bound components of the spindle pole body in fission yeast. *Mol. Genet. Genomics* 270, 449–461. doi: 10.1007/s00438-003-0938-8

Miki, F., Okazaki, K., Shimanuki, M., Yamamoto, A., Hiraoka, Y., and Niwa, O. (2002). The 14-kDa dynein light chain-family protein Dlc1 is required for regular oscillatory nuclear movement and efficient recombination during meiotic prophase in fission yeast. *Mol. Biol. Cell* 13, 930–946. doi: 10.1091/mbc.01-11-0543

Mislow, J. M., Kim, M. S., Davis, D. B., and Mcnally, E. M. (2002). Myne-1, a spectrin repeat transmembrane protein of the myocyte inner nuclear membrane, interacts with lamin A/C. *J. Cell Sci.* 115, 61–70.

Moens, P. B., Bernelotmoens, C., and Spyropoulos, B. (2011). Chromosome core attachment to the meiotic nuclear envelope regulates in *Chloeaktis* (Orthoptera). *Genome* 32, 601–610. doi: 10.1139/g89-488

Morimoto, A., Shibuya, H., Zhu, X., Kim, J., Ishiguro, K., Han, M., et al. (2012). A conserved KASH domain protein associates with telomeres, SUN1, and dynactin during mammalian meiosis. *J. Cell Biol.* 198, 165–172. doi: 10.1083/jcb.201204085

Mosleybishop, K. L., Li, Q., Patterson, L., and Fischer, J. A. (1999). Molecular analysis of the klarsicht gene and its role in nuclear migration within differentiating cells of the *Drosophila* eye. *Curr.Biol.* 9, 1211–1220. doi: 10.1016/S0960-9822(99)80501-6

Murphy, S. P., and Bass, H. W. (2012). The maize (*Zea mays*) desynaptic (dy) mutation defines a pathway for meiotic chromosome segregation, linking nuclear morphology, telomere distribution and synapsis. *J. Cell Sci.* 125, 3681–3690. doi: 10.1242/jcs.108290

Murphy, S. P., Gumber, H. K., Mao, Y., and Bass, H. W. (2014). A dynamic meiotic SUN belt includes the zygotene-stage telomere bouquet and is disrupted in chromosome segregation mutants of maize (*Zea mays* L.). *Front. Plant Sci.* 5:314. doi: 10.3389/fpls.2014.00314

Murphy, S. P., Simmons, C. R., and Bass, H. W. (2010). Structure and expression of the maize (*Zea mays* L.) SUN-domain protein gene family: evidence for the existence of two divergent classes of SUN proteins in plants. *BMC Plant Biol.* 10:269. doi: 10.1186/1471-2229-10-269

Oda, Y., and Fukuda, H. (2011). Dynamics of *Arabidopsis* SUN proteins during mitosis and their involvement in nuclear shaping. *Plant J.* 66, 629–641. doi: 10.1111/j.1365-313X.2011.04523.x

Ortega, S. P. I., Odajima, J., Martin, A., Dubus, P., Sotillo, R., Barbero, J. L., et al. (2003). Cyclin-dependent kinase 2 is essential for meiosis but not for mitotic cell division in mice. *Nat. Genet.* 33, 25–31. doi: 10.1038/ng1232

Padmakumar, V. C., Abraham, S. S., Noegel, A. A., Tunggal, B., Karakesisoglou, I., and Korenbaum, E. (2004). Enaptin, a giant actin-binding protein, is an element of the nuclear membrane and the actin cytoskeleton. *Exp. Cell Res.* 295, 330–339. doi: 10.1016/j.yexcr.2004.01.014

Padmore, R., Cao, L., and Kleckner, N. (1991). Temporal comparison of recombination and synaptonemal complex formation during meiosis in *S. cerevisiae*. *Cell* 66, 1239–1256. doi: 10.1016/0092-8674(91)90046-2

Park, S. H., and Craig, B. (2010). Further assembly required: construction and dynamics of the endoplasmic reticulum network. *EMBO Rep.* 11, 515–521. doi: 10.1038/embor.2010.92

Patterson, K., Molofsky, A. B., Robinson, C., Acosta, S., Cater, C., and Fischer, J. A. (2004). The functions of Klarsicht and nuclear lamin in developmentally regulated nuclear migrations of photoreceptor cells in the *Drosophila* eye. *Mol. Biol. Cell* 15, 600–610. doi: 10.1091/mbc.E03-06-0374

Pawlowski, W. P., Golubovskaya, I. N., Timofejeva, L., Meeley, R. B., Sheridan, W. F., and Cande, W. Z. (2004). Coordination of meiotic recombination, pairing, and synapsis by PHS1. *Science* 303, 89–92. doi: 10.1126/science.1091110

Penkner, A., Fridkin, A., Gloggnitzer, J., Baudrimont, A., Machacek, T., Woglar, A., et al. (2009). Meiotic chromosome homology search involves modifications of the nuclear envelope protein Matefin/SUN-1. *Cell* 139, 920–933. doi: 10.1016/j.cell.2009.10.045

Penkner, A., Tang, L., Novatchkova, M., Ladurner, M., Fridkin, A., Gruenbaum, Y., et al. (2007). The nuclear envelope protein Matefin/SUN-1 is required for homologous pairing in *C. elegans meiosis*. *Dev. Cell* 12, 873–885. doi: 10.1016/j.devcel.2007.05.004

Phillips, C. M., and Dernburg, A. F. (2006). A family of zinc-finger proteins is required for chromosome-specific pairing and synapsis during meiosis in *C. elegans*. *Dev. Cell* 11, 817–829. doi: 10.1016/j.devcel.2006.09.020

Phillips, C. M., Wong, C., Bhalla, N., Carlton, P. M., Weiser, P., Meneely, P. M., et al. (2005). HIM-8 binds to the X chromosome pairing center and mediates chromosome-specific meiotic synapsis. *Cell* 123, 1051–1063. doi: 10.1016/j.cell.2005.09.035

Razafsky, D., and Hodzic, D. (2009). Bringing KASH under the SUN: the many faces of nucleo-cytoskeletal connections. *J. Cell Biol.* 186, 461–472. doi: 10.1083/jcb.200906068

Richards, D. M., Greer, E., Martin, A. C., Moore, G., Shaw, P. J., and Howard, M. (2012). Quantitative dynamics of telomere bouquet

formation. *PLoS Comput. Biol.* 8, 1776–1776. doi: 10.1371/journal.pcbi.1002812

Rivero, F., Kuspa, A., Brokamp, R., Matzner, M., and Noegel, A. A. (1998). Interaptin, an actin-binding protein of the alpha-actinin superfamily in *Dictyostelium discoideum*, is developmentally and cAMP-regulated and associates with intracellular membrane compartments. *J. Cell Biol.* 142, 735–750. doi: 10.1083/jcb.142.3.735

Roeder, G. S. (1997). Meiotic chromosomes: it takes two to tango. *Genes Dev*. 11, 2600–2621.

Rog, O., and Dernburg, A. (2015). Direct visualization reveals kinetics of meiotic chromosome synapsis. *Cell Rep.* 10, 1639–1645. doi: 10.1016/j.celrep.2015.02.032

Rothballer, A., and Kutay, U. (2013). The diverse functional LINCs of the nuclear envelope to the cytoskeleton and chromatin. *Chromosoma* 122, 415–429. doi: 10.1007/s00412-013-0417-x

Rothballer, A., Schwartz, T. U., and Kutay, U. (2013). LINCing complex functions at the nuclear envelope: what the molecular architecture of the LINC complex can reveal about its function. *Nucleus* 4, 29–36. doi: 10.4161/nucl.23387

Roux, K. J., Crisp, M. L., Liu, Q., Kim, D., Kozlov, S., Stewart, C. L., et al. (2009). Nesprin 4 is an outer nuclear membrane protein that can induce kinesin-mediated cell polarization. *Proc. Natl. Acad. Sci. U.S.A*. 106, 2194–2199. doi: 10.1073/pnas.0808602106

Sato, A., Isaac, B., Phillips, C. M., Rillo, R., Carlton, P. M., Wynne, D. J., et al. (2009). Cytoskeletal forces span the nuclear envelope to coordinate meiotic chromosome pairing and synapsis. *Cell* 139, 907–919. doi: 10.1016/j.cell.2009.10.039

Scherthan, H. (2001). A bouquet makes ends meet. *Nat. Rev. Mol. Cell Biol.* 2, 621–627. doi: 10.1038/35085086

Scherthan, H. (2007). Telomere attachment and clustering during meiosis. *Cell. Mol. Life Sci.* 64, 117–124. doi: 10.1007/s00018-006-6463-2

Scherthan, H., Weich, S., Schwegler, H., Heyting, C., Härle, M., and Cremer, T. (1996). Centromere and telomere movements during early meiotic prophase of mouse and man are associated with the onset of chromosome pairing. *J. Cell Biol.* 134, 1109–1125. doi: 10.1083/jcb.134.5.1109

Schmitt, J., Benavente, R., Hodzic, D., Höög, C., Stewart, C. L., and Alsheimer, M. (2007). Transmembrane protein Sun2 is involved in tethering mammalian meiotic telomeres to the nuclear envelope. *Proc. Natl. Acad. Sci. U.S.A*. 104, 7426–7431. doi: 10.1073/pnas.0609198104

Shao, X., Tarnasky, H. A., Lee, J. P., Oko, R., and van der Hoorn, F. A. (1999). Spag4, a novel sperm protein, binds outer dense-fiber protein Odf1 and localizes to microtubules of manchette and axoneme. *Dev. Biol.* 211, 109–123. doi: 10.1006/dbio.1999.9297

Sheehan, M. J., and Pawlowski, W. P. (2009). Live imaging of rapid chromosome movements in meiotic prophase I in maize. *Proc. Natl. Acad. Sci. U.S.A*. 106, 20989–20994. doi: 10.1073/pnas.0906498106

Shibuya, H., Hernández-Hernández, A., Morimoto, A., Negishi, L., Höög, C., and Watanabe, Y. (2015). MAJIN links telomeric DNA to the nuclear membrane by exchanging telomere cap. *Cell* 163, 1252–1266. doi: 10.1016/j.cell.2015.10.030

Shibuya, H., Ishiguro, K., and Watanabe, Y. (2014). The TRF1-binding protein TERB1 promotes chromosome movement and telomere rigidity in meiosis. *Nat. Cell Biol.* 16, 145–156. doi: 10.1038/ncb2896

Shimanuki, M., Miki, F., Ding, D. Q., Chikashige, Y., Hiraoka, Y., Horio, T., et al. (1997). A novel fission yeast gene, *kms1+*, is required for the formation of meiotic prophase-specific nuclear architecture. *Mole Gen. Genet*. 254, 238–249. doi: 10.1007/s004380050412

Siderakis, M., and Tarsounas, M. (2007). Telomere regulation and function during meiosis. *Chromosome Res.* 15, 667–679. doi: 10.1007/s10577-007-1149-7

Sosa, B. A., Kutay, U., and Schwartz, T. U. (2013). Structural insights into LINC complexes. *Curr. Opin. Struc. Biol.* 23, 285–291. doi: 10.1016/j.sbi.2013.03.005

Sosa, B., Rothballer, A., Kutay, U., and Schwartz, T. (2012). LINC complexes form by binding of three KASH peptides to domain interfaces of trimeric SUN proteins. *Cell* 149, 1035–1047. doi: 10.1016/j.cell.2012.03.046

Starr, D. A. (2009). A nuclear-envelope bridge positions nuclei and moves chromosomes. *J. Cell Sci.* 122, 577–586. doi: 10.1242/jcs.037622

Starr, D. A. (2011). KASH and SUN proteins. *Curr. Biol.* 21, R414–R415. doi: 10.1016/j.cub.2011.04.022

Starr, D. A., and Fischer, J. A. (2005). KASH'n Karry: the KASH domain family of cargo-specific cytoskeletal adaptor proteins. *Bioessays* 27, 1136–1146. doi: 10.1002/bies.20312

Starr, D. A., and Fridolfsson, H. N. (2010). Interactions between nuclei and the cytoskeleton are mediated by SUN-KASH nuclear-envelope bridges. *Annu. Rev. Cell Dev. Biol.* 26, 421–444. doi: 10.1146/annurev-cellbio-100109-104037

Starr, D. A., and Han, M. (2002). Role of ANC-1 in tethering nuclei to the actin cytoskeleton. *J. Biol. Chem*. 298, 406–409. doi: 10.1126/science.1075119

Starr, D. A., Hermann, G. J., Malone, C. J., Fixsen, W., Priess, J. R., Horvitz, H. R., et al. (2001). unc-83 encodes a novel component of the nuclear envelope and is essential for proper nuclear migration. *Development* 128, 5039–5050.

Stewart, C. L., Roux, K. J., and Burke, B. (2007). Blurring the boundary: the nuclear envelope extends its reach. *Science* 318, 1408–1412. doi: 10.1126/science.1142034

Subramanian, V. V., and Hochwagen, A. (2014). The meiotic checkpoint network: step-by-step through meiotic prophase. *Cold Spring Harb. Perspect. Biol.* 6:a016675. doi: 10.1101/cshperspect.a016675

Tabata, M. (1962). Chromosome pairing in intercrosses between stocks of interchanges involving the same two chromosomes in maize. *Cytologia* 27, 410–417. doi: 10.1508/cytologia.27.410

Tamura, K., Iwabuchi, K., Fukao, Y., Kondo, M., Okamoto, K., Ueda, H., et al. (2013). Myosin XI-i links the nuclear membrane to the cytoskeleton to control nuclear movement and shape in *Arabidopsis*. *Curr. Biol.* 23, 1776–1781. doi: 10.1016/j.cub.2013.07.035

Tiang, C. L., He, Y., and Pawlowski, W. P. (2012). Chromosome organization and dynamics during interphase, mitosis, and meiosis in plants. *Plant Physiol.* 158, 26–34. doi: 10.1104/pp.111.187161

Trelles-Sticken, E., Loidl, J., and Scherthan, H. (1999). Bouquet formation in budding yeast: initiation of recombination is not required for meiotic telomere clustering. *J. Cell Sci.* 112(Pt 5), 651–658.

Tzur, Y. B., Wilson, K. L., and Gruenbaum, Y. (2006). SUN-domain proteins: 'Velcro' that links the nucleoskeleton to the cytoskeleton. *Nat. Rev. Mol. Cell Biol.* 7, 782–788. doi: 10.1038/nrm2003

Varas, J., Graumann, K., Osman, K., Pradillo, M., Evans, D. E., Santos, J. L., et al. (2015). Absence of SUN1 and SUN2 proteins in *Arabidopsis thaliana* leads to a delay in meiotic progression and defects in synapsis and recombination. *Plant J.* 81, 329–346. doi: 10.1111/tpj.12730

Viera, A., Alsheimer, M., Gómez, R., Berenguer, I., Ortega, S., Symonds, C. E., et al. (2015). CDK2 regulates nuclear envelope protein dynamics and telomere attachment in mouse meiotic prophase. *J. Cell Sci.* 128, 88–99. doi: 10.1242/jcs.154922

Viera, A., Rufas, J. I., Barbero, J. L., Ortega, S., and Suja, J. A. (2009). CDK2 is required for proper homologous pairing, recombination and sex-body formation during male mouse meiosis. *J. Cell Sci.* 122, 2149–2159. doi: 10.1242/jcs.046706

Wanat, J. J., Kim, K. P., Koszul, R., Zanders, S., Weiner, B., Kleckner, N., et al. (2008). Csm4, in collaboration with Ndj1, mediates telomere-led chromosome dynamics and recombination during yeast meiosis. *PLoS Genet.* 4:e1000188. doi: 10.1371/journal.pgen.1000188

Wang, H., Liu, R., Wang, J., Wang, P., Shen, Y., and Liu, G. (2014). The *Arabidopsis* kinesin gene AtKin - 1 plays a role in the nuclear division process during megagametogenesis. *Plant Cell Rep*. 33, 819–828. doi: 10.1007/s00299-014-1594-7

Wang, Q., Du, X., Cai, Z., and Greene, M. I. (2006). Characterization of the structures involved in localization of the SUN proteins to the nuclear envelope and the centrosome. *DNA Cell Biol.* 25, 554–562. doi: 10.1089/dna.2006.25.554

Wijnker, E., and Schnittger, A. (2013). Control of the meiotic cell division program in plants. *Plant Reprod*. 26, 143–158. doi: 10.1007/s00497-013-0223-x

Wilhelmsen, K., Ketema, M., Truong, H., and Sonnenberg, A. (2006). KASH-domain proteins in nuclear migration, anchorage and other processes. *J. Cell Sci.* 119, 5021–5029. doi: 10.1242/jcs.03295

Wilson, K. L., and Dawson, S. C. (2011). Evolution: functional evolution of nuclear structure. *J. Cell Biol.* 195, 171–181. doi: 10.1083/jcb.201103171

Woglar, A., and Jantsch, V. (2014). Chromosome movement in meiosis I prophase of *Caenorhabditis elegans*. *Chromosoma* 123, 15–24. doi: 10.1007/s00412-013-0436-7

Worman, H. J., and Gundersen, G. G. (2006). Here come the SUNs: a nucleocytoskeletal missing link. *Trends Cell Biol.* 16, 67–69. doi: 10.1016/j.tcb.2005.12.006

Wynne, D. J., Rog, O., Carlton, P. M., and Dernburg, A. F. (2012). Dynein-dependent processive chromosome motions promote homologous pairing in *C. elegans meiosis. J. Cell Biol.* 196, 47–64. doi: 10.1083/jcb.201106022

Xiong, H., Rivero, F., Euteneuer, U., Mondal, S., Mana-Capelli, S., Larochelle, D., et al. (2008). *Dictyostelium* Sun-1 connects the centrosome to chromatin and ensures genome stability. *Traffic* 9, 708–724. doi: 10.1111/j.1600-0854.2008.00721.x

Yamamoto, A. (2014). Gathering up meiotic telomeres: a novel function of the microtubule-organizing center. *Cell Mol. Life Sci.* 71, 2119–2134. doi: 10.1007/s00018-013-1548-1

Yu, J., Lei, K., Zhou, M., Craft, C. M., Xu, G., Xu, T., et al. (2011). KASH protein Syne-2/Nesprin-2 and SUN proteins SUN1/2 mediate nuclear migration during mammalian retinal development. *Hum. Mol. Genet.* 20, 1061–1073. doi: 10.1093/hmg/ddq549

Yu, J., Starr, D. A., Wu, X., Parkhurst, S. M., Zhuang, Y., Xu, T., et al. (2006). The KASH domain protein MSP-300 plays an essential role in nuclear anchoring during *Drosophila* oogenesis. *Dev. Biol.* 289, 336–345. doi: 10.1016/j.ydbio.2005.10.027

Zhang, X., Lei, K., Yuan, X., Wu, X., Zhuang, Y., Xu, T., et al. (2009). SUN1/2 and Syne/Nesprin-1/2 complexes connect centrosome to the nucleus during neurogenesis and neuronal migration in mice. *Neuron* 64, 173–187. doi: 10.1016/j.neuron.2009.08.018

Zhang, X., Xu, R., Zhu, B., Yang, X., Ding, X., Duan, S., et al. (2007). *Syne-1* and *Syne-2* play crucial roles in myonuclear anchorage and motor neuron innervation. *Development* 134, 901–908. doi: 10.1242/dev.02783

Zhou, K., Rolls, M. M., Hall, D. H., Malone, C. J., and Hanna-Rose, W. (2009). A ZYG-12-dynein interaction at the nuclear envelope defines cytoskeletal architecture in the *C. elegans* gonad. *J. Cell Biol.* 186, 229–241. doi: 10.1083/jcb.200902101

Zhou, X., and Meier, I. (2013). How plants LINC the SUN to KASH. *Nucleus* 4, 206–215. doi: 10.4161/nucl.24088

Zhou, X., Graumann, K., and Meier, I. (2015a). The plant nuclear envelope as a multifunctional platform LINCed by SUN and KASH. *J. Exp. Bot.* 66, 1649–1659. doi: 10.1093/jxb/erv082

Zhou, X., Graumann, K., Evans, D. E., and Meier, I. (2012a). Novel plant SUN-KASH bridges are involved in RanGAP anchoring and nuclear shape determination. *J. Cell Biol.* 196, 203–211. doi: 10.1083/jcb.201108098

Zhou, X., Graumann, K., Wirthmueller, L., Jones, J. D., and Meier, I. (2014). Identification of unique SUN-interacting nuclear envelope proteins with diverse functions in plants. *J. Cell Biol.* 205, 677–692. doi: 10.1083/jcb.201401138

Zhou, X., Graves, N. R., and Meier, I. (2015b). SUN anchors pollen WIP–WIT complexes at the vegetative nuclear envelope and is necessary for pollen tube targeting and fertility. *J. Exp. Bot.* 66, 7299–7307. doi: 10.1093/jxb/erv425

Zhou, Z., Du, X., Cai, Z., Song, X., Zhang, H., Mizuno, T., et al. (2012b). Structure of Sad1-UNC84 homology (SUN) domain defines features of molecular bridge in nuclear envelope. *J. Biol. Chem.* 287, 5317–5326. doi: 10.1074/jbc.M111.304543

Zickler, D. (2006). From early homologue recognition to synaptonemal complex formation. *Chromosoma* 115, 158–174. doi: 10.1007/s00412-006-0048-6

Zickler, D., and Kleckner, N. (1998). The leptotene-zygotene transition of meiosis. *Annu. Rev. Genet.* 32, 619–697.doi: 10.1146/annurev.genet.32.1.619

Conflict of Interest Statement: The authors declare that the research was conducted in the absence of any commercial or financial relationships that could be construed as a potential conflict of interest.

frontiers in Cell and Developmental Biology

OPINION
published: 27 November 2017
doi: 10.3389/fcell.2017.00100

Uterine Histone Secretion Likely Fosters Early Embryo Development So Efforts to Mitigate Histone Cytotoxicity Should Be Cautious

Lon J. Van Winkle[1, 2*]

[1] Department of Biochemistry, Midwestern University, Downers Grove, IL, United States, [2] Department of Medical Humanities, Rocky Vista University, Parker, CO, United States

Keywords: histones, blastocyst, implantation, antimicrobial, early development, amino acid transport systems

INTRODUCTION

The possible benefits of mitigating extracellular histone cytotoxicity have been outlined for the reproductive tract and other organs (e.g., Simon et al., 2013; Galuska et al., 2017; Lefrançais and Looney, 2017; Wygrecka et al., 2017; Yang et al., 2017). However, a reassessment of previously published data supports the notion that uterine histone secretion fosters early embryo development in multiple ways. (See below.) Hence, efforts to neutralize extracellular histone action in reproductive organs should be cautious. Thus far, there appears to be little discussion of how to preserve desirable histone effects while mitigating pathology caused by excessive extracellular histone actions.

MECHANISMS OF HISTONE CYTOTOXICITY ARE LIKELY RELATED TO THEIR ANTIMICROBIAL EFFECTS

Histones contribute to eukaryotic chromatin structure and function in a well-known manner (e.g., Harr et al., 2016). Less well known are the extra-nuclear functions of these macromolecules (e.g., Parseghian and Luhrs, 2006). Among these other functions, extracellular histones fight bacterial, fungal, viral, and other parasitic infections (Papayannopoulos, in press). At least two distinct mechanisms account for these antimicrobial effects.

First, histones are essential components of neutrophil extracellular traps (NETs). NETs are net-like structures that form from decondensed chromatin and cytosolic proteins. They usually form when neutrophils undergo cell death via a process termed NETosis. NETs trap and kill each of the pathogens listed above (Papayannopoulos, in press).

Free histones also have antimicrobial functions (Kawasaki and Iwamuro, 2008). For example, histones in amniotic fluid appear to fight bacteria by neutralizing the lipopolysaccharide (LPS) of microbes that gain access to this fluid (Witkin et al., 2011). Without such protection, LPS could cause pre-term labor and delivery (Hirsch et al., 2006).

The cytotoxic effects of histones are likely related to their mechanisms of antimicrobial action. For example, the hyperinflammatory response and death of mice given high doses of LPS appear to require free histones. Moreover, administration of free histones to mice causes their death (Xu et al., 2009). Similarly, histones contribute to organ damage by excessive NETosis especially in lungs (Silk et al., 2017; Papayannopoulos, in press). Clearly, NETosis and the actions of free histones need tight regulation in order to benefit mammals and prevent pathological effects.

OPEN ACCESS

Edited by:
Karin Lykke-Hartmann, Aarhus University, Denmark

Reviewed by:
Shuo Xiao, University of South Carolina, United States

***Correspondence:**
Lon J. Van Winkle
lvanwinkle@rvu.edu

Specialty section:
This article was submitted to Signaling, a section of the journal Frontiers in Cell and Developmental Biology

Received: *02 July 2017*
Accepted: *13 November 2017*
Published: *27 November 2017*

Citation:
Van Winkle LJ (2017) Uterine Histone Secretion Likely Fosters Early Embryo Development So Efforts to Mitigate Histone Cytotoxicity Should Be Cautious. Front. Cell Dev. Biol. 5:100. doi: 10.3389/fcell.2017.00100

ANTIMICROBIAL ACTIONS OF HISTONES IN THE REPRODUCTIVE TRACT

Extracellular histones also help to inhibit microbial proliferation in the reproductive tract. For example, in a mouse model, NETs appear to limit Group B Streptococcal infection via the vagina during pregnancy (Kothary et al., 2017). In addition, free histones in fluids from the reproductive tract of cows exhibit antimicrobial actions (Dráb et al., 2014). Since pathogens can cause inflammation in the reproductive tract of mammals, they can also adversely affect mammalian reproduction (Wiesenfeld et al., 2002; Mårdh, 2004; BonDurant, 2007). While extracellular histones protect against microbes in at least two ways, only one of these mechanisms of action likely apply to free histone molecules in follicular, oviductal, and uterine secretions.

DIRECT CONTRIBUTION OF HISTONES TO EARLY EMBRYO DEVELOPMENT

Background

Histones appear most abundantly in human uterine secretions at the time the uterus is receptive to blastocyst implantation (Beier and Beier-Hellwig, 1998). Similarly, histones are synthesized at increased rates in the uterine epithelium and stroma of ovariectomized mice upon administration of a hormonal protocol known to result in blastocyst implantation about 25 h later (Smith et al., 1970). Assuming histones appear in mouse uterine fluid when the uterus becomes receptive to blastocyst implantation, what other functions might histones serve there? One good possibility involves amino acid transport system $B^{0,+}$ in mouse and probably human blastocysts (Van Winkle et al., 2006). In order to consider this possibility in context, we first review system $B^{0,+}$ involvement in early embryo development and blastocyst implantation in the uterus.

The process of blastocyst implantation in the mouse is especially amenable to study owing to experimentally-controlled delay of implantation. While delay of implantation (diapause) occurs naturally in mice when blastocysts develop in nursing mothers, it can be produced experimentally in mice by removing their ovaries about 76 h after their eggs have been fertilized (Van Winkle and Campione, 1987; Van Winkle et al., 2006). Daily administration of progesterone followed by estrogen on day 7 of pregnancy then leads to blastocyst implantation 25 h later.

During this activation from delay of implantation, signaling owing to leucine uptake via amino acid transport system $B^{0,+}$ results specifically in development of trophoblast motility and penetration of the uterine epithelium by blastocysts (Van Winkle et al., 2006). This signaling occurs because increases in the Na^+ and K^+ concentrations in uterine secretions about 6 h after estrogen administration to ovariectomized, progesterone-treated rodents (Van Winkle et al., 1983; Nilsson and Ljung, 1985) drive net Na^+-dependent system $B^{0,+}$ leucine uptake by the blastocyst trophectoderm. Leucine then stimulates the mTOR signaling that is needed for development of trophoblast motility and penetration of the uterine epithelium, which occur about 19 h later (Van Winkle et al., 2006). Meanwhile the uterine environment somehow suppresses system $B^{0,+}$ activity beginning about 10 h after estrogen administration (Lindqvist et al., 1978; Van Winkle and Campione, 1987). For example, blastocysts take up a radiolabeled, nonmetabolizable amino acid *in utero*, when it is administered to their mothers about 6 h after estrogen administration, but little or no uptake occurs when the amino acid is administered 4 h *before* or *after* this time (Lindqvist et al., 1978). We calculated that the decrease, in the rate of amino acid uptake between about 6 and 10 h after estrogen administration, is statistically equivalent to finding a drug that lowers the death rate from 94 to 6% (based on the effect size that can be calculated from the data of Lindqvist et al., 1978). At the time of the latter report, however, the full physiological significance of these changes in amino acid uptake by blastocysts *in utero* were not understood.

Although system $B^{0,+}$ is relatively inactive *in utero* during the 15 h prior to blastocyst implantation, it can be reactivated to even greater levels of transport activity simply by removing blastocysts from the uterus near the time of blastocyst implantation (Van Winkle and Campione, 1987). This ability to reactivate system $B^{0,+}$ activity also likely serves an important physiological function (Van Winkle et al., 2006). After reactivation, system $B^{0,+}$ would help to remove tryptophan from the implantation chamber during the initial penetration of the uterus by motile trophoblasts and, thus, help to suppress T-cell proliferation and immunologic rejection of the blastocyst (Munn et al., 1998; Baban et al., 2004).

Possible Histone Involvement

But what reversibly suppresses system $B^{0,+}$ activity beginning about 15 h before blastocyst implantation? Good candidates include histones that are likely secreted by uterine epithelial and possibly stromal cells when the uterus becomes receptive to blastocyst attachment and penetration (Smith et al., 1970). At near the histone concentrations detected in uterine fluid (Beier and Beier-Hellwig, 1998; Dráb et al., 2014), we found these macromolecules to inhibit amino acid uptake by mouse blastocysts. System $B^{0,+}$ activity, in particular, was inhibited much more than the activities of several other amino acid transport systems in blastocysts (Table IV in Van Winkle, 1993). In fact, the extent to which histones inhibited each of four different amino acid transport systems in blasocysts, differed from each other ($p < 0.02$), and ranged from near 90% inhibition of system $B^{0,+}$ to no inhibition of system L. Hence, it seems unlikely that histone cytotoxicity alone caused histone inhibition of amino acid transport system $B^{0,+}$ activity in blastocysts.

Perhaps not coincidentally, the effect size of this system $B^{0,+}$ inhibition by histones equals the effect size reported above, for reduction of the rate of amino acid transport into blastocysts *in utero* between about 6 and 10 h after estrogen administration to progesterone-maintained ovariectomized mice (Lindqvist et al., 1978). In addition, histone H2A (one of the more conspicuous histones in secretions of the receptive human uterus; Beier and Beier-Hellwig, 1998) likely is more effective at inhibiting amino acid uptake by blastocysts than other histones (Doman and Van Winkle, 1979). Reactivation of system $B^{0,+}$ in blastocysts, at the time of blastocyst penetration of the uterine epithelium, could be accomplished simply by removing histones from the relatively small amount of uterine fluid in implantation chambers. In this regard, proteases, needed to hydrolyze histones to inactive

products, appear to abound in these chambers (e.g., Afonso et al., 1997).

While it is unclear why system $B^{0,+}$ activity needs to be suppressed after mTOR signaling, we observed one tantalizing possibility. When we incubated delayed-implantation blastocysts for 25 h *in vitro* in medium containing a relatively high Na^+ concentration, they irreversibly lost their Na^+-dependent component of amino acid uptake (Van Winkle, 1977). This apparent loss of Na^+-dependent system $B^{0,+}$ activity would likely mean that the ability of blastocysts to activate net Na^+-dependent tryptophan uptake would also be lost. If such loss were to occur in the implantation chamber *in utero*, then implanting blastocysts could face immunological rejection. Hence, suppression of system $B^{0,+}$ in blastocysts by histones after initiation of mTOR signaling, could preserve this activity for activation and concentration of tryptophan into trophoblast cells at the time of trophoblast penetration of the uterine epithelium.

CONCLUSIONS

We propose here that extracellular histones have at least two somewhat surprising functions during early development of blastocysts and their implantation in the uterus. First, free histones protect blastocysts and the uterus from the adverse effects of unwanted inflammation caused by infection. Histones appear in abundance in secretions of the uterus when it is receptive to blastocyst implantation. Thus, these macromolecules provide protection from infection when it is needed for peri-implantation development to continue. Second, histone secretion by the uterus beginning about 15 h before blastocyst implantation could cause the observed suppression of amino acid transport system $B^{0,+}$ activity in blastocysts *in utero*. Removal of histones from the implantation chamber at the time motile trophoblasts penetrate the uterine epithelium would reactivate system $B^{0,+}$ to take up tryptophan. Tryptophan is needed for T-cell proliferation, so its uptake and metabolism by blastocysts would help to prevent their immunologic rejection when they are most vulnerable owing to trophoblast penetration of the uterine epithelium. Because of these possible beneficial actions of extracellular histones, efforts to mitigate histone cytotoxicity in the reproductive tract should be cautious.

AUTHOR CONTRIBUTIONS

The author confirms being the sole contributor of this work and approved it for publication.

REFERENCES

Afonso, S., Romagnano, L., and Babiarz, B. (1997). The expression and function of cystatin C and cathepsin B and cathepsin L during mouse embryo implantation and placentation. *Development* 124, 3415–3425.

Baban, B., Chandler, P., McCool, D., Marshall, B., Munn, D. H., and Mellor, A. L. (2004). Indoleamine 2, 3-dioxygenase expression is restricted to fetal trophoblast giant cells during murine gestation and is maternal genome specific. *J. Reprod. Immunol.* 61, 67–77. doi: 10.1016/j.jri.2003.11.003

Beier, H. M., and Beier-Hellwig, K. (1998). Molecular and cellular aspects of endometrial receptivity. *Hum. Reprod. Update* 4, 448–458. doi: 10.1093/humupd/4.5.448

BonDurant, R. H. (2007). Selected diseases and conditions associated with bovine conceptus loss in the first trimester. *Theriogenology* 68, 461–473. doi: 10.1016/j.theriogenology.2007.04.022

Doman, D. R., and Van Winkle, L. J. (1979). A histone induced diminution of ^{14}C-amino acid uptake and incorporation in preimplantation mouse embryos. *Bios* 50, 67–73.

Dráb, T., Kračmerová, J., Hanzlíková, E., Cerná, T., Litváková, R., Pohlová, A., et al. (2014). The antimicrobial action of histones in the reproductive tract of cow. *Biochem. Biophys. Res. Commun.* 443, 987–990. doi: 10.1016/j.bbrc.2013.12.077

Galuska, S. P., Galuska, C. E., Tharmalingam, T., Zlatina, K., Prem, G., Husejnov, F. C., et al. (2017). *In vitro* generation of polysialylated cervical mucins by bacterial polysialyltransferases to counteract cytotoxicity of extracellular histones. *FEBS J.* 284, 1688–1699. doi: 10.1111/febs.14073

Harr, J. C., Gonzalez-Sandoval, A., and Gasser, S. M. (2016). Histones and histone modifications in perinuclear chromatin anchoring: from yeast to man. *EMBO Rep.* 17, 139–155. doi: 10.15252/embr.201541809

Hirsch, E., Filipovich, Y., and Mahendroo, M. (2006). Signaling via the type I IL-1 and TNF receptors is necessary for bacterially induced preterm labor in a murine model. *Am. J. Obstet. Gynecol.* 194, 1334–1340. doi: 10.1016/j.ajog.2005.11.004

Kawasaki, H., and Iwamuro, S. (2008). Potential roles of histones in host defense as antimicrobial agents. *Infect. Disord. Drug Targets* 8, 195–205. doi: 10.2174/1871526510808030195

Kothary, V., Doster, R. S., Rogers, L. M., Kirk, L. A., Boyd, K. L., Romano-Keeler, J., et al. (2017). Group B Streptococcus induces neutrophil recruitment to gestational tissues and elaboration of extracellular traps and nutritional immunity. *Front. Cell. Infect. Microbiol.* 7:19. doi: 10.3389/fcimb.2017.00019

Lefrançais, E., and Looney, M. R. (2017). Neutralizing extracellular histones in acute respiratory distress syndrome: a new role for an endogenous pathway. *Am. J. Respir. Crit. Care Med.* 196, 122–124. doi: 10.1164/rccm.201701-0095ED

Lindqvist, I., Einarsson, B., Nilsson, O., and Ronquist, G. (1978). The *in vivo* transport of ^{14}C-α-aminoisobuturic acid into mouse blastocysts during activation for implantation. *Acta Physiologica* 102, 477–483. doi: 10.1111/j.1748-1716.1978.tb06096.x

Mårdh, P. A. (2004). Tubal factor infertility, with special regard to chlamydial salpingitis. *Curr. Opin. Infect. Dis.* 17, 49–52. doi: 10.1097/00001432-200402000-00010

Munn, D. H., Zhou, M., Attwood, J. T., Bondarev, I., Conway, S. J., Marshall, B., et al. (1998). Prevention of allogeneic fetal rejection by tryptophan catabolism. *Science* 281, 1191–1193. doi: 10.1126/science.281.5380.1191

Nilsson, B. O., and Ljung, L. (1985). X-ray micro analyses of cations (Na, K, Ca) and anions (S, P, Cl) in uterine secretions during blastocyst implantation in the rat. *J. Exp. Zool.* 234, 415–421. doi: 10.1002/jez.1402340309

Papayannopoulos, V. (in press). Neutrophil extracellular traps in immunity and disease. *Nat. Rev. Immunol.* doi: 10.1038/nri.2017.105

Parseghian, M. H., and Luhrs, K. A. (2006). Beyond the walls of the nucleus: the role of histones in cellular signaling and innate immunity. *Biochem. Cell Biol.* 84, 589–595. doi: 10.1139/o06-082

Silk, E., Zhao, H., Weng, H., and Ma, D. (2017). The role of extracellular histone in organ injury. *Cell Death Dis.* 8:e2812. doi: 10.1038/cddis.2017.52

Simon, P., Bäumner, S., Busch, O., Röhrich, R., Kaese, M., Richterich, P., et al. (2013). Polysialic acid is present in mammalian semen as a post-translational modification of the neural cell adhesion molecule NCAM and the polysialyltransferase ST8SiaII. *J. Biol. Chem.* 288, 18825–18833. doi: 10.1074/jbc.M113.451112

Smith, J. A., Martin, L., King, R. J. B., and Vértes, M. (1970). Effects of oestradiol-17β and progesterone on total and nuclear-protein synthesis in epithelial and stromal tissues of the mouse uterus, and of progesterone on the ability of these tissues to bind oestradiol-17β. *Biochem. J.* 119, 773–784. doi: 10.1042/bj1190773

Van Winkle, L. J. (1977). Low Na^+ concentration: a factor contributing to diminished uptake and incorporation of amino acids by diapausing mouse blastocysts?. *J. Exp. Zool.* 202, 275–281. doi: 10.1002/jez.1402020218

Van Winkle, L. J. (1993). Endogenous amino acid transport systems and expression of mammalian amino acid transport proteins in *Xenopus oocytes*. *Biochim. Biophys. Acta* 1154, 157–172. doi: 10.1016/0304-4157(93)90009-D

Van Winkle, L. J., and Campione, A. L. (1987). Development of amino acid transport system $B^{0,+}$ in mouse blastocysts. *Biochim. Biophys. Acta* 925, 164–174. doi: 10.1016/0304-4165(87)90106-1

Van Winkle, L. J., Campione, A. L., and Webster, D. P. (1983). Sodium ion concentrations in uterine flushings from "implanting" and "delayed implanting" mice. *J. Exp. Zool.* 226, 321–324. doi: 10.1002/jez.1402260219

Van Winkle, L. J., Tesch, J. K., Shah, A., and Campione, A. L. (2006). System $B^{0,+}$ amino acid transport regulates the penetration stage of blastocyst implantation with possible long-term developmental consequences through adulthood. *Hum. Reprod. Update* 12, 145–157. doi: 10.1093/humupd/dmi044

Wiesenfeld, H. C., Hillier, S. L., Krohn, M. A., Amortegui, A. J., Heine, R. P., Landers, D. V., et al. (2002). Lower genital tract infection and endometritis: insight into subclinical pelvic inflammatory disease. *Obstet. Gynecol.* 100, 456–463. doi: 10.1097/00006250-200209000-00011

Witkin, S. S., Linhares, I. M., Bongiovanni, A. M., Herway, C., and Skupski, D. (2011). Unique alterations in infection-induced immune activation during pregnancy. *BJOG* 118, 145–153. doi: 10.1111/j.1471-0528.2010.02773.x

Wygrecka, M., Kosanovic, D., Wujak, L., Reppe, K., Henneke, I., Frey, H., et al. (2017). Antihistone properties of C1 esterase inhibitor protect against lung injury. *Am. J. Respir. Crit. Care Med.* 196, 186–199. doi: 10.1164/rccm.201604-0712OC

Xu, J., Zhang, X., Pelayo, R., Monestier, M., Ammollo, C. T., Semeraro, F., et al. (2009). Extracellular histones are major mediators of death in sepsis. *Nat. Med.* 15, 1318–1321. doi: 10.1038/nm.2053

Yang, R., Zou, X., Tenhunen, J., and Tønnessen, T. I. (2017). HMGB1 and extracellular histones significantly contribute to systemic inflammation and multiple organ failure in acute liver failure. *Mediators Inflamm.* 2017, 1–6. doi: 10.1155/2017/5928078

Conflict of Interest Statement: The author declares that the research was conducted in the absence of any commercial or financial relationships that could be construed as a potential conflict of interest.

frontiers in Cell and Developmental Biology

ORIGINAL RESEARCH
published: 28 September 2017
doi: 10.3389/fcell.2017.00089

Maternally Contributed Folate Receptor 1 Is Expressed in Ovarian Follicles and Contributes to Preimplantation Development

Trine Strandgaard[1†], Solveig Foder[1†], Anders Heuck[1], Erik Ernst[2], Morten S. Nielsen[1,3] and Karin Lykke-Hartmann[1,4,5]*

[1] Department of Biomedicine, Aarhus University, Aarhus, Denmark, [2] Department of Gynaecology and Obstetrics, Aarhus University Hospital, Aarhus, Denmark, [3] Lundbeck Foundation Research Initiative on Brain Barriers and Drug Delivery, Aarhus University, Aarhus, Denmark, [4] Department of Clinical Medicine, Aarhus University, Aarhus, Denmark, [5] Department of Clinical Genetics, Aarhus University Hospital, Aarhus, Denmark

OPEN ACCESS

Edited by:
Tomer Avidor-Reiss, University of Toledo, United States

Reviewed by:
Richard Eugene Frye, University of Arkansas for Medical Sciences, United States
Daniel Rossignol, Rossignol Medical Center, United States
Alfredo Ulloa-Aguirre, National Autonomous University of Mexico, Mexico

***Correspondence:**
Karin Lykke-Hartmann
kly@biomed.au.dk

[†] *These authors have contributed equally to this work.*

Specialty section:
This article was submitted to Cell Growth and Division, a section of the journal Frontiers in Cell and Developmental Biology

Received: *02 August 2017*
Accepted: *19 September 2017*
Published: *28 September 2017*

Citation:
Strandgaard T, Foder S, Heuck A, Ernst E, Nielsen MS and Lykke-Hartmann K (2017) Maternally Contributed Folate Receptor 1 Is Expressed in Ovarian Follicles and Contributes to Preimplantation Development. Front. Cell Dev. Biol. 5:89. doi: 10.3389/fcell.2017.00089

Folates have been shown to play a crucial role for proper development of the embryo as folate deficiency has been associated with reduced developmental capacity such as increased risk of fetal neural tube defects and spontanous abortion. Transcripts encoding the reduced folate carrier RFC1 (SLC19A1 protein) and the high-affinity folate receptor FOLR1 are expressed in oocytes and preimplantation embryos, respectively. In this study, we observed maternally contributed FOLR1 protein during mouse and human ovarian follicle development, and 2-cell mouse embryos. In mice, FOLR1 was highly enriched in oocytes from primary, secondary and tertiary follicles, and in the surrounding granulosa cells. Interestingly, during human follicle development, we noted a high and specific presence of FOLR1 in oocytes from primary and intermediate follicles, but not in the granulosa cells. The distribution of FOLR1 in follicles was noted as membrane-enriched but also seen in the cytoplasm in oocytes and granulosa cells. In 2-cell embryos, FOLR1-eGFP fusion protein was detected as cytoplasmic and membrane-associated dense structures, resembling the distribution pattern observed in ovarian follicle development. Knock-down of *Folr1* mRNA function was accomplished by microinjection of short interference (si)RNA targeting *Folr1*, into mouse pronuclear zygotes. This revealed a reduced capacity of *Folr1* siRNA-treated embryos to develop to blastocyst compared to the siRNA-scrambled control group, indicating that maternally contributed protein and zygotic transcripts sustain embryonic development combined. In summary, maternally contributed FOLR1 protein appears to maintain ovarian functions, and contribute to preimplantation development combined with embryonically synthesized FOLR1.

Keywords: folate receptor 1, follicle development, preimplantation development, siRNA, blastocyst

INTRODUCTION

It is well-established that folates are important for the development of the embryo. Pregnant women are advised to take a dietary supplement of 400 mg folic acid per day from 12 weeks before conception and during the first trimester of pregnancy (Hibbard, 1964; Cawley et al., 2016). Folate deficiency has been associated with increasing the risk of neural tube defects (NTD)

(Detrait et al., 2005; Pitkin, 2007), early spontaneous abortion (George et al., 2002), congenital heart defects (Rosenquist et al., 2010) and orofacial clefts (Taparia et al., 2007) amongst others.

The folate receptor is highly expressed in reproductive tissues thereby providing folate to the embryo (da Costa et al., 2003). Deficiency in folate uptake can cause pregnancy-related complication such as NTD, a well-established association (Centers for Disease Control, 1991a,b; MRC Vitamin Study Research Group, 1991; Czeizel and Dudas, 1992; Cragan et al., 1995). Interestingly, the identification of folate receptor autoantibodies in in women with recurrent NTD pregnancies might mechanistically explain how the embryo is deprived of folate (Rothenberg et al., 2004; Berrocal-Zaragoza et al., 2009; Sequeira et al., 2013). Additionally, variation in folate pathway genes are associated with female infertility (Altmae et al., 2010). In line with this, postnatally acquired FR autoantibodies blocking folate transport to the brain have been associated with the infantile-onset cerebral folate deficiency syndrome (Ramaekers et al., 2005), which in a number of patients manifests as low-functioning autism with neurological deficits (Ramaekers et al., 2007). Folic acid supplementation in pregnancy may have beneficial effects on the neurodevelopment of children, such as cerebral folate deficiency syndrome and autism spectrum disorders (Desai et al., 2016), beyond its proven effect on NTDs (Blencowe et al., 2010; De-Regil et al., 2015; Gao et al., 2016).

It is proposed that folate deficiency affects gene expression by disrupting DNA methylation patterns or by inducing base substitutions, DNA breaks, gene deletions and gene amplification (Crott et al., 2008). In line with this, mutations in the enzyme methionine synthase reductase (*Mtrr*), necessary for utilization of methyl groups from the folate cycle, affect the folate metabolism and cause epigenetic instability (Padmanabhan et al., 2013). The phenotypes of the *Mtrr*-deficient mice included congenital malformations with neural tube, heart and placental defects, which persisted for five generations, through transgenerational epigenetic inheritance (Padmanabhan et al., 2013). Folates are co-enzymes responsible for the 1-carbon (1C) unit transfer important for purine, pyrimidine and methionin synthesis, and glycine and serine metabolism (Fowler, 2001). The methionine synthesized from homocysteine in the folate cycle is the only significant source (in most cells) of the universal methyl donor, *S*-adenosyl methionine (SAM), and is essential for methylation processes (Stover, 2009). Although folates are recycled in the folate cycle, it is essential to accumulate as folates are degraded. Folates, where 5-methyl-THF is the predominant bioavailable form in mammals, can either be taken up directly from dietary sources or produced by metabolism of dietary folic acid (Kooistra et al., 2013).

Folate is principally taken up into cells by a reduced folate carrier, RFC1, and by two different folate receptors with high affinity for folate, FOLR1 and FOLR2 (Kooistra et al., 2013). Other members of the receptor family are FOLR3 and FOLR4. The folate receptors are attached to the extracellular side of the membrane by a glycosylphosphatidylinositol anchor (GPI-anchor). The folate receptors are heavily glycosylated and bind folic acid and 5-methyl-tetrahydrofolate (5-methyl-THF) with high affinity (Brigle et al., 1994; Chen et al., 2013). RFC1 has been reported expressed in cumulus-oocyte-complexes (COC) but not in preimplantation embryos, suggesting a role in folate accumulation in the COC cells, but without transport into the enclosed oocyte (Kooistra et al., 2013). FOLR1 has been shown to be an important receptor for the uptake of folates into the cells and has been found expressed in mouse preimplantation embryos, increasing from the 2-cell stage onwards (Kooistra et al., 2013). FOLR2 has not been reported expressed in neither COC nor preimplantation embryos (Kooistra et al., 2013) and binds folic acid with lower affinity than FOLR1 (Brigle et al., 1994). FOLR3 does bind folic acid, but it is a constitutively secreted protein rather than a membrane bound one, probably due to the lack of an efficient signal for glycosylphosphatidylinisotol (GPI)-anchor attachment (Shen et al., 1995). FOLR4 (Juno (FR-d in humans)) is not a typical member of the Folate Receptor Family, but share a high structural homology with FOLR1 (Spiegelstein et al., 2000). Juno-deficient mice are infertile (Bianchi et al., 2014).

The basis of folate supplementation of folate has been administrated as oral or intravenous folinic acid (5-formyltetrahydrofolate) treatments that has been shown to improve clinical status. Folinic acid can be transported through the RFC and participate in folate dependent reactions compared to both folic acid and MTHF that needs further processing (Desai et al., 2016; Frye et al., 2016; Ramaekers et al., 2016).

Mice deficient of *Folr1* are defective in early embryonic development (Piedrahita et al., 1999), in contrast to *Folr2*-deficient mice that developed normally (Piedrahita et al., 1999). *Folr1*$^{-/-}$ embryos died at day E10 with severe morphological abnormalities, and interestingly, these phenotypes could be reverted by maternal supplement of *Folr*$^{+/-}$ dams with folic acid (Piedrahita et al., 1999). The *curly tail* (*ct*) mouse provides a model for neuronal tube defects (spina bifida and exencephaly) (Van Straaten and Copp, 2001). However, folate supplement does not prevent NTD in *ct/ct* embryos (Burren et al., 2010), but formate supplementation enhanced the folate-dependent nucleotide biosynthesis and prevented spina bifida (Sudiwala et al., 2016). Interestingly, primary cultures of mouse embryonic fibroblasts established from *Folr1*$^{-/-}$ embryos revealed altered signal transduction in pathways including transforming growth factor beta 1 (TGFβ1) and the canonical Wnt signaling pathways suggesting that pathways for proper development are significantly altered (Warner et al., 2011).

Besides a role in signal transduction, it has been shown that FOLR1 can act as a transcription factor. In cell lines, FOLR1 translocated to the nucleus and interacted with FGFR4 and HES1, and was suggested to regulate a wide range of developmental genes (Boshnjaku et al., 2012).

In this study, we noted the presence of maternally contributed FOLR1 during mouse and human ovarian follicle development. In mouse follicles, the presence of FOLR1 was observed in both oocytes and the surrounding granulosa cells. In contrast, FOLR1 was restricted to oocytes in follicles from human tissue. In 2-cell embryos, FOLR1-eGFP fusion protein was detected as cytoplasmic and membrane-associated dense structures, resembling the observed cellular localization in ovarian follicle development.

Microinjections of short interference (si)RNA probes targeting the *Folr1* transcript revealed an efficient knock-down of the embryonic *Folr1* transcript. Interestingly, siRNA-mediated knock-down of *Folr1* in zygotes reduced the ability of embryos to develop to blastocyst. This indicates that maternally contributed FORLR1 protein and zygotically synthesized *Folr1* transcripts sustain embryonic development combined.

RESULTS

Folr1 Transcript is Detectable from 2-Cell Stage Onwards during Mouse Preimplanation Development

We first wished to analyse if the *Folr1* transcript would be expressed in germinal vesicle (GV) and metaphase II (MII) oocytes as well as during preimplantation development, and thus, if the transcript would be expressed solely from the zygotic genome. Toward this end, RT-qPCR was performed to analyse the expression pattern of *Folr1* during preimplantation stages of embryonic development (**Figure 1**). Histone *H2a.z* mRNA was used as the most stable internal reference gene during preimplanation development (Jeong et al., 2005; Albertsen et al., 2010). The expected size of *Folr1* and *H2af.z* PCR products were verified by gel electrohoresis (data not shown). The qPCR analysis revealed that *Folr1* was detectable at very low expression at the 2-cell stage, and then its transcript gradually increased to the blastocyst stages (**Figure 1**). We observed no detecable levels of *Folr1* in GV and MII oocytes (**Figure 1**). We used tissue from kidney to successfully verify the primer efficiency **Figure 1**.

This suggests that the *Folr1* transcription is initiated during the first wave of genomic transcripton activation during the 2-cell stage, and remains expressed during preimplantation development.

FOLR1 in Mouse Ovarian Tissue

As we did not detect any *Folr1* transcript before the 2-cell stage, we asked if there might be a maternal supply of FOLR1 protein during folliculogenesis. We set out to interrogate the presence and distribution of maternal FOLR1 in mouse ovarian tissue by immunohistochemistry (IHC). Firstly, Western blot analysis was performed to confirm the specificity of the FOLR1 antibody. Western blotting revealed a single protein band of approximately 50 kDa in both ovarian tissue and the kidney control sample (**Figure 2A**). FOLR1 was estimated to provide a band of approximately 30 kDa, indicating that post-translational modifications such as glycosylation might be added to the receptor. To verify this, the samples were treated with the Endoglycosidase H, a recombinant glycosidase that cleaves within the chitobiose core of high mannose and some hybrid oligosaccharides from *N*-linked glycoproteins. After endoglycosidase H treatment, FOLR1 was deglycosylated and a protein band of 30 kDa was observed in ovarie and kidney lysates (**Figure 2A**). The ability of the FOLR1 antibody to specifically detect FOLR1 in paraffin-embedded was verified on a positive kidney control (**Figure 2B**). A negative control (no primary

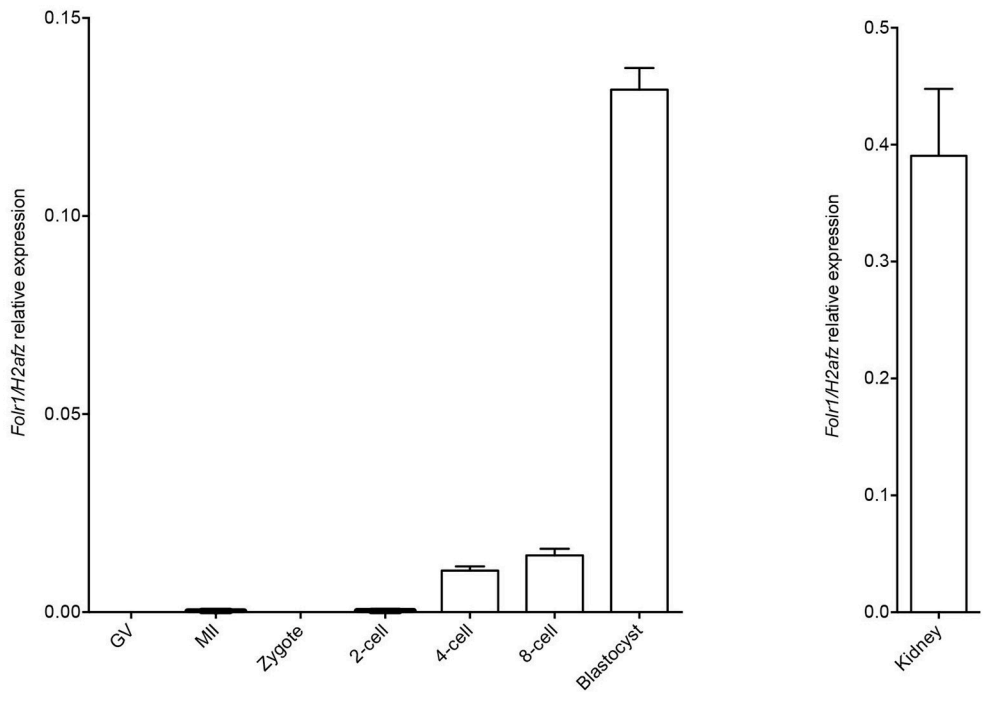

FIGURE 1 | *Folr1* gene expression in oocytes and preimplantation embryos. *Folr1* expression and relative abundan in GV and MII oocytes and preimplantation embryos, as indicated. Kidney tissue was included as a positive control. *Folr1* expression levels were normalized by *H2afz* and relative expression displayed. Data are presented as mean standard deviation SD (bars) of triplicate measurements including standard deviations.

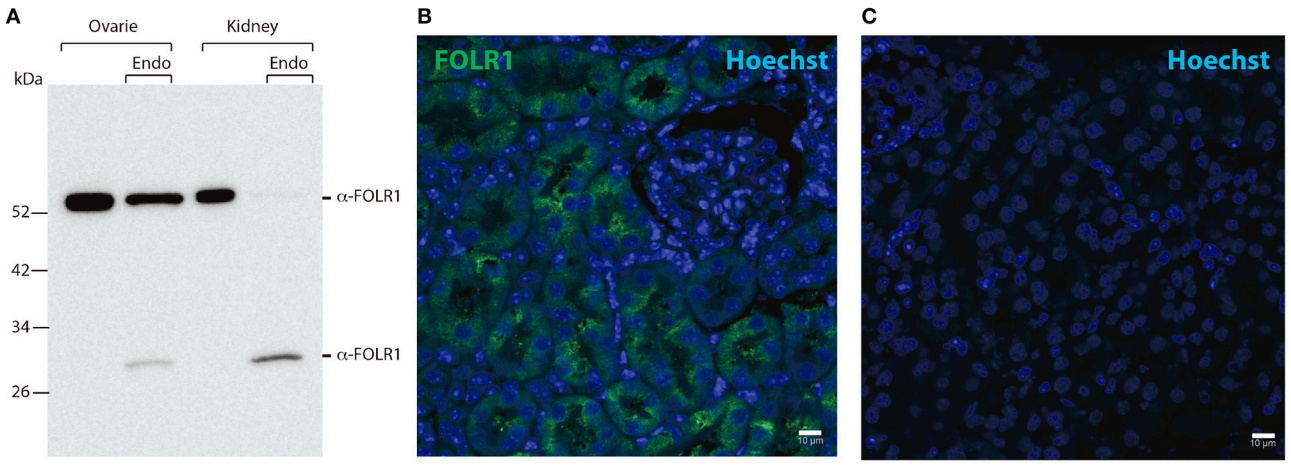

FIGURE 2 | Western blotting and immunohistochemistry controls. **(A)** Western blot of ovary and kidney lysates [with and without Endoglycosidase H (Endo) treatment] from adult mice with antibodies against FOLR1. **(B)** Immunofluorescence staining of kidney from adult mice using antibodies against the FOLR1 (green) **(C)** or without antibody against FOLR1, counterstained with Hoechst (blue) for nuclear stain. Scale bars: 10 µm.

antibody) was included and revealed no detectable staining (**Figure 2C**).

To determine the presence and intraovarian distribution of FOLR1 in the ovary, IHC was performed on paraffin-embedded and sectioned tissue. In the mouse ovary, the FOLR1 was observed in both oocytes and the surrounding granulosa cells in the tested stages of follicles (**Figure 3**), indicating that FOLR1 transport is possible in both germ and somatic cells. In human, the FOLR1 was strongly noted in the oocytes of the included follicle stages (**Figure 4**), and in contrast to the FOLR1 distribution in mice, no FOLR1 was detected in the granulosa cells.

In summary, a pronounced FOLR1 localization was observed in the periphery of the cells compared to the cytoplasm.

FOLR1 Distribution in Mouse 2-Cell Embryos

In order to test if the FOLR1 would display a dynamic intracellular distribution upon fertilization, FOLR1 was fused to enhanced green fluorescent protein (eGFP), to enable us to follow its dynamics and distribution. However, no dynamics was observed in the distribution of FOLR1 between zygotes and 2-cell stage embryos (data not shown). The FOLR1-EGFP distributed in vesicle-like structures in the periphery of the cell membrane, as well as in the cytoplasm (**Figure 5**). As a control, eGFP localization was observed in the 2-cell embryo, which revealed no specific distribution (**Figures 6A,B**). In the 2-cell stage (as in zygotes), the FOLR1-eGFP fusion protein resembled that observed for FOLR1 IHC in oocytes and granulosa cells in the ovaries.

siRNA-Mediated Knockdown of *Folr1* Compromised Early Developmental Potential

In order to reveal whether or not newly generated zygotic *Folr1* transcripts would be necessary to support early development (along side the maternally contributed FOLR1 protein), RNA interference (RNAi) was used as an approach to knock-down *Folr1* transcript. SiRNA-mediated knock-down of the *Folr1* transcript was accomplished by microinjection into mouse pronuclear zygotes. SiRNA probes targeting *Folr1* or scrambled (non-targeting) RNA (co-microinjected with rhodamine-conjugated dextran into zygotes in order to identify embryos that has received siRNAs) were microinjected into zygotes at the pronuclear stage (three independent experiments) (**Figure 7A**). After an overnight *in vitro* incubation, 2-cell stage embryos were collected for qPCR analysis, which revealed that the *Folr1* transcript was effectively reduced in *Folr1* siRNA-microinjected embryos (**Figure 7A**).

The embryos were subsequently monitored for their ability to develop into blastocysts. In the group of embryos injected with siRNA scrambled, 92% (21 out of 23) of the 2-cell stage embryos developed into blastocyst**,** where in the group that received siRNA targeting *Folr1*, only 56% (14 out of 25) of the 2-cell stage embryos developed into blastocysts **Figure 7B**.

This indicates that zygotic *Folr1* is indeed required to foster development, however, maternally contributed FOLR1 protein can sustain embryonic development. It might be that this is a fine-tuned gradient and dependent on the level of maternal FOLR1 protein contributed.

DISCUSSION

Dysfunctional maternal folate metabolism caused by folate deficiency or polymorphisms are associated with congenital abnormalities, intrauterine growth restrictions, placental and cardiovascular abnormalities as well as neural tube defects in human. While parts of the abnormalities can be directly associated with the embryonic expression of FOLR1, it is likely that maternally contributed FOLR1 might already mark ovarian cells before fertilization, and influence pre- and post-implantation development.

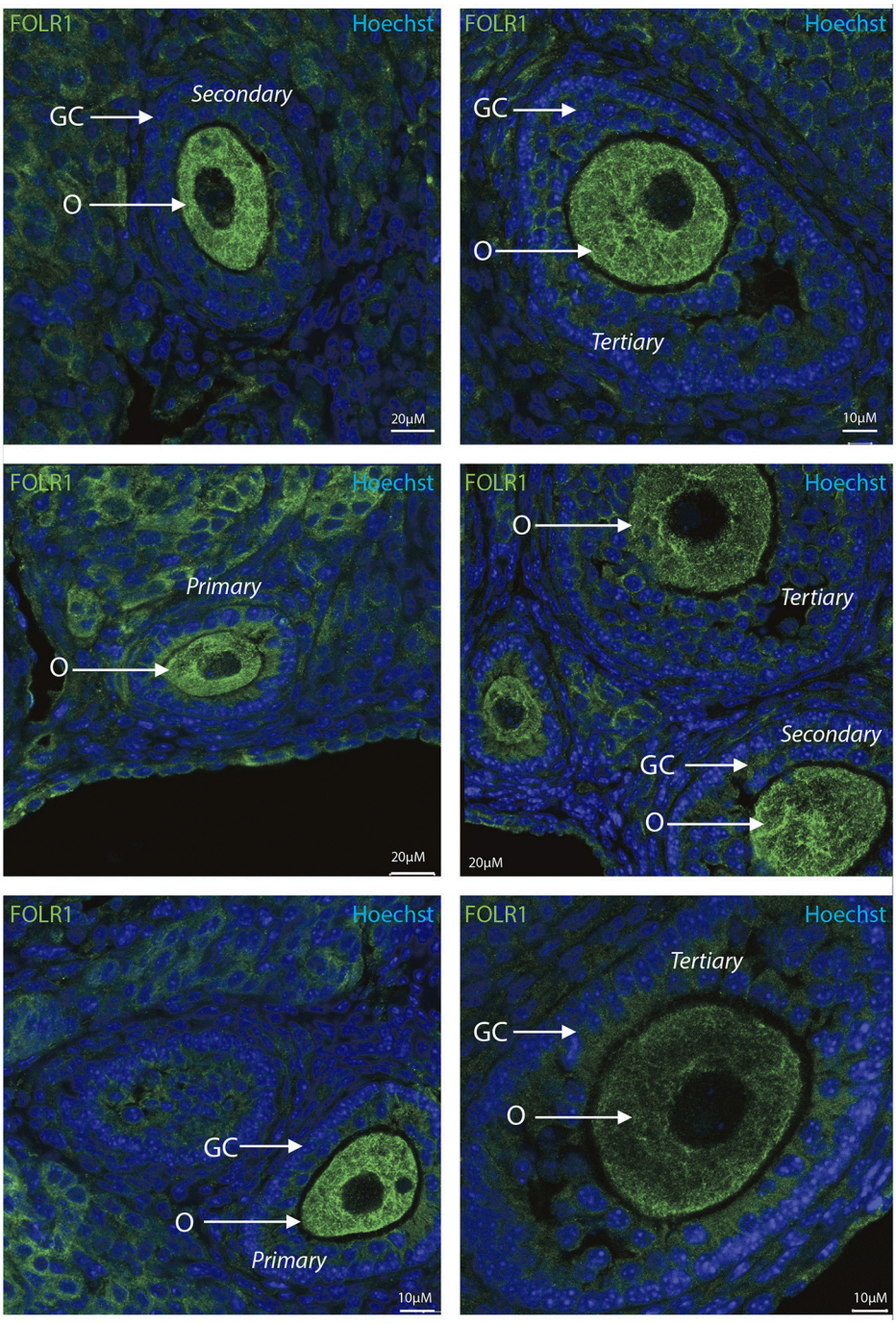

FIGURE 3 | Intraovarian distribution of FOLR in mouse ovary tissue. FOLR1 localized to oocytes in primary, secondary and tertiary follicles. Hoechts staining identifies the nucleus of cells in the slides and the surrounding granulosa cells. o, oocytes; GC, granulosa cells. Scale bars; 10 or 20 μm, as indicated.

Transcripts encoding the FOLR1 has not been investigated in ovarian follicles. However, a recent study enterrogated the transcriptomes in human oocytes from primordial and primary follicles, which did not detect expression of the *FOLR1* gene (Ernst et al., 2017). Whether granulosa cells from primordial and primary follicles express the *Folr1* transcript remains to be investigated.

In agreements with another study, we found that *Folr1* transcription appeared to initiate at the 2-cell stage, which is further emphasized in a study that interrogated amantidine-sensitive transcrips, which included *Folr1* (Zeng and Schultz, 2005). Interestingly, this appears to be conserved between different mice strains, as experiments were performed independently on three different strains [CF1 (Crl:CF1) females

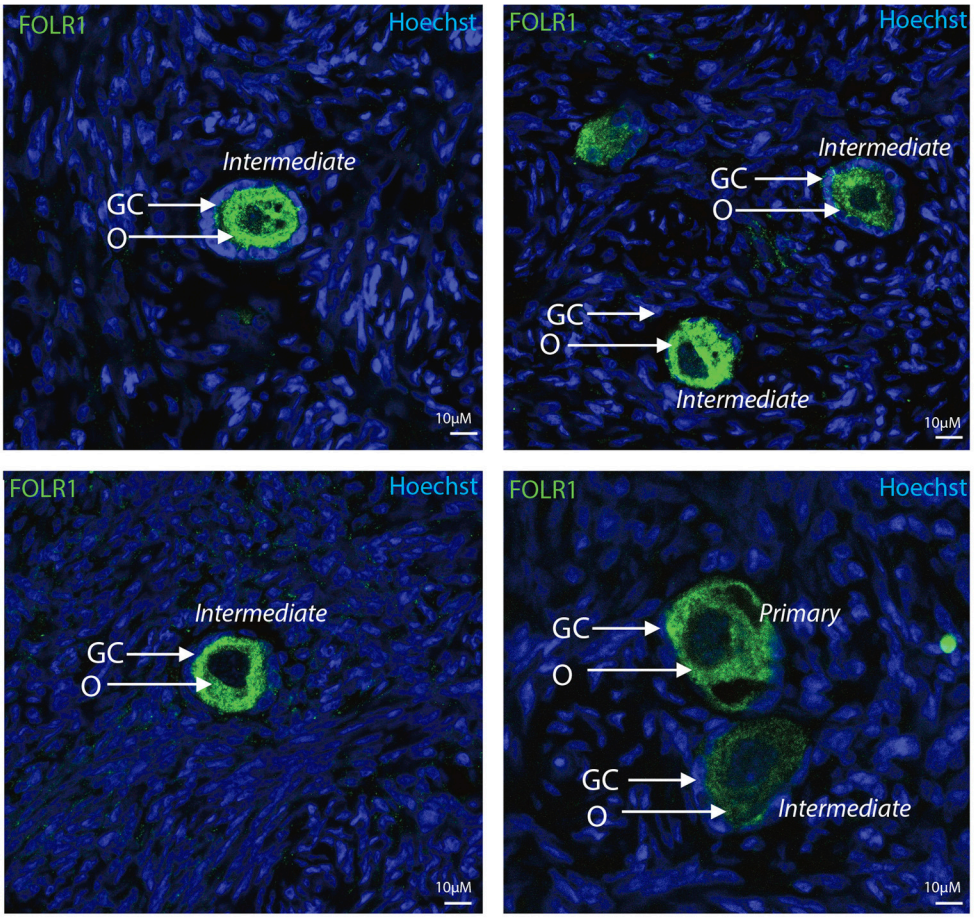

FIGURE 4 | Intraovarian distribution of FOLR in human ovary tissue. FOLR1 localized to oocytes in primary and intermediate follicles. Hoechts staining identifies the nucleus of cells in the slides and the surrounding granulosa cells. o, oocytes; GC, granulosa cells. Scale bars; 10 μm, as indicated.

(Charles River) and BDF1 (B6D2F1/Crl) males (Charles River) (Kooistra et al., 2013), superovulated female CF-1 mice (Harlan) mated to B6D2F1/J males (Jackson Laboratory) (Zeng and Schultz, 2005) and F1 [CBA (C57BL/6jxCBA) females and males (Janvier, this study).

Secreted FOLR1 proteins are either anchored to membranes via a glycosyl-phosphatidylinositol linkage or exist in a soluble form. The receptor-ligand complex is endocytosed into cytoplasmic vesicles and then recycled to the cell membrane. In our IHC, we accordingly observed FOLR1 at the cell membrane, but also noted it in the cytoplasm, resembling the intracellular transport of FOLR1. This might simply reflect the staus quo of the cell in the absence of active folate transport. Thus, in conclusion, it appears that oocyte folate accumulation must occur during follicle development, where folate is maternally supplied. The observation of the folate receptor in both oocytes and granulosa cells in the mouse follicles, but limited to oocytes in the follicles from human samples remains to be further investigated. Very low levels of the folate receptor and/or specific folate supplement might represent likely reasons that the folate receptor was not detected in human granulosa cells. FOLR1 appeared to be absent from the nucleus during follicle development, which suggest that during these stages in development, FOLR1 does not act as a transcription factor. This suggests that the function of FOLR1 during these stages is perhaps assigned predominantly to folate metabolism and signal transduction. Indeed, the role of TGFβ1 in ovarian physiology is well-know, and due to the fact that folate deficiency can alter this pathway, it might be that FOLR1 could influence this, as well, in ovarian follicles.

The FOLR1 distribution in 2-cell stage embryos was interogated using a eGFP fusion approach and the intracellular distribution of FOLR1-eGFP was comparable to that observed in the follicles. FOLR1-eGFP was concentrated at the cell membrane and further noted in cytoplasm, indicating that the FOLR1-eGFP follows the endogoues folate transport and makes this construct suitable for future studies on folate transport in embryonic cells.

Interestingly, while some of the embryos that were submitted to *Folr1* RNAi were indeed able to complete development to the blastocyst stage, several arrest development during later preimplantation stages. This indicates that during preimplantation development, the levels of *Folr1* transcript and FOLR1 protein are finely balanced to rely on maternally

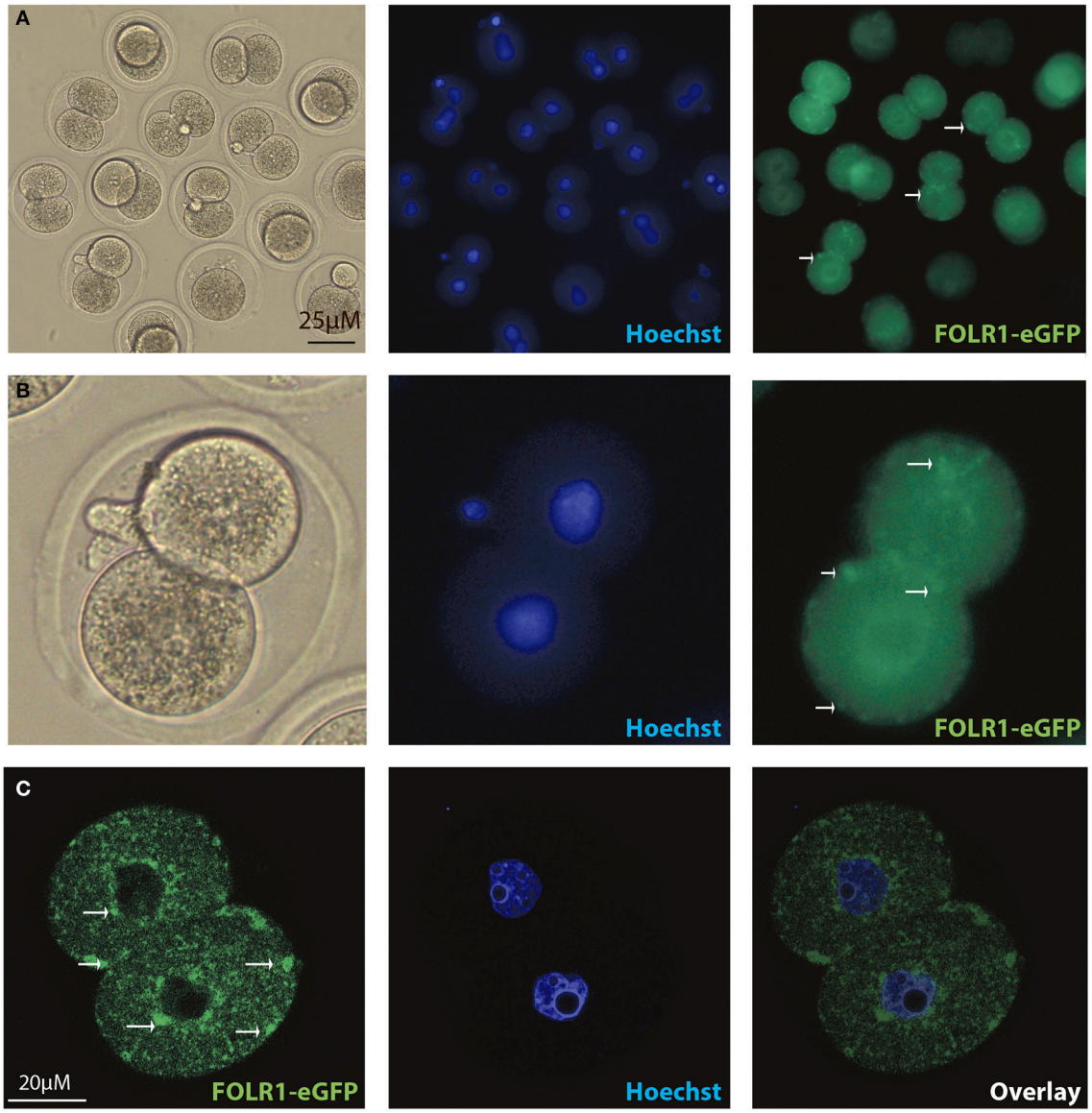

FIGURE 5 | Intracellular distribution of FOLR1-eGFP in mouse 2-cell embryos. Intracelluar immunofluorescent localization and distribution of FOLR1-eGFP in 2-cell mouse embryos using microscopic **(A,B)** confocal imaging **(C)**. Scale bars 20 or 25 μM, as indicated.

contributed proteins and the generation of zygotically-derived *Folr1*. Thus, this suggests that indeed the maternal supply of FOLR1 protein remain during preimplantation and is partly sufficient to support the development until blastocyst stage. Developmental competences might therefore be much more dependent on the maternal internal pool of folate than previously anticipated and variations might account for folate-associated deficiencies.

In this context, it is curious to note that most *in vitro*-based experiments today are performed without folate supplement to the media, even though the long term consequences of folate deficiency in the medium is unknown. It opens a question whether or not we should in fact supplement *in vitro* culture media with folate. Further studies are needed to address whether variations in folate storage might influence developmental potential accordingly.

The long-term effect of *Folr1* RNAi is not known, and it might be that depletion of *Folr1* could interfere with post-implantation. This is indeed in line with the fact that even low blood folate levels in pregnant women are correlated with higher risk of neural tube deficiency in their offspring (Smithells et al., 1976; Detrait et al., 2005), and periconceptional supplementation of folate reduces the occurrence of neural tube defects (Centers for Disease Control, 1991a,b; MRC Vitamin Study Research Group, 1991). Future studies are needed to elucidate the cellular and molecular mechanisms underlying folate and FOLR1 functions

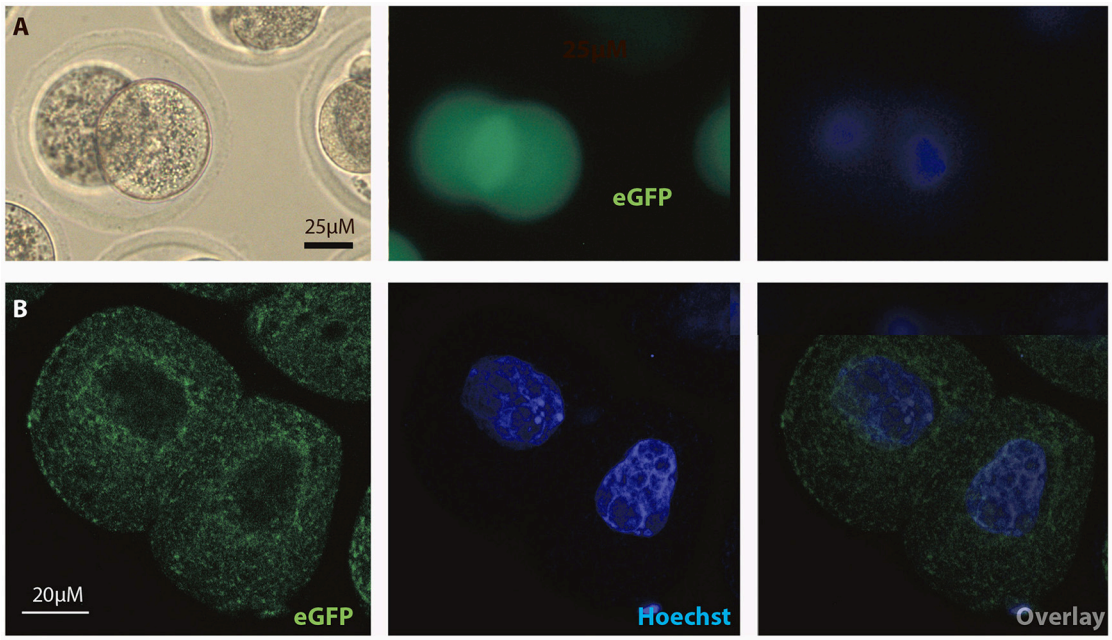

FIGURE 6 | Intracellular distribution of eGFP in mouse 2-cell embryos. Intracelluar immunofluorescent localization and distribution of eGFP in 2-cell mouse embryos using **(A)** microscopic and **(B)** confocal imaging. Scale bars 20 or 25 μM, as indicated.

and correlation between FOLR1 in preimplantation and early post-implantation development. This could include the CRISP-Cas9 technology and/or a conditional knock-out strategy to functionally knock-down the folate receptor before fertilization.

MATERIALS AND METHODS

Embryo Isolation

Embryo recovery and isolation F1 (C57BL/6xCBA) females were injected with 5 IU pregnant mare's serum gonadotrophin (PMSG; Folligon, Intervet) and with 5 IU human chorionic gonadotrophin (hCG; Chorulon; Intervet) 48 and 24 h later to induce ovulation, respectively, as described previously (Hogan et al., 1994), and mated with F1 (C57BL/6xCBA) males. Zygotes, 2-cell, 4-cell, and 8-cell embryos were collected at 26, 46, 56, and 64 h post hCG (Sigma), respectively. Blastocysts were collected at 72 h post hCG (Sigma). Zygotes for RNA injections were collected from female mice 25 h post-hCG. All procedures were approved by the Ethics Committee for the use of laboratory animals in Aarhus University (2015-15-0201-00800 to KLH). Zygotes were collected from the oviducts and treated with hyaluronidase (Sigma Aldrich)(50 μl of a 3 mg/ml solution in 250 μl M2 medium) to remove surrounding cumulus cells and cultured in M2 media (EmbryoMax® M2 medium with phenol red, Specialty Media, Millipore MR-015P-5F) at 37°C. Embryos were cultured overnight in drops of potassium simplex optimized medium (KSOM) (EmbryoMax KSOM Powdered Media Kit, Specialty Media, Millipore MR-020P-5F) supplemented with amino acids and 4 mg/mL BSA (Millipore) (no folate supplementation), under embryo-tested paraffin oil in an atmosphere of 5% CO_2 in air at 37°C.

RNA Isolation

Total RNA extraction was performed using the RNeasy® Mini Kit (Qiagen). For each stage, 10–20 oocytes or embryos were collected and 350 μl lysis buffer was used. Elution was performed with RNase-free water (Qiagen). For all RNA extractions, a DNase digestion step was performed, using the RNase-Free DNase Set (Qiagen). RNA was subsequently stored at −80°C.

cDNA Synthesis

Ovation® PicoSL WTA System V2 (Nugen) protocol was used to generate cDNA. For each cDNA synthesis reaction, 1.5–10 ng RNA was used.

qPCR

A qPCR analysis of the expression of the *Folr1* gene was made from GV and MII oocytes, 2-cell, 4-cell, 8-cell and blastocyst embryos using the TaqMan® Gene Expression Assay (Applied Biosystems). Reactions were set up for the *Folr1* gene and for the reference gene *H2afz* (Mamo et al., 2007). The reactions were run on a LightCycler® 96 (Roche) using LightCycler® 480 Probes Master (Roche) (Program: 50°C for 2 s, 95°C for 10 min, 45 cycles of 95°C for 15 s followed by 60°C for 60 s and finally 1 cycle of 40°C for 30 s). All reactions were done in triplets with 100 ng of template cDNA in a total volume of 10 μl containing 2 μl H_2O, 0.5 μl TaqMan Gene Expression Assays (Applied Biosystems) (see appendix 2), 5 μl Probes Master (Roche) and 2.5 μl template cDNA (40 ng/μl). Kidney was used as a positive control in the qPCR reaction. Experiments were repeated at least three times. Triplicate expression values of each gene was set relative to the reference gene via the $\Delta\Delta C_T$ methods (Schmittgen and Livak, 2008). As a negative control, cDNA from no template RT PCR

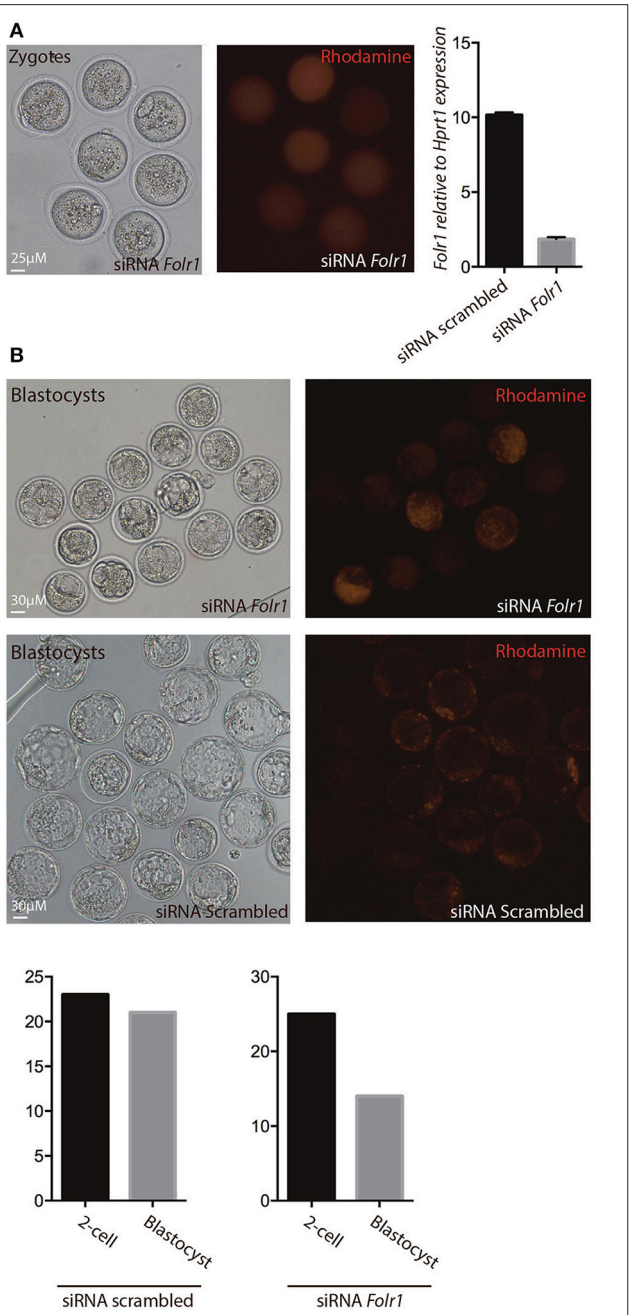

FIGURE 7 | siRNA-mediated knock-down of *Folr1* in mouse zygotes. **(A)** siRNA probes targeting Folr1 (or scrambled control (not shown) was microinjected in combination with rhodamine-conjugated dextrane, in order to identify injected embryos. At the 2-cell stage, qPCR showed that *Folr1* transcript is efficiently reduced after *Folr1* RNAi. **(B)** After *in vitro* culture, siRNA-injected embryos (both RNAi scrambled and *Folr1*) developed into blastocyst, however the capacity to form blastocysts was reduced in embryos that received siRNA targeting *Folr1* (56%) compared to the control RNAi group (92%). Scale bars 25 or 30 μM, as indicated.

reactions was used. All qPCR data was analyzed using Prism 6, version 6.0 (GraphPad Software Inc., CA, U.S.A.). Data are represented as mean ± SD.

Cloning of *Folr1*-e*Gfp*

Folr1 inserts were generated with SuperScript III One-Step RT-PCR System with Platinum Taq High Fidelity (Invitrogen) using kidney RNA as template, and the following primers: Folr1-Xma-F: 5′-NNNCCCGGGatggctcacctgatgactgtgc-3′ and Folr1-Xma-R: 5′-NNNCCCGGGGCTGATCACCCAGAGCAGCA-3′. Using *Xma*I restriction sites, the PCR-amplified *Folr1* insert was cloned into the *Xma*1-digested and dephosporylated pBS_RN3P-eGFP vector (Lemaire et al., 1995), in frame with e*Gfp*. Insert and orientation was verified by DNA sequencing.

Immunohistochemistry

Tissue Collection, Paraffin Embedding, and Sectioning

Mouse ovaries and kidneys were isolated from F1 females and kept overnight in 4% PFA before embedding into paraffin. Human ovarian cortical tissue was procured from patients who underwent unilateral oophorectomy prior to gonadotoxic treatment for a malignant disease (unrelated to any ovarian malignancies). Patients were normo-ovulatory, with normal reproductive hormones, and had not received ovarian stimulation with exogenous gonadotropins. All methods were carried out in accordance with relevant guidelines and regulations, and The Central Denmark Region Committees on Biomedical Research Ethics and the Danish Data Protection Agency approved the study. Written informed consent was obtained from all participants before inclusion. Patients consented to the research conducted. In subjects undergoing oophorectomy, a small pieCe of the ovarian cortex is used for evaluating the ovarian reserve and for research purposes (Danish Scientific Ethical Committee Approval Number: KF 299017 and J/KF/01/170/99) (Schmidt et al., 2003).

Paraffin tissues were cut in sections of 10 μm. Hereafter, the sections were deparaffinized in xylene and rehydrated in graded ethanol series (100, 95, 70%, water) for 5 min in each vessel. The tissue sections were transferred to 0.01 M citrate buffer (Citric acid and sodium citrate) for antigen retrieval and washed in PBS, and incubated with donkey serum (1 ml donkey serum and 4 ml PBS) for 30 min before adding primary FOLR1 antibody (diluted 1:100 (FOLR1 Rabbit anti-Human Polyclonal, LifeSpan BioSciences) overnight at 4°C. The next day the tissues were washed in PBS and then incubated for 1 h at room temperature with the secondary donkey-anti-rabbit antibody [Alexa Fluor® 488 donkey anti-rabbit IgG (Invitrogen)] (dilution of 1:300). In the following washing steps, the tissues were counterstained with Hoechst (Sigma) to stain the nucleus, added to PBS in a dilution of 1:7,500. The tissues were mounted using Fluorescent Mounting Medium (DAKO S3023). Sections were analyzed and confocal images were taken using a LSM780 laser-scanning confocal microscope with 20, 40 and 63xC-Apochromat water/oil immersion objectives (Carl Zeiss, Jena, Germany).

Western Blot

Ovary, kidney and brain cortex were taken out from mice and lysed in a lysis buffer containing 7 ml Tris-EDTA buffer (10 mM

Tris-HCl, 1mM EDTA), 1 tablet of Complete Mini EDTA-free protease inhibitor (Roche) and 1% (70 µl) IGEPAL®CA-630 (Sigma-Aldrich). 30 µg of proteins from ovary, kidney and cortex were used for Western blotting analysis. Primary FOLR1 antibody (see appendix 8) was applied in a concentration of 0.5 µg/ml in the blocking buffer and the membrane was incubated overnight at 4°C. The membrane was washed for 3 × 10 min in PBS-Tween and secondary HRP-conjugated polyclonal swine-anti-rabbit antibody (DAKO S3023) was applied in a dilution of 1:1,000 in blocking buffer and incubated for 1 h at RT. The membrane was incubated in a chemiluminescent detection reagent. [ECLTM Western Blotting Analysis system (GE Healthcare)] and developed for 45 s using a ImageQuant LAS-4000 (GE Healthcare).

Endoglycosidase H (New England Biolabs, P0702S) treatment was performed according to the manufactorers instructions (New England Biolabs protocol).

RNA Synthesis, Microinjections, and Confocal Imaging

Generation of mRNA encoding FOLR1-GFP and GFP and microinjection into zygotes were performed as described (Albertsen et al., 2010). Microinjection of embryos with siRNA (ON_TARGETplus Mouse *Folr1*, Smartpool, L-061448-01-0005 and ON-TARGETplus Non-targeting Pool D-001810-10-05) with the final concentration of 20 µM, together with Rhodamine-conjugated dextran as marker of injection) or mRNA (*Folr1-eGFP*, or *eGfp*, 200–400 ng/µl) was carried out in M2 media (EmbryoMax® M2 medium with phenol red, Specialty Media, Millipore MR-015P-5F) covered in oil on a glass depression slide using a Femtojet micro-injection system (Eppendorf). Embryos were cultured in KSOM (EmbryoMax KSOM Powdered Media Kit, Specialty Media, Millipore MR-020P-5F) under paraffin oil at 37.5°C in air enriched with 5% CO_2. The microinjected zygotes were incubated overnight (37°C, 5% CO_2) in KSOM (EmbryoMax KSOM Powdered Media Kit, Specialty Media, Millipore MR-020P-5F). The next day, 2-cell embryos were incubated for 15 min in a 1:7,500 dilution of Hoechst (Sigma) in DPBS (Life Technologies), washed three times in PBS-T and fixed for 15 min in 2% PFA, before mounting (Fluorescent Mounting Media, DAKO S3023). Embryos were analyzed using the fluorescent microscope (Leica DMI400B) and Leica LAS Software.

Confocal images were taken using a LSM800 laser-scanning confocal microscope with 20, 40, and 63xC-Apochromat water/oil immersion objectives NA 1.2 (Carl Zeiss, Jena, Germany). Confocal images were exported to ImageJ for image processing.

AUTHOR CONTRIBUTIONS

KL conceived the study. TS performed IHC/Western blot experiments. SF performed qPCR analyse. EE contributed with human tissue. MN and KL performed confocal analysis. AH conducted qPCR of siRNA experiments. KL performed siRNA microinjections and wrote the manuscript. All authors approved the final manuscript.

ACKNOWLEDGMENTS

The authors wish to thank past and current members of the Lykke-Hartmann laboratory (AU) for scientific discussions. We are particular grateful to Dr. Emil Hagen Ernst for his advice on human IHC. This work was supported by grants from Kong Christian Den Tiendes Fond, Th. Maigaards Eft. Fru Lily Benthine Lunds Fond, Toyota Fonden, Augustinus Fonden, and Fonden til Lægevidenskabens Fremme (to KL).

REFERENCES

Albertsen, M., Teperek, M., Elholm, G., Fuchtbauer, E. M., and Lykke-Hartmann, K. (2010). Localization and differential expression of the Kruppel-associated box zinc finger proteins 1 and 54 in early mouse development. *DNA Cell Biol.* 29, 589–601. doi: 10.1089/dna.2010.1040

Altmae, S., Stavreus-Evers, A., Ruiz, J. R., Laanpere, M., Syvanen, T., Yngve, A., et al. (2010). Variations in folate pathway genes are associated with unexplained female infertility. *Fertil. Steril.* 94, 130–137. doi: 10.1016/j.fertnstert.2009.02.025

Berrocal-Zaragoza, M. I., Fernandez-Ballart, J. D., Murphy, M. M., Cavalle-Busquets, P., Sequeira, J. M., and Quadros, E. V. (2009). Association between blocking folate receptor autoantibodies and subfertility. *Fertil. Steril.* 91, 1518–1521. doi: 10.1016/j.fertnstert.2008.08.104

Bianchi, E., Doe, B., Goulding, D., and Wright, G. J. (2014). Juno is the egg Izumo receptor and is essential for mammalian fertilization. *Nature* 508, 483–487. doi: 10.1038/nature13203

Blencowe, H., Cousens, S., Modell, B., and Lawn, J. (2010). Folic acid to reduce neonatal mortality from neural tube disorders. *Int. J. Epidemiol.* 39(Suppl. 1), i110–i121. doi: 10.1093/ije/dyq028

Boshnjaku, V., Shim, K. W., Tsurubuchi, T., Ichi, S., Szany, E. V., Xi, G., et al. (2012). Nuclear localization of folate receptor alpha: a new role as a transcription factor. *Sci. Rep.* 2:980. doi: 10.1038/srep00980

Brigle, K. E., Spinella, M. J., Westin, E. H., and Goldman, I. D. (1994). Increased expression and characterization of two distinct folate binding proteins in murine erythroleukemia cells. *Biochem. Pharmacol.* 47, 337–345. doi: 10.1016/0006-2952(94)90025-6

Burren, K. A., Scott, J. M., Copp, A. J., and Greene, N. D. (2010). The genetic background of the curly tail strain confers susceptibility to folate-deficiency-induced exencephaly. *Birth Defects Res. A Clin. Mol. Teratol.* 88, 76–83. doi: 10.1002/bdra.20632

Cawley, S., Mullaney, L., McKeating, A., Farren, M., McCartney, D., and Turner, M. J. (2016). A review of European guidelines on periconceptional folic acid supplementation. *Eur. J. Clin. Nutr.* 70, 143–154. doi: 10.1038/ejcn.2015.131

Centers for Disease Control (1991a). Use of folic acid for prevention of spina bifida and other neural tube defects–1983-1991. *JAMA* 266, 1190–1191. doi: 10.1001/jama.1991.03470090024009

Centers for Disease Control (1991b). Effectiveness in disease and injury prevention use of folic acid for prevention of spina bifida and other neural tube defects - 1983–1991. *MMWR Morb. Mortal. Wkly. Rep.* 40, 513–516.

Chen, C., Ke, J., Zhou, X. E., Yi, W., Brunzelle, J. S., Li, J., et al. (2013). Structural basis for molecular recognition of folic acid by folate receptors. *Nature* 500, 486–489. doi: 10.1038/nature12327

Cragan, J. D., Roberts, H. E., Edmonds, L. D., Khoury, M. J., Kirby, R. S., Shaw, G. M., et al. (1995). Surveillance for anencephaly and spina bifida and the impact of prenatal diagnosis–United States, 1985-1994. *MMWR CDC Surveill. Summ.* 44, 1–13.

Crott, J. W., Liu, Z., Keyes, M. K., Choi, S. W., Jang, H., Moyer, M. P., et al. (2008). Moderate folate depletion modulates the expression of selected genes involved in cell cycle, intracellular signaling and folate uptake in human colonic epithelial cell lines. *J. Nutr. Biochem.* 19, 328–335. doi: 10.1016/j.jnutbio.2007.05.003

Czeizel, A. E., and Dudas, I. (1992). Prevention of the first occurrence of neural-tube defects by periconceptional vitamin supplementation. *N. Engl. J. Med.* 327, 1832–1835. doi: 10.1056/NEJM199212243272602

da Costa, M., Sequeira, J. M., Rothenberg, S. P., and Weedon, J. (2003). Antibodies to folate receptors impair embryogenesis and fetal development in the rat. *Birth Defects Res. A Clin. Mol. Teratol.* 67, 837–847. doi: 10.1002/bdra.10088

De-Regil, L. M., Pena-Rosas, J. P., Fernandez-Gaxiola, A. C., and Rayco-Solon, P. (2015). Effects and safety of periconceptional oral folate supplementation for preventing birth defects. *Cochrane Database Syst. Rev.* 6:CD007950. doi: 10.1002/14651858.CD007950.pub3

Desai, A., Sequeira, J. M., and Quadros, E. V. (2016). The metabolic basis for developmental disorders due to defective folate transport. *Biochimie* 126, 31–42. doi: 10.1016/j.biochi.2016.02.012

Detrait, E. R., George, T. M., Etchevers, H. C., Gilbert, J. R., Vekemans, M., and Speer, M. C. (2005). Human neural tube defects: developmental biology, epidemiology, and genetics. *Neurotoxicol. Teratol.* 27, 515–524. doi: 10.1016/j.ntt.2004.12.007

Ernst, E. H., Grøndahl, M. L., Grund, S., Hardy, K., Heuck, A., Sunde, L., et al. (2017). Dormancy and activation of human oocytes from primordial and primary follicles: molecular clues to oocyte regulation. *Hum. Reprod.* 32, 1684–1700. doi: 10.1093/humrep/dex238

Fowler, B. (2001). The folate cycle and disease in humans. *Kidney Int. Suppl.* 78, S221–S229. doi: 10.1046/j.1523-1755.2001.07851.x

Frye, R. E., Slattery, J., Delhey, L., Furgerson, B., Strickland, T., Tippett, M., et al. (2016). Folinic acid improves verbal communication in children with autism and language impairment: a randomized double-blind placebo-controlled trial. *Mol. Psychiatry*. doi: 10.1038/mp.2016.168. [Epub ahead of print].

Gao, Y., Sheng, C., Xie, R. H., Sun, W., Asztalos, E., Moddemann, D., et al. (2016). New perspective on impact of folic acid supplementation during pregnancy on Neurodevelopment/Autism in the offspring children - a systematic review. *PLoS ONE* 11:e0165626. doi: 10.1371/journal.pone.0165626

George, L., Mills, J. L., Johansson, A. L., Nordmark, A., Olander, B., Granath, F., et al. (2002). Plasma folate levels and risk of spontaneous abortion. *JAMA* 288, 1867–1873. doi: 10.1001/jama.288.15.1867

Hibbard, B. M. (1964). The role of folic acid in pregnancy; with particular reference to anaemia, abruption and abortion. *J. Obstet. Gynaecol. Br. Commonw.* 71, 529–542. doi: 10.1111/j.1471-0528.1964.tb04317.x

Hogan, B., Beddington, R., Costantini, F., and Lacy, E. (1994). *Manipulating the Mouse Embryo: A Laboratory Manual, 2 Edn.* Cold Spring Habor Laboratory Press.

Jeong, Y. J., Choi, H. W., Shin, H. S., Cui, X. S., Kim, N. H., Gerton, G. L., et al. (2005). Optimization of real time RT-PCR methods for the analysis of gene expression in mouse eggs and preimplantation embryos. *Mol. Reprod. Dev.* 71, 284–289. doi: 10.1002/mrd.20269

Kooistra, M., Trasler, J. M., and Baltz, J. M. (2013). Folate transport in mouse cumulus-oocyte complexes and preimplantation embryos. *Biol. Reprod.* 89:63. doi: 10.1095/biolreprod.113.111146

Lemaire, P., Garrett, N., and Gurdon, J. B. (1995). Expression cloning of Siamois, a Xenopus homeobox gene expressed in dorsal-vegetal cells of blastulae and able to induce a complete secondary axis. *Cell* 81, 85–94. doi: 10.1016/0092-8674(95)90373-9

Mamo, S., Gal, A. B., Bodo, S., and Dinnyes, A. (2007). Quantitative evaluation and selection of reference genes in mouse oocytes and embryos cultured *in vivo* and *in vitro*. *BMC Dev. Biol.* 7:14. doi: 10.1186/1471-213X-7-14

MRC Vitamin Study Research Group (1991). Prevention of neural tube defects results of the Medical Research Council Vitamin Study. MRC Vitamin Study Research Group. *Lancet* 338, 131–137.

Padmanabhan, N., Jia, D., Geary-Joo, C., Wu, X., Ferguson-Smith, A. C., Fung, E., et al. (2013). Mutation in folate metabolism causes epigenetic instability and transgenerational effects on development. *Cell* 155, 81–93. doi: 10.1016/j.cell.2013.09.002

Piedrahita, J. A., Oetama, B., Bennett, G. D., Van Waes, J., Kamen, B. A., Richardson, J., et al. (1999). Mice lacking the folic acid-binding protein Folbp1 are defective in early embryonic development. *Nat. Genet.* 23, 228–232. doi: 10.1038/13861

Pitkin, R. M. (2007). Folate and neural tube defects. *Am. J. Clin. Nutr.* 85, 285S–288S.

Ramaekers, V. T., Blau, N., Sequeira, J. M., Nassogne, M. C., and Quadros, E. V. (2007). Folate receptor autoimmunity and cerebral folate deficiency in low-functioning autism with neurological deficits. *Neuropediatrics* 38, 276–281. doi: 10.1055/s-2008-1065354

Ramaekers, V. T., Rothenberg, S. P., Sequeira, J. M., Opladen, T., Blau, N., Quadros, E. V., et al. (2005). Autoantibodies to folate receptors in the cerebral folate deficiency syndrome. *N. Engl. J. Med.* 352, 1985–1991. doi: 10.1056/NEJMoa043160

Ramaekers, V. T., Sequeira, J. M., and Quadros, E. V. (2016). The basis for folinic acid treatment in neuro-psychiatric disorders. *Biochimie* 126, 79–90. doi: 10.1016/j.biochi.2016.04.005

Rosenquist, T. H., Chaudoin, T., Finnell, R. H., and Bennett, G. D. (2010). High-affinity folate receptor in cardiac neural crest migration: a gene knockdown model using siRNA. *Dev. Dyn.* 239, 1136–1144. doi: 10.1002/dvdy.22270

Rothenberg, S. P., Da Costa, M. P., Sequeira, J. M., Cracco, J., Roberts, J. L., Weedon, J., et al. (2004). Autoantibodies against folate receptors in women with a pregnancy complicated by a neural-tube defect. *N. Engl. J. Med.* 350, 134–142. doi: 10.1056/NEJMoa031145

Schmidt, K. L., Byskov, A. G., Nyboe Andersen, A., Muller, J., and Yding Andersen, C. (2003). Density and distribution of primordial follicles in single pieces of cortex from 21 patients and in individual pieces of cortex from three entire human ovaries. *Hum. Reprod.* 18, 1158–1164. doi: 10.1093/humrep/deg246

Schmittgen, T. D., and Livak, K. J. (2008). Analyzing real-time PCR data by the comparative C(T) method. *Nat. Protoc.* 3, 1101–1108. doi: 10.1038/nprot.2008.73

Sequeira, J. M., Ramaekers, V. T., and Quadros, E. V. (2013). The diagnostic utility of folate receptor autoantibodies in blood. *Clin. Chem. Lab. Med.* 51, 545–554. doi: 10.1515/cclm-2012-0577

Shen, F., Wu, M., Ross, J. F., Miller, D., and Ratnam, M. (1995). Folate receptor type gamma is primarily a secretory protein due to lack of an efficient signal for glycosylphosphatidylinositol modification: protein characterization and cell type specificity. *Biochemistry* 34, 5660–5665. doi: 10.1021/bi00016a042

Smithells, R. W., Sheppard, S., and Schorah, C. J. (1976). Vitamin deficiencies and neural tube defects. *Arch. Dis. Child.* 51, 944–950. doi: 10.1136/adc.51.12.944

Spiegelstein, O., Eudy, J. D., and Finnell, R. H. (2000). Identification of two putative novel folate receptor genes in humans and mouse. *Gene* 258, 117–125. doi: 10.1016/S0378-1119(00)00418-2

Stover, P. J. (2009). One-carbon metabolism-genome interactions in folate-associated pathologies. *J. Nutr.* 139, 2402–2405. doi: 10.3945/jn.109.113670

Sudiwala, S., De Castro, S. C., Leung, K. Y., Brosnan, J. T., Brosnan, M. E., Mills, K., et al. (2016). Formate supplementation enhances folate-dependent nucleotide biosynthesis and prevents spina bifida in a mouse model of folic acid-resistant neural tube defects. *Biochimie* 126, 63–70. doi: 10.1016/j.biochi.2016.02.010

Taparia, S., Gelineau-Van Waes, J., Rosenquist, T. H., and Finnell, R. H. (2007). Importance of folate-homocysteine homeostasis during early embryonic development. *Clin. Chem. Lab. Med.* 45, 1717–1727. doi: 10.1515/CCLM.2007.345

Van Straaten, H. W., and Copp, A. J. (2001). Curly tail: a 50-year history of the mouse spina bifida model. *Anat. Embryol.* 203, 225–237. doi: 10.1007/s004290100169

Warner, D. R., Webb, C. L., Greene, R. M., and Pisano, M. M. (2011). Altered signal transduction in Folr1-/- mouse embryo fibroblasts. *Cell Biol. Int.* 35, 1253–1259. doi: 10.1042/CBI20110025

Zeng, F., and Schultz, R. M. (2005). RNA transcript profiling during zygotic gene activation in the preimplantation mouse embryo. *Dev. Biol.* 283, 40–57. doi: 10.1016/j.ydbio.2005.03.038

Conflict of Interest Statement: The authors declare that the research was conducted in the absence of any commercial or financial relationships that could be construed as a potential conflict of interest.

Advantages of publishing in Frontiers

OPEN ACCESS
Articles are free to read for greatest visibility and readership

FAST PUBLICATION
Around 90 days from submission to decision

HIGH QUALITY PEER-REVIEW
Rigorous, collaborative, and constructive peer-review

TRANSPARENT PEER-REVIEW
Editors and reviewers acknowledged by name on published articles

Frontiers
Avenue du Tribunal-Fédéral 34
1005 Lausanne | Switzerland

Visit us: www.frontiersin.org
Contact us: info@frontiersin.org | +41 21 510 17 00

REPRODUCIBILITY OF RESEARCH
Support open data and methods to enhance research reproducibility

DIGITAL PUBLISHING
Articles designed for optimal readership across devices

FOLLOW US
@frontiersin

IMPACT METRICS
Advanced article metrics track visibility across digital media

EXTENSIVE PROMOTION
Marketing and promotion of impactful research

LOOP RESEARCH NETWORK
Our network increases your article's readership